DE GRUYTER

Tracey Rouault (Ed.)

IRON-SULFUR CLUSTERS IN CHEMISTRY AND BIOLOGY

VOLUME 2: BIOCHEMISTRY, BIOSYNTHESIS AND HUMAN DISEASES

2. EDITION

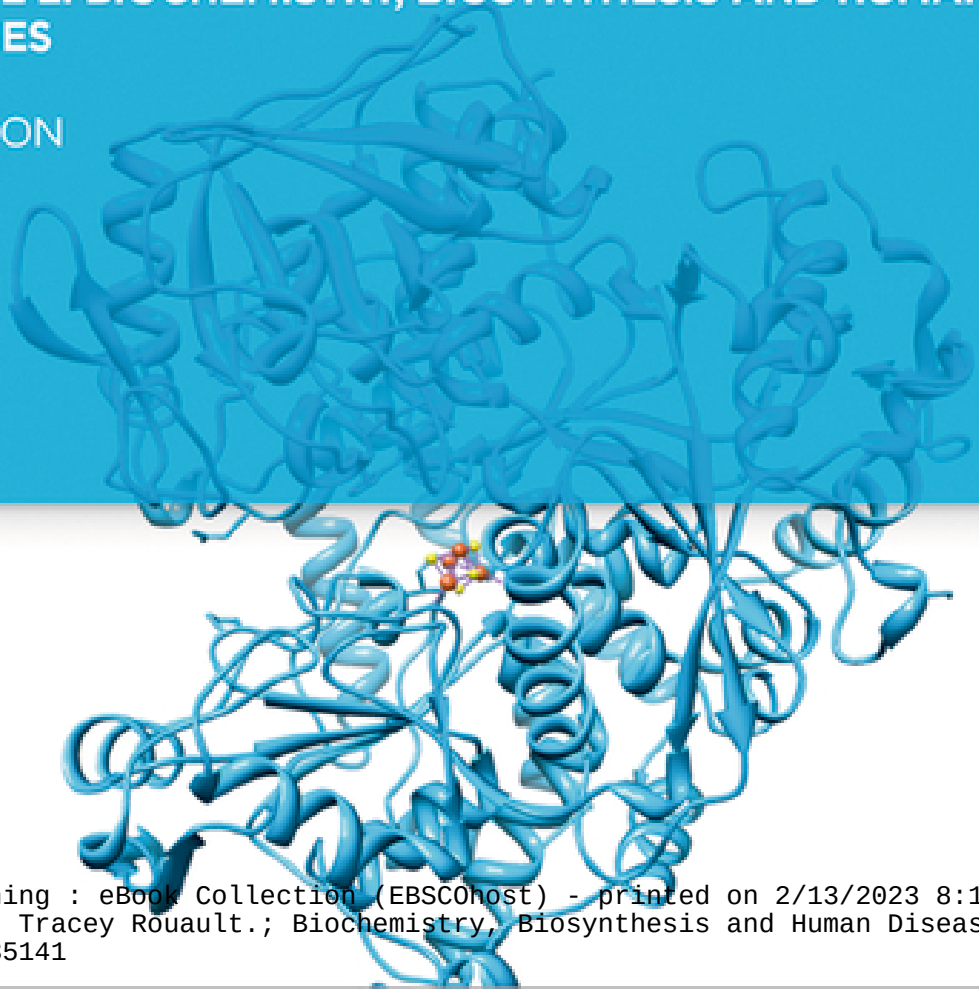

Rouault (Ed.)
Iron-Sulfur Clusters in Chemistry and Biology

Also of interest

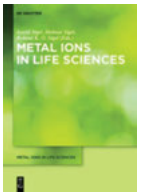

Metal Ions in Life Sciences
The Sigels' Series
Sigel, Astrid / Sigel, Helmut / Sigel, Roland K.O. (Eds.), 2017
ISSN 1559-0836, eISSN: 1868-0402

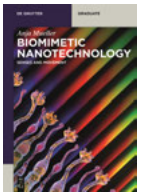

Biomimetic Nanotechnology
Senses and Movement
Mueller, 2017
ISBN 978-3-11-037914-3, e-ISBN 978-3-11-037916-7

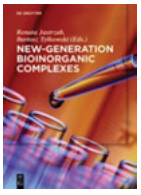

New-Generation Bioinorganic Complexes
Jastrzab, Tylkowski (Eds.), 2016
ISBN 978-3-11-034891-0, e-ISBN 978-3-11-034890-3

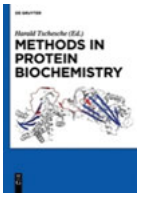

Methods in Protein Biochemistry
Tschesche, 2011
ISBN 978-3-11-025233-0, e-ISBN 978-3-11-025236-1

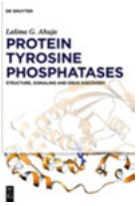

Protein Tyrosine Phosphatases
Structure, Signaling and Drug
Ahuja, 2018
ISBN 978-3-11-042643-4, e-ISBN 978-3-11-042177-4

Microbial Applications.
Recent Advancements and Future Developments
Kumar Gupta, Zeilinger, Ferreira Filho, Carmen Durán-Dominguez-de-Bazua, Purchase (Eds.), 2016
ISBN 978-3-11-041220-8, e-ISBN 978-3-11-041278-9

Iron-Sulfur Clusters in Chemistry and Biology

Biochemistry, Biosynthesis, and Human Diseases

Edited by
Tracey Rouault

Volume 2

DE GRUYTER

Editor
Tracey Rouault
Eunice Kennedy Shriver
National Institute of Child Health and Human Development
National Institutes of Health
Bethesda, MD. 20892
traceyrouault@icloud.com

ISBN 978-3-11-047939-3
e-ISBN (E-BOOK) 978-3-11-047985-0
e-ISBN (EPUB) 978-3-11-047952-2

Library of Congress Cataloging-in-Publication Data
A CIP catalog record for this book has been applied for at the Library of Congress.

Bibliographic information published by the Deutsche Nationalbibliothek
The Deutsche Nationalbibliothek lists this publication in the Deutsche Nationalbibliografie; detailed bibliographic data are available on the Internet at http://dnb.dnb.de.

Cover image: Rouault, Maio, 2017
Typesetting: Compuscript Ltd. Shannon, Ireland
Printing and binding: CPI books GmbH, Leck
∞ Printed on acid-free paper
Printed in Germany

www.degruyter.com

Preface

Iron-sulfur (Fe-S) clusters are versatile prosthetic groups that enable their associated proteins to perform numerous functions, ranging from electron transport to substrate ligation, structural support and DNA repair. Fe-S proteins did not become a focus of research until the late 1950's, when spectroscopy techniques evolved sufficiently to identify features that were specific for Fe-S clusters. Initially identified in mammalian succinate dehydrogenase, Fe-S clusters were subsequently found in numerous bacterial proteins that performed complex functions, including nitrogenase, which transforms atmospheric nitrogen into ammonia, generating an accessible source of nitrogen for synthesis of proteins and nucleic acids. Understanding how Fe-S clusters and proteins work has occupied many scientists for decades, and important breakthroughs regarding the mechanisms of nitrogenase and hydrogenase have occurred in just the last few years.

Not only is it a challenge to understand how Fe-S proteins work, but it is also a challenge to understand how Fe-S clusters are synthesized and inserted into Fe-S proteins in living organisms. Studies originally performed in bacterial model systems have revealed basic mechanisms of biogenesis that are conserved in all the kingdoms of life. Moreover, it has become apparent that flaws in the Fe-S assembly process cause several human diseases. As a result, biomedical researchers working on the pathophysiology of rare diseases such as Friedreich's ataxia have begun attending conferences at which chemists and physicists discuss Fe-S research based on complex spectroscopic studies and computational analyses. Researchers from different ends of the spectrum have struggled to bridge the large gap between the physics and chemistry of Fe-S clusters and the important biological questions associated with their functions.

Despite a growing need for cross-disciplinary communication, there was no single book devoted to Fe-S proteins that provided a basic and broad overview of the subject as it evolved over the last several decades until the first edition of this book was published in 2014. This book represents the second edition of "Iron-sulfur clusters in chemistry and biology", which was written to make the subject of Fe-S proteins more widely accessible to students and researchers by including a short history of Fe-S research, chapters that highlight the unique chemistry of Fe-S clusters and techniques important in analysis, and reviews from leading researchers on well-known Fe-S proteins such as nitrogenase and hydrogenase. In addition, numerous chapters focus on Fe-S synthesis and regulation in model organisms, and in mammalian biogenesis, DNA metabolism and human disease. Concluding with a discussion on the potential role of Fe-S clusters in capturing reducing power and contributing to the origin of life on earth, the final chapter touches on questions about how metabolic pathways initially developed. Because of the rapid growth of the field, this book is now divided into two volumes. The first volume focuses more on fundamental chemistry

and important enzymatic mechanisms. The second focuses more on Fe-S proteins in biological systems, the mechanisms by which Fe-S clusters are synthesized and correctly targeted to recipient proteins, and important regulatory functions of Fe-S proteins. Multiple chapters were updated to reflect rapid progress, and new chapters were added to expand coverage of methodologies used for characterization of Fe-S proteins, chemical principles that render Fe-S clusters unique, including their sensitivity to nitric oxide, and roles in DNA signaling and repair. Other new chapters cover the Fe-S biogenesis process in *E. coli*, new insights into how Fe-S recipient proteins acquire their clusters, and expansion of the chapters on human diseases that result from failures of Fe-S protein biogenesis and function.

I am indebted to my many outstanding and generous colleagues, who spent considerable time and effort in writing the chapters in this book. I hope that this book will be useful to those interested in the subject of Fe-S from many different perspectives, and that researchers from related disciplines will gain a greater sense for the context of their own work.

I want to thank Stephanie Dawson, who perceived that there was an unmet intellectual need and initiated this project in 2014 while she was an editor at De Gruyter. I also gratefully thank Julia Lauterbach, Ria Fritz, Anne Hirschelmann, and Vivien Schubert of De Gruyter for their tireless support and guidance in turning this book into a reality. My family and friends have graciously supported me when I needed time to work on the project long known to them as “the book”, and I’m thankful for their help.

Tracey Rouault, July, 2017

Tracey A. Rouault biography

Tracey A. Rouault is a leading researcher in the area of mammalian iron-sulfur proteins, an area she began to pursue after discovering an important role for an iron-sulfur protein in the regulation of mammalian iron metabolism. She received a degree in Biology from Yale College and an MD degree from Duke University Medical School, where she completed her training in internal medicine. She completed a medical fellowship at the National Institutes of Health in Bethesda, Maryland, and has since focused on the regulation of mammalian iron metabolism and its relationship to human diseases. Her main interests include elucidating mechanisms of mammalian iron-sulfur cluster biogenesis and exploring the pathophysiology of diseases related to ineffective iron-sulfur cluster biogenesis, several hematologic disorders, genetic cancer syndromes, and neurodegenerative diseases. Her early research in the role of iron-sulfur proteins in regulation led to a productive collaboration with Helmut Beinert, a researcher responsible for numerous ground-breaking advances related to iron-sulfur proteins. She has also collaborated with Richard Holm, whose pioneering work led to the inorganic synthesis of numerous iron-sulfur clusters and revealed that many properties of iron-sulfur proteins derive from intrinsic features of their iron-sulfur clusters. She is an active member of the rapidly growing iron-sulfur protein research community.

Contents

List of contributing authors

Michael W. W. Adams
Department of Biochemistry and Molecular Biology
University of Georgia
Athens, GA, USA
chapter 17

Laurent Aussel
Laboratoire de Chimie Bactérienne
Aix Marseille Université, CNRS
Marseille, France
chapter 2

Frédéric Barras
Laboratoire de Chimie Bactérienne
Aix Marseille Université, CNRS
Marseille, France
e-mail: barras@imm.cnrs.fr
chapter 2

Phillip L. Bartels
Division of Chemistry and Chemical Engineering
California Institute of Technology
Pasadena, CA, USA
e-mail: pbartels@caltech.edu
chapter 15

Jacqueline K. Barton
Division of Chemistry and Chemical Engineering
California Institute of Technology
Pasadena, CA, USA
e-mail: jkbarton@caltech.edu
chapter 15

Eric S. Boyd
Department of Microbiology
Montana State University
Bozeman, MT, USA
e-mail: eboyd@montana.edu
chapter 17

Joan B. Broderick
Department of Chemistry and Biochemistry
Montana State University
Bozeman, MT, USA
chapter 17

Sylvia Chareyre
Laboratoire de Chimie Bactérienne
Aix Marseille Université, CNRS
Marseille, France
chapter 2

Andrew Dancis
Biomedical Graduate Studies
University of Pennsylvania
Philadelphia, PA, USA
e-mail : adancis@mail.med.upenn.edu
chapter 6

Dennis Dean
Virginia Polytechnic Institute and State University
Blacksburg, VA, USA
e-mail : deandr@vt.edu
chapter 1

Patricia Dos Santos
Department of Chemistry
Wake Forest University
Winston-Salem, NC, USA
e-mail : dossanpc@wfu.edu
chapter 1 and 5

Yohann Duverger
Laboratoire de Chimie Bactérienne
Aix Marseille Université, CNRS
Marseille, France
chapter 2

Benjamin Ezraty
Laboratoire de Chimie Bactérienne
Aix Marseille Université, CNRS
Marseille, France
chapter 2

Kerstin Gari
Institute of Molecular Cancer Research
University of Zurich
Zurich, Switzerland
e-mail: gari@imcr.uzh.ch
chapter 13

Allison Huguenot
Laboratoire de Chimie Bactérienne
Aix Marseille Université, CNRS
Marseille, France
chapter 2

Patricia Kiley
Department of Biomolecular Chemistry
University of Wisconsin
Madison, WI, USA
e-mail : pjkiley@wisc.edu
chapter 4

Simon A.B. Knight
Perelman School of Medicine
University of Pennsylvania
Philadelphia, USA
chapter 11

Silke Leimkuhler
Molekulare Enzymologie
Universität Potsdam
Potsdam, Germany
e-mail : sleim@uni-potsdam.de
chapter 12

Roland Lill
Institut für Zytobiologie u.Zytopathologie
Philipps-Universität Marburg
Marburg, Germany
e-mail : Lill@staff.uni-marburg.de
chapter 14

Nunziata Maio
Eunice Kennedy Shriver National Institute of Child Health and Human Development
Bethesda, MD, USA
e-mail : nunziata.maio@nih.gov
chapter 9

Pierre Mandin
Laboratoire de Chimie Bactérienne
Aix Marseille Université, CNRS
Marseille, France
chapter 2

Erin L. Mettert
Department of Biomolecular Chemistry
University of Wisconsin
Madison, WI, USA
e-mail : elmettert@wisc.edu
chapter 4

Elizabeth O'Brien
Division of Chemistry and Chemical Engineering
California Institute of Technology
Pasadena, CA, USA
e-mail: eobrien@caltech.edu
chapter 15

Caryn Outten
Department of Chemistry and Biochemistry
University of South Carolina
Columbia, SC, USA
e-mail : outten@mailbox.sc.edu
chapter 7

Wayne Outten
Department of Chemistry and Biochemistry
University of South Carolina
Columbia, SC, USA
e-mail : outtenf@mailbox.sc.edu
chapter 3

Debkumar Pain
Department of Pharmacology and Physiology
New Jersey Medical School
Rutgers University
Newark, NJ, USA
e-mail: painde@njms.rutgers.edu
chapter 6

Nicole T. Perna
Department of Genetics,
University of Wisconsin
Madison, WI, USA
e-mail: ntperna@wisc.edu
chapter 4

John Peters
Department of Chemistry and Biochemistry
Montana State University
Bozeman, MT, USA
e-mail : john.peters.cab@gmail.com
chapter 17

Béatrice Py
Laboratoire de Chimie Bactérienne
Aix Marseille Université, CNRS
Marseille, France
chapter 2

Tracey Rouault
Eunice Kennedy Shriver National Institute of Child Health and Human Development
Bethesda, MD, USA
e-mail : traceyrouault@icloud.com
chapter 8 and 9

Eric M. Shepard
Department of Chemistry and Biochemistry
Montana State University
Bozeman, MT, USA
chapter 17

Gerrit J. Schut
Department of Biochemistry and Molecular Biology
University of Georgia
Athens, GA, USA
chapter 17

Marta Uzarska
Institut für Zytobiologie u.Zytopathologie
Philipps-Universität Marburg
Marburg, Germany
chapter 14

Robert B. Wilson
Children's Hospital of Philadelphia
Perelman School of Medicine
University of Pennsylvania
Philadelphia, USA
e-mail: wilsonr@mail.med.upenn.edu
chapter 11

Wing Hang Tong
Eunice Kennedy Shriver National Institute of Child Health and Human Development
Bethesda, MD, USA
e-mail : tongw@mail.nih.gov
chapter 10

James Wohlschlegel
Biology & Chemistry
UCLA
Los Angeles, CA, USA
e-mail : jwohl@mednet.ucla.edu
chapter 14

Hong Ye
Key Laboratory of Plant Resources Conservation and Sustainable Utilization
South China Botanical Garden
Chinese Academy of Sciences
Guangzhou, China
e-mail : hye@scib.ac.cn
chapter 16

Jordi Zamarreno
Laboratoire de Chimie Bactérienne
Aix Marseille Université, CNRS
Marseille, France
chapter 2

1 A retrospective on the discovery of [Fe-S] cluster biosynthetic machineries in *Azotobacter vinelandii*

Patricia C. Dos Santos and Dennis R. Dean

1.1 Introduction

Iron-sulfur clusters ([Fe-S]) clusters are inorganic prosthetic groups that participate in many essential life processes. Despite their relatively simple structures, the biological assembly of [Fe-S] clusters is complicated and the defining features of the process have only emerged over the past two decades. The biosynthetic process involves two principle interacting proteins, an L-cysteine desulfurase and a molecular assembly scaffold. In this chapter, a retrospective is provided that describes the initial discovery of the mechanism for the assembly of [Fe-S] clusters in the nitrogen-fixing organism *Azotobacter vinelandii*. Why and how the study of biological nitrogen fixation ultimately contributed the key insights into the general process of [Fe-S] cluster assembly is described.

Beinert, Holm, and Munck, pioneers in the field of bioinorganic chemistry, have aptly described biological iron-sulfur clusters ([Fe-S] clusters) as nature's modular, multipurpose structures [1]. What are [Fe-S] clusters, why do they exist in nature, and why are they so important to so many biological processes? [Fe-S] clusters were originally discovered as inorganic prosthetic groups composed exclusively of iron and sulfide contained in a class of redox-active proteins denominated as ferredoxins [2, 3]. Ferredoxins are electron/proton carrier proteins that contain [Fe-S] clusters, usually in the form of rhombic [2Fe-2S] or cubane [4Fe-4S] clusters (Fig. 1.1). [Fe-S] clusters are most often covalently attached to their cognate protein partners through cysteinyl thiolate ligation to their metal sites, although other ligation modes are also known to exist and not all of the metal sites are necessarily coordinated by a protein-donated ligand [4]. Ferredoxins represent a specialized class of a wide variety of proteins, now generically designated as [Fe-S] proteins, that contain one or more [Fe-S] clusters. It is the capacity of [Fe-S] clusters to exist in multiple oxidation states that endows [Fe-S] proteins with their ability to serve as electron/proton carriers. Indeed, the reversibility of redox properties of [Fe-S] proteins is an integral aspect of essential energy transducing processes in nitrogen fixation, photosynthesis, and respiration. The key involvement of [Fe-S] clusters in such life-sustaining processes is intimately linked to the wide range of redox potentials they can attain as a consequence of their respective polypeptide environments [5]. However, the ability of proteins to tune the redox potentials of their cognate [Fe-S] clusters is not the only feature of [Fe-S] clusters exploited by nature. The chemical and structural versatility of [Fe-S]

DOI 10.1515/9783110479850-001

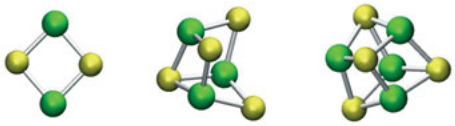

Fig. 1.1: Simple [Fe-S] cluster types found in nature.

clusters, uniquely achieved by combining the individual chemical properties of Fe and S, has enabled [Fe-S] proteins to fulfill other important biological roles including activation of substrates for chemical transformations, serving as environmental sensors, providing structural determinants within proteins, and functioning as agents of gene regulation [4, 6].

Although [Fe-S] clusters play a central role in many biological processes, there is also a significant penalty associated with their use. Indeed, Fe^{2+} and S^{2-}, necessary for both the assembly and disassembly of [Fe-S] clusters, are toxic to a wide variety of cellular processes in aerobic organisms. How then did [Fe-S] clusters become so pervasive in biology? The answer to this question is not known for certain but could be linked to the "iron-sulfur world" theory, which proposes that chemical reactions associated with formation of the organic building blocks necessary for the emergence of life on earth occurred on metal-sulfur surfaces in the highly reducing environment of prebiotic earth [7, 8]. Certain aspects of such chemistries might have been captured in primordial organisms in the form of [Fe-S] clusters, particularly when considering that facile "spontaneous" assembly of [Fe-S] clusters occurs under reducing conditions. This possibility finds some credence when it is considered that life likely originated in an anoxic environment in which free Fe^{2+} and free S^{2-} did not pose the same risk as is associated with the oxygen-saturated environment that dominates life on earth today. For example, the potential for lethal formation of reactive oxygen species (ROS) through Fenton chemistry did not exist for emergent life forms. This luxury was eliminated, however, by the advent of oxygenic photosynthesis, which gradually converted the biosphere from a reducing environment to a primarily oxidizing environment. Given that fundamental life sustaining processes requiring [Fe-S] clusters were almost certainly well developed by the time photosynthesis emerged, the spontaneous assembly of [Fe-S] clusters from free Fe^{2+} and S^{2-} could not possibly continue, even if that was the case in primordial life. What this means is that at some point during evolution and certainly upon transition of earth to an oxidizing atmosphere, living organisms needed to develop a way to construct [Fe-S] clusters such that free Fe^{2+} and free S^{2-} were not required [9, 10]. In other words, these elements needed to be trafficked and combined in nontoxic forms or living organisms needed to evolve alternative strategies to replace the many functions supplied by [Fe-S] proteins.

Considering the importance of [Fe-S] clusters in sustaining essential life processes [11] as well as the striking structural simplicity of most [Fe-S] clusters, it might

seem curious that so little was known about their biological assembly until relatively recently. However, as is discussed in this narrative, there are very good reasons why a fundamental understanding of the assembly of [Fe-S] clusters took so long to develop when compared with our understanding of the biosynthetic pathways for formation of many other organic cofactors. One reason is that the critical importance of [Fe-S] clusters to so many biological processes prevented fortuitous discovery of assembly factors in genetic screens because assembly factors were necessary for survival. Another reason is that the structural simplicity of [Fe-S] clusters, and the ability to form them spontaneously *in situ* from free Fe^{2+} and S^{2-}, failed to inspire serious inquiry into potential mechanisms for their biological formation. In this chapter, we provide a retrospective about the work using the bacterium *Azotobacter vinelandii*, and studies on the specialized process of biological N_2 fixation, that ultimately led to some of the key insights about the [Fe-S] cluster assembly process.

1.2 An introduction to nitrogenase

Serendipity is defined as the accident of finding something good or useful while not specifically searching for it. Initial work on nitrogenase was not aimed at understanding how simple [Fe-S] clusters are formed in biological systems. Instead, the focus was directed at understanding the genetic determinants and chemical mechanism of biological N_2 fixation, an essential contributor to the biogeochemical nitrogen cycle. Here we discuss some of the general features of the enzyme nitrogenase, the catalytic component of N_2 fixation, and the initial approaches that were used to explore its function [12, 13]. It will be seen that, by both chance and design, these approaches inexorably led to the discovery of unifying features involved in the assembly of simple [Fe-S] clusters necessary to sustain cellular metabolism.

Simple rhombic [2Fe-2S] and cubane [4Fe-4S] clusters (Fig. 1.1), composed only of Fe and S, represent the dominant forms of [Fe-S] clusters in biological systems [4]. However, there are also other types of [Fe-S] clusters that have higher nuclearity, those that contain another metal in addition to Fe, and those that also contain organic constituents [13, 14]. A broad spectrum of [Fe-S] cluster types can be found in nitrogenase, the enzyme that catalyzes the nucleotide-dependent reduction of N_2 to yield two molecules of ammonia (NH_3) (Fig. 1.2). Nitrogenase is a two component enzyme that contains a canonical [4Fe-4S] cluster, involved in electron transfer, a novel [8Fe-7S] cluster (P-cluster) that also serves as an agent of electron transfer, and a [7Fe-9S-Mo-C-homocitrate] cluster (FeMo cofactor, or FeMoco), which contains molybdenum (Mo) and provides the site for N_2 activation and reduction [15]. One component of nitrogenase is called the Fe protein, a name derived from the observation that it contains a single [4Fe-4S] cluster bridged between two identical subunits. Each Fe protein subunit also contains a nucleotide-binding site. The other component of nitrogenase is called the MoFe protein, a name derived from the fact it contains FeMoco. The MoFe

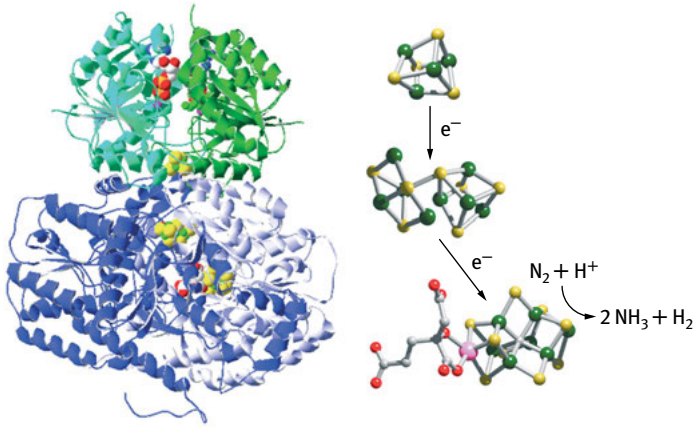

Fig. 1.2: Mo-dependent nitrogenase and its associated [Fe-S] clusters. (left) Ribbon representation of a Mo-dependent nitrogenase catalytic unit. The MoFe protein α-subunit is shown in light blue, and the β-subunit is shown in dark blue. The Fe protein is shown in a complex with the MoFe protein, and the identical Fe protein subunits are indicated in light and dark green. Nucleotides bound to the Fe protein and the associated [Fe-S] clusters are shown as space-filling models. (right) Ball-and-stick representations of the nitrogenase-associated [Fe-S] clusters: [4Fe-4S] cluster (top), [8Fe-7S] P-cluster (center), [7Fe-9S-C-Mo-homocitrate] FeMoco structure from PDB 3U7Q (bottom). The electron flow direction and site of nitrogen reduction is indicated.

protein is an $\alpha_2\beta_2$ heterotetramer that, in combination with two Fe proteins, appears to contain two independent catalytic units. One P-cluster is located at the interface of each MoFe protein αβ interface and one FeMoco is buried entirely within each MoFe protein α subunit. During catalysis, the Fe Protein and MoFe protein cycle through a series of sequential single electron transfer events and each cycle is coupled to the binding and hydrolysis of two ATPs. FeMoco becomes activated for N_2 binding and reduction once the MoFe protein has accumulated a sufficient number of electrons that have been delivered by the Fe protein [16].

Models for how intermolecular electron transfer is coupled to nucleotide hydrolysis, where and how nitrogenase substrates interact with FeMoco, and how FeMoco is activated for substrate binding have been proposed [17–19]. These models were developed through application of the biochemical-genetic approach described in a following section, advanced spectroscopic analyses, and consideration of high-resolution crystallographic structures of the Fe protein and MoFe protein. However, when the biochemical-genetic approach for analysis of nitrogenase structure and function was initiated, the structures of nitrogenase proteins and their associated metalloclusters were not known, nor was the identity, organization, and function of genes associated with formation of an active nitrogenase understood. During the late 1970s, a variety of approaches were undertaken with the goal of understanding how nitrogenase functions at the mechanistic level and how the complex [Fe-S] clusters

associated with its activity are formed [20, 21]. There were two practical reasons for wanting to understand the mechanism of nitrogenase at the chemical level as well as for understanding the pathways involved in assembly of its associated [Fe-S] clusters. First, a mechanistic understanding of nitrogenase might be useful for the development of synthetic biomimetic catalysts for N_2 reduction. Second, attempts to endow higher plants with the capacity to produce their own nitrogenous fertilizer necessarily depend on a fundamental understanding of the genetic and biochemical determinants required for formation of an active nitrogenase.

Attempts to elucidate the organization and function of genes associated with nitrogenase predated the availability of genomic sequences. The pioneering work in this area of research was performed in the late 1970s and early 1980s and used the N_2-fixing facultative anaerobe *Klebsiella pneumoniae* as an experimental organism. As a starting point, this work involved the isolation of mutant strains having point mutations or insertion mutations that resulted in a defective capacity for N_2 fixation [22, 23]. The chromosomal position of each mutation was subsequently determined by classical genetic mapping technologies using phage transduction and three factor crosses, and the individual proteins affected were identified by protein mobility shifts that could be recognized by analysis of mutant crude extracts using two-dimensional gel electrophoresis [24–28]. In retrospect, it is amazing that, without the benefit of DNA sequencing technology, nearly every gene associated with N_2 fixation in *K. pneumonia*, collectively designated as *nif* genes (for nitrogen fixation), was correctly identified in this way, as were their relative chromosomal locations, and their organization into transcriptional units (Fig. 1.3) [29, 30].

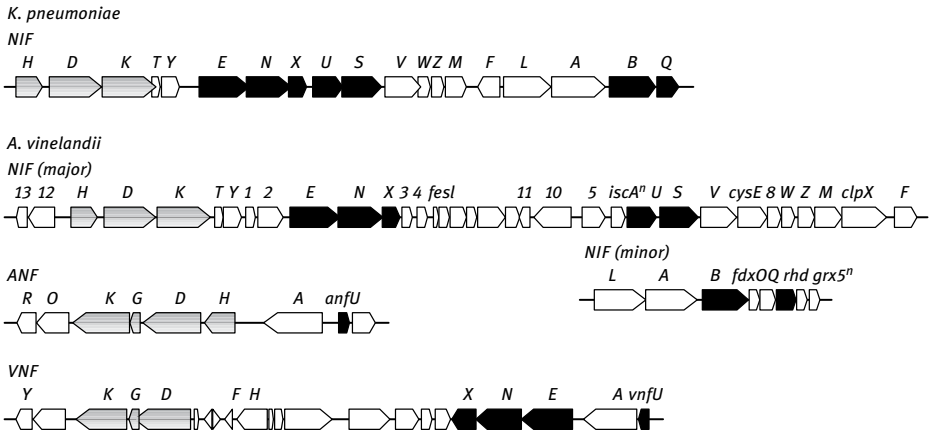

Fig. 1.3: Nitrogen fixation-associated gene regions in *K. pneumoniae* and *A. vinelandii*. The organization of gene regions for the three nitrogen fixation systems, Nif, Anf, and Vnf, is indicated. Genes encoding nitrogenase catalytic components are shown in light gray; genes known or suspected to be involved in [Fe-S] cluster assembly or trafficking are shown in black.

Once the fundamental genetic determinants necessary for N_2 fixation by *K. pneumoniae* were established, a variety of investigators turned their attention to *A. vinelandii* as the experimental organism because (i) *A. vinelandii* fixes N_2 under aerobic growth conditions, making large-scale growth possible without requiring specialized fermentation facilities, (ii) this bacterium abundantly produces nitrogenase when grown under conditions that impose a need for N_2 fixation, (iii) it is tractable to facile genetic manipulation, and (iv) it produces multiple, genetically distinct, forms of nitrogenase (discussed later). *A. vinelandii* turned out to be an excellent choice as an experimental organism and proved to be instrumental in advancing the current mechanistic understanding of N_2 fixation. For example, the highest resolution structures currently available were produced using nitrogenase isolated from *A. vinelandii* [31–33]. Also, current mechanistic models for nitrogenase are based on interpretation of biochemical and biophysical analyses of altered nitrogenases produced by mutant strains derived from *A. vinelandii* [15]. Finally, a comprehensive understanding of the mechanism for assembly of FeMoco, which provides the N_2 activation and reduction site, has emerged from studies on components isolated from *A. vinelandii* [34, 35].

Foundational work using *K. pneumoniae* proved to be valuable when investigators initiated serious studies on the biochemical-genetic analysis of N_2 fixation in *A. vinelandii* because it provided a genetic roadmap and a baseline analysis for establishing gene-product relationships. Early efforts to construct a physical map of genes involved in N_2 fixation in *A. vinelandii* revealed a much more complex picture than that established for *K. pneumoniae* (Fig. 1.3) [36, 37]. For example, not all *A. vinelandii* genes associated with N_2 fixation are physically linked on the genome, as was true for *K. pneumoniae*. Also, there are many more N_2 fixation-associated genes in *A. vinelandii* when compared with *K. pneumoniae*. Finally, it was discovered that *A. vinelandii* encodes three genetically distinct N_2-fixing systems, two of which do not require Mo for their respective activities [38]. One of these is designated as the "V-dependent" nitrogenase [genetically indicated as *vnf* because its counterpart to the FeMoco contains the transition metal, vanadium (V) in place of Mo]. The other is designated as "Fe-only" nitrogenase (genetically indicated as *anf*) because it represents a counterpart to the FeMoco in which Fe substitutes for the Mo atom [39–41]. There is a hierarchy of physiological expression of the different nitrogenases. Notably, the V-dependent enzyme is expressed only when Mo is not available in the growth medium but V is available. The Fe-only nitrogenase is expressed only when neither Mo nor V is available in the growth medium. Such hierarchical expression of genes that encode the different nitrogenases might reflect the catalytic efficiencies of the corresponding enzyme systems, with the Mo-dependent enzyme being the most efficient and the Fe-only enzyme being the least efficient [42]. Although the catalytic components of the different nitrogenases are genetically distinct, they all appear to share common mechanistic features. The entire suite of genes associated with all three systems was ultimately established by determination of the genome sequence of *A. vinelandii* and

transcriptome analyses of gene expression under conditions favoring each of the respective systems (Fig. 1.3) [43–46].

1.3 Approaches to identify gene-product and product-function relationships

Two related biochemical-genetic approaches were initially used to establish gene-product and product-function relationships in N_2 fixation [12] prior to the advent of the field now known as genomics. The first of these involved searching for mutant strains defective in N_2 fixation followed by identification of the affected gene, and subsequent characterization of the specific biochemical phenotype associated with loss of that function. The second approach used *in vitro* biochemical complementation experiments, involving the mixture of extracts, or purified proteins, prepared from separately isolated mutant strains that were each defective in a particular function, in an attempt to rescue a biochemical function. The power of such classical approaches, first developed in the 1940s, has been tremendously augmented over the past several decades through application of recombinant DNA technologies and the capacity for rapid and accurate DNA sequence analyses. Among the many tools now available to researchers that have been applied to the analysis of N_2 fixation are included: (1) prediction of possible functional features based on deduction of primary structures from DNA sequences; (2) heterologous production of proteins at prodigious levels using recombinant expression plasmids; (3) directed *in vitro* mutagenesis and gene replacement; and (4) placement of affinity tags within a gene that encodes a protein of particular interest to facilitate its purification for subsequent biochemical analysis. We now describe how these technologies, in combination with the classical biochemical-genetic approach, were applied to provide an understanding of some of the basic features associated with N_2 fixation-specific [Fe-S] cluster formation.

1.4 FeMoco and development of the scaffold hypothesis for complex [Fe-S] cluster formation

Two aspects of N_2 fixation make it particularly amenable to application of the biochemical-genetic approach for the study of [Fe-S] cluster biogenesis. First, the ability to fix N_2 is dispensable for the growth of N_2-fixing organisms when an alternative nitrogen source, for example, ammonia, is supplemented in the growth medium. In other words, mutant strains defective in N_2 fixation grow normally and are indistinguishable from wild-type strains, unless they are cultured under conditions that demand N_2 fixation [47]. The other reason N_2 fixation is amenable to biochemical-genetic analysis is that nitrogenase is a very poor catalyst [48], and therefore, it must be produced at very high levels to sustain growth under conditions that demand N_2

fixation. Consequently, N_2-fixing cells also have a high demand for the acquisition of the Fe and S needed for assembly of nitrogenase-associated [Fe-S] clusters. It is the conditional dispensability of the capacity for physiological N_2 reduction as well as the high levels of nitrogenase production in N_2 fixing cells that proved to be important aspects in the discovery of how Fe and S are combined for formation of both complex and simple [Fe-S] clusters.

It has already been noted that the FeMoco provides the site for N_2 binding and reduction. This feature was firmly established using a variety of experimental methods, but there were two, simple, but elegant, approaches that first led to discovery of FeMoco and subsequently to the concept of a molecular scaffold involvement in complex [Fe-S] cluster assembly. In the early analysis of mutant strains defective in N_2 fixation, several mutants that were specifically defective in MoFe protein activity but lacked mutations in the structural genes that encode the MoFe protein, *nifD* or *nifK*, were identified (Tab. 1.1). Rather, these mutant strains had mutations in genes designated *nifE*, *nifN*, or *nifB* [12, 30]. It was then discovered that extraction of purified MoFe protein using a chaotropic organic solvent, *N*-methyl formamide, released a factor that contained Fe and Mo, which could be added to extracts of *nifB, nifE*, or *nifN* mutants to reconstitute MoFe protein activity [49]. Because the released factor contained both Fe and Mo, it was designated FeMoco, and *nifB, nifE*, and *nifN* were recognized to be necessary for FeMoco formation.

Tab. 1.1: Gene-product relationships and phenotypes associated with selected *A. vinelandii nif* genes.

Gene	Product and function	Fe protein[a]	MoFe protein[b]	Required for V- and Fe-only nitrogenases
nifH	Fe protein subunit	NA	NA	No
*nif*D	MoFe protein α-subunit	A	NA	No
*nif*K	MoFe protein β-subunit	A	NA	No
*nif*E	FeMo-cofactor assembly scaffold α-subunit	A	NA	No
*nif*N	FeMo-cofactor assembly scaffold β-subunit	PA	NA	No
*nif*B	SAM-dependent C-insertion into FeMoco	A	NA	Yes
*nif*U	Simple [Fe-S] cluster assembly scaffold	PA	PA	Yes
*nif*S	Cysteine desulfurase	PA	PA	Yes
*nif*V	Homocitrate synthase	A	PA	Yes
*nif*M	Fe protein maturase *cis-trans* Prolyl-isomerase	NA	PA	Yes

[a] Fe protein activity (nmol of ethylene/min/mg of crude extracts) after addition of saturating levels of purified MoFe protein.
[b] MoFe protein activity (nmol of ethylene/min/mg of crude extracts) after addition of saturating levels of purified Fe protein.
A, activity detected (>50% of wild-type levels); NA, no activity (<1%); PA, partial activity detected (5%–40%).

It is now well understood that the biosynthesis of FeMoco involves the products of *nifE*, *nifN*, and *nifB* as well as the participation of other *nif* gene products, for example, *nifV*, which encodes a homocitrate synthase (Tab. 1.1) [50, 51]. However, none of the specific functions of these proteins was known during the early development of the scaffold hypothesis for complex [Fe-S] cluster assembly. With respect to assembly of FeMoco, one possibility was that Fe, S, Mo, and organic constituents could be separately inserted into the MoFe protein. Such an assembly path is analogous to on-site construction of a house within a neighborhood using brick, wood, and other construction materials separately delivered to the construction site. The other possibility was that FeMoco could be preassembled and then inserted into MoFe protein as an intact entity. This latter type of construction is analogous to the prefabrication of a house, followed by subsequent delivery of the house to the neighborhood. To differentiate between these possibilities, extracts of mutant strains that do not produce MoFe protein but express functional products of all of the other *nif* genes were mixed with extracts of strains that are defective in *nifE*, *nifN*, or *nifB*, which all produce an inactive FeMoco-less MoFe protein [52, 53]. In this experiment, MoFe protein activity was reconstituted, demonstrating that FeMoco can be assembled in the absence of MoFe protein (produced in extracts that do not contain MoFe protein) and therefore must be pre-constructed and subsequently inserted intact into a cofactorless form of MoFe protein (produced in extracts of strains lacking NifE, NifN, or NifB function).

The above experiments were executed in the absence of any knowledge about the primary structure of NifE, NifN, or NifB and without direct knowledge about the distribution of the [Fe-S] clusters contained within the MoFe protein. However, there were already some clues available that made it possible to advance the "scaffold hypothesis" for formation of FeMoco. The main premise of the scaffold hypothesis was that because FeMoco is synthesized separately from the MoFe protein, it could be anticipated that some aspect of assembly might occur on a molecular "scaffold" that duplicates certain structural features of the MoFe protein, particularly within FeMoco-binding regions [54]. This hypothesis was initially developed on the foundation of an apparent correlation between NifD (MoFe protein α-subunit) and NifE and between NifK (MoFe protein β-subunit) and NifN, respectively. Namely, it was already known from genetic mapping and two-dimensional gel electrophoresis analyses that *nifD* and *nifK* were co-transcribed and expressed at approximately equal levels to each other and that *nifE* and *nifN* were separately co-transcribed and expressed at approximately equal levels to each other, suggesting that the structural genes (NifD and NifK) were in a different operon from the cofactor assembly genes (NifE and NifN). Furthermore, NifD was similar in size and isoelectric point to NifE, and NifK was similar to NifN [28, 55]. Elucidation of primary structures, deduced from DNA sequence analysis, did, in fact, reveal significant conservation in primary structure between NifD and NifE and between NifK and NifN, respectively [54, 56]. Particularly rich sequence conservation between a segment of NifD and NifE, was observed in the region predicted to provide at least a portion of the FeMoco-binding pocket, on the basis of the NifD primary structure [57]. These observations provided powerful support for

the scaffold hypothesis and indicated that NifE and NifN might form a heterotetrameric complex that provides a transient site for an intermediate stage of FeMoco formation. The primary structural comparisons between NifD and NifE also suggested that FeMoco might be located entirely within the MoFe protein α-subunit and that the NifEN complex might contain another cluster, analogous to the MoFe protein P-cluster, bridged between the NifE and NifN subunits. All of these predictions turned out to be correct [58–60].

1.5 An approach for the analysis of *nif* gene product function

Details concerning other specialized aspects of FeMoco assembly, for example, the formation and attachment of the organic constituent, homocitrate, and the insertion of the central carbide atom [35], will not be discussed in detail here, although some of these are summarized in Tab. 1.1. The topic of FeMoco assembly has been exhaustively reviewed [34, 35] and is discussed elsewhere in this volume. Nevertheless, as will be discussed below, efforts to understand the biochemical and regulatory functions of all the *nif*-associated gene products ultimately led to the discovery of general principles concerning how simple [Fe-S] clusters can be assembled on molecular scaffolds. In this regard, it is interesting and instructive that analysis of the assembly of nature's most complex [Fe-S] cluster known to date, FeMoco, provided the conceptual starting point for understanding how simple [Fe-S] clusters are assembled on molecular scaffolds.

The size and complexity of the *nif* regulon, together with the fact that nitrogenase, and some of its assembly factors, are oxygen sensitive, prohibited transferring the entire system to a tractable host such as *Escherichia coli* for heterologous expression and subsequent analysis. Instead, the ability to efficiently transform *A. vinelandii* using isolated DNA, and the inherent capacity of this organism for frequent homologous recombination, was exploited to place in-frame deletions within the *A. vinelandii* genomic region for each of the *nif*-associated genes, separately, and in various combinations [61]. This simple strategy (Fig. 1.4) involved the use of restriction enzymes to delete known

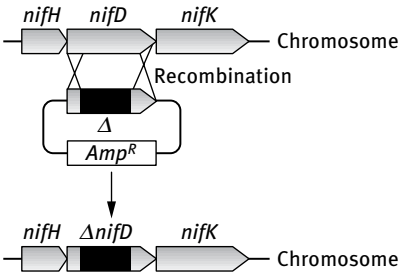

Fig. 1.4: Diagrammatic representation of *A. vinelandii* mutant strain construction. A specific deletion carried within a plasmid can be transferred to the chromosome by reciprocal recombination.

segments of *nif* genes contained in recombinant plasmids and subsequent transfer of such deletions to the corresponding region of the chromosome through transformation and reciprocal recombination. The values of this approach were that the native organism could be analyzed without disrupting the coordination and balance of *nif* gene expression and the precise nature of every genetic lesion was defined.

Because nitrogenase activity requires both the Fe protein and the MoFe protein and because neither protein exhibits any catalytic activity in the absence of the other, mutants that are specifically defective in one component or the other can be readily identified by adding either purified Fe protein or MoFe protein to mutant strain extracts in an attempt to reconstitute activity. One example of this type of experiment is that extracts of a mutant strain deleted for *nifB* exhibit no nitrogenase activity, but activity can be detected when isolated MoFe protein, or FeMoco extracted from MoFe protein, is added to the crude extract [12]. Hence, NifB is required for formation of an active MoFe protein and, more specifically, for formation of FeMoco. It was this type of analysis that launched the discovery of the roles of NifS and NifU as representing nature's minimum tool kit for formation of simple [Fe-S] clusters.

1.5.1 Phenotypes associated with loss of *NifS* or *NifU* function indicate their involvement in nitrogenase-associated [Fe-S] cluster formation

Strains in which either *nifS* or *nifU* were deleted revealed phenotypes that, in aggregate, distinguished them from all other N_2 fixation deficient mutant strains (Tab. 1.1). These phenotypes included the following: (1) negligible growth when cultured in the absence of a fixed nitrogen source under conditions that require expression of the Mo-dependent nitrogenase, the V-dependent nitrogenase, or the Fe-only nitrogenase; (2) significant descrease in the activities of both the Fe protein and the MoFe protein in crude extracts; (3) loss of the dark brown color characteristic of extracts prepared from N_2-fixing wild-type cells in extracts prepared from *nifU*- and *nifS*-deletion strains [62–65].

A common feature of all three nitrogenase systems is that they require [Fe-S] clusters for their respective activities. Similarly, the common feature of the Fe protein and MoFe protein is that they also both require [Fe-S] clusters to sustain a functional nitrogenase. These considerations indicated that NifS and NifU might have complementary functions related to the mobilization of the S and Fe necessary to assemble both the simple and the complex [Fe-S] clusters associated with nitrogenase. Because the characteristic dark brown color of extracts prepared from N_2-fixing cells is derived primarily from nitrogenase-associated [Fe-S] clusters, the relatively light color of NifS- and NifU-deficient extracts also implied that [Fe-S] cluster assembly was defective in *nifS* and *nifU* mutant strains. However, loss of NifS or NifU function does not completely eliminate nitrogenase activity [65] and therefore does not eliminate the assembly of nitrogenase-associated [Fe-S] clusters. This observation was interpreted to indicate that separate cellular functions, independent of N_2 fixation, might replace the functions of NifS and NifU but very inefficiently. In aggregate, these possibilities resulted

in the design of experiments that led to the discovery that NifS encodes a cysteine desulfurase involved in mobilization of S for [Fe-S] cluster assembly [66] and that NifU provides a molecular scaffold for the assembly of simple [Fe-S] clusters [67, 68]. They also led to an appreciation that the functions of NifS and NifU represent general features of [Fe-S] cluster formation throughout nature [6].

1.5.2 *NifS* is a cysteine desulfurase

One technical problem associated with functional analysis of proteins involved in maturation of nitrogenase components is that such proteins are only produced at very low levels because they engage in multiple turnovers. Therefore, as a way to gain insight into the possible function of its product, the *nifS* gene was heterologously expressed at very high levels in *E. coli* using a recombinant plasmid construct. Purification and initial analysis of NifS produced in this way revealed that it was a homodimer that exhibited a visible spectrum characteristic of pyridoxal-phosphate-dependent (PLP) enzymes [66]. Subsequent chemical analysis indeed confirmed that NifS contained PLP and, therefore, the possibility that L-cysteine is a substrate for NifS was investigated for the following reasons: (i) PLP enzymes are frequently involved in the elimination or rearrangement reactions involving amino acid substrates, (ii) a gene encoding a CysE homolog, which catalyzes the rate-limiting step in cysteine biosynthesis, is co-transcribed with *nifS*, and (iii) involvement for NifS in the mobilization of S was predicted based on the various phenotypes of a NifS-deficient strain. This possibility was confirmed by showing that, of all the amino acids, only the addition of L-cysteine to NifS resulted in a transient shift in its visible spectrum. Furthermore, prolonged incubation of L-cysteine with NifS resulted in the precipitation of colloidal sulfur and accumulation of L-alanine, demonstrating a role for NifS in S mobilization [69].

Basic features of the NifS L-cysteine desulfurization mechanism were elucidated using a combination of approaches [66, 69]. First, the production of colloidal S from L-cysteine indicated the likely participation of a protein thiol group in the S mobilization reaction, consistent with the observation that NifS catalytic activity is extremely sensitive to thiol alkylating reagents, such as *N*-ethylmaleimide. Second, phylogenetic comparisons of NifS primary structures from a variety of N_2-fixing microorganisms revealed that residue Cys325 is strictly conserved. Third, substitution of Cys325 by Ala325 resulted in complete loss of NifS activity and an *A. vinelandii* mutant strain that produces the Ala325-substituted protein exhibits the same phenotype as a strain deleted for *nifS*. Fourth, treatment of NifS with the L-cysteine analogues, L-allylglycine or vinylglycine, were shown to irreversibly inactivate NifS by respective formation of a γ-methylcystathionyl or cystathionyl residue derived from Cys325. Fifth, the formation of an enzyme-bound cysteinyl persulfide, located at the Cys325 position, was identified as an intermediate in the NifS-catalyzed L-cysteine desulfurization reaction.

Finally, evidence was obtained for the occurrence of an enamine intermediate in the NifS-catalyzed formation of L-alanine. These observations indicated that a cysteinyl persulfide could be formed on NifS through nucleophilic attack by the active site Cys325 thiol on a cysteine-PLP ketamine adduct and that formation of a NifS-bound cysteinyl persulfide could represent a benign way to activate and traffic S for nitrogenase [Fe-S] cluster formation. Subsequent to the initial characterization of the NifS cysteine desulfurase reaction, other studies established that NifS represents a broad class of enzymes that use L-cysteine and PLP chemistry to accomplish the activation and mobilization of S for biosynthesis of many S-containing biomolecules (Fig. 1.5) [70, 71]. Analysis of other cysteine desulfurases, including crystallographically determined high-resolution structures [72–76], has provided detailed insight into the probable NifS mechanism (Fig. 1.6).

The overall function of cysteine desulfurases can be considered to occur in two stages, formation of the enzyme-bound persulfide and subsequent delivery of S to an acceptor molecule. All cysteine desulfurases are thought to share similar mechanistic features in the first stage, whereas the second stage appears to vary with overall functionality of the cysteine desulfurase type and its corresponding delivery target (Fig. 1.5). The proposed intermediates formed during the first stage are shown in Fig. 1.6 [69, 77]. In the NifS resting state, PLP is covalently bound to the conserved Lys202 residue through a Schiff base (intermediate 1). The binding of cysteine to PLP is proposed to occur through formation of a tetrahedral C4′ intermediate, geminal diamine (intermediates 2–3). This results in the displacement of Lys202 from PLP and formation of an external Cys-aldimine Schiff base (intermediate 4). A key step involves proton abstraction by a protein residue serving as a general base (intermediate 5). Because a monoprotic residue facilitates intermediate 5 formation, this function is unlikely to involve the active site Lys202 residue [77]. Also, formation of the proposed quinonoid (intermediate 6) is independent of the active site cysteine residue because the NifS Ala325-substituted variant is still able to bind cysteine and to form intermediates 2–5. It appears likely that a histidine residue conducts the nucleophilic attack on the α-proton and either His100 or His201 are candidates to perform this role.

NifS inactivation studies using the suicide inhibitors, allylglycine and vinylglycine, have eliminated the possible involvement of Cys325 during conversion to the Cys-quinonoid form (intermediate 6) [69]. Instead, inhibition profiles favor the involvement of the active site Cys325 residue serving as a general acid during the protonation of C4′ of the Cys-PLP quinonoid adduct. Hydrogen bonding between the imine hydrogen and the phenolate oxygen allows expansion of the π-orbital system leading to a highly conjugated structure of PLP, therefore permitting electron delocalization. The committed step of the NifS reaction is characterized by nucleophilic attack of the deprotonated active site cysteine thiol on the thiol group of the substrate (intermediate 7). This event leads to formation of the persulfide bond, and conversion of cysteine to an alanine-enamine intermediate (intermediate 8). *In vitro* reactions performed in $^{2}H_{2}O$ confirmed that α and β hydrogens are exchanged during the reaction, supporting

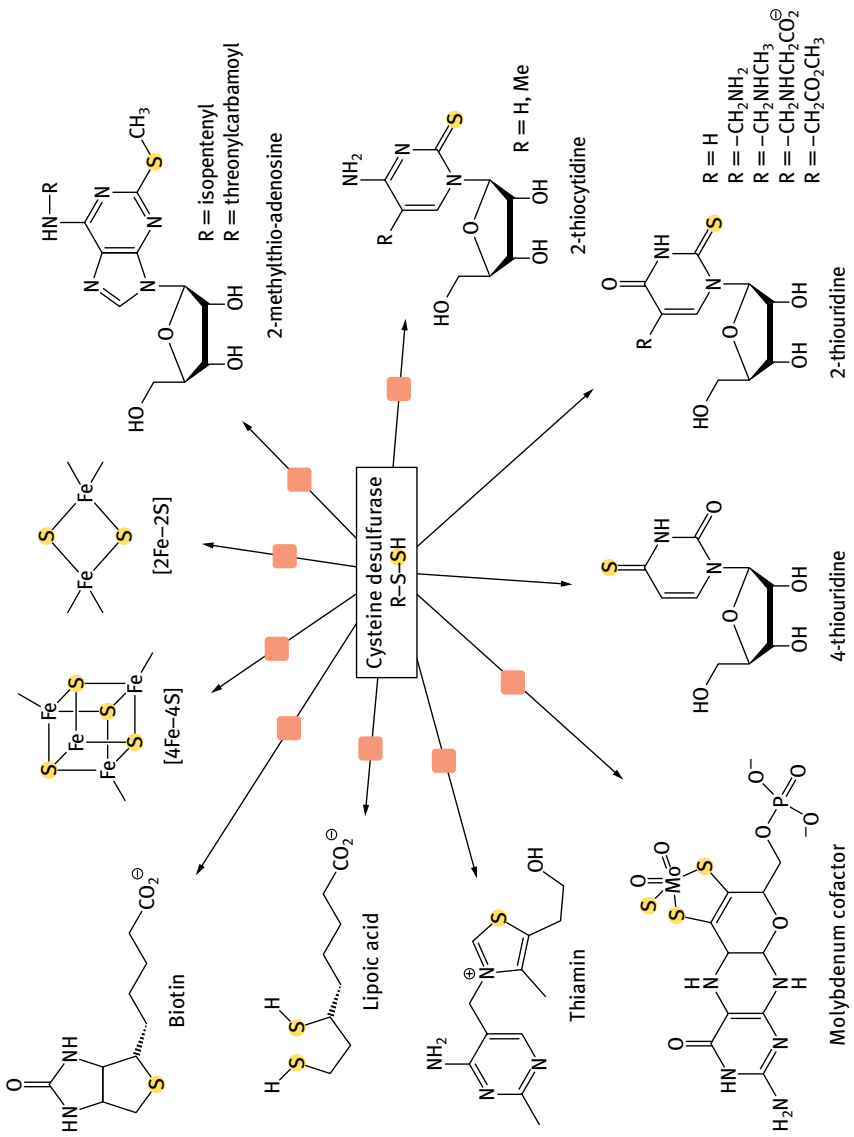

Fig. 1.5: Cysteine desulfurases are involved in the first step of sulfur mobilization in the biosynthesis of many thio-containing cofactors. Biosynthetic pathways requiring participation of at least one [Fe-S] protein are indicated by a red box.

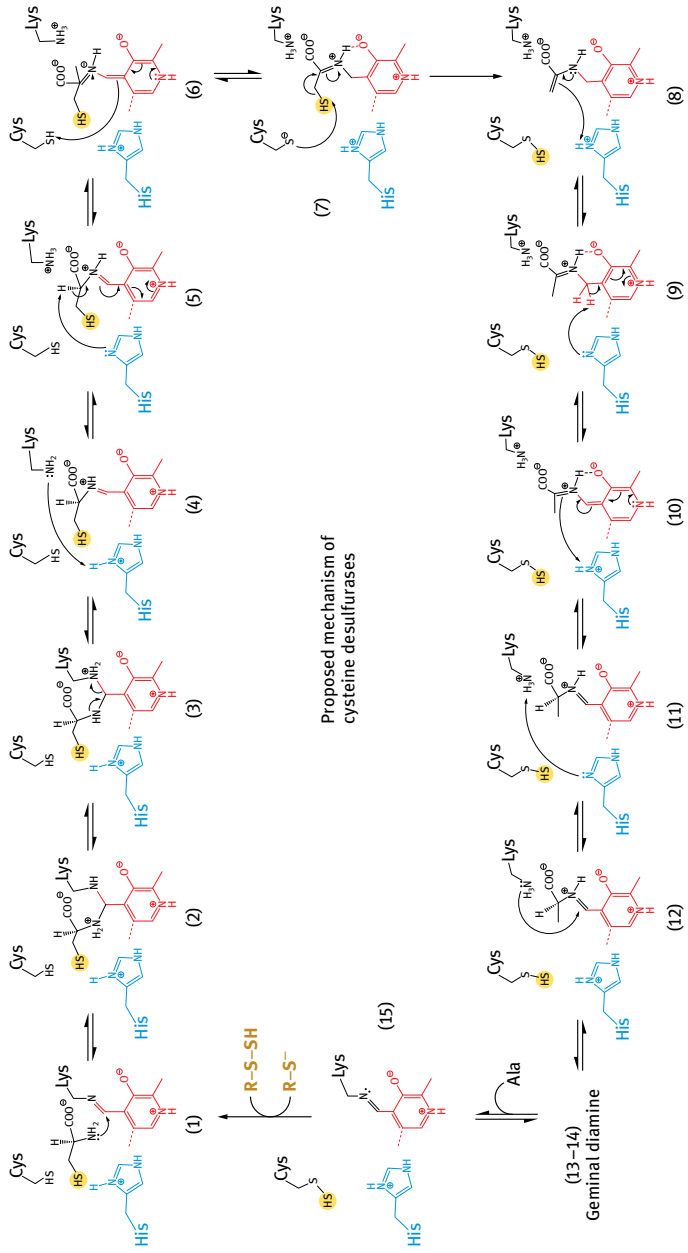

Fig. 1.6: Proposed L-cysteine desulfurase mechanism. The reaction involves two committed steps: the formation of the enzyme-bound persulfide bond and the subsequent transfer of the terminal persulfide sulfur to an acceptor molecule (R-S–). The proposed mechanism includes the PLP-coordinating lysine PLP (Lys202 of *A. vinelandii* NifS) and at least one histidine (shown in blue) serving as a general acid general base; His100 and His201 of *A. vinelandii* NifS are candidates for this role.

the occurrence of intermediate 8 [69]. Furthermore, the subsequent release of alanine is proposed to follow the same steps but in reverse order: ketamine (intermediate 9), quinonoid (intermediate 10), aldimine (intermediates 11–12), and gem-diamine (intermediates 13–14) to restore the internal Schiff base with Lys202 and form the persulfurated Cys325 residue. Formation of persulfurated NifS form (intermediate 15) marks the end of the first half of the cysteine desulfurase reaction, apparently common to all cysteine desulfurases. The second step, involving delivery of S for [Fe-S] cluster formation, is not yet clearly understood, but the mechanism of S delivery appears to differ among the different cysteine desulfurase types and their various targets (Fig. 1.5). The involvement of NifS in providing S for formation of [Fe-S] clusters on NifU is discussed in Section 1.5.3.

1.5.3 Extension of the scaffold hypothesis to NifU function

The apparent involvement of NifS in the mobilization of S for nitrogenase-associated [Fe-S] cluster assembly naturally led to an investigation of a possible complementary role for NifU in mobilizing Fe and/or serving as a scaffold for [Fe-S] cluster formation [78, 79]. A capacity for NifU to bind [Fe-S] clusters had in fact already been suspected on the basis of its primary structure [80] because phylogenetic comparisons indicated that NifU is comprised of three modules, and each module contains conserved cysteine residues (Fig. 1.7). The prediction that NifU might contain an [Fe-S] cluster was confirmed by analysis of the isolated protein heterologously produced in *E. coli*. This analysis, together with analysis of different recombinant NifU forms, each having one of the nine-conserved cysteine residues substituted by alanine, showed that NifU contains a redox-active [2Fe-2S] cluster, attached to the central domain through thiolate ligands provided by NifU residues Cys137, Cys139, Cys172, and Cys175.

Once it was discovered that overexpressed and purified NifU contained two [2Fe-2S] clusters, one cluster within each central domain of a NifU dimer [78], the possibility that such clusters represent precursors for nitrogenase-associated [Fe-S] clusters became an obvious consideration. It was expected that if the [2Fe-2S] clusters contained within recombinantly produced NifU were capable of being transferred to another protein, they would be labile and could easily be removed by treatment with metal chelating reagents. However, the [2Fe-2S] clusters attached to as-isolated NifU are quite stable, even when exposed to oxygen, and they are released only very slowly by treatment of NifU with Fe chelators, such as α-α′ dipyridyl [78]. Alternative possibilities for the function of the [2Fe-2S] clusters contained in the central domain of NifU, now designated as the "permanent clusters," include a redox role in the release of the persulfide from NifS, a redox role in the assembly of "transient" clusters contained in other NifU domains, or as a structural element. The function of the NifU permanent [2Fe-2S] clusters remains elusive. However, given the conservation of cysteines in the N- and C-terminal domains of NifU and the precedence of the role of NifEN as

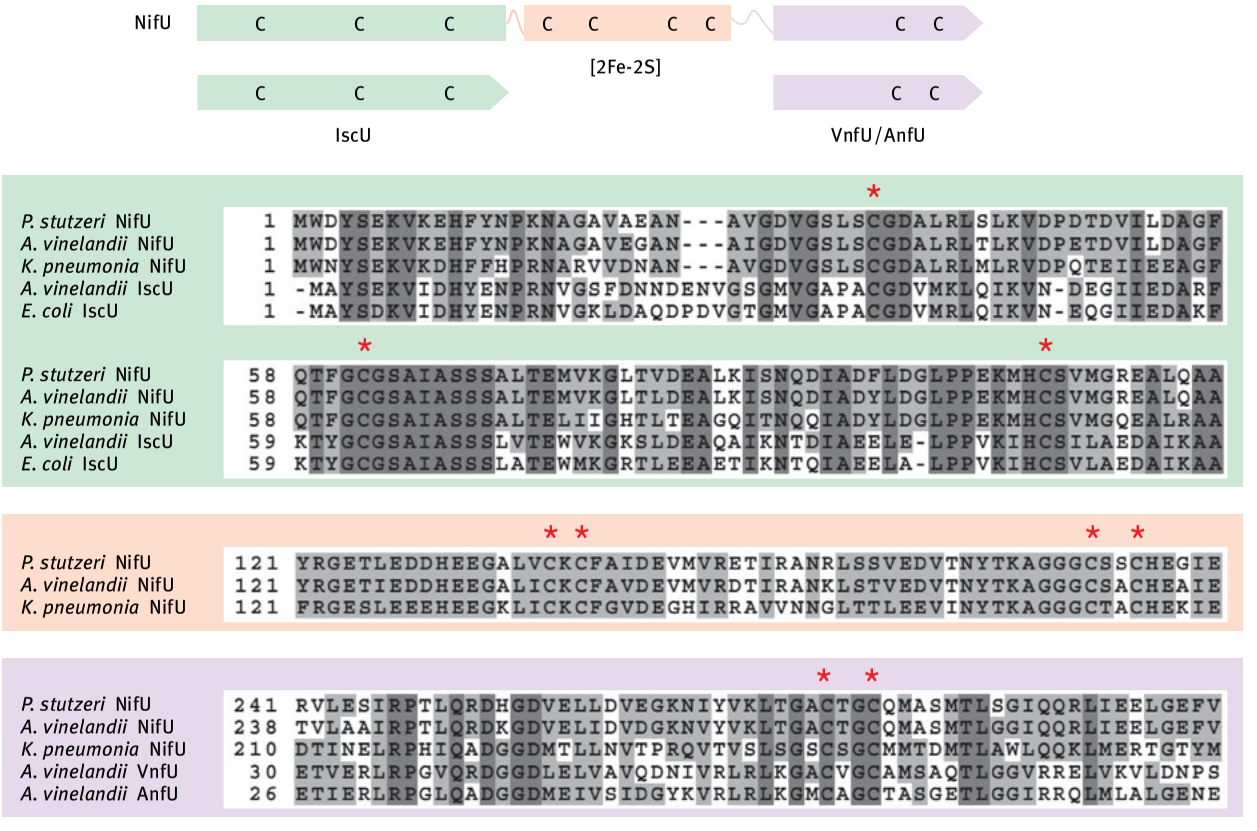

Fig. 1.7: NifU is a modular protein that contains conserved cysteine residues in each module. (top) Diagrammatic representation of NifU domains including the relative position of conserved cysteine residues and location of the permanent [2Fe-2S] cluster. (bottom) Sequence alignments comparing IscU and the N-terminal domain of NifU sequences (green box), central domain of NifU sequences (pink box), and VnfU, AnfU, and C-terminal domain of NifU sequences (violet box). Conserved cysteine residues are indicated with a star.

an assembly scaffold for FeMoco, the possibility that NifU serves as a scaffold for the formation of transient [Fe-S] clusters was an attractive one. Evidence supporting this possibility was obtained using a combination of approaches: (i) physiological analysis of defects associated with substitution of each of the conserved cysteine residues contained in the N- and C-terminal domains of NifU [68, 79], (ii) NifS-assisted assembly of [Fe-S] clusters within isolated NifU and NifU fragments [67], (iii) activation of a cluster-less nitrogenase Fe protein using either isolated NifU or NifU fragments that contain [Fe-S] clusters formed *in vitro* [68, 81], (v) isolation of NifU or NifU fragments produced *in vivo* that contain labile [Fe-S] clusters having the same biophysical features of [Fe-S] clusters formed on NifU *in vitro*.

1.5.3.1 Physiological characterization of *nifU* mutants

An important catalytic role for Cys325 was indicated for NifS by showing that the Ala325 substitution resulted in the same physiological phenotype as a strain deleted for *nifS*. However, a similar approach in the assessment of NifU function was much more complicated because nine conserved cysteines were identified, rather than the single conserved cysteine contained in NifS. Functional roles for conserved NifU cysteines were evaluated by substituting each of them, separately, and, in combination, by alanine. It was found that individual substitution of Cys35, Cys62, or Cys106 by alanine or the combined substitution of all three residues, resulted in the same moderate impairment in N_2-fixing growth when compared with the wild-type strain [68]. In other words, no cumulative effect was manifested upon combined substitution of conserved cysteines in the N-terminal domain, indicating these residues might all participate in the same quasi-dispensable function. Given the potential for cysteinyl residues to provide thiolate ligands for [Fe-S] clusters, the results suggested the possibility that, in aggregate, NifU residues Cys35, Cys62, and Cys106, could provide a nucleation site for the formation of "transient" [Fe-S] clusters destined for incorporation into nitrogenase. Similar to the situation with the N-terminal domain, there was only a very minor effect on the capacity for N_2-fixing growth when either of the two conserved cysteine residues in the C-terminal domain of NifU, Cys272 and Cys275, were substituted by alanine. However, a combination of alanine substitutions for conserved cysteines located in both the N- and C-terminal domain of NifU resulted in a severe defect in the ability for the respective strains to grow under N_2-fixing conditions. These results led to the proposal that the N- and C-terminal domains of NifU could have either redundant or complementary functions related to formation of transient [Fe-S] clusters at both sites [68].

1.5.3.2 *In vitro NifS*-assisted formation of [Fe-S] clusters on NifU

As a way to test if NifU can serve as an assembly scaffold for [Fe-S] cluster formation, isolated recombinant NifU, containing only the intact permanent [2Fe-2S] clusters, was incubated under anoxic conditions in the presence of Fe^{2+}, L-cysteine, and NifS. The results of these experiments demonstrated that NifS facilitated the

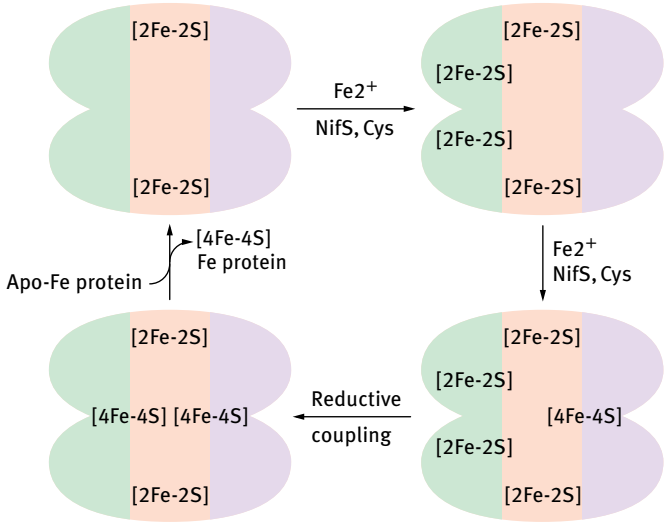

Fig. 1.8: NifU is an [Fe-S] cluster assembly scaffold that can be used to activate the nitrogenase Fe protein. As-isolated NifU dimer contains a redox-active [2Fe-2S] cluster located within the central domain of each NifU monomer (shown in pink). Upon incubation with NifS, cysteine, and Fe^{2+}, NifU undergoes sequential assembly of [2Fe-2S] clusters at the N-terminal IscU domain (shown in green). Prolonged incubation results in the formation of [4Fe-4S] at the C-terminal NfU domain (shown in violet) and subsequent appearance of a [4Fe-4S at the N-terminal domain.

formation of [Fe-S] clusters within NifU in a Fe^{2+}- and L-cysteine-dependent manner (Fig. 1.8). An analysis of the time-dependent [Fe-S] cluster formation process using spectroscopic and analytical methods indicated that, ultimately [4Fe-4S] clusters were assembled in both the N- and C-terminal NifU domains and that [2Fe-2S] clusters were initial intermediates in that process. Details of the process were further explored by testing if isolated NifU fragments, containing either the N- or C-terminal domain, could serve as *in vitro* assembly scaffolds [68, 81]. The results of these experiments revealed that NifS-dependent formation of the [4Fe-4S] cluster within the N-terminal NifU domain followed formation of [2Fe-2S] cluster intermediates, although no intermediates could be detected in formation of the [4Fe-4S] cluster within the C-terminal domain. It is not clear why there are two, apparently separate, [Fe-S] cluster-assembly sites located within NifU. However, it is noteworthy that there are genes associated with the *vnf* and *anf* systems that encode paralogues to the NifU C-terminal domain (Fig. 1.7) [44]. Given that NifU is required for all three nitrogenase systems and that the N-terminal domain of NifU apparently plays the dominant functional role, it could be that the NifU C-terminal domain and its corresponding VnfU and AnfU paralogues could function primarily as agents of delivery rather than assembly. In other words, [Fe-S] clusters formed on the N-terminal domain could be transferred to the C-terminal NifU domain types to provide target specificity.

1.5.3.3 Activation of Fe protein using cluster-loaded *NifU*

Assembly of [Fe-S] clusters within the N- and C-terminal domains of NifU, and demonstration that conserved cysteine residues within these domains are required for such assembly provided strong circumstantial evidence that NifU provides a scaffold for [Fe-S] cluster assembly. Nevertheless, two other experimental approaches were necessary to establish the role of NifU in simple [Fe-S] cluster formation. First, the capacity for [Fe-S] cluster-loaded NifU to activate a nitrogenase target protein was needed. Second, it was necessary to establish that [Fe-S] clusters assembled on NifU *in vitro* faithfully duplicated an *in vivo* process.

It was known that binding of MgATP produced a conformational change in the Fe protein that exposed its [4Fe-4S] cluster to solvent, and this property was exploited to produce apoprotein needed for [Fe-S] cluster transfer experiments. Solvent exposure of the cluster makes it susceptible to removal by treatment of metal chelators such as α-α′ -dipyridyl [82, 83]. Chelation of the [4Fe-4S] cluster, followed by a desalting step, performed in the presence of a reductant, such as dithionite, removed the released Fe^{2+} and S^{2-}. The resulting apo-Fe protein was then used as a target for cluster transfer experiments by mixing with cluster-loaded NifU prepared *in vitro*.

The initial [Fe-S] cluster-transfer experiments involved mixing NifU, NifS, Fe^{2+}, and L-cysteine to accomplish cluster assembly on the NifU scaffold. After removal of the excess Fe^{2+} and L-cysteine, the sample was mixed with apo-Fe protein, and activation was evaluated by subsequent measurement of recovered activity. The results showed that mixing with the reconstituted holo-NifU resulted in rapid and nearly complete restoration of Fe protein activity, whereas omission of any of the assembly ingredients resulted in no recovery of Fe protein activity in control experiments. In addition, removal of NifS from the reaction mixture, post-assembly, had only a very modest effect on the capacity for apo-Fe protein activation, indicating that, although NifS is required for *in vitro* assembly of [Fe-S] clusters on the NifU scaffold, transfer of the [Fe-S] cluster does not require the participation of NifS [68].

In light of the results from genetic and *in vitro* assembly experiments, indicating the capacity for [Fe-S] cluster formation on both the N- and C-terminal domains, the ability to transfer [Fe-S] clusters assembled on either NifU domain was evaluated. One approach involved using a full length NifU, in which either the N-terminal domain or the C-terminal domain was inactivated. In these experiments, activation of the Fe protein could be accomplished, whereas no activation occurred when a full length NifU inactivated in both the N-terminal and the C-terminal domains was used. A second series of experiments involved successful apo-Fe protein activation using preparations of [Fe-S] cluster-loaded N- or C-terminal fragments. In these experiments, the various NifU samples used for cluster transfer contained spectroscopically defined [Fe-S] cluster species shown primarily to be in the form of [4Fe-4S] clusters, suggesting that [4Fe-4S] clusters are transferred intact from NifU to the apo-Fe protein [81].

1.5.3.4 [Fe-S] clusters are assembled on NifU *in vivo*

A final approach used to establish that NifU functions as an [Fe-S] cluster assembly scaffold involved testing whether or not a cluster-loaded form of NifU could be produced *in vivo*. This effort faced a number of technical challenges. For example, [Fe-S] clusters assembled on NifU are labile because they must have a capacity for facile release to accomplish their delivery to target proteins. Such lability is manifested by rapid degradation when transient [Fe-S] clusters assembled on NifU *in vitro* are exposed to oxygen, reducing reagents, such as dithionite, or treated with chelating reagents. Consequently, a procedure for gentle and rapid purification of NifU was needed. Another challenge was related to the dynamic nature of *in vivo* cluster assembly and delivery. What this means is that [Fe-S] clusters assembled on NifU must be transiently located on the scaffold as they must be constantly delivered to other target proteins. Consequently, the occupancy level of the NifU cluster assembly sites could not be anticipated. Finally, because NifU is involved in the catalytic activation of other proteins, the physiological requirement for NifU is relatively low and it is accordingly produced in low quantities.

The technical aspects were overcome by decoupling the expression of *nifU* and *nifS* in *A. vinelandii* from nitrogen fixation by placing their expression under control of a strong, inducible promoter [84]. The rationale of the approach was to produce NifU and NifS at high levels in the absence of nitrogenase target proteins, reasoning that the absence of target recipients for [Fe-S] clusters might cause [Fe-S] clusters to accumulate on the NifU scaffold (Fig. 1.9). In addition, a benign affinity tag was placed within NifU such that its

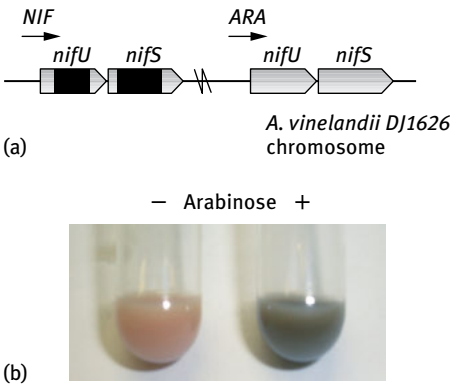

Fig. 1.9: *A. vinelandii* arabinose-controlled expression of NifU and NifS. (a) Schematic representation of gene regions containing *nifU* and *nifS* of *A. vinelandii* strain DJ1626. It contains two copies of the *nifU-nifS* genes. The *nif*-regulated copy contains an in frame deletion (black-colored region), whereas the second copy is located at a different chromosomal position. Expression of the second *nifUS* copy is under control of the arabinose regulatory system. (b) Resuspended cell pellet of *A. vinelandii* cells cultured in media supplemented with ammonia in the absence (–) or presence of arabinose (+). Note that the dark color of cells cultured in the presence of arabinose indicated a high level of [Fe-S] cluster accumulation.

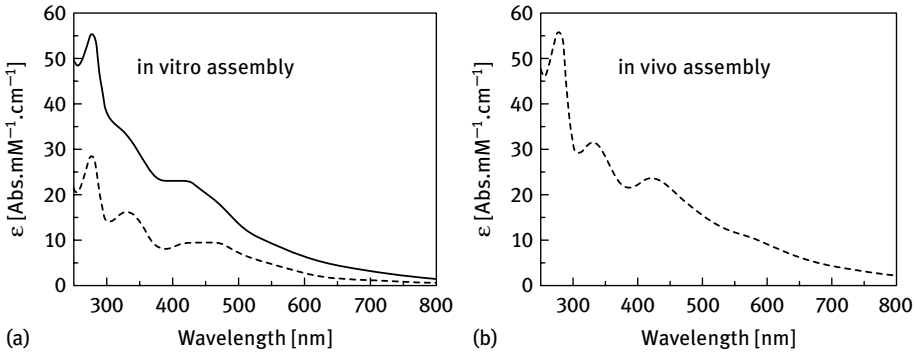

Fig. 1.10: UV-vis absorption spectra of NifU. (a) Spectra of NifU before (dashed line) and after (solid line) *in vitro* Fe-S cluster assembly. The dashed-line spectrum represents the as-isolated form of NifU that contains only the permanent [2Fe-2S] clusters. The solid line spectrum represents *in vitro* reconstituted NifU that contains both the permanent [2Fe-2S] clusters and transient [4Fe-4S] clusters. (b) Spectrum of [Fe-S] clusterloaded NifU produced by *A. vinelandii* strain DJ1626 (Fig. 1.8).

rapid and gentle purification could be accomplished. This strategy was successful, as shown in Figs. 1.9 and 1.10. Namely, NifU produced in *A. vinelandii*, under conditions where no other *nif* genes were expressed, and therefore, no acceptor proteins were produced, contained transient [Fe-S] clusters. The nearly identical spectra of cluster-loaded forms of NifU prepared *in vitro* or *in vivo* (Fig. 1.10) indicated that they were likely to be identical. These spectroscopic results, and the fact that cluster-loaded NifU produced *in vivo* can also be used for the effective *in vitro* activation of apo-Fe protein, provided a final compelling argument to support the scaffold hypothesis for the assembly of simple [Fe-S] clusters. It should be noted that the function of NifU is not limited to the activation of Fe protein. Indeed, there is now also *in vitro* evidence that simple [Fe-S] units assembled on NifU provide the building blocks necessary for the assembly of the more complex FeMoco [64]. Also, the scaffold hypothesis, originally developed for FeMoco, has been further developed to include the participation of a series of assembly scaffolds as well as carrier proteins that traffic [Fe-S] cluster intermediates.

1.5.4 Discovery of *isc* system for [Fe-S] cluster formation and functional cross-talk among [Fe-S] cluster biosynthetic systems

A variety of considerations indicated that the functions of NifU, and NifS might represent a duplication of "housekeeping" functions involved in the assembly of general [Fe-S] clusters, involved in other aspects of cellular metabolism unrelated to nitrogen fixation. First, there are many cellular processes that depend on [Fe-S] proteins, so there must be a mechanism for the assembly of their associated [Fe-S] clusters [11]. Second, nitrogenase is produced at very high levels in N_2 fixing cells, so it seemed

reasonable to expect that NifU and NifS could represent a mechanism to specifically satisfy an increased demand for [Fe-S] cluster formation. Third, there was already evidence in the literature that L-cysteine can serve as the ultimate S source for formation of [Fe-S] clusters in *E. coli*, a non-N_2-fixing organism [85]. Fourth, *E. coli* extracts exhibited L-cysteine desulfurase activity and, based on this feature, a protein having PLP-dependent L-cysteine desulfurase activity and primary structure similarity to NifS was isolated [86]. Finally, elimination of NifU or NifS function did not fully eliminate the capacity for producing active nitrogenase components, indicating that limited functional replacement of NifS and NifU activities were mediated by some other cellular components [65].

A search for a "housekeeping" [Fe-S] biosynthetic system in *A. vinelandii* was initiated by purification of a protein having L-cysteine desulfurase activity from extracts of a mutant strain in which *nifS* was deleted [87]. Because this effort predated the genomics era, the gene region that encoded the protein with cysteine desulfurase activity was isolated using a reverse genetics approach that relied on using the sequence of peptides generated by trypsin digestion to predict the DNA sequence. Examination of this region revealed that the gene encoding a NifS-like protein was contained in an apparent transcriptional unit that contained a total of seven genes. These genes were, respectively, designated *iscR*, *iscS*, *iscU*, i*scA*, *hscB*, *hscA*, *fdx*, and *iscX* (Fig. 1.11) and their proposed functions are shown in Tab. 1.2. Primary structural comparisons revealed strong similarity between components of the Nif and Isc systems: NifS was homologous to IscS, the N-terminal domain of NifU was homologous to IscU, and a *nif* gene product, now designated $IscA^{Nif}$, was homologous to IscA. Fdx does not bear primary structure similarity to any of the *nif* gene products, but it does contain a [2Fe-2S] cluster that might serve a function similar to the permanent [2Fe-2S] cluster located in the NifU central domain. There is no counterpart to the NifUC-terminal domain encoded within the *isc* gene cluster, but there is a gene, designated NfuA [88], located elsewhere on the genome that shares primary structure similarity when compared with the NifU-terminal domain, including the two conserved cysteinyl residues. There are no *nif* counterparts to *iscR*, *hscB*, *hscA*, or *iscX*. A description of the details of the Isc system is beyond the scope of the present discussion, and this topic

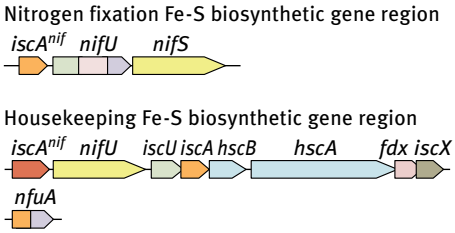

Fig. 1.11: [Fe-S] cluster biosynthetic gene regions in *A. vinelandii*. Genes whose products display primary structure similarities are color-coded accordingly.

Tab. 1.2: Selected *A. vinelandii* proteins known or suspected to be involved in simple [Fe-S] cluster assembly and their proposed functions.

Gene product	Proposed function
NifU	[Fe-S] cluster assembly scaffold/ [Fe-S] cluster carrier
NifS	Cysteine desulfurase
$IscA^{nif}$	[Fe-S] cluster carrier
IscR	[Fe-S] cluster transcription regulator
IscS	Cysteine desulfurase
IscU	[Fe-S] cluster assembly scaffold
IscA	[Fe-S] cluster carrier
HscB	[Fe-S] cluster delivery chaperone
HscA	[Fe-S] cluster delivery chaperone
Fdx	Ferredoxin, specific function unknown
IscX	Unknown
NfuA	[Fe-S] cluster carrier

is reviewed elsewhere [4, 6]. However, it is noteworthy that, although the Isc system for the assembly and delivery of [Fe-S] clusters appears to be more complicated than the Nif system, both are unified by the involvement of an L-cysteine desulfurase and an assembly scaffold. All of the essential mechanistic elements discovered for the Nif system have also been independently established for the Isc system.

1.6 The Isc system is essential in *A. vinelandii*

Identification of the Isc system provided insight into why the mechanism for assembly of such an important and simple prosthetic group took so long to discover. The answer to this question was expected to be associated with the participation of [Fe-S] proteins in so many essential biological processes. In other words, impairment in the ability to assemble [Fe-S] clusters would be manifested in the loss of many, apparently unrelated, essential metabolic processes. Circumstantial evidence for this possibility was found in the instability of mutant strains when attempts were made to incorporate targeted genetic lesions into the *isc* gene region [87]. A more direct and definitive approach to assess the importance of [Fe-S] cluster formation involved the development of a system for the controlled expression of the *isc* genes [89].

The controlled expression of *isc* genes was accomplished by introducing a second copy of the *isc* gene region within the *A. vinelandii* genome [89]. In this genetic construction, the expression of the duplicated *isc* gene copy was decoupled from the normal *isc* regulatory elements. Instead, their expression was placed under control of the sucrose catabolic regulatory elements, designated as *scr* (Fig. 1.12). When cells containing the duplicated genes are grown in the presence of sucrose, they produce Isc components from both the *isc*-regulated genes and the *scr*-regulated genes. However,

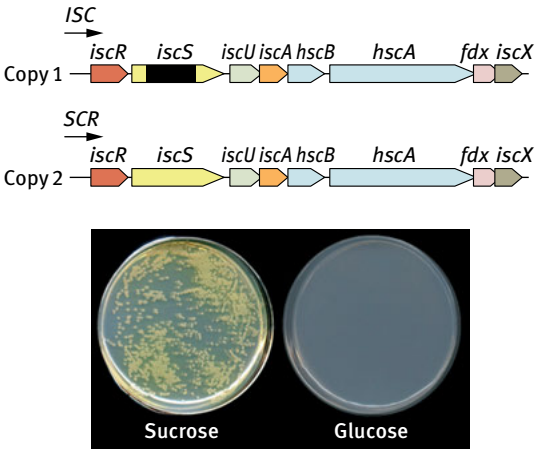

Fig. 1.12: Sucrose-dependent expression of *iscS*. (top) Schematic representation of duplicate *isc* gene regions contained in *A. vinelandii* strain DJ1422. The *isc*-regulated copy carries an in-frame deletion within the *iscS* coding sequence (black-colored region within *iscS*), whereas the second copy, whose expression is under control of the scr regulatory elements, is intact. (bottom) *A. vinelandii* strain DJ1422 cultured on Petri plates using sucrose or glucose as the only carbon source.

when such cells are grown in the absence of sucrose, for example, when glucose is used as the sole carbon source, only the *isc*-regulated copy is expressed. The approach of using an inducible copy of each Isc gene enabled researchers to assess whether or not individual Isc components were essential. An example of this approach is illustrated in Fig. 1.12, which shows how growth of a strain deleted for the *isc*-regulated *iscS* gene can be supported by activation of the *scr*-regulated copy of *iscS*. This strain cannot grow when cultured in the absence of sucrose because the capacity to produce IscS is eliminated. In contrast, when sucrose is added to the growth medium robust growth is restored. Using this controlled gene expression approach, IscS, IscU, and Fdx were also demonstrated to be essential in *A. vinelandii* [89].

1.7 There is limited functional cross-talk between the Nif and Isc systems

The fact that neither a *nifU* nor a *nifS* deletion eliminates the capacity for assembly of an active nitrogenase represented a major clue that ultimately led to the discovery of the Isc system. On the basis of minimal retention of activity, it was suspected that, under N_2-fixing conditions, NifU and NifS might represent a specialized way to meet the increased demand for [Fe-S] clusters in the abundantly produced [Fe-S] cluster-containing nitrogenase components. It was not possible to directly test this possibility by asking if the combined elimination of NifS and IscS function or

combined elimination of NifU and IscU function completely eliminated the capacity for producing an active nitrogenase because IscS and IscU are both essential. Instead, an orthogonal approach, which exploited the negative regulation of *isc* genes by IscR, was used. Inactivation of IscR results in highly elevated expression of all the other housekeeping [Fe-S] cluster biosynthetic components. Therefore, the ability of elevated expression of the Isc system to increase the capacity for N_2 fixation in strains deleted for *nifU* or *nifS* was tested, and rescue of the very slow N_2-fixing growth phenotypes associated with deletion of *nifU* or *nifS* was achieved through high Isc expression [84]. Although this result does not eliminate the possibility that other factors can also replace NifU and NifS function in *A. vinelandii*, it does establish that the capacity for limited functional cross-talk exists between the Nif and the Isc systems.

1.8 Closing remarks

In this chapter, we have not attempted to provide a comprehensive summary of the overall process of the assembly of [Fe-S] clusters. This topic represents a very active and rapidly advancing area of research. Among the many important and fascinating features not addressed in this narrative are included the regulation of [Fe-S] cluster formation, trafficking of [Fe-S] clusters, and the repair of damaged [Fe-S] proteins. Here we have only provided a personalized perspective on the conceptual and experimental basis from which the field emerged. Emphasized here is the role of nitrogen fixation research as providing some of the foundational discoveries that underpin the importance of S trafficking and participation of molecular assembly scaffolds for the assembly of [Fe-S] clusters, in most, and perhaps all, biological systems. It is of particular interest that the peculiarities of the N_2-fixing system for specialized [Fe-S] cluster formation contributed so significantly to these discoveries.

Acknowledgments

Work in the laboratory of Dennis R. Dean is supported by NSF MCB-071770, and work in the laboratory of Patricia C. Dos Santos is supported by NSF MCB-1054623.

References

[1] Beinert H, Holm RH, Munck E. Iron-sulfur clusters: nature's modular, multipurpose structures. Science 1997;277:653–9.
[2] Mortenson LE, Valentine RC, Carnahan JE. An electron transport factor from Clostridium pasteurianum. Biochem Biophys Res Commun 1962;7:448–52.
[3] Tagawa K, Arnon DI. Ferredoxins as electron carriers in photosynthesis and in the biological production and consumption of hydrogen gas. Nature 1962;195:537–43.
[4] Johnson DC, Dean DR, Smith AD, Johnson MK. Structure, function, and formation of biological iron-sulfur clusters. Annu Rev Biochem 2005;74:247–81.

[5] Ewen KM, Kleser M, Bernhardt R. Adrenodoxin: the archetype of vertebrate-type [2Fe-2S] cluster ferredoxins. Biochim Biophys Acta 2011;1814:111–25.
[6] Roche B, Aussel L, Ezraty B, Mandin P, Py B, Barras F. Iron/sulfur proteins biogenesis in prokaryotes: formation, regulation and diversity. Biochim Biophys Acta 2013;1827:455–69.
[7] Wachtershauser G. Groundworks for an evolutionary biochemistry: the iron-sulphur world. Prog Biophys Mol Biol 1992;58:85–201.
[8] Wachtershauser G. Origin of life. Life as we don't know it. Science 2000;289:1307–8.
[9] Peters JW, Williams LD. The origin of life: look up and look down. Astrobiology 2012;12:1087–92.
[10] Imlay JA. Iron-sulphur clusters and the problem with oxygen. Mol Microbiol 2006;59:1073–82.
[11] Py B, Barras F. Building Fe-S proteins: bacterial strategies. Nat Rev Microbiol 2010;8:436–46.
[12] Brill WJ. Biochemical genetics of nitrogen fixation. Microbiol Rev 1980;44:449–67.
[13] Rees DC, Howard JB. The interface between the biological and inorganic worlds: iron-sulfur metalloclusters. Science 2003;300:929–31.
[14] Peters JW, Broderick JB. Emerging paradigms for complex iron-sulfur cofactor assembly and insertion. Annu Rev Biochem 2012;81:429–50.
[15] Seefeldt LC, Hoffman BM, Dean DR. Mechanism of Mo-dependent nitrogenase. Annu Rev Biochem 2009;78:701–22.
[16] Hoffman BM, Lukoyanov D, Dean DR, Seefeldt LC. Nitrogenase: a draft mechanism. Acc Chem Res 2013;46:587–95.
[17] Seefeldt LC, Hoffman BM, Dean DR. Electron transfer in nitrogenase catalysis. Curr Opin Chem Biol 2012;16:19–25.
[18] Duval S, Danyal K, Shaw S, et al. Electron transfer precedes ATP hydrolysis during nitrogenase catalysis. Proc Natl Acad Sci USA 2013;110:16414–9.
[19] Yang ZY, Khadka N, Lukoyanov D, Hoffman BM, Dean DR, Seefeldt LC. On reversible H2 loss upon N2 binding to FeMo-cofactor of nitrogenase. Proc Natl Acad Sci USA 2013;110:16327–32.
[20] Mortenson LE, Thorneley RN. Structure and function of nitrogenase. Annu Rev Biochem 1979;48:387–418.
[21] Dixon RAY, Cannon F, Kondorosi A. Construction of a P plasmid carrying nitrogen fixation genes from Klebsiella pneumoniae. Nature 1976;260:268–71.
[22] Streicher S, Gurney E, Valentine RC. Transduction of the nitrogen-fixation genes in Klebsiella pneumoniae. Proc Natl Acad Sci USA 1971;68:1174–7.
[23] Cannon FC, Dixon RA, Postgate JR. Derivation and properties of F-prime factors in Escherichia coli carrying nitrogen fixation genes from Klebsiella pneumoniae. J Gen Microbiol 1976;93:111–25.
[24] Kennedy C. Linkage map of the nitrogen fixation (nif) genes in Klebsiella pneumoniae. Mol Gen Genet 1977;157:199–204.
[25] Dixon R, Kennedy C, Kondorosi A, Krishnapillai V, Merrick M. Complementation analysis of Klebsiella pneumoniae mutants defective in nitrogen fixation. Mol Gen Genet 1977;157:189–98.
[26] St John RT, Johnston HM, Seidman C, et al. Biochemistry and genetics of Klebsiella pneumoniae mutant strains unable to fix N2. J Bacteriol 1975;121:759–65.
[27] MacNeil T, MacNeil D, Roberts GP, Supiano MA, Brill WJ. Fine-structure mapping and complementation analysis of nif (nitrogen fixation) genes in Klebsiella pneumoniae. J Bacteriol 1978;136:253–66.
[28] Roberts GP, Brill WJ. Gene-product relationships of the nif regulon of Klebsiella pneumoniae. J Bacteriol 1980;144:210–6.
[29] Dixon R, Eady RR, Espin G, et al. Analysis of regulation of Klebsiella pneumoniae nitrogen fixation (nif) gene cluster with gene fusions. Nature 1980;286:128–32.
[30] Roberts GP, Brill WJ. Genetics and regulation of nitrogen fixation. Annu Rev Microbiol 1981;35:207–35.
[31] Spatzal T, Aksoyoglu M, Zhang L, et al. Evidence for interstitial carbon in nitrogenase FeMo cofactor. Science 2011;334:940.

[32] Schindelin H, Kisker C, Schlessman JL, Howard JB, Rees DC. Structure of ADP × AlF4(-)-stabilized nitrogenase complex and its implications for signal transduction. Nature 1997;387:370–6.
[33] Strop P, Takahara PM, Chiu H, Angove HC, Burgess BK, Rees DC. Crystal structure of the all-ferrous [4Fe-4S]^0 form of the nitrogenase iron protein from Azotobacter vinelandii. Biochemistry 2001;40:651–6.
[34] Rubio LM, Ludden PW. Biosynthesis of the iron-molybdenum cofactor of nitrogenase. Annu Rev Microbiol 2008;62:93–111.
[35] Hu Y, Ribbe MW. Biosynthesis of the iron-molybdenum cofactor of nitrogenase. J Biol Chem 2013;288:13173–7.
[36] Jacobson MR, Brigle KE, Bennett LT, et al. Physical and genetic map of the major nif gene cluster from Azotobacter vinelandii. J Bacteriol 1989;171:1017–27.
[37] Joerger RD, Bishop PE. Nucleotide sequence and genetic analysis of the nifB-nifQ region from Azotobacter vinelandii. J Bacteriol 1988;170:1475–87.
[38] Bishop PE, Joerger RD. Genetics and molecular biology of alternative nitrogen fixation systems. Ann Rev Plant Physiol Plant Mol Biol 1990;41:109–25.
[39] Pau RN, Mitchenall LA, Robson RL. Genetic-evidence for an Azotobacter vinelandii nitrogenase lacking molybdenum and vanadium. J Bacteriol 1989;171:124–9.
[40] Joerger RD, Jacobson MR, Premakumar R, Wolfinger ED, Bishop PE. Nucleotide-sequence and mutational analysis of the structural genes (anfhdgk) for the 2nd alternative nitrogenase from Azotobacter vinelandii. J Bacteriol 1989;171:1075–86.
[41] Luque F, Pau RN. Transcriptional regulation by metals of structural genes for Azotobacter vinelandii nitrogenases. Mol Gen Genet 1991;227:481–7.
[42] Eady RR. Structure-function-relationships of alternative nitrogenases. Chem Rev 1996;96:3013–30.
[43] Hamilton TL, Ludwig M, Dixon R, et al. Transcriptional profiling of nitrogen fixation in Azotobacter vinelandii. J Bacteriol 2011;193:4477–86.
[44] Setubal JC, dos Santos P, Goldman BS, et al. Genome sequence of Azotobacter vinelandii, an obligate aerobe specialized to support diverse anaerobic metabolic processes. J Bacteriol 2009;191:4534–45.
[45] Dos Santos PC, Fang Z, Mason SW, Setubal JC, Dixon R. Distribution of nitrogen fixation and nitrogenase-like sequences amongst microbial genomes. BMC Genomics 2013;13:162.
[46] O'Carroll IP, Dos Santos PC. Genomic analysis of nitrogen fixation. Methods Mol Biol 2011;766:49–65.
[47] Bishop PE, Brill WJ. Genetic analysis of Azotobacter vinelandii mutant strains unable to fix nitrogen. J Bacteriol 1977;130:954–6.
[48] Thorneley RN, Lowe DJ. Nitrogenase of Klebsiella pneumoniae. Kinetics of the dissociation of oxidized iron protein from molybdenum-iron protein: identification of the rate-limiting step for substrate reduction. Biochem J 1983;215:393–403.
[49] Shah VK, Brill WJ. Isolation of a molybdenum-iron cluster from nitrogenase. Proc Natl Acad Sci USA 1981;78:3438–40.
[50] Hoover TR, Robertson AD, Cerny RL, et al. Identification of the V factor needed for synthesis of the iron-molybdenum cofactor of nitrogenase as homocitrate. Nature 1987;329:855–7.
[51] Zheng LM, White RH, Dean DR. Purification of the Azotobacter vinelandii NifV-encoded homocitrate synthase. J Bacteriol 1997;179:5963–6.
[52] Shah VK, Imperial J, Ugalde RA, Ludden PW, Brill WJ. Invitro synthesis of the iron-molybdenum cofactor of nitrogenase. Proc Natl Acad Sci USA 1986;83:1636–40.
[53] Ugalde RA, Imperial J, Shah VK, Brill WJ. Biosynthesis of iron-molybdenum cofactor in the absence of nitrogenase. J Bacteriol 1984;159:888–93.
[54] Dean DR, Brigle KE. Azotobacter vinelandii nifD and nifE-encoded polypeptides share structural homology. Proc Natl Acad Sci USA 1985;82:5720–3.

[55] Roberts GP, MacNeil T, MacNeil D, Brill WJ. Regulation and characterization of protein products coded by the nif (nitrogen fixation) genes of Klebsiella pneumoniae. J Bacteriol 1978;136:267–79.
[56] Brigle KE, Weiss CM, Newton WE, Dean DR. Products of the iron-molybdenum cofactor-specific biosynthetic genes, nifE and nifN, are structurally homologous to the products of the nitrogenase molybdenum-iron protein genes, nifD and nifK. J Bacteriol 1987;169:1547–53.
[57] Brigle KE, Newton WE, Dean DR. Complete nucleotide-sequence of the Azotobacter vinelandii nitrogenase structural gene-cluster. Gene 1985;37:37–44.
[58] Goodwin PJ, Agar JN, Roll JT, Roberts GP, Johnson MK, Dean DR. The Azotobacter vinelandii NifEN complex contains two identical [4Fe-4S] clusters. Biochemistry 1998;37:10420–8.
[59] Hu Y, Ribbe MW. Biosynthesis of Nitrogenase FeMoco. Coord Chem Rev 2011;255:1218–24.
[60] Kaiser JT, Hu Y, Wiig JA, Rees DC, Ribbe MW. Structure of precursor-bound NifEN: a nitrogenase FeMo cofactor maturase/insertase. Science 2011;331:91–4.
[61] Dos Santos PC. Molecular biology and genetic engineering in nitrogen fixation. Methods Mol Biol 2012;766:81–92.
[62] Kennedy C, Dean D. The nifU, nifS and nifV gene products are required for activity of all three nitrogenases of Azotobacter vinelandii. Mol Gen Genet 1992;231:494–8.
[63] Dos Santos PC, Dean DR, Hu Y, Ribbe MW. Formation and insertion of the nitrogenase iron-molybdenum cofactor. Chem Rev 2004;104:1159–73.
[64] Zhao D, Curatti L, Rubio LM. Evidence for nifU and nifS participation in the biosynthesis of the iron-molybdenum cofactor of nitrogenase. J Biol Chem 2007;282:37016–25.
[65] Jacobson MR, Cash VL, Weiss MC, Laird NF, Newton WE, Dean DR. Biochemical and genetic analysis of the nifUSVWZM cluster from Azotobacter vinelandii. Mol Gen Genet 1989;219:49–57.
[66] Zheng L, White RH, Cash VL, Jack RF, Dean DR. Cysteine desulfurase activity indicates a role for NIFS in metallocluster biosynthesis. Proc Natl Acad Sci USA 1993;90:2754–8.
[67] Yuvaniyama P, Agar JN, Cash VL, Johnson MK, Dean DR. NifS-directed assembly of a transient [2Fe-2S] cluster within the NifU protein. Proc Natl Acad Sci USA 2000;97:599–604.
[68] Dos Santos PC, Smith AD, Frazzon J, Cash VL, Johnson MK, Dean DR. Iron-sulfur cluster assembly: NifU-directed activation of the nitrogenase Fe protein. J Biol Chem 2004;279:19705–11.
[69] Zheng L, White RH, Cash VL, Dean DR. Mechanism for the desulfurization of L-cysteine catalyzed by the nifS gene product. Biochemistry 1994;33:4714–20.
[70] Mueller EG. Trafficking in persulfides: delivering sulfur in biosynthetic pathways. Nat Chem Biol 2006;2:185–94.
[71] Kessler D. Enzymatic activation of sulfur for incorporation into biomolecules in prokaryotes. FEMS microbiology reviews 2006;30:825–40.
[72] Kaiser JT, Clausen T, Bourenkow GP, Bartunik HD, Steinbacher S, Huber R. Crystal structure of a NifS-like protein from Thermotoga maritima: implications for iron sulphur cluster assembly. J Mol Biol 2000;297:451–64.
[73] Tirupati B, Vey JL, Drennan CL, Bollinger JM Jr. Kinetic and structural characterization of Slr0077/SufS, the essential cysteine desulfurase from Synechocystis sp. PCC 6803. Biochemistry 2004;43:12210–9.
[74] Cupp-Vickery JR, Urbina H, Vickery LE. Crystal structure of IscS, a cysteine desulfurase from Escherichia coli. J Mol Biol 2003;330:1049–59.
[75] Shi R, Proteau A, Villarroya M, et al. Structural basis for Fe-S cluster assembly and tRNA thiolation mediated by IscS protein-protein interactions. PLoS Biol 2010;8:e1000354.
[76] Marinoni EN, de Oliveira JS, Nicolet Y, et al. $(IscS\text{-}IscU)_2$ complex structures provide insights into Fe_2S_2 biogenesis and transfer. Angew Chem Int Ed Engl 2012;51:5439–42.
[77] Behshad E, Bollinger JM Jr. Kinetic analysis of cysteine desulfurase CD0387 from Synechocystis sp. PCC 6803: formation of the persulfide intermediate. Biochemistry 2009;48:12014–23.

[78] Fu W, Jack RF, Morgan TV, Dean DR, Johnson MK. The nifU gene product from Azotobacter vinelandii is a homodimer that contains two identical [2Fe-2S] clusters. Biochemistry 1994;33:13455–63.
[79] Agar JN, Yuvaniyama P, Jack RF, et al. Modular organization and identification of a mononuclear iron-binding site within the NifU protein. J Biol Inorg Chem 2000;5:167–77.
[80] Beynon J, Ally A, Cannon M, et al. Comparative organization of nitrogen fixation-specific genes from Azotobacter vinelandii and Klebsiella pneumoniae: DNA sequence of the nifUSV genes. J Bacteriol 1987;169:4024–9.
[81] Smith AD, Jameson GN, Dos Santos PC, et al. NifS-mediated assembly of [4Fe-4S] clusters in the N- and C-terminal domains of the NifU scaffold protein. Biochemistry 2005;44:12955–69.
[82] Zheng L, Dean DR. Catalytic formation of a nitrogenase iron-sulfur cluster. J Biol Chem 1994;269:18723–6.
[83] Walker GA, Mortenson LE. Effect of magnesium adenosine 5'-triphosphate on the accessibility of the iron of clostridial azoferredoxin, a component of nitrogenase. Biochemistry 1974;13:2382–8.
[84] Dos Santos PC, Johnson DC, Ragle BE, Unciuleac MC, Dean DR. Controlled expression of nif and isc iron-sulfur protein maturation components reveals target specificity and limited functional replacement between the two systems. J Bacteriol 2007;189:2854–62.
[85] White RH. Origin of the labile sulfide in the iron-sulfur proteins of Escherichia coli. Biochem Biophys Res Commun 1983;112:66–72.
[86] Flint DH. Escherichia coli contains a protein that is homologous in function and N-terminal sequence to the protein encoded by the nifS gene of Azotobacter vinelandii and that can participate in the synthesis of the Fe-S cluster of dihydroxy-acid dehydratase. J Biol Chem 1996;271:16068–74.
[87] Zheng L, Cash VL, Flint DH, Dean DR. Assembly of iron-sulfur clusters. Identification of an iscSUA-hscBA-fdx gene cluster from Azotobacter vinelandii. J Biol Chem 1998;273:13264–72.
[88] Bandyopadhyay S, Naik SG, O'Carroll IP, et al. A proposed role for the Azotobacter vinelandii NfuA protein as an intermediate iron-sulfur cluster carrier. J Biol Chem 2008;283:14092–9.
[89] Johnson DC, Unciuleac MC, Dean DR. Controlled expression and functional analysis of iron-sulfur cluster biosynthetic components within Azotobacter vinelandii. J Bacteriol 2006;188:7551–61.

2 The ISC system and the different facets of Fe-S biology in bacteria

Laurent Aussel, Sylvia Chareyre, Yohann Duverger, Benjamin Ezraty, Allison Huguenot, Pierre Mandin, Béatrice Py, Jordi Zamarreno, and Frédéric Barras

2.1 Introduction

As early as the 1970s, it was shown that *in vitro* iron-sulfur (Fe-S) clusters can be spontaneously assembled from ferrous and sulfide salts and ligated to proteins [1]. The *in vivo* situation proved to be more complex, and in the 1990s, Dean and collaborators discovered that cells employ complex protein machineries for cluster biosynthesis [2] (see Dos Santos and Dean, pp. 1–30, this volume). The Fe-S biogenesis machineries are widespread and highly conserved in eubacteria and eukaryotes (reviewed in [3–6]). One obvious advantage is that like for any cellular process, Fe-S biosynthesis-assisted systems allow for better specificity and higher speed. Moreover, with respect to Fe-S biology, Fe-S cluster biogenesis systems may also protect the surrounding cellular components from deleterious effects of free Fe^{2+}, Fe^{3+}, and S^{2-} ions, especially under oxidative conditions. To date, three machineries have been described, NIF, ISC, and SUF. In all three cases, the process of Fe-S cluster biogenesis can be described in two steps: assembly and delivery (Fig. 2.1). The assembly step is the actual building of the Fe-S cluster and the delivery step is routes taken by clusters to reach their final apo-targets. Hereafter, we shall summarize the state of knowledge on the *Escherichia coli* ISC system, which has homologs in yeast, plants, and humans.

2.2 The ISC system, the general housekeeping system for Fe-S biogenesis

2.2.1 Description and function

The ISC system of *E. coli* is comprised of eight proteins (Fig. 2.2) (reviewed in [5, 6]). The eukaryotic ISC system is primarily located in the mitochondria and shares many components and mechanistic details with prokaryotes [3, 4]. IscS (Nfs1 in eucaryotes), is a cysteine desulfurase that releases sulfur from L-cysteine [7–9]. IscU (Isu/IscU in eucaryotes) acts as a scaffold for the actual assembly of the Fe-S cluster by capturing both IscS-produced sulfur and iron [10–15]. The source of iron remains elusive and a dedicated donor might not exist. Fdx (Arh in eucaryotes), a ferredoxin, interacts both with IscS and IscU and could act as an electron donor for sulfur transfer from IscS to

DOI 10.1515/9783110479850-002

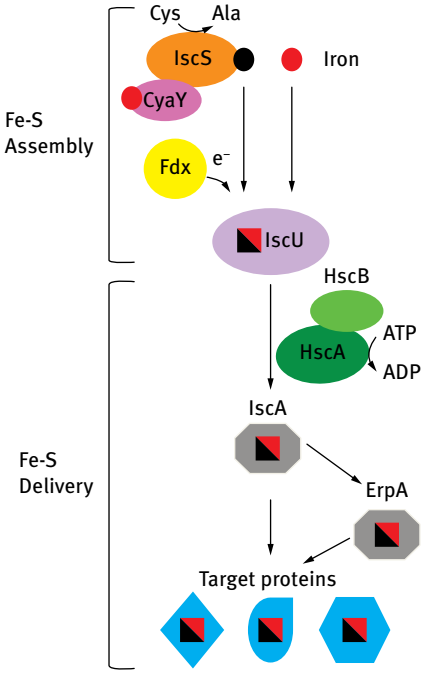

Fig. 2.1: Model of functioning of the *E. coli* ISC system. Sulfur (black dot) is produced from cysteine (Cys) by the action of the cysteine desulfurase IscS and is then transferred to the sulfur acceptor IscU. The activity of IscS can be controlled by CyaY and IscX. The ferredoxin might provide electrons $^{(e-)}$ at the assembly step. The Fe-S cluster (half black/red square) assembly takes place on IscU. The chaperone/co-chaperone HscAB assists Fe-S transfer from IscU (or possibly the IscS/IscU complex) to IscA, with concomitant ATP hydrolysis. Depending on the environmental conditions, the Fe-S cluster is transferred from holo-IscA to target cellular apo-proteins directly or indirectly *via* an Fe-S relay involving another ATC, such as ErpA in aerobic conditions.

IscU [14, 16–18]. CyaY (frataxin [Fxn] or Yfh1 in eucaryotes) and IscX could act as regulatory proteins that tune the activity of IscS-IscU-assisted Fe-S assembly according to bioavailable iron concentrations [19–22]. The HscB and HscA are specialized co-/chaperones from the DnaJ/DnaK family that initiate the delivery step by facilitating release of the IscU-bound Fe-S cluster [23, 24]. The cluster is then transferred to IscA, a Fe-S cluster transporter, which will hand it over either directly to an apo-target or to another set of carriers (ErpA, NfuA) [25–29]. The actual function of A-type carrier proteins (ATCs-IscA, SufA, ErpA) has been long debated. Initially proposed as scaffolds, they were later thought to be iron donors and are presently thought to be Fe-S carriers. The arguments for and against all of these possibilities were discussed in detail in Roche et al. [5]. Main arguments supporting the view of A-type proteins as carriers are that (i) *in vitro*, they receive clusters from scaffolds and transfer them to apo-targets and to other scaffolds, and (ii) *in vivo*, they cannot substitute for scaffolds

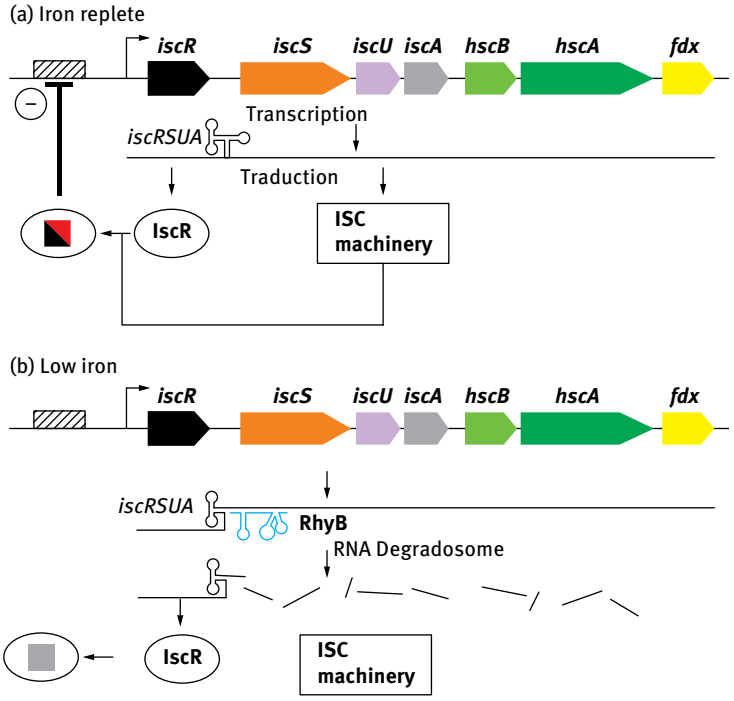

Fig. 2.2: Regulation of the *isc* operon in *E. coli*. The *isc* operon is depicted and its expression is shown to be under the influence of IscR and of the small noncoding RNA, RyhB. (A) Under normal conditions, the IscR regulator acquires its Fe-S from the ISC system and represses its expression to give rise to an autoregulatory circuit that senses the Fe-S state of the cell. The *ryhB* gene is not expressed under such conditions. (B) Regulation of the *isc* operon in low-iron conditions is also illustrated. The sRNA RyhB, which is regulated by ferric-uptake-regulation protein (Fur), causes differential degradation of the polycistronic *isc* mRNA. Under low-iron conditions, RyhB is expressed and pairs with the 5′ untranslated region of *iscS*. This promotes recruitment of the RNA degradosome and degradation of the downstream *isc* mRNAs whereas the strong secondary structure at the 3′ end of *iscR* protects this transcript from degradation. Expression of RyhB leads to increased expression at the *iscR* promoter owing to the fact that IscR no longer acquires its Fe-S cluster from the downstream Isc operon.

but they are important for cluster acquisition by many apo-proteins. The *iscA* deletion mutant exhibits milder phenotypes than deletion of the scaffold mutant *iscU* regarding growth parameters and activity of the Fe-S-containing enzymes, such as GltS and Sdh [30]. Construction of the double deletion mutants, *iscA sufA* and *iscA erpA*, revealed more growth impairments, likely because of redundancy between IscA and the two other ATCs [27]. IscA is thought to assist delivery to most, if not all cellular apo-proteins, when cells grow under favorable conditions such as anaerobiosis and/or nutrient-rich environments. Under less favorable conditions (aerobiosis) or Fe-S destabilizing conditions (oxidative stress, iron limitation), other delivery routes that rely on ErpA, NfuA, and/or SufA are utilized. IscA might contribute to these routes,

depending upon the conditions and which particular apoprotein is the intended Fe-S recipient protein such as in the case of IscR, whose activity was decreased by the same order of magnitude in the *iscA* and *iscU* mutant. The case of IscR may relate to its specific recruitment in the *isc* operon to sense the functional status of the ISC machinery.

2.2.2 The putative role of Fxn in early Fe-S biogenesis by the ISC system

In humans, defects in ISC factors lead to pathological disorders as they provoke defects in Fe-S-dependent proteins, such as respiratory complex I or the TCA cycle enzymes, aconitase and succinate dehydrogenase. Another illuminating case is Fxn. In eucaryotes, Fxn deficiency causes Friedreich's ataxia, an autosomal recessive neurodegenerative disease [31, 32]. A consequence of Fxn deficiency is decreased Fe-S enzyme activities. However, the precise role of Fxn has remained unclear, in particular because Fxn deficiency is responsible for multiple phenotypes, and associated defects in Fe-S biosynthesis might be indirect [33]. However, thanks to studies establishing the chronology of pathological events, it is now clear that defects in Fe-S biogenesis represent an early event, strongly supporting the idea that Fe-S deficiency is a direct consequence of loss of Fxn [34, 35]. Moreover, Fxn is part of a quaternary complex including NFS1, the cysteine desulfurase-stabilizing factor Isd11, a stabilizing factor absent in *E. coli*, and Isu [36–39]. Surprisingly, in *E. coli*, Fe-S biogenesis is only marginally affected by the absence of CyaY, the bacterial homologue of Fxn [40–42]. We recently elucidated that this is due to the nature of the 108th residue in IscU [43]. Hence, an Ile residue at that position allows the ISC machinery to work in the absence of Fxn, while a Met residue leads to Fxn dependency of the system. Remarkably, the same rule holds true for the yeast mitochondrial ISC system [44]. Additional studies both with human and *E. coli* models established Fxn as a *bona fide* ISC factor, possibly acting as a positive factor within the assembly step [45, 46].

2.2.3 Stress represses ISC functions and enhances SUF pathway activity

Genetic and physiological observations established that the ISC system carries out Fe-S cluster assembly under normal conditions, whereas the SUF pathway is the stress-responsive system that functions in the presence of exogenous ROS and iron-limited conditions (see Outten, F., this volume). Recently, kinetic analysis demonstrated that the IscU-bound Fe-S cluster exhibits a much shorter half-life [fivefold to sevenfold] than the SufB-bound cluster when exposed to O_2 or oxygen peroxide [47]. The IscU-bound cluster is also much more easily destabilized by iron limitation. The presence of the chaperone components failed to significantly enhance the stability

of the FeS cluster bound to IscU [47]. Structural data of the IscU-bound cluster are eagerly awaited to provide molecular rationale for its features.

2.3 Genetic regulation of ISC synthesis

Transcription of the *iscRSUAhscBAfdx*, encoding the ISC machinery, is mainly driven by the transcriptional regulator IscR, itself the product of the first gene of this operon (see Kiley et al., p. 75–92 in this book and [48, 49]). IscR is a 2Fe-2S-containing protein, which can be found either in its holo or apo form depending on the physiological state of the cell and on Fe-S demand [50, 51]. Holo-IscR acts as a transcriptional repressor of the expression of many genes (>150) in addition to the *isc* operon [52]. Crucial to the understanding of the homeostatic regulation of ISC synthesis is that IscR acquires its cluster from the ISC system itself. Hence, under favorable conditions, IscR is present in its repressing holo-form and very few ISC proteins are synthesized (Fig. 2.2A). However, if cells experience a slight increase in Fe-S demand, the apo-IscR form can predominate, thereby ceasing to repress the *isc* operon whose expression will increase to satisfy the demand for Fe-S synthesis. This autoregulatory circuit functions as a rheostat that regulates Fe-S cluster homeostasis under routine conditions. This model implies that IscR is a poor ISC substrate, so that general Fe-S cluster demand must be met before IscR acquires its cluster and represses *isc* expression. In line with this idea, coordination of the 2Fe-2S cluster on IscR involves an atypical His residue in place of one Cys, which might endow it with peculiar sensing/stability properties [53].

In addition to this homeostatic regulation of Isc, IscR will also react to conditions that are unfavorable to the Fe-S production or that may be detrimental to Fe-S stability, such as iron starvation, ROS production, NO, or toxic metals such as cobalt [54–58]. In such conditions, the apo form of IscR will also tend to accumulate, inducing the transcriptional expression of the *isc* operon.

Transcriptional activation of the *isc* operon during iron starvation has long been puzzling since it was earlier noted that SUF, not ISC, was the dedicated system for Fe-S biogenesis when iron is scarce [54]. The key to the understanding of this apparent paradox came with the discovery of the posttranscriptional regulation of *isc* expression by the small regulatory RNA (sRNA) RyhB. RyhB is an sRNA whose expression is under the direct control of the Fur repressor, the major iron homeostasis regulator [59]. When iron concentration is low, Fur repression is alleviated and RyhB is expressed [60]. With the help of the RNA chaperone Hfq, RyhB will in turn basepair to and repress expression from numerous mRNAs encoding nonessential iron using proteins, thereby redirecting iron usage to crucial iron-using proteins [61]. RyhB basepairs to the *iscRSU* mRNA directly upstream of the *iscS* gene [59], and it is critical for the regulation of Fe-S biogenesis. Binding upstream of *iscS* induces degradation of the 3′ part of the *iscRSUA* mRNA by the RNA degradosome, leaving the 5′

end that encodes *iscR* intact (Fig. 2.2B). Thus, under such conditions, ISC expression is turned down, but IscR expression remains high, ultimately leading to the accumulation of apo-IscR, which has been shown to be critical to the induction of SUF.

The double regulation by IscR and RyhB under iron starvation is not restricted to *isc*. Indeed, it was recently shown that another gene shares the same double regulation by RyhB and IscR: *erpA*, which encodes an Fe-S carrier essential under aerobic growth [62]. In this case, it was shown that this mechanism allows fine-tuning of *erpA* expression relative to iron concentrations. Indeed, *erpA* expression relative to iron concentrations has a typical "bell shape": *erpA* expression is minimal either when iron is abundant (because of IscR repression) or when it is scarce (because of RyhB repression) but maximal at moderate iron concentrations (because both repressions are alleviated). Indeed, the ISC system is also subject to the same regulation by RyhB and IscR. It is thus very likely that a parallel mechanism may be at work behind expression of the *isc* operon to favor its expression under certain conditions; however, this concept requires further investigation.

2.4 The role of the ISC system in antibiotic resistance

Fe-S cluster biology influences the level of antibiotic resistance/sensitivity of *E. coli*. The connections between Fe-S biology and antibiotic resistance are multiple, and we shall illustrate two of them as they are highly dependent upon ISC.

2.4.1 The proton motive force link

Recently, Fe-S cluster biology was put in the center of the question of how bactericidal antibiotics kill [63–71]. The proposal was that bactericidal antibiotics would alter functions of the respiratory chain, thereby inducing ROS production. Enhanced ROS production would in turn be destabilizing to solvent exposed Fe-S clusters, which would release Fe atoms that would fuel Fenton chemistry, thereby amplifying the ROS-dependent damage and cell death. In this context, the enhanced resistance pattern of the *iscS* mutant was concluded to be due to a lack of Fe-S clusters [66]. A problem arose when it was realized that a *iscU* mutant, which experiences a drop in Fe-S biogenesis comparable to a *iscS* mutant, failed to exhibit resistance to all bactericidal antibiotics comparable to those of mutant *iscS* strains [68]. Other interpretations were sought for and proposed as briefly accounted below.

The energy-converting NADH:ubiquinone oxidoreductase, respiratory complex I, plays a central role in cellular energy metabolism, as it couples NADH oxidation to proton translocation, thereby giving rise to proton motive force (PMF) for energy-consuming processes such as ATP synthesis, active transport, and motion. Complex I from *E. coli* is made up of 14 different subunits and one flavin mononucleotide and nine

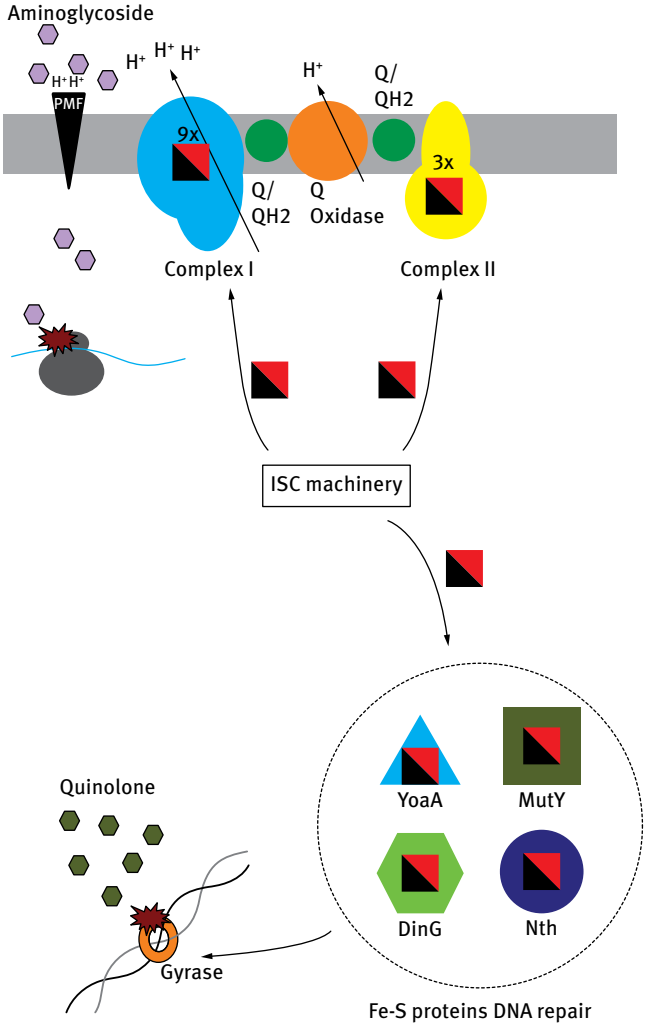

Fig. 2.3: The influence of the ISC machinery on susceptibility to antibiotics. The connection between the ISC system and aminoglycoside is shown (top of the figure). The ISC system provides Fe-S clusters to complex I (nine Fe-S clusters) and complex II (three Fe-S clusters), thereby generating the PMF that is necessary for the transport of aminoglycosides. The connection between the ISC system and quinolone is represented (bottom of the figure). *E. coli* contains at least four Fe-S proteins that are involved in DNA damage repair (Nth, MutY, DinG, and YoaA). The ISC system supplies Fe-S clusters to these proteins, and thereby participates in the repair of quinolone-induced damages. The contribution of SUF to the maturation of these proteins remains to be investigated.

Fe-S clusters as cofactors for the electron transfer reaction. Because PMF is central to bacterial import of many antibiotics, the level of antibiotic resistance is expected to depend on complex I activity levels. Accordingly, it was shown that an *iscU* deletion conferred enhanced resistance to aminoglycoside because it hampers complex I

activity and reduces PMF production sufficiently to prevent gentamicin uptake [68]. A strain lacking ISC but engineered such that it makes Fe-S clusters with SUF under all conditions showed that levels of complex I activity were too low to support gentamicin uptake, and as a consequence, this strain was found to exhibit enhanced resistance to gentamicin. As explained above, *E. coli* uses ISC under iron-replete conditions and SUF under iron-limiting conditions. Hence, this study demonstrated that Fe-S cluster production does not potentiate the action of gentamicin, but rather influences the level of PMF produced as a function of whether the ISC or the SUF system is involved in providing Fe-S clusters to complex I (Fig. 2.3). Presumably, and for unknown reasons, complex I is less accessible to SUF components. Hence, this study fully demonstrated that iron levels influence levels of gentamicin resistance by determining at the genetic level which Fe-S cluster assembly machinery is functional [68].

2.4.2 The DNA repair connection

Another type of link between Fe-S cluster and antibiotic susceptibility is to be found with Fe-S proteins involved in the repair of DNA damage. In *E. coli*, there are four known enzymes: the Nth endonuclease III, the MutY glycosylase, the DinG, and the YoaA helicases, all of which contain a 4Fe-4S cluster [72–76]. Hence, perturbing the ISC system is likely to alter Fe-S acquisition of these proteins and their efficiency in repairing fluoroquinolone-induced damages (Fig. 2.3).

2.5 The role of the ISC system in bacterial pathogenesis

During the course of the infection, bacterial pathogens encounter environments with variable levels of oxygen and iron. Because iron limitation and oxidative stress are detrimental for Fe-S enzyme biogenesis, several studies addressed the involvement of the ISC and SUF machineries in sustaining bacterial virulence. Recently, it was shown that in *Salmonella enterica*, the ISC machinery is required during the first step of its infectious cycle [77]. The ISC mutant was found to be impaired in the expression of a Type Three Secretion System (TTSS)—which is essential for the first stage of *Salmonella* infection—and exhibited a reduced invasion in epithelial cells and virulence attenuation in mouse. Moreover, the Fe-S cluster sensor IscR was shown to repress *hilD*—which encodes the master regulator of the TTSS—supporting the idea that the ISC machinery is important for *Salmonella* virulence through the ability of IscR to regulate the TTSS gene expression [77] (Fig. 2.4). Interestingly, *Yersinia pseudotuberculosis* IscR was shown to bind upstream of the operon encoding the TTSS master regulator LcrF, endowing IscR with a positive role in transcription of *Yersinia* TTSS genes [78]. Thus, IscR plays a primary role in the virulence program of both

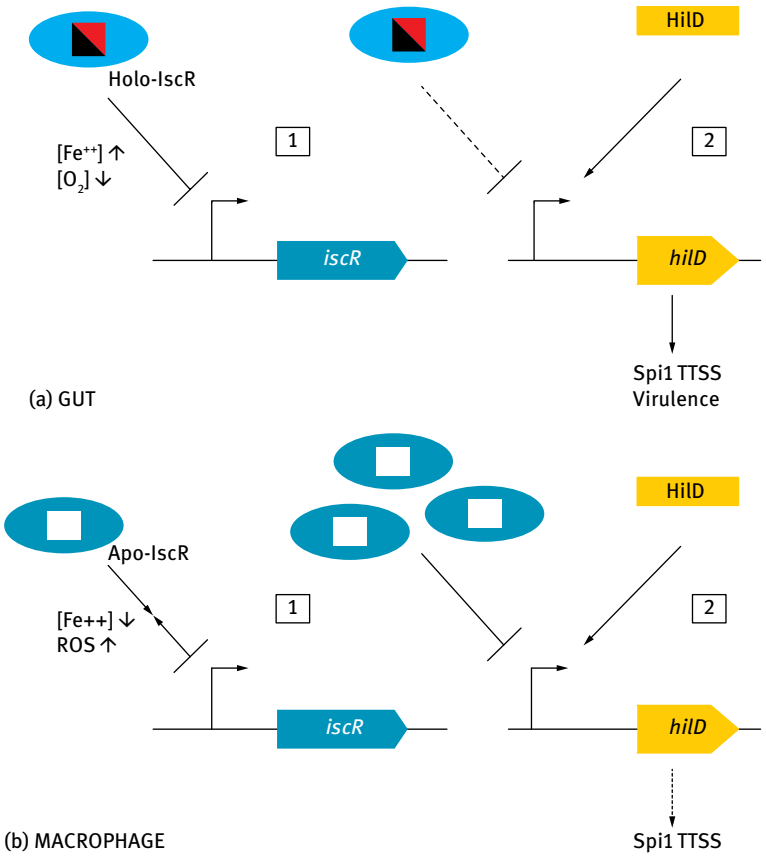

Fig. 2.4: A simplified model for the regulation of the *Salmonella* TTSS Spi1. (A) The first step of *Salmonella* infection process occurs in the gut, where iron is available and oxygen concentrations are low. Such environments favor Fe-S cluster stability, resulting in *iscR* repression by holo-IscR (1). Low levels of holo-IscR will poorly compete with HilD, yielding an activation of *hilD*, Spi1 TTSS gene full expression, and invasion of epithelial cells (2). (B) During the second step of the infection, *Salmonella* survives and replicates in macrophages within a membrane-bound compartment called the *Salmonella*-containing vacuole using a TTSS encoded by Spi2. The oxidizing and iron-poor environment of this compartment is detrimental for the biogenesis and stability of Fe-S clusters. Therefore, apo-IscR predominates and alleviates *iscR* repression, leading to an increase in apo-IscR cellular content (1). In this context, the repression of *hilD* by apo-IscR is stronger, reducing the expression of Spi1 TTSS genes and limiting energetic expenses as Spi1 is not required for *Salmonella* proliferation within macrophages (2).

pathogens in targeting TTSS regulation in opposite ways, as an activator in *Yersinia* and a repressor in *Salmonella*.

In *Shigella flexneri*, inactivation of the ISC system prevents formation of plaques because the strain is noninvasive [79], whereas in *Mycobacterium tuberculosis*, the

SUF system was shown to be essential for survival and required for virulence [80]. More recently, deletion of *Mycobacterium iscS* was found to render the cells microaerophilic, hypersensitive to oxidative stress, and impaired in Fe-S cluster-dependent enzyme activity, indicating that IscS was associated with Fe-S cluster assembly in this bacterium [81]. Earlier, we had found the SUF and ISC systems to be required for full virulence of the plant pathogen *Dickeya dadantii* [82, 83]. Surprisingly, the *iscR* mutant was shown to be noninvasive on *Saintpaulia ionantha* plants (because the SUF system could not be activated by IscR), whereas this mutant exhibited a wild-type phenotype on *Arabidopsis thaliana*, probably because the demand in Fe-S clusters was satisfied by the ISC machinery [83]. Mutations in *iscR* also reduce the virulence of other pathogens like *Pseudomonas aeruginosa* and *Xanthomonas campestris*, whereas in enterotoxigenic *E. coli*, IscR was shown to bind upstream of *cfaA* to activate CFA/I fimbriae production in response to iron starvation [84–86]. In *Vibrio vulnificus*, the disruption of *iscR* resulted in a reduction in motility and adhesion to epithelial cells, as well as resistance to ROS [87]. Together, these studies indicate that the ISC and SUF machineries contribute to the success in the pathogenesis of many bacterial species. Particular attention must be given to IscR, which was shown to regulate the expression of virulence genes in addition to Fe-S cluster biogenesis operons.

2.6 Conclusions

Two decades of studies have provided a detailed understanding of many aspects of the ISC system, from structural description to physiological roles. Uncertainties remain on the specific contributions of some of the components, either isolated or as part of the ensemble. For instance, the actual role of Fxn within the assembly step is still open to question as it could be involved in iron sensing, cysteine desulfurase activity, or structural rearrangements of the initial Fe-S synthesis complex. The actual source of iron remains a mystery, and whether there is a single dedicated iron donor or a series of iron-binding components from which ISC extracts iron remains unknown. Recent years have widened the physiological role of ISC and its impact in cell biology. A most spectacular aspect is the connection between ISC and antibiotic resistance/sensitivity of host target cells. Another important topic involves the role that ISC plays in bacterial pathogenicity. In all of these cases, a key question is to know how directly ISC function can be linked to the phenotype under consideration. In any case, these recent studies clearly reinforce the view that bacteria exploit features of Fe-S based biology using an impressive array of maneuvers to enhance their growth. In this regard, studies aimed at appreciating the contribution of ISC biology within the contexts of medical or environmental microbiology are likely to gain increasing importance in the near future.

References

[1] Malkin R, Rabinowit JC. The reconstitution of clostridial ferredoxin. Biochem Biophys Res Commun 1966;23:822–7.
[2] Jacobson MR, Cash VL, Weiss MC, Laird NF, Newton WE, Dean DR. Biochemical and genetic analysis of the nifUSVWZM cluster from Azotobacter vinelandii. Mol Gen Genet 1989;219:49–57.
[3] Lill R. Function and biogenesis of iron-sulfur proteins. Nature 2009;460:831–8.
[4] Balk J, Schaedler TA. Iron cofactor assembly in plants. Annu Rev Plant Biol 2014;65:125–53.
[5] Roche B, Aussel L, Ezraty B, Mandin P, Py B, Barras F. Iron/sulfur proteins biogenesis in prokaryotes: formation, regulation and diversity. Biochim Biophys Acta 2013;1827:455–69.
[6] Blanc B, Gerez C, Ollagnier de Choudens S. Assembly of Fe/S proteins in bacterial systems: Biochemistry of the bacterial ISC system. Biochim Biophys Acta 2015;1853:1436–47.
[7] Schwartz CJ, Djaman O, Imlay JA, Kiley PJ. The cysteine desulfurase, IscS, has a major role in vivo Fe-S cluster formation in Escherichia coli. Proc Nat Acad Sci USA 2000;97:9009–14.
[8] Kurihara T, Mihara H, Kato SI, Yoshimura T, Esaki N. Assembly of iron-sulfur clusters mediated by cysteine desulfurases, IscS, CsdB and CSD from Escherichia coli. Biochim Biophys Acta 2003;1647:303–9.
[9] Zheng L, White RH, Cash VL, Jack RF, Dean DR. Cysteine desulfurase activity indicates a role for NIFS in metallocluster biosynthesis. Proc Natl Acad Sci USA 1993;90:2754–8.
[10] Agar JN, Krebs C, Frazzon J, Huynh BH, Dean DR, Johnson MK. IscU as a scaffold for iron-sulfur cluster biosynthesis: sequential assembly of [2Fe-2S] and [4Fe-4S] clusters in IscU. Biochemistry 2000;39:7856–62.
[11] Smith AD, Agar JN, Johnson KA, Frazzon J, Amster IJ, Dean DR, Johnson MK. Sulfur transfer from IscS to IscU: the first step in iron-sulfur cluster biosynthesis. J Am Chem Soc 2001;123:11103–4.
[12] Urbina HD, Silberg JJ, Hoff KG, Vickery LE. Transfer of sulfur from IscS to IscU during Fe/S cluster assembly. J Biol Chem 2001;276:44521–6.
[13] Smith AD, Frazzon J, Dean DR, Johnson MK. Role of conserved cysteines in mediating sulfur transfer from IscS to IscU. FEBS Lett 2005;579:5236–40.
[14] Chandramouli K, Unciuleac MC, Naik S, Dean DR, Huynh BH, Johnson MK, Formation and properties of [4Fe-4S] clusters on the IscU scaffold protein. Biochemistry 2007;46:6804–11.
[15] Raulfs EC, O'Carroll IP, Dos Santos PC, Unciuleac MC, Dean DR. In vivo iron-sulfur cluster formation. Proc Natl Acad Sci USA 2008;105:8591–6.
[16] Yan R, Adinolfi S, Pastore A. Ferredoxin, in conjunction with NADPH and ferredoxin-NADP reductase, transfers electrons to the IscS/IscU complex to promote iron-sulfur cluster assembly. Biochim Biophys Acta 2015;1854:1113–7.
[17] Yan R, Konarev PV, Iannuzzi C, Adinolfi S, Roche B, Kelly G, Simon L, Martin SR, Py B, Barras F, Svergun DI, Pastore A. Ferredoxin competes with bacterial frataxin in binding to the desulfurase IscS. J Biol Chem 2013;288:24777–87.
[18] Kim JH, Frederick RO, Reinen NM, Troupis AT, Markley JL. [2Fe-2S]-ferredoxin binds directly to cysteine desulfurase and supplies an electron for iron-sulfur cluster assembly but is displaced by the scaffold protein or bacterial frataxin. J Am Chem Soc 2013;135:8117–20.
[19] Roche B, Huguenot A, Barras F, Py B. The iron-binding CyaY and IscX proteins assist the ISC-catalyzed Fe-S biogenesis in Escherichia coli. Mol Microbiol 2015;95:605–23.
[20] Tsai CL, Barondeau DP. Human frataxin is an allosteric switch that activates the Fe-S cluster biosynthetic complex. Biochemistry 2010;49:9132–9.
[21] Iannuzzi C, Adinolfi S, Howes BD, Garcia-Serres R, Clémancey M, Latour JM, Smulevich G, Pastore A. The role of CyaY in iron sulfur cluster assembly on the E. coli IscU scaffold protein. PLoS One 2011;6:e21992.

[22] Kim JH, Bothe JR, Frederick RO, Holder JC, Markley JL. Role of IscX in iron-sulfur cluster biogenesis in Escherichia coli. J Am Chem Soc 2014;136:7933–42.
[23] Chandramouli K, Johnson MK. HscA and HscB stimulate [2Fe-2S] cluster transfer from IscU to apoferredoxin in an ATP-dependent reaction. Biochemistry 2006;45:11087–95.
[24] Bonomi F, Iametti S, Morleo A, Ta D, Vickery LE. Facilitated transfer of IscU-[2Fe-2S] clusters by chaperone-mediated ligand exchange. Biochemistry 2011;50:9641–50.
[25] Loiseau L, Gerez C, Bekker M, Ollagnier-de-Choudens S, Py B, Sanakis Y, Teixeira-de-Mattos J, Fontecave M, Barras F, ErpA, an iron-sulfur (Fe-S) protein of the A-type essential for respiratory metabolism in Escherichia coli. Proc Natl Acad Sci USA 2007;104:13626–31.
[26] Ollagnier-de Choudens S, Sanakis Y, Fontecave M. SufA/IscA: reactivity studies of a class of scaffold proteins involved in [Fe-S] cluster assembly. J Biol Inorg Chem 2004;9:828–38.
[27] Vinella D, Brochier-Armanet C, Loiseau L, Talla E, Barras F, Iron-sulfur (Fe/S) protein biogenesis: phylogenomic and genetic studies of A-type carriers. PLoS Gen 2009;5:e1000497.
[28] Py B, Gerez C, Angelini S, Planel R, Vinella D, Loiseau L, Talla E, Brochier-Armanet C, Garcia-Serres R, Latour JM, Ollagnier-de Choudens S, Fontecave M, Barras F. Molecular organization, biochemical function, cellular role and evolution of NfuA, an atypical Fe-S carrier. Mol Mic 2012;86:155–71.
[29] Angelini S, Gerez C, Ollagnier-de-Choudens S, Sanakis Y, Fontecave M, Barras F, Py B, NfuA, a new factor required for maturing Fe/S proteins in Escherichia coli under oxidative stress and iron starvation conditions. J Biol Chem 2008;283:14084–91.
[30] Tokumoto U, Takahashi Y. Genetic analysis of the isc operon in Escherichia coli involved in the biogenesis of cellular iron-sulfur proteins. J Biochem 2001;130:63–71.
[31] Campuzano V, Montermini L, Moltò MD, Pianese L, Cossée M, Cavalcanti F, Monros E, Rodius F, Duclos F, Monticelli A, Zara F, Cañizares J, Koutnikova H, Bidichandani SI, Gellera C, Brice A, Trouillas P, De Michele G, Filla A, De Frutos R, Palau F, Patel PI, Di Donato S, Mandel JL, Cocozza S, Koenig M, Pandolfo M. Friedreich's ataxia: autosomal recessive disease caused by an intronic GAA triplet repeat expansion. Science 1996;271:1423–7.
[32] Campuzano V, Montermini L, Lutz Y, Cova L, Hindelang C, Jiralerspong S, Trottier Y, Kish SJ, Faucheux B, Trouillas P, Authier FJ, Dürr A, Mandel JL, Vescovi A, Pandolfo M, Koenig M. Frataxin is reduced in Friedreich ataxia patients and is associated with mitochondrial membranes. Hum Mol Genet 1997;6:1771–80.
[33] Martelli A, Puccio H. Dysregulation of cellular iron metabolism in Friedreich ataxia: from primary iron-sulfur cluster deficit to mitochondrial iron accumulation. Front Pharmacol 2014;5:130.
[34] Puccio H, Simon D, Cossée M, Criqui-Filipe P, Tiziano F, Melki J, Hindelang C, Matyas R, Rustin P, Koenig M. Mouse models for Friedreich ataxia exhibit cardiomyopathy, sensory nerve defect and Fe-S enzyme deficiency followed by intramitochondrial iron deposits. Nat Genet 2001;27:181–6.
[35] Martelli A, Wattenhofer-Donzé M, Schmucker S, Bouvet S, Reutenauer L, Puccio H. Frataxin is essential for extramitochondrial Fe-S cluster proteins in mammalian tissues. Hum Mol Genet 2007;16:2651–8.
[36] Gerber J, Mühlenhoff U, Lill R. An interaction between frataxin and Isu1/Nfs1 that is crucial for Fe/S cluster synthesis on Isu1. EMBO Rep 2003;4:906–11.
[37] Shan Y, Napoli E, Cortopassi G. Mitochondrial frataxin interacts with ISD11 of the NFS1/ISCU complex and multiple mitochondrial chaperones. Hum Mol Genet 2007;16:929–41.
[38] Prischi F, Konarev PV, Iannuzzi C, Pastore C, Adinolfi S, Martin SR, Svergun DI, Pastore A. Structural bases for the interaction of frataxin with the central components of iron-sulphur cluster assembly. Nat Commun 2010;1:95. doi: 10.1038/ncomms1097.
[39] Schmucker S, Martelli A, Colin F, Page A, Wattenhofer-Donzé M, Reutenauer L, Puccio H. Mammalian frataxin: an essential function for cellular viability through an interaction with a preformed ISCU/NFS1/ISD11 iron-sulfur assembly complex. PLoS One 2011;6:e16199.

[40] Li DS, Ohshima K, Jiralerspong S, Bojanowski MW, Pandolfo M. Knock-out of the cyaY gene in Escherichia coli does not affect cellular iron content and sensitivity to oxidants. FEBS 1999;456:13–6.
[41] Vivas E, Skovran E, Downs DM. Salmonella enterica strains lacking the frataxin homolog CyaY show defects in Fe-S cluster metabolism in vivo. J Bact 2006;188:1175–9.
[42] Pohl T, Walter J, Stolpe S, Soufo JH, Grauman PL, Friedrich T. Effects of the deletion of the Escherichia coli frataxin homologue CyaY on the respiratory NADH: ubiquinone oxidoreductase. BMC Biochem 2007;8:1–10.
[43] Roche B, Agrebi R, Huguenot A, Ollagnier de Choudens S, Barras F, Py B. Turning Escherichia coli into a frataxin-dependent organism. PLoS Genet 2015;11:e1005134.
[44] Yoon H, Knight SA, Pandey A, Pain J, Turkarslan S, Pain D, Dancis A. Turning Saccharomyces cerevisiae into a Frataxin-Independent Organism. PLoS Genet 2015;11:e1005135.
[45] Bridwell-Rabb J, Iannuzzi C, Pastore A, Barondeau DP. Effector role reversal during evolution: the case of frataxin in Fe-S cluster biosynthesis. Biochemistry 2012;51:2506–14.
[46] Bridwell-Rabb J, Fox NG, Tsai CL, Winn AM, Barondeau DP. Human frataxin activates Fe-S cluster biosynthesis by facilitating sulfur transfer chemistry. Biochemistry 2014;53:4904–13.
[47] Blanc B, Clémancey M, Latour JM, Fontecave M, Ollagnier de Choudens S. Molecular investigation of iron-sulfur cluster assembly scaffolds under stress. Biochemistry 2014;53:7867–9.
[48] Giel JL, Nesbit AD, Mettert EL, Fleischhacker AS, Wanta BT, Kiley PJ. Regulation of iron-sulphur cluster homeostasis through transcriptional control of the Isc pathway by [2Fe-2S]-IscR in Escherichia coli. Mol Microbiol 2013;87:478–92.
[49] Mettert EL, Kiley PJ. Fe-S proteins that regulate gene expression. Biochim Biophys Acta. 2015;1853:1284–93.
[50] Schwartz CJ, Giel JL, Patschkowski T, Luther C, Ruzicka FJ, Beinert H, et al. IscR, an Fe-S cluster-containing transcription factor, represses expression of Escherichia coli genes encoding Fe-S cluster assembly proteins. Proc Natl Acad Sci USA 2001;98:14895–900.
[51] Fleischhacker AS, Stubna A, Hsueh K-L, Guo Y, Teter SJ, Rose JC, et al. Characterization of the [2Fe-2S] cluster of Escherichia coli transcription factor IscR. Biochemistry (Mosc) 2012;51:4453–62.
[52] Giel JL, Rodionov D, Liu M, Blattner FR, Kiley PJ. IscR-dependent gene expression links iron-sulphur cluster assembly to the control of O2-regulated genes in Escherichia coli. Mol Microbiol 2006;60:1058–75.
[53] Rajagopalan S, Teter SJ, Zwart PH, Brennan RG, Phillips KJ, Kiley PJ. Studies of IscR reveal a unique mechanism for metal-dependent regulation of DNA binding specificity. Nat Struct Mol Biol 2013;20:740–7.
[54] Outten FW, Djaman O, Storz G. A suf operon requirement for Fe-S cluster assembly during iron starvation in Escherichia coli. Mol Microbiol 2004;52:861–72.
[55] Fantino J-R, Py B, Fontecave M, Barras F. A genetic analysis of the response of Escherichia coli to cobalt stress. Environ Microbiol 2010;12:2846–57.
[56] Vinella D, Loiseau L, Ollagnier de Choudens S, Fontecave M, Barras F. In vivo [Fe-S] cluster acquisition by IscR and NsrR, two stress regulators in Escherichia coli. Mol Microbiol 2013;87:493–508.
[57] Pullan ST, Gidley MD, Jones RA, Barrett J, Stevanin TM, Read RC, et al. Nitric oxide in chemostat-cultured Escherichia coli is sensed by Fnr and other global regulators: unaltered methionine biosynthesis indicates lack of S nitrosation. J Bacteriol 2007;189:1845–55.
[58] Yeo W-S, Lee J-H, Lee K-C, Roe J-H. IscR acts as an activator in response to oxidative stress for the suf operon encoding Fe-S assembly proteins. Mol Microbiol 2006;61:206–18.
[59] Desnoyers G, Morissette A, Prévost K, Massé E. Small RNA-induced differential degradation of the polycistronic mRNA iscRSUA. EMBO J 2009;28:1551–61.

[60] Massé E, Gottesman S. A small RNA regulates the expression of genes involved in iron metabolism in Escherichia coli. Proc Natl Acad Sci USA 2002;99:4620–5.
[61] Massé E, Vanderpool CK, Gottesman S. Effect of RyhB small RNA on global iron use in Escherichia coli. J Bacteriol 2005;187:6962–71.
[62] Mandin P, Chareyre S, Barras F. A Regulatory circuit composed of a transcription factor, IscR, and a regulatory RNA, RyhB, controls Fe-S cluster delivery. mBio 2016;7(5):e00966–16 doi: 10.1128/mBio.00966–16.
[63] Dwyer DJ, Kohanski MA, Hayete B, Collins JJ. Gyrase inhibitors induce an oxidative damage cellular death pathway in Escherichia coli. Mol Syst Biol 2007;3:91.
[64] Dwyer DJ, Belenky PA, Yang JH, et al. Antibiotics induce redox-related physiological alterations as part of their lethality. Proc Natl Acad Sci USA 2014;111:100–9.
[65] Dwyer DJ, Collins JJ, Walker GC. Unraveling the Physiological Complexities of antibiotic lethality. Annu Rev Pharmacol Toxicol 2015;55:313–32.
[66] Kohanski MA, Dwyer DJ, Hayete B, Lawrence CA, Collins JJ. A common mechanism of cellular death induced by bactericidal antibiotics. Cell 2007;130:797–810.
[67] Kohanski MA, Dwyer DJ, Wierzbowski J, Cottarel G, Collins JJ. Mistranslation of membrane proteins and two-component system activation trigger antibiotic-mediated cell death. Cell 2008;135:679–90.
[68] Ezraty B, Vergnes A, Banzhaf M, et al. Fe-S cluster biosynthesis controls uptake of aminoglycosides in a ROS-less death pathway. Science 2013;340:1583–7.
[69] Keren I, Wu Y, Inocencio J, Mulcahy LR, Lewis K. Killing by bactericidal antibiotics does not depend on reactive oxygen species. Science 2013;339:1213–6.
[70] Liu Y, Imlay JA. Cell death from antibiotics without the involvement of reactive oxygen species. Science 2013;339:1210–3.
[71] Imlay JA. Diagnosing oxidative stress in bacteria: not as easy as you might think. Curr Opin Microbiol 2015;24:124–31.
[72] Cunningham RP, Asahara H, Bank JF, et al. Endonuclease III is an iron-sulfur protein. Biochemistry 1989;28:4450–5.
[73] Boal AK, Yavin E, Lukianova OA, O'Shea VL, David SS, Barton JK. DNA-bound redox activity of DNA repair glycosylases containing [4Fe-4S] clusters. Biochemistry 2005;44:8397–407.
[74] Lukianova OA, David SS. A role for iron-sulfur clusters in DNA repair. Curr Opin Chem Biol 2005;9:145–51.
[75] Ren B, Duan X, Ding H. Redox control of the DNA damage-inducible protein DinG helicase activity via its iron-sulfur cluster. J Biol Chem 2009;284:4829–35.
[76] Brown LT, Sutera VA, Zhou S, Weitzel CS, Cheng Y, Lovett ST. Connecting replication and repair: YoaA, a helicase-related protein, promotes azidothymidine tolerance through association with chi, an accessory clamp loader protein. PLoS Genet 2015;11:e1005651
[77] Vergnes A, Viala JPM, Ouadah-Tsabet R, Pocachard B, Loiseau L, Méresse S, Barras F, Aussel L. The iron-sulfur cluster sensor IscR is a negative regulator 1 of Spi1 type III secretion system in Salmonella enterica. Cell Microbiol 2007;19:e12680.
[78] Miller HK, Kwuan L, Schwiesow L, Bernick DL, Mettert E, Ramirez HA, et al. IscR is essential for Yersinia pseudotuberculosis type III secretion and virulence. PLoS Pathog 2014;10:e1004194.
[79] Runyen-Janecky L, Daugherty A, Lloyd B, Wellington C, Eskandarian H, Sagransky M. Role and regulation of iron-sulfur cluster biosynthesis genes in Shigella flexneri virulence. Infect Immun 2008;76:1083–92.
[80] Huet G, Daffé M, Saves I. Identification of the Mycobacterium tuberculosis SUF machinery as the exclusive mycobacterial system of [Fe-S] cluster assembly: evidence for its implication in the pathogen's survival. J Bacteriol 2005;187:6137–46.

[81] Rybniker J, Pojer F, Marienhagen J, Kolly GS, Chen JM, van Gumpel E, Hartmann P, Cole ST. The cysteine desulfurase IscS of Mycobacterium tuberculosis is involved in iron-sulfur cluster biogenesis and oxidative stress defence. Biochem J 2014;459:467–78.
[82] Nachin L, El Hassouni M, Loiseau L, Expert D, Barras F. SoxR-dependent response to oxidative stress and virulence of Erwinia chrysanthemi: the key role of SufC, an orphan ABC ATPase. Mol Microbiol 2001;39:960–72.
[83] Rincon-Enriquez G, Crété P, Barras F, Py B. Biogenesis of Fe-S proteins and pathogenicity: IscR plays a key role in allowing Erwinia chrysanthemi to adapt to hostile conditions. Mol Microbiol 2008;67:1257–73.
[84] Kim SH, Lee BY, Lau GW, Cho YH. IscR modulates catalase A (KatA) activity, peroxide resistance and full virulence of Pseudomonas aeruginosa PA14. J Microbiol Biotechnol 2009;19:1520–6.
[85] Fuangthong M, Jittawuttipoka T, Wisitkamol R, Romsang A, Duang-nkern J, Vattanaviboon P, Mongkolsuk S. IscR plays a role in oxidative stress resistance and pathogenicity of a plant pathogen, Xanthomonas campestris. Microbiol Res 2015;170:139–46.
[86] Haines S, Arnaud-Barbe N, Poncet D, Reverchon S, Wawrzyniak J, Nasser W, Renauld-Mongénie G. IscR regulates synthesis of colonization factor antigen I fimbriae in response to iron starvation in enterotoxigenic Escherichia coli. J Bacteriol 2015;197:2896–907.
[87] Lim JG, Choi SH. IscR is a global regulator essential for pathogenesis of Vibrio vulnificus and induced by host cells. Infect Immun 2014;82:569–78.

3 A stress-responsive Fe-S cluster biogenesis system in bacteria – the *suf* operon of Gammaproteobacteria

F. Wayne Outten

3.1 Introduction to Fe-S cluster biogenesis

Iron-sulfur (Fe-S) clusters are minerals captured by the biosphere and integrated into cellular metabolism at the earliest stages of life [1, 2]. The elegant work of Holm and others suggests that early Fe-S cluster incorporation into metabolism may not have required any biogenesis machinery [3–6]. Fe-S clusters are thermodynamically stable, especially in anaerobic environments, and can undergo facile ligand exchange with small molecule (i.e. nonproteinaceous) ligands *in vitro*. Iron and sulfide were both abundant in certain environmental niches of the early anaerobic earth, for example, in hydrothermal vents where some of the most phylogenetically ancient organisms still thrive [7]. The earliest precursors of modern cells may have simply encapsulated preformed Fe-S clusters, concentrating them within membranes to be bound by metalloproteins or other metabolites with suitable ligands and/or binding site geometry (see discussion in Chapter 17 in volume 2 by Boyd *et al.*). It is likely that the first piece of the biogenesis machinery to have evolved is the Fe-S scaffold protein, which allows cells to physically sequester Fe-S clusters and direct them into specific target metalloproteins. A scaffold protein helps to limit nonspecific incorporation of Fe-S clusters into proteins with potential metal-binding amino acid residues. Such cluster misincorporation is still a technical problem that must be overcome by experimentalists characterizing new candidate Fe-S proteins [8].

What makes a good Fe-S cluster scaffold protein? The scaffold structure must promote formation of a stable cluster during assembly but be flexible enough to efficiently release the Fe-S cluster for insertion into a target metalloprotein. These requirements are further complicated by the potential need for the scaffold to accommodate multiple cluster types with very different geometries (planar *vs* cuboidal, for example). Elegant biophysical characterization of the IscU Fe-S cluster scaffold protein from *E. coli* has clearly shown that the scaffold is metamorphic, that is, it can exist in two interconvertible conformations that are similar in their free energies [9–11]. The partially disordered (D) state of IscU promotes sulfur acquisition during cluster assembly as well as transfer of the fully formed cluster. In contrast, the structured (S) conformation of IscU facilitates iron binding and iron-sulfide interactions to initially assemble the *de novo* cluster. Interconversion between these different conformations is partially controlled by *cis-trans* isomerization of two peptidyl-prolyl peptide bonds in IscU as well as by interaction with molecular chaperones that preferentially bind a specific conformation [9].

DOI 10.1515/9783110479850-003

As Fe-S cluster metabolism became more predominant among early lineages of life, there was likely selection for specific iron and sulfide donation pathways. Organisms that filled some environmental niches may have struggled with limited access to bioavailable iron and sulfur sources, a problem that was certainly exacerbated by the accumulation of oxygen after the development of oxygenic photosynthesis [12–14]. This scarcity selected for the evolution of high affinity uptake transporters and dedicated intracellular homeostasis systems for iron and sulfur, at least partially to ensure continued biogenesis of Fe-S clusters required for core metabolism. We will discuss each in turn, beginning with sulfur trafficking, which is better characterized than *in vivo* iron donation.

3.2 Sulfur trafficking for Fe-S cluster biogenesis

Among the Bacteria and Eukarya, the cysteine desulfurase enzyme family controls sulfide donation for Fe-S cluster assembly (Fig. 3.1). Cysteine desulfurases are homodimeric enzymes that utilize pyridoxal-5′-phosphate (PLP) as a cofactor to catalyze the removal of sulfur from L-cysteine substrate [15, 16]. The sulfur is abstracted from L-cysteine by nucleophilic attack from the thiolate anion of a Cys residue in the desulfurase active site on the PLP-L-cysteine protonated quinonoid adduct. This results in the sulfur atom forming a persulfide bond (R-S-SH) at the active site Cys residue of the cysteine desulfurase enzyme. The remaining backbone of L-cysteine is released from PLP as L-alanine. The persulfide sulfur is then transferred from the cysteine desulfurase to a partner protein (usually the scaffold) *via* a thiol exchange reaction in which a Cys residue from the partner protein carries out a nucleophilic attack on the persulfide of the donor (Fig. 3.1). This sulfur trafficking pathway likely limits the release of sulfide *in vivo* during cluster biogenesis. Because sulfide is toxic to most aerobic organisms, the controlled trafficking of a persulfide species avoids deleterious side reactions during cluster assembly. The persulfide is S^0 and must be reduced to S^{2-} during the subsequent steps of cluster assembly. Recent evidence suggests that the source of reducing equivalents for this may be provided by partner redox proteins, such as [2Fe-2S] Fdx in the Isc pathway, that directly donate electrons for sulfur reduction [17, 18]. It also has been proposed that oxidation of Fe^{2+} to Fe^{3+} during formation of the first $[2Fe\text{-}2S]^{2+}$ cluster intermediate may provide some of the reducing power for sulfide formation. Despite numerous published results, it is still difficult to establish if persulfide and iron are donated sequentially (and if so, which comes first) or if they must be provided simultaneously for proper cluster assembly. Results obtained *in vitro* are often complicated by the lack of one or more potential partner proteins for the cysteine desulfurase and/or scaffold protein, which may significantly alter the biochemical behavior of the system. Context is everything in Fe-S cluster biogenesis.

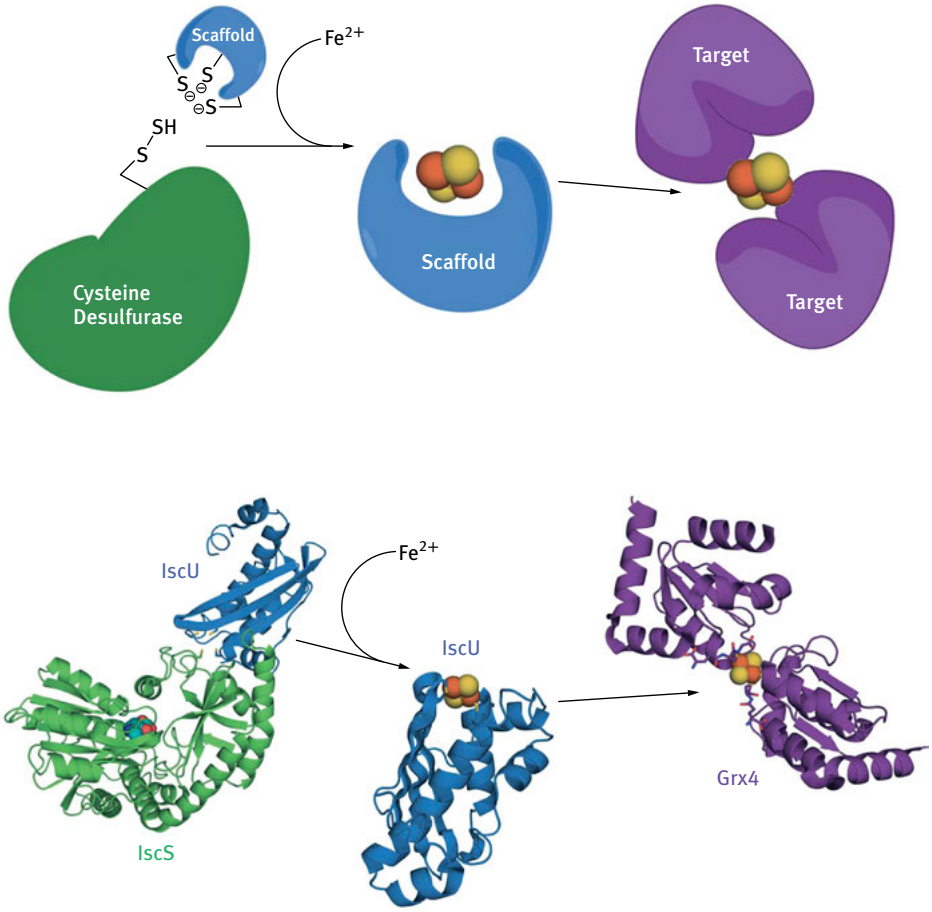

Fig. 3.1: Core components of Fe-S cluster assembly. (top) Diagram of persulfide transfer from cysteine desulfurase to scaffold protein. Iron donation and cluster assembly proceed and then cluster transfer occurs to a target Fe-S metalloprotein. (bottom) Structures of IscS cysteine desulfurase (green) and IscU scaffold (blue) are shown (from co-structure of $IscS_2$-$IscU_2$ in PDB 4EB5) [19]. [2Fe-2S] monothiol glutaredoxin 4 (Grx4) is shown in purple as a target protein (from PDB 2WCI) [68].

3.3 Iron donation for Fe-S cluster biogenesis

The donation of iron for Fe-S cluster biogenesis is still largely uncharacterized. It is generally accepted (although not proven experimentally) that iron used for Fe-S cluster biogenesis comes from a ferrous pool of "labile" iron. The nature of the labile iron pool is still under investigation, but it is thought to consist of weakly chelated Fe^{2+} that is routed into iron metallocofactor biogenesis. This pool also is sensed by iron metalloregulatory proteins that control cellular iron homeostasis. To direct labile

iron into Fe-S cluster biogenesis, the scaffold protein could directly bind iron from this pool. Multiple studies to address this question have not resulted in a clear answer. Although *Azotobacter vinelandii* and *Escherichia coli* IscU scaffolds do not appear to have appreciable iron binding capability, *Thermotoga maritima* SufU can bind either Fe^{2+} or Fe^{3+} with affinities that range from the high nanomolar to low micromolar [20–22].

Alternatively, iron donation may require a separate iron "chaperone" protein that specifically interacts with the scaffold protein. Metallochaperones have been identified for other essential metals, such as copper and cobalt. Examples of well-studied copper chaperones include Atx1 in eukaryotes and CopZ in bacteria. Atx1 efficiently traffics copper and releases it upon direct protein-protein contact with its cognate acceptor Ccc2 [23–25]. An analogous iron chaperone would ensure that a subpopulation of the labile iron pool is dedicated for Fe-S cluster biogenesis as opposed to heme biosynthesis or maturation of mono- and di-nuclear iron enzymes. A number of candidate iron donor proteins have been put forth over the last two decades, of which frataxin is the most thoroughly studied (see volume 2, chapter 10 by Tong). There is clear evidence that frataxin is intimately involved in Fe-S cluster biogenesis by the Isc (iron-sulfur cluster) pathway, both in Bacteria as well as in the mitochondria of Eukarya. *E. coli* contains a microbial frataxin (CyaY). CyaY binds two Fe^{2+} ions with a weak affinity (K_d = 3.8 μM) [26]. The weak affinity of CyaY for Fe^{2+} is in contrast to other metallochaperones that typically have metal-binding affinities of picomolar or lower for their target metals [27, 28].

CyaY can also mediate the controlled oxidation of ferrous iron to ferric iron in the presence of H_2O_2, thereby avoiding hydroxyl radical generation [26]. This reaction is fundamentally similar to that of the mini-ferritin protein Dps (see Section 3.8.2), which sequesters ferric iron under oxidative stress in *E. coli*. CyaY can accommodate approximately 26 Fe^{3+}, likely in the form of polynuclear iron hydroxo(oxo) species that are only partially associated with the protein. Iron associates with CyaY at the carboxyl side chain of conserved aspartate and glutamate residues [29]. Since carboxyl groups are less susceptible to oxidation than the thiol side chain of cysteine ligands that are prevalent in ferrous iron-binding proteins, it is proposed that CyaY sequesters ferric iron in the presence of hydrogen peroxide to help minimize the production of hydroxyl radicals [27]. Based on these studies and analogous work on eukaryotic frataxins, it was originally proposed that CyaY may be an iron donor for the Isc pathway [30].

However, a role for CyaY in iron donation has recently been called into question [31–34]. In *E. coli*, CyaY has been shown to inhibit *in vitro* [2Fe-2S] cluster formation on IscU when using IscS as the sulfur donor. The presence of CyaY does not facilitate iron delivery for cluster reconstitution on IscU, regardless of whether iron is added in solution or bound directly to CyaY. CyaY inhibition likely occurs through direct binding of CyaY to the IscS-IscU co-complex such that CyaY inhibits a step in cluster assembly, such as persulfide transfer from IscS to IscU. It was shown that CyaY residues that bind iron are also involved in binding to IscS because mutation of these residues diminished the ability of CyaY to inhibit IscS. The presence of iron slightly enhanced the inhibitory effect of CyaY on IscS-IscU cluster formation, leading to the

proposal that CyaY may act as a gatekeeper to control Fe-S cluster assembly based on *in vivo* iron levels [31]. One could imagine a model where *in vivo* oxidation of Fe^{2+} to Fe^{3+} on CyaY during oxidative stress might enhance CyaY repression of IscS-IscU to limit Isc-mediated cluster assembly. Such regulation would be consistent with other post-transcriptional repression of Isc under certain stress conditions (see below in Section 3.5). Further studies are necessary to confirm the exact function of frataxin.

In addition to frataxin, in eukaryotes the poly(rC)-binding proteins (PCBPs) were shown to be required for efficient *in vivo* iron loading into the ferritin iron storage protein as well as iron- and 2-oxoglutarate-dependent dioxygenases [35–37]. PCBP1 can bind up to 3 iron ions with high nanomolar to low micromolar affinity and was shown to directly interact with ferritin in a Fe^{2+}-dependent manner. However, close PCBP homologues are largely absent in currently sequenced microbial genomes; thus, it is not clear if they play any role in iron trafficking in non-eukaryotic organisms.

Unlike copper, specific high-affinity metallochaperones for individual iron-containing enzymes have not been identified in bacteria. This difference may be due to the abundance of iron containing enzymes in the cell, which requires a large labile iron pool and makes a "one chaperone per metalloenzyme" system less tenable. The labile copper pool is quite small (less than femtomolar) due to tight buffering by metallochaperones and glutathione (GSH) [29, 38, 39]. In contrast, the labile iron pool is thought be considerable (low micromolar) in most cell types. It is possible that the use of metallochaperones for other metals besides iron may have arisen to protect weakly chelated iron pools from direct competition by metals like copper and zinc. Cu^{II} and Zn^{II} should bind more tightly to cellular ligands than Fe^{II} based on their relative positions in the Irving-Williams series. This explanation certainly seems plausible in the case of copper, which has been shown to disrupt iron homeostasis when present in excess of the cell's copper buffering capacity [40, 41]. In that particular case, Cu^{I} may be the culprit due to its thiophilic nature, which allows it to compete strongly for binding to Cys thiolates in cluster-binding sites. At present iron donation for Fe-S cluster biogenesis is perhaps the least well-defined step of the entire pathway. We will come back to this topic in more detail later.

3.4 Fe-S cluster assembly and trafficking

As iron and persulfide are mobilized to the scaffold protein, the cluster assembly proceeds. In the well characterized U-type scaffolds (such as IscU and the N-terminus of NifU), the first observable intermediate in cluster assembly is a $[2Fe\text{-}2S]^{2+}$ cluster [42–47]. This cluster type can then be transferred from IscU to target apo-proteins with the assistance of heat shock cognate molecular chaperones (HscA and HscB in *E. coli*) [48–51]. Depending on the target apo-protein, the chaperones can enhance cluster transfer rates from $[2Fe\text{-}2S]^{2+}$ IscU up to 700-fold [50]. Structural analysis and biochemical experiments suggest that the molecular chaperones are required to initiate ligand exchange during cluster transfer by promoting dissociation of one of

the IscU Cys ligands from the Fe-S cluster [48, 50–53]. Opening this coordinate site presumably allows the target apo-protein to access the cluster and initiate the transfer process. Molecular chaperone proteins also help control the equilibrium between structured and partially disordered conformations of IscU *via* an ATP-dependent binding cycle [49, 54, 55].

With additional iron and sulfide donation, the $[2Fe\text{-}2S]^{2+}$ form of the IscU dimer can further assemble a second $[2Fe\text{-}2S]^{2+}$ cluster. At this stage, the addition of one electron to each cluster will catalyze reductive coupling of the 2 × $[2Fe\text{-}2S]^{+}$ clusters into a single $[4Fe\text{-}4S]^{2+}$ cluster on IscU [44, 48]. The $[4Fe\text{-}4S]^{2+}$ cluster can be transferred to a target apo-protein but does not require molecular chaperones for the transfer [56]. The $[4Fe\text{-}4S]^{2+}$ cluster on IscU is sensitive to oxygen, and upon oxidation, it may "disassemble" back to the $[2Fe\text{-}2S]^{2+}$ form *in vitro*. The oxygen-sensitive cluster conversion process may create an *in vivo* pool of IscU that contains both $[4Fe\text{-}4S]^{2+}$ and $[2Fe\text{-}2S]^{2+}$ clusters, which are, by far, the most common cluster types required by Fe-S metalloproteins. The equilibrium between cluster forms of IscU would be controlled by oxygen and by the specific target apo-proteins that are drawing Fe-S clusters from the biogenesis pool. The number and types of various target Fe-S apo-proteins would in turn be controlled by cellular metabolic requirements.

Recently, it has also become clear that *in vivo* Fe-S cluster metabolism requires an array of Fe-S cluster trafficking proteins, including the A-type carrier (ATC) family [54–63] and the monothiol glutaredoxins [16, 64–68]. ATC proteins directly interact with the scaffold proteins and are highly efficient at accepting the clusters and passing them to target apo-proteins. Meanwhile, retrograde cluster transfer from the carrier back to the scaffold is typically unfavorable. The Fe-S cluster trafficking carrier proteins may provide an additional layer of *in vivo* specificity that would be difficult to encode directly in a single scaffold. For example, both ErpA, and IscA are required for full maturation of the Fe-S subunits of formate-hydrogen lyase complex in *E. coli* [69]. Similarly, Fe-S cluster acquisition by the Fe-S metalloregulatory proteins IscR and NsrR is controlled by different ATC proteins *in vivo* [70, 71]. Another possible use of carrier proteins *in vivo* is to act as a way station where clusters can accumulate while they await cellular demand. If sulfur trafficking, iron donation, and *de novo* cluster assembly are the slowest and/or most sensitive steps of Fe-S cluster biogenesis, there may be a physiological advantage to loading a pool of Fe-S carrier proteins to minimize reliance on the early steps in biogenesis. There is also strong evidence that the ATC proteins can reversibly interconvert $[4Fe\text{-}4S]^{2+}$ and $[2Fe\text{-}2S]^{2+}$ clusters in response to oxygen [72, 73]. Monothiol glutaredoxins are also known to accommodate multiple cluster types [74]. Cluster interconversion could allow them to load Fe-S clusters into multiple types of enzymes. Cluster interconversion may also provide the various trafficking proteins with a mechanism to "protect" sensitive $[4Fe\text{-}4S]^{2+}$ clusters by carrying out a controlled oxidation and disassembly to the $[2Fe\text{-}2S]^{2+}$ form in response to oxygen toxicity. In some cases all-ferric $[2Fe\text{-}2S]^{2+}$ clusters are more resistant to oxidation than $[4Fe\text{-}4S]^{2+}$ clusters that contain a mixture of Fe^{2+}/Fe^{3+}.

3.5 Iron and oxidative stress are intimately intertwined

From the observations described in Section 3.4, it is clear that oxygen is a major antagonist of Fe-S cluster metabolism, likely through the production of ROS such as H_2O_2 and superoxide (O_2•). Superoxide is electrostatically attracted to the iron cations of the Fe-S cluster and can directly oxidize Fe^{2+} to Fe^{3+} [75]. Cuboidal [4Fe-4S] clusters in most proteins are not stable in the $[4Fe\text{-}4S]^{3+}$ state. Cluster oxidation leads to ejection of iron and further oxidation of the remaining iron or sulfide (S^{2-}) causes cluster disassembly (described in detail in Chapter 12, volume 1 by Nicolet and Fontecilla-Camps) (Fig. 3.2). Some Fe-S clusters are protected from direct disruption by being buried in a solvent-protected environment within the metalloprotein. However, many Fe-S cluster-dependent dehydratase enzymes require that an open coordination site on one Fe atom be exposed to solvent to bind and activate the enzyme substrate. Fe-S clusters in this class of dehydratase are some of the most sensitive targets of oxidative stress [75–83]. ROS such as H_2O_2 also react readily with the thiolate anion form of cysteine, resulting in oxidation of the organosulfur to sulfenic, sulfinic, and sulfonic acids (Fig. 3.2) [84]. Because Cys residues are often used to coordinate Fe-S clusters, oxidative modifications of the active sites of Fe-S metalloproteins (including Fe-S cluster scaffolds) would block binding of Fe-S clusters. The protein-bound persulfide species carried on the cysteine desulfurases and trafficked by Fe-S cluster biogenesis proteins is also sensitive to oxidation providing a further mechanism by which Fe-S cluster biogenesis can be disrupted by oxygen toxicity.

Oxygen also has an indirect effect on the ability of organisms to acquire iron. In the presence of oxygen, Fe^{2+} is readily oxidized to the ferric ion Fe^{3+}. In aqueous solutions near neutral pH, Fe^{3+} will hydrolyze H_2O to generate $iron^{III}$ oxide-hydroxide compounds. Iron hydroxides can then polymerize *via* a pH-dependent process known as olation, thereby forming insoluble iron hydroxide precipitates. The aqueous chemistry of ferric iron results in vary low amounts of bioavailable iron in many environments that are otherwise favorable for life and often makes iron a limiting nutrient for growth. Although multiple strategies have evolved to circumvent iron limitation (including use of non-iron alternatives in many metabolic pathways), there appear to be a subset of absolutely essential iron metalloproteins in many organisms [60, 85].

Clearly, iron metalloproteins are a target of oxidative stress; however, iron also directly contributes to oxidative stress. This is because weakly chelated Fe^{2+} participates in the production of hydroxyl radicals *via* Fenton chemistry ($Fe^{2+} + H_2O_2 \rightarrow Fe^{3+} + {-}OH + {\cdot}OH$). To avoid toxicity, bacterial cells dynamically regulate iron distribution to maintain iron homeostasis [86, 87]. Multiple strategies are used to maintain necessary intracellular iron levels: secretion of iron-scavenging siderophores, regulation of iron import systems, utilization of iron storage proteins, and controlled distribution of iron to various pathways [88]. Intracellular iron availability is sensed by several global transcriptional regulators, including the ferric uptake regulator (Fur) and the iron-sulfur cluster regulator IscR (see Chapter 13 by Mettert *et al.*). Fur directly binds

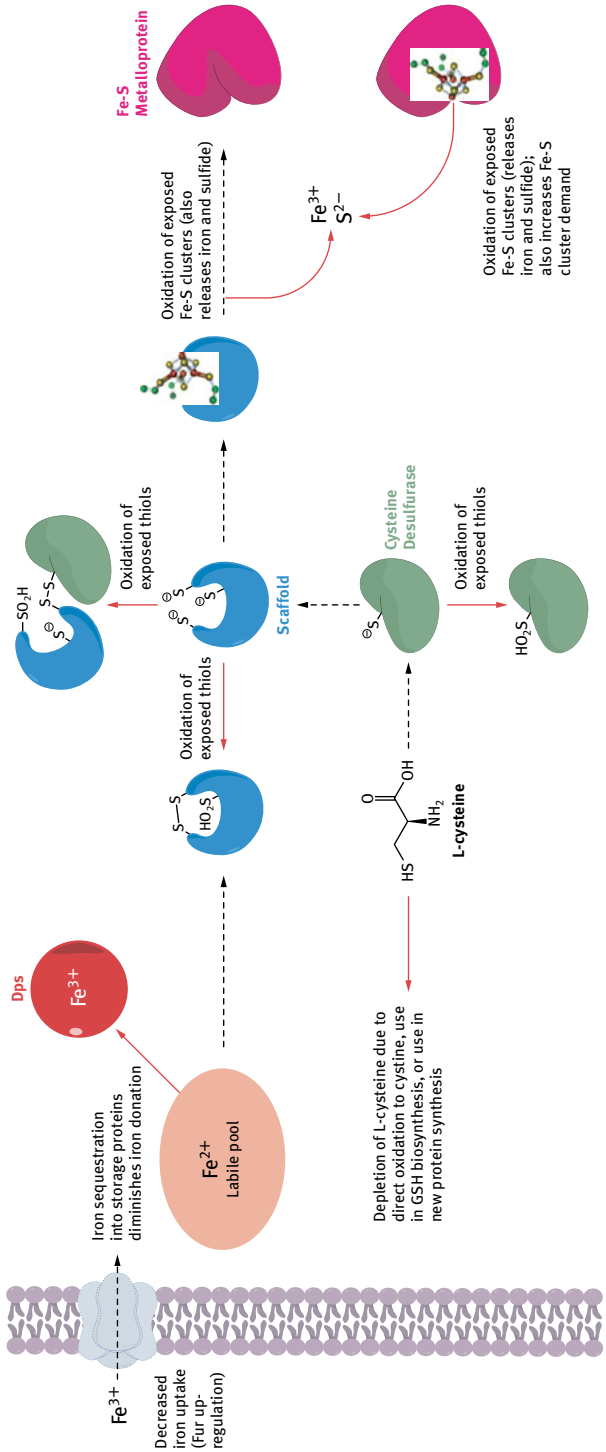

Fig. 3.2: Effects of oxidative stress on Fe-S cluster metabolism in *E. coli*, steps of iron or Fe-S homeostasis that may be perturbed by oxidative stress are indicated by dashed arrows. Reactions/processes that occur in response to stress and disrupt iron or Fe-S homeostasis are indicated by red arrows.

iron, and under iron-replete conditions Fe^{2+}-Fur represses the transcription of genes that encode iron starvation stress response proteins (such as siderophore biosynthesis systems, iron uptake transporters, and non-iron alternative enzymes) [87, 89]. As cellular Fe^{2+} levels drop, apo-Fur dissociates from its binding site at target promoters and thereby allows RNA polymerase access to initiate transcription. For example, Fe^{2+}-Fur represses *suf* transcription when cellular iron levels are adequate, but this repression is abolished under iron starvation conditions [90, 91]. Fur also indirectly regulates many mRNA transcripts in *E. coli* by repressing the transcription of the RyhB small RNA under iron-replete conditions [92–94]. Under low iron conditions, the RyhB small RNA is expressed and binds to target mRNAs to regulate their stability or translation. For example, when RyhB is expressed, the small RNA binds to the *isc* mRNA and promotes RnaseE-mediated degradation of *isc* transcript under iron starvation conditions (Fig. 3.3).

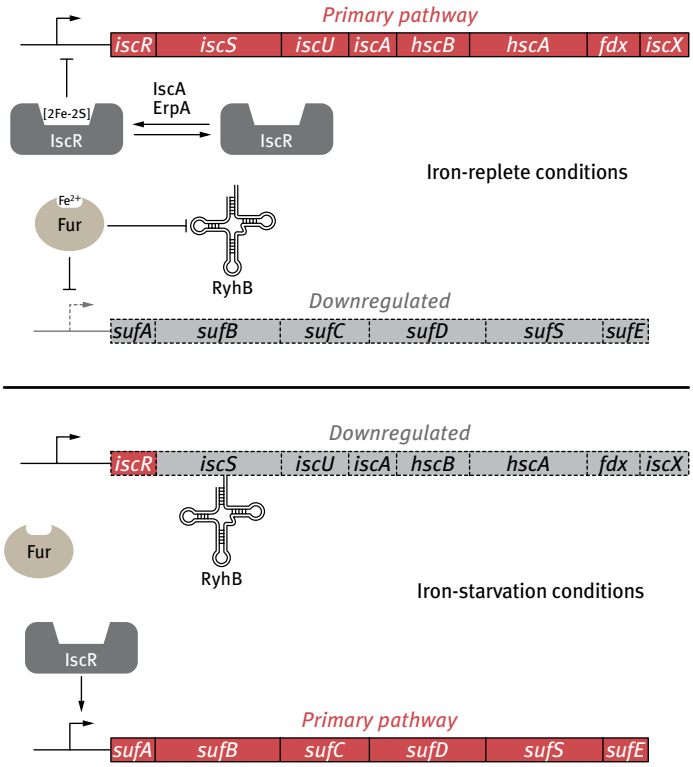

Fig. 3.3: Iron-dependent regulation of *isc* and *suf* operons in *E. coli*. Gray dashed boxes indicate transcriptional or post-transcriptional downregulation of mRNA. Red boxes indicate increased expression of mRNA. RyhB interacts with the *iscS* region of the polycistronic *isc* mRNA and does not appear to decrease *iscR* expression.

Deletion of Fur leads to a decrease of total cellular iron (due to the reduced expression of some iron storage proteins) but causes an increase in the labile pool of iron due to increased iron uptake and decreased iron utilization by iron metalloproteins. The increase in labile iron causes increased sensitivity to hydrogen peroxide (H_2O_2) and other ROS that react with Fe^{2+} *via* the Fenton reaction [78, 95, 96]. It has also been shown that *fur* expression is upregulated in response to H_2O_2 induction *via* the OxyR transcriptional activator that senses peroxide stress. Increased Fur expression helps to replace Fur protein damaged by ROS [97] and allows Fur to both sequester labile iron released from damaged iron metalloproteins and to tightly repress any further iron uptake during the oxidative stress.

These complex regulatory loops show that iron starvation and oxidative stress responses are intimately intertwined in *E. coli*. Both conditions result in disruption of iron metabolism and *de facto* iron limitation for iron cofactor biosynthesis *in vivo*. In the case of oxidative stress, iron limitation occurs due to increased iron demand to replace damaged iron enzymes, decreased iron uptake due to Fur upregulation, and increased iron sequestration in iron storage proteins (such as Dps and Bfr, see Section 3.8.2) (Fig. 3.2). *E. coli* attempts to circumvent iron limitation by expressing non-iron alternative enzymes and by decreasing production of non-essential iron metalloproteins. However, as noted above, there are at least a handful of iron-dependent enzymes that cannot be replaced and their maturation must be maintained for cell survival.

3.6 Stress-response Fe-S cluster biogenesis in *E. coli*

Oxygen-dependent disruption of Fe-S cluster metabolism has selected for the evolution of Fe-S cluster biogenesis pathways that are able to maintain cluster biogenesis under stress. The most well-studied example of a stress-response Fe-S biogenesis pathway is the Suf system found in many facultative anaerobes among the Gammaproteobacteria, such as *E. coli*. The Suf pathway is broadly distributed among Archaea and Bacteria, where it is often the primary housekeeping pathway for cluster biogenesis (see Chapter 1, volume 2 by Dos Santos and Dean for more discussion of housekeeping Suf systems in Gram-positive Bacteria) [98]. However, in some Bacteria, and in a limited set of Eukaryotes, Suf appears to have taken on the role of either a stress-response system or an organelle-specific system for Fe-S cluster biogenesis (for Eukaryotic Suf systems, note the role of Suf in some plant chloroplasts as described in Chapter 16, volume 2 by Ye). In those cases, Suf augments other housekeeping cluster biogenesis pathways (typically the Isc pathway, see Chapter 4, volume 2) and is a *bona fide* stress-response system for maintaining Fe-S cluster biogenesis under a variety of stress conditions.

E. coli switches between the Isc and the Suf systems based on environmental conditions using multiple transcriptional and post-transcriptional regulatory mechanisms (Fig. 3.3). Transcription of the *iscRSUA-hscBA-fdx-iscX* operon is controlled by the IscR metalloregulatory protein (for a comprehensive description of IscR, see

Chapter 4, volume 2 by Mettert *et al.*) [99]. Briefly, IscR regulates global Fe-S metabolism in response to Fe-S cluster demand [71, 100–102]. IscR itself binds a [2Fe-2S] cluster and holo-IscR represses *isc* transcription. As Fe-S cluster demand exceeds the ability of the biogenesis machinery to load the [2Fe-2S] cluster into IscR, the apo-IscR predominates, leading to increased *isc* transcription. Interestingly, apo-IscR is not inactive. Instead, loss of the Fe-S cluster allows apo-IscR to acquire a new set of target promoters for which it activates transcription [101, 103]. Although *isc* transcription is generally responsive to a certain window of Fe-S cluster demand, under severe iron limitation, the *isc* mRNA is selectively degraded by RNaseE due to the action of the RyhB small RNA regulator (Fig. 3.3) [104]. Under such conditions, the cell begins to utilize the Suf pathway for Fe-S cluster biogenesis while minimizing its reliance on Isc.

Transcription of the *sufABCDSE* operon is increased under iron starvation stress *via* two mechanisms. First, the *suf* promoter is activated by apo-IscR, which will predominate when iron is limiting for Fe-S cluster biogenesis [101, 103]. Second, under iron-replete conditions, the transcription of *suf* is repressed by Fe^{2+}-Fur, an iron metalloregulatory protein (Fig. 3.3) [90, 91]. During iron starvation, Fe^{2+}-Fur repression is abolished, allowing *suf* transcription to increase. Transcription of *suf* also increases under oxidative stress by the concerted efforts of the OxyR peroxide stress response regulator and integration host factor (IHF) as well as through separate activation by apo-IscR [90, 105]. Due to this complex regulation, *suf* transcription should generally increase under any stress condition in which iron or Fe-S metabolism is disrupted, including iron limitation and oxidative stress.

The reciprocal regulation of Isc and Suf is also reflected in their respective mutant phenotypes [41, 62, 63, 90, 98, 106–110]. Although deletion of the *isc* locus causes a general defect in Fe-S cluster biogenesis under normal conditions, increased expression of *suf* is able to compensate for the lack of Isc function. Similarly, deletion of the *suf* operon has little effect on Fe-S cluster biogenesis under normal growth conditions, but the *suf* mutants are sensitive to stresses that disrupt Fe-S metabolism. The alternate regulation and phenotypes associated with Isc and Suf raises the question of what are the specific adaptations of the Suf pathway in organisms such as *E. coli* that allow it to maintain Fe-S cluster biogenesis when the housekeeping Isc pathway is compromised?

3.7 Sulfur trafficking in the stress-response Suf pathway

SufS is the cysteine desulfurase that mobilizes sulfur from L-cysteine during Fe-S cluster biogenesis. This pyridoxal-5′-phospate (PLP) dependent reaction results in an enzyme bound persulfide (R-S-SH) species on Cys364 of SufS. The steady-state activity of SufS is many-fold lower than that of the IscS cysteine desulfurase used by the Isc pathway. Comparison of the structures of the two provides a partial explanation for this difference (Fig. 3.4). Both cysteine desulfurases are homodimers with PLP binding sites located in the vicinity of the active site Cys residues used for sulfur abstraction

from L-cysteine substrate. The active site Cys328 residue of IscS is on a flexible, solvent exposed loop. In most *E. coli* IscS structures, the active site loop is disordered and cannot be resolved. Figure 3.4 shows the *A. fulgidus* IscS co-crystallized with IscU, which has a well-defined active site loop containing Cys321 (analogous to Cys328). In contrast, the SufS active site loop is largely covered by a "lid" structure provided by the neighboring SufS monomer (Fig. 3.4). The active site lid restricts solvent access to SufS Cys364, and this important structural element is not present in IscS (Fig. 3.4). Cysteine desulfurase enzyme turnover requires release of the persulfide from the active site Cys residue, which depends on the ability of a reductant (usually DTT or TCEP *in vitro* or a partner protein thiol *in vivo*) to gain access to the persulfide species in the active site.

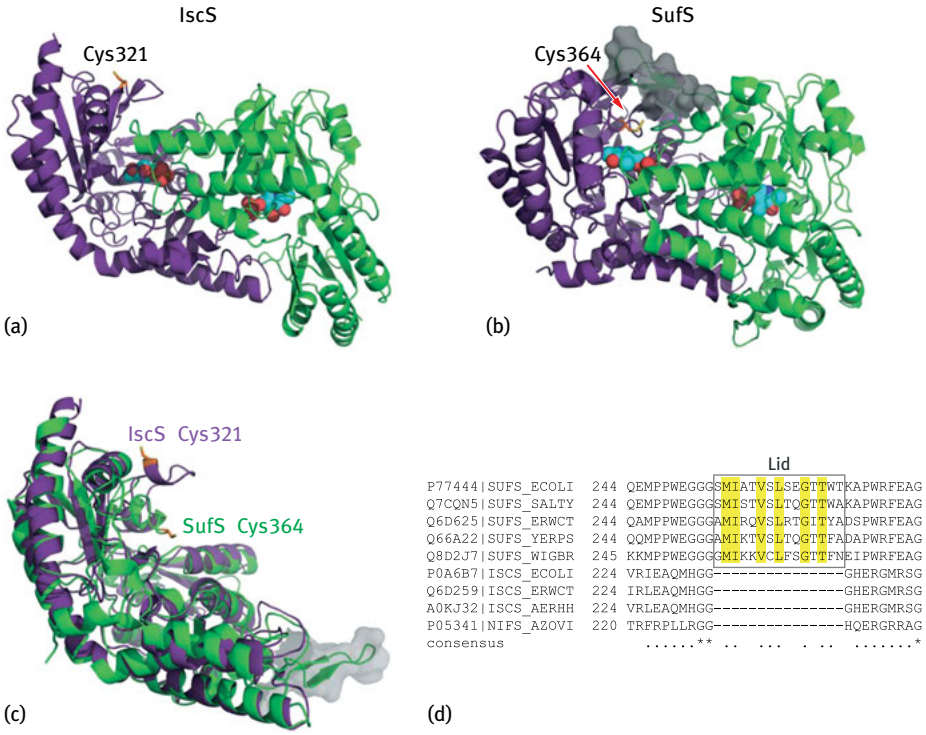

Fig. 3.4: Comparison of IscS and SufS cysteine desulfurases. (a) *A. fulgidus* IscS homodimer with one monomer in green and one in violet (taken from IscU-IscS co-structure in PDB 4EB5). Active Cys321 is shown in orange with PLP cofactor in cyan. (b) *E. coli* SufS homodimer with one monomer in green and one in violet (take from PDB 1KMJ) [111]. Active Cys364 is shown in orange with PLP cofactor in cyan. Active site "lid" structure highlighted in surface representation (transparent gray). (c) FATCAT structural alignment of IscS (violet) and SufS (green) monomers from A and B [112]. Active site Cys residues are in orange. PLP is not shown and IscU is omitted for comparison of IscS and SufS structures. (d) Partial amino acid alignment of select cysteine desulfurases generated by FASTA. The lid region conserved in SufS family members is boxed with highly conserved residues highlighted in yellow.

The structural lid over the SufS active site limits access of reductants to the Cys364 persulfide and results in low steady-state activity of SufS compared with IscS [113–119]. At present, it is not clear if the rate at which SufS forms the enzyme persulfide is actually slower than IscS as direct quantitative comparisons have not been done between the two enzymes under pre-steady-state conditions. Possibly SufS reacts quickly to form the persulfide but then turns over at a much slower rate than IscS in the *in vitro* assays due to the failure to release persulfide [113].

Is there an advantage to this structural limitation of SufS? Recently, we determined that SufS Cys364 is more resistant to direct oxidation by H_2O_2 compared with IscS Cys328, indicating that the active site lid may prevent disruption of sulfur mobilization by SufS in the presence of hydrogen peroxide [120]. These experiments had to be conducted in the absence of strong reductants such as DTT to prevent "repair" of partially oxidized Cys residues. As one might imagine, DTT and TCEP are not the physiological reductants for the persulfides on IscS or SufS *in vivo*. In both cases, the persulfide species is released from the cysteine desulfurase enzyme by the nucleophilic attack of a thiol residue from a specific partner protein. For IscS, the Fe-S scaffold protein IscU is the partner protein that accepts the persulfide. The *E. coli* Suf system lacks a true IscU homologue (in contrast to Gram-positive Bacteria, as discussed in Chapter 5, volume 2 by Dos Santos) but SufS does interact with the SufE protein.

Although there is poor sequence conservation between the two proteins, SufE is structurally similar to IscU [121]. In contrast to IscU, there is no evidence that SufE can act as an Fe-S cluster scaffold because it lacks two of the three conserved Cys residues used by IscU to coordinate its cluster. Instead, SufE has a single conserved Cys residue at position 51 (analogous to IscU Cys63) that is used to accept sulfur from SufS. As a result, addition of SufE to the SufS activity assay results in a dramatic enhancement of basal SufS activity such that it reaches the level of IscS [116, 117, 122]. Addition of IscU can also mildly enhance IscS activity *in vitro* but only if the strong chemical reductants (DTT, TCEP) are omitted from the reaction until it is quenched. If the reductants are present during the reaction, they apparently release IscS persulfide much more efficiently than IscU such that activity enhancement by IscU is not observed [120].

Although the SufE Cys51 residue is on a loop structure near the surface of SufE, the Cys51 side chain is actually oriented into a protected groove in the SufE structure (Fig. 3.5) [121]. The groove is lined with hydrophobic residues and has limited solvent exposure. SufE Cys51 can be oxidized by H_2O_2 but is much less sensitive to oxidation than IscU Cys63, which is part of a more extended and exposed Fe-S cluster-binding site in IscU [120]. Recently, a co-structure was solved containing two close homologues of SufS and SufE, named CsdA and CsdE, respectively, which were identified in a third bacterial cysteine desulfurase system known as the Csd (cysteine sulfinate desulfinase) system (Fig. 3.5) [123]. These proteins catalyze a cysteine desulfurase reaction, but the resulting persulfide appears to be donated to a partner protein known as CsdL for the synthesis of an unknown sulfur-containing metabolite or protein [124]. However, the co-structure of CsdA-CsdE is illuminating. In the structure, the SufE

homologue CsdE has adopted a confirmation in which the active site Cys residue that accepts persulfide sulfur is flipped out of its groove on the CsdE surface and is extended into the active site of the cysteine desulfurase CsdA [123]. Apparently protein-protein interactions between CsdA and CsdE trigger this conformational change to facilitate sulfur transfer from the desulfurase to the acceptor proteins (Fig. 3.5). One would assume that SufE undergoes a similar conformational change upon interacting with SufS. In fact, using hydrogen deuterium exchange mass spectrometry, we have observed changes in solvent accessibility around SufE Cys51 when it interacts with SufS [125].

Does the presence of the partner proteins alter the sensitivity of SufS or IscS to oxidative stress? We determined that addition of IscU to IscS actually made IscS activity more sensitive to disruption by oxidative stress [120]. In contrast, SufS activity was still enhanced in the presence of SufE and was not sensitive to H_2O_2 exposure. SufS-SufE maintained a higher level of absolute activity than IscS or IscS-IscU over the entire range of H_2O_2 concentrations tested (ranging from low to mid micromolar concentrations). When we measured the level of Cys oxidation at the active site Cys residues of each protein after H_2O_2 exposure, we observed that IscU was readily oxidized at its active site Cys63 and Cys106 residues and formed mixed disulfide species with Cys328 of IscS. In contrast, we observed little oxidation of SufS Cys364 and only mild oxidation of SufE Cys51 in response to H_2O_2 exposure. Thus, it appears that the Isc sulfur transfer pathway is inherently more sensitive to oxidative stress than the Suf pathway, providing a partial rationale for the cell to utilize Suf under oxidative stress conditions.

In addition to their differential sensitivity to oxidation, SufS-SufE and IscS-IscU also show differences in their relative activity levels under low L-cysteine concentrations [120]. SufS-SufE are up to 6-fold more active at low L-cysteine concentrations

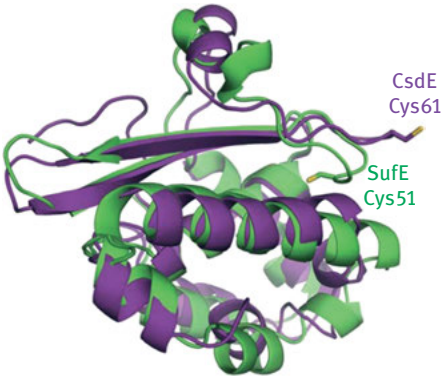

Fig. 3.5: Comparison of resting and active SufE/CsdE sulfur transfer shuttles. CsdE from co-structure with CsdA (PDB 4LW4) is shown in purple with active site Cys61 in stick representation [123]. SufE (PDB 1MZG) is shown in green with active site Cys51 in stick representation [121]. Structures were aligned using FATCAT [112].

than IscS-IscU. The greater ability of Suf to maintain sulfide mobilization under low L-cysteine conditions may have *in vivo* relevance. Under oxidative stress, cellular L-cysteine pools may become transiently depleted as L-cysteine is used for GSH synthesis or to replace damaged thiols in oxidized proteins. Recently, it was also shown that L-cysteine biosynthesis is downregulated under iron starvation stress by RyhB to divert L-serine for siderophore production [126]. L-Serine is a common intermediate in both L-cysteine and enterobactin biosynthesis pathways. Thus, Suf may be better adapted than Isc to acquire sulfide under stress conditions in which the L-cysteine substrate is limiting (Fig. 3.2).

3.8 Stress-responsive iron donation for the Suf pathway

The complexity of *in vivo* iron homeostasis poses a significant challenge for understanding iron trafficking to Fe-S cluster biogenesis pathways. Iron is a required nutrient in *E. coli* (with total cellular iron content typically in the hundreds of micromolar range depending on environmental iron levels) [127]. Identification of an *in vivo* iron donor for Suf is complicated by a number of obstacles. Confirming a role for an iron donor *in vitro* is difficult because scaffold proteins can easily incorporate weakly chelated iron into nascent clusters. Any passive source of iron ions will "donate" iron to cluster assembly *in vitro*, making it difficult to evaluate the physiological significance of previous studies [27, 31, 128, 129]. Based on the role of Suf during iron starvation and oxidative stress conditions that disrupt iron homeostasis, it is reasonable to posit that *E. coli* Suf must acquire iron from a protected source that is resistant to these stresses. At present, the *in vivo* iron donation process is still under study. Here we will summarize the likely suspects for Suf iron donation and discuss the evidence for and against their role in iron trafficking to the Suf pathway.

3.8.1 SufD

The SufB, SufC, and SufD proteins are localized in the cytoplasm and interact as a stable $SufBC_2D$ complex (Fig. 3.6) [58, 116, 130–134]. The $SufBC_2D$ complex forms a novel Fe-S scaffold upon which iron and sulfide assemble into a stable cluster prior to transfer to target Fe-S proteins [58, 134, 135]. SufB is the final destination of iron and the site of cluster assembly, SufC has intrinsic ATPase activity, and the role of SufD in cluster assembly is not fully characterized. SufD is homologous to SufB (26% identical, 45% similar over the C-terminal ~150 residues) and likely resulted from a gene duplication of SufB. However, SufD does not appear to coordinate an Fe-S cluster on its own. $SufB_2C_2$ and $SufC_2D_2$ complexes have also been isolated, but the role of these sub-complexes has not been fully studied [59, 133, 133, 136]. We found that the absence of SufD diminishes *in vivo* iron incorporation into SufB with only a modest effect on

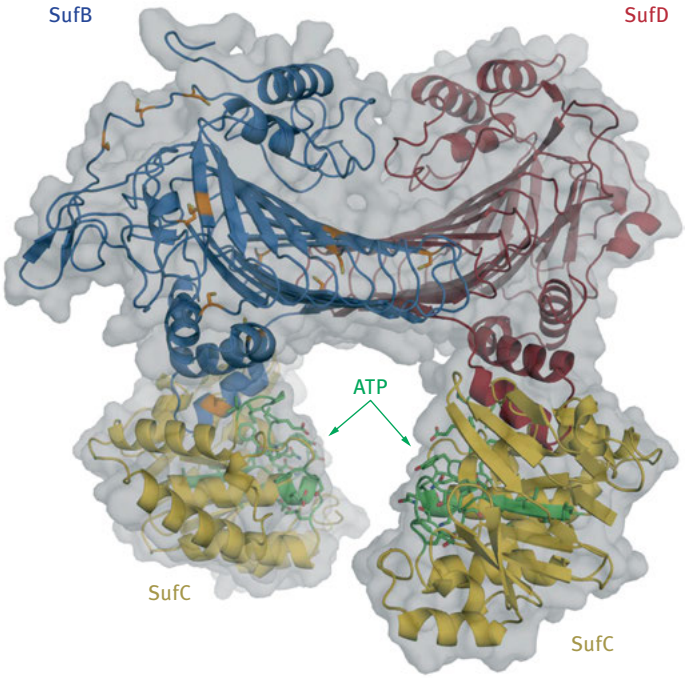

Fig. 3.6: Model structure of complete $SufBC_2D$ structure. SufB is in blue, SufD is in red, and SufC monomers are in yellow. ATP binding sites on SufC are highlighted in green in stick representations. All Cys residues in SufB are highlighted in orange in stick representations. Surface representation is in transparent gray. SufB was modeled onto one SufD subunit from the $SufC_2D_2$ complex (PDB 2ZU0) [130].

sulfide, suggesting that SufD may be required for iron acquisition [136]. A selective depletion of iron on SufB was also observed when SufC ATPase activity was altered by a point mutation that did not otherwise alter $SufBC_2D$ interactions. Based on these results, we proposed that SufC ATPase activity works in concert with SufD to facilitate iron delivery into the Suf pathway [136]. The iron donation step may require energy in the form of ATP hydrolysis to obtain iron and concentrate it for cluster assembly against an unfavorable concentration gradient.

The $SufBC_2D$ complex is isolated associated with 1 equiv. of $FADH_2$ per complex [134, 136]. All three proteins are required for the full binding of $FADH_2$ with a K_d for $FADH_2$ of 12 μM. Reduced flavins are very efficient ferric iron-reducing agents and $SufBC_2D$-$FADH_2$ was shown to mobilize iron from ferric citrate and the iron-bound bacterial frataxin CyaY, presumably *via* a reductive mechanism [134]. It was proposed that $SufBC_2D$ uses $FADH_2$ as a redox cofactor to mobilize iron for the Suf pathway although the *in vivo* iron donor remains unclear. CyaY does not appear to play a direct role in Suf mediated Fe-S cluster biogenesis and is instead closely linked to the Isc system (W. Outten, unpublished results) [137–139].

3.8.2 Iron storage proteins

E. coli contains four potential iron storage proteins that could release iron for Suf cluster assembly: ferritin A (FtnA), ferritin B (FtnB), heme-binding bacterioferritin (Bfr), and "DNA-binding protein from starved cells" (Dps) [140]. FtnA, Bfr, and Dps form multisubunit protein shells that oxidize Fe^{2+} to Fe^{3+} to store iron as ferric hydroxide cores. Stored iron must be reduced to Fe^{2+} for iron to be mobilized for cell use. Bfr and FtnA are similar, and each forms a 12-faced polyhedron structure consisting of 24 subunits. Both proteins also have a similar ferroxidase center that utilizes O_2 to catalyze ferrous iron oxidation during storage. One key difference between FtnA and Bfr is that Bfr incorporates twelve inter-subunit heme groups that are not present in FtnA [141–143]. Kinetic profiles of iron release from *E. coli* and *A. vinelandii* Bfr indicate that heme increases iron release by 2- to 4-fold using $FMNH_2$ as the reductant [144]. It is not clear if FtnB is functionally similar to the other ferritins because it lacks the residues critical for ferroxidase activity and those residues important for multimeric protein assembly [145]. However, a role for FtnB in some step of Fe-S cluster repair was observed in *Salmonella* [146].

In contrast to FtnA, and Bfr, Dps quaternary structure only consists of 12 subunits, leading to a smaller overall capacity for iron storage (approximately 500 iron atoms compared with 4,500 iron atoms). Dps also contains a novel ferroxidase center that utilizes H_2O_2 to oxidize Fe^{2+} in a controlled reaction that produces H_2O rather than hydroxyl radicals (in contrast to the Fenton reaction) [147–149]. Dps also has the additional ability to bind to DNA, possibly to protect DNA from Fenton chemistry through its iron sequestration and H_2O_2 reduction activities [150]. Dps is highly regulated in response to oxidative stress as well as during stationary phase in *E. coli* [151, 152]. At present, it is not clear if iron stored in Dps can be directly used as an iron source for metallocofactor assembly or if Dps is exclusively an iron detoxification system. However, its co-regulation with the Suf pathway under oxidative stress suggests it could serve as an iron source for that pathway.

In *E. coli*, transcription of both *bfr* and *ftnA* increases under iron-replete conditions [153]. For *bfr,* it is not entirely clear how this regulation occurs, although it may be a target of the small RNA RyhB [94]. In the case of *ftnA*, this regulation is mediated through a complex regulatory mechanism whereby Fe^{2+}-Fur binds upstream of the *ftnA* promoter and blocks H-NS repression of *ftnA* [154]. By relieving H-NS repression of *ftnA*, Fe^{2+}-Fur indirectly activates *ftnA* transcription under high iron conditions. Consequently, FtnA stores up to 50% of total cellular iron under iron-sufficient growth conditions, with the majority of *ftnA* expression occurring during the post-exponential phase of growth [155]. In contrast, Bfr accounts for only 1% of total cellular iron under iron-replete conditions in *E. coli*. However, when cells are grown under more moderate iron levels (6 μM in minimal media), the relationship between Bfr and FtnA changes. Under low to moderate iron conditions, Bfr accounts for approximately 14% of protein-bound iron, whereas FtnA accounts for only 5% [156]. Thus, it appears

that FtnA is primarily a storage protein for conditions of iron excess, whereas Bfr may be preferentially used for iron storage in growth conditions with low to moderate iron availability. Bfr expression is also controlled by the nutrient starvation regulator RpoS, such that it is likely to be more highly expressed in stationary or lag phase growth conditions.

The complex regulation of FtnA and Bfr complicates the interpretation of their physiological roles in iron trafficking. However, genetic evidence indirectly links the Suf pathway to Bfr in the Gram-negative plant pathogen *Erwinia chrysanthemi* [157]. In *E. chrysanthemi* strains lacking the *sufC* gene, iron release from Bfr is somehow impaired leading to iron accumulation in Bfr. In contrast, deletions of *sufA*, *sufB*, *sufD*, *sufS*, or *sufE* reduced the amount of iron loaded into Bfr *in vivo*. The results suggest that the Suf proteins directly or indirectly influence iron cycling through Bfr. Because of these phenotypes, it is tempting to speculate that Suf directly acquires iron from Bfr or another iron storage protein to bypass the labile iron pool. A dedicated iron trafficking pathway from storage proteins to Suf could be advantageous under iron starvation and oxidative stress conditions in which the labile pool of iron will be diminished.

3.8.3 Other candidates

YtfE contains a di-iron center and plays a role in *in vivo* Fe-S cluster repair after nitrosative and oxidative stresses. Deletion of *ytfE* caused defects in Fe-S enzyme activity in *E. coli*. Addition of holo-YtfE to cell lysates promoted the repair of the [4Fe-4S] clusters of fumarase and aconitase. The results suggest YtfE donates iron for the repair of damaged [4Fe-4S] clusters *in vivo* [158–162]. To date, no results have been published indicating a direct relationship between Suf and YtfE.

YggX (*yggX*) and GSH contribute in an overlapping manner to the maintenance of labile iron homeostasis in *Salmonella enterica* [139, 163–165]. YggX is a small soluble protein that is regulated in response to oxidative stress [166]. Deletion of *yggX* in *E. coli* or *S. enterica* leads to specific defects in iron and Fe-S cluster metabolism [163, 164, 166]. It was hypothesized that YggX may be an intracellular iron chaperone; however, subsequent studies suggest YggX cannot bind iron *in vitro* [163, 167]. It is clear that YggX plays some role in Fe-S metabolism, but the exact function of YggX in this process is not known. GSH is present at millimolar levels in the cell and is considered the main cellular reductant. GSH can chelate metals as well as reduce ferric iron and has been proposed as an iron chelator. It was also proposed that GSH facilitates binding of iron by Fur [165]. A *gshA* deletion mutant that is unable to synthesize GSH showed sensitivity to H_2O_2 and impairment of Fe-S cluster repair [165]. The phenotype of a *gshA* deletion is aggravated when combined with the *yggX* gene deletion. An *yggX gshA* double-deletion mutant strain showed enhanced sensitivity

to streptonigrin and further increased sensitivity to H_2O_2 [165]. These results suggest that the pool of iron available for participation in Fenton chemistry increased. Interestingly, the *yggX gshA cyaY* triple mutant strain has a strong phenotype, with increased nutritional auxotrophies and decreased activity of iron-containing and Fe-S enzymes [139]. At present, it is not clear if YggX (and GSH) are directly important for iron trafficking or if their effects on Fe-S cluster metabolism are indirectly caused by increased oxidative stress.

3.9 Unanswered questions about Suf and Isc roles in *E. coli*

There is growing evidence that Suf mobilization of iron and sulfide is more robust than Isc under stress conditions. However, there are other steps of cluster biogenesis where Suf and Isc may diverge in function. The inherent flexibility of the IscU scaffold protein likely renders it sensitive to disruption, especially by oxidation of exposed thiol ligands. It is possible that SufB and IscU are not equally sensitive to stress. SufB does not appear to catalyze cluster assembly *via* a stable $[2Fe\text{-}2S]^{2+}$ intermediate as observed for IscU, although $[4Fe\text{-}4S]^{2+}$ SufB can by converted into the $[2Fe\text{-}2S]^{2+}$ form by air exposure [135, 136]. Interestingly, SufB contains some linear [3Fe-4S] cluster (in addition to $[4Fe\text{-}4S]^{2+}$) after *in vivo* expression with SufCDSE [136]. The linear [3Fe-4S] cluster may represent a cluster intermediate or a cluster degradation product. Regardless, it is easily convertible back to the $[4Fe\text{-}4S]^{2+}$ form by the addition of iron and one electron [168, 169]. Possibly, the ability to stabilize this particular cluster type provides some advantage under oxidative stress conditions.

The Fe-S cluster trafficking steps may also be sensitive to disruption, but here, there is less divergence between Suf and Isc. Both pathways encode an ATC protein (SufA and IscA) that appear to overlap considerably in their *in vivo* function and *in vitro* biochemical characteristics [61, 62, 109, 170–172]. Although the downstream targets of the ATC proteins are likely to be specific for each ATC, the ATCs seem to share some ability to interact with both SufB and IscU scaffolds. Monothiol glutaredoxins may be used for Suf stress-responsive cluster trafficking, but the ability of the Grx4 to interface with Suf and Isc has not been carefully compared [173, 174]. It is likely that Suf and Isc differentially interact with currently uncharacterized pieces of the Fe-S cluster metabolism machinery *in vivo*. Future work in this field should help delineate the complex relationship between housekeeping and stress-responsive Fe-S cluster biogenesis.

Acknowledgment

Work in the laboratory of F. Wayne Outten was supported by NIH GM 81706.

References

[1] Dupont CL, Butcher A, Valas RE, Bourne PE, Caetano-Anolles G. History of biological metal utilization inferred through phylogenomic analysis of protein structures. Proc Natl Acad Sci USA 2010;107:10567–72.

[2] Meyer J. Iron-sulfur protein folds, iron-sulfur chemistry, and evolution. J Biol Inorg Chem 2008;13:157–70.

[3] Hagen KS, Reynolds JG, Holm RH. Definition of reaction sequences resulting in self-assembly of $[Fe_4S_4(Sr)4]^{2-}$ clusters from simple reactants. J Am Chem Soc 1981;103:4054–63.

[4] Hagen KS, Watson AD, Holm RH. Synthetic routes to Fe_2S_2, Fe_3S_4, Fe_4S_4, and Fe_6S_9 clusters from the common precursor $[Fe(Sc_2H_5)4]^{2-}$ – structures and properties of $[Fe_3S_4(Sr)4]^{3-}$ and $[Fe_6S_9(Sc_2H_5)2]^{4-}$, examples of the newest types of Fe-S-Sr Clusters. J Am Chem Soc 1983;105:3905–13.

[5] Beinert H, Holm RH, Munck E. Iron-sulfur clusters: nature's modular, multipurpose structures. Science 1997;277:653–9.

[6] Venkateswara Rao P, Holm RH. Synthetic analogues of the active sites of iron-sulfur proteins. Chem Rev 2004;104:527–59.

[7] Liu Y, Beer LL, Whitman WB. Methanogens: a window into ancient sulfur metabolism. Trends Microbiol 2012.

[8] Yang J, Bitoun JP, Ding H. Interplay of IscA and IscU in biogenesis of iron-sulfur clusters. J Biol Chem 2006;281:27956–63.

[9] Dai Z, Tonelli M, Markley JL. Metamorphic protein IscU changes conformation by cis-trans isomerizations of two peptidyl-prolyl peptide bonds. Biochemistry 2012;51:9595–602.

[10] Kim JH, Tonelli M, Kim T, Markley JL. Three-dimensional structure and determinants of stability of the iron-sulfur cluster scaffold protein IscU from Escherichia coli. Biochemistry 2012;51:5557–63.

[11] Kim JH, Tonelli M, Markley JL. Disordered form of the scaffold protein IscU is the substrate for iron-sulfur cluster assembly on cysteine desulfurase. Proc Natl Acad Sci USA 2012;109:454–9.

[12] Anbar AD. Oceans elements and evolution. Science 2008;322:1481–3.

[13] Anbar AD, Knoll AH. Proterozoic ocean chemistry and evolution: a bioinorganic bridge? Science 2002;297:1137–42.

[14] Kim KM, Qin T, Jiang YY, et al. Protein domain structure uncovers the origin of aerobic metabolism and the rise of planetary oxygen. Structure 2012;20:67–76.

[15] Zheng L, White RH, Cash VL, Dean DR. Mechanism for the desulfurization of L-cysteine catalyzed by the nifS gene product. Biochemistry 1994;33:4714–20.

[16] Zheng L, White RH, Cash VL, Jack RF, Dean DR. Cysteine desulfurase activity indicates a role for NIFS in metallocluster biosynthesis. Proc Natl Acad Sci USA 1993;90:2754–8.

[17] Kim JH, Frederick RO, Reinen NM, Troupis AT, Markley JL. [2Fe-2S]-ferredoxin binds directly to cysteine desulfurase and supplies an electron for iron-sulfur cluster assembly but is displaced by the scaffold protein or bacterial frataxin. J Am Chem Soc 2013;135:8117–20.

[18] Yan R, Konarev PV, Iannuzzi C, et al. Ferredoxin competes with bacterial frataxin in binding to the desulfurase IscS. J Biol Chem 2013;288:24777–87.

[19] Marinoni EN, de Oliveira JS, Nicolet Y, et al. (IscS-IscU)2 complex structures provide insights into Fe_2S_2 biogenesis and transfer. Angew Chem Int Ed Engl 2012;51:5439–42.

[20] Adinolfi S, Rizzo F, Masino L, et al. Bacterial IscU is a well folded and functional single domain protein. Eur J Biochem 2004;271:2093–100.

[21] Nuth M, Yoon T, Cowan JA. Iron-sulfur cluster biosynthesis: characterization of iron nucleation sites for assembly of the $[2Fe\text{-}2S]^{2+}$ cluster core in IscU proteins. J Am Chem Soc 2002;124:8774–5.

[22] Smith AD, Agar JN, Johnson KA, et al. Sulfur transfer from IscS to IscU: the first step in iron-sulfur cluster biosynthesis. J Am Chem Soc 2001;123:11103–4.

[23] Lin SJ, Pufahl RA, Dancis A, O'Halloran TV, Culotta VC. A role for the Saccharomyces cerevisiae ATX1 gene in copper trafficking and iron transport. J Biol Chem 1997;272:9215–20.
[24] Pufahl RA, Singer CP, Peariso KL, et al. Metal ion chaperone function of the soluble Cu(I) receptor Atx1. Science 1997;278:853–6.
[25] Robinson NJ, Winge DR. Copper metallochaperones. Annu Rev Biochem 2010;79:537–62.
[26] Bou-Abdallah F, Adinolfi S, Pastore A, Laue TM, Dennis Chasteen N. Iron binding and oxidation kinetics in frataxin CyaY of Escherichia coli. J Mol Biol 2004;341:605–15.
[27] Banci L, Bertini I, Ciofi-Baffoni S, et al. Human Sco1 functional studies and pathological implications of the P174L mutant. Proc Natl Acad Sci USA 2007;104:15–20.
[28] Changela A, Chen K, Xue Y, et al. Molecular basis of metal-ion selectivity and zeptomolar sensitivity by CueR. Science 2003;301:1383–7.
[29] Nair M, Adinolfi S, Pastore C, Kelly G, Temussi P, Pastore A. Solution structure of the bacterial frataxin ortholog, CyaY: mapping the iron binding sites. Structure 2004;12:2037–48.
[30] Layer G, Ollagnier de Choudens S, Sanakis Y, Fontecave M. Iron-sulfur cluster biosynthesis: characterization of Escherichia coli CyaY as an iron donor for the assembly of [2Fe-2S] clusters in the scaffold IscU. J Biol Chem 2006;281:16256–63.
[31] Adinolfi S, Iannuzzi C, Prischi F, et al. Bacterial frataxin CyaY is the gatekeeper of iron-sulfur cluster formation catalyzed by IscS. Nat Struct Mol Biol 2009;16:390–6.
[32] Prischi F, Konarev PV, Iannuzzi C, et al. Structural bases for the interaction of frataxin with the central components of iron-sulphur cluster assembly. Nat Commun 2010;1:95.
[33] Iannuzzi C, Adinolfi S, Howes BD, et al. The role of CyaY in iron sulfur cluster assembly on the E. coli IscU scaffold protein. PLoS One 2011;6:e21992.
[34] Bridwell-Rabb J, Iannuzzi C, Pastore A, Barondeau DP. Effector role reversal during evolution: the case of frataxin in Fe-S cluster biosynthesis. Biochemistry 2012;51:2506–14.
[35] Leidgens S, Bullough KZ, Shi H, et al. Each member of the poly-r(C)-binding protein 1 (PCBP) family exhibits iron chaperone activity toward ferritin. J Biol Chem 2013;288:17791–802.
[36] Nandal A, Ruiz JC, Subramanian P, et al. Activation of the HIF prolyl hydroxylase by the iron chaperones PCBP1 and PCBP2. Cell Metab 2011;14:647–57.
[37] Shi H, Bencze KZ, Stemmler TL, Philpott CC. A cytosolic iron chaperone that delivers iron to ferritin. Science 2008;320:1207–10.
[38] Rae TD, Schmidt PJ, Pufahl RA, Culotta VC, O'Halloran TV. Undetectable intracellular free copper: the requirement of a copper chaperone for superoxide dismutase. Science 1999;284:805–8.
[39] Rae TD, Schmidt PJ, Pufahl RA, Culotta VC, O'Halloran TV. The function of the copper chaperone for Cu,Zn-superoxide dismutase implies a negligible concentration of intracellular free copper. J Inorg Biochem 1999;74:271.
[40] Macomber L, Imlay JA. The iron-sulfur clusters of dehydratases are primary intracellular targets of copper toxicity. Proc Natl Acad Sci USA 2009;106:8344–9.
[41] Chillappagari S, Seubert A, Trip H, Kuipers OP, Marahiel MA, Miethke M. Copper stress affects iron homeostasis by destabilizing iron-sulfur cluster formation in Bacillus subtilis. J Bacteriol 2010;192:2512–24.
[42] Fu W, Jack RF, Morgan TV, Dean DR, Johnson MK. nifU gene product from Azotobacter vinelandii is a homodimer that contains two identical [2Fe-2S] clusters. Biochemistry 1994;33:13455–63.
[43] Agar JN, Krebs C, Frazzon J, Huynh BH, Dean DR, Johnson MK. IscU as a scaffold for iron-sulfur cluster biosynthesis: sequential assembly of [2Fe-2S] and [4Fe-4S] clusters in IscU. Biochemistry 2000;39:7856–62.
[44] Agar JN, Zheng L, Cash VL, Dean DR, Johnson MK. Role of the IscU Protein in Iron-Sulfur Cluster Biosynthesis: IscS-mediated Assembly of a 2Fe-2S Cluster in IscU. J Am Chem Soc 2000;122:2136–7.
[45] Yuvaniyama P, Agar JN, Cash VL, Johnson MK, Dean DR. NifS-directed assembly of a transient [2Fe-2S] cluster within the NifU protein. Proc Natl Acad Sci USA 2000;97:599–604.

[46] Smith AD, Jameson GN, Dos Santos PC, et al. NifS-mediated assembly of [4Fe-4S] clusters in the N- and C-terminal domains of the NifU scaffold protein. Biochemistry 2005;44:12955–69.
[47] Chandramouli K, Unciuleac MC, Naik S, Dean DR, Huynh BH, Johnson MK. Formation and properties of [4Fe-4S] clusters on the IscU scaffold protein. Biochemistry 2007;46:6804–11.
[48] Cupp-Vickery JR, Peterson JC, Ta DT, Vickery LE. Crystal structure of the molecular chaperone HscA substrate binding domain complexed with the IscU recognition peptide ELPPVKIHC. J Mol Biol 2004;342:1265–78.
[49] Silberg JJ, Tapley TL, Hoff KG, Vickery LE. Regulation of the HscA ATPase reaction cycle by the co-chaperone HscB and the iron-sulfur cluster assembly protein IscU. J Biol Chem 2004;279:53924–31.
[50] Chandramouli K, Johnson MK. HscA and HscB stimulate [2Fe-2S] cluster transfer from IscU to apoferredoxin in an ATP-dependent reaction. Biochemistry 2006;45:11087–95.
[51] Vickery LE, Cupp-Vickery JR. Molecular chaperones HscA/Ssq1 and HscB/Jac1 and their roles in iron-sulfur protein maturation. Crit Rev Biochem Mol Biol 2007;42:95–111.
[52] Bonomi F, Iametti S, Morleo A, Ta D, Vickery LE. Studies on the mechanism of catalysis of iron-sulfur cluster transfer from IscU[2Fe2S] by HscA/HscB chaperones. Biochemistry 2008;47:12795–801.
[53] Bonomi F, Iametti S, Morleo A, Ta D, Vickery LE. Facilitated transfer of IscU-[2Fe2S] clusters by chaperone-mediated ligand exchange. Biochemistry 2011;50:9641–50.
[54] Silberg JJ, Hoff KG, Tapley TL, Vickery LE. The Fe/S assembly protein IscU behaves as a substrate for the molecular chaperone Hsc66 from Escherichia coli. J Biol Chem 2001;276:1696–700.
[55] Silberg JJ, Vickery LE. Kinetic characterization of the ATPase cycle of the molecular chaperone Hsc66 from Escherichia coli. J Biol Chem 2000;275:7779–86.
[56] Unciuleac MC, Chandramouli K, Naik S, et al. In vitro activation of apo-aconitase using a [4Fe-4S] cluster-loaded form of the IscU [Fe-S] cluster scaffolding protein. Biochemistry 2007;46:6812–21.
[57] Chahal HK, Dai Y, Saini A, Ayala-Castro C, Outten FW. The SufBCD Fe-S scaffold complex interacts with SufA for Fe-S cluster transfer. Biochemistry 2009;48:10644–53.
[58] Chahal HK, Outten FW. J Inorg Biochem 2012;116:126–34.
[59] Gupta V, Sendra M, Naik SG, et al. Native Escherichia coli SufA, coexpressed with SufBCDSE, purifies as a [2Fe-2S] protein and acts as an Fe-S transporter to Fe-S target enzymes. J Am Chem Soc 2009;131:6149–53.
[60] Loiseau L, Gerez C, Bekker M, et al. ErpA, an iron sulfur (Fe-S) protein of the A-type essential for respiratory metabolism in Escherichia coli. Proc Natl Acad Sci USA 2007;104:13626–31.
[61] Lu J, Yang J, Tan G, Ding H. Complementary roles of SufA and IscA in the biogenesis of iron-sulfur clusters in Escherichia coli. Biochem J 2008;409:535–43.
[62] Vinella D, Brochier-Armanet C, Loiseau L, Talla E, Barras F. Iron-sulfur (Fe/S) protein biogenesis: phylogenomic and genetic studies of A-type carriers. PLoS Genet 2009;5:e1000497.
[63] Wollenberg M, Berndt C, Bill E, Schwenn JD, Seidler A. A dimer of the FeS cluster biosynthesis protein IscA from cyanobacteria binds a [2Fe-2S] cluster between two protomers and transfers it to [2Fe-2S] and [4Fe-4S] apo proteins. Eur J Biochem 2003;270:1662–71.
[64] Rodriguez-Manzaneque MT, Tamarit J, Belli G, Ros J, Herrero E. Grx5 is a mitochondrial glutaredoxin required for the activity of iron/sulfur enzymes. Mol Biol Cell 2002;13:1109–21.
[65] Achebach S, Tran QH, Vlamis-Gardikas A, Mullner M, Holmgren A, Unden G. Stimulation of Fe-S cluster insertion into apoFNR by Escherichia coli glutaredoxins 1:2 and 3 in vitro. FEBS Lett 2004;565:203–6.
[66] Rouhier N, Unno H, Bandyopadhyay S, et al. Functional, structural, and spectroscopic characterization of a glutathione-ligated [2Fe-2S] cluster in poplar glutaredoxin C1. Proc Natl Acad Sci USA 2007;104:7379–84.

[67] Bandyopadhyay S, Gama F, Molina-Navarro MM, et al. Chloroplast monothiol glutaredoxins as scaffold proteins for the assembly and delivery of [2Fe-2S] clusters. EMBO J 2008;27:1122–33.
[68] Iwema T, Picciocchi A, Traore DA, Ferrer JL, Chauvat F, Jacquamet L. Structural basis for delivery of the intact $[Fe_2S_2]$ cluster by monothiol glutaredoxin. Biochemistry 2009;48:6041–3.
[69] Pinske C, Sawers RG. A-type carrier protein ErpA is essential for formation of an active formate-nitrate respiratory pathway in Escherichia coli K-12. J Bacteriol 2012;194:346–53.
[70] Vinella D, Loiseau L, Ollagnier de Choudens S, Fontecave M, Barras F. In vivo [Fe-S] cluster acquisition by IscR and NsrR, two stress regulators in Escherichia coli. Mol Microbiol 2013;87:493–508.
[71] Giel JL, Nesbit AD, Mettert EL, Fleischhacker AS, Wanta BT, Kiley PJ. Regulation of iron-sulphur cluster homeostasis through transcriptional control of the Isc pathway by [2Fe-2S]-IscR in Escherichia coli. Mol Microbiol 2013;87:478–92.
[72] Ollagnier-de-Choudens S, Sanakis Y, Fontecave M. SufA/IscA: reactivity studies of a class of scaffold proteins involved in [Fe-S] cluster assembly. J Biol Inorg Chem 2004;9:828–38.
[73] Mapolelo DT, Zhang B, Naik SG, Huynh BH, Johnson MK. Spectroscopic and functional characterization of iron-sulfur cluster-bound forms of Azotobacter vinelandii (Nif)IscA. Biochemistry 2012;51:8071–84.
[74] Zhang B, Bandyopadhyay S, Shakamuri P, et al. Monothiol glutaredoxins can bind linear $[Fe_3S_4]^+$ and $[Fe_4S_4]^{2+}$ clusters in addition to $[Fe_2S_2]^{2+}$ clusters: spectroscopic characterization and functional implications. J Am Chem Soc 2013;135:15153–64.
[75] Flint DH, Tuminello JF, Emptage MH. The inactivation of Fe-S cluster containing hydro-lyases by superoxide. J Biol Chem 1993;268:22369–76.
[76] Djaman O, Outten FW, Imlay JA. Repair of oxidized iron-sulfur clusters in Escherichia coli. J Biol Chem 2004;279:44590–9.
[77] Imlay JA. Iron-sulphur clusters and the problem with oxygen. Mol Microbiol 2006;59:1073–82.
[78] Keyer K, Imlay JA. Superoxide accelerates DNA damage by elevating free-iron levels. Proc Natl Acad Sci USA 1996;93:13635–40.
[79] Keyer K, Imlay JA. Inactivation of dehydratase [4Fe-4S] clusters and disruption of iron homeostasis upon cell exposure to peroxynitrite. J Biol Chem 1997;272:27652–9.
[80] Varghese S, Tang Y, Imlay JA. Contrasting sensitivities of Escherichia coli aconitases A and B to oxidation and iron depletion. J Bacteriol 2003;185:221–30.
[81] Gardner PR, Fridovich I. Superoxide sensitivity of the Escherichia coli aconitase. J Biol Chem 1991;266:19328–33.
[82] Gardner PR, Fridovich I. Superoxide sensitivity of the Escherichia coli 6-phosphogluconate dehydratase. J Biol Chem 1991;266:1478–83.
[83] Gardner PR, Fridovich I. Inactivation-reactivation of aconitase in Escherichia coli. A sensitive measure of superoxide radical. J Biol Chem 1992;267:8757–63.
[84] Leonard SE, Carroll KS. Chemical 'omics' approaches for understanding protein cysteine oxidation in biology. Curr Opin Chem Biol 2011;15:88–102.
[85] Gari K, Ortiz AML, Borel V, Flynn H, Skehel JM, Boulton SJ. MMS19 links cytoplasmic iron-sulfur cluster assembly to DNA metabolism. Science 2012;337:243–45.
[86] Amir A, Meshner S, Beatus T, Stavans J. Damped oscillations in the adaptive response of the iron homeostasis network of E. coli. Mol Microbiol 2010;76:428–36.
[87] Andrews SC, Robinson AK, Rodriguez-Quinones F. Bacterial iron homeostasis. FEMS Microbiol Rev 2003;27:215–37.
[88] Semsey S, Andersson AM, Krishna S, Jensen MH, Masse E, Sneppen K. Genetic regulation of fluxes: iron homeostasis of Escherichia coli. Nucleic Acids Res 2006;34:4960–7.
[89] Hantke K. Regulation of ferric iron transport in Escherichia coli K12: isolation of a constitutive mutant. Mol Gen Genet 1981;182:288–92.
[90] Outten FW, Djaman O, Storz G. A suf operon requirement for Fe-S cluster assembly during iron starvation in Escherichia coli. Mol Microbiol 2004;52:861–72.

[91] Patzer SI, Hantke K. SufS is a NifS-like protein, and SufD is necessary for stability of the [2Fe-2S] FhuF protein in Escherichia coli. J Bacteriol 1999;181:3307–9.
[92] Masse E, Escorcia FE, Gottesman S. Coupled degradation of a small regulatory RNA and its mRNA targets in Escherichia coli. Genes Dev 2003;17:2374–83.
[93] Masse E, Gottesman S. A small RNA regulates the expression of genes involved in iron metabolism in Escherichia coli. Proc Natl Acad Sci USA 2002;99:4620–5.
[94] Masse E, Vanderpool CK, Gottesman S. Effect of RyhB small RNA on global iron use in Escherichia coli. J Bacteriol 2005;187:6962–71.
[95] Maringanti S, Imlay JA. An intracellular iron chelator pleiotropically suppresses enzymatic and growth defects of superoxide dismutase-deficient Escherichia coli. J Bacteriol 1999;181:3792–802.
[96] Woodmansee AN, Imlay JA. Reduced flavins promote oxidative DNA damage in non-respiring Escherichia coli by delivering electrons to intracellular free iron. J Biol Chem 2002;277:34055–66.
[97] Varghese S, Wu A, Park S, Imlay KR, Imlay JA. Submicromolar hydrogen peroxide disrupts the ability of Fur protein to control free-iron levels in Escherichia coli. Mol Microbiol 2007;64:822–30.
[98] Takahashi Y, Tokumoto U. A third bacterial system for the assembly of iron-sulfur clusters with homologs in archaea and plastids. J Biol Chem 2002;277:28380–3.
[99] Schwartz CJ, Giel JL, Patschkowski T, et al. IscR, an Fe-S cluster-containing transcription factor, represses expression of Escherichia coli genes encoding Fe-S cluster assembly proteins. Proc Natl Acad Sci USA 2001;98:14895–900.
[100] Giel JL, Rodionov D, Liu M, et al. IscR-dependent gene expression links iron-sulphur cluster assembly to the control of O_2-regulated genes in Escherichia coli. Mol Microbiol 2006;60:1058–75.
[101] Yeo WS, Lee JH, Lee KC, Roe JH. IscR acts as an activator in response to oxidative stress for the suf operon encoding Fe-S assembly proteins. Mol Microbiol 2006;61:206–18.
[102] Fleischhacker AS, Stubna A, Hsueh KL, et al. Characterization of the [2Fe-2S] cluster of Escherichia coli transcription factor IscR. Biochemistry 2012;51:4453–62.
[103] Nesbit AD, Giel JL, Rose JC, Kiley PJ. Sequence-specific binding to a subset of IscR-regulated promoters does not require IscR Fe-S cluster ligation. J Mol Biol 2009;387:28–41.
[104] Desnoyers G, Morissette A, Prevost K, Masse E. Small RNA-induced differential degradation of the polycistronic mRNA iscRSUA. EMBO J 2009;28:1551–61.
[105] Lee JH, Yeo WS, Roe JH. Induction of the sufA operon encoding Fe-S assembly proteins by superoxide generators and hydrogen peroxide: involvement of OxyR, IHF and an unidentified oxidant-responsive factor. Mol Microbiol 2004;51:1745–55.
[106] Nachin L, Loiseau L, Expert D, Barras F. SufC: an unorthodox cytoplasmic ABC/ATPase required for [Fe-S] biogenesis under oxidative stress. EMBO J 2003;22:427–37.
[107] Tokumoto U, Kitamura S, Fukuyama K, Takahashi Y. Interchangeability and distinct properties of bacterial Fe-S cluster assembly systems: functional replacement of the isc and suf operons in Escherichia coli with the nifSU-like operon from Helicobacter pylori. J Biochem (Tokyo) 2004;136:199–209.
[108] Ranquet C, Ollagnier de Choudens S, Loiseau L, Barras F, Fontecave M. Cobalt stress in Escherichia coli: the effect on the iron-sulfur proteins. J Biol Chem 2007;282:30442–51.
[109] Tan G, Lu J, Bitoun JP, Huang H, Ding H. IscA/SufA paralogues are required for the [4Fe-4S] cluster assembly in enzymes of multiple physiological pathways in Escherichia coli under aerobic growth conditions. Biochem J 2009;420:463–72.
[110] Jang S, Imlay JA. Hydrogen peroxide inactivates the Escherichia coli Isc iron-sulphur assembly system, and OxyR induces the Suf system to compensate. Mol Microbiol 2010;78:1448–67.
[111] Lima CD. Analysis of the E. coli NifS CsdB protein at 2.0 Å reveals the structural basis for perselenide and persulfide intermediate formation. J Mol Biol 2002;315:1199–208.
[112] Ye Y, Godzik A. FATCAT: a web server for flexible structure comparison and structure similarity searching. Nucleic Acids Res 2004;32:W582–5.

[113] Selbach BP, Pradhan PK, Dos Santos PC. Protected sulfur transfer reactions by the Escherichia coli Suf system. Biochemistry 2013;52:4089–96.
[114] Turowski VR, Busi MV, Gomez-Casati DF. Structural and functional studies of the mitochondrial cysteine desulfurase from Arabidopsis thaliana. Mol Plant 2012;5:1001–10.
[115] Tirupati B, Vey JL, Drennan CL, Bollinger JM Jr. Kinetic and structural characterization of Slr0077/SufS, the essential cysteine desulfurase from Synechocystis sp. PCC 6803. Biochemistry 2004;43:12210–19.
[116] Outten FW, Wood MJ, Munoz FM, Storz G. The SufE protein and the SufBCD complex enhance SufS cysteine desulfurase activity as part of a sulfur transfer pathway for Fe-S cluster assembly in Escherichia coli. J Biol Chem 2003;278:45713–9.
[117] Ollagnier-de-Choudens S, Lascoux D, Loiseau L, Barras F, Forest E, Fontecave M. Mechanistic studies of the SufS-SufE cysteine desulfurase: evidence for sulfur transfer from SufS to SufE. FEBS Lett 2003;555:263–7.
[118] Mihara H, Kurihara T, Yoshimura T, Esaki N. Kinetic and mutational studies of three NifS homologs from Escherichia coli: mechanistic difference between L-cysteine desulfurase and L-selenocysteine lyase reactions. J Biochem (Tokyo) 2000;127:559–67.
[119] Mihara H, Maeda M, Fujii T, Kurihara T, Hata Y, Esaki N. A nifS-like gene, csdB, encodes an Escherichia coli counterpart of mammalian selenocysteine lyase. Gene cloning, purification, characterization and preliminary x-ray crystallographic studies. J Biol Chem 1999;274:14768–72.
[120] Dai Y, Outten FW. The E. coli SufS-SufE sulfur transfer system is more resistant to oxidative stress than IscS-IscU. FEBS Lett 2012;586:4016–22.
[121] Goldsmith-Fischman S, Kuzin A, Edstrom WC, et al. The SufE sulfur-acceptor protein contains a conserved core structure that mediates interdomain interactions in a variety of redox protein complexes. J Mol Biol 2004;344:549–65.
[122] Loiseau L, Ollagnier-de-Choudens S, Nachin L, Fontecave M, Barras F. Biogenesis of Fe-S cluster by the bacterial Suf system: SufS and SufE form a new type of cysteine desulfurase. J Biol Chem 2003;278:38352–9.
[123] Kim S, Park S. Structural changes during cysteine desulfurase CsdA and sulfur acceptor CsdE interactions provide insight into the trans-persulfuration. J Biol Chem 2013;288:27172–80.
[124] Trotter V, Vinella D, Loiseau L, Ollagnier de Choudens S, Fontecave M, Barras F. The CsdA cysteine desulphurase promotes Fe/S biogenesis by recruiting Suf components and participates to a new sulphur transfer pathway by recruiting CsdL (ex-YgdL), a ubiquitin-modifying-like protein. Mol Microbiol 2009;74:1527–42.
[125] Singh H, Dai Y, Outten FW, Busenlehner LS. Escherichia coli SufE sulfur transfer protein modulates the SufS cysteine desulfurase through allosteric conformational dynamics. J Biol Chem 2013;288: 36189–200.
[126] Salvail H, Lanthier-Bourbonnais P, Sobota JM, et al. A small RNA promotes siderophore production through transcriptional and metabolic remodeling. Proc Natl Acad Sci USA 2010;107:15223–8.
[127] Outten CE, O'Halloran TV. Femtomolar sensitivity of metalloregulatory proteins controlling zinc homeostasis. Science 2001;292:2488–92.
[128] Ding H, Yang J, Coleman LC, Yeung S. Distinct iron binding property of two putative iron donors for the iron-sulfur cluster assembly: IscA and the bacterial frataxin ortholog CyaY under physiological and oxidative stress conditions. J Biol Chem 2007;282:7997–8004.
[129] Wang W, Huang H, Tan G, et al. In vivo evidence for the iron-binding activity of an iron-sulfur cluster assembly protein IscA in Escherichia coli. Biochemical J 2010;432:429–36.
[130] Nachin L, El Hassouni M, Loiseau L, Expert D, Barras F. SoxR-dependent response to oxidative stress and virulence of Erwinia chrysanthemi: the key role of SufC, an orphan ABC ATPase. Mol Microbiol 2001;39:960–72.
[131] Rangachari K, Davis CT, Eccleston JF, et al. SufC hydrolyzes ATP and interacts with SufB from Thermotoga maritima. FEBS Lett 2002;514:225–8.

[132] Eccleston JF, Petrovic A, Davis CT, Rangachari K, Wilson RJ. The kinetic mechanism of the SufC ATPase: the cleavage step is accelerated by SufB. J Biol Chem 2006;281:8371–8.
[133] Wada K, Sumi N, Nagai R, et al. Molecular dynamism of Fe-S cluster biosynthesis implicated by the structure of SufC2-SufD2 complex. J Mol Biol 2009;387:245–58.
[134] Wollers S, Layer G, Garcia-Serres R, et al. Iron-sulfur (Fe-S) cluster assembly: the SufBCD complex is a new type of Fe-S scaffold with a flavin redox cofactor. J Biol Chem 2010;285:23331–41.
[135] Layer G, Gaddam SA, Ayala-Castro CN, et al. SufE transfers sulfur from SufS to SufB for iron-sulfur cluster assembly. J Biol Chem 2007;282:13342–50.
[136] Saini A, Mapolelo DT, Chahal HK, Johnson MK, Outten FW. SufD and SufC ATPase activity are required for iron acquisition during in vivo Fe-S cluster formation on SufB. Biochemistry 2010;49:9402–12.
[137] Li DS, Ohshima K, Jiralerspong S, Bojanowski MW, Pandolfo M. Knock-out of the cyaY gene in Escherichia coli does not affect cellular iron content and sensitivity to oxidants. FEBS Lett 1999;456:13–6.
[138] Vivas E, Skovran E, Downs DM. Salmonella enterica strains lacking the frataxin homolog CyaY show defects in Fe-S cluster metabolism in vivo. J Bacteriol 2006;188:1175–9.
[139] Thorgersen MP, Downs DM. Oxidative stress and disruption of labile iron generate specific auxotrophic requirements in Salmonella enterica. Microbiology 2009;155:295–304.
[140] Andrews SC. The Ferritin-like superfamily: evolution of the biological iron storeman from a rubrerythrin-like ancestor. Biochim Biophys Acta 2010;1800:691–705.
[141] Cheesman MR, le Brun NE, Kadir FH, et al. Haem and non-haem iron sites in Escherichia coli bacterioferritin: spectroscopic and model building studies. Biochem J 1993;292:47–56.
[142] Le Brun NE, Cheesman MR, Thomson AJ, et al. An EPR investigation of non-haem iron sites in Escherichia coli bacterioferritin and their interaction with phosphate. A study using nitric oxide as a spin probe. FEBS Lett 1993;323:261–6.
[143] Andrews SC, Le Brun NE, Barynin V, et al. Site-directed replacement of the coaxial heme ligands of bacterioferritin generates heme-free variants. J Biol Chem 1995;270:23268–74.
[144] Yasmin S, Andrews SC, Moore GR, Le Brun NE. A new role for heme, facilitating release of iron from the bacterioferritin iron biomineral. J Biol Chem 2011;286:3473–83.
[145] Le Brun NE, Crow A, Murphy ME, Mauk AG, Moore GR. Iron core mineralisation in prokaryotic ferritins. Biochim Biophys Acta 2010;1800:732–44.
[146] Velayudhan J, Castor M, Richardson A, Main-Hester KL, Fang FC. The role of ferritins in the physiology of Salmonella enterica sv. typhimurium: a unique role for ferritin B in iron-sulphur cluster repair and virulence. Mol Microbiol 2007;63:1495–507.
[147] Ilari A, Ceci P, Ferrari D, Rossi GL, Chiancone E. Iron incorporation into Escherichia coli Dps gives rise to a ferritin-like microcrystalline core. J Biol Chem 2002;277:37619–23.
[148] Zhao G, Ceci P, Ilari A, et al. Iron and hydrogen peroxide detoxification properties of DNA-binding protein from starved cells. A ferritin-like DNA-binding protein of Escherichia coli. J Biol Chem 2002;277:27689–96.
[149] Chiancone E, Ceci P. The multifaceted capacity of Dps proteins to combat bacterial stress conditions: detoxification of iron and hydrogen peroxide and DNA binding. Biochim Biophys Acta 2010;1800:798–805.
[150] Martinez A, Kolter R. Protection of DNA during oxidative stress by the nonspecific DNA-binding protein Dps. J Bacteriol 1997;179:5188–94.
[151] Almiron M, Link AJ, Furlong D, Kolter R. A novel DNA-binding protein with regulatory and protective roles in starved Escherichia coli. Genes Dev 1992;6:2646–54.
[152] Altuvia S, Almiron M, Huisman G, Kolter R, Storz G. The dps promoter is activated by OxyR during growth and by IHF and sigma S in stationary phase. Mol Microbiol 1994;13:265–72.
[153] McHugh JP, Rodriguez-Quinones F, Abdul-Tehrani H, et al. Global iron-dependent gene regulation in Escherichia coli. A new mechanism for iron homeostasis. J Biol Chem 2003;278:29478–86.

[154] Nandal A, Huggins CC, Woodhall MR, et al. Induction of the ferritin gene (ftnA) of Escherichia coli by Fe^{2+}-Fur is mediated by reversal of H-NS silencing and is RyhB independent. Mol Microbiol 2010;75:637–57.
[155] Abdul-Tehrani H, Hudson AJ, Chang YS, et al. Ferritin mutants of Escherichia coli are iron deficient and growth impaired, and fur mutants are iron deficient. J Bacteriol 1999;181:1415–28.
[156] Sevcenco AM, Pinkse MW, Wolterbeek HT, Verhaert PD, Hagen WR, Hagedoorn PL. Exploring the microbial metalloproteome using MIRAGE. Metallomics 2011;3:1324–30.
[157] Expert D, Boughammoura A, Franza T. Siderophore-controlled iron assimilation in the enterobacterium Erwinia chrysanthemi: evidence for the involvement of bacterioferritin and the Suf iron-sulfur cluster assembly machinery. J Biol Chem 2008;283:36564–72.
[158] Justino MC, Vicente JB, Teixeira M, Saraiva LM. New genes implicated in the protection of anaerobically grown Escherichia coli against nitric oxide. J Biol Chem 2005;280:2636–43.
[159] Justino MC, Almeida CC, Goncalves VL, Teixeira M, Saraiva LM. Escherichia coli YtfE is a di-iron protein with an important function in assembly of iron-sulphur clusters FEMS Microbiol Lett 2006;257:278–84.
[160] Justino MC, Almeida CC, Teixeira M, Saraiva LM. Escherichia coli di-iron YtfE protein is necessary for the repair of stress-damaged iron-sulfur clusters. J Biol Chem 2007;282:10352–9.
[161] Overton TW, Justino MC, Li Y, et al. Widespread distribution in pathogenic bacteria of di-iron proteins that repair oxidative and nitrosative damage to iron-sulfur centers. J Bacteriol 2008;190:2004–13.
[162] Todorovic S, Justino MC, Wellenreuther G, et al. Iron-sulfur repair YtfE protein from Escherichia coli: structural characterization of the di-iron center. J Biol Inorg Chem 2008;13:765–70.
[163] Gralnick JA, Downs DM. The YggX protein of Salmonella enterica is involved in Fe(II) trafficking and minimizes the DNA damage caused by hydroxyl radicals: residue CYS-7 is essential for YggX function. J Biol Chem 2003;278:20708–15.
[164] Skovran E, Lauhon CT, Downs DM. Lack of YggX results in chronic oxidative stress and uncovers subtle defects in Fe-S cluster metabolism in Salmonella enterica. J Bacteriol 2004;186: 7626–34.
[165] Thorgersen MP, Downs DM. Analysis of yggX and gshA mutants provides insights into the labile iron pool in Salmonella enterica. J Bacteriol 2008;190:7608–13.
[166] Pomposiello PJ, Koutsolioutsou A, Carrasco D, Demple B. SoxRS-regulated expression and genetic analysis of the yggX gene of Escherichia coli. J Bacteriol 2003;185:6624–32.
[167] Osborne MJ, Siddiqui N, Landgraf D, Pomposiello PJ, Gehring K. The solution structure of the oxidative stress-related protein YggX from Escherichia coli. Protein Sci 2005;14:1673–8.
[168] Kennedy MC, Emptage MH, Dreyer JL, Beinert H. The role of iron in the activation-inactivation of aconitase. J Biol Chem 1983;258:11098–105.
[169] Kennedy MC, Kent TA, Emptage M, Merkle H, Beinert H, Munck E. Evidence for the formation of a linear [3Fe-4S] cluster in partially unfolded aconitase. J Biol Chem 1984;259:14463–71.
[170] Balasubramanian R, Shen G, Bryant DA, Golbeck JH. Regulatory roles for IscA and SufA in iron homeostasis and redox stress responses in the cyanobacterium Synechococcus sp. strain PCC 7002. J Bacteriol 2006;188:3182–91.
[171] Pinske C, Sawers RG. Delivery of iron-sulfur clusters to the hydrogen-oxidizing [NiFe]-hydrogenases in Escherichia coli requires the A-type carrier proteins ErpA and IscA. PLoS One 2012;7:e31755.
[172] Mapolelo DT, Zhang B, Randeniya S, et al. Monothiol glutaredoxins and A-type proteins: partners in Fe-S cluster trafficking. Dalton Trans 2013;42:3107–15.
[173] Butland G, Babu M, Diaz-Mejia JJ, et al. eSGA: E. coli synthetic genetic array analysis. Nat Methods 2008;5:789–95.
[174] Yeung N, Gold B, Liu NL, et al. The E. coli monothiol glutaredoxin GrxD forms homodimeric and heterodimeric Fe-S cluster containing complexes. Biochemistry 2011;50:8957–69.

4 Sensing the cellular Fe-S cluster demand: a structural, functional, and phylogenetic overview of *Escherichia coli* IscR

Erin L. Mettert, Nicole T. Perna, and Patricia J. Kiley

4.1 Introduction

Given the versatile chemical reactivity of iron-sulfur (Fe-S) cluster cofactors, it is perhaps not surprising that in addition to serving structural, catalytic, or electron transfer roles for a variety of enzymes, Fe-S clusters enable many transcriptional regulatory proteins to sense specific environmental signals and respond appropriately by altering gene expression [1–4]. For the bacterium *Escherichia coli*, Fe-S cluster transcription factors are known to differentially regulate gene expression in response to several redox active compounds or gases, such as O_2, reactive oxygen species (ROS; e.g., hydrogen peroxide, superoxide), nitric oxide (NO), and redox-cycling drugs [3, 4]. As such, these transcription factors—by altering mRNA levels through transcriptional regulation—play an important role in managing redox stress in cells.

Perhaps the most well-known example, and the subject of many reviews, is the global regulator FNR, which directly senses O_2 through the lability of its $[4Fe\text{-}4S]^{2+}$ cluster [3–8]. During anaerobic growth of *E. coli*, acquisition of the $[4Fe\text{-}4S]^{2+}$ cluster by FNR promotes protein dimerization, enabling FNR to bind site-specifically to DNA sites within promoter regions to control the transcription of genes encoding for proteins involved in metabolism, among numerous other functions. This transcriptional response enables *E. coli* to adapt its metabolism to anaerobic environments. In the presence of O_2, the $[4Fe\text{-}4S]^{2+}$ cluster is converted to a $[2Fe\text{-}2S]^{2+}$ cluster, thereby inactivating FNR through loss of dimerization. This mechanism of cluster conversion serves as a paradigm for the O_2 sensitivity of Fe-S clusters in general.

Although the sensitivity of the $[4Fe\text{-}4S]^{2+}$ cluster to O_2 is optimized for the role of FNR in regulating relevant pathways under anaerobic conditions, the activities of many Fe-S enzymes are essential under both aerobic and anaerobic growth conditions. Thus, the innate instability of some Fe-S clusters to O_2 and ROS [9–11] suggests that *in vivo*, the cellular requirements for Fe-S cluster biogenesis should vary with environmental changes in O_2 tension. An initial clue that *E. coli* responds to changes in Fe-S cluster demand was based on the finding that expression of the housekeeping Fe-S cluster biogenesis system (the Isc pathway) [12] is upregulated under aerobic conditions compared to anaerobic conditions. Furthermore, we discovered that the transcription factor IscR, the first gene in the operon encoding the Isc proteins (*iscRSUAhscBAfdx*), is responsible for this O_2-mediated differential expression by negatively regulating expression of the *isc* operon. Within the last 10 years, extensive studies have focused on how IscR

DOI 10.1515/9783110479850-004

makes use of the ligation state of its own Fe-S cluster to assess the cellular Fe-S demand and accordingly globally alter gene transcription to maintain Fe-S cluster homeostasis. These studies have also revealed that, unlike FNR, IscR is a novel type of regulator in that both the Fe-S cluster-containing form and the clusterless, apo-protein form are active to modulate gene expression. Furthermore, these two forms of IscR differentially regulate gene expression by site-specifically binding to two distinct DNA motifs in response to O_2 availability. In this chapter, we highlight the key structural features of IscR and relate these to the major findings that have established its critical physiological role in Fe-S homeostasis. In addition, we discuss the results of phylogenetic analyses, which have revealed insights into evolutionary aspects of IscR function.

4.2 General properties of IscR

IscR is a member of the Rrf2 family of transcription factors that are widely distributed in bacteria and are responsible for sensing a variety of signals [13]. Other members include the nitric oxide sensor NsrR [14]; the *Rhizobiaceae* iron-responsive regulator RirA [15]; and the global cysteine regulator CymR of *Bacillus subtilis* [13]. Although this protein family has not been extensively studied, the crystal structures of several Rrf2 family members, including IscR, have been solved in recent years (Fig. 4.1) [13, 16, 17]. These

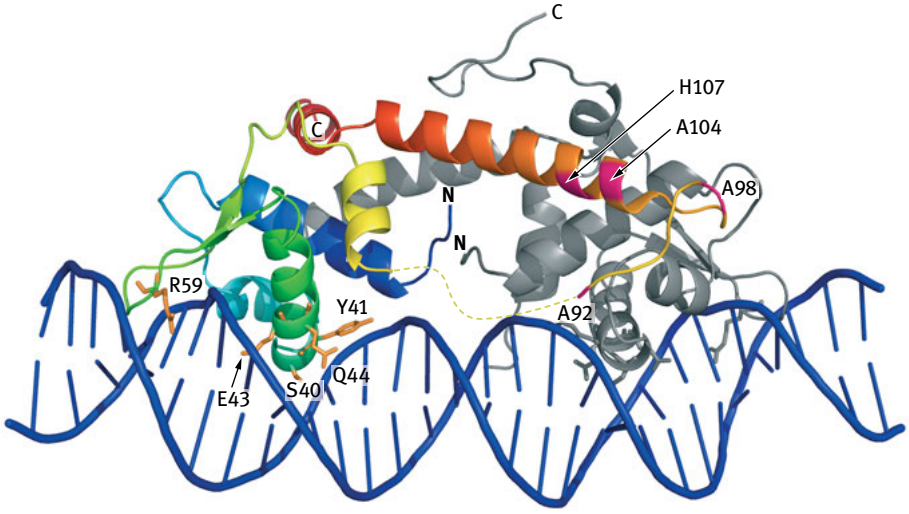

Fig. 4.1: Overall structure of an apo-IscR dimer bound to a 29-bp type 2 site derived from the *hyaA* promoter. In this crystal form, an IscR variant with three (Cys92, Cys98, and Cys104) of the four cluster ligands substituted with alanine (shown in magenta) was used. The IscR dimer is shown as a ribbon representation, with one subunit in gray and the other subunit in rainbow colors. Side chains making specific contacts to the *hyaA* DNA (shown in blue) are shown as sticks, and the dashed line indicates residues for which electron density was missing.

structures have revealed some key features common to members of the Rrf2 family, such as the presence of an N-terminal winged helix-turn-helix (wHTH) DNA-binding motif and a long dimerization helix. This long dimerization helix positions the wHTH at the extreme ends of the protein dimer, enabling these relatively small proteins to span 23–27 bp of DNA [13]. In addition, sequence comparisons among Rrf2 members have revealed that a subset contain three conserved cysteine residues in their C-terminal region, suggesting that some family members may ligate Fe-S clusters [13, 18].

While the apo-protein form of IscR was used to solve its crystal structure [16], several lines of evidence have demonstrated that IscR can indeed ligate an Fe-S cluster. Upon overexpression and isolation under anaerobic conditions, IscR is red in color and exhibits an absorption spectrum typical of a protein containing a [2Fe-2S] cluster [12]. The presence of a mostly reduced $[2Fe\text{-}2S]^{1+}$ cluster in isolated IscR was supported by EPR and Mössbauer spectroscopies. Furthermore, Mössbauer studies using whole cells indicate that *in vivo*, the IscR [2Fe-2S] cluster is predominantly in the reduced (1+) state [12, 19]. Substitution of all three C-terminal cysteine residues (Cys92, Cys98, and Cys104) or just Cys92 with alanine, followed by purification yields IscR protein that does not contain any Fe-S cluster [18]. Thus, these results indicate that the conserved cysteine residues, in fact, serve as ligands for the IscR [2Fe-2S] cluster.

Until recently, it was unclear what residue provides the fourth ligand to the [2Fe-2S] cluster since IscR only contains the three aforementioned cysteine residues. Analysis of purified [2Fe-2S]-IscR by resonance Raman and NMR spectroscopies revealed that the [2Fe-2S] cluster has partial noncysteinyl coordination. Indeed, subsequent mutational analysis identified His107 as the fourth ligand of the [2Fe-2S] cluster [19]. Although His107 is highly conserved among IscR orthologues, it is not conserved across all Rrf2 family members [13]. Furthermore, the $(Cys)_3(His)_1$ ligation is atypical since most [2Fe-2S] clusters have all cysteinyl $(Cys)_4$ ligation, or in the case of Rieske proteins, a $(Cys)_2(His)_2$ ligation. Interestingly, the few proteins known to bind a [2Fe-2S] cluster with $(Cys)_3(His)_1$ ligation, such as the yeast Fra2-Grx3/4 protein complexes [20] and the mitochondrial mitoNEET protein [21], appear to have possible roles as sensors. Further work is needed to determine whether the unique cluster ligation scheme allows IscR to more efficiently carry out its function in sensing the cellular Fe-S demand.

The apo-IscR crystal structure revealed that the electron density for residues encompassing the cluster-binding region were either weak or missing (Fig. 4.1) [16], suggesting conformational flexibility of this region in the absence of the [2Fe-2S] cluster. Nevertheless, the location of the weak electron density indicated that the cluster-binding site is exposed to solvent, perhaps allowing for efficient incorporation and/or loss of the [2Fe-2S] cluster. Additionally, the cluster-binding region from one monomer was proximal to the wHTH DNA binding domain of the other monomer, thus raising the possibility that upon [2Fe-2S] cluster ligation, a conformational change within IscR could influence DNA binding. Recent studies to address the mechanism of DNA binding by apo- and holo-IscR are described in further detail later in this chapter.

4.3 [2Fe-2S]-IscR represses Isc expression *via* a negative feedback loop

The significance of the [2Fe-2S] cluster for IscR transcriptional activity was recognized by the initial observation that a functional Isc pathway is required for IscR to repress transcription of the *iscRSUAhscBAfdx* operon *in vivo* [12]. Presumably, the Isc pathway provides IscR its [2Fe-2S] cluster and provides a link between IscR [2Fe-2S] cluster occupancy and the level of synthesis of the Isc pathway. Since this discovery, the IscR-dependent autoregulatory mechanism of Isc expression has been investigated in detail to better understand how Isc Fe-S cluster biogenesis machinery is regulated and, accordingly, how Fe-S cluster homeostasis is maintained.

DNase I footprinting experiments revealed that [2Fe-2S]-IscR binds to three individual sites within the *iscR* promoter region (P_{iscR}; Fig. 4.2a) [22]; however, only two of these sites, designated site A and site B, are necessary for IscR-mediated repression of P_{iscR} *in vivo* [23]. Because these sites partially overlap promoter elements recognized by RNA polymerase (RNAP), we predicted that [2Fe-2S]-IscR represses P_{iscR} by preventing RNAP from binding to the promoter. In support of this notion, DNase I footprinting revealed that simultaneous incubation of [2Fe-2S]-IscR and RNAP with DNA containing the *iscR* promoter region resulted in a pattern of protection from DNase I cleavage identical to the one when just [2Fe-2S]-IscR was present (Fig. 4.2b) [24]. This result indicates that binding of [2Fe-2S]-IscR to P_{iscR} prevents RNAP from binding to the promoter and activating transcription.

The requirement of the [2Fe-2S] cluster in IscR-mediated repression of P_{iscR} was definitively established by demonstrating that P_{iscR} repression is relieved in strains expressing IscR mutants containing alanine substitutions of the cluster ligands (Cys92, Cys98, Cys104, and His107) [19, 23]. [2Fe-2S]-IscR is the form needed for DNA binding because fluorescence anisotropy assays revealed that *in vitro*, [2Fe-2S]-IscR binds to DNA fragments containing either site A or B from P_{iscR} with much higher affinity than the clusterless variant IscR-C92A/C98A/C104A [23]. In addition, strains lacking individual components of the Isc pathway, such as IscS, IscU, or Fdx, yielded similar defects in P_{iscR} repression as a strain lacking the entire Isc pathway (Δ*iscSUAhscBAfdx*) [12, 23, 25]. Although this defect was less severe in a strain lacking the A-type carrier (ATC) protein IscA [23, 25], recent studies demonstrated that another ATC, ErpA, also participates in IscR [2Fe-2S] cluster delivery [25]. Finally, in contrast to the Isc pathway, deletion of the *sufABCDSE* operon, encoding the alternate, stress-induced Suf Fe-S cluster biogenesis pathway, had no effect on the ability of [2Fe-2S]-IscR to repress P_{iscR} *in vivo* [23, 25]. Taken together, these findings support the conclusion that the Isc pathway provides the [2Fe-2S] cluster required for IscR to repress P_{iscR} expression.

In characterizing the Fe-S cluster maturation pathway for IscR, it was shown that while the ATC proteins IscA and ErpA participate in cluster transfer to IscR *in vivo* and *in vitro*, evidence also suggests that IscR may receive clusters directly from a scaffold protein (e.g. IscU) without the assistance of any ATC. This was in contrast to the Rrf2 paralogue NsrR, which exhibited a strict cluster transfer requirement from a scaffold

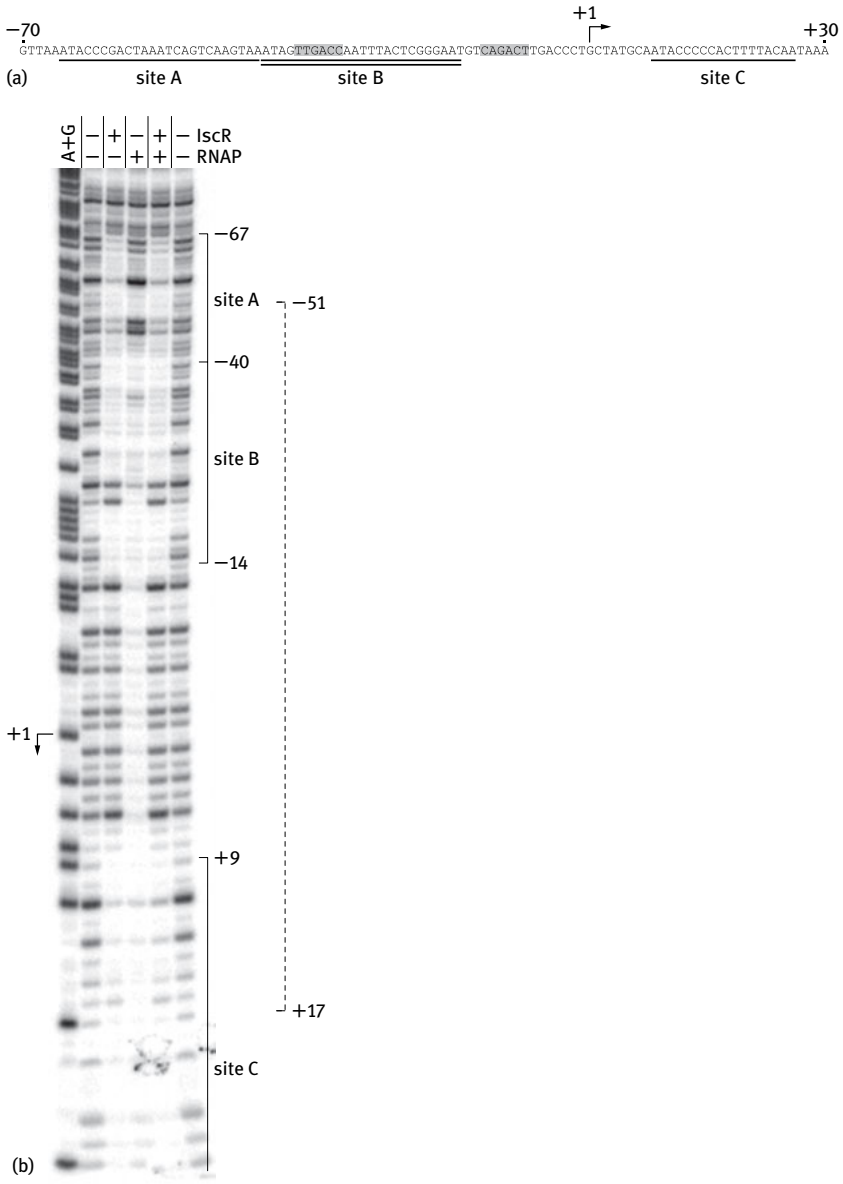

Fig. 4.2: IscR prevents binding of RNAP to the *iscR* promoter *in vitro*. (a) Diagram of the *iscR* promoter region with the IscR binding sites A (underlined), B (double underlined), and C (underlined); the transcriptional start site (arrow); and the –35 and –10 promoter elements (shaded) indicated. (b) Results of a DNase I footprinting assay, carried out as previously described [22], to evaluate binding of IscR (500 nM dimers) or σ^{70}-RNAP (100 nM) to the top strand of the *iscR* promoter. IscR, RNAP, or both were incubated with DNA radiolabeled at one end for 30 minutes at 37°C before the addition of DNase I for 30 seconds. Electrophoresis of the samples revealed the IscR- or RNAP-specific patterns of protection of the DNA from DNase I cleavage. The presence (+) or absence (-) of the proteins in the reaction and the extent of the IscR (solid line) and σ^{70}-RNAP (dashed line) footprints relative to the +1 transcription start site are noted. Samples were electrophoresed with a Maxam-Gilbert (A + G) ladder.

to either IscA or SufA and, subsequently, to ErpA [25]. These findings, together with those of additional studies [26–28] suggest that while cluster delivery is a versatile process, specific routes may depend on intrinsic features of the apo-protein substrate and/or environmental conditions. Furthermore, growing evidence has indicated that several non-A-type proteins, such as NfuA, GrxD, and Mrp, may also participate in cluster delivery [29–32]. With the exception of SufA, cellular levels of carrier proteins appear to be quite abundant under standard aerobic growth conditions [33]. Thus, a systematic approach will be necessary to further define the delivery routes by which IscR, and other apo-protein substrates, acquire Fe-S clusters.

4.4 IscR adjusts synthesis of the Isc pathway based on the cellular Fe-S demand

E. coli is predicted to contain greater than 150 proteins that contain Fe-S clusters, some of which are known to be sensitive to destruction or damage by O_2 and ROS. Although it is not known in general how levels of these proteins compare between aerobic and anaerobic growth conditions, gene expression studies suggest that Fe-S proteins are highly expressed under both conditions [34]. Thus, to mitigate the damage to Fe-S clusters by O_2 or ROS, the need for Fe-S cluster biogenesis or repair is likely increased in the presence of O_2. Consistent with this notion, there is fivefold less P_{iscR} repression under aerobic conditions than anaerobic conditions. Furthermore, this aerobic derepression of P_{iscR} occurs despite IscR protein levels being ~10-fold higher under aerobic than anaerobic conditions [23]. Hence, we interpret this as indicating that the cellular Fe-S demand appears to be higher when O_2 is present.

Recent research has focused on how IscR may sense these changes in cellular Fe-S demand. Based on previous studies with FNR [35–37], it was reasonable to hypothesize that O_2 may destabilize the IscR $[2Fe\text{-}2S]^{1+}$ cluster, or as in the case for SoxR in response to redox cycling drugs [38], the oxidation state of the cluster may be altered, thereby affecting holo-IscR activity. However, results from *in vitro* experiments suggest that O_2-mediated destruction of the IscR $[2Fe\text{-}2S]^{1+}$ cluster does not occur at a biologically relevant rate [12] (Kiley and Fleischhacker, unpublished results). Furthermore, although Mössbauer spectroscopy revealed that the $[2Fe\text{-}2S]^{+1}$ cluster is indeed subject to immediate oxidation to the (2+) state upon exposure to O_2, [2Fe-2S]-IscR was shown to have similar affinity for DNA containing the P_{iscR} site B *in vitro* regardless of the cluster oxidation state [19].

Rather, the current hypothesis is that IscR cluster occupancy differs between aerobic and anaerobic conditions due to competition between IscR and other Fe-S substrates for the Isc machinery (Fig. 4.3). This competition would be elevated under aerobic conditions due to increased rates of O_2- or ROS-mediated Fe-S cluster turnover for proteins containing labile clusters. In turn, this would lead to low IscR [2Fe-2S] cluster occupancy and, thus, less repression of the *iscRSUAhscBAfdx* operon. Under anaerobic conditions, Fe-S clusters are predicted to be more stable, and thus, less competition

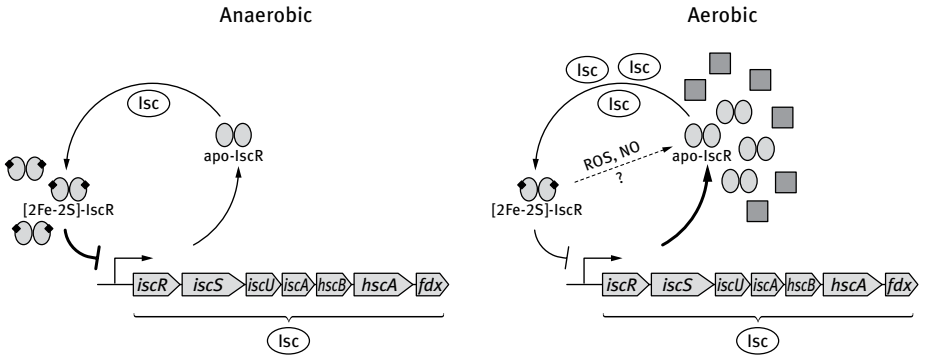

Fig. 4.3: Model describing how IscR responds to the differential demand in Fe-S cluster biogenesis between aerobic and anaerobic growth conditions. (Adapted from Giel JL, Nesbit AD, Mettert EL, Fleischhacker AS, Wanta BT, Kiley PJ, *Mol Microbiol*, 87, 478–92, 2013.) When O_2 is present, the rate of general Fe-S cluster turnover is predicted to be high, resulting in an increased demand for Fe-S cluster assembly. This leads to competition between IscR and apo-protein substrates (gray squares) for the Isc machinery, resulting in low IscR [2Fe-2S] cluster occupancy and, thus, derepression of the *iscRSUAhscBAfdx* operon. ROS and NO may also directly destabilize the IscR [2Fe-2S] cluster to generate apo-IscR, although this has yet to be confirmed. In contrast, when O_2 is absent, the demand for Fe-S cluster biogenesis is low due to heightened stability of Fe-S clusters. As a result, IscR [2Fe-2S] cluster occupancy is increased, culminating in repression of the Isc pathway. Although not depicted, under iron-limiting conditions, synthesis of [2Fe-2S]-IscR may be decreased, leading to elevated levels of apo-IscR.

would exist between IscR and apo-protein substrates. As a result, IscR would be predominantly in the holo-protein form to repress expression of the Isc pathway. Consistent with this model, IscR titration experiments revealed that half-maximal repression of P_{iscR} *in vivo* required ~ninefold more IscR protein under aerobic conditions relative to anaerobic conditions [23]. If the concentration of holo-IscR is presumed to be equivalent to the IscR protein concentration required for 50% P_{iscR} repression, these results indicate that IscR [2Fe-2S] cluster occupancy is lower under aerobic conditions. Although direct measurement of IscR cluster occupancy would further support this hypothesis, we currently lack robust methods to assess cluster occupancy at physiological levels of Fe-S proteins. Nevertheless, overexpression of FNR, or FNR-L28H, which contains a leucine-to-histidine substitution that renders the [4Fe-4S] cluster resistant to oxygen, diminished aerobic P_{iscR} repression, whereas anaerobic P_{iscR} expression remained unaffected [23]. This finding argues that under anaerobic conditions, there is sufficient Isc machinery present to efficiently respond to changes in Fe-S demand, thereby decreasing the competition between IscR and substrate proteins for Fe-S clusters.

Although this model provides an explanation for how *E. coli* exploits changes in IscR [2Fe-2S] cluster occupancy to sense and respond to differential requirements for Fe-S biogenesis, many questions regarding this proposed mechanism still remain. For example, as mentioned earlier in this chapter, it is not known whether the atypical $(Cys)_3(His)_1$ cluster ligation scheme or some other feature makes IscR a less efficient

competitor for the Isc machinery compared with other Fe-S substrate proteins. If IscR is less able to acquire its Fe-S cluster, then other important cellular Fe-S cluster requirements would be satisfied before IscR acquires its [2Fe-2S] cluster. Furthermore, whether $(Cys)_3(His)_1$ ligation makes IscR more prone to cluster loss upon exposure to ROS remains to be established. While expression of the *iscRSUAhscBAfdx* operon was induced upon exposure of cultures to H_2O_2 and the O_2^--generating drug paraquat [39–42], further work is needed to establish whether ROS can directly target the stability of the IscR [2Fe-2S] cluster, in addition to increasing the general cellular need for Fe-S synthesis.

It is also possible that [2Fe-2S]-IscR responds to other environmental signals. For example, in response to excess amounts of cobalt, expression of *iscRSUAhscBAfdx* was increased [43], suggesting that [2Fe-2S]-IscR may indirectly sense cobalt stress. [2Fe-2S]-IscR may also sense NO, known to damage some Fe-S clusters [44, 45], and/or levels of Fe. Indeed, in cells treated with the Fe^{2+}-specific chelator 2,2'-dipyridyl, transcription of the *iscRSUAhscBAfdx* operon was upregulated [25, 39, 46]. Under these same growth conditions, however, the small regulatory RNA RyhB was found to target the *iscSUAhscBAfdx* transcript for degradation. In contrast, the *iscR* transcript remained relatively stable, presumably due to secondary structure within the transcript that protected the transcript from degradation by ribonucleases [47]. Thus, this differential transcript degradation could allow for IscR-mediated gene regulation while simultaneously decreasing Isc-mediated Fe-S biogenesis under conditions when Fe is limiting. However, this mechanism could also simply increase expression of the regulator without coupling it to changes in levels of the biogenesis machinery, which are already fairly abundant [24, 33, 48, 49]. Resolving the role of Fe in the regulation of IscR and Isc-mediated cluster assembly will require determining whether Fe limitation significantly alters IscR protein levels. Ultimately, these and future studies to decipher how IscR is regulated will provide key insights into understanding how Fe-S homeostasis is maintained throughout *E. coli*'s ever-changing environment.

4.5 IscR has a global role in maintaining Fe-S homeostasis

Subsequent to discovering that IscR functions as a repressor of the *iscRSUAhscBAfdx* operon [12], genome-wide transcription profiling data, in addition to findings from biochemical and genetic studies, have revealed that IscR either directly or indirectly controls the expression of more than 40 genes in *E. coli* [22, 40, 50–53]. Similar to the *isc* operon, IscR also represses the expression of ErpA and NfuA, proteins that have roles in Fe-S cluster assembly [22]. In addition, IscR is predicted to bind the promoter region of *cysE* [22]. CysE is a serine acetyltransferase that catalyzes a rate-limiting step in biosynthesis of cysteine [54], which is needed for Fe-S cluster assembly. Surprisingly, IscR directly activates transcription of the *sufABCDSE* operon that encodes the alternate Suf Fe-S biogenesis pathway [22, 40]. Although Isc is considered to be

the housekeeping Fe-S biogenesis pathway, the Suf system is proposed to function primarily under oxidative and nitrosative stress and Fe-limiting conditions [39, 41, 55, 56]. Thus, the role of IscR in maintaining Fe-S cluster homeostasis goes beyond that of simply regulating the Isc pathway.

4.6 Fe-S cluster ligation broadens DNA site specificity for IscR

To establish the consensus IscR DNA binding site, sequences of the IscR protected regions in DNase I footprinting experiments were analyzed. This analysis, in addition to further investigation by phylogenetic footprinting, revealed that IscR specifically binds to two classes of DNA target sites, referred to as type 1 and type 2 sites (Fig. 4.4) [22]. However, as later studies revealed, the promoters of genes controlled by type 1 and type 2 sites show differences in their regulation by IscR according to the availability of O_2. The different roles of these two sites in allowing IscR to maintain Fe-S homeostasis will be discussed later in the chapter. Because the nucleotide sequences of these sites differ, it was not immediately apparent how an IscR dimer, predicted to have a single wHTH DNA binding domain in each subunit, could distinguish between the two sites. Even more intriguing was the finding that IscR binding to type 1 and type 2 sites is differentially regulated depending on whether the IscR [2Fe-2S] cluster is present. *In vitro* studies revealed that only [2Fe-2S]-IscR binds with high affinity to a type 1 site (found in the *iscR* promoter), whereas both [2Fe-2S]-IscR and apo-IscR bind with similar high affinity to a type 2 site (found in the *hyaA* and *suf*A promoters) [18, 23]. Because other known Fe-S cluster-containing transcription factors (e.g. FNR, SoxR) do not regulate transcription when they lack a cluster [6, 57], the finding that both holo- and apo-IscR are both active forms of the protein was truly unexpected. Furthermore, since Fe-S cluster occupancy of IscR is regulated by O_2 availability, broadening of IscR target site recognition upon [2Fe-2S] ligation revealed a very unique mechanism for differential gene regulation.

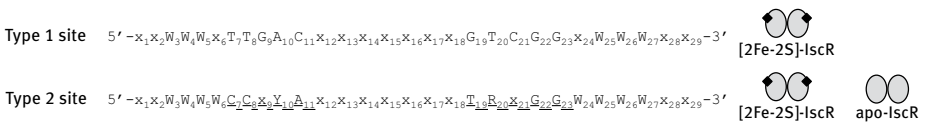

Fig. 4.4: The proposed consensus DNA binding sites for IscR are shown. [2Fe-2S]-IscR binds with high affinity to type 1 sites, whereas both [2Fe-2S]-IscR and apo-IscR bind with equally high affinity to type 2 sites. For the type 2 site, underlined is the symmetrical sequence present in each half site shown to be important for base-specific recognition by IscR. A, T, C, and G represent adenine, thymine, cytosine, and guanine, respectively; R represents A or G, Y represents C or T, W represents A or T, and x is undefined. Prototypical promoters that contain type 1 sites are *iscR*, *erpA,* and *nfuA,* whereas those that contain type 2 sites are *hyaA*, *sufA*, and *hybO*.

The crystal structure of apo-IscR bound to the type 2 site of the *hyaA* promoter has provided the major framework to understand how IscR distinguishes between two different DNA sites (Fig. 4.1). Although nonspecific interactions to the minor groove and DNA backbone provide much of the binding energy required to form the IscR-*hyaA* complex, the structure also revealed nucleotide-specific contacts between the IscR recognition helix and major groove of the DNA [16]. These findings corroborated earlier mutational analysis of the *hyaA* type 2 site that identified the same nucleotides important for IscR site-specific binding [18]. In addition, alanine substitution of the residues participating in these specific contacts (Ser40, Tyr41, Glu43, Gln44, and Arg59) established their relative importance in IscR recognition of the symmetrical ^{7}CCxYA^{11} sequence (where x is undefined and Y is a cytosine or thymine) present in each half site of the type 2 motif (Fig. 4.4) [16].

The presence of Glu43 within the IscR-*hyaA* interface was particularly compelling since acidic residues are not typically involved in nucleotide recognition due to potential electrostatic repulsion with the DNA backbone. Nevertheless, Glu43 was determined to be an important specificity-determining contact with the ^{7}CC^{8} dinucleotides in each type 2 half site. While mutation of ^{7}CC^{8} in one half site disrupted *in vitro* binding affinity for wild-type IscR, binding affinity of the mutant protein IscR-E43A was unaffected. Furthermore, unlike wild-type IscR, IscR-E43A did not discriminate between nucleotide bases at positions 7 or 8 [16]. These results suggest that the Glu43 contacts with the symmetrical ^{7}CC^{8} dinucleotides are critical for specific recognition of type 2 sites.

In contrast to the symmetrical type 2 site, the type 1 site is asymmetrical, containing ^{7}CC^{8} in one half site and a $^{7'}$TT$^{8'}$ in the other half site (Fig. 4.4). Since apo-IscR binds only type 2 sites with high affinity, it was proposed that an unfavorable interaction between Glu43 and $^{7'}$TT$^{8'}$ may inhibit apo-IscR from binding type 1 sites. In support of this hypothesis, both apo- and holo-forms of the IscR-E43A mutant bound the *iscRB* type 1 site with similar high affinity *in vitro* [16]. Thus, Glu43 of the wild-type protein is vital for discrimination against apo-IscR binding to the type 1 site. Furthermore, this finding implies that in order for [2Fe-2S]-IscR to bind to the type 1 site, the electrostatic repulsion between Glu43 and $^{7'}$TT$^{8'}$ must be removed. The current model proposes that ligation of the [2Fe-2S] cluster may induce a conformational change within IscR that repositions Glu43 away from $^{7'}$TT$^{8'}$, allowing for favorable contacts with the type 1 site.

Additional sequence differences in the two IscR binding motifs may also account for the differential regulation of type 1 and type 2 sites. Indeed, simply replacing the $^{7'}$TT$^{8'}$ dinucleotide of the *iscRB* type 1 site with cytosines was not sufficient to allow high-affinity binding by apo-IscR [16]. This suggests that the potentially favorable interaction between Glu43 and the CC dinucleotide may lock the IscR-DNA complex in such a conformation that essential contacts to other nucleotides in the type 1 site are not made. Although residues Ser40, Tyr41, Gln44, and Arg59 were found to be important for [2Fe-2S]-IscR binding to both type 1 and type 2 sites, the relative influence of

contacts made by Ser40 and Gln44 varied between the two sites [16]. Thus, it appears that upon [2Fe-2S] ligation, repositioning of Glu43 allows for a more flexible protein conformation such that IscR can make different nucleotide contacts to accommodate binding to type 1 sites. Studies to establish a structural basis for this model and to further characterize important nucleotides within the type 1 site are ongoing.

Although IscR from *E. coli* represents the paradigm for understanding mechanistically how a transcription factor is capable of binding site-specifically to two different sites, this may be an emerging property of other transcription factors. For example, the Fur proteins from *Campylobacter jejuni* and *Bradyrhizobium japonicum* and the Fur homolog BosR from *Borrelia burgdorferi* apparently recognize multiple DNA sequences, although the exact relationship between sequence specificity and affinity has not been established [58–60]. In addition, the functionality of both apo- and holo-forms may not be unique to IscR, whereas Fur requires its Fe^{2+} cofactor to repress transcription in most bacteria, apo-Fur appears to regulate expression of a few genes in *C. jejuni* and *Helicobacter pylori* [58, 61].

4.7 Phylogenetic analysis of IscR

To establish the extent to which IscR is conserved among bacteria and, more specifically, how well the key IscR residues that allow differential DNA site regulation are conserved, we conducted evolutionary analyses. The primary IscR amino acid sequence from *E. coli* strain MG1655 was used to query the NCBI reference protein database. This blastp search, plus further verification by sequence alignment, produced 4,527 proteins similar to MG1655 IscR. Among these proteins, we identified four major clades (Fig. 4.5a): the first clade (1,209 proteins) includes *E. coli* IscR; the second clade (1,310 proteins) includes *E. coli* NsrR; and the third clade (1,292 proteins) includes *B. subtilis* CymR. This observation is consistent with the fact that all three of these proteins belong to the Rrf2 protein family. The fourth clade (715 proteins, designated here as Unknown clade) does not appear to contain any well-characterized transcription factors, and literature in the PubMed database linked to these proteins almost exclusively consisted of genome sequence reports. Only one taxon, *Gemmatimonas aurantiaca* T-27 gi|226227389, could not be definitively assigned to one of these clades. Although taxonomic distribution does not reveal any obviously strict patterns, some interesting trends emerge among the four clades, which encompass a wide range of bacterial diversity (Tab. 4.1). For instance, the Unknown clade is dominated by Alphaproteobacteria and Actinobacteria. Gammaproteobacteria and Betaproteobacteria tend to have IscR and NsrR, but very few CymR and Unknown clade members. In addition, Bacilli and other Firmicutes tend to have NsrR and CymR, although there is some evidence for a few IscR and/or Unknown clade members in these taxa.

We found that IscR is most prevalent in the Proteobacteria (primarily gamma, then beta and alpha), similar to what was observed previously [62]. However, it is

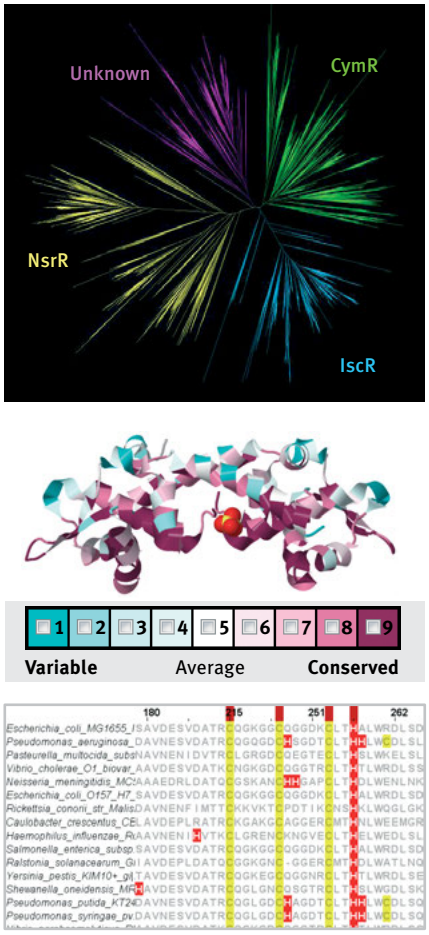

Fig. 4.5: (a) Shown is an unrooted tree for 4,527 proteins similar to *E. coli* MG1655 IscR. The MG1655 IscR protein sequence was used to query the reference protein (refseq protein) database using blastp with an *E* value cutoff of 0.0001 and a maximum number of hits (20,000) that exceeded the number of matches retrieved. The search returned 4,529 hits. These, plus MG1655 IscR, were aligned with MAFFT (version 7) using the FFT-NS-1 option (PMID: 23329690). Three sequences from one organism were very poorly aligned (*Saccharopolyspora spinosa*), so they were removed, and the remaining sequences were realigned using the same options. Phylogenetic analysis was conducted using FastTree2 with default parameters (PMID: 19377059). Trees were visualized using Archeopteryx (PMID: 19860910). (b) Shown is the structure of apo-IscR colorized according to amino acid conservation. The conservation scores and mapping onto the structure (PDB ID: 4hf0) were performed using the ConSurf server (PMID: 20478830) with a MAFFT alignment of the 1,209 IscR clade proteins. (c) Shown is an alignment of a subset of IscR proteins. This is a portion of the 1,209 protein IscR clade MAFFT alignment visualized using Jalview2.8 (PMID: 19151095) with gaps relative to the *E. coli* MG1655 IscR protein hidden. Red blocks mark columns of the alignment corresponding to Cys92, Cys98, Cys104, and His107. All cysteines (yellow) and histidines (orange) in this region are highlighted.

Tab. 4.1: Taxonomic distribution of four clades of Rrf2 family proteins.

Taxonomy[a]	Clade[b]				Total
	IscR	CymR	NsrR	Unknown	
Proteobacteria; Gammaproteobacteria	733	4	387	17	1,140
Proteobacteria; Alphaproteobacteria	162	56	276	268	762
Firmicutes; Clostridia	5	437	86	5	533
Firmicutes; Bacilli	0	224	191	9	424
Proteobacteria; Betaproteobacteria	259	10	104	0	373
Actinobacteria; Actinobacteridae	0	0	47	218	265
Proteobacteria; Deltaproteobacteria	8	91	44	20	163
Cyanobacteria; Oscillatoriophycideae	0	108	0	0	108
Firmicutes; Negativicutes	0	63	7	0	70
Cyanobacteria; Nostocales	0	57	0	0	57
Bacteroidetes; Flavobacteriia	1	1	21	32	55
Proteobacteria; Epsilonproteobacteria	0	22	5	27	54
Actinobacteria; Coriobacteridae	0	34	13	0	47
Bacteroidetes; Cytophagia	0	0	12	31	43
Spirochaetes; Spirochaetales	9	25	3	0	37
Deinococcus-Thermus; Deinococci	0	25	0	10	35
Bacteroidetes; Sphingobacteriia	0	6	9	17	32
Planctomycetes; Planctomycetia	0	0	8	19	27
Thermotogae; Thermotogales	16	1	5	0	22
Fusobacteria; Fusobacteriales	0	16	4	0	20
Cyanobacteria; Stigonematales	0	18	0	0	18
Synergistetes; Synergistia	0	6	6	4	16
Firmicutes; Erysipelotrichia	1	13	1	0	15
Bacteroidetes; Bacteroidia	0	5	6	3	14
Chlorobi; Chlorobia	0	1	12	0	13
Acidobacteria; Acidobacteriales	0	2	8	1	11
Deferribacteres; Deferribacterales	4	0	2	4	10
Nitrospirae; Nitrospirales	0	1	8	1	10
Actinobacteria; Rubrobacteridae	0	2	1	6	9
Cyanobacteria; Pleurocapsales	0	9	0	0	9
Proteobacteria; Zetaproteobacteria	6	0	3	0	9
Verrucomicrobia; Verrucomicrobiae	0	1	2	6	9
candidate division OP9	0	5	2	0	7
Aquificae; Aquificales	0	0	6	0	6
Bacteroidetes; Bacteroidetes Order II	0	0	6	0	6
Chloroflexi; Chloroflexales	0	6	0	0	6
Chloroflexi; Ktedonobacteria	0	2	3	0	5
Ignavibacteriae; Ignavibacteria	0	2	3	0	5
Actinobacteria; Acidimicrobidae	0	0	2	2	4
Cyanobacteria	0	4	0	0	4
Dictyoglomi; Dictyoglomales	0	4	0	0	4
Verrucomicrobia; Opitutae	0	0	0	4	4

Tab. 4.1 Continued

Taxonomy[a]	Clade[b]				Total
	IscR	CymR	NsrR	Unknown	
Acidobacteria; Holophagae	0	3	0	0	3
Acidobacteria; Solibacteres	0	1	1	1	3
candidate division OD1	0	2	1	0	3
candidate division OP8	0	1	1	1	3
Chloroflexi; Dehalococcoidia	0	3	0	0	3
Cyanobacteria; Gloeobacteria	0	2	1	0	3
Firmicutes; environmental samples	0	3	0	0	3
Thermodesulfobacteria	1	1	1	0	3
Verrucomicrobia	0	0	0	3	3
Armatimonadetes; Chthonomonadetes	0	1	1	0	2
Chloroflexi; Anaerolineae	0	0	2	0	2
Chloroflexi; Sphaerobacteridae	0	2	0	0	2
Firmicutes	0	2	0	0	2
Thermobaculum	0	1	0	1	2
Acidobacteria; Chloracidobacterium	0	1	0	0	1
Acidobacteria; Koribacter	0	0	1	0	1
Actinobacteria; Microthrix	0	0	0	1	1
Caldiserica; Caldisericia	0	0	0	1	1
Caldithrix;	0	0	1	0	1
Candidate division KSB1	1	0	0	0	1
Candidate division NC10	0	0	0	1	1
Candidate division NKB19	0	0	1	0	1
Candidate division OP3	0	0	0	1	1
Candidate division WS1	0	0	1	0	1
Chlamydiae; Chlamydiales	0	0	1	0	1
Chloroflexi; Herpetosiphonales	0	1	0	0	1
Chloroflexi; Thermomicrobiales	0	1	0	0	1
Chrysiogenetes; Chrysiogenales	0	1	0	0	1
Cyanobacteria; Prochlorales	0	1	0	0	1
dsDNA viruses; unclassified dsDNA phages	0	1	0	0	1
Euryarchaeota; Thermoplasmata	0	1	0	0	1
Fibrobacteres; Fibrobacterales	0	1	0	0	1
Lentisphaerae; Lentisphaeria	0	0	1	0	1
Metazoa; Ecdysozoa	1	0	0	0	1
Planctomycetes; Phycisphaerae	0	0	1	0	1
Synergistetes	0	1	0	0	1
Verrucomicrobia; Spartobacteria	0	0	0	1	1
Total	1,207	1,292	1,308	715	4,521

[a] Taxonomic information was extracted from Reference Protein XML records.

[b] Clades were assigned according to phylogenetic analysis (Fig. 4.5).

also present in distantly related organisms, such as Spirochaetes and Thermotogae. Notably, the presence of IscR appears to be widespread among pathogenic bacteria and, accordingly, was demonstrated to be important for virulence by the plant pathogens *Dickeya dadantii* (formerly known as *Erwinia chyrsanthemi*) and *Xanthomonas campestris* and the human pathogens *Pseudomonas aeruginosa*, *Vibrio vulnificus, Yersina pseudotuberculosis*, and *Shigella flexneri* [63–68]. Remarkably, the key residues involved in IscR [2Fe-2S] cluster ligation and DNA binding are all highly conserved among members of the IscR clade (Fig. 4.5b and c). This finding implies that the mechanism by which IscR regulates two different DNA target sites may also be highly conserved among numerous bacteria.

Despite this high degree of conservation, we and others [62, 69] observed an intriguing variation among the Alphaproteobacteria; whereas most IscR proteins possess the [2Fe-2S] cluster ligands, these residues are not conserved in the Rhodobacterales. Rather, a C-terminal cysteine residue that is not present at the same position in *E. coli* IscR was recently shown to be required for *Rhodobacter sphaeroides* IscR to exhibit an absorbance spectrum that may be characteristic of a Fe-S protein [70]. More direct methods need to be employed to validate this finding. Additionally, the genomic context of Rhodobacterales is a combination of *isc* (*iscRS*) and *suf* (*sufBCDS*) genes. Since IscR-dependent repression of this hybrid pathway was relieved in iron-limiting media, it was proposed that the function of the cysteine residue in *Rhodobacter sphaeroides* IscR may be required for proper regulation of the *iscRSsufBCDS* operon [70]. Interestingly, the Alphaproteobacteria *Caulobacter crescentus* also has this hybrid operon, but its IscR protein has all of the conserved cluster ligands [71]. Thus, dissecting the mechanism by which IscR regulates this hybrid operon among Alphaproteobacteria will be important in determining how Fe-S homeostasis in maintained within this diverse class of bacteria.

4.8 Binding to two classes of DNA sites allows IscR to differentially regulate transcription in response to O_2

By identifying which IscR-regulated promoters contain a type 1 site *vs* a type 2 site, it is apparent that the ability of IscR to discriminate between these two sites poses a major advantage for maintaining Fe-S cluster homeostasis. For example, type 1 site-containing promoters include those of the *iscRSUAhscBAfdx* operon, *erpA*, *nfuA*, and *cysE*, all of which are known or are predicted to be repressed by [2Fe-2S]-IscR and encode proteins involved in Fe-S cluster assembly [22]. Because the Fe-S demand under anaerobic conditions is low, it makes physiological sense to have these genes repressed by [2Fe-2S]-IscR (Fig. 4.3). In contrast, under aerobic conditions, when the Fe-S demand is high and levels of apo-IscR increase due to competition with other substrate proteins for the Isc machinery, de-repression of *iscRSUAhscBAfdx*, *erpA*, *nfuA*, and *cysE* occurs so that the cellular Fe-S requirements can be met. Interestingly,

although all IscR-dependent promoters identified thus far contain a single target site, the one exception is the *iscR* promoter, which contains two type 1 sites [22], perhaps emphasizing the significance of regulating Isc Fe-S biogenesis *in vivo*.

Although promoters containing a type 2 site can be bound by both apo- and holo-IscR *in vitro* [18], transcription profiling results indicate that most of these promoters are limited to regulation by IscR under aerobic growth conditions when apo-IscR is the predominant form of the protein [22]. As previously mentioned, promoters with a type 2 site include that of the *hyaABCDEF* operon, encoding the anaerobic Fe-S enzyme hydrogenase 1. Two other anaerobic Fe-S enzymes, hydrogenase 2 and the periplasmic nitrate reductase, are also regulated by type 2 site-containing promoters, *hybO* and *napF*, respectively. Under aerobic conditions, IscR represses transcription of these enzymes, perhaps directing Fe-S cluster biogenesis toward Fe-S proteins that exhibit essential cellular functions in the presence of O_2 [22]. IscR also activates the expression of some promoters that have a type 2 site. These include those of the *sufABCDSE* operon and *sodA*, encoding the Mn^{2+}-containing superoxide dismutase (Mn^{2+}-SOD) [22, 40]. Thus, IscR-dependent regulation of type 2 sites enables *E. coli* to maintain Fe-S cluster homeostasis not only by directly controlling Fe-S biogenesis but also by decreasing ROS and possibly protecting Fe-S clusters from destruction under conditions of oxidative stress.

Further investigation of promoters having a type 2 site revealed that several are regulated by additional transcription factors. For instance, *sufA* is regulated by Fur, OxyR, IHF, and NsrR [39, 41, 72–74]; and *sodA* is regulated by Fur, ArcA, IHF, and SoxS [75–77]. Therefore, it was hypothesized that coordinate regulation of type 2 site-containing promoters by multiple transcription factors may at least partially account for the decreased regulation by [2Fe-2S]-IscR under anaerobic conditions of this class of promoters. Indeed, this mechanism of O_2-dependent regulation was recently demonstrated for the *hyaA* and *sufA* promoters [78, 79]. In the case of *hyaA*, apo-IscR represses this promoter under aerobic conditions, whereas the anaerobic transcription factors ArcA and AppY promote P_{hyaA} transcription under anaerobic conditions by antagonizing IscR-mediated repression. Although the mechanism by which AppY prevents IscR repression remains to be elucidated, ArcA was shown to compete with IscR in binding P_{hyaA} *in vitro*. Furthermore, it was demonstrated that, *in vivo*, [2Fe-2S]-IscR exhibits weaker repressor activity at *hyaA* compared with apo-IscR [78]. This weaker repressor activity, in combination with antirepression by ArcA and AppY and the fact that anaerobic levels of [2Fe-2S]-IscR are low due to negative autoregulation, would ultimately lead to increased P_{hyaA} expression under anaerobic conditions. Thus, in contrast to type 1 sites where O_2-dependent regulation appears to primarily depend on changes in IscR [2Fe-2S] cluster occupancy, O_2-dependent regulation of type 2 sites may involve the combinatorial action of multiple transcription factors. Since the identity and number of transcription factors that regulate each type 2 site-containing promoter varies, further investigation is required to dissect the mechanism by which each promoter is coordinately regulated. In summary, the ability of IscR to recognize

two classes of DNA target sites provides a novel and efficient mechanism for sculpting the *E. coli* transcriptome in response to O_2.

4.9 Roles of IscR beyond Fe-S homeostasis

IscR also regulates type 2 sites in promoters of genes whose functional ties to Fe-S homeostasis are not currently obvious. For example, under iron-limiting conditions, IscR directly activates transcription of *fimE*, encoding the FimE recombinase that decreases expression of type I fimbriae, thus reducing biofilm formation [50]. Also under iron-limiting conditions, IscR promotes expression of NrdEF, the Mn^{2+}-containing ribonucleotide reductase [53]. Because IscR also upregulates Mn^{2+}-SOD [22], it is intriguing that IscR upregulates several isoenzymes that contain Mn^{2+}, which, unlike their counterparts that contain Fe^{2+}, would not be sensitive to oxidation. In conjunction with LexA, IscR represses *cka*, encoding the pore-forming toxin colicin K [52]; this coordinate gene regulation has shown to be important for delayed production of colicin K following induction of the SOS response, a global response to DNA damage that prompts DNA repair. In addition, IscR directly represses *rnlA*, an essential gene for the activity of RNase LS, an endoribonuclease important for RNA metabolism and antagonizing bacteriophage T4 [51]. Overall, these findings suggest that IscR may respond to stresses in addition to changes in the cellular Fe-S demand. Further investigation of the direct IscR regulon is needed to gain insight on ancillary regulatory roles of IscR.

4.10 Additional aspects of IscR regulation

Although the critical findings establishing IscR's role in Fe-S homeostasis have been reviewed here, further research is needed to shed light on additional factors that enable IscR to carry out this vital function. For example, while IscR is a target of the ClpXP protease [80], it is not known how regulating IscR protein levels may influence expression of the IscR regulon. However, in the case of *cka*, decreased IscR levels in cells entering late exponential phase and early stationary phase are important for derepression of colicin K production. This is apparently due to the fact that when IscR levels are sufficient, such as in nonstressed, exponentially growing cells, IscR stabilizes LexA at the *cka* promoter to prevent transcription [52]. Given that IscR levels in aerobic cells are very abundant (~10, 300 molecules per cell [23], compared with ~5,000 and ~4,100 molecules per cell for the global regulators Fur [81] and FNR [82], respectively), it is possible that posttranslational regulation may be important for decreasing the cellular concentration of IscR. Furthermore, stabilization of LexA by IscR at the *cka* promoter raises the question as to whether IscR employs a similar mechanism with other transcription factors to alter gene expression. Thus, future

studies will likely provide exciting new insight on additional mechanisms that regulate IscR.

4.11 Summary

Here, we have reviewed the structural and functional analyses of IscR that have advanced our understanding of how *E. coli* maintains Fe-S cluster homeostasis. Critical to this process is the ability of IscR to sense the demand for Fe-S synthesis through its [2Fe-2S] cluster and, accordingly, adjust transcription of relevant target genes through binding two different DNA sites. The capacity of IscR to distinguish between type 1 and type 2 sites based on its cluster ligation state is an extremely versatile trait, providing an efficient means to alter gene expression in response to environmental changes in O_2 availability. As our phylogenetic analysis of IscR suggests, this mechanism of differential gene expression by a single transcription factor appears to be conserved in numerous bacteria, further demonstrating the significance of IscR versatility.

Acknowledgments

The authors are grateful to past and current members of Patricia Kiley's laboratory, who have contributed much of the work discussed in this chapter. We specifically thank Jennifer Giel for providing the data shown in Fig. 4.2. This work was supported by NIH grant GM45844 to P.J.K. and by NSF AToL grant DEB-0936214 to N.T.P.

References

[1] Beinert H. Iron-sulfur proteins: ancient structures, still full of surprises. J Biol Inorg Chem 2000;5:2–15.
[2] Fontecave M. Iron-sulfur clusters: ever-expanding roles. Nat Chem Biol 2006;2:171–4.
[3] Kiley PJ, Beinert H. The role of Fe-S proteins in sensing and regulation in bacteria. Curr Opin Microbiol 2003;6:181–5.
[4] Fleischhacker AS, Kiley PJ. Iron-containing transcription factors and their roles as sensors. Curr Opin Chem Biol 2011;15:335–41.
[5] Unden G, Achebach S, Holighaus G, Tran HG, Wackwitz B, Zeuner Y. Control of FNR function of Escherichia coli by O_2 and reducing conditions. J Mol Microbiol Biotechnol 2002;4:263–8.
[6] Kiley PJ, Beinert H. Oxygen sensing by the global regulator, FNR: the role of the iron-sulfur cluster. FEMS Microbiol Rev 1998;22:341–52.
[7] Green J, Crack JC, Thomson AJ, LeBrun NE. Bacterial sensors of oxygen. Curr Opin Microbiol 2009;12:145–51.
[8] Sawers G. The aerobic/anaerobic interface. Curr Opin Microbiol 1999;2:181–7.
[9] Imlay JA. Iron-sulphur clusters and the problem with oxygen. Mol Microbiol 2006;59:1073–82.
[10] Imlay JA. Cellular defenses against superoxide and hydrogen peroxide. Annu Rev Biochem 2008;77:755–76.

[11] Imlay JA. The molecular mechanisms and physiological consequences of oxidative stress: lessons from a model bacterium. Nat Rev Microbiol 2013;11:443–54.
[12] Schwartz CJ, Giel JL, Patschkowski T, et al. IscR, an Fe-S cluster-containing transcription factor, represses expression of Escherichia coli genes encoding Fe-S cluster assembly proteins. Proc Natl Acad Sci USA 2001;98:14895–900.
[13] Shepard W, Soutourina O, Courtois E, England P, Haouz A, Martin-Verstraete I. Insights into the Rrf2 repressor family—the structure of CymR, the global cysteine regulator of Bacillus subtilis. FEBS J 2011;278:2689–701.
[14] Bodenmiller DM, Spiro S. The yjeB (nsrR) gene of Escherichia coli encodes a nitric oxide-sensitive transcriptional regulator. J Bacteriol 2006;188:874–81.
[15] Todd JD, Wexler M, Sawers G, Yeoman KH, Poole PS, Johnston AW. RirA, an iron-responsive regulator in the symbiotic bacterium Rhizobium leguminosarum. Microbiology 2002;148:4059–71.
[16] Rajagopalan S, Teter SJ, Zwart PH, Brennan RG, Phillips KJ, Kiley PJ. Studies of IscR reveal a unique mechanism for metal-dependent regulation of DNA binding specificity. Nat Struc Mol Biol 2013;20:740–7.
[17] Berman HM, Westbrook J, Feng Z, et al. The Protein Data Bank. Nucleic Acids Res 2000;28:235–42.
[18] Nesbit AD, Giel JL, Rose JC, Kiley PJ. Sequence-specific binding to a subset of IscR-regulated promoters does not require IscR Fe-S cluster ligation. J Mol Biol 2009;387:28–41.
[19] Fleischhacker AS, Stubna A, Hsueh KL, et al. Characterization of the [2Fe-2S] Cluster of Escherichia coli transcription factor IscR. Biochemistry 2012;51:4453–62.
[20] Li H, Mapolelo DT, Dingra NN, et al. The yeast iron regulatory proteins Grx3/4 and Fra2 form heterodimeric complexes containing a [2Fe-2S] cluster with cysteinyl and histidyl ligation. Biochemistry 2009;48:9569–81.
[21] Paddock ML, Wiley SE, Axelrod HL, et al. MitoNEET is a uniquely folded 2Fe 2S outer mitochondrial membrane protein stabilized by pioglitazone. Proc Natl Acad Sci USA 2007;104:14342–7.
[22] Giel JL, Rodionov D, Liu M, Blattner FR, Kiley PJ. IscR-dependent gene expression links iron-sulphur cluster assembly to the control of O_2-regulated genes in Escherichia coli. Mol Microbiol 2006;60:1058–75.
[23] Giel JL, Nesbit AD, Mettert EL, Fleischhacker AS, Wanta BT, Kiley PJ. Regulation of iron-sulphur cluster homeostasis through transcriptional control of the Isc pathway by [2Fe-2S]-IscR in Escherichia coli. Mol Microbiol 2013;87:478–92.
[24] Giel JL. Role of IscR in regulation of iron-sulfur biogenesis in Escherichia coli: Identification of the IscR regulon and mechanisms of autoregulation. PhD dissertation. University of Wisconsin-Madison; 2007.
[25] Vinella D, Loiseau L, de Choudens SO, Fontecave M, Barras F. In vivo [Fe-S] cluster acquisition by IscR and NsrR, two stress regulators in Escherichia coli. Mol Microbiol 2013;87:493–508.
[26] Loiseau L, Gerez C, Bekker M, et al. ErpA, an iron-sulfur (Fe-S) protein of the A-type essential for respiratory metabolism in Escherichia coli. Proc Natl Acad Sci USA 2007;104:13626–31.
[27] Vinella D, Brochier-Armanet C, Loiseau L, Talla E, Barras F. Iron-sulfur (Fe/S) protein biogenesis: phylogenomic and genetic studies of A-type carriers. PLoS Genet 2009;5:e1000497.
[28] Mandin P, Chareyre S, Barras F. A regulatory circuit composed of a transcription factor, IscR, and a regulatory RNA, RyhB, Controls Fe-S Cluster delivery. MBio 2016;7:e00966.
[29] Angelini S, Gerez C, Ollagnier-de Choudens S, et al. NfuA, a new factor required for maturing Fe/S proteins in Escherichia coli under oxidative stress and iron starvation conditions. J Biol Chem 2008;283:14084–91.
[30] Py B, Gerez C, Angelini S, et al. Molecular organization, biochemical function, cellular role and evolution of NfuA, an atypical Fe-S carrier. Mol Microbiol 2012;86:155–71.

[31] Yeung N, Gold B, Liu NL, et al. The E. coli monothiol glutaredoxin GrxD forms homodimeric and heterodimeric FeS cluster containing complexes. Biochemistry 2011;50:8957–69.
[32] Boyd JM, Pierik AJ, Netz DJ, Lill R, Downs DM. Bacterial ApbC can bind and effectively transfer iron-sulfur clusters. Biochemistry 2008;47:8195–202.
[33] Li GW, Burkhardt D, Gross C, Weissman JS. Quantifying absolute protein synthesis rates reveals principles underlying allocation of cellular resources. Cell 2014;157:624–35.
[34] Py B, Barras F. Building Fe-S proteins: bacterial strategies. Nat Rev Microbiol 2010;8:436–46.
[35] Jordan PA, Thomson AJ, Ralph ET, Guest JR, Green J. FNR is a direct oxygen sensor having a biphasic response curve. FEBS Lett 1997;416:349–52.
[36] Khoroshilova N, Popescu C, Münck E, Beinert H, Kiley PJ. Iron-sulfur cluster disassembly in the FNR protein of Escherichia coli by O_2: [4Fe-4S] to [2Fe-2S] conversion with loss of biological activity. Proc Natl Acad Sci USA 1997;94:6087–92.
[37] Popescu CV, Bates DM, Beinert H, Münck E, Kiley PJ. Mössbauer spectroscopy as a tool for the study of activation/inactivation of the transcription regulator FNR in whole cells of Escherichia coli. Proc Natl Acad Sci USA 1998;95:13431–5.
[38] Gu M, Imlay JA. The SoxRS response of Escherichia coli is directly activated by redox-cycling drugs rather than by superoxide. Mol Microbiol 2011;79:1136–50.
[39] Outten FW, Djaman O, Storz G. A suf operon requirement for Fe-S cluster assembly during iron starvation in Escherichia coli. Mol Microbiol 2004;52:861–72.
[40] Yeo WS, Lee JH, Lee KC, Roe JH. IscR acts as an activator in response to oxidative stress for the suf operon encoding Fe-S assembly proteins. Mol Microbiol 2006;61:206–18.
[41] Zheng M, Wang X, Templeton LJ, Smulski DR, LaRossa RA, Storz G. DNA microarray-mediated transcriptional profiling of the Escherichia coli response to hydrogen peroxide. J Bacteriol 2001;183:4562–70.
[42] Blanchard JL, Wholey WY, Conlon EM, Pomposiello PJ. Rapid changes in gene expression dynamics in response to superoxide reveal SoxRS-dependent and independent transcriptional networks. PloS One 2007;2:e1186.
[43] Fantino JR, Py B, Fontecave M, Barras F. A genetic analysis of the response of Escherichia coli to cobalt stress. Environ Microbiol 2010;12:2846–57.
[44] Spiro S. Regulators of bacterial responses to nitric oxide. FEMS Microbiol Rev 2007;31:193–211.
[45] Tucker NP, Le Brun NE, Dixon R, Hutchings MI. There's NO stopping NsrR, a global regulator of the bacterial NO stress response. Trends Microbiol 2010;18:149–56.
[46] Lee KC, Yeo WS, Roe JH. Oxidant-responsive induction of the suf operon, encoding a Fe-S assembly system, through Fur and IscR in Escherichia coli. J Bacteriol 2008;190:8244–7.
[47] Desnoyers G, Morissette A, Prévost K, Massé E. Small RNA-induced differential degradation of the polycistronic mRNA iscRSUA. EMBO J 2009;28:1551–61.
[48] Hoff KG, Silberg JJ, Vickery LE. Interaction of the iron-sulfur cluster assembly protein IscU with the Hsc66/Hsc20 molecular chaperone system of Escherichia coli. Proc Natl Acad Sci USA 2000;97:7790–5.
[49] Vickery LE, Silberg JJ, Ta DT. Hsc66 and Hsc20, a new heat shock cognate molecular chaperone system from Escherichia coli. Protein Sci 1997;6:1047–56.
[50] Wu Y, Outten FW. IscR controls iron-dependent biofilm formation in Escherichia coli by regulating type I fimbria expression. J Bacteriol 2009;191:1248–57.
[51] Otsuka Y, Miki K, Koga M, et al. IscR regulates RNase LS activity by repressing rnlA transcription. Genetics 2010;185:823–30.
[52] Butala M, Sonjak S, Kamensek S, et al. Double locking of an Escherichia coli promoter by two repressors prevents premature colicin expression and cell lysis. Mol Microbiol 2012;86:129–39.
[53] Martin JE, Imlay JA. The alternative aerobic ribonucleotide reductase of Escherichia coli, NrdEF, is a manganese-dependent enzyme that enables cell replication during periods of iron starvation. Mol Microbiol 2011;80:319–34.

[54] Zheng L, Cash VL, Flint DH, Dean DR. Assembly of iron-sulfur clusters. Identification of an iscSUA-hscBA-fdx gene cluster from Azotobacter vinelandii. J Biol Chem 1998;273: 13264–72.
[55] Justino MC, Vicente JB, Teixeira M, Saraiva LM. New genes implicated in the protection of anaerobically grown Escherichia coli against nitric oxide. J Biol Chem 2005;280:2636–43.
[56] Mukhopadhyay P, Zheng M, Bedzyk LA, LaRossa RA, Storz G. Prominent roles of the NorR and Fur regulators in the Escherichia coli transcriptional response to reactive nitrogen species. Proc Natl Acad Sci USA 2004;101:745–50.
[57] Hidalgo E, Demple B. An iron-sulfur center essential for transcriptional activation by the redox-sensing SoxR protein. EMBO J 1994;13:138–46.
[58] Butcher J, Sarvan S, Brunzelle JS, Couture JF, Stintzi A. Structure and regulon of Campylobacter jejuni ferric uptake regulator Fur define apo-Fur regulation. Proc Natl Acad Sci USA 2012;109:10047–52.
[59] Ouyang Z, Deka RK, Norgard MV. BosR (BB0647) controls the RpoN-RpoS regulatory pathway and virulence expression in Borrelia burgdorferi by a novel DNA-binding mechanism. PLoS Pathog 2011;7:e1001272.
[60] Friedman YE, O'Brian MR. A novel DNA-binding site for the ferric uptake regulator (Fur) protein from Bradyrhizobium japonicum. J Biol Chem 2003;278:38395–401.
[61] Miles S, Carpenter BM, Gancz H, Merrell DS. Helicobacter pylori apo-Fur regulation appears unconserved across species. J Microbiol 2010;48:378–86.
[62] Rodionov DA, Gelfand MS, Todd JD, Curson AR, Johnston AW. Computational reconstruction of iron- and manganese-responsive transcriptional networks in alpha-proteobacteria. PLoS Comput Biol 2006;2:e163.
[63] Rincon-Enriquez G, Crete P, Barras F, Py B. Biogenesis of Fe/S proteins and pathogenicity: IscR plays a key role in allowing Erwinia chrysanthemi to adapt to hostile conditions. Mol Microbiol 2008;67:1257–73.
[64] Fuangthong M, Jittawuttipoka T, Wisitkamol R, et al. IscR plays a role in oxidative stress resistance and pathogenicity of a plant pathogen, Xanthomonas campestris. Microbiol Res 2015;170:139–46.
[65] Kim SH, Lee BY, Lau GW, Cho YH. IscR modulates catalase A (KatA) activity, peroxide resistance and full virulence of Pseudomonas aeruginosa PA14. J Microbiol and Biotechn 2009;19:1520–6.
[66] Lim JG, Bang YJ, Choi SH. Characterization of the Vibrio vulnificus 1-Cys peroxiredoxin Prx3 and regulation of its expression by the Fe-S cluster regulator IscR in response to oxidative stress and iron starvation. J Biol Chem 2014;289:36263–74.
[67] Miller HK, Kwuan L, Schwiesow L, et al. IscR is essential for Yersinia pseudotuberculosis type III secretion and virulence. PLoS Pathog 2014;10:e1004194.
[68] Runyen-Janecky L, Daugherty A, Lloyd B, Wellington C, Eskandarian H, Sagransky M. Role and regulation of iron-sulfur cluster biosynthesis genes in Shigella flexneri virulence. Infect Immun 2008;76:1083–92.
[69] Imam S, Noguera DR, Donohue TJ. An integrated approach to reconstructing genome-scale transcriptional regulatory networks. PLoS Comput Biol 2015;11:e1004103.
[70] Remes B, Eisenhardt BD, Srinivasan V, Klug G. IscR of Rhodobacter sphaeroides functions as repressor of genes for iron-sulfur metabolism and represents a new type of iron-sulfur-binding protein. Microbiologyopen 2015;4:790–802.
[71] da Silva Neto JF, Lourenco RF, Marques MV. Global transcriptional response of Caulobacter crescentus to iron availability. BMC Genomics 2013;14:549.
[72] Partridge JD, Bodenmiller DM, Humphrys MS, Spiro S. NsrR targets in the Escherichia coli genome: new insights into DNA sequence requirements for binding and a role for NsrR in the regulation of motility. Mol Microbiol 2009;73:680–94.

[73] Lee JH, Yeo WS, Roe JH. Induction of the *sufA* operon encoding Fe-S assembly proteins by superoxide generators and hydrogen peroxide: involvement of OxyR, IHF and an unidentified oxidant-responsive factor. Mol Microbiol 2004;51:1745–55.
[74] Lee JH, Yeo WS, Roe JH. Regulation of the *sufABCDSE* operon by Fur. J Microbiol 2003;41:109–14.
[75] Tardat B, Touati D. Iron and oxygen regulation of Escherichia coli MnSOD expression: competition between the global regulators Fur and ArcA for binding to DNA. Mol Microbiol 1993;9:53–63.
[76] Presutti DG, Hassan HM. Binding of integration host factor (IHF) to the Escherichia coli sodA gene and its role in the regulation of a sodA-lacZ fusion gene. Mol Genet 1995;246:228–35.
[77] Fawcett WP, Wolf RE, Jr. Purification of a MalE-SoxS fusion protein and identification of the control sites of Escherichia coli superoxide-inducible genes. Mol Microbiol 1994;14:669–79.
[78] Nesbit AD, Fleischhacker AS, Teter SJ, Kiley PJ. ArcA and AppY antagonize IscR repression of hydrogenase-1 expression under anaerobic conditions, revealing a novel mode of O2 regulation of gene expression in Escherichia coli. J Bacteriol 2012;194:6892–9.
[79] Mettert EL, Kiley PJ. Coordinate regulation of the Suf and Isc Fe-S cluster biogenesis pathways by IscR is essential for viability of Escherichia coli. J Bacteriol 2014;196:4315–23.
[80] Flynn JM, Neher SB, Kim YI, Sauer RT, Baker TA. Proteomic discovery of cellular substrates of the ClpXP protease reveals five classes of ClpX-recognition signals. Mol Cell 2003;11:671–83.
[81] Zheng M, Doan B, Schneider TD, Storz G. OxyR and SoxRS regulation of fur. J Bacteriol 1999;181:4639–43.
[82] Sutton VR, Mettert EL, Beinert H, Kiley PJ. Kinetic analysis of the oxidative conversion of the [4Fe-4S]2+ cluster of FNR to a [2Fe-2S]2+ Cluster. J Bacteriol 2004;186:801.

5 Fe-S assembly in Gram-positive bacteria

Patricia C. Dos Santos

5.1 Introduction

Biosynthetic pathways involved in the assembly and trafficking of Fe-S clusters in Gram-positive bacteria are distinct from those found in Gram-negative bacteria and Eukaryotes. Inspection of Gram-positive bacterial genome sequences showed that only one type of biosynthetic pathway is represented in each species, which suggests that each pathway will be vital for function. These single pathways varied across taxonomic classes of Gram-positive bacteria where three types of genetically distinct pathways were identified: Clostridia-ISC, Actinobacteria-SUF, and Bacilli-SUF encoded by *iscRSU, sufRCDBSUT*, and *sufCDSUB* gene regions, respectively. Close inspection of these systems show that they differ in the number of genes contained in each operon, genomic organization, and composition from previously studied systems. Although components of the Clostridia-ISC are more similar to the components of the Gram-negative ISC system, the components of the Actinobacteria- and Bacilli-SUF system share high levels of sequence similarities to each other and have more in common with SUF systems. The assembly of Fe-S clusters in Gram-positive bacteria containing the SUF systems involves SufS, which catalyzes the PLP-dependent Cys:SufU sulfurtransferase reaction. The subsequent assembly of Fe-S clusters is proposed to be mediated by SufU and/or the SufBDC complex. The distinct biosynthetic makeup of these systems combined with the essential role of their individual components render this pathway a potential target for specific pharmacological interventions in infections caused by Gram-positive pathogens.

5.2 Fe-S proteins in Gram-positive bacteria

The requirement for Fe-S clusters in promoting life-sustaining reactions discussed in previous chapters for nitrogen-fixing and Gram-negative bacteria is also an important metabolic feature in Gram-positive bacteria. As in other forms of life, Fe-S clusters, when associated with proteins, facilitate numerous reactions ranging from electron transfer, to substrate activation, to sulfur mobilization, to molecular signaling, to transcriptional and post-translational regulation of gene expression [1, 2]. The inherent oxygen sensitivity of Fe-S proteins and the existence of species-specific Fe-S cluster assembly machineries pose technical challenges for identification of their functionalities and their protein partners.

DOI 10.1515/9783110479850-005

With the development of affordable technologies for genome sequencing, computational tools have aided in the identification of putative Fe-S proteins and gene products involved in the biosynthesis and cellular trafficking of Fe-S clusters. Although bioinformatic predictions are *in silico* estimations of biological processes, they have provided direction for experimental validation of the involvement of Fe-S enzymes in metabolism. Sequence analysis of Fe-S cluster binding motifs using manually curated genomes showed that some microbial genomes encode a large number of Fe-S proteins (Tab. 5.1). The genome of the well-studied *Escherichia coli*, for example, encodes 143 known and putative Fe-S proteins, one-third of which are of unidentified function [1, 3]. Similarly, the genome of other Gram-negative bacteria, including *Azotobacter vinelandii* and *Salmonella enterica*, encode over 100 proteins containing Fe-S binding motifs. In contrast, the genomes of selected Gram-positive bacteria encode fewer proteins that contain Fe-S binding motifs (Tab. 5.1), with the exception of the microaerophilic *Clostridium difficile*, which is predicted to encode nearly 100 proteins that have Fe-S binding motifs [3].

The reduced number of Fe-S proteins in Gram-positive bacteria may be attributable to multiple causes. First, these selected genomes often lack the duplicated genes that encode multiple versions of Fe-S enzymes that perform similar and overlapping functions. For example, the *E. coli* and *A. vinelandii* genomes encode two copies of aconitase, whereas *Bacillus subtilis* only expresses one. Second, some of the reactions

Tab. 5.1: Number of bacterial proteins known or suspected to contain Fe-S cluster(s).

	Fe-S proteins[a] (total proteins)
Gram-negative bacteria	
A. vinelandii DJ	129 (5,050)
E. coli MG1655	143 (4,519)
Pseudomonas aeruginosa DK2	92 (5,884)
S. enterica enterica serovar Heidelberg str. B182	113 (4,333)
Gram-positive bacteria	
B. subtilis subtilis 168	63 (4,229)
C. botulinum B1 str. Okra	101 (3,862)
C. difficile CD196	109 (3,444)
En. faecalis OG1RF	25 (2,579)
Lactobacillus casei BL23	8 (3,015)
Listeria monocytogenes 07PF0776	29 (2,797)
M. tuberculosis H37Ra	63 (4,034)
St. aureus 04-02981	35 (2,650)
Streptomyces avermitilis MA-4680	83 (7,681)

[a] Number of gene products identified through gene ontology classes: GO: 0051536, Fe-S cluster binding; GO: 0051537, 2Fe-2S cluster binding; GO: 0051538, 3Fe-4S cluster binding; GO: 0051539, 4Fe-4S cluster binding.

catalyzed by Fe-S enzymes in *E. coli* are performed by Fe-S independent enzymes in *B. subtilis*, as in the case of fumarase and ribonucleotide reductase. Third, in some species, pathways that contain Fe-S enzymes are not present at all, such as the isoprenoid and quinolinic acid biosynthetic pathways in *Staphylococcus aureus* [3]. These modifications may be seen as evolutionary adaptation events in response to nutritional and environmental challenges faced by certain bacteria. Consequently, pathways involved in the assembly of Fe-S cofactors differ in their biosynthetic components and are subjected to distinct types of regulation.

5.3 Fe-S cluster assembly orthologous proteins

The Fe-S cluster biosynthetic pathways found in Gram-positive bacteria are different from those of well-studied Gram-negative bacteria. Initial identification of gene products suspected to be involved in Fe-S cluster formation was based on amino acid sequence similarity to proteins known to participate in the metabolism of Fe-S clusters in other organisms (Tab. 5.2). Prior to experimental validation, their functions are proposed to be analogous to those identified in other bacterial model systems. Genomes of Gram-positive bacteria, despite a few exceptions, contain one single pathway for the assembly and trafficking of Fe-S clusters. The apparent lack of redundancy suggests that gene-encoding components of this pathway are essential. In fact, high-throughput genomic analysis established that *suf* genes are essential in *B. subtilis* [4]; likewise, inactivation of the *Mycobacterium tuberculosis sufB* demonstrated that *SufB* was essential [5, 6]. Disruption of the *Str. thermophilus sufD* gene resulted in a slow-growth phenotype under iron-limiting conditions [7]. Identification of main Fe-S biosynthetic components in Gram-positive species, exemplified for selected species in Tab. 5.2, showed the occurrence of three types of genomic arrangements found in Actinobacteria, Bacilli, and Clostridia taxonomic classes (Fig. 5.1). When compared with the systems found in Gram-negative bacteria, they vary in composition and gene organization.

5.3.1 Clostridia-ISC system

A shorter version of the ISC system from *E. coli* is found in Clostridium species, a group of mainly rod-shaped anaerobes that includes *C. difficile*, *C. botulinum*, *C. beijerinckii*, *C. cellulolyticum*, *C. perfringens*, *C. thermocellum*, and *Carboxydothermus hydrogenoformans* (Fig. 5.1). The first gene in the operon encodes a transcriptional regulator similar to IscR. The clostridial IscR consensus sequence retains the three conserved cysteine residues proposed to coordinate a Fe-S cluster in the IscR homologue of *E. coli* but lacks the homologous histidine cluster ligand (His107 in *E. coli*). In

Tab. 5.2: Proteins known or suspected to be involved in Fe-S cluster biogenesis in Gram-positive bacteria.

	B. subtilis	*St. aureus*	*En. faecalis*	*L. casei*	*Li. monocytogenes*	*M. tuberculosis*	*M. smegmatis*	*Str. avermitilis*	*C. botulinum*	*C. difficile*
Cysteine desulfurase										
CD-Class I	BSU27150 (YrvO)[a]	SA2981_1580[a]	OG1RF_11765[a]	LCABL_15200[a]	MUO_07795[a]	MRA_3056[a]	MSMEI_2297[a]	SAV_2933	CLD_1997[d]	CD196_1141[d]
	BSU29590 (NifZ)[b]	SA2981_1674	OG1RF_10258	LCABL_14780[b]	MUO_08195[b]		MSMEI_1207	SAV_2756	CLD_3387	CD196_0700
	BSU27800 (NifS)[c]		OG1RF_11949		MUO-10340[c]		MSMEI_6085	SAV_6046		
							MSMEI_6196			
Class II	BSU32690 (SufS)[e]	SA2981_0799[e]	OG1RF_11827[e]	LCABL_14040[e]	MUO-12040[e]	MRA_1473[e]	MSMEI_3046[e]	SAV_6329[e]	CLD_0389	D196_3484
						MRA_3818	MSMEI_4425	SAV_6057	CLD_0841	CD196_2820
								SAV_7203		
								SAV_1061		
Sulfur transfer protein										
E-type (SufE)	–	–	–	–	–	–	–	–	–	–
U-type (SufU)	BSU32680 (SufU)	SA2981_0800	OG1RF_11826	LCABL_14050	MUO_12035	MRA_1474	MSMEI_3047	SAV_6330	–	–
Fe-S scaffold										
IscU	–	–	–	–	–	–	–	–	CLD_1998	CD196_1142
SufBCD	BSU32710 (SufC)	SA2981_0797	OG1RF_11829	LCABL_14020	MUO_12050	MRA_1472	MSMEI_3045	SAV_6328	–	–
	BSU32700 (SufD)	SA2981_0798	OG1RF_11828	LCABL_14030	MUO_12045	MRA_1471	MSMEI_3044	SAV_6326	–	–
	BSU32670 (SufB)	SA2981_0801	OG1RF_11825	LCABL_14060	MUO_12030	MRA_1470	MSMEI_3043	SAV_6325	–	–

Tab. 5.2 (continued)

Fe-S carrier										
A-type	BSU32160 (SufA)	SA2981_0895	–	–	–	MRA_2220	MSMEI_4171	SAV6042	–	–
Nfu-type	BSU32220 (Nfu)	SA2981_0891	–	–	MUO_11975	–	MSMEI_2651	–	–	CD196_0799
Iron sensor/donor										
Frataxin	BSU05750 (Fra)	–	–	LCABL_24650	MUO_02090	–	–	–	–	–
Unknown function										
SufT	BSU11160 (SufT)	SA2981_0927	OG1RF_11226	LCABL_17190	MUO_11595	MRA_1475	MSMEI_3048	SAV6331	–	–

B. subtilis, *St. aureus*, *En. faecalis*, *L. casei*, and *Li. monocytogenes* contain the Bacilli-SUF system; *M. tuberculosis*, *M. smegmatis*, and *Str. avermitilis* contain the Actinobacteria-SUF system; *C. botulinum* and *C. difficile* contain the Clostridia-ISC system.

Relevant genomic location coding sequence adjacent to [a] *mnmA*, [b] *thiI*, [c] *nadBCA* operon, [d] *iscU*, and [e] *sufU*.

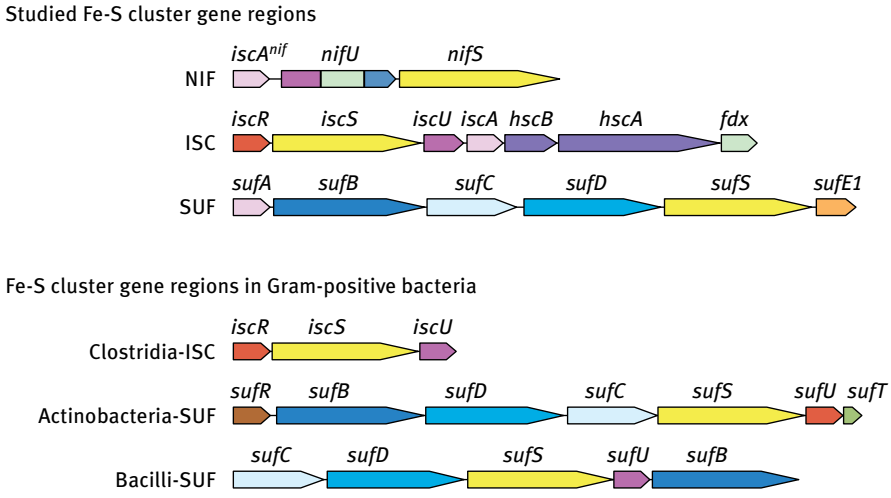

Fig. 5.1: Bacterial Fe-S cluster biosynthetic gene regions. Diagram representation shows the gene regions containing genes coding for the main Fe-S cluster biosynthetic components. Gene products displaying similar amino acid sequences are color-coded accordingly. Although not shown, some species of Actinobacteria class contain a ferredoxin-like coding sequence between *sufD* and *sufC*.

addition, clostridial IscR sequences also contain the conserved residues Tyr41, Glu43, Gln44, Arg59, which are involved in binding of IscR to DNA regulatory sequences [8]. Sequence similarities suggest that the mechanism by which clostridial IscR transcription regulates transcription is likely similar to the one described for *E. coli* (Mettert *et al.*, Chapter 13). Downstream of *iscR*, the *iscS* and *iscU* orthologous genes are located. Clostridial IscS is a class I cysteine desulfurase, similar to *E. coli* IscS and *A. vinelandii* IscS and NifS. It contains the conserved lysine involved in PLP binding and a conserved cysteine involved in the persulfide formation and sulfur transfer. The IscU protein sequences share more than 50% identity with the well-studied Fe-S cluster scaffold protein, IscU of *E. coli*, including (i) three conserved cysteine residues along with an aspartate located two residues away from the first cysteine, (ii) the LPP(V/A)K chaperone binding motif, and (iii) a histidine that precedes the third cysteine (Fig. 5.2). Although clostridial species lack the *hscA* and *hscB* chaperone and co-chaperone genes, their genomes encode one to two copies of *dnaK, grpE,* and *dnaJ* genes, which are always remotely located but may function as chaperones. It has previously been shown that the *Thermatoga maritima* DnaK is able to bind to *T. maritima* and *Homo sapiens* IscU and that complex formation affects the rate of cluster transfer [9]. Based on these observations, it seems plausible to propose that the Clostridia-ISC system uses the generic DnaKJ pair as chaperones during Fe-S cluster assembly.

In most clostridial species, the *mnmA* gene, which encodes tRNA-specific 2-thiouridylate, is located downstream of the *iscU* coding sequence. The proximity of the gene coding for the 2-thiouridylase MnmA to IscS suggests that IscS is involved in 2-thiouridine tRNA formation in clostridial species. Among Gram-positive bacteria

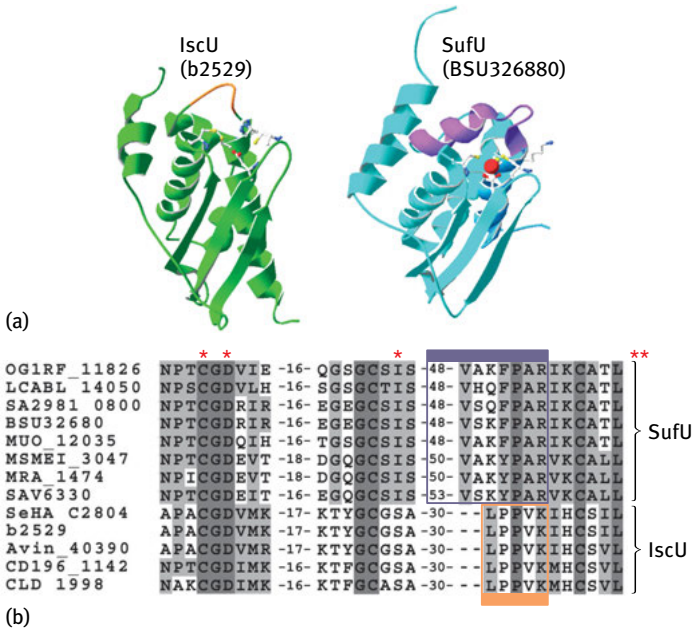

Fig. 5.2: Structural and amino acid sequence comparison among SufU and IscU sequences. (a) Ribbon representation of *E. coli IscU* (3LVIL) and *B. subtilis* SufU (1XJS). (b) Amino acid sequence alignment of IscU and SufU sequences from Gram-positive bacteria included in Tab. 5.1 and IscU sequences from *E. coli* (b2529) and *S. enterica* (SeHA_C2804). The alignment shows the three most conserved regions among IscU and SufU. The number of residues between regions are indicated. Strictly conserved residues in both SufU and IscU are highlighted in dark gray, whereas residues partially conserved are highlighted in light gray. The chaperone binding motif within IscU is colored in orange in the structure and the alignment. SufU sequences do not contain a standard LPPVK motif, but residues occupying equivalent positions show conservation within the last three residues (PAR), including the proline, followed by a small hydrophobic residue, and further followed by a positively charged residue. The 18–23 residue insertion unique to SufU sequences is colored in purple in the structure and the alignment. Although not shown in the figure, the consensus sequence of this insertion is FsemvqgkexvedxxxxilgD. Residues known to be important for the function of IscU and SufU are displayed in the structure as a stick-and-ball model and indicated with a star mark in the alignment. The zinc present in the SufU structure is displayed in space filling representation in red.

with sequenced genomes, components of the Clostridia-ISC are phylogenetically closer to components of the ISC system found in Gram-negative bacteria but are very different from systems found in other Gram-positive bacteria (Actinobacteria-SUF and Bacilli-SUF). This observation is not only supported by sequence identity of pathway components but also by potential involvement of the cysteine desulfurase IscS in the biosynthesis of Fe-S clusters and other thio-cofactors such as tRNA thio-modification, which is a feature of other Isc systems.

Notable exceptions to the generalization that clostridial species rely mainly on Isc systems were found in the nitrogen fixing *C. beijerinckii*, *C. lentocellum*,

and *C. acetobutylicum*. These species contain one copy of the Bacilli-SUF gene region (Fig. 5.1 and Tab. 5.2). Interestingly, *C. beijerinckii* contains two proposed Fe-S biosynthetic gene regions: one Clostridia-ISC and one Bacilli-SUF. Among 22 (known or proposed) diazotrophic (nitrogen-fixing) Gram-positive bacteria with sequenced genomes, 20 are species of the Clostridia taxonomic class. None of nitrogen fixing Clostridia contain components of the nitrogen fixing (NIF) Fe-S cluster biosynthetic pathway, suggesting that the general Fe-S cluster biosynthetic machinery is able to provide Fe-S clusters for both housekeeping and nitrogen fixation purposes [10].

5.3.2 Actinobacteria-SUF

In the species of Actinobacteria, aerobic bacteria that sometimes form branching filaments, the main Fe-S cluster gene region includes genes with sequence similarity to the *E. coli suf* genes (Fig. 5.1). The first gene in the operon encodes a transcriptional regulator SufR, which is similar to the transcriptional regulator of *sufBCDS* operon in Synechococcus, a marine cyanobacterium. SufR orthologous sequences from Actinobacteria also contain the three conserved cysteine residues thought to be the ligands of a 4Fe-4S cluster in Synechococcal IscR [11]. Despite utilizing a similar mechanism of transcription regulation, SufR is not homologous to IscR; their amino acid sequences show less than 20% identity and the cysteine residues proposed to coordinate a Fe-S cluster do not occupy equivalent positions within the primary sequence.

The Actinobacteria-SUF system also includes the SufB, SufC, and SufD proteins similar to the SufBCD complex found in Gram-negative bacteria. In *E. coli*, SufC is a soluble ATPase that forms a complex with SufD and/or SufB [12]. The latter is thought to serve as a platform for the synthesis of Fe-S clusters [13]. In *M. tuberculosis*, SufB is thought to be essential because a viable deletion strain could not be obtained [5]. Interestingly, in this organism, the *sufB* gene contains an intein domain, and its post-translational splicing of the peptide is crucial for the ability of SufB to interact with other SUF components, namely SufC and SufD [6]. Amino acid sequence alignment of SufB sequences indicated that there are only two cysteine residues, both of which are conserved and present in the *E. coli* SufB sequence (Cys254 and Cys405).

The sulfur mobilization step of Actinobacteria species is thought to involve the class II cysteine desulfurase, SufS. Its amino acid sequence is 64% and 60% similar to the *B. subtilis* and *E. coli* SufS enzymes, respectively. In this reaction, the sulfur is mobilized from the free amino acid cysteine to the proposed sulfur acceptor SufU *via* a PLP-dependent mechanism mediated by SufS. SufU shows 25% and 37% amino acid sequence identity to the Fe-S cluster scaffold IscU from *E. coli* and SufU from *B. subtilis*, respectively (Fig. 5.2). In some Actinobacteria species such as *Arthrobacter aurescens* and *Rothia dentocariosa*, *sufSU* genes are located in a separate gene region away from *sufRBDCT* operon. As discussed later in this chapter, the

co-occurrence of a cysteine desulfurase SufS and a U-type protein SufU is not a unique feature of Actinobacteria-SUF because Bacilli species also contain the *sufSU* gene pair.

Downstream of *sufU* is located *sufT*, whose function remains unidentified. SufT is a member of the Domain of Unknown Function 59 family (DUF59), which also includes components of eukaryotic Fe-S cluster biosynthetic pathways, such as AE7 [14], CIA2 [15], and the N-terminus of HC101 [16]. SufT orthologous sequences are also found in other Gram-positive species containing the Bacilli-SUF system but not in Clostridia-ISC or Gram-negative bacteria containing the ISC system (Tab. 5.2). The Cys62 residue in the *M. tuberculosis* sequence is conserved throughout SufT sequences from both Actinobacteria and Bacilli species.

5.3.3 Bacilli-SUF

The third and best studied Fe-S cluster biosynthetic gene region in Gram-positive bacteria is the Bacilli-SUF. Genes encoding the SUF components are located in the *sufCDSUB* operon, which displays an alternate order of genes of the Actinobacteria *suf* gene region operon and lacks the regulator *sufR*. In this system, the cysteine desulfurase SufS along with the sulfur acceptor protein SufU catalyzes the sulfur mobilization step [17]. The Bacilli-SUF also includes the SufC, SufD, and SufB proteins similar to the SufBCD from Actinobacteria and Gram-negative bacteria. In *B. subtilis*, SufC is an ATPase that forms a transient complex with SufD, and the binding of SufD to SufC enhances the rate of ATP hydrolysis by nearly 30-fold (unpublished data). Neither the mechanisms of SufC activation nor the step(s) in Fe-S cluster biogenesis and trafficking that involves ATP hydrolysis have been determined in any arrangement of SUF system found in either Gram-positive or Gram-negative bacteria. In *E. coli*, the $SufBC_2D$ complex is proposed to be the scaffold for the synthesis of Fe-S clusters during iron starvation and oxidative stress conditions [18]. Although a similar role is anticipated for Gram-positive SufBCD proteins, this proposal remains to be verified in Gram-positive bacteria.

Transcriptomic and proteomic analyses indicated that patterns of expression of genes involved in Fe-S biogenesis change in species containing the Bacilli-SUF system according to changes in environmental conditions. In a genome-wide expression study, Nicolas *et al.* quantified expression levels of 5,874 unique transcript sequences of *B. subtilis* samples [19]. Levels of whole genome transcript expression varied under 144 growth conditions, growth stages, and stress conditions such as temperature (16°C–51°C) and exposure to salt, H_2O_2, and paraquat. The *suf* genes were included in a subset of genes (<3% of coding sequences) that were always highly expressed, regardless of the condition tested. Additionally, a two-dimensional proteomics approach showed that SufC and SufB proteins accumulated upon challenge with salt and paraquat [20]. Expression of genes involved in Fe-S metabolism including biosynthetic SUF and Fe-S enzymes were also sensitive to copper stress through the copper-responsive transcriptional repressor, CsoR

[21]. In *B. anthracis*, proteomic and transcriptomic analysis after challenge with H_2O_2 and paraquat also showed increased expression of *suf* along with genes involved in Fe acquisition [22]. Likewise, *Str. thermophilus suf* genes have been associated with the defense against oxidative stress, as inactivation of *sufD* and *sufU* genes caused higher sensitivity to superoxide [7]. In group A Streptococcus, the expression of these genes was enhanced 2- to 4-fold upon challenge with H_2O_2 in both wild-type and *perR* deletion strains [23], indicating that upregulation of the Fe-S cluster biosynthetic system in this organism is not regulated by the peroxide stress response transcriptional regulator, PerR. Despite mounting evidence showing the expression of the *suf* genes, regulatory elements directly controlling expression of Bacilli-SUF have not been identified to date.

5.3.3.1 Sulfurtransferase reaction of SufS

The kinetic mechanism of the *B. subtilis* cysteine desulfurase SufS has been determined [17]. Although the overall mechanism of all cysteine desulfurases is thought to follow the same general path [24, 25], their physiological roles and catalytic reactivities are very distinct *in vitro*. Like other cysteine desulfurases, the first half of the *B. subtilis* SufS reaction involves the binding of free cysteine to the active site pyridoxal-5′-phosphate (PLP), leading to the formation of a Cys-PLP internal aldimine intermediate. This event triggers the activation of the substrate for the nucleophilic attack of the active site cysteine (Cys361 in *B. subtilis* SufS), which is the first committed step of the SufS reaction. The first half of this reaction is marked by the formation of a covalent enzyme S-intermediate (Cys361-persulfide) and release of the first product, alanine [17]. *In vitro*, the *B. subtilis* SufS can be partially regenerated through release of free sulfide by artificial reducing agents, such as DTT. *In vivo*, the second half of the reaction involves transfer of the terminal persulfide sulfur to the acceptor molecule SufU, which regenerates the SufS enzyme for the next catalytic cycle.

The *B. subtilis* SufS displayed very modest activity *in vitro* (~5 nmol alanine/min/mg) [17, 26]. These levels are comparable to the activities found for the *E. coli* SufS enzyme [27, 28]. Kinetic assays following the profile of alanine release showed that a kinetic burst was associated with the first turnover of the reaction. Interestingly, the amplitude of the burst phase (nanomoles of alanine product/nanomole of enzyme) was close to 0.5, suggesting that only one active site of the SufS dimer would be active at a time. This behavior, also observed in dimers and tetramers of other PLP-dependent enzymes, is characteristic of a flip-flop mechanism [17]. Analysis of the crystal structure of Synechocystis SufS enzyme (50% identical to *B. subtilis* SufS) shows that the protein environment surrounding the access of the active site is partially occupied by 13-residue loop from the other subunit of the dimer (residues 259–272 of the of Synechocystis SufS) [29]. This structural element could provide communication between subunits and serve as basis for a flip-flop mechanism. This segment is unique to class II cysteine desulfurases including enzymes from both Gram-positive and Gram-negative bacteria.

In the presence of its physiological substrate SufU, the catalytic rate of alanine and sulfide formation by SufS is enhanced nearly 200-fold. The kinetic scheme of this reaction has been characterized as a double displacement mechanism (ping-pong), wherein the release of the first product alanine precedes the binding of the second substrate, SufU. Besides the occurrence of the aforementioned kinetic burst, the characteristic activity profile of substrate saturation curves along with the essential role of the SufS Cys361 residue provided evidence for the proposed kinetic scheme (Fig. 5.3). The affinity of *B. subtilis* SufS for cysteine (K_{mCys} of 86 μM) was found to be near the physiological concentration of reduced cysteine. The K_m of the SufS for SufU was much lower (3 μM), indicating the high affinity of SufS for its sulfur acceptor molecule, SufU [17]. The cysteine:SufU sulfurtransferase reaction of the *B. subtilis* enzyme led to the proposal that other cysteine desulfurases would follow the same scheme. In fact, a recent study showed a similar kinetic profile for the cysteine:SufE sulfurtransferase reaction of the *E. coli* SufS enzyme [28]. However, in this case, the sulfur transfer reaction was resistant to reductive cleavage by DTT [27].

SufS is proposed to be the major S-donor for the biosynthesis of Fe-S clusters in Bacilli species. The reaction is thought to involve the direct sulfur transfer to SufU. However, it is possible that SufS also forms partnerships with yet-unidentified sulfur acceptor molecules and participates in additional sulfur transfer reactions for the biosynthesis of other thio-cofactors that do not contain metals.

5.3.3.2 Sulfur acceptor SufU

The second half of the cysteine desulfurase reaction is controlled by the nucleophilic attack of a thiolate group of SufU onto the persulfide sulfur of SufS Cys361. SufU has three conserved cysteine residues (Cys41, Cys63, and Cys128 in *B. subtilis*), which are mandatory for its sulfurtransferase activity [26]. Alkylation of SufU

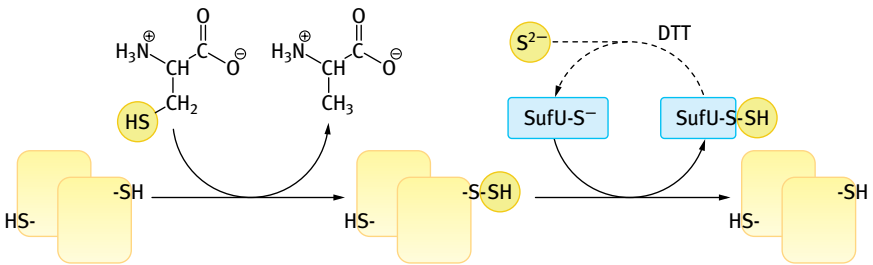

Fig. 5.3: Kinetic scheme of the cysteine:SufU sulfur transferase reaction of SufS. The reaction proceeds *via* a ping-pong mechanism where the formation of a covalent S-enzyme intermediate at Cys361 of SufS and release of alanine precede the binding of the second substrate, SufU. In *in vitro* reactions in the presence of DTT, the second product, SufU-SSH, is recycled through release of sulfide (dashed lines).

with iodoacetamide ($SufU_{alk}$) eliminates its ability to participate in the sulfurtransferase reaction of SufS; $SufU_{alk}$ acts as a noncompetitive inhibitor of Suf in competition assays, although $SufU_{alk}$ is still able to interact with SufS. The strong inhibition of $SufU_{alk}$ (IC_{50} of 0.37 μM) displays positive cooperative behavior, suggesting that one molecule of $SufU_{alk}$ inhibits two active sites of SufS. This pattern of inhibition is consistent with the flip-flop mechanism of SufS where the binding of one molecule of $SufU_{alk}$ to one subunit of SufS inhibits both subunits of the SufS dimer [17]. Site-directed mutagenesis revealed that substitution of Cys41 to Ala uniquely elicited an inhibitory effect similar to that of $SufU_{alk}$. Interestingly, the tight binding of SufS to the SufUC41A variant occurs only in the presence of cysteine, indicating that the SufUC41A does not interfere with the free form of the cysteine desulfurase [26].

In *Enterococcus faecalis*, another member of the Bacillus genus, SufU also enhances the activity of SufS [30]. Similar to *B. subtilis*, the three conserved cysteine residues (Cys35, Cys41, and Cys128) are also critical for the sulfurtransferase activity of the *En. faecalis* SufU. Mass spectrometry analysis of a trypsin digest of a reaction containing *En. faecalis* SufU, SufS, and cysteine showed that there was a +64 mass shift (i.e. two additional sulfur atoms) associated with the peptide containing the SufS active site Cys365. This analysis did not show the presence of any modifications in peptides containing the three conserved cysteine residues, but a +32 mass shift was identified in the peptide containing the Cys153 of SufU. Unlike other SufU sequences, the *En. faecalis* protein contains a fourth nonconserved cysteine residue (Cys153) near the C-terminal end [30].

SufU displays primary and tertiary structural similarities to IscU, with some notable differences. The structural alignment of the *B. subtilis* SufU NMR and IscU crystal structures shows on average 3-Å root mean square deviation, a measure of tertiary alignment according to a network service that compare three-dimensional protein structures, the DALI server (Fig. 5.2). The three conserved cysteines along with the aspartate (Asp43) are located in close proximity to both IscU and SufU structures. In the *B. subtilis* SufU structure, these residues provide the tetracoordination to a zinc atom [31]. Notably, zinc was also found in structures of IscU [32, 33]. However, the binding of zinc to IscU seems to be adventitious and does not interfere with the Fe-S cluster assembly reaction. Meanwhile, the binding of zinc to SufU is tight and it is not displaced under conditions known to retain a Fe-S cluster on scaffold protein [62], indicating important differences between these two subfamilies for proteins. Diagnostic features of SufU sequences are the absence of a complete chaperone binding motif (LPPVK) and presence of an 18- to 21-amino acid sequence inserted before the third cysteine (Fig. 5.2) [34]. Interestingly, all SufU sequences also contain a conserved lysine residue (Lys127) in place of the essential histidine immediately preceding the last cysteine (His105 in *E. coli* IscU) [35]. Neither the function of the histidine on IscU nor the function of the lysine on SufU has been determined.

In *B. subtilis*, inactivation of *sufU* has been suggested to be lethal [4], whereas a conditional knockout strain showed pronounced growth defects [36]. Cell extracts depleted of SufU have impaired Fe-S metabolism as evidenced by more than 50% reduction in the levels of aconitase and succinate dehydrogenase activity. Additionally, SufU was able to accelerate the rate of *in vitro* reconstitution of the yeast 4Fe-4S cluster-containing Leu1 enzyme upon incubation with iron and sulfide, leading to the proposal that this protein could serve as a platform for the synthesis of Fe-S clusters [36]. However, unlike the standard scaffold IscU, Fe-S cluster-loaded SufU has not been isolated, an observation that justifies additional investigation on the role of this protein.

5.3.3.3 Cysteine desulfurases involved in the biosynthesis of other thio-cofactors

The SufU-dependent activity of SufS suggests the existence of alternate routes for sulfur transfer. In fact, the *B. subtilis* genome contains four additional putative cysteine desulfurases genes: *yrvO, nifS, nifZ,* and *ycbU*. Amino acid sequence comparison to known cysteine desulfurases shows that all four are members of group I, which includes the studied NifS and IscS from Gram-negative bacteria [37]. Initial analyses of the kinetic properties of these enzymes showed that, with the exception of YcbU, all enzymes displayed reactivity toward cysteine [38, 39]. In *E. coli* and other organisms containing the ISC system, the biosynthesis of Fe-S clusters is coupled to the formation of other sulfur-containing cofactors [40]. First, IscS catalyzes the first step of sulfur mobilization for the synthesis other thio-cofactors. Second, Fe-S enzymes are essential participants in the biosynthesis of sulfur-containing cofactors such as thiamine (ThiH [41] and ThiC [42]), thio-tRNA (MiaB [43, 44] and TtcA [45]), biotin (BioB [43]), Mo-cofactor (MoaA [46]), and lipoic acid (LipA [47]). In Bacilli and Actinobacteria, the presence of additional cysteine desulfurases suggests that sulfur mobilization for the synthesis of thio-cofactors is not coupled to Fe-S cluster biogenesis, and their genomic locations gives hints into their physiological functions.

NifZ is a cysteine desulfurase devoted to the biosynthesis of 4-thiouridine tRNA [38]. In *B. subtilis* and most Gram-positive bacteria, a cysteine desulfurase gene (*nifZ*) is located adjacent to *thiI*. The co-occurrence of the *nifZ-thiI* gene pair in several Gram-positive bacterial species suggests that they are partners in mediating sulfur transfer reactions. In *E. coli* and *S. enterica*, IscS and ThiI participate in the biosynthesis of thiamine and 4-thiouridine (s^4U8) [48]. Gene inactivation studies in *B. subtilis* indicated that both NifZ and ThiI are essential for the synthesis of s^4U8 but not thiamine. Interestingly, complementation studies in *ΔiscS* or *ΔthiI* strains of *E. coli* showed that s^4U8 synthesis was restored only when both NifZ and ThiI were present [38], indicating their mutual dependence. It is possible that Gram-positive ThiI sequences, which lack the rhodanase sulfurtransferase domain, required a dedicated cysteine desulfurase, as they do not compete well with other sulfur acceptors for the general cysteine desulfurase, IscS.

A similar pattern of specific partnership between cysteine desulfurase and sulfur acceptor might also involve the cysteine desulfurase, YrvO from *B. subtilis*. Following a similar biosynthetic scheme as s^4U8, post-transcriptional modification of the wobble base on $tRNA^{Lys/Gln/Glu}$ involves the insertion of a sulfur atom at the C2 position of a uridine base (s^2U34) [49]. In *E. coli*, this pathway also includes IscS, which transfers the sulfur indirectly to the activating thiouridylase, MnmA, *via* a five-component sulfur-relay system, TusABCDE [50]. In *B. subtilis*, the *mnmA* (*trmU*) gene coding for tRNA (5-methylaminomethyl-2-thiouridylate)-methyltransferase is adjacent to the *yrvO* coding sequence, and most Gram-positive bacteria lack the *tusABCDE* genes, leading to the hypothesis that YrvO provides sulfur directly to MnmA. Gene inactivation studies in *B. subtilis* indicate that both *yrvO* and *mnmA* are essential genes [4], suggesting that the sulfur transfer reaction from YrvO to MnmA is indispensible.

Located upstream of *yrvO* is *cymR*, which encodes the global regulator of cysteine metabolism. In *St. aureus* [51], this transcriptional regulator mediates changes in gene expression upon response to oxidative stress. It has been proposed that oxidative challenge with H_2O_2 induces oxidation through formation of sulfenic acid on the single cysteine residue (Cys25) of CymR. This modification decreases its DNA binding affinity by nearly 20-fold [52]. In *B. subtilis*, deletion of *cymR* causes several metabolic defects manifested by (i) slow growth rate, (ii) sensitivity to H_2O_2 and paraquat, (iii) depletion of branched chain amino acids, and (iv) elevated cysteine levels and hydrogen sulfide production [53]. CymR is a member of the Rrf2 family of transcription regulators along with IscR and NsrR, but it differs in that it lacks residues involved in Fe-S cluster coordination [54]. In fact, the *B. subtilis* CymR sequence does not contain any cysteine residues, indicating that it employs a distinctive mode of regulation. Unlike *St. aureus*, CymR affinity for DNA in *B. subtilis* is modulated upon complex formation with CysK [55]. Nevertheless, the *cymR-yrvO-mnmA* operon connects distinct aspects of sulfur acquisition and metabolism to oxidative stress, conditions known to affect Fe-S metabolism.

NifS was the first cysteine desulfurase to be studied at the genetic level in *B. subtilis*. In 1993, Sun and Setlow [56] identified two genes upstream of the *B. subtilis nadBCA* operon associated with the biosynthesis of nicotinamide adenine dinucleotide (NAD). The first gene, *nifS*, encodes a cysteine desulfurase, and *nadR* encodes a transcriptional repressor of both the *nadBCA* and *nifS-nadR* operons (Fig. 5.4) [57]. The *B. subtilis* Δ*nifS* strain is unable to synthesize quinolinic acid, an intermediate of the NAD pathway [56]. This metabolic defect can be circumvented by activating the salvage pathway through provision of nicotinic acid in the growth media. Neither nicotinic acid nor NAD are thio-cofactors, but the enzyme that catalyzes the second step in the *de novo* pathway, NadA, is a [4Fe-4S] cluster-containing enzyme [58]. Therefore, it has been suggested that NifS participation in NAD synthesis is indirect, as it facilitates the synthesis of the Fe-S cofactor of NadA, although a potential scaffold partner for this NifS has not been identified.

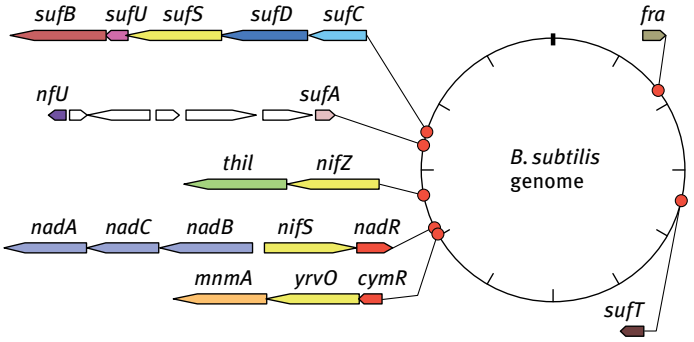

Fig. 5.4: Genomic location of genes known or suspect to be involved in Fe-S metabolism in *B. subtilis*. Diagram representation shows the relative chromosomal location, size, and orientation of genes included in Tab. 5.1 and the relevant genomic neighborhood.

5.3.3.4 Additional proteins involved in Fe-S metabolism

Besides the main Fe-S biosynthetic system, additional coding sequences similar to proteins involved in Fe-S metabolism were identified in Gram-positive bacteria (Tab. 5.2). Single copies of A-type Fe-S carrier similar to ErpA, IscA, and SufA are present in some species [59]. Amino acid sequence alignments showed that these sequences are more similar to ErpA than IscA and SufA. In *E. coli*, the three A-type carriers exert partial redundant functions in Fe-S metabolism and ErpA has been shown to be an essential respiratory protein required for activation of Fe-S enzymes IspH and IspG [60]. Although IspH and IspG are essential enzymes in *B. subtilis*, inactivation of the single A-type carrier gene *sufA* (*yutM*) showed no growth phenotype or any defects in Fe-S enzymes [36]. These observations indicate that in Gram-positive bacteria, A-type carriers may serve alternative cellular purposes or that the route of Fe-S delivery may also utilize a distinct subset of cluster carriers. Approximately 5 kb downstream of *sufA*, an *nfu* gene that encodes a second type of Fe-S cluster scaffold/carrier is found in Gram-positive bacteria. Similarly to A-type carriers, genes encoding Nfu domain proteins are present as single copies, within small proteins that are devoid of additional domains. Nfu sequences from Gram-positive bacteria also contain a CxxC motif, suggesting that these Nfu proteins may coordinate transient Fe-S clusters. Transcriptomic analysis in *B. subtilis* cultured under a variety of growth conditions and stress challenges showed that *sufA* and *nfu* were always expressed regardless of growth stage or condition similar to the expression pattern of the *sufCDSUB* genes. Interestingly, these seven genes, proposed to promote the assembly and trafficking of Fe-S clusters, were expressed on average five times higher than other *B. subtilis* genes [19].

Lastly, frataxin orthologous genes (related to Yfh of *Saccharomyces cerevisisiae* and human frataxin, which causes Friedreich ataxia when deficient) are scattered across Gram-positive bacterial genomes. In *B. subtilis*, Fra (YdhG) is important for maintaining iron homeostasis. When cultured in minimum medium, *B. subtilis*

strains lacking Fra displayed severe growth defects. In rich medium, *B. subtilis fra* knockout strains lacked the bacillibactin siderophore and showed increased levels of iron and decreased activity of the Fe-S enzyme, aconitase [61]. *In vitro* assays showed that iron-bound Fra could serve as the iron donor for the SufU-mediated activation of aconitase. These observations led to a model of which Fra could serve as a cellular iron donor for the synthesis of Fe-S clusters by the SUF system [61]. Although Fra is an important component of iron-metabolism in *B. subtilis*, its function(s) are not limited to its role in Gram-positive SUF systems because phenotypes associated with its deletion are distinct from those observed upon *sufU* deletion. In addition, *fra* is absent in most Gram-positive species that contain the SUF system.

5.4 Concluding remarks and remaining questions

In the last few years, the availability of genomic information has resulted in the identification of numerous proteins involved in Fe-S biogenesis, which has propelled initial biochemical investigation of their associated functions. However, many biochemical steps involved in the synthesis of Fe-S clusters remain to be explored. Apart from the involvement of SufS in sulfur mobilization, the subsequent reactions involving the synthesis and delivery of the Fe-S clusters have not been well defined. The identity and roles of proposed scaffold protein(s), the involvement of an ATP-dependent reaction during synthesis and/or delivery of clusters, and the participation of protein carriers constitute some of the key questions to be addressed in future studies. The Actinobacteria- and Bacilli-SUF systems contain SufU, a sulfur acceptor of SufS that is proposed to be a Fe-S cluster scaffold based on its sequence similarity to IscU and its ability to enhance the activation of Fe-S enzymes. This system also includes SufBCD, which is orthologous to the Fe-S cluster scaffold of the *E. coli* SUF system. The occurrence of two potential scaffolds within the main pathway seems paradoxical [62]. Whether these components have evolved to serve different cellular purposes or to assist Fe-S cluster biogenesis in a single concerted pathway remains to be identified. Interestingly, like the Gram-negative-SUF system, the Gram-positive SUF systems also include the SufC ATPase, whose activity is crucial for function of the pathway. The mechanisms by which ATPase activity of SufC enables cluster synthesis and/or delivery is not understood. Furthermore, the involvement of additional cellular components such as SufA and Nfu remains to be identified. The lack of phenotypes associated with the inactivation of SufA raises questions about its function: When are additional biosynthetic components recruited? Do they serve a specific clientele of Fe-S targets? Are they recruited during specific physiological conditions?

Although the essential role of SUF components in Gram-positive bacteria provides relevance for the study of Fe-S cluster biogenesis, it also poses a technical challenge for *in vivo* validation of proposed biosynthetic schemes. The dependency of Fe-S biosynthetic components for cell survival can be seen as a consequence of

the requirement for participation of certain Fe-S enzymes catalyzing indispensable reactions. The identification of Fe-S proteins performing critical reactions not only opens an avenue for the discovery of new metabolic targets to treat infections caused by Gram-positive pathogens but also enables the development of viable genetic approaches to study the functions of their biosynthetic components. It appears that species that contain fewer Fe-S enzymes (Tab. 5.1) may offer good model systems for dissecting the specific roles of Fe-S biogenesis enzymes.

References

[1] Py B, Barras F. Building Fe-S proteins: bacterial strategies. Nat Rev Microbiol 2010;8:436–46.
[2] Saini V, Farhana A, Glasgow JN, Steyn AJ. Iron sulfur cluster proteins and microbial regulation: implications for understanding tuberculosis. Curr Opin Chem Biol 2012;16:45–53.
[3] Caspi R, Altman T, Dreher K, et al. The MetaCyc database of metabolic pathways and enzymes and the BioCyc collection of pathway/genome databases. Nucleic Acids Res 2012;40:D742–53.
[4] Kobayashi K, Ehrlich SD, Albertini A, et al. Essential Bacillus subtilis genes. Proc Natl Acad Sci USA 2003;100:4678–83.
[5] Huet G, Daffe M, Saves I. Identification of the Mycobacterium tuberculosis SUF machinery as the exclusive mycobacterial system of [Fe-S] cluster assembly: evidence for its implication in the pathogen's survival. J Bacteriol 2005;187:6137–46.
[6] Huet G, Castaing JP, Fournier D, Daffe M, Saves I. Protein splicing of SufB is crucial for the functionality of the Mycobacterium tuberculosis SUF machinery. J Bacteriol 2006;188:3412–4.
[7] Thibessard A, Borges F, Fernandez A, Gintz B, Decaris B, Leblond-Bourget N. Identification of Streptococcus thermophilus CNRZ368 genes involved in defense against superoxide stress. Appl Environ Microbiol 2004;70:2220–9.
[8] Rajagopalan S, Teter SJ, Zwart PH, Brennan RG, Phillips KJ, Kiley PJ. Studies of IscR reveal a unique mechanism for metal-dependent regulation of DNA binding specificity. Nat Struct Mol Biol 2013;20:740–7.
[9] Wu SP, Mansy SS, Cowan JA. Iron-sulfur cluster biosynthesis. Molecular chaperone DnaK promotes IscU-bound [2Fe-2S] cluster stability and inhibits cluster transfer activity. Biochemistry 2005;44:4284–93.
[10] Dos Santos PC, Fang Z, Mason SW, Setubal JC, Dixon R. Distribution of nitrogen fixation and nitrogenase-like sequences amongst microbial genomes. BMC Genomics 2012;13:162.
[11] Shen G, Balasubramanian R, Wang T, et al. SufR coordinates two [4Fe-4S]2+,1+ clusters and functions as a transcriptional repressor of the sufBCDS operon and an autoregulator of sufR in cyanobacteria. J Biol Chem 2007.
[12] Outten FW, Wood MJ, Munoz FM, Storz G. The SufE protein and the SufBCD complex enhance SufS cysteine desulfurase activity as part of a sulfur transfer pathway for Fe-S cluster assembly in Escherichia coli. J Biol Chem 2003;278:45713–9.
[13] Layer G, Gaddam SA, Ayala-Castro CN, et al. SufE Transfers Sulfur from SufS to SufB for Iron-Sulfur Cluster Assembly. J Biol Chem 2007;282:13342–50.
[14] Luo D, Bernard DG, Balk J, Hai H, Cui X. The DUF59 family gene AE7 acts in the cytosolic iron-sulfur cluster assembly pathway to maintain nuclear genome integrity in Arabidopsis. Plant Cell 2012;24:4135–48.
[15] Stehling O, Mascarenhas J, Vashisht AA, et al. Human CIA2A-FAM96A and CIA2B-FAM96B integrate iron homeostasis and maturation of different subsets of cytosolic-nuclear iron-sulfur proteins. Cell Metab 2013;18:187–98.

[16] Schwenkert S, Netz DJ, Frazzon J, et al. Chloroplast HCF101 is a scaffold protein for [4Fe-4S] cluster assembly. Biochem J 2009;425:207–14.
[17] Selbach B, Earles E, Dos Santos PC. Kinetic analysis of the bisubstrate cysteine desulfurase SufS from Bacillus subtilis. Biochemistry 2010;49:8794–802.
[18] Saini A, Mapolelo DT, Chahal HK, Johnson MK, Outten FW. SufD and SufC ATPase activity are required for iron acquisition during in vivo Fe-S cluster formation on SufB. Biochemistry 2010;49:9402–12.
[19] Nicolas P, Mader U, Dervyn E, et al. Condition-dependent transcriptome reveals high-level regulatory architecture in Bacillus subtilis. Science 2012;335:1103–6.
[20] Tam le T, Antelmann H, Eymann C, Albrecht D, Bernhardt J, Hecker M. Proteome signatures for stress and starvation in Bacillus subtilis as revealed by a 2-D gel image color coding approach. Proteomics 2006;6:4565–85.
[21] Chillappagari S, Miethke M, Trip H, Kuipers OP, Marahiel MA. Copper acquisition is mediated by YcnJ and regulated by YcnK and CsoR in Bacillus subtilis. J Bacteriol 2009;191:2362–70.
[22] Pohl S, Tu WY, Aldridge PD, et al. Combined proteomic and transcriptomic analysis of the response of Bacillus anthracis to oxidative stress. Proteomics 2011;11:3036–55.
[23] Le Breton Y, Mistry P, Valdes KM, et al. Genome-wide identification of genes required for fitness of group A Streptococcus in human blood. Infect Immun 2013;81:862–75.
[24] Zheng L, White RH, Cash VL, Dean DR. Mechanism for the desulfurization of L-cysteine catalyzed by the nifS gene product. Biochemistry 1994;33:4714–20.
[25] Behshad E, Bollinger JM Jr. Kinetic analysis of cysteine desulfurase CD0387 from Synechocystis sp. PCC 6803: formation of the persulfide intermediate. Biochemistry 2009;48:12014–23.
[26] Albrecht AG, Peuckert F, Landmann H, Miethke M, Seubert A, Marahiel MA. Mechanistic characterization of sulfur transfer from cysteine desulfurase SufS to the iron-sulfur scaffold SufU in Bacillus subtilis. FEBS Lett 2011;585:465–70.
[27] Selbach BP, Pradhan PK, Dos Santos PC. Protected sulfur transfer reactions by the Escherichia coli Suf system. Biochemistry 2013;52:4089–96.
[28] Dai Y, Outten FW. The E. coli SufS-SufE sulfur transfer system is more resistant to oxidative stress than IscS-IscU. FEBS Lett 2012;586:4016–22.
[29] Tirupati B, Vey JL, Drennan CL, Bollinger JM Jr. Kinetic and structural characterization of Slr0077/SufS, the essential cysteine desulfurase from Synechocystis sp. PCC 6803. Biochemistry 2004;43:12210–9.
[30] Riboldi GP, de Oliveira JS, Frazzon J. Enterococcus faecalis SufU scaffold protein enhances SufS desulfurase activity by acquiring sulfur from its cysteine-153. Biochim Biophys Acta 2011;1814:1910–8.
[31] Kornhaber GJ, Snyder D, Moseley HN, Montelione GT. Identification of zinc-ligated cysteine residues based on 13Calpha and 13Cbeta chemical shift data. J Biomol NMR 2006;34:259–69.
[32] Liu J, Oganesyan N, Shin DH, et al. Structural characterization of an iron-sulfur cluster assembly protein IscU in a zinc-bound form. Proteins 2005;59:875–81.
[33] Ramelot TA, Cort JR, Goldsmith-Fischman S, et al. Solution NMR structure of the iron-sulfur cluster assembly protein U (IscU) with zinc bound at the active site. J Mol Biol 2004;344:567–83.
[34] Johnson DC, Dean DR, Smith AD, Johnson MK. Structure, function, and formation of biological iron-sulfur clusters. Annu Rev Biochem 2005;74:247–81.
[35] Johnson DC, Unciuleac MC, Dean DR. Controlled expression and functional analysis of iron-sulfur cluster biosynthetic components within Azotobacter vinelandii. J Bacteriol 2006;188:7551–61.
[36] Albrecht AG, Netz DJ, Miethke M, et al. SufU is an essential iron-sulfur cluster scaffold protein in Bacillus subtilis. J Bacteriol 2010.

[37] Mihara H, Esaki N. Bacterial cysteine desulfurases: their function and mechanisms. Appl Microbiol Biotechnol 2002;60:12–23.
[38] Rajakovich LJ, Tomlinson J, Dos Santos PC. Functional analysis of Bacillus subtilis genes involved in the biosynthesis of 4-thiouridine in tRNA. J Bacteriol 2012;194:4933–40.
[39] Park JH, Dorrestein PC, Zhai H, Kinsland C, McLafferty FW, Begley TP. Biosynthesis of the thiazole moiety of thiamin pyrophosphate (vitamin B1). Biochemistry 2003;42:12430–8.
[40] Mueller EG. Trafficking in persulfides: delivering sulfur in biosynthetic pathways. Nat Chem Biol 2006;2:185–94.
[41] Leonardi R, Fairhurst SA, Kriek M, Lowe DJ, Roach PL. Thiamine biosynthesis in Escherichia coli: isolation and initial characterisation of the ThiGH complex. FEBS Lett 2003;539:95–9.
[42] Raschke M, Burkle L, Muller N, et al. Vitamin B1 biosynthesis in plants requires the essential iron sulfur cluster protein, THIC. Proc Natl Acad Sci USA 2007;104:19637–42.
[43] Booker SJ, Cicchillo RM, Grove TL. Self-sacrifice in radical S-adenosylmethionine proteins. Curr Opin Chem Biol 2007;11:543–52.
[44] Anton BP, Russell SP, Vertrees J, et al. Functional characterization of the YmcB and YqeV tRNA methylthiotransferases of Bacillus subtilis. Nucleic Acids Res 2010.
[45] Jager G, Leipuviene R, Pollard MG, Qian Q, Bjork GR. The conserved Cys-X1-X2-Cys motif present in the TtcA protein is required for the thiolation of cytidine in position 32 of tRNA from Salmonella enterica serovar Typhimurium. J Bacteriol 2004;186:750–7.
[46] Hanzelmann P, Schindelin H. Crystal structure of the S-adenosylmethionine-dependent enzyme MoaA and its implications for molybdenum cofactor deficiency in humans. Proc Natl Acad Sci USA 2004;101:12870–5.
[47] Cicchillo RM, Lee KH, Baleanu-Gogonea C, Nesbitt NM, Krebs C, Booker SJ. Escherichia coli lipoyl synthase binds two distinct [4Fe-4S] clusters per polypeptide. Biochemistry 2004;43:11770–81.
[48] Martinez-Gomez NC, Palmer LD, Vivas E, Roach PL, Downs DM. The rhodanese domain of ThiI is both necessary and sufficient for synthesis of the thiazole moiety of thiamine in Salmonella enterica. J Bacteriol 2011;193:4582–7.
[49] Numata T, Ikeuchi Y, Fukai S, Suzuki T, Nureki O. Snapshots of tRNA sulphuration via an adenylated intermediate. Nature 2006;442:419–24.
[50] Ikeuchi Y, Shigi N, Kato J, Nishimura A, Suzuki T. Mechanistic insights into sulfur relay by multiple sulfur mediators involved in thiouridine biosynthesis at tRNA wobble positions. Mol Cell 2006;21:97–108.
[51] Soutourina O, Dubrac S, Poupel O, Msadek T, Martin-Verstraete I. The pleiotropic CymR regulator of Staphylococcus aureus plays an important role in virulence and stress response. PLoS Pathog 2010;6:e1000894.
[52] Ji Q, Zhang L, Sun F, et al. Staphylococcus aureus CymR is a new thiol-based oxidation-sensing regulator of stress resistance and oxidative response. J Biol Chem 2012;287:21102–9.
[53] Hullo MF, Martin-Verstraete I, Soutourina O. Complex phenotypes of a mutant inactivated for CymR, the global regulator of cysteine metabolism in Bacillus subtilis. FEMS Microbiol Lett 2010;309:201–7.
[54] Shepard W, Soutourina O, Courtois E, England P, Haouz A, Martin-Verstraete I. Insights into the Rrf2 repressor family – the structure of CymR, the global cysteine regulator of Bacillus subtilis. FEBS J 2011;278:2689–701.
[55] Tanous C, Soutourina O, Raynal B, et al. The CymR regulator in complex with the enzyme CysK controls cysteine metabolism in Bacillus subtilis. J Biol Chem 2008;283:35551–60.
[56] Sun D, Setlow P. Cloning, nucleotide sequence, and regulation of the Bacillus subtilis nadB gene and a nifS-like gene, both of which are essential for NAD biosynthesis. J Bacteriol 1993;175:1423–32.

[57] Rossolillo P, Marinoni I, Galli E, Colosimo A, Albertini AM. YrxA is the transcriptional regulator that represses de novo NAD biosynthesis in Bacillus subtilis. J Bacteriol 2005;187:7155–60.
[58] Marinoni I, Nonnis S, Monteferrante C, et al. Characterization of L-aspartate oxidase and quinolinate synthase from Bacillus subtilis. FEBS J 2008;275:5090–107.
[59] Vinella D, Brochier-Armanet C, Loiseau L, Talla E, Barras F. Iron-sulfur (Fe/S) protein biogenesis: phylogenomic and genetic studies of A-type carriers. PLoS Genet 2009;5:e1000497.
[60] Loiseau L, Gerez C, Bekker M, et al. ErpA, an iron sulfur (Fe S) protein of the A-type essential for respiratory metabolism in Escherichia coli. Proc Natl Acad Sci USA 2007;104:13626–31.
[61] Albrecht AG, Landmann H, Nette D, et al. The frataxin homologue Fra plays a key role in intracellular iron channeling in Bacillus subtilis. Chembiochem 2011;12:2052–61.
[62] Selbach BP, Chung AH, Scott AD, George SJ, Cramer SP, Dos Santos PC. Fe-S cluster biogenesis in Gram-positive bacteria: SufU is a zinc-dependent sulfur transfer protein. Biochemistry 2014;53:152–60.

6 Fe-S cluster assembly and regulation in yeast

Debkumar Pain and Andrew Dancis

6.1 Introduction

The general scheme by which iron-sulfur (Fe-S) clusters are assembled has come into clearer view recently through work in the model eukaryote *Saccharomyces cerevisiae*. Fe-S cluster assembly components have been discovered by a variety of genetic screens based on iron homeostasis, amino acid biosynthesis, ribosome biogenesis, DNA repair, tRNA thiolation, and oxidant stress protection, all linking to Fe-S cluster assembly components. The mitochondrial system, termed ISC for Fe-S cluster assembly, is a complete machinery and is able to synthesize Fe-S clusters on its own. The central feature is the Isu scaffold, and many components are involved in making the Fe-S cluster intermediate on the Isu scaffold. These include Nfs1/Isd11, which provides cysteine desulfurase activity and contributes sulfur from the amino acid cysteine. Several regulatory conformational changes in Nfs1 are associated with the cysteine desulfurase activity, including stimulation by frataxin and Isd11. The Fe-S cluster intermediate on the Isu scaffold is transferred to recipients in a process involving ATP-dependent chaperones, Ssq1 and Jac1, and Grx5, a glutaredoxin able to coordinate Fe-S clusters in the presence of glutathione. Glutathione is involved in multiple stages of Fe-S cluster assembly *via* interactions with monothiol glutaredoxins inside and outside mitochondria. A parallel cytoplasmic Fe-S cluster machinery, termed CIA for cytoplasmic Fe-S protein assembly, has never been reconstituted, but its constituents, including scaffold, reductase, and transfer components, are required for formation of cytoplasmic and nuclear Fe-S cluster proteins. The Atm1 transporter is an exporter of the mitochondrial inner membrane with its substrate-binding site oriented toward the mitochondrial interior, and thus, it may export a substrate or a signal from mitochondria to the cytoplasm. Defects of ISC components, but not the CIA components, lead to a special iron homeostatic phenotype, characterized by activation of the cellular iron uptake system and accumulation of iron in mitochondria.

6.2 Yeast and Fe-S cluster assembly – evolutionary considerations

All kingdoms of life contain Fe-S cluster proteins, and all kingdoms possess at least one Fe-S cluster assembly machinery. Prokaryotes use ISC, plants and Archaea use SUF (for sulfur mobilization), and high-output systems such as *Azotobacter vinelandii* with abundant nitrogenase use NIF (for nitrogen fixation) [1]. The systems have common features such as the use of cysteine desulfurase to provide sulfur, the central role of scaffold proteins for Fe-S cluster synthesis, and the chaperone functions to transfer Fe-S cluster intermediates to recipient proteins [2]. In eukaryotes, such as the yeast *S. cerevisiae*, the ISC

DOI 10.1515/9783110479850-006

machinery was acquired from purple bacteria as part of the endosymbiotic events that gave rise to mitochondria. Thus, many of the components of the yeast mitochondrial Fe-S cluster system are conserved and are recognizable by orthology or homology with the bacterial counterparts [3].

6.2.1 Nfs1 and the surprise of Isd11

The sulfur for Fe-S cluster synthesis is derived exclusively from the amino acid cysteine *via* the action of enzymes called cysteine desulfurases (Fig. 6.1). The role of these enzymes in Fe-S cluster assembly was discovered by the pioneering work of Dennis Dean. The *A. vinelandii* NIF operon carries NifS, the founding member of this enzyme group [4]. Key features of the enzyme include a substrate-binding site containing the cofactor pyridoxal phosphate that interacts with the substrate cysteine, and a cysteine residue in the active site that performs a nucleophilic attack on the enzyme-bound substrate for sulfur abstraction [5]. The bacterial ISC operon carries a cysteine desulfurase with these features [2], and the yeast nuclear genome contains a single essential gene, *NFS1*, encoding the cysteine desulfurase [6]. In yeast, the Nfs1 protein is initially synthesized on cytoplasmic ribosomes with an N-terminal mitochondrial targeting signal. Upon import into mitochondria, the targeting signal is removed by two distinct mitochondrial peptidases, generating the mature form of the enzyme [7]. Thus, Nfs1 is present primarily in mitochondria, although a small amount of the enzyme is found in the cytoplasm and nucleus [7]. The protein is essential for viability and functions to provide an activated form of sulfur for Fe-S cluster assembly and other vital cellular processes. The bacterial and mature yeast proteins exhibit 48.4% identity and 62.8% amino acid similarity. The *E. coli* protein has a characteristic biochemical activity – it acts on the amino acid cysteine, releasing sulfide that can be detected by a colorimetric assay [2]. A surprising result was that the mature yeast enzyme, even in the presence of the pyridoxal phosphate cofactor, was inactive [8]. This result was later explained by the discovery of Isd11 [9, 10], a small mitochondrial protein that forms a tight complex with Nfs1 and is required for the Nfs1 cysteine desulfurase activity [8]. *In vivo*, Isd11 is required for cysteine desulfurase activity [8], Nfs1 protein stability, and cellular Fe-S cluster assembly [9, 10]. Isd11 has no prokaryotic homologue and seems to be an entirely eukaryotic invention. Homologous proteins, however, are found in all eukaryotic subgroups, including plants, animals and lineages with reduced organelle contents such as hydrogenosomes of *Trichomonas*, and mitosomes of *Cryptosporidium* species [11]. In hydrogenosomes or mitosomes, the oxidative phosphorylation function has been lost, and only rudimentary components of Fe-S cluster assembly remain as organelle contents. The retention of Nfs1/Isd11 in these organelles suggests that the Fe-S cluster synthesis may be the most essential and irreplaceable function. The evolutionary origin of Isd11 is unclear; it might have been originated at the time of the key endosymbiotic event shared by all eukaryotes [12]. The way in which this special eukaryotic component influences the process of Fe-S cluster assembly is still being worked out, and distinct regulatory features are being uncovered.

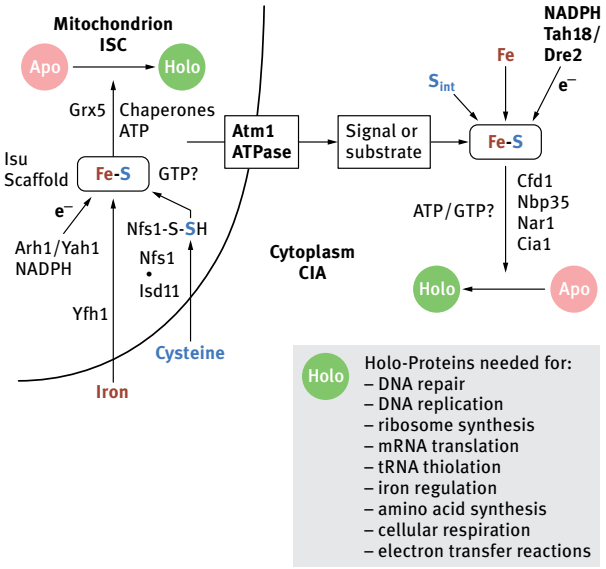

Fig. 6.1: General scheme for Fe-S cluster assembly in yeast. A mitochondrial system termed ISC for Fe-S cluster assembly is complete and able to synthesize Fe-S clusters on its own [49]. The central feature is the Isu scaffold, and many components are involved in making an Fe-S cluster intermediate on the Isu scaffold [50]. These include Nfs1/Isd11, which contribute sulfur from cysteine [8], Arh1/Yah1, which provide electrons [51, 52], and Yfh1, which provides iron and/or regulates the sulfur donation [22, 23]. The intermediate on the Isu scaffold is transferred to recipients in a process involving ATP-dependent chaperones, Ssq1 and Jac1 [29], and Grx5, a glutaredoxin able to coordinate Fe-S clusters in the presence of glutathione [53]. A parallel cytoplasmic Fe-S cluster system termed CIA for cytoplasmic Fe-S protein assembly, has never been reconstituted and may be incomplete. It is made up of scaffold components (Cfd1, Npb35), reductase components (Dre2, Tah18), and transfer components (Nar1, Cia1) [3]. The iron source is not well defined. The sulfur intermediate, S_{int}, presumably originates from cysteine *via* cysteine desulfurase activity of Nfs1/Isd11, but it is also not well defined in terms of its chemical nature or its cellular source. The Atm1 transporter is an exporter of the mitochondrial inner membrane [54], and this may export a substrate or a signal from mitochondria to the cytoplasm. The output of the Fe-S cluster assembly systems is made up of critical Fe-S cluster holoproteins that perform many functions [1], some of which are listed.

6.2.2 Scaffold proteins in yeast mitochondria

The basic scheme for Fe-S cluster assembly in cells involves transient assembly of a cluster on a scaffold protein and subsequent transfer of the intermediate to recipients (Fig. 6.1) [2]. In yeast mitochondria, Isu1 and Isu2 are redundant scaffold proteins encoded by separate genes [13]. These proteins are synthesized on cytoplasmic ribosomes and are imported into mitochondria. Inside mitochondria, the targeting sequence is removed by the processing peptidase, and the proteins interact with other components of the Fe-S cluster assembly machinery. The yeast proteins are highly homologous to the *E. coli* IscU scaffold, exhibiting 62.4% identity and 74.4% similarity at the amino acid

level. Accordingly, the bacterial protein targeted to yeast mitochondria by addition of a matrix targeting sequence, is able to complement the essential function of the yeast Isu scaffolds [14]. The yeast protein is also highly conserved with metazoan mitochondrial scaffold proteins exhibiting 64.9% identity and 73.9% similarity, and the human protein likewise can complement the yeast mutant lacking Isu1/2. The retention of high sequence similarity and orthologous relationships likely reflect constraints that result from multiple conserved protein-protein interactions with the scaffold that are required during the process of Fe-S cluster assembly [15].

6.2.3 Frataxin's roles throughout evolution

Frataxin is a highly conserved protein, found in prokaryotes such as *E. coli*, in primitive eukaryotes such as yeast, and in metazoans such as humans. The human frataxin was cloned in 1996 after identifying the disease locus of patients with the inherited neurodegenerative disease, Friedreich ataxia [16]. The homologous yeast gene (*YFH1*) was knocked out, and the phenotypic characterization of the deletion strain led to realization of its role in iron homeostasis, and Fe-S cluster assembly [17]. Recently frataxin was found to be a constituent of an Fe-S cluster assembly complex in mitochondria (Fig. 6.1), associated with Nfs1/Isd11, and Isu, and cells lacking components of the complex were found to be deficient in Fe-S cluster proteins [18, 19]. A regulatory function of frataxin was hinted at early on because yeast mutants completely lacking the frataxin homologue (Yfh1) were still viable and exhibited a small amount of basal Fe-S cluster assembly [20]. The Δ*yfh1* deletion strain accumulated extragenic suppressor mutants [21]. By contrast, knockouts of integral components (e.g. Nfs1) of the Fe-S cluster assembly machinery were completely nonviable with no detectable escape mutants. Frataxin might be involved in promoting and coordinating sulfur [22] and iron [23] delivery to Isu for the synthesis of Fe-S cluster intermediates, although the mechanistic details are still being clarified.

The *E. coli* genome carries a frataxin protein called CyaY, and it is not present on the ISC operon. CyaY was shown to function in yeast if properly targeted to mitochondria; it was able to complement the Fe-S cluster assembly defect of the Δ*yfh1* mutant, presumably by interacting with yeast Nfs1 and the Fe-S cluster assembly complex [24]. Whereas the eukaryotic Nfs1/Isd11 exhibited low cysteine desulfurase activity that was stimulated by frataxin, the prokaryotic Nfs1 homologue, IscS, showed constitutively high activity that was inhibited by frataxin [25]. Thus, the regulatory effects of frataxin were different for prokaryotes and eukaryotes. These differences were further underscored by the finding of a genetic suppressor of the yeast Δ*yfh1* deletion that promoted growth and Fe-S cluster assembly independent of frataxin. Specifically a single point mutation in Isu1 was identified with frataxin-bypassing activity. The substitution changed methionine 107, an amino acid present in all eukaryotic Isu proteins, to isoleucine, an amino acid present in *E. coli*, and many other prokaryotic Isu homologues [26]. The basal cysteine desulfurase of the yeast Δ*yfh1* mitochondria was increased

in the presence of Isu1 (M107I), thus mimicking the situation in prokaryotes [27]. In summary, there appear to be fundamental differences between prokaryotic and mitochondrial Fe-S cluster assembly apparatus in the way the components are wired. A critical function of frataxin in stimulating cysteine desulfurase in yeast can be bypassed by a mutation that renders the Isu scaffold more "prokaryote-like."

6.2.4 Ssq1 is a specialized Hsp70 chaperone arising by convergent evolution

Hsp70 chaperones and co-chaperones in mitochondria are required for the transfer of Fe-S cluster intermediates formed on Isu to recipient proteins (Fig. 6.1) [28]. In yeast, there are two mitochondrial Hsp70 (mtHsp70) proteins. The major one, Ssc1, is involved in protein import and protein folding in the organelle, and thus, it has innumerable substrates. The less abundant one, Ssq1, apparently arose by a gene duplication event about 300 million years ago, and over evolutionary time it became adapted to interacting with a single client protein, Isu. The Isu scaffold contains the LPPVK motif that binds to the Ssq1 substrate-binding site, and this interaction is highly specific, as Ssq1 does not interact with more general mitochondrial targeting peptides. The Ssq1 ATPase activity is optimally stimulated by the LPPVK peptide in conjunction with the specialized co-chaperone, Jac1, a J protein that is not stimulated by other peptides [29]. In yeast mitochondria, Mge1 is required to release ADP from both Ssc1 and Ssq1, allowing initiation of another catalytic cycle. For the human and *E. coli* systems, the evolutionary aspects of the chaperones are somewhat different. In humans, the gene duplication giving rise to Ssq1 did not occur. Therefore, there is a single mtHsp70 that must handle all clients, including protein import substrates and Isu. The existence of a specific J protein, orthologous to the yeast Jac1 and adapted to interacting with Isu, however, may provide some degree of specificity to the system and allow efficient handling of Fe-S cluster protein substrates [29]. In *E. coli*, a specialized Hsp70 and J protein, called HscA and HscB, respectively, are found on the ISC operon. However, these proteins arose from the major cellular Hsp70, DnaK, by an independent gene duplication. They are not considered to be orthologues of the yeast proteins but rather the products of independent convergent evolution. Remarkably, the substrate binding specificity of the HscA is identical to that of Ssq1, and the cognate scaffold protein has the identical LPPVK motif [30]. Other subtle differences in the systems have been found; for example, the *E. coli* chaperones do not need a recycling factor because of their lower binding affinities for nucleotides [31].

6.2.5 Atm1 and CIA components

Atm1 is an ABC transporter, with its substrate-binding site oriented toward the mitochondrial matrix, suggesting that it exports its substrate(s) from the matrix to other compartments of the cell (Fig. 6.1). Atm1 in yeast has been implicated in Fe-S

cluster assembly and iron homeostasis. Strong homologues exist in proteobacteria, suggesting that it could have come along during the original endosymbiotic event. The importance of a transporter that would move its substrate from the inside to the outside of the bacterial cell is unclear, although one could imagine that some key activities for Fe-S cluster assembly take place in the periplasm. The substrate for the bacterial transporter is unknown, and phenotypes of the knockout have not been characterized. Therefore, this evolutionary link does not shed much light on the function of these proteins, but rather adds to the mystery.

CIA components are involved in cytoplasmic Fe-S cluster assembly (Fig. 6.1), and in yeast there are now eight constituents that have been identified [3]. They are thought to perform reductase (Dre2 and Tah18), scaffold (Nbp35 and Cfd1), and transfer functions (Cia1, Cia2, Nar1, and Mms18), somewhat analogous to counterparts in the mitochondrial system. In terms of evolution, however, these genes are found in the last common eukaryotic ancestor before the diversification of eukaryotic lineages, and thus, they are present in protists and primitive eukaryotes [32]. Their prior origins in prokaryotes are harder to discern. In fact, only the scaffold components, Nbp35 and Cfd1, have a clear prokaryotic homologue. This protein, called ApbC, was studied in *Salmonella enterica* and shown to function in Fe-S cluster biogenesis. Furthermore, *in vitro* biochemical analysis showed that the purified ApbC could function as a scaffold in binding and transferring Fe-S cluster intermediates to Leu1, the yeast cytoplasmic Fe_4S_4 enzyme [33]. Interestingly, Archaea also have ApbC homologues that were able to functionally complement the *S. enterica* mutant, indicating that at least for this case, the CIA machinery seems to have origins in Archaea [34].

6.2.6 Yeast components are conserved with their human counterparts

Moving up the evolutionary ladder, the components of the human Fe-S cluster assembly machineries (ISC and CIA) are conserved with yeast, with a few exceptions. Many human proteins have yeast orthologues, and the human proteins expressed in yeast often correct the Fe-S cluster assembly defects of the corresponding yeast mutants, demonstrating real functional equivalence. This is true for Isu1/2 (our unpublished data), frataxin [35], Atm1 [36], Dre2 [37], Tah18 [38], and others. Grx5 from zebrafish rescued the corresponding yeast mutant, and so this mitochondrial glutaredoxin is also conserved between yeast and metazoans [39]. The story for the yeast ferredoxin Yah1 is complicated by existence of two human ferredoxins encoded by separate genes, Fdx1 and Fdx2. In one study, Fdx2 but not Fdx1 was able to complement the phenotypes of the Yah1-depleted yeast, including Fe-S cluster assembly, overall heme levels, and heme O formation [40]. In another study, knockdown of either Fdx1 or Fdx2 in various human cell lines impaired Fe-S cluster assembly [41]. The basis for the specificity of the Fdx2 yeast complementation is unclear as both isoforms are very similar. As mentioned above (Section 6.2.4), human mitochondria make use of a single Hsp70 chaperone for handling protein import, protein folding, and Fe-S cluster

assembly. Thus, the human Hsp70 has multiple client proteins, including Isu1, as contrasted with the yeast specialized Hsp70, Ssq1, which interacts with Isu as its sole client [29]. The human Hsc20, which encodes a J protein with similarity to yeast Jac1, interacts with the human Isu1, although other substrates have not been ruled out. The presence of an insertion sequence between the aspartic acid of the HPD motif and an invariant serine in the helix 3 apparently enhances the interaction of the Hsc20 with the generic mtHsp70 (called HspA9). In any case, the human Hsc20 is able to complement the yeast Jac1 deletion strain [42].

6.2.7 Yeast Fe-S cluster assembly mutants modeling aspects of human diseases

The yeast frataxin homologue (Yfh1), the scaffold proteins of mitochondria (Isu1/2), and the mitochondrial exporter (Atm1) all have human homologues. Human diseases may result from deficiency of each of these conserved Fe-S cluster components [43]. Because Fe-S cluster assembly is essential for viability of all cells, the disease-causing mutations are usually hypomorphic rather than complete loss-of-function mutations. The phenotype-genotype correlations for Fe-S cluster diseases are very complicated, especially as regards to tissue specificity. It remains unclear why one tissue is targeted in some cases and another is affected in other cases. Friedreich ataxia results from a GAA expansion in the first intron of the frataxin gene, resulting in decreased expression of frataxin [16]. The disease primarily affects certain nerves, especially dorsal root ganglion cells. Cardiomyocytes are also sensitive to lack of frataxin, and cardiomyopathy is a major feature of the disease [44]. Blood cells of various lineages are spared, even though frataxin is deficient in these cells and Fe-S cluster assembly is necessary for blood cell development [45]. In ISCU myopathy, skeletal muscles are particularly affected due to low levels of ISCU (homologous to yeast Isu1/2), with characteristic episodes of muscle fatigue and lactic acidosis. More severe stress leads to rhabdomyolysis and myoglobinuria as a result of muscle cell death. A tissue specific splicing defect interfering with expression of the ISCU gene may partly explain the predilection for skeletal muscle [46]. In a disease called XLSA/A, X-linked sideroblastic anemia with ataxia, a defect in ABCB7 (homologous to yeast Atm1) has been implicated. A nonprogressive neurological defect causing ataxia and anemia are the principal manifestations. The anemia is characterized by ringed sideroblasts, indicating red cell precursors with mitochondrial iron accumulations that stain with Prussian blue. The ring pattern derives from the propensity of iron-loaded mitochondria to encircle the nucleus in these cells [47]. Although these diseases are very different, each one is caused by deficiency of a protein involved in Fe-S cluster assembly [43]. In addition, in each case the diseased tissues show deficiency of Fe-S cluster proteins and perturbed iron metabolism, thereby resembling the corresponding yeast mutants. The perturbed iron metabolism, also similar to the yeast mutants, is characterized by increased cellular iron and increased mitochondrial iron, primarily in a nonproteinaceous form [48].

6.3 Yeast genetic screens pointing to the Fe-S cluster assembly apparatus

The constituents of the Fe-S cluster machinery were initially discovered by homology with components from other species, especially *E. coli*, or by genetic screens. The discovery of NifS in *A. vinelandii* by Dennis Dean opened the field and showed that Fe-S cluster assembly in cells was a catalyzed process [4]. This finding provided a fulcrum for uncovering other components of the Fe-S cluster assembly machinery, initially by association with operon groupings of genes in prokaryotes. The identification of the NIF operon for nitrogenase production and the ISC operon for housekeeping Fe-S cluster assembly in *A. vinelandii* led to the identification of cysteine desulfurase, reductase, scaffold, and chaperone components [55]. These were found to have homologues in eukaryotes that localized primarily to mitochondria. Studies in yeast allowed for phenotypic characterization of the corresponding genes and processes. Some components were not found on the operons, either because they were elsewhere in the prokaryotic genome (e.g. Arh1, frataxin) or because they were not present at all in prokaryotes (e.g. Isd11) [56]. The discovery of the role of frataxin was made possible following cloning of the human disease gene and identification of the yeast homologue. The yeast frataxin homologue was deleted, with striking phenotypic effects on iron homeostasis and Fe-S clusters [17].

The yeast *S. cerevisiae* is conducive to genetic screens, and many informative screens were performed. In general, mutants were identified with easy-to-score phenotypes: some mutants exhibited altered iron homeostasis [57], amino acid auxotrophies [58, 59], ribosome assembly abnormalities [60], DNA replication defects [61], or absent tRNA modifications [62]. The phenotypes were traced back to one or more Fe-S cluster proteins (in some cases, the relevant Fe-S cluster protein has not yet been identified) and to an underlying problem with Fe-S cluster synthesis. In this way, hypomorphic mutants in many of the constituents of the Fe-S cluster machinery were found (Tab. 6.1).

6.3.1 Misregulation of iron uptake

In yeast, the high affinity cellular iron uptake system consists of an externally directed surface reductase encoded by *FRE1* and *FRE2*, and an oxidase-permease complex encoded by *FET3*/*FTR1* [63]. The entirety is homeostatically regulated by iron availability *via* the Aft1 transcriptional regulator and the Cth1 and Cth2 RNA stability regulators, driving increased expression of the iron uptake system in response to iron deprivation [64]. For the screen, the *FRE1* promoter was fused to the *HIS3* open reading frame, and mutants were selected under iron replete conditions that constitutively expressed His3. The selected mutants showed constitutively high iron uptake and included components of the mitochondrial Fe-S cluster assembly machinery,

Tab. 6.1: Yeast genetic screens leading to Fe-S cluster assembly components.

	Genetic screen	Mutant phenotype	Fe-S cluster(s) targeted	Assembly components found	References
1	FRE1-HIS3 selection	Misregulated iron uptake	Aft1, Fra1, Grx3/4	Ssq1, Nfs1, Jac1, Atm1	[57]
2	Sod1 suppression	Lysine, methionine auxotrophy	Unknown	Nfs1, Ssq1, Jac1	[59]
3	IRP1 in yeast	Glutamate auxotrophy	IRP1 in cytoplasm	Cfd1	[58]
4	Pol3 interaction	*pol3-13* synthetic lethality	Rad3, Met10, Dna2, Ntg2	Dre2, Tah18, Nbp35, Mms19	[61]
5	Mrs3/4 interaction	Δ*mrs3* Δ*mrs4* synthetic lethality	Unknown	Dre2	[37]
6	Ribosome processing	Rpl25-GFP in nucleus	Rli1	Cfd1, Nbp35, Nar1	[60]
7	Cytosolic tRNA thiolation	Sensitive to *K. lactis* killer toxin	Unknown	Cfd1, Npb35, Cia1	[62, 65]
8	Yap5 high iron response	No Ccc1 induction	?Yap5 cluster	Ssq1	[66]

including a hypomorphic allele of Nfs1 [6], loss-of-function mutants of Ssq1 [57], Jac1 [67], and Atm1 [68]. Cytoplasmic Fe-S cluster assembly components such as Dre2 and others were not selected. The iron homeostatic effects of perturbing mitochondrial Fe-S cluster assembly led to activation of *FRE1-HIS3* expression, allowing selection of the mutants.

6.3.2 Suppression of Δ*sod1* amino acid auxotrophies

The Cu-Zn superoxide dismutase, Sod1, is responsible for defense against oxidative stress by dismutation of superoxide to peroxide and water. The yeast Δ*sod1* mutant is sensitive to oxygen exposure, and in air, it develops lysine and methionine auxotrophies [59]. The most likely explanation for the auxotrophies is that a key step in the biosynthesis of these amino acids is sensitive to oxidants that are ordinarily inactivated by Sod1. In a genetic screen, mutants of Δ*sod1* were selected for the ability to grow in the absence of lysine and methionine. These mutants included partial loss-of-function alleles of Nfs1, Ssq1, and Jac1 i.e. mitochondrial Fe-S cluster assembly components [59]. The manner in which partial loss-of-function of Fe-S cluster assembly rescues Sod1 deficiency is not immediately clear. Interestingly, all of these mutants were associated with mitochondrial iron accumulation, and mutations minimizing this effect also abrogated the Δ*sod1* suppression. Thus, the mitochondrial iron might cause a stress response in the mutants that enhanced specific pathways of amino acid synthesis [59].

6.3.3 tRNA modification and the *SPL1-1* allele

Nfs1 was first identified in a complicated genetic screen involving splicing of certain nuclear-cytoplasmic tRNAs [69]. Briefly, an opal stop codon was inserted into the *HIS4* and *LEU2* genes, leading to auxotrophy for histidine and leucine. A cytoplasmic/nuclear tRNA with a spliced intron introduced into this strain was able to relieve the auxotrophy by stop codon suppression. A modified and nonfunctional version of the suppressor tRNA with an altered splice site was introduced instead, and this was the starting point for the screen. A randomly selected mutant that conferred splicing activity and stop codon suppression was identified, and the activity was found to depend on a dominant allele of Nfs1 called *SPL1-1* for its newly acquired splicing activity [69]. It remains to be explained how the altered Nfs1 enhanced splicing of the inactive opal tRNA suppressor. However, subsequent studies have shown that some tRNA modifications such as tRNA thiolation are dependent on Fe-S cluster synthesis in general and cytoplasmic Fe-S cluster synthesis in particular [65]. One can imagine that an Nfs1 mutant could result in an altered tRNA, maybe incompletely thiolated, which might be a more efficient splicing substrate.

6.3.4 tRNA thiolation and resistance to killer toxin

Certain cytoplasmic tRNAs such as cy-tRNA-Lys2$_{UUU}$ and cy-tRNA-Glu3$_{UUC}$ carry a thiol modified uridine in the 5′ wobble position, the so-called mcm^{5}s^{2}U (5-methoxycarbonylmethyl-2-thiouridine). The modification is essential for correct base pairing and for viability of the organism. A role for Fe-S clusters in cytoplasmic tRNA modifications was indirectly shown by cellular depletion experiments. The depletion of CIA components (Cfd1, Nbp35, or Cia1) was associated with decreased tRNA modification [65]. The presumption is that a critical Fe-S cluster protein is involved in uridine thiolation, although the identity and role of the presumed Fe-S cluster protein has not been clarified. A global genetic screen was undertaken to find the genes required for modification of the 5′ wobble nucleoside [70]. The idea for the screen comes from the observation that the γ subunit of the *Kluyveromyces lactis* killer toxin is a tRNA endonuclease that cleaves modified tRNAs 3′ of the wobble nucleoside, utilizing the modified base as a recognition motif. Mutants that fail to modify the uridine were identified based on their resistance to the killer toxin. Various resistant mutants including Urm1, Uba4, Ncs2, Ncs6, and Tum1 were found in this screen, and it is possible that one of these proteins carries an Fe-S cluster or requires an Fe-S cluster for its activation [70].

6.3.5 Cytoplasmic aconitase maturation

Aconitase, a [Fe$_4$S$_4$] cluster protein, is responsible for isomerizing citrate to isocitrate, which in turn gives rise to α-ketoglutarate as part of the tricarboxylic acid cycle. The

yeast Δ*aco1* deletion strain is viable but develops auxotrophy for glutamate because of the inadequate supply of the α-ketoglutarate precursor. Interestingly, although yeast aconitase is primarily found in mitochondria, expression of aconitase (in this case, the human IRP1 [71]) in the cytoplasm of a Δ*aco1* strain corrects the glutamate auxotrophy, probably *via* exchange of intermediates in and out of mitochondria [72]. The yeast Δ*aco1* strain expressing IRP1 in the cytoplasm was the starting point for a genetic screen. Mutants with glutamate auxotrophy included a hypomorphic allele of Cfd1 in which the AUG start codon was changed to a less efficient AUA initiator. The auxotrophy for glutamate developed because the cytoplasmic IRP1 was no longer properly loaded with its [Fe_4S_4] cluster, and as a consequence, the enzyme was less active [58]. The results demonstrated that Cfd1 was required for cytoplasmic Fe-S cluster assembly, making it the first member of the CIA machinery to be discovered. The Cfd1-depletion phenotype was instructive and novel because the defect was restricted to cytoplasmic Fe-S clusters, with preservation of the mitochondrial Fe-S cluster enzyme activities [58].

6.3.6 Ribosome assembly

The biogenesis of eukaryotic ribosomes is a highly coordinated process, beginning in the nucleus and ending with the assembly of 60S and 40S subunits in the cytoplasm. The nuclear export of various ribosomal components is subjected to quality control, and improper processing of ribosomal proteins leads to their retention in the nucleus [73]. For the screen, a fusion of the ribosomal protein Rpl25 (or Rps2) to GFP was inserted into a library of temperature-sensitive mutants [60]. After shifting to non-permissive temperature, mutants were identified with enhanced nuclear GFP fluorescence due to nuclear retention of the ribosomal precursor protein. The mutants identified in this manner, so called rix or ribosomal protein export mutants, included CIA components Cfd1, Nbp35, and Nar1 [60]. The explanation for the ribosomal phenotype of CIA mutants was provided by the protein Rli1. Rli1 is required for rRNA maturation and nuclear export of 60S and 40S subunits, and Rli1 possesses two [Fe_4S_4] clusters that are critical to its function [74]. Thus, mutations interfering with Fe-S cluster assembly resulted in defects in Rli1 function and indirectly led to a block in nuclear-cytoplasmic trafficking of ribosomal proteins. The mutants could only have been discovered with such a library of temperature-sensitive alleles because the corresponding genes are essential and complete loss-of-function mutants are nonviable.

6.3.7 Synthetic lethality with the *pol3-13* allele

DNA polymerases are multi-subunit enzyme complexes that are responsible for priming, initiating, and extending the lagging and leading strands of the double stranded genome during the process of DNA replication. The catalytic subunits, Pol1,

Pol2, and Pol3, contain conserved sets of cysteine residues in an essential carboxyl terminal domain [75]. A change of ^{104}Cys to Ser in the carboxyl terminal domain of Pol3 conferred a temperature-sensitive growth phenotype, presumably because of compromised efficiency of replication [61]. This finding was the basis for a synthetic lethal sectoring screen, starting with the *pol3-13* allele covered by a plasmid with the wild-type *POL3*. Synthetic lethal screens are commonly used in model organisms to identify other genes that function in the same genetic pathway. They identify other genes that are needed for survival in a compromised strain. The strain with the ^{104}Cys to Ser in the carboxyl terminal domain of Pol3 was mutagenized, and mutants were recognized that were unable to survive without the plasmid-borne copy of wild-type *POL3*. The procedure identified second site mutations (mutations in other genes) that worsened the phenotype of the *pol3-13* allele, and these included alleles of CIA components such as Dre2, Tah18, Nbp35, and Mms19 [61]. These genes have been implicated in assembly of cytoplasmic or nuclear Fe-S clusters. The observation linking Pol3 and Fe-S cluster assembly was subsequently explained when Pol3 itself was found to coordinate an Fe-S cluster [76]. The cluster plays a role in stabilizing the protein and mediating critical protein-protein interactions among the DNA polymerase subunits. Thus, the synthetic lethal genetic relationship occurred because the *pol3-13* allele with ^{104}Cys replaced by Ser was less effective in coordinating its Fe-S cluster, and second site mutations interfering with Fe-S cluster assembly made matters even worse. Another genetic screen was based on the putative mitochondrial iron carriers, Mrs3 and Mrs4. Cells lacking both of these carrier proteins grow robustly on rich media, and a synthetic lethal screen identified Dre2, an essential component of the CIA [37]. The *dre2-137* mutant allele was synthetically lethal with the double mutant Δ*mrs3*Δ*mrs4*. Other Fe-S cluster assembly components including Cfd1 and Atm1 showed a similar synthetic lethality when combined with Δ*mrs3*Δ*mrs4*, and the synthetic lethality was made worse by iron deprivation [37]. A possible explanation for these findings is that mitochondrial iron (involving Mrs3/4) and cytoplasmic Fe-S cluster assembly (involving Dre2, Cfd1, and Atm1) are dependent on each other.

6.3.8 Factors needed for Yap5 response to high iron

The cellular responses to iron exposure involve downregulation of the cell surface iron uptake systems (Aft1 and Cth1/2 mediated) [64] and upregulation of vacuolar iron transport *via* increased Ccc1 expression (Yap5 mediated) [77]. The signals for the Yap5 effects were unknown, and so a genetic screen was undertaken [66]. The Yap5 regulatory domain responsible for conveying the iron signal was fused to Gal4, thereby conferring an iron-dependent response to the *GAL1* promoter. The *GAL1* promoter was fused to *HIS3*, and the hybrid gene was used to identify mutants that are unresponsive to the iron signal. In a second construct, the *CCC1* promoter was fused to *lacZ*. Selection of mutants that were histidine auxotrophs and were white identified genes that

were required for the Yap5-dependent iron induction. Interestingly Ssq1 mutants were identified in this screen, and mutants of Yfh1 and Isu1 were also shown to prevent the high iron response. The implication is that both low-iron (Aft1) and high-iron (Yap5) responses involve Fe-S cluster intermediates in the sensing pathways. An attractive possibility is that Yap5 itself might form an Fe-S cluster in its cysteine-rich domain [66].

6.3.9 Screening of essential genes coding for mitochondrial proteins

A genome-wide screen in yeast was performed by deletion and sporulation to identify essential genes. Isd11 was shown to be essential by this approach [78]. A separate screen for protein localization using GFP fusions identified Isd11 as a mitochondrial protein [79]. The essentiality and mitochondrial localization led to the conjecture that Isd11 must be involved in a critical function of mitochondria. Mitochondrial protein import has been known for a long time to be an essential process. However, Isd11 mutants or conditional alleles exhibited normal protein import activity [9, 80]. Fe-S cluster synthesis is also an essential function of mitochondria. Therefore, Fe-S cluster assembly was examined in Isd11 mutants, and shown to be defective. No prokaryotic homologue exists, and so Isd11 could not have been found by comparison with prokaryotes [9, 80]. The Isd11 protein was found to form a tight complex with the cysteine desulfurase Nfs1 and to participate in stabilization of the protein in mitochondria [9, 80]. Isd11 was also found to activate Nfs1, enabling its cysteine desulfurase activity and promoting persulfide formation [8].

6.4 Mitochondrial Fe-S cluster assembly

Mitochondria possess a complete and functional Fe-S cluster assembly machinery. The basic pieces were acquired during evolution from purple bacteria, although important tweaking and major modifications occurred over evolutionary time [11]. Intact mitochondria isolated from yeast and "fed" metabolic precursors are capable of synthesizing new $[Fe_2S_2]$ or $[Fe_4S_4]$ clusters, and inserting them into endogenous or freshly imported apo-proteins [49]. For mitochondrial Fe-S cluster assembly to proceed, iron, sulfur, and various nucleotides are required.

1. Iron supply: Iron is already present inside mitochondria in a form that can be utilized for Fe-S cluster synthesis. The functionally important mitochondrial iron pool may correspond to the nonheme high-spin (NHHS) Fe^{2+} iron pool described by Lindahl and colleagues [81] in Mössbauer spectroscopic studies of isolated mitochondria. In some settings, iron in this pool is present at concentrations of 100–200 μM, and the abundance is subjected to regulatory shifts depending on growth conditions. The precise chemical form and its ligands have not been ascertained, but the iron pool is sensitive to membrane permeable ferrous iron

chelators such as *o*-phenanthroline [81]. The iron in this pool can be "chased" into new Fe-S clusters as shown by experiments with isolated mitochondria, suggesting that it functions as a true intermediate [82]. The source of this mitochondrial iron pool remains poorly defined. It is presumed to originate from cytoplasmic iron that is transported into mitochondria. The transporters responsible have not been clearly identified either, so this entire issue remains somewhat nebulous. Mrs3 and Mrs4 are redundant mitochondrial carrier proteins, and extensive work has shown that they play a role in providing iron to mitochondria for Fe-S cluster and heme synthesis [83, 84]. However, these proteins have never been reconstituted into liposomes and shown to transport iron or any iron ligand, and so their transport substrate remains unknown. Another mitochondrial carrier protein, the pyrimidine exchanger Rim2, also plays a role in iron delivery into mitochondria, and overexpression is able to completely rescue the phenotype of a Δ*mrs3*Δ*mrs4* deletion [85]. Once inside mitochondria, iron must be delivered to the scaffold Isu, and frataxin may play a role here [18, 23].

2. Sulfur supply: The sulfur for Fe-S cluster assembly is derived from cysteine by the action of cysteine desulfurase [4]. Although Fe-S clusters can be made *in vitro* using sulfide and iron under defined conditions, only the cysteine desulfurase can supply sulfur for Fe-S cluster synthesis in intact cells or in isolated mitochondria, and sulfur in other chemical forms cannot substitute [2]. The yeast cysteine desulfurase, similar to the bacterial enzymes, interacts with cysteine and forms a persulfide on the enzyme [82]. The persulfide sulfur is the real precursor, and is used in Fe-S cluster assembly following transfer to Isu. In the eukaryotic setting, the cysteine desulfurase Nfs1 requires Isd11 for its activity [8].
3. Nucleotide requirements: Mitochondria depleted of nucleotides are unable to synthesize Fe-S clusters, and thus, *in vitro* assays with isolated mitochondria must be supplemented with nucleotides for supporting efficient Fe-S cluster assembly [49, 86]. This is because key steps depend on NAD(P)H, ATP, or GTP. More specifically, NAD(P)H is required for reductases, such as the ferredoxin reductase (Arh1) that provides electrons to ferredoxin (Yah1) and then probably to an Fe-S cluster assembly complex. The reducing equivalents are needed for converting the persulfide sulfur (S^0) on Nfs1 to S^{2-} for incorporation into the nascent cluster on Isu [87]. Likewise, only ferrous iron is useful for the assembly process, and the Arh1/Yah1 reductase chain may also be involved in maintaining iron in reduced (Fe^{2+}) form, as this may have a tendency to reoxidize. Furthermore, the conversion of [Fe_2S_2] to [Fe_4S_4] clusters requires additional electrons in a process called reductive coupling, and this might also depend on the mitochondrial NAD(P)H reductase system [88]. Like NAD(P)H, ATP is also required for one or more steps in the assembly process. The role of Hsp70 chaperones in Fe-S cluster assembly was discovered at the time of the discovery of the ISC operon because the Hsp70 HscA was found on the operon and linked to IscS and the other key elements for Fe-S cluster assembly [55]. The yeast

mitochondrial Ssq1, although not orthologous to HscA, is an Hsp70 that interacts with Isu as its sole client. The requirement of ATP for the Hsp70 reaction cycle likely explains the requirement of ATP for mitochondrial Fe-S cluster assembly [29, 89]. Finally, GTP is required, although the target for this nucleotide requirement has not yet been identified. The role of GTP was discovered because mutant mitochondria lacking the GTP/GDP carrier, Ggc1, were deficient in both mitochondrial GTP and in Fe-S cluster assembly activity [90]. Presumably, there exists a GTPase that interacts with the assembly machinery and conveys a signal or performs a key catalytic function. Thus, mitochondria provided with cysteine, iron, NAD(P)H, ATP, and GTP are able to catalyze efficient synthesis of new Fe-S clusters (Fig. 6.1).

4. Synthesis of Fe-S cluster intermediates on Isu *vs* transfer of cluster intermediates to apo-proteins: The scaffold proteins, Isu1 and Isu2, in yeast mitochondria are redundant proteins, but at least one of them is absolutely essential [13]. The Fe-S cluster biogenesis can be understood in terms of two steps: formation of an Fe-S cluster intermediate on Isu and transfer of the intermediate from Isu to apo-protein recipients (Fig. 6.1) [50]. A number of independent components must interact in a complex choreography to perform each of these steps and to switch between them. To classify different components in terms of their importance for the synthesis or transfer step, an iron-labeling approach was undertaken. The yeast deletion mutant (or depleted strain if the corresponding gene was found to be essential) was labeled with radioactive iron (^{55}Fe), and Isu was recovered by immunoprecipitation. If the mutant was defective in formation of the Isu intermediate, ^{55}Fe label on Isu was decreased. Conversely, if the mutant was capable of generating the Isu intermediate but defective in transfer of the intermediate to apo-proteins, ^{55}Fe label on Isu was increased. In this manner, Fe-S cluster synthesis/assembly components (Nfs1, Isd11, Yfh1, and Yah1) were distinguished from Fe-S cluster transfer components (Ssq1, Jac1, and Grx5) [50].

6.4.1 Mitochondrial cysteine desulfurase

Cysteine desulfurases are conserved enzymes that act on the substrate cysteine, removing sulfur and forming a covalent persulfide on the active site cysteine. It is this form of sulfur that is exclusively utilized in the synthesis of cofactors such as Fe-S clusters, biotin, lipoic acid, and thiamine [91, 92] and also for the thio modification of tRNAs [65]. In *S. cerevisiae*, Nfs1 is the only known cysteine desulfurase, and the enzyme is required for activities of the Fe-S cluster proteins throughout the cell, including aconitase (Aco1) in mitochondria and isopropylmalate isomerase (Leu1) in the cytoplasm [6, 93]. These enzymes require a [Fe_4S_4] cluster for activity. In the absence of adequate levels of Nfs1, cellular Fe-S cluster biogenesis does not occur, leading to global deficiency of these cofactors. Likewise, a hypomorphic mutant allele, *nfs1-14*,

was associated with low activities of Fe-S proteins in mitochondria and constitutively induced cellular and mitochondrial iron uptake activities [6]. Lipoic acid proteins and enzyme activities were also deficient in the *nfs1* mutant because of deficiency of lipoic acid synthase, which requires Fe-S cluster cofactors [94].

Nfs1 forms a persulfide intermediate in mitochondria. Cysteine desulfurase activity can be assessed by incubating the enzyme with cysteine and DTT, and then assessing the amount of sulfide released utilizing methylene blue and ferric chloride [95]. However, this colorimetric assay is too insensitive and is not suitable for detecting the cysteine desulfurase activity in mitochondria. The assay requires a minimum of 2–5 μg of the purified Nfs1/Isd11 complex or *A. vinelandii* NifS. Such an insensitive assay therefore cannot be reliably used for measuring the cysteine desulfurase activity in mitochondria in which Nfs1 is present in small amounts. Furthermore, mitochondria with no detectable Nfs1 exhibit strong background sulfide-generating activity [8], likely due to cystathionine β-synthase or similar enzymes that release H_2S and perform transulfuration reactions. A highly sensitive radioactive assay has therefore been developed based on the fact that the enzymatic cycle of cysteine desulfurase involves formation of a covalent persulfide on the active site. If the active enzyme is incubated with ^{35}S-cysteine, the covalently attached ^{35}S can be visualized on a nonreducing SDS gel. The radioactivity on the active enzyme can be removed by reduction of the persulfide with DTT. By contrast with the spectrophotometric assays, the radioactive assay using ^{35}S-cysteine is at least 50–100 times more sensitive, and ^{35}S-persulfide formation can be easily detected with as little as 5–50 ng of the purified Nfs1/Isd11 complex or 50–200 μg of total mitochondrial proteins [8]. Nfs1 persulfide formation (a necessary step in cysteine desulfurase activity) requires Isd11. Nfs1-S-^{35}SH, the Nfs1 persulfide, cannot be detected in Nfs1-depleted or *nfs1-14* mutant mitochondria. In these assays, several other radiolabeled proteins are also detected regardless of the presence or absence of Nfs1 in mitochondria. However, the authentic Nfs1-bound persulfide (Nfs1-S-^{35}SH) can be easily separated and distinguished from the Nfs1-independent radiolabeled background bands by nonreducing SDS-PAGE [8].

Isd11 is required for Nfs1 to form a persulfide. Nfs1 cannot form persulfide in mitochondria lacking Isd11, and consequently, Fe-S cluster synthesis does not occur in these mitochondria. Cells depleted of Isd11 or carrying a temperature-sensitive allele that has been shifted to the nonpermissive temperature fail to make Fe-S clusters [9, 10]. Bacterially expressed and purified Isd11 imported into these isolated mitochondria restores both of these processes [8]. Importantly, Isd11-independent and Isd11-dependent steps involved in the Nfs1-mediated cysteine desulfuration reaction can be distinguished. Nfs1 is able to bind the substrate cysteine but is unable to form the persulfide. Then Nfs1 with prebound cysteine, after interacting with Isd11, is able to form the persulfide bound to its active site. An interaction of Isd11 with Nfs1 may induce a conformational change in the enzyme that brings the active site cysteine and the bound substrate cysteine together, thereby allowing persulfide formation [8].

Nfs1 persulfide formation is stimulated by frataxin. Another level of Nfs1 regulation involves a unique role of frataxin/Yfh1. A stimulatory effect of frataxin on cysteine desulfurase was first noted for the human enzyme [22]. In studies of the yeast proteins, frataxin directly interacts with Nfs1, exposing substrate-binding sites and enhancing the binding of cysteine. This function of frataxin does not require iron, Isu1, or Isd11. Once bound to Nfs1, the thiol of the substrate cysteine can be used to form the persulfide on the active site cysteine of the enzyme. Persulfide formation depends on the interaction with Isd11. Thus, for full activation of cysteine desulfurase activity, the mitochondrial enzyme must undergo at least two conformational changes. One change is mediated by frataxin/Yfh1 interaction that promotes substrate binding. A second change is induced by Isd11 binding that brings the bound substrate in proximity to the active site cysteine for persulfide formation [27] (Fig. 6.2).

The Nfs1-bound persulfide functions as an intermediate in mitochondrial Fe-S cluster assembly. Upon incubation of isolated mitochondria with ^{35}S-cysteine, a radiolabeled persulfide was detected on Nfs1 (Nfs1-S-^{35}SH). The ^{35}S label detected on Nfs1 depended on the cysteine desulfurase activity of the enzyme, and the radioactive signal varied reciprocally with conditions that blocked or allowed Fe-S cluster

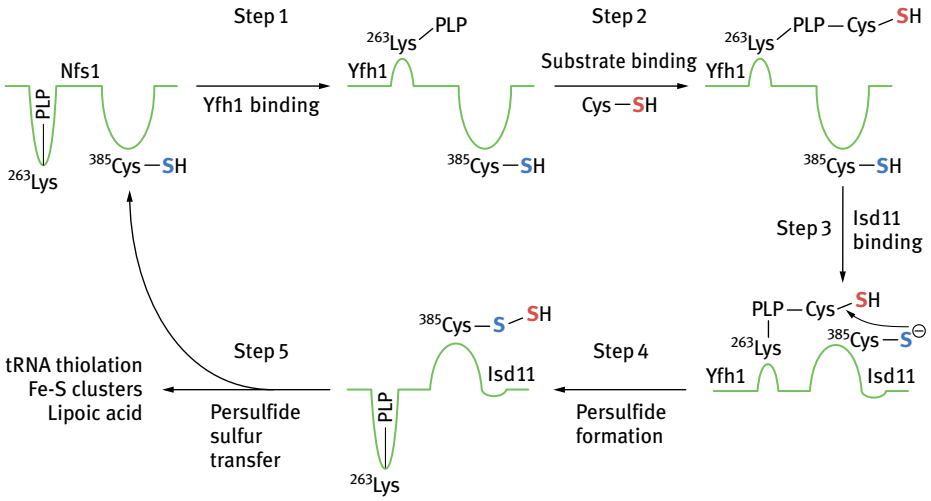

Fig. 6.2: Scheme for steps involved in cysteine desulfurase activation [27]. Yeast Nfs1 (green) contains pyridoxal phosphate (PLP) bound to lysine (^{263}Lys) in the substrate-binding site. A free thiol is present on a cysteine of the active site loop (^{385}Cys-SH, blue S). Step 1: Yfh1 binds to Nfs1-exposing substrate-binding sites. Step 2: The substrate cysteine (Cys-SH, red S) binds to substrate-binding sites on Nfs1, including sites exposed by the Yfh1 interaction. Step 3: Isd11 binds to Nfs1, producing a conformational change that brings the active site close to the substrate site with substrate already bound. Step 4: The persulfide (blue S and red S) is formed on the active site ^{385}Cys of Nfs1. Step 5: Persulfide sulfur (red S) on Nfs1 is transferred from Nfs1 to recipients for Fe-S cluster synthesis and other uses including tRNA thiolation and lipoic acid synthesis.

synthesis in mitochondria. Nucleotide and/or iron depletion of mitochondria block Fe-S cluster synthesis, and the Nfs1-bound persulfide persisted under these conditions. When nucleotides, and iron were added, the radiolabeled Nfs1 persulfide was greatly reduced and radiolabeled aconitase was formed. Thus, the persulfide sulfur was productively chased from Nfs1 and utilized for Fe-S cluster synthesis under optimal metabolic conditions of mitochondria [82].

In summary, the mitochondrial cysteine desulfurase activity is highly regulated, with important controls exerted by interactions with frataxin and Isd11. The optimal control of cysteine desulfurase activity is important for normal cellular functions, and it must be tightly regulated. Too little cysteine desulfurase activity leads to Fe-S cluster deficiency in mitochondria (e.g. *nfs11-14* or Isd11-depleted mitochondria). Conversely, too much activity is toxic. Overexpression of the active Nfs1/Isd11 cysteine desulfurase complex causes the cells to become nonviable, whereas overexpression of Nfs1 alone (inactive without Isd11) is not toxic and does not confer a growth/viability phenotype (Fig. 6.3). Regulation of cysteine desulfurase is thus critical for cell viability. The stimulatory effects of frataxin and Isd11 on cysteine desulfurase activity are apparently eukaryotic features, and the prokaryotic enzymes behave differently in terms of their regulation [25]. The mitochondrial Nfs1 is different from the bacterial cysteine desulfurases that are active in the absence of accessory proteins [4, 5].

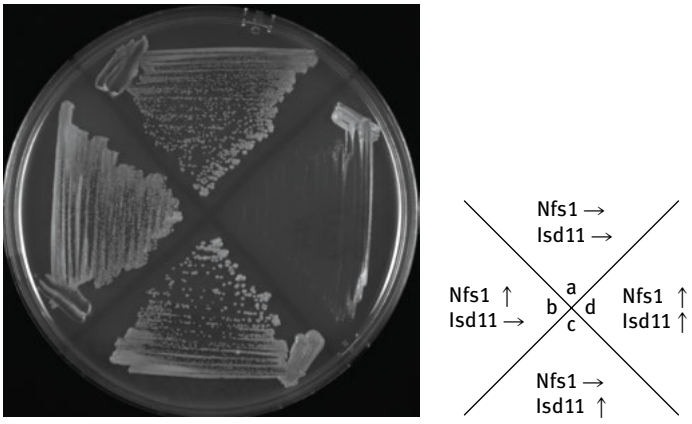

Fig. 6.3: Toxicity of too much cysteine desulfurase. The following strains were tested for growth and viability on galactose plates. (a) Wild type. (b) Promoter swap strain overexpressing Nfs1 from the Gal1 promoter. Isd11 was expressed from the genomic locus [6]. (c) Promoter swap strain overexpressing Isd11 from the Gal1 promoter. Nfs1 was expressed from the genomic locus. (d) Promoter swap strain overexpressing Isd11 from the Gal1 promoter [8] and overexpressing Nfs1 from a high-copy-number plasmid YEp352-Nfs1. Note that the slow growth of (d) indicating toxicity of too much cysteine desulfurase was observed only when both Nfs1 and Isd11 were overexpressed together. Nfs1 overexpression alone (b) was not toxic because it was inactive as a cysteine desulfurase without Isd11.

6.4.2 Formation of the Isu Fe-S cluster intermediate in mitochondria

Isu physically interacts with Nfs1/Isd11 and frataxin [19]. The multi-protein complex forms a core machinery for Fe-S cluster biosynthesis, facilitating and accelerating the formation of cluster intermediates on Isu [22]. The protein complex was isolated from yeast [19] and human [96] mitochondria, although no crystal structures are available and there is little overall structural information. Two particularly informative prokaryotic complexes have been structurally characterized. In one case, the Nfs1 (bacterial IscS) dimer was viewed in head to tail configuration [97]. Two Isu (bacterial IscU) monomers were seen binding at the ends of each Nfs1, maximally separated from each other and precluded from interacting with each other. Frataxin (bacterial CyaY) monomers were found in a groove between each Isu and the Nfs1 surface. The molecular stoichiometry (2 Nfs1:2 Isu:2 frataxin) and orientation of the components suggest that Fe-S cluster intermediates might be formed separately on each Isu monomer (Fig. 6.4). Isd11 was not present in this structure because it is not present in prokaryotes [97]. In another structural study, the *A. vinelandii* NifS (Nfs1 homologue) with a D39A substitution was co-crystallized with the IscU scaffold (Isu homologue), and the Fe-S cluster intermediate was captured in the crystal [98]. The cluster was liganded by three cysteine residues from IscU, and surprisingly, the fourth ligand was provided by the active site cysteine from NifS. The presence of a complete Fe_2S_2 cluster within the NifS/IscU complex showed that the complex did not have to be dissociated for each cycle of cysteine desulfuration; two sulfur atoms were contained in the cluster intermediate and two cycles would be required to form it. Importantly, the fact that the cluster intermediate on IscU was captured in the crystal showed that synthesis could occur separately from transfer [98].

The protein-protein interactions in the Fe-S cluster assembly complex of mitochondria are important for formation of the Fe-S cluster intermediate on Isu (Fig. 6.4). The sulfur for the intermediate is probably directly transferred from the Nfs1 active site to Isu thiol, thus involving direct interaction between Nfs1 and Isu proteins [99]. The flow of sulfur to Isu must be regulated because too little sulfur is deleterious and too much is toxic (Fig. 6.3). The components of the Fe-S cluster assembly complex, frataxin and Isd11, both exert regulatory effects on the cysteine desulfurase for controlling sulfur flow, but these effects are mediated differently. Frataxin stimulates cysteine binding to Nfs1 by exposing new substrate-binding sites. By contrast Isd11, induces a conformational change of Nfs1 that brings the protein loop with the active site cysteine into proximity with the substrate-binding site, so that the persulfides can be formed [27]. At this point, sulfur transfer to Isu can proceed, even without dissociation of the protein complex. Fe-S cluster assembly on Isu involves iron insertion as well as sulfur donation, and this process too is stimulated in the setting of this protein complex (Nfs1/Isd11/Isu/frataxin), as assessed by *in vitro* assays using cysteine, ferrous iron, and dithiothreitol as a reductant [100].

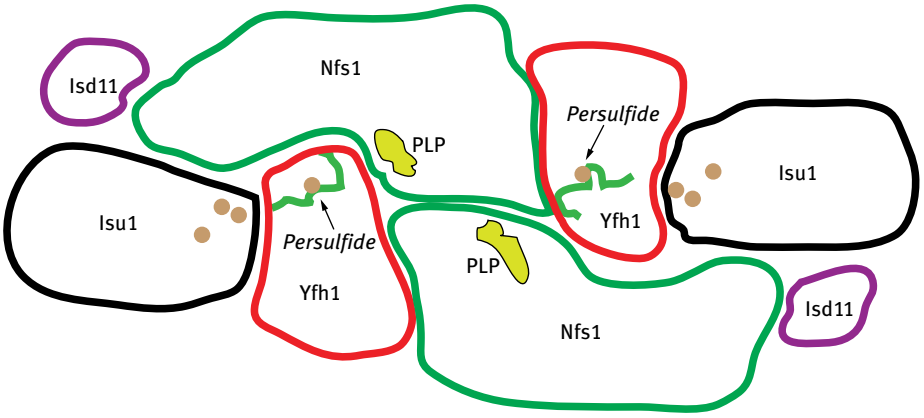

Fig. 6.4: Fe-S cluster assembly complex of the mitochondria. No structure for a eukaryotic or mitochondrial assembly complex has been obtained. The possible locations of key components were outlined based on the positions of the *E. coli* counterparts in the SASX structure [97]. Nfs1 is outlined in green, and it is shown as a head to tail dimer, with substrate-binding sites indicated as yellow "lakes" of PLP in each monomer. The Nfs1 protein loop with the active site cysteine is shown as a green "squiggle," and the active site cysteine is shown as a brown circle labeled "persulfide" because this is the site of persulfide formation. The Isu1 scaffold proteins are shown as black polygons with three brown circles inside, indicating the cysteine residues that coordinate the Fe-S cluster intermediate [97]. The position of the active site loop is such that it could toggle between the Nfs1 substrate-binding site and the Isu1-liganding cysteines without dissociating the Nfs1-Isu1 complex. The Yfh1 proteins are shown in red, and they fit neatly in a space between Isu1 and Nfs1. Isd11 is not present in prokaryotes [11], and so the binding sites in the complex are unknown. Isd11 is shown modeled in purple interacting with Nfs1 and participating in the Nfs1/Isd11/Isu1/Yfh1 Fe-S cluster assembly complex. The manner in which Fe-S cluster assembly on each Isu1 monomer is coordinated (if at all) is unknown.

6.4.3 Roles of frataxin

Frataxin is the protein implicated in the inherited neurodegenerative disease Friedreich ataxia [16]. The finding that the yeast homologue associates with Nfs1/Isd11 and Isu in mitochondria underscores its important role in Fe-S cluster assembly [19]. Two functions ascribed to frataxin relate to sulfur and iron effects, and these are not mutually exclusive. Frataxin stimulates cysteine desulfurase activity of Nfs1 as noted above (Section 6.4.1; Fig. 6.2). Frataxin also plays a role in iron donation for forming the Isu intermediate. Evidence for this function is that iron was found to interact with an acidic surface of purified frataxin with a stoichiometry of 2 atoms per molecule, albeit with a low micromolar (3 μM) affinity [23]. In addition, the interaction of frataxin with the other core assembly components in mitochondria was shown to be iron dependent because it was enhanced by the addition of iron and inhibited by iron chelation [18]. Using purified proteins, Yfh1-Isu1 interaction was found to take place in 1:1 stoichiometry as assessed by ITC measurements, and the interaction occurred only if iron was added to the reaction [23]. Further evidence of frataxin's role was provided by detailed

studies using EXAFS, in which iron was tracked during transfer from frataxin to Isu. Oxygen and nitrogen liganding was detected for iron intermediates bound to frataxin or bound to Isu1, and only when a sulfur source was provided did sulfur ligation supersede the oxygen environment [23]. A picture can be imagined according to which the iron cofactor for Fe-S cluster assembly is bound to frataxin, an iron-dependent interaction with Isu occurs, and iron is then transferred to Isu. When sulfur becomes available in the Fe-S cluster-binding site on Isu, iron migrates to that location and assembles to form the Fe-S cluster intermediate. Of course, iron and sulfur delivery for Fe-S cluster intermediate formation need to be coordinated because it does no good to have one without the other. To address this issue, an interesting set of experiments was performed with protein complexes reconstituted from the mammalian components [100]. In the three-component complex (Nfs1/Isd11/Isu), iron supplied as ferrous ammonium sulfate could be loaded on Isu, up to a stoichiometry of two atoms per complex. In the four-component complex (Nfs1/Isd11/Isu/frataxin), however, iron could not be loaded at all. Only when iron and cysteine were added together to the four-component complex was iron loading achieved, and in that case, a complete Fe-S cluster intermediate was formed on Isu [100]. The implication is that frataxin was blocking iron entry into the Fe-S cluster assembly site on Isu until sulfur was provided *via* the cysteine desulfurase, and only then did it allow iron donation and cluster assembly. How such an iron-gating function would operate is unknown, but multiple conformational changes have been ascribed to Isu [15], and such a change induced by frataxin might close or open a pathway for iron entry into Isu.

6.4.4 Bypass mutation in Isu

A spontaneously occurring mutation in Isu1 was found to confer improved growth and improved Fe-S cluster assembly to a Δ*yfh1* mutant [26]. The mutant Isu1 was able to stimulate cysteine desulfurase of purified Nfs1/Isd11 or of Nfs1 in isolated mitochondria lacking frataxin [27]. These effects explain the frataxin bypass activity because the mutant Isu1 was performing frataxin's function. Interestingly, the bypass substitution mutation altered an amino acid M107 that is conserved with all eukaryotic Isu scaffold proteins. By contrast, the substituted amino acid, isoleucine, occurs in many prokaryotic Isu scaffolds, including *E. coli*. The change can be envisaged as rendering the eukaryotic Fe-S cluster machinery into a more prokaryotic form. The stimulatory effect of frataxin on cysteine desulfurase is a feature of eukaryotic enzyme and contrasts with the prokaryotic enzymes, which are constitutively active. Thus, by changing M107 of Isu1 to I, the need for the stimulatory effect of frataxin was lessened. A detailed examination of the bypass mutant phenotype, however, showed a more nuanced picture. Under usual laboratory conditions, the growth and Fe-S cluster proteins were restored to normal levels. However, under stress conditions exerted by peroxide exposure, the bypass suppressor grew more slowly than the wild-type strain expressing frataxin. The reason for this phenotype is that the bypass Isu mutant corrected the cysteine desulfurase deficit but did not restore the rate of Fe-S cluster assembly to normal [101].

These data suggest that frataxin possesses an additional function (other than cysteine desulfurase stimulation) that is not replaced by the Isu suppressor substitution. A possibility is that iron donation or regulation of iron donation represents the function of frataxin that is not corrected in the bypass mutant.

6.4.5 Transfer of the mitochondrial Isu Fe-S cluster intermediate

The Hsp70s are a large group of chaperones that perform essential functions in protein folding and protein import [101]. They contain two domains – a substrate-binding domain and an enzymatic domain with ATP-binding and hydrolysis activity. The two domains talk to each other, such that substrate binding in one domain is influenced by the nucleotide binding state in the other. The higher affinity substrate binding state is conferred by ADP interaction in the nucleotide-binding site. Co-chaperones or special J proteins are important for conferring functional specificity, bringing the substrate to the substrate-binding site and enhancing nucleotide hydrolysis. Finally, recycling factors are needed to facilitate release of ADP and replacement by ATP [102].

The remarkable story of the mechanism of Isu cluster transfer in mitochondria relates to the special adaptation of a mitochondrial Hsp70 chaperone for this purpose. Ssq1 is an Hsp70 chaperone that has become specialized for handling a single client protein, Isu. The manner in which this specialized reaction cycle functions for accelerating Fe-S cluster transfer is as follows. The Fe-S cluster intermediate is formed on the Isu scaffold, and the holo-Isu thus formed interacts with Jac1, a specialized co-chaperone [103]. Jac1 targets the holo-Isu1 to the ATP-bound Hsp70 chaperone, Ssq1, where it binds in the substrate-binding cleft *via* the conserved LPPVK motif of Isu [104]. Substrate binding to the Hsp70, especially in the context of Jac1 interaction, triggers a burst of ATP hydrolysis and a conformational change in the chaperone [29]. The conformational change compels release of the Isu-bound cluster intermediates with concomitant transfer to the recipient apo-protein. Finally, recycling of ADP and binding of ATP to the nucleotide-binding domain of Ssq1 is facilitated by Mge1, the recycling factor, and this step induces release of apo-Isu1 and initiation of another reaction cycle [31]. In this way, the transfer of Fe-S cluster intermediates is coupled to the activity of the Hsp70, which has been especially adapted for this purpose. The design of the chaperone machinery also adds another level of regulatory control because cluster transfer depends on the ATPase activity of Ssq1, and the latter is activated only when presented with the Isu1 client in the context of Jac1 [29].

6.4.6 Role of Grx5

Grx5, the monothiol glutaredoxin, is a conserved protein required in the later stages of mitochondrial Fe-S cluster assembly [105]. The Δ*grx5* mutant accumulates Fe-S cluster intermediates on Isu, showing that it is not required for the formation of the

intermediates but that it is required for transfer of the intermediates [50]. In addition, the Grx5 protein is able to coordinate an Fe-S cluster *via* thiols of two monomers and two glutathione molecules [106]. A missing link in the larger scheme then was to show that Grx5 interacts with the chaperones in some fashion and that the Grx5-bound cluster functions as an intermediate in Fe-S cluster synthesis. Two recent papers provide some new information on these points. In experiments with the bacterial constituents, Johnson and colleagues [106] were able to show that Fe-S clusters assembled on IscU were transferred to Grx5-gluathione much more efficiently in the presence of chaperones HscA and HscB. In experiments with yeast proteins and yeast mutants, Uzarska *et al.* showed that holo-Isu1 and apo-Grx5 were able to bind Ssq1 simultaneously, with the Grx5 binding outside of the substrate-binding pocket [107]. Such interactions would be well poised to facilitate transfer of the Fe-S cluster intermediate from Isu to Grx5, while all the constituents were still bound on the surface of the Hsp70 chaperone. After forming on Grx5, Fe-S cluster intermediates are probably further modified and distributed to specialized branch pools. Some [Fe_4S_4] proteins such as mitochondrial aconitase apparently need special components (e.g. Iba57) for maturation of its cofactor [108] and others such as lipoic acid synthase use different maturation factors (e.g. Nfu1) [109, 110].

6.4.7 The switch between cluster synthesis and cluster transfer

Fe-S cluster synthesis in mitochondria involves assembly protein complexes (Nfs1 containing) and transfer protein complexes (Jac1 containing) that are set to function sequentially. Recently, it was found that Nfs1 and Jac1 interact with Isu1 at the same site, implying that there must be a switch such that Nfs1 comes off Isu and Jac1 comes on [111]. The physiological signal for the switch has not been identified with certainty, but a logical scheme would be for the switch to depend on the presence or absence of the Isu Fe-S cluster. A proposal for how this might work is as follows: if Isu is in the apo form, it assumes an unstructured conformation, as described for the disordered form of the bacterial IscU [15]. In this form, it is more adapted to Nfs1 binding and Fe-S cluster formation. Meanwhile, if Isu is in the holo form, it assumes a compact conformation, as described for the structured form of the bacterial IscU [15]. In this form, it is more adapted to Jac1 binding and Fe-S cluster transfer. Thus, the formation of the Fe-S cluster on Isu may generate the structural features suited to interacting with the chaperone system, initiating the switch from cluster forming to cluster transferring protein complexes [111].

In summary, Fe-S cluster assembly in mitochondria involves the formation of intermediates on the Isu scaffold, as performed by closely coordinated cysteine desulfurase activation and iron donation steps. More than one cycle of cysteine desulfurase can occur without disassembling the protein complex, and the cluster assembly can occur independent from transfer. The iron source and means of coordinating iron

with sulfur delivery are still poorly characterized, although frataxin plays a role. A switch probably initiated by a conformational change in Isu promotes formation of the Fe-S cluster transfer complexes with Hsp70 chaperones and co-chaperones. The Hsp70 reaction cycle, specially adapted to Isu, facilitates Fe-S cluster transfer. Following this, glutathione and Grx5 receive and distribute the clusters. Insights into the molecular details of this process have been achieved over the last few years, and genetic and biochemical experiments using *S. cerevisiae* have played an important part in providing these insights.

6.5 Role of glutathione

Glutathione is a conserved tripepide consisting of glutamate, cysteine, and glycine [112]. It is synthesized in sequential steps mediated by Gsh1 and Gsh2, and the process is independent of ribosomal protein synthesis [113]. Although these enzymes reside in the cytoplasm, glutathione is found in millimolar amounts in all cellular compartments (cytoplasm, nucleus, endoplasmic reticulum, and mitochondria), implying that specific transporters exist for distributing the compound within the cell, although these putative transporters have not been molecularly identified [114]. Glutathione serves two different roles: on the one hand, it performs a redox buffering function, and on the other hand, it interacts with iron and Fe-S clusters. For the redox buffering function, the effect is mediated by interconversions between reduced (GSH) and oxidized (GSSG) forms, controlled by oxidative stresses and enzymes such as glutathione reductases [114]. The balance between the two forms defines a redox state characteristic of each cellular subcompartment, and this may be important for protein folding within that compartment [115]. For the iron-related function, it is significant that glutathione can interact directly with Fe^{2+} *via* its free thiol, reducing and maintaining solubility of the metal. According to one hypothesis Fe^{2+} glutathione may serve as a labile pool in cells, facilitating trafficking and transfer steps before being incorporated into Fe-S clusters and other cofactors [116]. A new insight into the functions of glutathione came with the discovery of a unique property of monothiol glutaredoxins. These proteins were found to be capable of coordinating Fe-S clusters using the thiols from their CGFS peptide motif and thiols from glutathione [117]. The $[Fe_2S_2]$ ligation was achieved by the contribution of two glutaredoxin molecules and two molecules of reduced glutathione. The lability of these glutaredoxin-glutathione clusters under some *in vitro* conditions led to the suggestion that these molecules might function as biosynthetic intermediates, binding and transferring cofactors or cofactor constituents for downstream utilization. Molecular genetic approaches in yeast have highlighted the roles of monothiol glutaredoxins in mitochondrial Fe-S cluster assembly, both inside mitochondria (Grx5) [118] and outside mitochondria (Grx3 and Grx4) [119]. These proteins appear to act by forming Fe-S cluster intermediates with glutathione.

The yeast Δ*gsh1* mutant was instrumental in the discovery of a role for glutathione in Fe-S cluster assembly. The deletion mutant was found to be auxotrophic for glutathione [120]. Growth of Δ*gsh1* yeast slowed progressively as the intracellular glutathione level declined, reaching about 60 μM after three divisions (down from 3 mM), and growth stopped completely after about ten divisions [121]. Examination of the phenotypes as the fuel ran down, so to speak, revealed striking changes. Genes involved in iron uptake were strongly induced, and genes involved in iron utilization were repressed, consistent with Aft1 activation and an iron starvation response [121]. Tests of iron homeostasis showed induction of cellular iron uptake and simultaneous mitochondrial iron accumulation as nanoparticles, similar to some mutants with Fe-S cluster deficiency [122]. In terms of Fe-S cluster proteins and activities, the observed effects depended on the degree of glutathione depletion achieved. In the early stages, cytoplasmic Fe-S clusters were more strongly affected [122], whereas in later stages, mitochondrial Fe-S cluster proteins were also deficient [121]. Leu1, a cytoplasmic Fe-S cluster protein, was deficient and activity was almost undetectable after seven divisions, whereas mitochondrial aconitase, Aco1, was relatively preserved but also deficient at this point. Interestingly, during the time course of depletion, oxidant stress genes were not induced. Yap1, a redox sensor transcriptional activator, remained in the reduced state and so was not turned on. Aft1, an iron sensor and transcriptional activator, was turned on, indicating that the iron uptake response was occurring earlier (at a higher glutathione threshold) than the oxidative stress response [121]. The experiment of progressive cellular glutathione depletion may be pointing to the existence of different thresholds that titrate different targets of glutathione action: one for cytoplasmic Fe-S cluster synthesis, another one for mitochondrial Fe-S cluster synthesis, and a third one for oxidative stress responses [121].

6.5.1 Glutathione and monothiol glutaredoxins in mitochondria

In yeast, Grx5 is the only monothiol glutaredoxin found in mitochondria. The deletion mutant phenotype was associated with deficiencies of Fe-S cluster proteins and iron homeostasis abnormalities [118]. This phenotypic analysis suggested that it was acting in the same pathway as other mitochondrial ISC components. Additional observations placed Grx5 as a late acting component. In an iron-labeling epistasis experiment, the deletion strain was found to accumulate ^{55}Fe on Isu, suggesting that synthesis of the Fe-S cluster intermediate was able to proceed, whereas transfer of the Fe-S cluster intermediate was blocked [50]. The phenotype was similar to the Ssq1 Hsp70 chaperone mutant, and Ssq1 and Grx5 were recently shown to physically interact. Interestingly, the Ssq1 interaction with Grx5 could occur simultaneously with Isu1 interaction i.e. outside the substrate-binding site and without stimulation of ATP hydrolysis [107]. Thus, Isu1 with bound scaffold intermediate was probably interacting with the Ssq1 chaperone and Grx5, facilitating transfer of the Fe-S cluster

intermediate to Grx5. Glutathione was presumed to be an essential ligand of the cluster intermediate on the glutaredoxin Grx5 and therefore required for the transfer step. Change of the cysteine residue of the CGFS motif in Grx5 to alanine or serine abrogated or decreased the transfer activity [107].

A direct demonstration of a role for glutathione in Fe-S cluster transfer to Grx5 was achieved by elegant experiments with *A. vinelandii* constituents [106]. Fe-S cluster transfer between IscU and Grx5 was monitored by circular dichroism. There was very little basal transfer even in the presence of glutathione; however, a tremendous rate enhancement was achieved by the addition of the chaperones HscA, HscB (homologues of the yeast Ssq1 and Jac1), and MgATP in the presence of glutathione. The second-order rate constant of the transfer of the $[Fe_2S_2]$ clusters increased from 30 to 20,000 M^{-1} min^{-1} [106]. Such a tremendous *in vitro* effect reflecting synergistic interaction among these components almost certainly reflects a physiological role in Fe-S cluster transfer. This experiment also directly demonstrated a role for glutathione because glutathione had to be included in the assays for cluster transfer to occur. Identification of the downstream acceptors for Grx5-glutathione intermediates has not been accomplished as of yet, but candidates include cluster apo-proteins, both $[Fe_2S_2]$ and $[Fe_4S_4]$ proteins, and carrier proteins of branch pathways such as A-type and Nfu1-type carriers. Although these experiments were performed with bacterial proteins, the eukaryotic homologues, Isu1/2, Ssq1, Jac1, and Grx5, will very likely interact with glutathione and behave in a fashion similar to their prokaryotic counterparts during Fe-S cluster transfers.

6.5.2 Glutathione and monothiol glutaredoxins Grx3 and Grx4 outside of mitochondria

In yeast, two redundant monothiol glutaredoxins, Grx3 and Grx4, reside outside of mitochondria, primarily in the cytoplasm and nucleus [53]. In addition to a glutaredoxin domain, these proteins also possess an amino terminal thioredoxin domain and a carboxy terminal Aft1-binding domain [53]. The Grx3 and Grx4 proteins, like Grx5, were shown to coordinate Fe-S clusters [123]. This ability required the presence of the critical cysteine of the CGFS motif and glutathione, as demonstrated by *in vivo* ^{55}Fe immunoprecipitation studies [119] as well as by *in vitro* reconstitution [123]. The loss-of-function Δ*grx3*/Δ*grx4* mutant or the C-to-A (AGFS) allele, exhibited a complicated iron regulatory phenotype, in part due to Aft1 activation and in part due to other downstream effects [119]. In these mutants, cellular iron uptake was increased, reflecting Aft1 activation, and a direct interaction of the C-terminal domain of Grx3 or Grx4 with Aft1 was shown [124, 125]. The manner in which the iron regulatory signal was conveyed to Aft1 is thought to involve the Fe-S clusters on Grx3/4. When the Fe-S clusters on Grx3/4 were present, there was a direct physical interaction with Aft1 protein and other intermediate regulators, e.g. Fra1, causing Aft1 to be retained in

the cytoplasm and preventing the translocation of Aft1 to the nucleus. Conversely, in the absence of the Fe-S clusters on Grx3/4, Aft1 did not interact and nuclear translocation occurred concurrent with transcriptional activation of iron uptake and other effects [124].

The iron-related phenotypes, however, were more complicated and not entirely explained by the Grx3/4-Aft1 axis. In the Δ*grx3*Δ*grx4* mutant, iron uptake was activated but mitochondrial iron accumulation did not occur, distinguishing this phenotype from other mutants with Fe-S cluster assembly deficits [119]. Another unique aspect of the phenotype was a more global iron deficiency, affecting iron proteins in various cellular compartments and with various types of cofactors. Heme and di-iron proteins were also found to be deficient in these mutants, suggesting that a global problem with biological iron was affecting all types of cellular iron proteins. The problem affected both cytoplasmic and mitochondrial proteins. For example, nuclear-cytoplasmic ribonucleotide reductase, which requires a di-iron cofactor for generating a critical sulfur radical was deficient in *grx3/4* mutants [126]. Similarly, Coq7, a protein located on the matrix face of the mitochondrial inner membrane, utilizes a di-iron cofactor for synthesis of ubiquinone in mitochondria. This enzyme was also deficient in the *grx3/4* mutant as shown by accumulation of the DMQ6 precursor metabolite in the matrix fraction [119]. The implication is that Grx3/4-glutathione Fe-S clusters may be involved, either directly or indirectly, in providing iron for synthesis of cellular iron proteins. It is not yet clear how this works. Possibly, iron atoms of the Grx3/4-glutathione Fe-S clusters are cannibalized in a process that generates iron intermediates for biosynthesis of iron cofactors. In one scheme that has been proposed, an iron-glutathione conjugate with iron bound to the free thiol of a GSH molecule acts as the low molecular weight labile iron pool [116]. Measurements of this pool suggest it may measure about 1 μM in the cytoplasm of most cell types [116]. The cytoplasmic pool could then be tapped for cytoplasmic cofactor synthesis and transfer into mitochondria for mitochondrial Fe-S cluster and heme synthesis.

6.6 Role of Atm1, an ABC transporter of the mitochondrial inner membrane

Atm1 is an ABC transporter of the mitochondrial inner membrane [54]. A key feature has to do with its topology, with its predicted ATP- and substrate-binding sites oriented toward the interior or matrix side of mitochondria [54]. The implication of this finding is that Atm1 likely exports its substrate(s) from inside to outside of mitochondria. A major missing piece of the puzzle is the unknown identity of the substrate(s).

The *ATM1* gene was disrupted, and the mutant phenotypes were determined. The mutant grew slowly on rich medium and did not grow at all on minimal medium. The mitochondrial genome was destabilized, and the isolated mitochondria were completely white, indicating a lack of cytochromes [54]. Fe-S cluster proteins were

also deficient in the mutant. In some studies, both mitochondrial and cytoplasmic Fe-S clusters were deficient [127], whereas in others, mitochondrial Fe-S clusters were relatively preserved [93]. The iron accumulation phenotype characteristic of Fe-S cluster deficiency was prominently displayed by the Δ*atm1* mutant, with loss of homeostasis and iron accumulation in mitochondria [68, 128]. The biophysical characteristics of the mitochondrial iron were investigated [127]. Similar to the situation for mitochondrial Fe-S cluster assembly mutants (e.g. Yah1- or Yfh1-deficient cells), mitochondrial iron in Atm1-depleted cells accumulated as ferric phosphate nanoparticles. Fe-S clusters and heme detected by Mössbauer and spectroscopic methods were decreased, but an NHHS Fe^{2+} (nonheme high-spin ferrous) species was noted [127]. Evidence has been presented that this mitochondrial iron species, abundant in *atm1* mutant and also present in wild-type cells, could represent an iron intermediate for Fe-S cluster and heme synthesis [129].

Microarray analysis of Atm1-depleted cells revealed a large number of induced and repressed transcripts [130]. The effects reflected a general iron starvation response. The Aft1 regulon was strongly induced, causing activation of the cellular iron uptake systems. Transcripts for Isu1/2 scaffold proteins were increased, whereas Grx5 was repressed. The genes for citric acid cycle enzymes and for proteins involved in oxidative phosphorylation and ergosterol biosynthesis were repressed, consistent with an effort to conserve iron by minimizing utilization. The effects were virtually identical to the phenotypes of Fe-S cluster deficiency associated with depletion of the mitochondrial ferredoxin, Yah1 [130]. However, there was a set of genes that did not match. The retrograde response genes encoding citrate synthase (*CIT2*), dicarboxylic amino acid permease (*DIP5*), and isocitrate dehydrogenase (*IDH2*) were induced by Yah1 depletion and not by Atm1 depletion [130]. The retrograde response refers to the effects of an unknown signal, produced by dysfunctional mitochondria and acting on rest of the cell, likely mediating different types of compensatory responses [131]. The inability of *atm1* mutant mitochondria to induce a retrograde response could mean that Atm1 in some fashion mediates this signaling pathway.

6.6.1 Cells lacking Atm1 lose mtDNA

Iron accumulates in Atm1-deficient cells, causing oxidative damage to cellular constituents, and iron proteins are deficient in mitochondria and cytoplasm. Thus, the pleiomorphic phenotypes of these cells make it very difficult to determine the primary function of the exporter. Two types of experiments have aided in further parsing these phenotypes. If Gal-Atm1 cells were grown under repressing conditions (glucose) and at the same time were kept anaerobic, Atm1 was depleted from the cells, but the characteristic iron accumulation was abrogated. The lack of iron accumulation was associated with improved heme and improved Fe-S cluster levels. Oxidative damage to mitochondrial proteins as assessed by carbonyl adducts was also prevented [127]. By contrast, cytoplasmic isopropylmalate isomerase (Leu1), which requires

a [Fe_4S_4] cluster for catalyzing a critical step in the leucine biosynthetic pathway, was diminished in both anaerobic and aerobic conditions [127]. However, in another work [132], both wild-type and Gal-Atm1 cells grown in glucose were shown to be Leu1 deficient, raising the question of whether the enzyme deficiency was a carbon source effect rather than an Atm1 effect. In another type of experiment, the Gal-Atm1 cells were shifted from the inducing carbon source, galactose, to a repressing carbon source, glucose, and Atm1 was progressively depleted. Cytoplasmic Leu1 activity declined, whereas mitochondrial aconitase and succinate dehydrogenase were relatively preserved [93]. However, the differences very much depended on experimental conditions, such that with shorter depletion times only minor effects were noted, whereas with extremely long depletion times, mtDNA effects ensued and both mitochondrial and cytoplasmic Fe-S clusters were compromised. In the human disease resulting from missense mutations in the gene for the homologous protein ABCB7, the principal manifestation is anemia. In studies of blood cells from such individuals, protoporphyrin was found to accumulate, indicating that these mitochondria were abnormal and exhibited problems with iron metabolism [133]. Both mitochondrial and cytoplasmic aconitases were deficient in HeLa cell knockdowns of the homologous ABCB7, indicating an effect of ABCB7 on Fe-S cluster biogenesis in both compartments [133]. Thus, the precise roles of Atm1 in mitochondrial *vs* cytoplasmic iron metabolism and Fe-S cluster assembly remain to be elucidated.

The answers to Atm1 function may ultimately come from better understanding of the protein itself and by the identification of its transport substrate(s). Atm1 is encoded by a nuclear gene with an N-terminal mitochondrial targeting signal [54]. The protein is synthesized on cytoplasmic ribosomes and is post-translationally imported and matured by cleavage of the targeting sequence within mitochondria. Atm1 is an integral membrane protein of the inner membrane with both N- and C-termini oriented toward the matrix side, suggesting that six transmembrane domains span the inner membrane. The finding that the C-terminal domain of the protein is in the matrix is especially important because this domain includes the nucleotide-binding site as well as the putative substrate-binding site [54]. These topology data led to the prediction that the Atm1 substrate originates within mitochondria and that Atm1 must function to export its substrate from the mitochondrial matrix to the intermembrane space. The protein self-assembles to form homodimers *in vivo*, and this has been experimentally demonstrated [134]. Other mitochondrial ABC half transporters with similar topology include Mdl1 and Mdl2. These proteins are called half transporters because of their requirement for dimerization. The former may be a peptide exporter, and as for the latter, the substrate is undefined [135]. ABC transporters often show stimulation of their ATPase activity when challenged with the correct transport substrate. Experiments have been performed with Atm1-containing liposomes, seeking to identify the substrate, and stimulation was observed with micromolar concentrations of thiol rich peptides [136]. Further identification of the substrate has not been achieved, however. Thus, it will be important to identify the Atm1 substrate(s)

to finally ascertain its function. The phenotypes of Atm1-depleted cells suggest that its transport substrate has something to do with Fe, S, Fe-S, and/or heme. The iron accumulation phenotype and gene regulation phenotype coincide closely with the phenotypes of other Fe-S cluster assembly mutants [135]. A role of Atm1 in Fe-S cluster assembly therefore seems likely. It is possible that the Atm1 transport substrate is a constituent needed for Fe-S cluster assembly such as iron, an activated form of sulfur, or glutathione. Alternatively, a molecule mediating a form of retrograde signaling might be exported by Atm1, and this could be a peptide, nucleotide, siderophore, or other specialized molecule.

6.7 Relationship between Fe-S cluster biogenesis and iron homeostasis

A distinctive iron homeostatic phenotype was first observed in yeast mutants with defects in frataxin [17] or Ssq1 [57]. It was subsequently recognized that these mutants were also deficient in Fe-S cluster assembly and that there was a connection between Fe-S cluster assembly and iron homeostasis [56, 137]. Yeast deploys cellular iron uptake systems that homeostatically respond to iron availability, increasing cellular uptake in response to iron starvation and repressing cellular uptake in response to iron repletion. In various mutants (e.g. *nfs1-14*) with Fe-S cluster defects, however, the iron uptake systems were constitutively induced and unresponsive to iron availability. If more iron was added to the growth medium, more was taken up into the cells. Furthermore, the excess cellular iron was diverted to mitochondria, reaching levels of 100 times or more the normal range [6]. Mitochondrial iron accumulating in these mutants was also different from that of the wild-type in terms of the physical properties. When mitochondria isolated from the mutants were treated with a non-ionic detergent such as Triton X-100, most of the proteins were solubilized, leaving the majority of the iron in the insoluble fraction. This iron insolubility correlated with a lack of iron availability for cofactor synthesis. In Yfh1-depleted cells, for example, heme synthesis was deficient because iron was unavailable to the ferrochelatase enzyme in mitochondria; instead, zinc was inserted in place of iron, generating zinc protoporphyrin [21].

A more sophisticated and quantitative approach to characterizing iron in mitochondria has been undertaken by Lindahl and colleagues. Briefly, a combination of methods including Mössbauer, EPR, and UV-Vis spectroscopy combined with ICP-MS for metal quantification was applied to studies of isolated mitochondria. A packing efficiency parameter was measured for preparations of isolated mitochondria so that concentrations of different iron species could be calculated [138]. In wild-type mitochondria, the total iron was found to be present at very high concentrations of about 700–800 μM, and this could be divided into different pools. In respiring cells, 70% of the mitochondrial iron was present in Fe-S cluster and heme cofactors of respiratory

complexes. An iron pool within mitochondria was recognized by a distinctive signature in Mössbauer studies, the nonheme high-spin ferrous pool (NHHS Fe^{2+}). This was proposed to act as feedstock for biosynthetic activities by supplying iron for heme, Fe-S cluster, and probably di-iron-containing proteins. Accordingly, shifting of growth conditions from fermentable to non-fermentable carbon source induced a shift in the mitochondrial iron distribution, with a marked decrease in the NHHS Fe^{II}, and an increase in the protein-bound iron pools, consistent with utilization of iron intermediates and a metabolic shift to oxidative phosphorylation [81]. Iron nanoparticles were also detected in mitochondria. These particles, with characteristic Mössbauer features, are 2- to 4-nm-diameter spheroids containing magnetically interacting Fe^{3+} ions coordinated by oxygen donor ligands, including phosphate and polyphosphate. A small quantity of iron nanoparticles was detected in wild-type mitochondria grown under respiring conditions and more were detected under fermenting conditions. In the Fe-S cluster assembly mutants the total mitochondrial iron could be as high as 10 mM, mostly in the form of nanoparticles [139]. Thus, the nanoparticles represent the pool of insoluble iron noted in biochemical studies of the same mutants. In various Fe-S cluster assembly mutant cells examined by electron microscopy, iron nanoparticles were visible as electron dense bodies in the mitochondrial matrix (Fig. 6.5). Aggregates or nanoparticles were found sporadically in different parts of the mitochondria. Some areas were spared and others were heavily involved, consistent with the importance of local conditions; iron aggregation may depend on local ferroxidation and nucleation events (Fig. 6.5).

The question has been posed whether mitochondrial iron overload produces the Fe-S cluster assembly defect or vice versa. Experiments performed with Yfh1 (or Nfs1) under control of a regulated promoter allowed the protein to be depleted from cells and then reintroduced. During these time course experiments, the Fe-S cluster assembly defect appeared prior to mitochondrial iron accumulation [6, 21]. Conversely, recovery of the Fe-S cluster defect occurred rapidly upon re-expression of the protein and prior to clearing of mitochondrial iron [21]. Thus, the Fe-S cluster defect was considered to be primary, and the iron homeostatic effect was considered to be secondary. However, iron accumulation can worsen the Fe-S cluster defect in a situation with some residual activity, such as in a deletion of Yfh1 [140]. Under anaerobic conditions, no accumulation occurred during Gal-Atm1 depletion, perhaps because iron uptake was blocked in the absence of ferroxidase requiring Fet3 or because iron oxidation in mitochondria was a driving force and did not occur in the absence of oxygen. Under these conditions, iron proteins and enzyme activities were much improved because iron toxicity was lessened [127]. Thus, iron toxicity does contribute to the Fe-S cluster defect, although the major causal arrows seem to point the other way, from Fe-S cluster defect to the iron homeostatic defect.

The iron homeostatic phenotype can be viewed as Fe-S cluster deficiency and increased cellular uptake associated with mitochondrial iron accumulation in the form of nanoparticles. Various Fe-S cluster assembly mutants have been associated

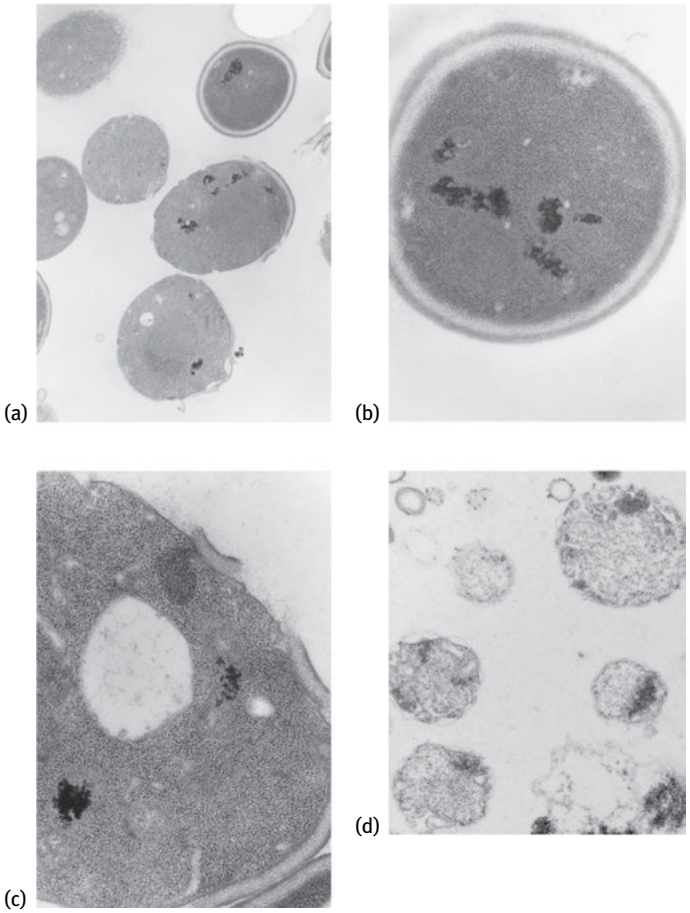

Fig. 6.5: Iron accumulation phenotype. A mutant carrying a truncated form of Ssq1 was identified in a genetic screen [57]. The *ssq1* mutant cells were grown in defined medium with 10 μM ferric chloride, fixed with glutaraldehyde, lightly stained with osmium tetroxide and potassium ferrocyanide, and visualized using a Jeol 100CX model electron microscope as described [57]. Shown are (a) multiple cells, most of which contain electron dense iron aggregates in mitochondria, (b) and (c) higher magnification views of affected cells, (d) isolated intact mitochondria with iron accumulations. Aggregates or nanoparticles occur sporadically in different parts of the mitochondria, which may contain larger or smaller deposits of iron.

with the homeostatic phenotype. These include mutations in components affecting formation of the mitochondrial Isu intermediate (Nfs1 [6], Isd11 [9, 10], Yfh1 [17], Yah1 [51], Arh1 [52]) (Tab. 6.2, item 1) and components involved in transfer of the Isu intermediate to recipients (Ssq1 [57], Jac1 [67, 141], Grx5 [117]) (Tab. 6.2, item 2). The Fe-S cluster scaffold Isu1 is redundant with Isu2, and so the single mutants exhibited a mild phenotype, although some iron accumulation was noted [13]. Depletion of Isu1

in an Δ*isu2* mutant [14] or hypomorphic alleles of Isu1 (M107E) in the Δ*isu2* mutant produced a strong iron accumulation phenotype (Tab. 6.2, item 3). The existence of branch pathways required for distribution of Fe-S cluster intermediates to specialized pools has recently been discovered in yeast and *E. coli*. The purview and substrates for these pathways are subjects of active research [1]. The Nfu1 mutant, originally isolated by its synthetic lethality with Ssq1 [89], was recently found to be associated with deficiencies of maturation of lipoate-containing 2-oxoacid dehydrogenases and assembly of some respiratory chain complexes [109, 110]. No iron homeostatic changes were noted in this mutant. Similarly, other proteins associated with subsets of Fe-S cluster protein maturation, such as Iba57 [108] and Mms19 [141], were not associated with perturbed iron homeostasis. By contrast, mutants of Isa1 and Isa2 did show the phenotype [142]. These proteins were originally proposed to act as alternative scaffold proteins in mitochondria but they did not show redundancy with Isu proteins, and later they were shown to be involved in iron donation for $[Fe_4S_4]$ cluster assembly in mitochondria [143]. Isa1 and Isa2 proteins are not redundant with each other, and the corresponding deletion strains were independently associated with activation of the iron uptake system and iron homeostatic abnormalities [142] (Tab. 6.2, item 4).

Mutation or deletion of the ABC transporter Atm1 also gave a strong iron homeostatic phenotype, with iron accumulation in the cell and mitochondria [68, 128]. The role of Atm1 in Fe-S cluster assembly is still unresolved and quite controversial (see Section 6.6). However, the iron homeostatic effects are unambiguous, and they strongly resemble the iron homeostatic effects caused by defects in the core mitochondrial Fe-S cluster assembly components (Tab. 6.2, item 5). Erv1 is a sulfhydryl oxidase of the mitochondrial intermembrane space and is required for protein import and trapping of precursor proteins in that compartment. Interestingly, it is also involved in some aspects of Fe-S cluster assembly, and temperature-sensitive mutations have been associated with mitochondrial iron accumulation [144]. Glutathione appears to participate in multiple steps of Fe-S cluster assembly *via* interactions with monothiol glutaredoxins (Grx5 and Grx3/Grx4) and perhaps by other mechanisms. Depletion of cellular glutathione has been experimentally achieved by depriving the Δ*gsh1* mutant of exogenous glutathione, and in this setting, iron homeostatic abnormalities ensued, including increased cellular uptake and iron accumulation in mitochondria [121, 122]. It is unknown which of the cellular targets primarily mediates the glutathione iron homeostasis effects, but targets may include Grx3 and Grx4 (Tab. 6.2, item 6). A machinery dedicated to cytoplasmic and nuclear Fe-S cluster assembly has been characterized in yeast [3]. The components are encoded by essential genes, and they perform reductase, scaffold, ATPase, and transfer functions. These include Dre2, Tah18, Nbp35, Cfd1, Nar1, Cia1, Cia2, and Mms19 (Tab. 6.2, item 7). Depletion or mutation of these genes has been associated with deficiencies of many cytoplasmic and nuclear Fe-S cluster proteins, but cellular iron uptake was unaffected, and mitochondrial iron accumulation was not observed. Fe-S cluster assembly mutants of the CIA components did not perturb iron regulation [3].

Tab. 6.2: Yeast mutants that do or do not accumulate iron in mitochondria.

Gene(s)	Function	Aft1 activation	Mitochondrial iron accumulation	References
1. Core assembly component involved in formation of the Isu intermediate in mitochondria				
Nfs1	Cysteine desulfurase	+	+	[6]
Isd11	Accessory protein	+	+	[9, 10]
Yah1	Ferredoxin	+	+	[51]
Arh1	Ferredoxin reductase	+	+	[52]
Yfh1	Yeast frataxin homologue	+	+	[17]
2. Core assembly component involved in transfer of the Isu intermediate to recipient proteins in mitochondria				
Ssq1	Hsp70 chaperone	+	+	[57]
Jac1	J protein co-chaperone	+	+	[67, 145]
Grx5	Monothiol glutaredoxin	+	+	[118]
3. Mitochondrial scaffold protein				
Isu1 Isu1 (M107E)	Mitochondrial scaffold	+	+	[13, 14]
4. Branch pathway proteins mediating Fe-S cluster assembly of a subset of proteins				
Nfu1	Lipoic acid synthase requires	–	–	[109, 110]
Iba57	Aconitase requires	–	–	[108]
Isa1, Isa2	$[Fe_4S_4]$ clusters require	+	+	[142, 143]
5. Mitochondrial export and associated proteins				
Atm1	ABC transporter	+	+	[68, 128]
Erv1	Sulfhydryl oxidase of intermembrane space	+	+	[144]
6. Glutathione				
Gsh1	Glutathione synthesis	+	+	[121, 122]
Grx3, Grx4	Monothiol glutaredoxins	+	–	[119]
7. Cystosolic Fe-S cluster assembly components				
Dre2, Tah18	Reductase components	–	–	[37, 38]
Cfd1, Nbp35	Scaffold components	–	–	[76]
Nar1, Cia1, Cia2, Mms19	Transfer components	–	–	[3]
8. Mitochondrial carrier proteins				
Mtm1	Unknown substrate	+	+	[146]
Ggc1	GTP/GDP exchanger	+	+	[147, 148]
Mrs3, Mrs4	Putative iron importers	+	–	[84]
9. Iron regulatory				
Aft1-1^{up}	Iron transcriptional regulator	+	–	[17]
Fra1, Fra2	Co-regulatory factors	+	–	[149]
10. Heme biosynthesis				
Hem1, Hem15	Porphyrin synthesis	–	–	[150]

Mitochondrial carrier proteins Mtm1 [146] and Ggc1 [147] were also required for iron homeostasis (Tab. 6.2, item 8). The carrier proteins belong to a family of proteins with uncertain evolutionary origin and are responsible for moving varied substrates in and out of mitochondria by transport across the mitochondrial inner membrane [151]. Mtm1 exhibits a network of cytoplasmic and matrix salt bridges and therefore is expected to function as an obligate exchanger, with substrate binding in the intermembrane space followed by exchange for a matrix substrate [152]. The identity of the substrates, either imported from the cytoplasm or exported from the mitochondria, is unknown. A guess is that they may resemble amino acids, as indicated by an evolutionary analysis that groups Mtm1 with known amino acid transporters [152]. The phenotype of the Δ*mtm1* deletion strain is similar to that of other mitochondrial iron accumulators. Iron uptake is induced, mitochondrial iron builds up in the form of nanoparticles, and Fe-S cluster proteins are deficient [153, 154]. Thus, it is possible that Mtm1 transports a critical but unknown substrate that is required for mitochondrial Fe-S cluster assembly. The deficiency of this unknown molecule might impair mitochondrial Fe-S cluster assembly, triggering a secondary signal that disrupts iron homeostasis. A role for Mtm1 in heme synthesis has also been proposed [155]. Because both heme synthesis and Fe-S cluster synthesis are affected in the mutant, an explanation could be that the Mtm1 substrate mediates iron delivery for cofactor synthesis in the mitochondrial matrix.

Ggc1 is another mitochondrial carrier protein (Tab. 6.2, item 8). In this case, the substrate is known and transport has been demonstrated by vesicle studies [148]. The yeast protein was expressed in *E. coli* and reconstituted into liposomes. Based on the transport studies showing exchange activity for GTP and GDP, the function of the transporter was proposed to deliver GTP into the mitochondrial matrix for important processes such as nucleic acid and protein synthesis [148]. An additional function was revealed by studies with the Δ*ggc1* mutant showing defective mitochondrial Fe-S cluster assembly and iron homeostasis [147]. The GTP dependence of the Fe-S cluster assembly defect was demonstrated by a bypass experiment. In this experiment, the mammalian GTP-generating enzyme, Nm23-H4, was targeted to the mitochondrial matrix of the yeast Δ*ggc1* mutant. The Δ*ggc1* mitochondria expressing the bypass enzyme, although they could still not transport GTP from the cytoplasm, were now able to synthesize GTP inside mitochondria. The mutant phenotypes were thereby reverted, including recovery of normal Fe-S cluster assembly and normal iron regulation [147]. These studies showed yet again that Fe-S cluster assembly and iron homeostasis are linked; GTP depletion of the mitochondria was associated with both defective Fe-S cluster assembly and perturbed iron homeostasis, and GTP repletion was associated with recovery of Fe-S cluster assembly and normal iron homeostasis [90]. The results also suggest that there is a GTP-dependent enzyme in mitochondria, perhaps a GTPase, involved in Fe-S cluster assembly. The identification of this enzyme is the objective of an ongoing search.

At the cellular level, the uptake systems are regulated by the Aft1 sensor/regulator with important inputs *via* the Cth1/2 mRNA stability modulators [156]. Recent discoveries have shown that Aft1 is retained in the cytoplasm by interactions with Fe-S cluster

proteins Grx3/4-Fra1. In the absence of the regulatory clusters such as occurs in Fe-S cluster assembly mutants, Aft1 is translocated to the nucleus, and there it activates a set of target genes (including Fet3 and Ftr1, the iron transporters of the plasma membrane) by direct interaction with sequences in the target promoters [157]. Thus, lack of Fe-S clusters turns on the cellular iron uptake system. Aft1-1^{up}, an activating mutation in Aft1, is associated with constitutive cellular iron uptake but not mitochondrial iron accumulation [17] (Tab. 6.2, item 9). Similarly, *fra1* or *fra2* mutants activate cellular but not mitochondrial uptake [149] (Tab. 6.2, item 9). The means by which lack of Fe-S clusters augments mitochondrial iron levels is less clear. The lack of heme synthesis in some mammalian cells (e.g. from mutant alleles of erythroid 5-aminolevulinic acid synthase) is associated with mitochondrial iron accumulation and sideroblastic anemia [158]. However, the regulatory circuits are different for yeast, and *hem1* or *hem15* mutants do not accumulate iron in mitochondria [150] (Tab. 6.2, item 10).

A hypothetical scheme for explaining the iron accumulation phenotype of Fe-S cluster assembly mutants is as follows. Iron in mitochondria is regulated, and the functional iron pool, perhaps the NHHS Fe^{II} pool [138] or the soluble iron pool, is maintained in a narrow range by homeostatic controls. If the level declines, more is taken up by transport from the cytoplasm, and if the level increases, less is taken up. In the pathological situation of the iron accumulation mutants, the functional iron pool in mitochondria becomes non-utilizable because of precipitation and aggregation. Precipitated iron is inert to the sensing/feedback system in mitochondria, and so more iron enters, continuously feeding the insoluble pool, while the functional pool remains diminished. The defect in Fe-S cluster assembly leads to a decrease in the soluble iron pool, which in turn leads to more mitochondrial iron uptake and accumulation of the nanoparticles. Unfortunately, many of the key variables for this scheme are undefined. The chemical form of the soluble iron pool in cytoplasm is unknown. The transport of iron into mitochondria is thought to be mediated by the carrier proteins, Mrs3 and Mrs4 [80, 84], Rim2 [85], and Mtm1 [146]. Mmt1/2 [159] may also be involved, but the iron-related substrates for these transporters are not well defined, and feedback controls for iron transport are unknown. Finally, the key Fe-S cluster protein(s) responsible for the complex iron regulatory phenotype has not been identified. Recently a number of regulatory Fe-S clusters have been discovered. Aft1, Fra1, Grx3, Grx4, and maybe Yap5 are extra-mitochondrial proteins shown to interact with clusters that perform regulatory functions in iron homeostasis [157]. However, none of these (when interrupted or mutated) fully account for the mitochondrial iron accumulation phenotype. The precise manner in which Fe-S clusters control mitochondrial iron remains to be clarified.

6.8 Conclusion and missing pieces

A variety of biochemical and genetic approaches undertaken through studies in yeast have yielded the outlines of a picture of the Fe-S cluster assembly process in eukaryotes. However, key pieces are still obscured. In mitochondria, the Fe-S cluster assembly

complex and Fe-S cluster transfer complexes are better defined, but how the switch between them occurs is not known. How is the assembly process calibrated so that enough Fe-S clusters are made to satisfy the demands of new protein synthesis and to keep up with turnover occurring during the course of cellular stresses? The regulatory controls that occur within mitochondria are just beginning to be defined. Cysteine desulfurase in mitochondria appears to be highly regulated, but this is probably just the first glimpse of the types of extensive regulatory controls involved. The iron source for Fe-S cluster synthesis is still mysterious, and the manner in which iron and sulfur availability are coordinated is not known. The existence of mitochondrial and cytoplasmic Fe-S cluster proteins necessitates assembly systems that function inside and outside of mitochondria. However, the signaling between these compartments and the coordination of the Fe-S cluster synthesis in mitochondria and cytoplasm needs to be better understood. Finally, the iron homeostatic abnormality resulting from Fe-S cluster synthesis defects represents the failure of a regulatory signal, and the nature of the signal needs to be better defined.

Acknowledgments

A.D. and D.P. are supported by National Institutes of Health Grants R37DK053953 and RO1AG030504, respectively. We thank Alok Pandey for help with some of the graphics.

References

[1] Roche B, Aussel L, Ezraty B, Mandin P, Py B, Barras F. Iron/sulfur proteins biogenesis in prokaryotes: formation, regulation and diversity. Biochim Biophys Acta 2013;1827:455–69.
[2] Johnson DC, Dean DR, Smith AD, Johnson MK. Structure, function, and formation of biological iron-sulfur clusters. Annu Rev Biochem 2005;74:247–81.
[3] Stehling O, Lill R. The role of mitochondria in cellular iron-sulfur protein biogenesis: mechanisms, connected processes, and diseases. Cold Spring Harb Perspect Med 2013;3:1–17.
[4] Zheng L, White RH, Cash VL, Jack RF, Dean DR. Cysteine desulfurase activity indicates a role for NIFS in metallocluster biosynthesis. Proc Natl Acad Sci USA 1993;90:2754–8.
[5] Zheng L, White RH, Cash VL, Dean DR. Mechanism for the desulfurization of L-cysteine catalyzed by the nifS gene product. Biochemistry 1994;33:4714–20.
[6] Li J, Kogan M, Knight SA, Pain D, Dancis A. Yeast mitochondrial protein, Nfs1p, coordinately regulates iron-sulfur cluster proteins, cellular iron uptake, and iron distribution. J Biol Chem 1999;274:33025–34.
[7] Naamati A, Regev-Rudzki N, Galperin S, Lill R, Pines O. Dual targeting of Nfs1 and discovery of its novel processing enzyme, Icp55. J Biol Chem 2009;284:30200–8.
[8] Pandey A, Golla R, Yoon H, Dancis A, Pain D. Persulfide formation on mitochondrial cysteine desulfurase: enzyme activation by a eukaryote-specific interacting protein and Fe-S cluster synthesis. Biochem J 2012;448:171–87.
[9] Adam AC, Bornhovd C, Prokisch H, Neupert W, Hell K. The Nfs1 interacting protein Isd11 has an essential role in Fe/S cluster biogenesis in mitochondria. EMBO J 2006;25:174–83.

[10] Wiedemann N, Urzica E, Guiard B, et al. Essential role of Isd11 in mitochondrial iron-sulfur cluster synthesis on Isu scaffold proteins. EMBO J 2006;25:184–95.
[11] Richards TA, van der Giezen M. Evolution of the Isd11-IscS complex reveals a single alpha-proteobacterial endosymbiosis for all eukaryotes. Mol Biol Evol 2006;23:1341–4.
[12] Goldberg AV, Molik S, Tsaousis AD, et al. Localization and functionality of microsporidian iron-sulphur cluster assembly proteins. Nature 2008;452:624–8.
[13] Garland SA, Hoff K, Vickery LE, Culotta VC. Saccharomyces cerevisiae ISU1 and ISU2: members of a well-conserved gene family for iron-sulfur cluster assembly. J Mol Biol 1999;294:897–907.
[14] Gerber J, Neumann K, Prohl C, Muhlenhoff U, Lill R. The yeast scaffold proteins Isu1p and Isu2p are required inside mitochondria for maturation of cytosolic Fe/S proteins. Mol Cell Biol 2004;24:4848–57.
[15] Markley JL, Kim JH, Dai Z, et al. Metamorphic protein IscU alternates conformations in the course of its role as the scaffold protein for iron-sulfur cluster biosynthesis and delivery. FEBS Lett 2013;587:1172–9.
[16] Campuzano V, Montermini L, Molto MD, et al. Friedreich's ataxia: autosomal recessive disease caused by an intronic GAA triplet repeat expansion. Science 1996;271:1423–7.
[17] Babcock M, de Silva D, Oaks R, et al. Regulation of mitochondrial iron accumulation by Yfh1p, a putative homolog of frataxin. Science 1997;276:1709–12.
[18] Gerber J, Muhlenhoff U, Lill R. An interaction between frataxin and Isu1/Nfs1 that is crucial for Fe/S cluster synthesis on Isu1. EMBO Rep 2003;4:906–11.
[19] Wang T, Craig EA. Binding of yeast frataxin to the scaffold for Fe-S cluster biogenesis, Isu. J Biol Chem 2008;283:12674–9.
[20] Duby G, Foury F, Ramazzotti A, Herrmann J, Lutz T. A non-essential function for yeast frataxin in iron-sulfur cluster assembly. Hum Mol Genet 2002;11:2635–43.
[21] Lesuisse E, Santos R, Matzanke BF, Knight SA, Camadro JM, Dancis A. Iron use for haeme synthesis is under control of the yeast frataxin homologue (Yfh1). Hum Mol Genet 2003;12: 879–89.
[22] Tsai CL, Barondeau DP. Human frataxin is an allosteric switch that activates the Fe-S cluster biosynthetic complex. Biochemistry 2010;49:9132–9.
[23] Cook JD, Kondapalli KC, Rawat S, et al. Molecular details of the yeast frataxin-Isu1 interaction during mitochondrial Fe-S cluster assembly. Biochemistry 2010;49:8756–65.
[24] Bedekovics T, Gajdos GB, Kispal G, Isaya G. Partial conservation of functions between eukaryotic frataxin and the Escherichia coli frataxin homolog CyaY. FEMS Yeast Res 2007;7:1276–84.
[25] Bridwell-Rabb J, Iannuzzi C, Pastore A, Barondeau DP. Effector role reversal during evolution: the case of frataxin in Fe-S cluster biosynthesis. Biochemistry 2012;51:2506–14.
[26] Yoon H, Golla R, Lesuisse E, et al. Mutation in the Fe-S scaffold protein Isu bypasses frataxin deletion. Biochem J 2012;441:473–80.
[27] Pandey A, Gordon DM, Pain J, Stemmler TL, Dancis A, Pain D. Frataxin directly stimulates mitochondrial cysteine desulfurase by exposing substrate-binding sites and a mutant Fe-S cluster scaffold protein with frataxin-bypassing ability acts similarly. J Biol Chem 2013;288:36773–86.
[28] Hoff KG, Silberg JJ, Vickery LE. Interaction of the iron-sulfur cluster assembly protein IscU with the Hsc66/Hsc20 molecular chaperone system of Escherichia coli. Proc Natl Acad Sci USA 2000;97:7790–5.
[29] Schilke B, Williams B, Knieszner H, et al. Evolution of mitochondrial chaperones utilized in Fe-S cluster biogenesis. Curr Biol 2006;16:1660–5.
[30] Tapley TL, Cupp-Vickery JR, Vickery LE. Structural determinants of HscA peptide-binding specificity. Biochemistry 2006;45:8058–66.

[31] Dutkiewicz R, Schilke B, Knieszner H, Walter W, Craig EA, Marszalek J. Ssq1, a mitochondrial Hsp70 involved in iron-sulfur (Fe/S) center biogenesis. Similarities to and differences from its bacterial counterpart. J Biol Chem 2003;278:29719–27.
[32] Tsaousis AD, Gentekaki E, Eme L, Gaston D, Roger AJ. Evolution of the cytosolic Iron/sulfur cluster assembly machinery in Blastocystis sp. and other microbial eukaryotes. Eukaryot Cell 2013;13:143–53.
[33] Boyd JM, Pierik AJ, Netz DJ, Lill R, Downs DM. Bacterial ApbC can bind and effectively transfer iron-sulfur clusters. Biochemistry 2008;47:8195–202.
[34] Boyd JM, Drevland RM, Downs DM, Graham DE. Archaeal ApbC/Nbp35 homologs function as iron-sulfur cluster carrier proteins. J Bacteriol 2009;191:1490–7.
[35] Wilson RB, Roof DM. Respiratory deficiency due to loss of mitochondrial DNA in yeast lacking the frataxin homologue. Nat Genet 1997;16:352–7.
[36] Csere P, Lill R, Kispal G. Identification of a human mitochondrial ABC transporter, the functional orthologue of yeast Atm1p. FEBS Lett 1998;441:266–70.
[37] Zhang Y, Lyver ER, Nakamaru-Ogiso E, et al. Dre2, a conserved eukaryotic Fe/S cluster protein, functions in cytosolic Fe/S protein biogenesis. Mol Cell Biol 2008;28:5569–82.
[38] Netz DJ, Stumpfig M, Dore C, Muhlenhoff U, Pierik AJ, Lill R. Tah18 transfers electrons to Dre2 in cytosolic iron-sulfur protein biogenesis. Nat Chem Biol 2010;6:758–65.
[39] Wingert RA, Galloway JL, Barut B, et al. Deficiency of glutaredoxin 5 reveals Fe-S clusters are required for vertebrate haem synthesis. Nature 2005;436:1035–9.
[40] Sheftel AD, Stehling O, Pierik AJ, et al. Humans possess two mitochondrial ferredoxins, Fdx1 and Fdx2, with distinct roles in steroidogenesis, heme, and Fe/S cluster biosynthesis. Proc Natl Acad Sci USA 2010;107:11775–80.
[41] Shi Y, Ghosh M, Kovtunovych G, Crooks DR, Rouault TA. Both human ferredoxins 1 and 2 and ferredoxin reductase are important for iron-sulfur cluster biogenesis. Biochim Biophys Acta 2012;1823:484–92.
[42] Uhrigshardt H, Singh A, Kovtunovych G, Ghosh M, Rouault TA. Characterization of the human HSC20, an unusual DnaJ type III protein, involved in iron-sulfur cluster biogenesis. Hum Mol Genet 2010;19:3816–34.
[43] Rouault TA. Biogenesis of iron-sulfur clusters in mammalian cells: new insights and relevance to human disease. Dis Model Mech 2012;5:155–64.
[44] Payne RM, Pride PM, Babbey CM. Cardiomyopathy of Friedreich's ataxia: use of mouse models to understand human disease and guide therapeutic development. Pediatr Cardiol 2011;32:366–78.
[45] Selak MA, Lyver E, Micklow E, et al. Blood cells from Friedreich ataxia patients harbor frataxin deficiency without a loss of mitochondrial function. Mitochondrion 2011;11:342–50.
[46] Crooks DR, Jeong SY, Tong WH, et al. Tissue specificity of a human mitochondrial disease: differentiation-enhanced mis-splicing of the Fe-S scaffold gene ISCU renders patient cells more sensitive to oxidative stress in ISCU myopathy. J Biol Chem 2012;287:40119–30.
[47] Allikmets R, Raskind WH, Hutchinson A, Schueck ND, Dean M, Koeller DM. Mutation of a putative mitochondrial iron transporter gene (ABC7) in X-linked sideroblastic anemia and ataxia (XLSA/A). Hum Mol Genet 1999;8:743–9.
[48] Whitnall M, Suryo Rahmanto Y, Huang ML, et al. Identification of nonferritin mitochondrial iron deposits in a mouse model of Friedreich ataxia. Proc Natl Acad Sci USA 2012;109:20590–95.
[49] Amutha B, Gordon DM, Dancis A, Pain D. Chapter 14 Nucleotide-dependent iron-sulfur cluster biogenesis of endogenous and imported apoproteins in isolated intact mitochondria. Methods Enzymol 2009;456:247–66.
[50] Muhlenhoff U, Gerber J, Richhardt N, Lill R. Components involved in assembly and dislocation of iron-sulfur clusters on the scaffold protein Isu1p. EMBO J 2003;22:4815–25.

[51] Lange H, Kaut A, Kispal G, Lill R. A mitochondrial ferredoxin is essential for biogenesis of cellular iron-sulfur proteins. Proc Natl Acad Sci USA 2000;97:1050–5.
[52] Li J, Saxena S, Pain D, Dancis A. Adrenodoxin reductase homolog (Arh1p) of yeast mitochondria required for iron homeostasis. J Biol Chem 2001;276:1503–9.
[53] Herrero E, Belli G, Casa C. Structural and functional diversity of glutaredoxins in yeast. Curr Protein Peptide Sci 2010;11:659–68.
[54] Leighton J, Schatz G. An ABC transporter in the mitochondrial inner membrane is required for normal growth of yeast. EMBO J 1995;14:188–95.
[55] Zheng L, Cash VL, Flint DH, Dean DR. Assembly of iron-sulfur clusters. Identification of an iscSUA-hscBA-fdx gene cluster from Azotobacter vinelandii. J Biol Chem 1998;273:13264–72.
[56] Lill R, Hoffmann B, Molik S, et al. The role of mitochondria in cellular iron-sulfur protein biogenesis and iron metabolism. Biochim Biophys Acta 2012;1823:1491–508.
[57] Knight SA, Sepuri NB, Pain D, Dancis A. Mt-Hsp70 homolog, Ssc2p, required for maturation of yeast frataxin and mitochondrial iron homeostasis. J Biol Chem 1998;273:18389–93.
[58] Roy A, Solodovnikova N, Nicholson T, Antholine W, Walden WE. A novel eukaryotic factor for cytosolic Fe-S cluster assembly. EMBO J 2003;22:4826–35.
[59] Strain J, Lorenz CR, Bode J, et al. Suppressors of superoxide dismutase (SOD1) deficiency in Saccharomyces cerevisiae. Identification of proteins predicted to mediate iron-sulfur cluster assembly. J Biol Chem 1998;273:31138–44.
[60] Yarunin A, Panse VG, Petfalski E, Dez C, Tollervey D, Hurt EC. Functional link between ribosome formation and biogenesis of iron-sulfur proteins. EMBO J 2005;24:580–8.
[61] Chanet R, Heude M. Characterization of mutations that are synthetic lethal with pol3–13, a mutated allele of DNA polymerase delta in Saccharomyces cerevisiae. Curr Genet 2003;43:337–50.
[62] Huang B, Lu J, Bystrom AS. A genome-wide screen identifies genes required for formation of the wobble nucleoside 5-methoxycarbonylmethyl-2-thiouridine in Saccharomyces cerevisiae. RNA 2008;14:2183–94.
[63] Stearman R, Yuan DS, Yamaguchi-Iwai Y, Klausner RD, Dancis A. A permease-oxidase complex involved in high-affinity iron uptake in yeast. Science 1996;271:1552–7.
[64] Puig S, Vergara SV, Thiele DJ. Cooperation of two mRNA-binding proteins drives metabolic adaptation to iron deficiency. Cell Metab 2008;7:555–64.
[65] Nakai Y, Nakai M, Lill R, Suzuki T, Hayashi H. Thio modification of yeast cytosolic tRNA is an iron-sulfur protein-dependent pathway. Mol Cell Biol 2007;27:2841–7.
[66] Li L, Miao R, Bertram S, Jia X, Ward DM, Kaplan J. A role for iron-sulfur clusters in the regulation of transcription factor Yap5-dependent high iron transcriptional responses in yeast. J Biol Chem 2012;287:35709–21.
[67] Kim R, Saxena S, Gordon DM, Pain D, Dancis A. J-domain protein, Jac1p, of yeast mitochondria required for iron homeostasis and activity of Fe-S cluster proteins. J Biol Chem 2001;276:17524–32.
[68] Chen S, Sanchez-Fernandez R, Lyver ER, Dancis A, Rea PA. Functional characterization of AtATM1, AtATM2, and AtATM3, a subfamily of Arabidopsis half-molecule ATP-binding cassette transporters implicated in iron homeostasis. J Biol Chem 2007;282:21561–71.
[69] Kolman C, Soll D. SPL1–1, a Saccharomyces cerevisiae mutation affecting tRNA splicing. J Bacteriol 1993;175:1433–42.
[70] Bjork GR, Huang B, Persson OP, Bystrom AS. A conserved modified wobble nucleoside (mcm5s2U) in lysyl-tRNA is required for viability in yeast. RNA 2007;13:1245–55.
[71] Rouault TA, Stout CD, Kaptain S, Harford JB, Klausner RD. Structural relationship between an iron-regulated RNA-binding protein (IRE-BP) and aconitase: functional implications. Cell 1991;64:881–3.
[72] Brown NM, Kennedy MC, Antholine WE, Eisenstein RS, Walden WE. Detection of a [3Fe-4S] cluster intermediate of cytosolic aconitase in yeast expressing iron regulatory protein 1. Insights into the mechanism of Fe-S cluster cycling. J Biol Chem 2002;277:7246–54.

[73] Tschochner H, Hurt E. Pre-ribosomes on the road from the nucleolus to the cytoplasm. Trends Cell Biol 2003;13:255–63.
[74] Kispal G, Sipos K, Lange H, et al. Biogenesis of cytosolic ribosomes requires the essential iron-sulphur protein Rli1p and mitochondria. EMBO J 2005;24:589–98.
[75] Johansson E, Macneill SA. The eukaryotic replicative DNA polymerases take shape. Trends Biochem Sci 2010;35:339–47.
[76] Netz DJ, Pierik AJ, Stumpfig M, et al. A bridging [4Fe-4S] cluster and nucleotide binding are essential for function of the Cfd1-Nbp35 complex as a scaffold in iron-sulfur protein maturation. J Biol Chem 2012;287:12365–78.
[77] Li L, Bagley D, Ward DM, Kaplan J. Yap5 is an iron-responsive transcriptional activator that regulates vacuolar iron storage in yeast. Mol Cell Biol 2008;28:1326–37.
[78] Winzeler EA, Shoemaker DD, Astromoff A, et al. Functional characterization of the S. cerevisiae genome by gene deletion and parallel analysis. Science 1999;285:901–6.
[79] Huh WK, Falvo JV, Gerke LC, et al. Global analysis of protein localization in budding yeast. Nature 2003;425:686–91.
[80] Wiesenberger G, Link TA, von Ahsen U, Waldherr M, Schweyen RJ. MRS3 and MRS4, two suppressors of mtRNA splicing defects in yeast, are new members of the mitochondrial carrier family. J Mol Biol 1991;217:23–37.
[81] Holmes-Hampton GP, Miao R, Garber Morales J, Guo Y, Munck E, Lindahl PA. A nonheme high-spin ferrous pool in mitochondria isolated from fermenting Saccharomyces cerevisiae. Biochemistry 2010;49:4227–34.
[82] Pandey A, Yoon H, Lyver ER, Dancis A, Pain D. Identification of a Nfs1p-bound persulfide intermediate in Fe-S cluster synthesis by intact mitochondria. Mitochondrion 2012;12:539–49.
[83] Muhlenhoff U, Stadler JA, Richhardt N, et al. A specific role of the yeast mitochondrial carriers MRS3/4p in mitochondrial iron acquisition under iron-limiting conditions. J Biol Chem 2003;278:40612–20.
[84] Zhang Y, Lyver ER, Knight SA, Pain D, Lesuisse E, Dancis A. Mrs3p, Mrs4p, and frataxin provide iron for Fe-S cluster synthesis in mitochondria. J Biol Chem 2006;281:22493–502.
[85] Yoon H, Zhang Y, Pain J, et al. Rim2, a pyrimidine nucleotide exchanger, is needed for iron utilization in mitochondria. Biochem J 2011;440:137–46.
[86] Pain J, Balamurali MM, Dancis A, Pain D. Mitochondrial NADH kinase, Pos5p, is required for efficient iron-sulfur cluster biogenesis in Saccharomyces cerevisiae. J Biol Chem 2010;285:39409–24.
[87] Lill R. Function and biogenesis of iron-sulphur proteins. Nature 2009;460:831–8.
[88] Agar JN, Krebs C, Frazzon J, Huynh BH, Dean DR, Johnson MK. IscU as a scaffold for iron-sulfur cluster biosynthesis: sequential assembly of [2Fe-2S] and [4Fe-4S] clusters in IscU. Biochemistry 2000;39:7856–62.
[89] Schilke B, Voisine C, Beinert H, Craig E. Evidence for a conserved system for iron metabolism in the mitochondria of Saccharomyces cerevisiae. Proc Natl Acad Sci USA 1999;96:10206–11.
[90] Amutha B, Gordon DM, Gu Y, Lyver ER, Dancis A, Pain D. GTP is required for iron-sulfur cluster biogenesis in mitochondria. J Biol Chem 2008;283:1362–71.
[91] Kessler D. Enzymatic activation of sulfur for incorporation into biomolecules in prokaryotes. FEMS Microbiol Rev 2006;30:825–40.
[92] Mueller EG. Trafficking in persulfides: delivering sulfur in biosynthetic pathways. Nat Chem Biol 2006;2:185–94.
[93] Kispal G, Csere P, Prohl C, Lill R. The mitochondrial proteins Atm1p and Nfs1p are essential for biogenesis of cytosolic Fe/S proteins. EMBO J 1999;18:3981–89.
[94] Onder O, Yoon H, Naumann B, Hippler M, Dancis A, Daldal F. Modifications of the lipoamide-containing mitochondrial subproteome in a yeast mutant defective in cysteine desulfurase. Mol Cell Proteomics 2006;5:1426–36.

[95] Jaschkowitz K, Seidler A. Role of a NifS-like protein from the cyanobacterium Synechocystis PCC 6803 in the maturation of FeS proteins. Biochemistry 2000;39:3416–23.
[96] Schmucker S, Martelli A, Collin F, et al. Mammalian frataxin: an essential function for cellular viability through an interaction with a preformed ISCU/NFS1/ISD11 iron-sulfur assembly complex. PLoS One 2011;26:e16199.
[97] Prischi F, Konarev PV, Iannuzzi C, et al. Structural bases for the interaction of frataxin with the central components of iron-sulphur cluster assembly. Nat Commun 2010;1:95.
[98] Marinoni EN, de Oliveira JS, Nicolet Y, et al. (IscS-IscU)2 complex structures provide insights into Fe_2S_2 biogenesis and transfer. Angewandte Chemie 2012;51:5439–42.
[99] Bonomi F, Iametti S, Morleo A, Ta D, Vickery LE. Facilitated transfer of IscU-[2Fe2S] clusters by chaperone-mediated ligand exchange. Biochemistry 2011;50:9641–50.
[100] Colin F, Martelli A, Clemancey M, et al. Mammalian frataxin controls sulfur production and iron entry during de novo Fe4S4 cluster assembly. J Am Chem Soc 2013;135:733–40.
[101] Yoon H, Knight AB, Pandey A, Pain J, Zhang Y, Pain D, Dancis A. Frataxin-bypassing Isu1: characterization of the bypass activity in cells and mitochondria. Biochem J 2014;459:71–81.
[102] Kampinga HH, Craig EA. The HSP70 chaperone machinery: J proteins as drivers of functional specificity. Nat Rev Mol Cell Biol 2010;11:579–92.
[103] Andrew AJ, Dutkiewicz R, Knieszner H, Craig EA, Marszalek J. Characterization of the interaction between the J-protein Jac1p and the scaffold for Fe-S cluster biogenesis, Isu1p. J Biol Chem 2006;281:14580–7.
[104] Dutkiewicz R, Schilke B, Cheng S, Knieszner H, Craig EA, Marszalek J. Sequence-specific interaction between mitochondrial Fe-S scaffold protein Isu and Hsp70 Ssq1 is essential for their in vivo function. J Biol Chem 2004;279:29167–74.
[105] Molina-Navarro MM, Casas C, Piedrafita L, Belli G, Herrero E. Prokaryotic and eukaryotic monothiol glutaredoxins are able to perform the functions of Grx5 in the biogenesis of Fe/S clusters in yeast mitochondria. FEBS Lett 2006;580:2273–80.
[106] Shakamuri P, Zhang B, Johnson MK. Monothiol glutaredoxins function in storing and transporting [Fe(2)S(2)] clusters assembled on IscU scaffold proteins. J Am Chem Soc 2012;134:15213–6.
[107] Uzarska MA, Dutkiewicz R, Freibert SA, Lill R, Muhlenhoff U. The mitochondrial Hsp70 chaperone Ssq1 facilitates Fe/S cluster transfer from Isu1 to Grx5 by complex formation. Mol Biol Cell 2013;24:1830–41.
[108] Gelling C, Dawes IW, Richhardt N, Lill R, Muhlenhoff U. Mitochondrial Iba57p is required for Fe/S cluster formation on aconitase and activation of radical SAM enzymes. Mol Cell Biol 2008;28:1851–61.
[109] Cameron JM, Janer A, Levandovskiy V, et al. Mutations in iron-sulfur cluster scaffold genes NFU1 and BOLA3 cause a fatal deficiency of multiple respiratory chain and 2-oxoacid dehydrogenase enzymes. Am J Hum Genet 2011;89:486–95.
[110] Navarro-Sastre A, Tort F, Stehling O, et al. A fatal mitochondrial disease is associated with defective NFU1 function in the maturation of a subset of mitochondrial Fe-S proteins. Am J Hum Genet 2011;89:656–67.
[111] Majewska J, Ciesielski SJ, Schilke B, et al. Binding of the chaperone Jac1 protein and cysteine desulfurase Nfs1 to the iron-sulfur cluster scaffold Isu protein is mutually exclusive. J Biol Chem 2013;288:29134–42.
[112] Meister A, Anderson ME. Glutathione. Annu Rev Biochem 1983;52:711–60.
[113] Grant CM, MacIver FH, Dawes IW. Glutathione synthetase is dispensable for growth under both normal and oxidative stress conditions in the yeast Saccharomyces cerevisiae due to an accumulation of the dipeptide gamma-glutamylcysteine. Mol Biol Cell 1997;8:1699–707.
[114] Toledano MB, Delaunay-Moisan A, Outten CE, Igbaria A. Functions and cellular compartmentation of the thioredoxin and glutathione pathways in yeast. Antioxid Redox Signal 2013;18:1699–711.
[115] Hu J, Dong L, Outten CE. The redox environment in the mitochondrial intermembrane space is maintained separately from the cytosol and matrix. J Biol Chem 2008;283:29126–34.

[116] Hider RC, Kong XL. Glutathione: a key component of the cytoplasmic labile iron pool. Biometals 2011;24:1179–87.
[117] Picciocchi A, Saguez C, Boussac A, Cassier-Chauvat C, Chauvat F. CGFS-type monothiol glutaredoxins from the cyanobacterium Synechocystis PCC6803 and other evolutionary distant model organisms possess a glutathione-ligated [2Fe-2S] cluster. Biochemistry 2007;46:15018–26.
[118] Rodriguez-Manzaneque MT, Tamarit J, Belli G, Ros J, Herrero E. Grx5 is a mitochondrial glutaredoxin required for the activity of iron/sulfur enzymes. Mol Biol Cell 2002;13:1109–21.
[119] Muhlenhoff U, Molik S, Godoy JR, et al. Cytosolic monothiol glutaredoxins function in intracellular iron sensing and trafficking via their bound iron-sulfur cluster. Cell Metab 2010;12:373–85.
[120] Wu AL, Moye-Rowley WS. GSH1, which encodes gamma-glutamylcysteine synthetase, is a target gene for yAP-1 transcriptional regulation. Mol Cell Biol 1994;14:5832–9.
[121] Kumar C, Igbaria A, D'Autreaux B, et al. Glutathione revisited: a vital function in iron metabolism and ancillary role in thiol-redox control. EMBO J 2011;30:2044–56.
[122] Sipos K, Lange H, Fekete Z, Ullmann P, Lill R, Kispal G. Maturation of cytosolic iron-sulfur proteins requires glutathione. J Biol Chem 2002;277:26944–9.
[123] Li H, Mapolelo DT, Dingra NN, et al. The yeast iron regulatory proteins Grx3/4 and Fra2 form heterodimeric complexes containing a [2Fe-2S] cluster with cysteinyl and histidyl ligation. Biochemistry 2009;48:9569–81.
[124] Hoffmann B, Uzarska MA, Berndt C, et al. The multidomain thioredoxin-monothiol glutaredoxins represent a distinct functional group. Antioxid Redox Signal 2011;15:19–30.
[125] Ojeda L, Keller G, Muhlenhoff U, Rutherford JC, Lill R, Winge DR. Role of glutaredoxin-3 and glutaredoxin-4 in the iron regulation of the Aft1 transcriptional activator in Saccharomyces cerevisiae. J Biol Chem 2006;281:17661–9.
[126] Zhang Y, Liu L, Wu X, An X, Stubbe J, Huang M. Investigation of in vivo diferric tyrosyl radical formation in Saccharomyces cerevisiae Rnr2 protein: requirement of Rnr4 and contribution of Grx3/4 AND Dre2 proteins. J Biol Chem 2011;286:41499–509.
[127] Miao R, Kim H, Koppolu UM, Ellis EA, Scott RA, Lindahl PA. Biophysical characterization of the iron in mitochondria from Atm1p-depleted Saccharomyces cerevisiae. Biochemistry 2009;48:9556–68.
[128] Kispal G, Csere P, Guiard B, Lill R. The ABC transporter Atm1p is required for mitochondrial iron homeostasis. FEBS Lett 1997;418:346–50.
[129] Garber Morales J, Holmes-Hampton GP, Miao R, Guo Y, Munck E, Lindahl PA. Biophysical characterization of iron in mitochondria isolated from respiring and fermenting yeast. Biochemistry 2010;49:5436–44.
[130] Hausmann A, Samans B, Lill R, Muhlenhoff U. Cellular and mitochondrial remodeling upon defects in iron-sulfur protein biogenesis. J Biol Chem 2008;283:8318–30.
[131] Liu Z, Butow RA. Mitochondrial retrograde signaling. Annu Rev Genet 2006;40:159–85.
[132] Bedekovics T, Li H, Gajdos GB, Isaya G. Leucine biosynthesis regulates cytoplasmic iron-sulfur enzyme biogenesis in an Atm1p-independent manner. J Biol Chem 2011;286:40878–88.
[133] Cavadini P, Biasiotto G, Poli M, et al. RNA silencing of the mitochondrial ABCB7 transporter in HeLa cells causes an iron-deficient phenotype with mitochondrial iron overload. Blood 2007;109:3552–9.
[134] Chloupkova M, Reaves SK, LeBard LM, Koeller DM. The mitochondrial ABC transporter Atm1p functions as a homodimer. FEBS Lett 2004;569:65–69.
[135] Zutz A, Gompf S, Schagger H, Tampe R. Mitochondrial ABC proteins in health and disease. Biochim Biophys Acta 2009;1787:681–90.
[136] Kuhnke G, Neumann K, Muhlenhoff U, Lill R. Stimulation of the ATPase activity of the yeast mitochondrial ABC transporter Atm1p by thiol compounds. Mol Membr Biol 2006;23:173–84.
[137] Rouault TA, Tong WH. Iron-sulfur cluster biogenesis and human disease. Trends Genet 2008;24:398–407.

[138] Lindahl PA, Holmes-Hampton GP. Biophysical probes of iron metabolism in cells and organelles. Curr Opin Chem Biol 2011;15:342–6.
[139] Miao R, Martinho M, Morales JG, et al. EPR and Mossbauer spectroscopy of intact mitochondria isolated from Yah1p-depleted Saccharomyces cerevisiae. Biochemistry 2008;47:9888–99.
[140] Bulteau AL, Dancis A, Gareil M, Montagne JJ, Camadro JM, Lesuisse E. Oxidative stress and protease dysfunction in the yeast model of Friedreich ataxia. Free Radic Biol Med 2007;42:1561–70.
[141] Stehling O, Vashisht AA, Mascarenhas J, et al. MMS19 assembles iron-sulfur proteins required for DNA metabolism and genomic integrity. Science 2012;337:195–9.
[142] Jensen LT, Culotta VC. Role of Saccharomyces cerevisiae ISA1 and ISA2 in iron homeostasis. Mol Cell Biol 2000;20:3918–27.
[143] Muhlenhoff U, Richter N, Pines O, Pierik AJ, Lill R. Specialized function of yeast Isa1 and Isa2 proteins in the maturation of mitochondrial [4Fe-4S] proteins. J Biol Chem 2011;286:41205–16.
[144] Lange H, Lisowsky T, Gerber J, Muhlenhoff U, Kispal G, Lill R. An essential function of the mitochondrial sulfhydryl oxidase Erv1p/ALR in the maturation of cytosolic Fe/S proteins. EMBO Rep 2001;2:715–20.
[145] Voisine C, Cheng YC, Ohlson M, et al. Jac1, a mitochondrial J-type chaperone, is involved in the biogenesis of Fe/S clusters in Saccharomyces cerevisiae. Proc Natl Acad Sci USA 2001;98:1483–8.
[146] Yang M, Cobine PA, Molik S, et al. The effects of mitochondrial iron homeostasis on cofactor specificity of superoxide dismutase 2. EMBO J 2006;25:1775–83.
[147] Gordon DM, Lyver ER, Lesuisse E, Dancis A, Pain D. GTP in the mitochondrial matrix plays a crucial role in organellar iron homoeostasis. Biochem J 2006;400:163–8.
[148] Vozza A, Blanco E, Palmieri L, Palmieri F. Identification of the mitochondrial GTP/GDP transporter in Saccharomyces cerevisiae. J Biol Chem 2004;279:20850–57.
[149] Lesuisse E, Knight SA, Courel M, Santos R, Camadro JM, Dancis A. Genome-wide screen for genes with effects on distinct iron uptake activities in Saccharomyces cerevisiae. Genetics 2005;169:107–22.
[150] Crisp RJ, Pollington A, Galea C, Jaron S, Yamaguchi-Iwai Y, Kaplan J. Inhibition of heme biosynthesis prevents transcription of iron uptake genes in yeast. J Biol Chem 2003;278:45499–506.
[151] Palmieri F, Pierri CL, De Grassi A, Nunes-Nesi A, Fernie AR. Evolution, structure and function of mitochondrial carriers: a review with new insights. Plant J Cell Mol Biol 2011; 66:161–81.
[152] Robinson AJ, Overy C, Kunji ER. The mechanism of transport by mitochondrial carriers based on analysis of symmetry. Proc Natl Acad Sci USA 2008;105:17766–71.
[153] Park J, McCormick SP, Chakrabarti M, Lindahl PA. Insights into the iron-ome and manganese-ome of Δmtm1 Saccharomyces cerevisiae mitochondria. Metallomics 2013;5:656–72.
[154] Yang Y, Yamashita T, Nakamaru-Ogiso E, et al. Reaction mechanism of single subunit NADH-ubiquinone oxidoreductase (Ndi1) from Saccharomyces cerevisiae: evidence for a ternary complex mechanism. J Biol Chem 2011;286:9287–97.
[155] Nilsson R, Schultz IJ, Pierce EL, et al. Discovery of genes essential for heme biosynthesis through large-scale gene expression analysis. Cell Metab 2009;10:119–30.
[156] Puig S, Askeland E, Thiele DJ. Coordinated remodeling of cellular metabolism during iron deficiency through targeted mRNA degradation. Cell 2005;120:99–110.
[157] Outten CE, Albetel AN. Iron sensing and regulation in Saccharomyces cerevisiae: ironing out the mechanistic details. Curr Opin Microbiol 2013;16:662–8.
[158] Bottomley SS. Congenital sideroblastic anemias. Curr Hematol Rep 2006;5:41–9.
[159] Li L, Kaplan J. Characterization of two homologous yeast genes that encode mitochondrial iron transporters. J Biol Chem 1997;272:28485–93.

7 The role of Fe-S clusters in regulation of yeast iron homeostasis

Caryn E. Outten

7.1 Introduction

The intracellular concentration and subcellular speciation of iron in eukaryotic cells is tightly regulated to maintain sufficient levels of this essential micronutrient while avoiding the toxic effects of iron overload. Iron is present in all subcellular compartments in a variety of chemical forms, including as protein-bound cofactors in Fe-S clusters, heme, and mononuclear and dinuclear iron-binding sites, as ferric oxide biominerals in iron storage proteins, as ferric oxyhydroxide nanoparticles, and as chelatable or "free" ferrous and/or ferric iron bound to low-molecular-weight ligands. Which of these forms is used as a gauge for intracellular iron concentrations and what are the molecular mechanisms for sensing and regulating iron bioavailability within eukaryotic cells? An emerging theme from recent studies in yeast model systems is that Fe-S clusters play key roles in iron regulation, which parallels previous findings in mammalian cells. This chapter highlights studies in the budding yeast *Saccharomyces cerevisiae*, and the fission yeast *Schizosaccharomyces pombe* that demonstrate the importance of Fe-S clusters as signals of intracellular iron bioavailability. A brief overview of yeast iron uptake and trafficking is provided, followed by detailed descriptions of the transcriptional regulators in *S. cerevisiae* and *S. pombe* that coordinate the cell's response to both high- and low-iron-growth conditions. Current knowledge on the role of Fe-S clusters in modulating the activity of yeast transcriptional regulators is discussed for each model eukaryote. The chapter concludes with a section comparing and contrasting the mechanisms of iron regulation in *S. cerevisiae* and *S. pombe*.

7.2 Iron acquisition and trafficking in yeast

Microbial iron acquisition is complicated by the low bioavailability of iron in oxygenated environments at neutral pH. Thus, eukaryotic microbes such as *S. cerevisiae* and *S. pombe* have devised multiple strategies for scavenging this essential resource (Fig. 7.1). One strategy involves acquisition and transport of ionic iron at the cell surface. Transmembrane proton pumps help acidify the extracellular environment to increase Fe^{3+} solubility. Environmental Fe^{3+} is converted to Fe^{2+} by cell surface ferrireductases (Fre1 and Fre2 in *S. cerevisiae*, Frp1 in *S. pombe*) [1]. Fe^{2+} is the substrate for the high-affinity oxidase-permease complexes (*S. cerevisiae* Fet3 and Ftr1, *S. pombe* Fio1 and Fip1) that first oxidize Fe^{2+} to Fe^{3+} prior to transporting Fe^{3+} into the cell. Another strategy is to scavenge iron from the environment using highly specific small-molecule Fe^{3+} chelators

DOI 10.1515/9783110479850-007

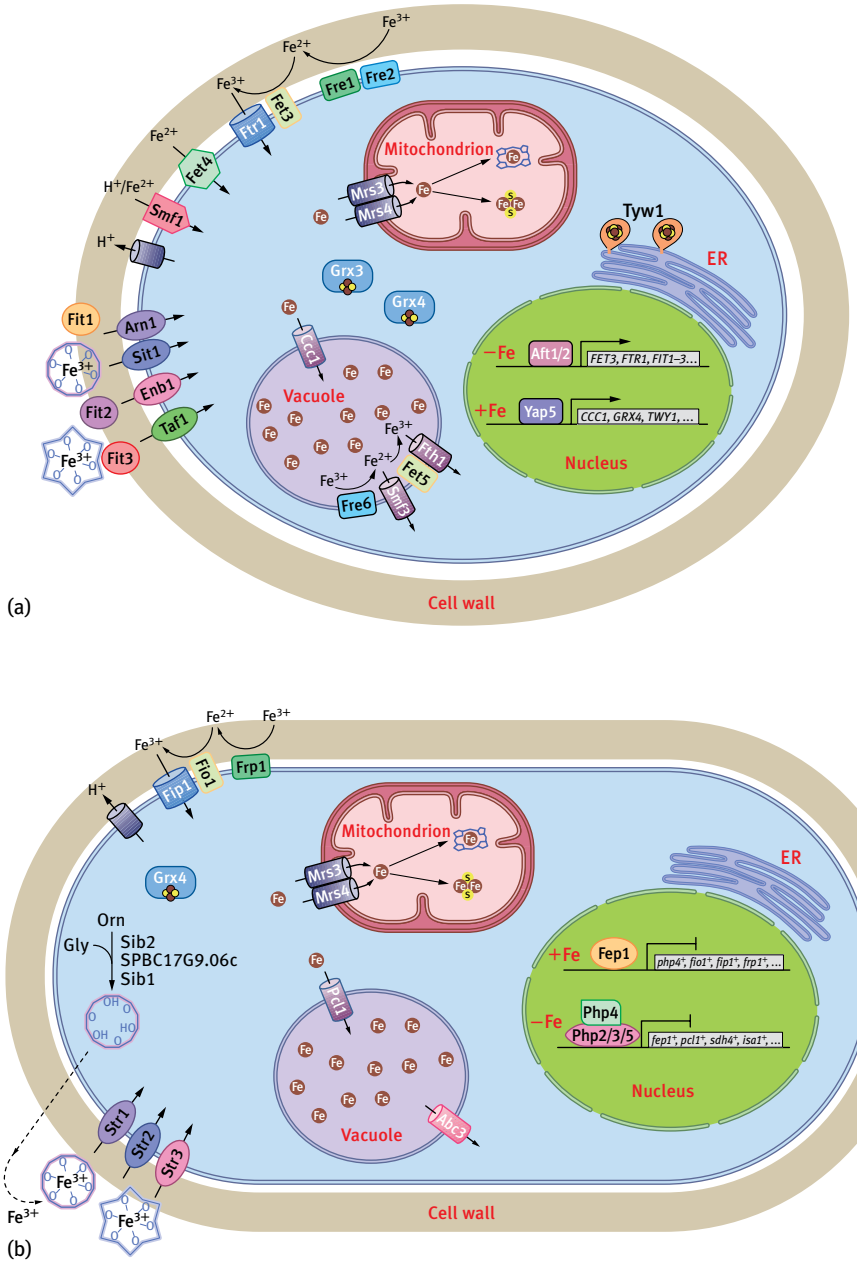

Fig. 7.1: Iron uptake, trafficking, and regulation systems in (a) *S. cerevisiae* and (b) *S. pombe*. (a) *S. cerevisiae* Fit1, Fit2, and Fit3 are siderophore-binding mannoproteins anchored in the cell wall. Arn1, Sit1, Enb1, and Taf1 are cell surface transporters for Fe^{3+}-siderophore complexes. The ferrireductases Fre1 and Fre2 reduce environmental Fe^{3+} to Fe^{2+}. Fet3 and Ftr1 form the cell surface high-affinity iron uptake system in which Fet3 oxidizes Fe^{2+} to Fe^{3+} and Ftr1 transports Fe^{3+} across the plasma membrane. Fet4 is a low-affinity transporter responsible for cell surface uptake under

iron-replete conditions. Smf1 is a H^+/M^+ symporter for transition metals such as Fe^{2+}, Mn^{2+}, and Zn^{2+}. Vacuolar iron transport systems include the importer Ccc1, the ferrireductase Fre6, and the exporters Smf3 and Fet5/Fth1. Grx3 and Grx4 are cytosolic [2Fe-2S]-binding proteins implicated in intracellular iron trafficking and Aft1/2 regulation. Mrs3 and Mrs4 import iron into the mitochondria, which is used for both heme and Fe-S cluster biogenesis, whereas Tyw1 is an ER-anchored radical SAM enzyme that sequesters Fe-S clusters during iron overload. Iron homeostasis in *S. cerevisiae* is coordinated by the low-iron-responsive activators, Aft1 and Aft2, which activate the expression of iron acquisition pathways, and the high-iron-responsive activator Yap5, which activates expression of proteins involved in iron sequestration. (b) *S. pombe* synthesizes the siderophore ferrichrome from ornithine and glycine using the ornithine N^5 monooxygenase Sib2, the gene product of *SPBC17G9*.06c, and the non-ribosomal peptide synthetase Sib1. Str1, Str2, and Str3 are plasma membrane transporters that import iron-siderophore complexes. Iron is imported into vacuoles *via* Pcl1 and exported *via* Abc3. *S. pombe* also has orthologues to *S. cerevisiae* Mrs3 and Mrs4 that likely import iron into mitochondria for Fe-S cluster and heme biosynthesis. The CGFS monothiol glutaredoxin Grx4 signals iron availability to the two transcriptional repressors Fep1 and Php4 that regulate iron homeostasis in *S. pombe*.

known as siderophores. *S. pombe* synthesizes and excretes ferrichrome, a siderophore with hydroxamate groups for high-affinity Fe^{3+} binding [2]. Ferrichrome is synthesized in the cytosol using three glycines and three modified ornithines. Sib2 and the product of the gene *SPBC17G9.06c* are predicted to catalyze N^5-hydroxylation and acetylation of ornithine, respectively [3]. A third unidentified enzyme may catalyze formation of ornithine-glycine dipeptides, whereas Sib1 is a non-ribosomal peptide synthetase that polymerizes and circularizes the ornithine-glycine dipeptides to form the finished ferrichrome siderophore [4]. Fe^{3+}-loaded ferrichrome is taken up by the transporters Str1 and Str2 [5]. In addition to iron acquisition, ferrichrome may also play a role in intracellular iron storage because *S. pombe* accumulates intracellular ferrichrome under both high- and low-iron conditions [2].

Unlike *S. pombe*, *S. cerevisiae* does not synthesize siderophores; nevertheless, it expresses proteins at the cell surface for capturing (Fit1, Fit2, and Fit3) and internalizing (Arn1, Sit1, Enb1, and Taf1) a variety of siderophores produced by other microorganisms [6]. Likewise, *S. pombe* is capable of importing exogenous Fe^{3+}-bound siderophores (*via* Str1, Str2, and Str3) in addition to ferrichrome as sources of iron [5]. In addition to these high-affinity systems, *S. cerevisiae* possesses nonspecific low-affinity transporters (Fet4 and the NRAMP homologue Smf1) that import Fe^{2+} as well as Cu^{2+}, Mn^{2+}, and Zn^{2+} (Fig. 7.1) [7].

A number of pathways for trafficking iron from the cytosol to other subcellular compartments have been identified. The two main hubs for iron trafficking in yeast are the mitochondria and vacuoles. Iron import into mitochondria in *S. cerevisiae* is primarily mediated by the paralogous mitochondrial carrier proteins Mrs3 and Mrs4 [8, 9], whereas the vacuolar transporter Ccc1 facilitates storage and sequestration of iron in this organelle [10]. Orthologues for these mitochondrial and vacuolar iron importers are found in *S. pombe*, although only the function of the vacuolar importer (Pcl1) has been verified [11, 12]. *S. cerevisiae* additionally expresses a low-affinity NRAMP vacuolar transporter, Smf3, that is homologous to Smf1 [13]. Under conditions of iron depletion, vacuolar iron

stores are mobilized by Smf3 and the oxidase-permease complex Fet5/Fth1, which is analogous to the Fet3/Ftr1 complex at the plasma membrane [7]. Orthologues for Smf3 and Fet5/Fth1 have not been identified in *S. pombe*. However, the *S. pombe* ABC-type transporter Abc3 carries out a similar function to Smf3 and Fet5/Fth1 by transporting vacuolar iron or iron conjugates to the cytosol when iron is scarce (Fig. 7.1) [12].

7.3 Regulation of iron homeostasis in *S. cerevisiae*

7.3.1 Aft1/Aft2 low-iron transcriptional regulators and target genes

S. cerevisiae responds to iron deficiency by activating the high-affinity ionic iron and iron-siderophore uptake systems as well as the vacuolar iron export systems to increase cytosolic iron levels. Activation of these systems is primarily controlled at the transcriptional level by the DNA binding regulator Aft1 and its paralogue Aft2 [6, 14–17]. Both Aft1 and Aft2 have an N-terminal DNA-binding domain and a C-terminal activation domain (Fig. 7.2). The N-terminal DNA-binding domains are homologous to the WRKY-GCM1 superfamily of eukaryotic transcriptional factors and have conserved Cys/His residues that are zinc finger (ZF) ligands in some WRKY-GCM1 family members [18]. A crystal structure for Aft2 bound to DNA confirms that Aft2 binds a structural ZF with these residues, and the same is likely true for Aft1 (C. Outten

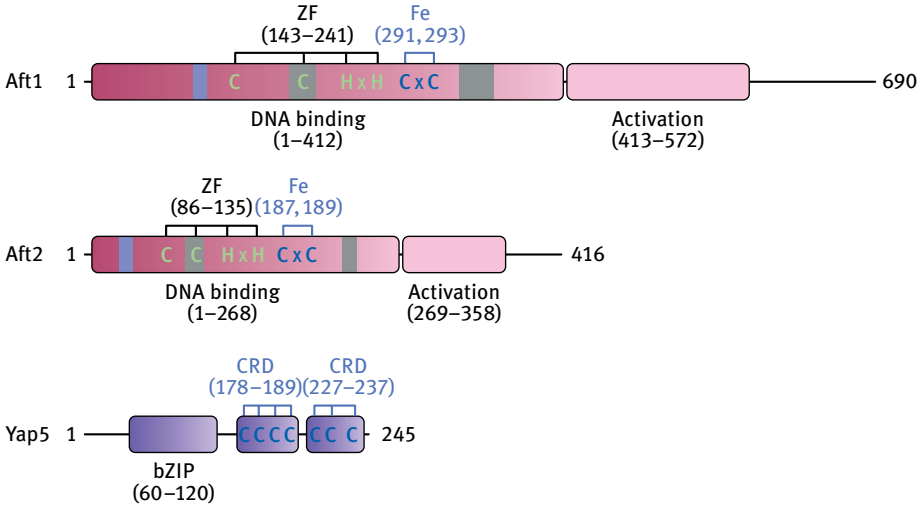

Fig. 7.2: Domain structure of iron-responsive transcriptional regulators Aft1, Aft2, and Yap5 from *S. cerevisiae*. Conserved ZF ligands in Aft1 and Aft2 are shown in green, and iron-responsive cysteine residues are shown in blue. The dark blue boxes indicate the positions of nuclear export signals, whereas the gray boxes show the locations of nuclear import signals. The conserved cysteines in the Yap5 cysteine-rich domains (CRDs) are shown in blue.

and C. He, unpublished data). Downstream of this ZF in the DNA-binding domain is a CDC motif that is essential to regulate Aft1 and Aft2 activity in response to iron, as discussed in Section 7.3.3 (Fig. 7.2). In total, Aft1 and Aft2 activate expression of 27 different genes that together comprise the iron regulon (Tab. 7.1) [1]. In addition to the plasma membrane and vacuolar iron transport systems, the iron regulon includes genes encoding the mitochondrial iron importer Mrs4, the Fe-S cluster assembly

Tab. 7.1: *S. cerevisiae* genes regulated by Aft1 and Aft2.

Gene name	Protein function and location
Cell surface siderophore iron uptake	
ARN1	Cell surface iron-siderophore transporter
ARN2/TAF1	Cell surface iron-siderophore transporter
ARN3/SIT1	Cell surface iron-siderophore transporter
ARN4/ENB1	Cell surface iron-siderophore transporter
FIT1	Cell wall iron-siderophore-binding protein
FIT2	Cell wall iron-siderophore-binding protein
FIT3	Cell wall iron-siderophore-binding protein
Cell surface ionic iron uptake	
FRE1	Cell surface ferrireductase
FRE2	Cell surface ferrireductase
FRE3	Cell surface ferrireductase
FET3	Cell surface multicopper oxidase
FTR1	Cell surface Fe^{2+} permease
CCC2	Golgi Cu^{2+}-transporting ATPase required for Fet3/Fet5 assembly
ATX1	Cytosolic Cu chaperone required for Cu delivery to Ccc2
Vacuolar metal transport	
FRE6	Vacuolar ferrireductase
FET5	Vacuolar multicopper oxidase
FTH1	Vacuolar Fe^{2+} permease
SMF3	Vacuolar Fe^{2+} exporter
COT1	Vacuolar Co^{2+}/Zn^{2+} importer
Mitochondrial iron metabolism	
ISU1	Mitochondrial Fe-S cluster assembly scaffold protein
MRS4	Mitochondrial Fe^{2+} importer
Post-transcriptional iron regulation	
CTH1	Nuclear/cytosolic mRNA-binding protein
CTH2	Nuclear/cytosolic mRNA-binding protein
Other functions	
VHT1	Cell surface biotin importer
AKR1	Golgi palmitoyl transferase
HMX1	ER heme oxygenase
BNA2	Cytosolic tryptophan 2,3 dioxygenase required for *de novo* NAD biosynthesis (predicted)
ECM4	Cytosolic glutathione S-transferase

scaffold protein Isu1, and the mRNA-binding proteins Cth1 and Cth2 [1]. Cth1 and Cth2 play roles in post-transcriptional control of iron homeostasis by facilitating targeted turnover of transcripts encoding proteins in nonessential, Fe-rich metabolic pathways. The net result is to redirect diminishing iron pools to essential Fe-dependent functions [19]. For example, Cth1 and Cth2 downregulate mRNA transcripts for TCA cycle Fe-S enzymes such as succinate dehydrogenase and aconitase, as well as components of the respiratory chain including the Rieske Fe-S protein, and cytochromes *c* and c_1. Consequently, cellular metabolism shifts from Fe-dependent respiration to Fe-independent fermentation to conserve iron [19–21].

Aft1 and Aft2 have overlapping as well as independent DNA targets. Aft1 preferentially binds Fe response elements with the consensus sequence TGCACCC, whereas Aft2 binds the related but shorter consensus sequence G/ACACCC [22, 23]. Aft1 has a more dominant role in iron homeostasis because *aft1Δ* mutants exhibit a stronger iron-deficiency phenotype than *aft2Δ* mutants. However, an *aft1Δaft2Δ* double mutant is more sensitive to iron-deficient conditions than an *aft1Δ* single mutant, indicating that Aft2 can partially compensate for loss of Aft1 in iron regulation [16, 17, 23]. Transcriptional analysis of Aft1 and Aft2 target genes suggest that Aft1 is primarily involved in cellular iron uptake, whereas Aft2 specifically regulates intracellular trafficking to vacuoles and mitochondria [22, 23].

7.3.2 Yap5 high-iron transcriptional regulator and target genes

In addition to the low-iron-sensing transcriptional activators Aft1 and Aft2, *S. cerevisiae* possesses a high-iron-sensing transcriptional activator named Yap5. Yap5 is a member of the basic leucine zipper (bZIP) transcriptional activator family (Fig. 7.2), which includes eight homologues in the *S. cerevisiae* genome. The list of genes regulated by Yap5 is much shorter than the Aft1/Aft2 regulon, limited to genes encoding the vacuolar iron importer Ccc1, Fe-S cluster-binding proteins Twy1 and Grx4, and the metallothionein Cup1 (Tab. 7.2) [24, 25]. Each of these Yap5-regulated genes has a known or potential role in sequestering excess iron, albeit *via* different mechanisms.

Tab. 7.2: *S. cerevisiae* genes regulated by Yap5.

Gene name	Protein function and location
Vacuolar iron import	
CCC1	Vacuolar iron importer
Metal-binding proteins	
GRX4	Nuclear/cytosolic multidomain [2Fe-2S]-binding glutaredoxin
TYW1	ER-tethered radical SAM [4Fe-4S] enzyme required for synthesis of wybutosine-modified tRNA
CUP1	Cytosolic Cu^{2+}-binding metallothionein

Activation of *CCC1* allows iron import into the vacuole to decrease the cytosolic iron pool (Fig. 7.1) [24]. Tyw1 is an ER-anchored, [4Fe-4S] cluster-binding radical SAM enzyme involved in modification of tRNA bases; however, the catalytic function of Tyw1 is not implicated in protection against iron toxicity. Instead, the data suggest that Yap5 protects the cell from excess iron by increasing Tyw1 levels, which sequesters iron as protein-bound Fe-S clusters [24]. Upregulation of Grx4 expression may serve a similar role because this [2Fe-2S]-binding protein is implicated in iron trafficking [26]. In addition, Grx4 plays a key role in inhibiting Aft1 and Aft2 during iron sufficiency (see Section 7.3.3), and increased levels of this protein may thereby enhance Aft1 and Aft2 inactivation. *CUP1* encodes a Cu-binding metallothionein that is important for resistance to copper toxicity [27]. Interestingly, biophysical studies indicate that Cup1 also binds four Fe^{2+} atoms/monomer *in vitro* [28] and thus could play a role in iron sequestration under toxic iron conditions. Taken together, these studies suggest that Yap5 responds to high cellular iron levels by decreasing free cytosolic iron through sequestration in vacuoles or incorporation into Fe- or Fe-S cluster-binding proteins [24].

7.3.3 Links between mitochondrial Fe-S cluster biogenesis, the Grx3/Grx4/Fra2/Fra1 signaling pathway, and Aft1/Aft2 regulation

A number of studies have started to shed light on the specific molecular mechanism by which Aft1 and Aft2 sense intracellular iron levels, revealing the critical role of Fe-S clusters. The first clues to the Aft1/2 regulation mechanism were provided by *in vivo* DNA footprinting studies demonstrating that Aft1 binds its genetic targets under iron-deplete, but not iron-replete conditions [29]. In addition, Aft1 nuclear localization is controlled by the cellular iron status: in iron-starved cells, Aft1 accumulates in the nucleus, whereas under iron-replete conditions, Aft1 dissociates from its DNA targets and is shuttled to the cytosol by the nuclear exportin Msn5 [30, 31]. Interaction with Msn5 and export of Aft1/2 to the cytosol requires multimerization of Aft1 or Aft2, which is dependent on a conserved CDC located in the DNA-binding domain (Fig. 7.2). Mutation of either Cys residue in the CDC motif (termed Aft1/2^{up} mutations) leads to constitutive nuclear localization of Aft1/2 and activation of the iron regulon [14, 30, 32]. Interestingly, Aft1/2 localization and DNA binding are independent of changes in cytosolic iron levels. Instead, the activity of Aft1 and Aft2 is dependent one the ability of mitochondria to assemble Fe-S clusters [33]. When Fe-S cluster biogenesis is disrupted, Aft1 and Aft2 are constitutively active regardless of cytosolic iron levels. In addition, iron signaling to Aft1/2 also requires the mitochondrial ABC transporter Atm1 [34]. Atm1 is proposed to export an unknown sulfur-containing substrate from mitochondria that is used to build and/or insert Fe-S clusters into cytosolic proteins [35]. However, deletion of proteins in the CIA (cytosolic iron-sulfur assembly) pathway has no effect on Aft1 and Aft2 activity, indicating that iron sensing is only linked to the mitochondrial pathway [32].

Aft1/2 inhibition in response to mitochondrial Fe-S cluster (ISC) biogenesis is mediated by a signaling pathway involving four cytosolic proteins: Grx3, Grx4, Fra2, and Fra1, all of which have homologues in mammalian cells [36–38]. Components of this signaling pathway were primarily identified by gene deletion and *in vivo* protein-protein interaction studies. The two cytosolic *S. cerevisiae* CGFS Grxs perform essential but redundant functions in iron metabolism because single *grx3Δ* and *grx4Δ* deletion strains have no discernable growth phenotypes, whereas *grx3grx4* double mutants are severely growth impaired or inviable, depending on the strain background [26, 36, 37]. Intracellular iron overaccumulates in *grx3grx4* strains due to constitutive activation of the iron regulon, although mitochondrial iron levels are decreased. In addition, the enzymatic activity and *in vivo* iron binding for a variety of Fe-S cluster, heme, and nonheme iron-binding proteins in both the cytosol and mitochondria are dramatically reduced in a *grx3grx4* strain, indicating that intracellular iron is much less bioavailable [26]. Thus, in addition to regulation of Aft1/2 activity, the cytosolic, multidomain CGFS Grxs in *S. cerevisiae* are suggested to play an essential role in intracellular iron trafficking. In *fra2Δ* and *fra1Δ* strains, the iron regulon is also constitutively activated, although disruption of iron homeostasis is less severe in these strains [38, 39]. Iron signaling to Aft1 and Aft2 is controlled by specific protein-protein interactions between components of this signaling pathway. Physical interactions between Aft1 and Grx3/4, Grx3/4 and Fra2, and Fra1 and Fra2 have been demonstrated *in vivo* by high-throughput and targeted yeast two-hybrid, co-immunoprecipitation, and affinity capture studies [36–38, 40].

7.3.4 Fe-S cluster binding by Grx3/4 and Fra2 is important for their function in *S. cerevisiae* iron regulation

S. cerevisiae Grx3 and Grx4 are paralogous members of the monothiol glutaredoxin (Grx) family found a wide variety of prokaryotes and eukaryotes. Members of this family possess a signature CGFS active site sequence that differs from the classical CPY/FC active site found in dithiol Grxs. Dithiol Grxs are glutathione (GSH)-dependent thiol-disulfide oxidoreductases, whereas monothiol CGFS Grxs have little or no oxidoreductase activity when tested with standard Grx model substrates [41–46]. CGFS-type monothiol Grxs can be further classified into two groups: single-domain Grxs that have a single Grx-like domain and multidomain Grxs that possess an N-terminal thioredoxin (TRX)-like domain and one or more Grx-like domains. Single-domain CGFS Grxs are found in prokaryotes and in the mitochondria and chloroplasts of eukaryotes, whereas multidomain CGFS Grxs are exclusively eukaryotic, exhibiting cytosolic/nuclear localization. Both single and multidomain CGFS Grxs form $[2Fe\text{-}2S]^{2+}$-bridged homodimers with all-cysteinyl ligation provided by the two CGFS active site cysteines in the Grx-like domain and two GSH molecules (Fig. 7.3a) [46–53]. Members of the single-domain subfamily are proposed to facilitate maturation of Fe-S cluster proteins (see Chapter 15 by Debkumar Pain and

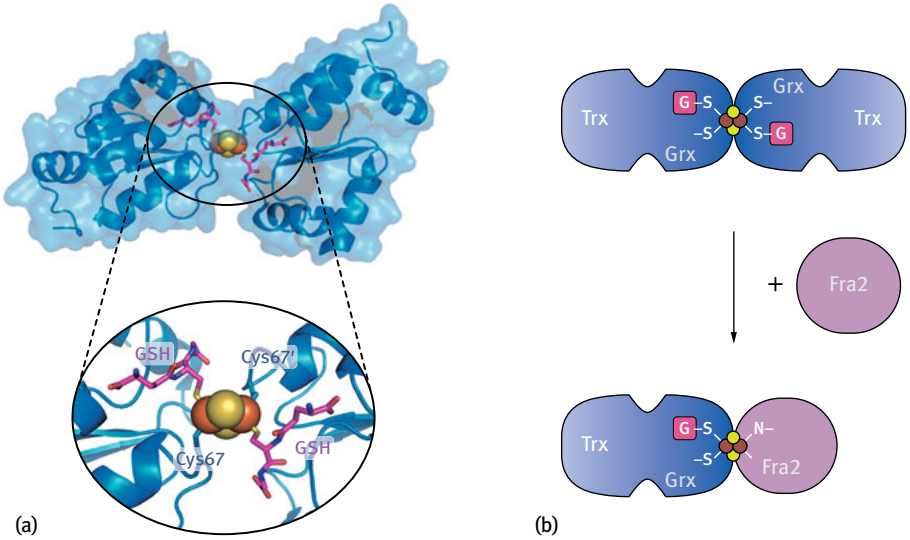

Fig. 7.3: Structures of [2Fe-2S]-bridged CGFS Grx complexes. (a) X-ray crystal structure of *H. sapiens* GLRX5 (PDB 2WUL) [47] with close-up view of the GSH-ligated [2Fe-2S] cluster. Cys67 is the conserved cysteine in the CGFS active site of human Glrx5. Glrx5 crystallizes as two interacting homodimers but only one homodimer is shown in the figure. (b) Model for $[2Fe\text{-}2S]^{2+}$ Grx3/4 homodimer (top) and $[2Fe\text{-}2S]^{2+}$ Fra2-Grx3/4 heterodimer (bottom) characterized from *S. cerevisiae*. The $[2Fe\text{-}2S]^{2+}$ Fra2-Grx3/4 heterodimer is formed by titration of $[2Fe\text{-}2S]^{2+}$ Grx3/4 homodimers with apo Fra2. For the Grx3/4 homodimer, the active site cysteines in the GRX-like domains and 2 GSH [G] molecules ligate the Fe-S cluster. For the Fra2-Grx3/4 heterodimer, the Fe-S cluster is ligated by one GRX domain active site cysteine, one GSH, a histidine from Fra2 (N), and an unidentified fourth ligand.

Andrew Dancis and Chapter 18 by Wing-Hang Tong), whereas multidomain CGFS Grxs are proposed to play dual roles in cytosolic iron trafficking (see Section 7.3.3) and iron regulation [26, 36–38, 54]. The Fe-S cluster biogenesis function of single-domain CGFS Grxs and the trafficking and regulatory functions of multidomain CGFS Grxs in yeast are all dependent on the presence of the conserved Cys in the CGFS active site, suggesting that coordination of the [2Fe-2S] cluster is essential to these functions [26, 36, 54–57]. Formation of this Fe-S complex *in vivo* is supported by studies in *S. cerevisiae* demonstrating that iron binding to CGFS Grxs requires the GRX domain CGFS motif, sufficient intracellular GSH levels, and functional mitochondrial Fe-S cluster biogenesis [26]. The role of the less well-conserved TRX domain in multidomain Grxs has also been studied, although its specific function remains elusive. Mutation of a conserved Cys in the TRX domain of Grx3/4 disrupts neither Fe-S binding or homodimer formation *in vitro* [51] nor iron binding, iron trafficking, and Aft1/2 iron regulation *in vivo* [26]. Complete removal of this domain also does not impact Fe-S binding to the GRX domain *in vivo* and *in vitro* [51, 58], although the TRX domain is essential for Grx3/4 trafficking and regulation functions *in vivo* [58]. Based on these studies, the current hypothesis is that the TRX domain mediates specific protein-protein interactions with Grx3/4 binding partners.

In vitro biochemical and biophysical studies have demonstrated that *S. cerevisiae* Grx3 and Grx4 form $[2Fe\text{-}2S]^{2+}$-bridged heterodimers with Fra2 in addition to $[2Fe\text{-}2S]^{2+}$-bridged homodimers (Fig. 7.3b) [51, 59]. Fra2-Grx3/4 heterodimers exhibit significant differences in cluster stability and coordination environment in comparison to Grx3/4 homodimers. The Fe-S cluster in Fra2-Grx3/4 heterodimers is more stable to oxidation/reduction than the Fe-S cluster in Grx3/4 homodimers. Furthermore, the [2Fe-2S] Grx3 homodimer can be rapidly and efficiently converted to a [2Fe-2S] Grx3-Fra2 heterodimer by titration with apo-Fra2, demonstrating that formation of the heterodimer is thermodynamically and kinetically favored. In Fra2-Grx3/4 heterodimers, Fra2 replaces one Grx3/4 monomer and one GSH, providing a histidine ligand (His103) and presumably a fourth ligand that has not yet been identified. Mutation of Fra2 His103 to a Cys or Ala does not abolish formation of a [2Fe-2S]-bridged heterodimer with Grx3/4 *in vitro*; however, EPR and EXAFS data indicate that the stability of the mutant complex is compromised [59]. The H103A Fra2 mutant is also unable to rescue the iron regulation defects in *fra2Δ* strains, suggesting that a stable and/or redox-active cluster may be important for Fra2-Grx3/4 function [59]. Fra2 His103 is highly conserved in both prokaryotic and eukaryotic BolA homologues; therefore, it may play an important structural or functional role for other members of this protein family [60].

7.3.5 Working model for Fe-dependent regulation of Aft1/2 *via* the Fra1/Fra2/Grx3/Grx4 signaling pathway

The available data lend itself to a working model for Fe-dependent regulation of Aft1/2 *via* the Fra1/Fra2/Grx3/Grx4 signaling pathway (Fig. 7.4). According to the model, the mitochondrial inner membrane transporter Atm1 exports a sulfur-containing substrate produced by the mitochondrial ISC assembly machinery during conditions of iron sufficiency. This substrate and GSH are both essential for Fe-S cluster binding to Grx3/4 homodimers. The mechanism by which the [2Fe-2S] cluster is assembled and/or delivered to Grx3 and Grx4 is unknown. However, the cytosolic iron-sulfur assembly (CIA) system is not required for *in vivo* iron incorporation into Grx3/4 [26] or iron-dependent inhibition of Aft1/2 activity [32]. Thus, an unidentified parallel pathway must exist for Fe-S loading into Grx3/4 complexes. Formation of [2Fe-2S] Fra2-Grx3/4 heterodimers may proceed *via* a simple substitution reaction whereby apo-Fra2 displaces GSH and one of the Grx3/4 monomers. This mechanism is supported by *in vitro* results demonstrating that apo-Fra2 binds tightly and stoichiometrically to Grx3/4 homodimers leading to [2Fe-2S] Fra2-Grx3/4 heterodimer formation [59]. The [2Fe-2S] Fra2-Grx3/4 complex is then proposed to facilitate oligomerization of Aft1/2. The specific compartment in which the Fra-Grx inhibitory complex interacts with Aft1/2 is unclear. An initial study using overexpressed, GFP-tagged Grx3 suggested that this protein is primarily localized to the nucleus [55]. However, natively expressed, untagged Grx3 was found to exhibit mainly cytosolic localization. In addition, restriction of Grx4 to the cytosol *via* tethering to the mitochondrial outer

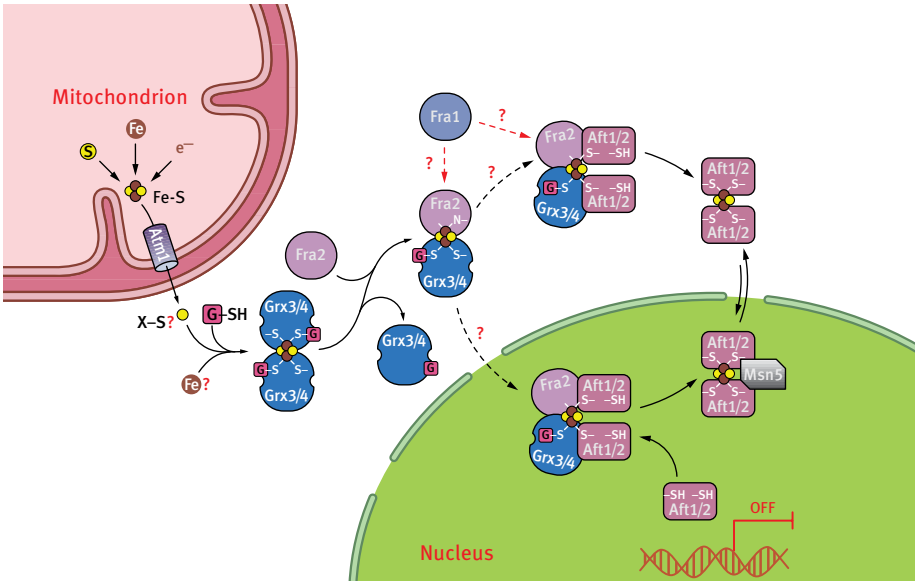

Fig. 7.4: Proposed model for *S. cerevisiae* iron regulation *via* Aft1 and Aft2 under iron-replete conditions. During conditions of iron sufficiency, Fe-S clusters are synthesized in mitochondria *via* integration of iron, sulfur, and redox control pathways. An unknown substrate produced by the mitochondrial ISC machinery is exported out to the cytosol by the transporter Atm1. GSH is also required for export of this signal. Grx3 and Grx4, which form GSH-ligated, Fe-S-bridged homodimers, are proposed to form heterodimers with Fra2 to relay this signal to Aft1 and Aft2. Fra1 interacts with Fra2; however, its specific role is not known. In addition, the specific compartment (nucleus, cytosol, or both) in which the Fra-Grx inhibitory complex interacts with Aft1 and Aft2 is unclear. Interaction of Grx3/4 with Aft1 promotes dissociation of the transcriptional activator from its target DNA and export to the cytosol, leading to deactivation of Aft1/2-regulated genes. The exportin Msn5 facilitates iron-dependent export of both Aft1 and Aft2.

membrane was shown to have little effect on inhibition of Aft1 activity in response to iron, suggesting that the Fra-Grx inhibitory complex acts in the cytosol [38]. In either case, oligomerization of Aft1 and Aft2 requires the conserved CDC motif. This motif in Aft1/2 is key to the regulation mechanism because substitution of these Cys residues disrupts the *in vivo* interaction between Grx3/4 and Aft1/2 and prevents Aft1/2 oligomerization. The CDC motif is also required for Aft1/2 interaction with the exportin Msn5- and Fe-dependent nuclear export, although recent evidence suggests that Msn5-mediated export of Aft1/2 is not essential to the inhibition mechanism because Aft1 functions normally in an *msn5Δ* strain despite constitutive localization to the nucleus [34]. Nevertheless, the essential role of the CDC motif in iron-dependent Aft1/2 inhibition, taken together with the dependence of Grx3/4 and Fra2 function on [2Fe-2S] cluster binding, strongly suggests that thiol redox chemistry and/or Fe-S or Fe binding to Aft1/2 drives multimerization, DNA dissociation, and translocation of Aft1/2 to the cytosol under iron-replete conditions (Fig. 7.4).

Despite considerable progress in defining the genetic and molecular interactions among Aft1/2, Grx3/4, Fra2, and Fra1, some key aspects of the iron sensing and regulation mechanism still remain unresolved. Most importantly, what is the specific molecular mechanism for inhibiting Aft1/2 activity in response to iron? Recent work by our group suggests that dimerization of Aft2 is driven by transfer of a [2Fe-2S] cluster from Fra2-Grx3 to Aft2, with two Cys from each Aft2 monomer ligating the [2Fe-2S] cluster (Fig. 7.4) (C. Outten and C. He, unpublished data). Furthermore, we find that Fe-S cluster binding to Aft2 lowers its DNA-binding affinity, which agrees with *in vivo* data suggesting that Grx3/4 induces Aft1 dissociation from DNA [34]. Experiments to further test this regulation model are ongoing in our laboratory. Fra1 also plays a role in Aft1-mediated iron signaling and interacts with Fra2 *in vivo*, but how is it specifically involved in the signaling pathway? Additionally, the Fra-Grx signaling pathway may not be the only method for inhibiting Aft1/2 activity under iron-replete conditions. Transcriptional reporter assays of Aft1/2-regulated genes indicate that the iron regulon is not fully activated in iron-sufficient medium in *fra1Δ* or *fra2Δ* mutants or upon disruption of mitochondrial ISC biogenesis pathways, suggesting that a separate signal may partially inhibit Aft1/2 activity in these mutants [38]. Finally, it is unknown how Fe-S dependent inhibition of Aft1 and Aft2 influences their interaction with transcriptional co-activators. Ssn6/Tup1 and Nhp6 associate with Aft1 *in vivo* and *in vitro* and are required for transcriptional activation of certain Aft1-regulated genes [61, 62]. It is possible that Aft1/2 metal binding and/or dimerization decreases these interactions, which in turn facilitates deactivation of Aft1/2 target genes.

7.3.6 Yap5 regulation and mitochondrial Fe-S cluster biogenesis

Unlike Aft1 and Aft2, Yap5 is constitutively localized to the nucleus and bound to its DNA targets under both high- and low-iron conditions. Thus, the iron-dependent switch that controls Yap5 activity does not involve changes in DNA-binding affinity as suggested for Aft1 and Aft2. However, similar to Aft1/2, cysteine residues are involved in controlling Yap5 function. In the case of Yap5, changes in iron availability are proposed to modify sulfhydryls located in two cysteine-rich domains (CRDs) downstream of the DNA-binding domain (Fig. 7.2). Single mutations in these Cys residues decrease Yap5 transcriptional activity to varying degrees, with mutations in the N-terminal CRD having the strongest effect. Mutation of all seven Cys residues leads to complete loss of Yap5 transcriptional activity without affecting DNA binding [63]. Furthermore, thiol modification assays on cellular extracts suggested that high iron induces disulfide formation on Yap5, implicating thiol redox chemistry in the regulation mechanism (Fig. 7.5). Interestingly, mitochondrial Fe-S cluster biogenesis also plays a key role in the response to high iron mediated by the *S. cerevisiae* transcription factor Yap5. As previously demonstrated for Aft1 and Aft2, iron-dependent control of Yap5-regulated genes is independent of changes in cytosolic iron levels or vacuolar/mitochondrial iron

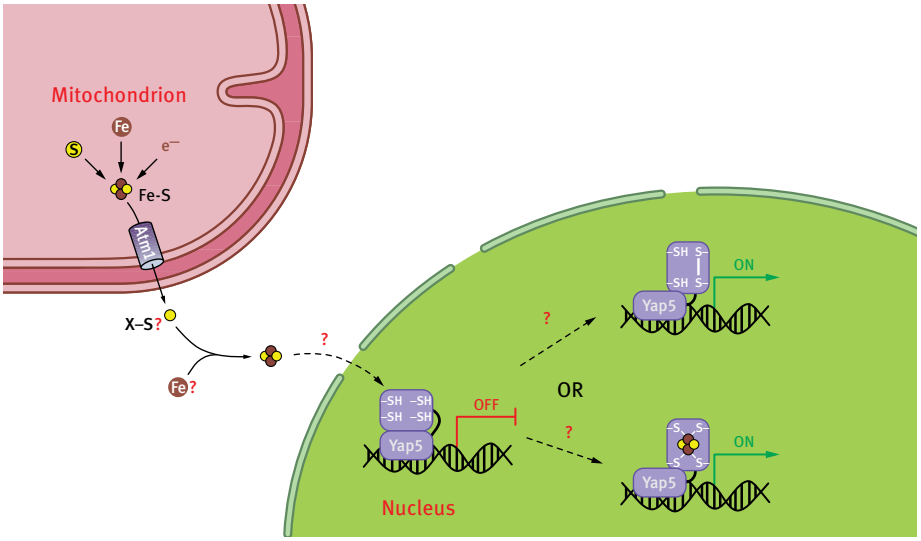

Fig. 7.5: Proposed model for *S. cerevisiae* iron regulation *via* Yap5 under iron-replete conditions. Under iron-replete conditions, the mitochondria ISC-dependent signal exported by Atm1 is relayed to Yap5 *via* as-yet-unidentified factor(s). This mitochondrial Fe-S-dependent signal stimulates Yap5 activation of its target genes *via* thiol modification and/or Fe-S cluster binding to conserved cysteine residues located in the C-terminal domain. Yap5 is bound to DNA in both high- and low-iron conditions.

sequestration. Instead, the transcriptional response is tuned to the availability of Fe-S clusters assembled in the mitochondria [64]. This intriguing result raises the alternate possibility that Yap5 directly binds an Fe-S cluster as suggested for Aft1/2 (Fig. 7.5); however, at present there is no direct evidence for this hypothesis.

Although both Aft1/2 and Yap5 are connected to mitochondrial Fe-S cluster assembly, one significant difference is the pathway by which the Fe-S cluster-dependent signal is relayed to the low- *vs* high-iron transcriptional regulators. Both are dependent on Atm1 function, but iron signaling to Yap5 is independent of the cytosolic Fe-S cluster-binding proteins Grx3 and Grx4, which play an essential role in Aft1/2 regulation [64]. The CIA assembly pathway is also not required for iron signaling to Yap5 [64]. Thus, identifying the molecular pathway for activating Yap5 in response to Fe-S cluster availability requires further study.

7.4 Regulation of iron homeostasis in *S. pombe*

7.4.1 Fep1 and Php4 transcriptional repressors and target genes

Although the pathways for iron uptake and trafficking are similar between *S. pombe* and *S. cerevisiae*, the mechanisms for regulation of iron homeostasis in these two fungi are significantly different, reflecting their evolutionary divergence. The genome of

S. pombe does not encode homologues of *S. cerevisiae* Aft1 and Aft2. Instead, iron homeostasis in *S. pombe* is primarily modulated by two repressors designated Fep1 and Php4, which are responsible for regulating iron uptake and iron utilization, respectively [1, 3, 65]. Fep1 is a GATA-type transcription factor that represses the expression of iron uptake and transport genes. Fep1-regulated genes encode proteins involved in siderophore iron uptake (*str1*$^+$, *str2*$^+$, and *str3*$^+$) and ionic iron uptake (*fio1*$^+$, *frp1*$^+$, and *fip1*$^+$) at the cell surface, as well as vacuolar iron export (*abc3*$^+$) (Tab. 7.3) [5, 12, 66]. Fep1 binds to GATA-containing sequences in promoters of these genes in iron-replete conditions, thereby repressing their expression to avoid iron overload. The co-repressors Tup11 and Tup12 bind to DNA-bound Fep1 in an iron-independent manner, facilitating repression of the target genes. These co-repressors downregulate numerous genes involved in a variety of different pathways [67]. When iron levels are low, Fep1 is released from the promoter region and the Fep1 regulon is turned on to promote iron uptake [68].

As mentioned in Section 7.3.1, metabolic remodeling in response to low iron availability in *S. cerevisiae* is controlled at the post-transcriptional level by the mRNA-binding proteins Cth1 and Cth2, whose expression is activated by Aft1 and Aft2 when iron is limiting. These regulators facilitate degradation of mRNA-encoding enzymes that function in nonessential Fe-rich metabolic pathways to preserve iron pools for essential functions. In contrast, iron-dependent metabolic remodeling in *S. pombe* is primarily controlled at the transcriptional level by the repressor Php4. Php4 binds to a heterotrimeric CCAAT-binding complex composed of Php2, Php3, and Php5. Under iron-replete conditions, the Php2/Php3/Php5 complex activates expression of its target genes by binding to CCAAT sequences in their promoters. Php2/Php3/Php5-regulated

Tab. 7.3: *S. pombe* genes regulated by Fep1.

Gene name	Protein function and location
Ferrichrome synthesis	
sib1$^+$	Cytosolic ferrichrome synthetase
sib2$^+$	Cytosolic ornithine N^5 monooxygenase (predicted)
Cell surface siderophore iron uptake	
str1$^+$	Cell surface iron-siderophore transporter
str2$^+$	Cell surface iron-siderophore transporter
str3$^+$	Cell surface iron-siderophore transporter
Cell surface ionic iron uptake	
fio1$^+$	Cell surface multicopper oxidase
fip1$^+$	Cell surface Fe^{2+} permease
frp1$^+$	Cell surface ferrireductase
Vacuolar iron export	
abc3$^+$	Vacuolar iron exporter
Transcriptional iron regulation	
php4$^+$	Cytosolic/nuclear Fe-sensing transcriptional repressor, subunit of CCAAT-binding factor complex

genes encode proteins involved in iron-rich metabolic pathways such as the mitochondrial electron transport chain (*cyt1*$^+$, *cyc1*$^+$), the tricarboxylic acid cycle (*sdh2*$^+$, *sdh3*$^+$, *sdh4*$^+$), amino acid biosynthesis (*leu2*$^+$, *glt1*$^+$), and iron-sulfur cluster (*isa1*$^+$) and heme biosynthesis (*hem3*$^+$) (Tab. 7.4) [11]. Under low-iron conditions, Php4 binds to the Php2/Php3/Php5 complex, causing it to switch from an activator to a repressor. Thus, nonessential iron-utilizing pathways are downregulated as an iron-sparing response.

Php4 and Fep1 each regulate expression of the other iron-responsive transcription factor creating a reciprocal regulatory loop. The *php4*$^+$ gene contains GATA elements

Tab. 7.4: *S. pombe* genes regulated by Php4.[a]

Gene name	Protein function and location
Vacuolar iron import	
pcl1$^+$	Vacuolar iron importer
Mitochondrial energy metabolism	
sdh2$^+$	Mitochondrial Fe-S subunit of succinate dehydrogenase
sdh3$^+$	Mitochondrial cytochrome *b* subunit of succinate dehydrogenase
sdh4$^+$	Mitochondrial inner membrane anchor subunit of succinate dehydrogenase
cyc1$^+$	Mitochondrial heme-binding cytochrome *c* (predicted)
cyt1$^+$	Mitochondrial heme-binding cytochrome c_1 (predicted)
SPAC20G8.04C	Mitochondrial electron-transfer flavoprotein-ubiquinone oxidoreductase (predicted)
SPAC24C9.06C	Mitochondrial Fe-S binding aconitase (predicted)
Amino acid biosynthesis	
leu2$^+$	Cytosolic Fe-S binding isopropylmalate dehydratase (predicted)
glt1$^+$	Mitochondrial Fe-S binding glutamate synthase (predicted)
sir1$^+$	Cytosolic Fe-S binding sulfite reductase, beta subunit
Cofactor biosynthesis	
isa1$^+$	Mitochondrial Fe-S cluster trafficking protein (Fe-S cluster assembly)
bio2$^+$	Mitochondrial Fe-S binding biotin synthase
hem3$^+$	Cytosolic/nuclear hydroxymethylbilane synthase (heme biosynthesis)
Transcriptional iron regulation	
fep1$^+$	Nuclear Fe-sensing GATA-type transcriptional repressor
Other functions	
aif1$^+$	Mitochondrial Fe-S binding apoptosis-inducing factor homologue (predicted)
ctt1$^+$	Cytosolic/nuclear heme-binding catalase
erg11$^+$	ER heme-binding sterol 14-demethylase, cytochrome P450 member (predicted)

[a] A recent microarray study identified 86 potential Php4-regulated genes [69]. Only the target genes confirmed by RNase protection assays are shown here.

within its promoter allowing Fep1 repression [11]. Likewise, the *fep1*$^+$ gene contains CCAAT *cis*-acting elements in its promoter region and is downregulated in a Php4-dependent manner. Php2, Php3, and Php5 are constitutively synthesized so the Php2/Php3/Php5 complex itself is not directly responsive to iron levels [11]. Thus, when iron levels are high, Fep1 is expressed and binds to the promoter of *php4*$^+$, thereby inactivating its transcription (Fig. 7.6, left). Without the Php4 repressor, the Php2/Php3/Php5 complex activates expression of *fep1*$^+$. Conversely, when iron levels are low, *php4*$^+$ is expressed enabling repression of *fep1*$^+$ *via* Php4 binding to the Php2/Php3/Php5 complex (Fig. 7.6, right). Reduced Fep1 levels, in turn, relieve the Fep1-dependent repression of the *php4*$^+$ gene. This reciprocal regulatory loop thus allows direct crosstalk between iron acquisition and iron utilization pathways to fine tune iron homeostasis in *S. pombe*.

7.4.2 Roles for Grx4 in regulation of Fep1 and Php4 activity

In addition to iron-dependent cross-regulation at the transcriptional level, the activities of both Fep1 and Php4 are controlled at the post-translational level by *S. pombe* Grx4, a member of the multidomain CGFS Grx subfamily. Thus, as demonstrated for *S. cerevisiae* Aft1 and Aft2 iron regulators, a CGFS Grx plays a key role in *S. pombe* iron regulation, even though Fep1 and Php4 do not share significant sequence identity with Aft1 or Aft2 and use different regulation mechanisms. Although *S. cerevisiae* has two paralogous cytosolic CGFS Grxs (Grx3/4), the *S. pombe*

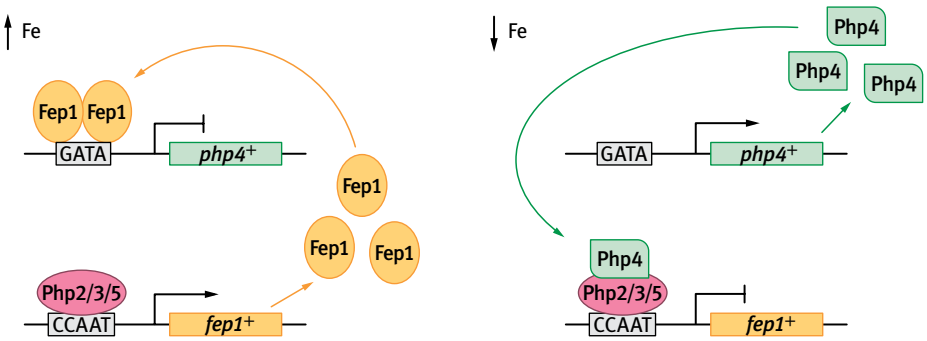

Fig. 7.6: Mutual transcriptional regulation by Php4 and Fep1 in *S. pombe*. When iron levels are high, *php4*$^+$ expression is repressed by Fep1 binding to GATA-containing sequences in the promoter region of this gene. Without Php4, the heterotrimeric Php2/Php3/Php5 CCAAT-binding factor complex that is bound to the CCAAT *cis*-activating elements in the promoter region of the *fep1*$^+$ gene is able to activate expression of *fep1*$^+$. In iron-deficient conditions, Fep1 dissociates from the promoter of *php4*$^+$, allowing expression of this gene. Increased Php4 levels, in turn, facilitate repression of *fep1*$^+$ *via* binding of Php4 to the CCAAT-binding factor complex, switching this complex from an activator to a repressor.

genome only encodes one, designated Grx4 [60, 70]. Grx4 impacts both Fep1 and Php4 function because Fep1- and Php4-regulated genes are constitutively repressed in *grx4* deletion strains [54, 57, 71]. Control of Fep1 and Php4 activity by Grx4 is governed by specific protein-protein interactions. Grx4 physically interacts with Fep1 and Php4 *in vivo* in an iron-independent manner as demonstrated by yeast two-hybrid and bimolecular fluorescence complementation experiments [54, 57, 71, 72]. Under iron-replete conditions, Grx4 promotes Php4 export to the cytosol by facilitating interaction with the nuclear exportin Crm1 (Fig. 7.7b). However, as demonstrated for Aft1/2, nucleocytoplasmic shuttling is not the primary mechanism for control of Php4 activity because Php4-regulated genes are activated in iron-replete conditions upon inhibition of Crm1 nuclear export activity [71]. Thus, in addition to promoting nuclear export of Php4 when iron is abundant, the interaction of Grx4 with Php4 also prevents Php4 from repressing the Php2/Php3/Php5 complex [71]. In

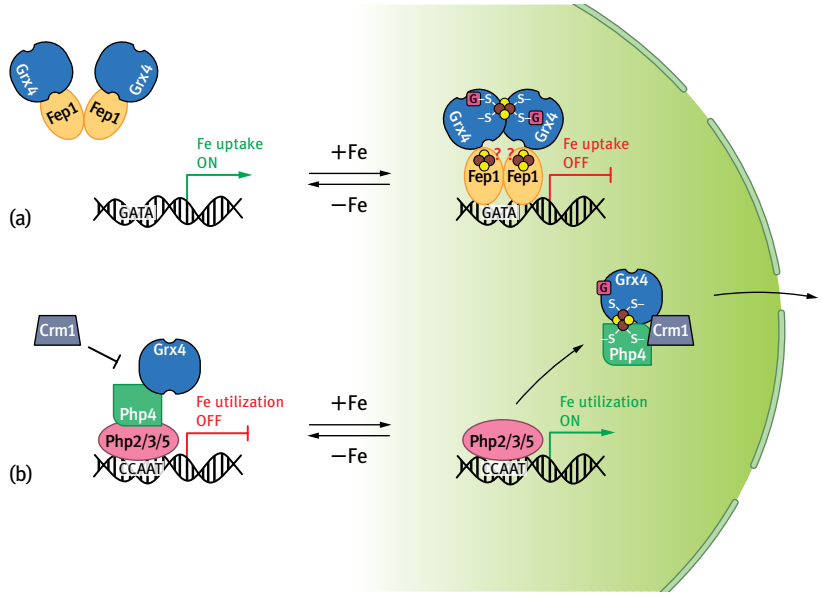

Fig. 7.7: Proposed model for *S. pombe* iron regulation under iron-replete and iron-depleted conditions for (a) Fep1 and (b) Php4. (a) (left) When iron is limiting, Fep1 dissociates from DNA but maintains an interaction with both the TRX and GRX domains of Grx4. (right) Under iron-replete conditions when Grx4 forms [2Fe-2S]-bridged homodimers, Fep1 binds DNA and interacts only with the TRX domain of Grx4. Fep1 itself may also bind iron or an Fe-S cluster. The Fep1 co-repressors Tup11 and Tup12 are not included in the model for the sake of simplicity. (b) (left) When iron levels are low, Php4 interacts with the TRX domain of Grx4 while binding the Php2/3/5 heterotrimeric complex, thereby repressing expression of iron utilization genes. Under these conditions, the exportin Crm1 is unable to interact with Php4. When iron is abundant, Php4 interacts with both the GRX domain and the TRX domain of Grx4, likely forming an Fe-S cluster-bound heterocomplex. Php4 dissociates from the Php2/3/4 heterotrimer and the Php4-Grx4 complex is exported by Crm1.

contrast, the interaction between Fep1 and Grx4 does not involve iron-dependent nucleocytoplasmic shuttling. Grx4 constitutively interacts with Fep1 in the nucleus regardless of intracellular iron status. When iron is limited, Grx4 inhibits Fep1 function, leading to dissociation of Fep1 from DNA and derepression of the Fep1 regulon. When iron is abundant, Grx4 is unable to inhibit Fep1 repressor function, although it still physically interacts with Fep1 (Fig. 7.7a) [54, 57].

7.4.3 Molecular basis of iron-dependent control of Fep1 activity

The specific domains and residues that mediate protein-DNA and protein-protein interactions for Fep1 have been mapped out by a variety of techniques. The N-terminal DNA-binding domain of Fep1 (and other iron-dependent GATA-type transcription factors found in similar fungi) includes two ZF domains (ZF1 and ZF2) that are required for high-affinity DNA binding *in vivo* and *in vitro* (Fig. 7.8) [68, 73]. Sandwiched between the two ZF domains is a conserved 27 amino acid cysteine-rich region [65, 74]. The four conserved Cys residues in this region are also required for high-affinity DNA binding and have been implicated in Fe^{3+} binding [11, 74]. Whether or not this cysteine-rich region binds an Fe-S cluster has not yet been tested, although the UV-visible absorption spectrum of as-purified recombinant SRE [75], a Fep1 homologue from *Neurospora crassa*, is reminiscent of a $[2Fe\text{-}2S]^{2+}$-binding protein [76]. Substitution of these conserved cysteines in recombinant Fep1 (and in its orthologues *N. crassa* SRE and *Histoplasma capsulatum* Sre1) leads to loss of this characteristic reddish-brown color, confirming the role of

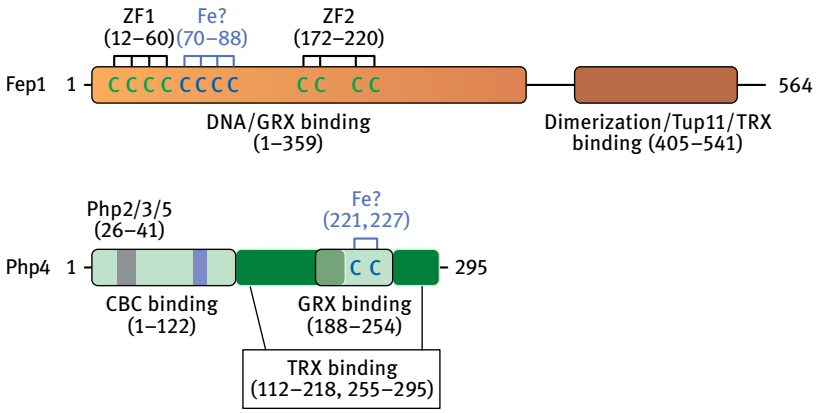

Fig. 7.8: Domain structure of iron-responsive transcriptional regulators Fep1 and Php4 from *S. pombe*. Conserved ZF ligands are shown in green and putative iron-responsive cysteine residues are shown in blue. The dark blue box in Php4 indicates the position of the nuclear export signal, whereas the gray box in the Php4 CCAAT-binding complex (CBC)-binding domain depicts the specific location of the Php2/3/5-binding residues.

these residues in metal binding [65, 74, 75]. Nevertheless, Fep1 remains bound to DNA and represses its target genes under both low- and high-iron conditions when *grx4* is deleted, suggesting that iron or Fe-S binding is not absolutely necessary for Fep1 DNA binding *in vivo* [54, 57].

The C-terminus of Fep1 includes a predicted leucine zipper coiled-coil region that favors Fep1-Fep1 dimer formation and is required for efficient repression of Fep1 target genes [73]. The Tup11 interaction domain has been mapped to the C-terminal domain as well (Fig. 7.8) [77]. The interaction between Fep1 and Grx4 involves both the N- and the C-terminal regions of both proteins. The N-terminal TRX domain of Grx4 invariably and strongly interacts with the C-terminus of Fep1, whereas the C-terminal GRX domain of Grx4 weakly interacts with the N-terminus of Fep1 only in iron-depleted conditions. The association between the N-terminus of Fep1 and the GRX domain of Grx4 requires Grx4 Cys172 located in the CGFS motif, whereas the interaction between the C-terminus of Fep1 and the TRX domain of Grx4 is dependent on Cys35 located in the putative active site of the TRX domain [54]. Analysis of Fep1 function upon expression of C35A or C35S Grx4 in *grx4* mutant strains indicated that Cys35 in the TRX domain is dispensable for Grx4-dependent inhibition of Fep1 activity. In contrast, mutation of Cys172 in the GRX domain of Grx4 led to constitutive repression by Fep1, demonstrating that the weak interaction between the GRX domain of Grx4 and the N-terminal domain of Fep1 is critical to the inhibition mechanism [54, 57]. A key difference between the role of CGFS Grxs in iron regulation for *S. pombe* in comparison to *S. cerevisiae* is that inhibition of Fep1 activity *via* interaction with Grx4 occurs under low-iron conditions in *S. pombe*, whereas Grx3/4-mediated inhibition of Aft1/2 occurs under iron-replete conditions in *S. cerevisiae*. This suggests that the CGFS Grx-dependent inhibition mechanisms for *S. cerevisiae* Aft1/2 and *S. pombe* Fep1 are distinctly different.

7.4.4 Molecular basis of iron-dependent control of Php4 activity

In contrast to Fep1, *S. pombe* Php4 is inhibited by Grx4 in iron-replete conditions and undergoes iron-dependent nucleocytoplasmic shuttling similar to *S. cerevisiae* Aft1/2. The Php4 nuclear export signal is located in the N-terminal domain along with the putative interaction site for the Php2/3/5 complex (Fig. 7.8) [11, 71]. Interestingly, Php4 and its orthologues in other fungi have conserved cysteine-rich regions in the C-terminal domain that are proposed to bind iron [78]. *S. pombe* Php4 has two conserved cysteines in this region, Cys221 and Cys227 (Fig. 7.8), that are essential for the iron-dependent interaction between the Php4 C-terminal domain (residues 188–254) and the GRX domain of Grx4 [72]. Grx4 Cys172 located in the CGFS Fe-S binding site is also required for this interaction with Php4. In addition, transcriptional analysis of Php4-regulated genes upon expression of C172S/A Grx4 mutants demonstrates that Cys172 is absolutely required for Grx4-dependent inhibition of Php4 activity [57, 72].

Based on these findings, Php4 and Grx4 are proposed to form an Fe-S binding complex that inhibits Php4 activity in iron-replete conditions (Fig. 7.7b) [72].

The interaction between Php4 and Grx4 is also partially mediated by the TRX domain of Grx4. Yet, in contrast to the GRX domain, the TRX domain of Grx4 binds to Php4 in an iron-independent manner. The TRX domain interaction site on Php4 has been mapped to two regions between residues 112–218 and 255–295 (Fig. 7.8). Grx4 Cys35 is required for the strong interaction between the TRX domain and Php4 [72]; however, unlike the conserved Cys in the GRX domain, mutation of the conserved Cys in the TRX domain has no effect on Php4 activity *in vivo* [57]. This interaction pattern between Grx4 and Php4 parallels the Grx4-Fep1 interaction: the TRX domain Cys35 facilitates a strong, iron-independent interaction with the repressor that is dispensable for repressor inhibition, whereas the GRX domain Cys172 maintains a weak, iron-dependent interaction that is essential for repressor inhibition. However, one key difference is that the GRX domain of Grx4 binds to Php4 under iron-replete conditions *in vivo* but interacts with Fep1 exclusively when iron is depleted.

7.5 Summary

The budding yeast *S. cerevisiae* and the fission yeast *S. pombe* utilize different mechanisms for regulation of iron homeostasis because *S. cerevisiae* regulators (Aft1, Aft2, Yap5) are transcriptional activators, whereas *S. pombe* regulators (Fep1, Php4) are transcriptional repressors. However, a common theme in yeast iron regulation is the central role of Fe-S clusters. In both model eukaryotes, the transcriptional response to changing iron bioavailability is specifically tuned to the ability of the cell to assemble Fe-S clusters. These versatile and ancient cofactors are a logical choice for this role due to their involvement in a wide variety of cellular functions, including mitochondrial energy metabolism, cofactor biosynthesis (e.g. heme, lipoate), amino acid biosynthesis, nucleotide metabolism, ribosome assembly, and DNA replication and repair. Tapping into the available pool of Fe-S clusters likely provides a sensitive gauge of intracellular iron availability.

An additional similarity between iron regulation in *S. cerevisiae* and *S. pombe* is the important regulatory role of cytosolic CGFS Grxs. Formation of GSH-ligated Fe-S cluster-binding complexes has been demonstrated for a wide variety of CGFS Grxs [60], and in most cases, the Fe-S cluster has proven essential for Grx function. This observation holds true for the two model yeasts described in this chapter because the available evidence suggests that Fe-S binding *via S. cerevisiae* Grx3/4 and *S. pombe* Grx4 is required for inhibition of *S. cerevisiae* Aft1/2 as well as *S. pombe* Php4 and Fep1. In each case, mutation of the CGFS motif in Grx3/Grx4 disrupts Fe-dependent inhibition of the transcriptional regulators, leading to constitutive activation by Aft1/Aft2 or constitutive repression by Php4 and Fep1. In addition, GSH depletion in both *S. cerevisiae* and *S. pombe* leads to a similar loss of iron-dependent inhibition of Aft1/

Aft2 and Php4. This phenomenon presumably stems from the requirement for GSH as a [2Fe-2S] cluster ligand in CGFS Grx complexes and/or for export of the Atm1 substrate [33, 69, 79]. The discovery of GSH-ligated Fe-S clusters thus uncovers a novel function for this ubiquitous thiol-containing tripeptide and highlights the intimate connection between thiol redox homeostasis and iron metabolism.

Despite the common themes in iron regulation in *S. cerevisiae* and *S. pombe*, there are some key differences between the regulation mechanisms. For instance, Aft1/Aft2 regulation involves two additional proteins to some extent, the BolA homologue Fra2 and the aminopeptidase P-like protein Fra1. Roles for either of these proteins in *S. pombe* iron homeostasis have not been reported. Another important distinction is that Aft1/Aft2 and Php4 activities are inhibited by cytosolic CGFS Grxs under iron-replete conditions, whereas Fep1 activity is inhibited under low-iron conditions. Thus, if ligation of a [2Fe-2S] cluster by Grx3/Grx4 is a key factor, Fe-S cluster binding must promote the inhibitive interaction between Aft1/Aft2/Php4 and Grx3/Grx4 while it prevents the inhibitive interaction between Fep1 and Grx4. Finally, *S. cerevisiae* Yap5 is unique compared with the other regulators because deletion of the genes encoding Grx3 and Grx4 does not affect the transcriptional activity of this regulator. Nevertheless, the available information on Yap5 confirms that both Fe-S cluster assembly and thiol redox biochemistry impact the function of this regulator as demonstrated for the other iron-responsive regulators in *S. cerevisiae* and *S. pombe*.

Acknowledgments

Work in the laboratory of Dr. Caryn E. Outten has been supported by National Institutes of Health grants K22 ES103780, R01 GM086619, and R01 GM100069.

References

[1] Kaplan CD, Kaplan J. Iron acquisition and transcriptional regulation. Chem Rev 2009; 109:4536–52.
[2] Schrettl M, Winkelmann G, Haas H. Ferrichrome in Schizosaccharomyces pombe – an iron transport and iron storage compound. Biometals 2004;17:647–54.
[3] Labbé S, Khan MG, Jacques JF. Iron uptake and regulation in Schizosaccharomyces pombe. Curr Opin Microbiol 2013;16:669–76.
[4] Pluskal T, Nakamura T, Villar-Briones A, Yanagida M. Metabolic profiling of the fission yeast S. pombe: quantification of compounds under different temperatures and genetic perturbation. Mol Biosyst 2010;6:182–98.
[5] Pelletier B, Beaudoin J, Philpott CC, Labbé S. Fep1 represses expression of the fission yeast Schizosaccharomyces pombe siderophore-iron transport system. Nucleic Acids Res 2003;31:4332–44.
[6] Protchenko O, Ferea T, Rashford J, et al. Three cell wall mannoproteins facilitate the uptake of iron in Saccharomyces cerevisiae. J Biol Chem 2001;276:49244–50.

[7] Kosman DJ. Molecular mechanisms of iron uptake in fungi. Mol Microbiol 2003;47:1185–97.
[8] Li L, Kaplan J. A mitochondrial-vacuolar signaling pathway in yeast that affects iron and copper metabolism. J Biol Chem 2004;279:33653–61.
[9] Mühlenhoff U, Stadler JA, Richhardt N, et al. A specific role of the yeast mitochondrial carriers MRS3/4p in mitochondrial iron acquisition under iron-limiting conditions. J Biol Chem 2003;278:40612–20.
[10] Li L, Chen OS, McVey Ward D, Kaplan J. CCC1 is a transporter that mediates vacuolar iron storage in yeast. J Biol Chem 2001;276:29515–9.
[11] Mercier A, Pelletier B, Labbé S. A transcription factor cascade involving Fep1 and the CCAAT-binding factor Php4 regulates gene expression in response to iron deficiency in the fission yeast Schizosaccharomyces pombe. Eukaryot Cell 2006;5:1866–81.
[12] Pouliot B, Jbel M, Mercier A, Labbé S. *abc3*$^{+}$ encodes an iron-regulated vacuolar ABC-type transporter in Schizosaccharomyces pombe. Eukaryot Cell 2010;9:59–73.
[13] Portnoy ME, Liu XF, Culotta VC. Saccharomyces cerevisiae expresses three functionally distinct homologues of the Nramp family of metal transporters. Mol Cell Biol 2000;20:7893–902.
[14] Yamaguchi-Iwai Y, Dancis A, Klausner RD. AFT1: a mediator of iron regulated transcriptional control in Saccharomyces cerevisiae. EMBO J 1995;14:1231–9.
[15] Casas C, Aldea M, Espinet C, Gallego C, Gil R, Herrero E. The AFT1 transcriptional factor is differentially required for expression of high-affinity iron uptake genes in Saccharomyces cerevisiae. Yeast 1997;13:621–37.
[16] Blaiseau PL, Lesuisse E, Camadro JM. Aft2p, a novel iron-regulated transcription activator that modulates, with Aft1p, intracellular iron use and resistance to oxidative stress in yeast. J Biol Chem 2001;276:34221–6.
[17] Rutherford JC, Jaron S, Ray E, Brown PO, Winge DR. A second iron-regulatory system in yeast independent of Aft1p. Proc Natl Acad Sci USA 2001;98:14322–7.
[18] Babu MM, Iyer LM, Balaji S, Aravind L. The natural history of the WRKY-GCM1 zinc fingers and the relationship between transcription factors and transposons. Nucleic Acids Res 2006;34:6505–20.
[19] Puig S, Vergara SV, Thiele DJ. Cooperation of two mRNA-binding proteins drives metabolic adaptation to iron deficiency. Cell Metab 2008;7:555–64.
[20] Puig S, Askeland E, Thiele DJ. Coordinated remodeling of cellular metabolism during iron deficiency through targeted mRNA degradation. Cell 2005;120:99–110.
[21] Philpott CC, Leidgens S, Frey AG. Metabolic remodeling in iron-deficient fungi. Biochim Biophys Acta 2012;1823:1509–20.
[22] Courel M, Lallet S, Camadro JM, Blaiseau PL. Direct activation of genes involved in intracellular iron use by the yeast iron-responsive transcription factor Aft2 without its paralog Aft1. Mol Cell Biol 2005;25:6760–71.
[23] Rutherford JC, Jaron S, Winge DR. Aft1p and Aft2p mediate iron-responsive gene expression in yeast through related promoter elements. J Biol Chem 2003;278:27636–43.
[24] Li L, Jia X, Ward DM, Kaplan J. Yap5 protein-regulated transcription of the TYW1 gene protects yeast from high iron toxicity. J Biol Chem 2011;286:38488–97.
[25] Pimentel C, Vicente C, Menezes RA, Caetano S, Carreto L, Rodrigues-Pousada C. The role of the Yap5 transcription factor in remodeling gene expression in response to Fe bioavailability. PLoS One 2012;7:e37434.
[26] Mühlenhoff U, Molik S, Godoy JR, et al. Cytosolic monothiol glutaredoxins function in intracellular iron sensing and trafficking via their bound iron-sulfur cluster. Cell Metab 2010;12:373–85.
[27] Winge DR, Nielson KB, Gray WR, Hamer DH. Yeast metallothionein. Sequence and metal-binding properties. J Biol Chem 1985;260:14464–70.

[28] Ding XQ, Bill E, Trautwein AX, Hartmann HJ, Weser U. Mossbauer studies on iron(II)-substituted yeast metallothionein. Eur J Biochem 1994;223:841–5.
[29] Yamaguchi-Iwai Y, Stearman R, Dancis A, Klausner RD. Iron-regulated DNA binding by the AFT1 protein controls the iron regulon in yeast. EMBO J 1996;15:3377–84.
[30] Ueta R, Fujiwara N, Iwai K, Yamaguchi-Iwai Y. Mechanism underlying the iron-dependent nuclear export of the iron-responsive transcription factor Aft1p in Saccharomyces cerevisiae. Mol Biol Cell 2007;18:2980–90.
[31] Yamaguchi-Iwai Y, Ueta R, Fukunaka A, Sasaki R. Subcellular localization of Aft1 transcription factor responds to iron status in Saccharomyces cerevisiae. J Biol Chem 2002;277:18914–8.
[32] Rutherford JC, Ojeda L, Balk J, Mühlenhoff U, Lill R, Winge DR. Activation of the iron regulon by the yeast Aft1/Aft2 transcription factors depends on mitochondrial but not cytosolic iron-sulfur protein biogenesis. J Biol Chem 2005;280:10135–40.
[33] Chen OS, Crisp RJ, Valachovic M, Bard M, Winge DR, Kaplan J. Transcription of the yeast iron regulon does not respond directly to iron but rather to iron-sulfur cluster biosynthesis. J Biol Chem 2004;279:29513–8.
[34] Ueta R, Fujiwara N, Iwai K, Yamaguchi-Iwai Y. Iron-induced dissociation of the Aft1p transcriptional regulator from target gene promoters is an initial event in iron-dependent gene suppression. Mol Cell Biol 2012;32:4998–5008.
[35] Lill R, Hoffmann B, Molik S, et al. The role of mitochondria in cellular iron-sulfur protein biogenesis and iron metabolism. Biochim Biophys Acta 2012;1823:1491–508.
[36] Ojeda L, Keller G, Mühlenhoff U, Rutherford JC, Lill R, Winge DR. Role of glutaredoxin-3 and glutaredoxin-4 in the iron regulation of the Aft1 transcriptional activator in Saccharomyces cerevisiae. J Biol Chem 2006;281:17661–9.
[37] Pujol-Carrion N, Bellí G, Herrero E, Nogues A, de la Torre-Ruiz MA. Glutaredoxins Grx3 and Grx4 regulate nuclear localisation of Aft1 and the oxidative stress response in Saccharomyces cerevisiae. J Cell Sci 2006;119:4554–64.
[38] Kumánovics A, Chen OS, Li L, et al. Identification of FRA1 and FRA2 as genes involved in regulating the yeast iron regulon in response to decreased mitochondrial iron-sulfur cluster synthesis. J Biol Chem 2008;283:10276–86.
[39] Lesuisse E, Knight SA, Courel M, Santos R, Camadro JM, Dancis A. Genome-wide screen for genes with effects on distinct iron uptake activities in Saccharomyces cerevisiae. Genetics 2005;169:107–22.
[40] Huynen MA, Spronk CA, Gabaldon T, Snel B. Combining data from genomes, Y2H and 3D structure indicates that BolA is a reductase interacting with a glutaredoxin. FEBS Lett 2005;579:591–6.
[41] Ken CF, Chen IJ, Lin CT, Liu SM, Wen L. Monothiol glutaredoxin cDNA from Taiwanofungus camphorata: a novel CGFS-type glutaredoxin possessing glutathione reductase activity. J Agric Food Chem 2011;59:3828–35.
[42] Mesecke N, Mittler S, Eckers E, Herrmann JM, Deponte M. Two novel monothiol glutaredoxins from Saccharomyces cerevisiae provide further insight into iron-sulfur cluster binding, oligomerization, and enzymatic activity of glutaredoxins. Biochemistry 2008;47:1452–63.
[43] Tamarit J, Bellí G, Cabiscol E, Herrero E, Ros J. Biochemical characterization of yeast mitochondrial Grx5 monothiol glutaredoxin. J Biol Chem 2003;278:25745–51.
[44] Zaffagnini M, Michelet L, Massot V, Trost P, Lemaire SD. Biochemical characterization of glutaredoxins from Chlamydomonas reinhardtii reveals the unique properties of a chloroplastic CGFS-type glutaredoxin. J Biol Chem 2008;283:8868–76.
[45] Fernandes AP, Fladvad M, Berndt C, et al. A novel monothiol glutaredoxin (Grx4) from Escherichia coli can serve as a substrate for thioredoxin reductase. J Biol Chem 2005;280:24544–52.

[46] Johansson C, Roos AK, Montano SJ, et al. The crystal structure of human GLRX5: iron-sulfur cluster co-ordination, tetrameric assembly and monomer activity. Biochem J 2010;433:303–11.
[47] Picciocchi A, Saguez C, Boussac A, Cassier-Chauvat C, Chauvat F. CGFS-type monothiol glutaredoxins from the cyanobacterium Synechocystis PCC6803 and other evolutionary distant model organisms possess a glutathione-ligated [2Fe-2S] cluster. Biochemistry 2007;46:15018–26.
[48] Bandyopadhyay S, Gama F, Molina-Navarro MM, et al. Chloroplast monothiol glutaredoxins as scaffold proteins for the assembly and delivery of [2Fe-2S] clusters. EMBO J 2008;27:1122–33.
[49] Iwema T, Picciocchi A, Traore DA, Ferrer JL, Chauvat F, Jacquamet L. Structural basis for delivery of the intact [Fe2S2] cluster by monothiol glutaredoxin. Biochemistry 2009;48:6041–3.
[50] Haunhorst P, Berndt C, Eitner S, Godoy JR, Lillig CH. Characterization of the human monothiol glutaredoxin 3 (PICOT) as iron-sulfur protein. Biochem Biophys Res Commun 2010;394:372–6.
[51] Li H, Mapolelo DT, Dingra NN, et al. The yeast iron regulatory proteins Grx3/4 and Fra2 form heterodimeric complexes containing a [2Fe-2S] cluster with cysteinyl and histidyl ligation. Biochemistry 2009;48:9569–81.
[52] Yeung N, Gold B, Liu NL, et al. The E. coli monothiol glutaredoxin GrxD forms homodimeric and heterodimeric FeS cluster containing complexes. Biochemistry 2011;50:8957–69.
[53] Ye H, Jeong SY, Ghosh MC, et al. Glutaredoxin 5 deficiency causes sideroblastic anemia by specifically impairing heme biosynthesis and depleting cytosolic iron in human erythroblasts. J Clin Invest 2010;120:1749–61.
[54] Jbel M, Mercier A, Labbé S. Grx4 monothiol glutaredoxin is required for iron limitation-dependent inhibition of Fep1. Eukaryot Cell 2011;10:629–45.
[55] Molina MM, Bellí G, de la Torre MA, Rodriguez-Manzaneque MT, Herrero E. Nuclear monothiol glutaredoxins of Saccharomyces cerevisiae can function as mitochondrial glutaredoxins. J Biol Chem 2004;279:51923–30.
[56] Bellí G, Polaina J, Tamarit J, et al. Structure-function analysis of yeast Grx5 monothiol glutaredoxin defines essential amino acids for the function of the protein. J Biol Chem 2002;277:37590–6.
[57] Kim KD, Kim HJ, Lee KC, Roe JH. Multi-domain CGFS-type glutaredoxin Grx4 regulates iron homeostasis via direct interaction with a repressor Fep1 in fission yeast. Biochem Biophys Res Commun 2011;408:609–14.
[58] Hoffmann B, Uzarska MA, Berndt C, et al. The multidomain thioredoxin-monothiol glutaredoxins represent a distinct functional group. Antioxid Redox Signal 2011;15:19–30.
[59] Li H, Mapolelo DT, Dingra NN, et al. Histidine 103 in Fra2 is an iron-sulfur cluster ligand in the [2Fe-2S] Fra2-Grx3 complex and is required for in vivo iron signaling in yeast. J Biol Chem 2011;286:867–76.
[60] Li H, Outten CE. Monothiol CGFS glutaredoxins and BolA-like proteins: [2Fe-2S] binding partners in iron homeostasis. Biochemistry 2012;51:4377–89.
[61] Lesuisse E, Blaiseau PL, Dancis A, Camadro JM. Siderophore uptake and use by the yeast Saccharomyces cerevisiae. Microbiology 2001;147:289–98.
[62] Fragiadakis GS, Tzamarias D, Alexandraki D. Nhp6 facilitates Aft1 binding and Ssn6 recruitment, both essential for FRE2 transcriptional activation. EMBO J 2004;23:333–42.
[63] Li L, Bagley D, Ward DM, Kaplan J. Yap5 is an iron-responsive transcriptional activator that regulates vacuolar iron storage in yeast. Mol Cell Biol 2008;28:1326–37.
[64] Li L, Miao R, Bertram S, Jia X, Ward DM, Kaplan J. A role for iron-sulfur clusters in the regulation of transcription factor Yap5-dependent high iron transcriptional responses in yeast. J Biol Chem 2012;287:35709–21.
[65] Labbé S, Pelletier B, Mercier A. Iron homeostasis in the fission yeast Schizosaccharomyces pombe. Biometals 2007;20:523–37.

[66] Pelletier B, Beaudoin J, Mukai Y, Labbé S. Fep1, an iron sensor regulating iron transporter gene expression in Schizosaccharomyces pombe. J Biol Chem 2002;277:22950–8.
[67] Fagerstrom-Billai F, Wright AP. Functional comparison of the Tup11 and Tup12 transcriptional corepressors in fission yeast. Mol Cell Biol 2005;25:716–27.
[68] Jbel M, Mercier A, Pelletier B, Beaudoin J, Labbé S. Iron activates in vivo DNA binding of Schizosaccharomyces pombe transcription factor Fep1 through its amino-terminal region. Eukaryot Cell 2009, 8;649–64.
[69] Mercier A, Watt S, Bahler J, Labbé S. Key function for the CCAAT-binding factor Php4 to regulate gene expression in response to iron deficiency in fission yeast. Eukaryot Cell 2008;7:493–508.
[70] Chung WH, Kim KD, Roe JH. Localization and function of three monothiol glutaredoxins in Schizosaccharomyces pombe. Biochem Biophys Res Commun 2005;330:604–10.
[71] Mercier A, Labbé S. Both Php4 function and subcellular localization are regulated by iron via a multistep mechanism involving the glutaredoxin Grx4 and the exportin Crm1. J Biol Chem 2009;284:20249–62.
[72] Vachon P, Mercier A, Jbel M, Labbé S. The monothiol glutaredoxin Grx4 exerts an iron-dependent inhibitory effect on Php4 function. Eukaryot Cell 2012;11:806–19.
[73] Pelletier B, Trott A, Morano KA, Labbé S. Functional characterization of the iron-regulatory transcription factor Fep1 from Schizosaccharomyces pombe. J Biol Chem 2005;280:25146–61.
[74] Chao LY, Marletta MA, Rine J. Sre1, an iron-modulated GATA DNA-binding protein of iron-uptake genes in the fungal pathogen Histoplasma capsulatum. Biochemistry 2008;47:7274–83.
[75] Harrison KA, Marzluf GA. Characterization of DNA binding and the cysteine rich region of SRE, a GATA factor in Neurospora crassa involved in siderophore synthesis. Biochemistry 2002;41:15288–95.
[76] Dailey HA, Finnegan MG, Johnson MK. Human ferrochelatase is an iron-sulfur protein. Biochemistry 1994;33:403–7.
[77] Znaidi S, Pelletier B, Mukai Y, Labbé S. The Schizosaccharomyces pombe corepressor Tup11 interacts with the iron-responsive transcription factor Fep1. J Biol Chem 2004;279:9462–74.
[78] Hortschansky P, Eisendle M, Al-Abdallah Q, et al. Interaction of HapX with the CCAAT-binding complex – a novel mechanism of gene regulation by iron. EMBO J 2007;26:3157–68.
[79] Kumar C, Igbaria A, D'Autreaux B, et al. Glutathione revisited: a vital function in iron metabolism and ancillary role in thiol-redox control. EMBO J 2011;30:2044–56.

8 Biogenesis of Fe-S proteins in mammals

Tracey Rouault

8.1 Introduction

Although mammalian cells were known to contain Fe-S proteins as early as 1960 [2], little was known about how Fe-S clusters were assembled. Extensive work on mammalian mitochondrial aconitase had proven that mitochondrial aconitase contained a cubane [4Fe-4S] cluster to which the aconitase substrates, citrate, or isocitrate bound during the enzymatic reaction. The Fe-S cluster of mitochondrial aconitase could be assembled from sulfide and iron *in vitro* under anaerobic conditions using high concentrations of sulfide, iron, and reductant, but the assembly process was arduous and inefficient. In 1990, when the bifunctional protein now known as iron regulatory protein 1 (IRP1) was purified and cloned, it became apparent that this protein functioned as a cytosolic aconitase in iron-replete cells. In iron-deficient cells, the Fe-S cluster was absent, and binding of apo-IRP1 to RNA stem-loop structures in transcripts repressed translation of some transcripts such as ferritin and extended the half-life of some others. The presence or absence of the Fe-S cluster determined whether the protein functioned in posttranscriptional regulation or as an enzyme, and this kindled interest in how the Fe-S cluster was assembled and degraded. Building on the progress that had been made in identifying Fe-S biogenesis proteins in bacteria [3], human homologues of these proteins were identified through sequence homology, and when the human genome was fully sequenced, it was possible to identify a full complement of Fe-S biogenesis proteins in the genome based on homology and function. What follows is an account of how the field of mammalian Fe-S biogenesis progressed upon discovery of Fe-S biogenesis proteins and unexpectedly proved to be key to understanding a group of rare human diseases.

8.2 The Fe-S regulatory switch of IRP1

In the 1980s, several genes important in mammalian iron metabolism were cloned and sequenced, including genes that encoded ferritin H and L chains [4], which form heteropolymers that sequester iron [5] and transferrin receptor 1 (TFR1), which internalizes iron from circulating diferric transferrin [6]. Direct measurements of protein expression had shown that cells expressed high amounts of TFR1 and low ferritin when they were iron starved, whereas they synthesized low amounts of TFR1 and more ferritin when they were rich in iron. To determine how cells achieved these desirable changes in ferritin and TFR1 expression and maintained iron homeostasis, the sequences of the newly cloned genes were used to

DOI 10.1515/9783110479850-008

quantify expression levels of the mRNA that encoded each gene in cell lysates. There was very little change in ferritin mRNA levels when cells were iron starved or loaded with iron [7], consistent with earlier indirect observations [8]. The fact that protein levels varied up to 50-fold, whereas mRNA levels did not change, led to focus on translation of the mRNA itself as the point of regulation. A deletional analysis focusing on the 5′ end of the mRNA led to the conclusion that an RNA stem-loop in the untranslated region near the 5′ end of the mRNA was both necessary and sufficient to confer translational regulation upon the mRNA [9]. This RNA stem-loop became known as the iron-responsive element (IRE), and it was soon apparent in gel-shift experiments that the IRE could tightly bind a cellular protein that slowed migration of the negatively charged radiolabelled IRE in an acrylamide gel [10, 11]. Five IREs were found in the 3′ untranslated region of the TFR1 mRNA [12] that were later shown to flank and protect the mRNA from endonucleolytic cleavage when cells were depleted of iron [13] (Fig. 8.1).

Cellular lysates contained a protein or proteins that bound to the IRE in low or high amounts, depending on whether the cells from which lysates were made were iron rich or iron deficient when the lysates were made [10, 11]. Using the gel-shift assay, the IRE binding protein (IRE-BP) was purified and cloned, using peptide sequences to predict the mRNA sequence [14–17], and a remarkable sequence homology to the peptide sequence of mitochondrial aconitase was noted, which included the identity of all of the residues involved in the formation of the enzymatic active site [18]. The presence of a cytosolic aconitase had been previously identified in mammalian cells [19, 20], raising the possibility that the IRE-BP could also function as an aconitase. Indeed, the IRE-BP readily acquired aconitase function in iron-rich cells [21–23], and EPR and sulfide measurements verified that a [4Fe-4S] cluster was present [24] in purified cytosolic aconitase.

The novel discovery that the presence or absence of a Fe-S cluster determined whether a protein functioned as an enzyme or as a regulatory protein raised questions about how clusters were synthesized and degraded. To cover its two functions, the protein was renamed iron regulatory protein 1, and much work indicated that the Fe-S cluster of both aconitases was relatively solvent exposed and could be readily disassembled by oxidants ranging from oxygen and superoxide to nitric oxide [25, 26], whereas measurements of the half-life of IRP1 protein indicated that the protein itself was relatively stable [27]. Thus, the regulatory switch might depend on the ability of the cell to rebuild an Fe-S cluster that was readily disassembled because of its exposed position in the aconitase active site cleft [28]. Moreover, the two activities of IRP1 appeared to be mutually exclusive, as each depended on portions of the enzymatic active site for function [29–32]; opening of the active site cleft was predicted to be required for the IRE to fit into the active site cleft. Indeed, years later, the structure was solved for the cytosolic aconitase form of IRP1 [33] and for the apo-IRP1-IRE complex [34], and conformational changes that accommodated access of the IRE to otherwise inaccessible internal sites and identification of its high affinity contact

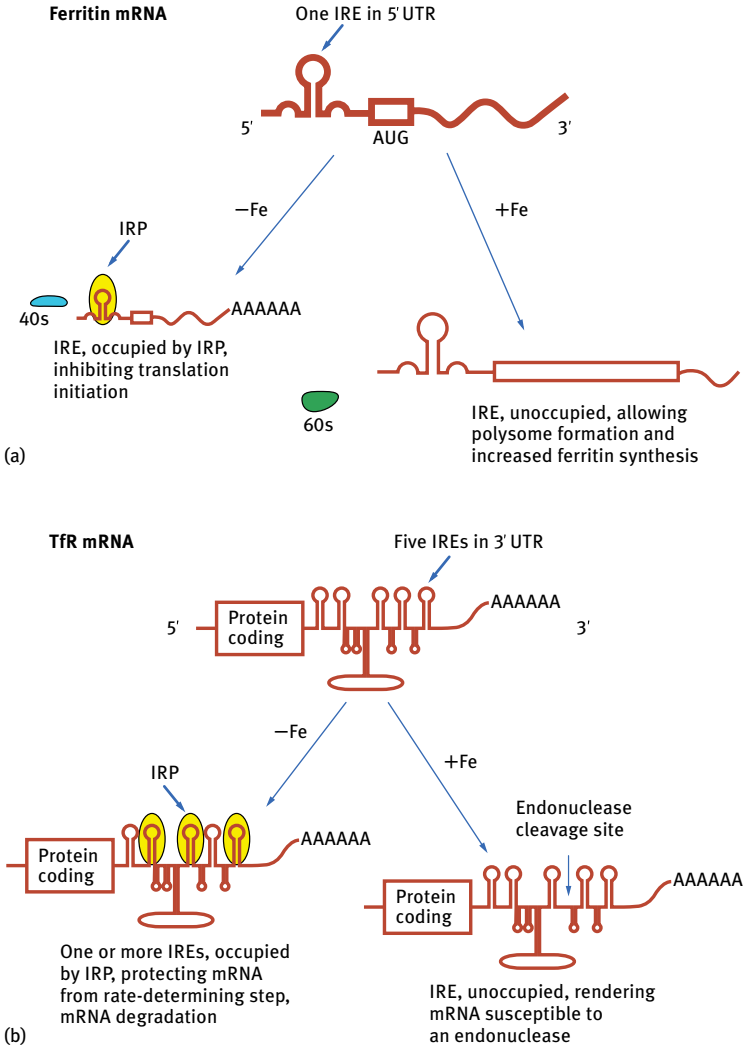

Fig. 8.1: Model of how binding of IRP (IRP1 and IRP2) to RNA stem-loops in the transcripts of ferritin (a) and transferrin receptor (TfR mRNA) regulates synthesis of each protein (reproduced from [35]). In iron-depleted cells, when IRP1 lacks an Fe-S cluster, it binds to IRE stem-loops in many different mRNAs. Binding to a IRE near the 5′ end of the transcript prevents ribosomal subunits from binding to the 5′ end and then synthesizing the protein encoded by the open reading frame (box). New translation of ferritin (and other proteins encoded by transcripts that contain an IRE near the 5′ end of the transcript) is repressed, with the result that there is little synthesis of the iron sequestration protein, ferritin, when cells are depleted of iron. In the TfR transcript, binding of IRPs protects the mRNA from degradation, which leads to more synthesis of TfR. Conversely, when cells are iron-replete, ferritin is actively synthesized, whereas TfR synthesis is reduced because the TfR mRNA is degraded. Thus, expression of the iron uptake protein, TfR, increases when cells are depleted of iron. By regulating expression of ferritin, the major iron sequestration protein, and TfR, a major iron uptake protein, the IRP regulatory system adjusts iron homeostasis to maintain optimal intracellular iron levels.

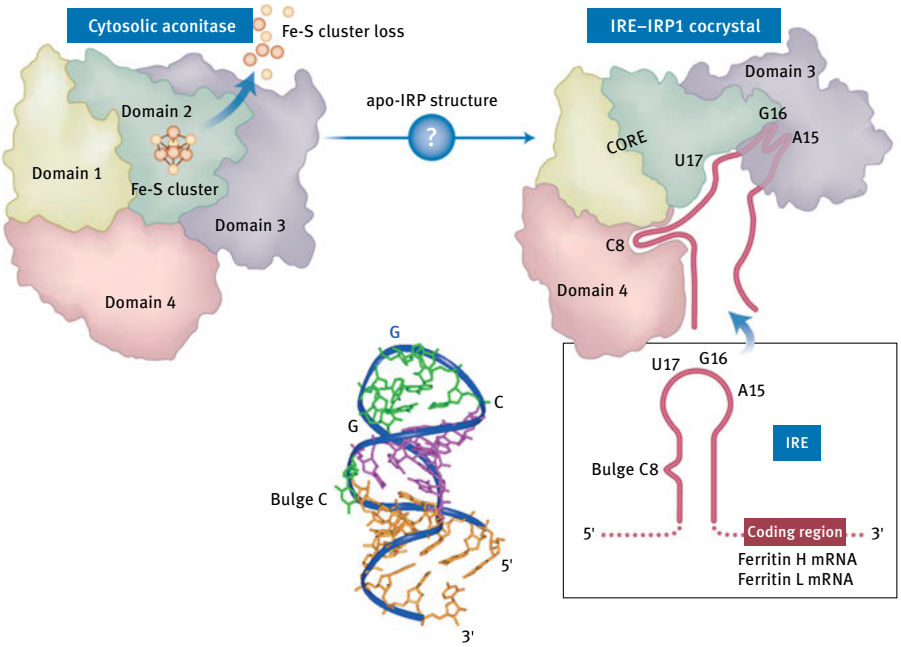

Fig. 8.2: The presence or absence of an Fe-S cluster determines whether IRP1 will function as an active aconitase or as an IRE-BP. Upon loss of the Fe-S cluster, which is readily degraded by oxidants, IRP1 undergoes a conformational shift in several of its four domains, creating a binding pocket that contains interstices into which residues C8, G16 A15, and U17 of the IRE can insert. Multiple hydrogen bonds form between these highly conserved residues of the IRE, which are optimally spatially separated from one another by the length of the upper stem and the loop structure of the IRE. Conserved structural features of the IRE function as molecular rulers that separate specific contact points [36] that bind simultaneously. Multiple contacts between residues of the IRE with peptide sequences that are accessible in the open conformation of IRP1 contribute to high affinity binding of IRP1 to the IRE. Figure from [37].

points in apo-IRP1 were identified. Phosphorylation also was shown to influence reversibility of IRP functions [38] (Fig. 8.2).

Therefore, attention increasingly centered on identifying the mechanisms involved in synthesis of Fe-S clusters. The large body of work by Richard Holm and colleagues had shown that Fe-S clusters could spontaneously assemble [39], but reassembly of the Fe-S cluster on apo-IRP1 was difficult to achieve using inorganic materials alone. When news about a cysteine desulfurase important in Fe-S assembly in bacteria traveled, it seemed that a mechanism for enzymatic mobilization of sulfur might be the answer to the challenge of how to generate the sulfur needed for Fe-S biogenesis [40]. Indeed, addition of a bacterial cysteine desulfurase to Fe-S reconstitutions of aconitase revealed that efficiency of reconstitution was greatly increased (Kennedy MC, personal communication).

8.3 IRP2, a highly homologous gene, also posttranscriptionally regulates iron metabolism, but iron sensing occurs through regulation of its degradation rather than through a Fe-S switch mechanism

When IRP1 was cloned, a second highly homologous gene was cloned [14], which proved to encode a second IRP, IRP2 [41, 42], that functioned equally well as IRP1 in translational regulation [43]. IRP2 lacked an Fe-S cluster, but rather was degraded by the proteasome in iron-replete cells [44, 45]. Ultimately, iron sensing was attributed to the protein FBXL5, which contained a hemerythrin-type iron binding site, and orchestrated ubiquitination and proteasomal degradation of IRP2 in iron-replete cells [46, 47] (Fig. 8.3). *IRP1* and *IRP2* likely represent a duplicated gene pair, a common feature of mammalian genomes [48] in which gene function is largely conserved, but redundancy makes it possible for a system to evolve and, in this case, perhaps to enable a different mechanism of iron sensing to prevail. From one perspective, degradation of IRP2 in iron-replete cells represents a more robust solution to the problem of sensing and regulation, because the protein is rendered physically absent in iron-replete cells, whereas IRP1 is still present, though its Fe-S cluster eliminates its IRE binding activity.

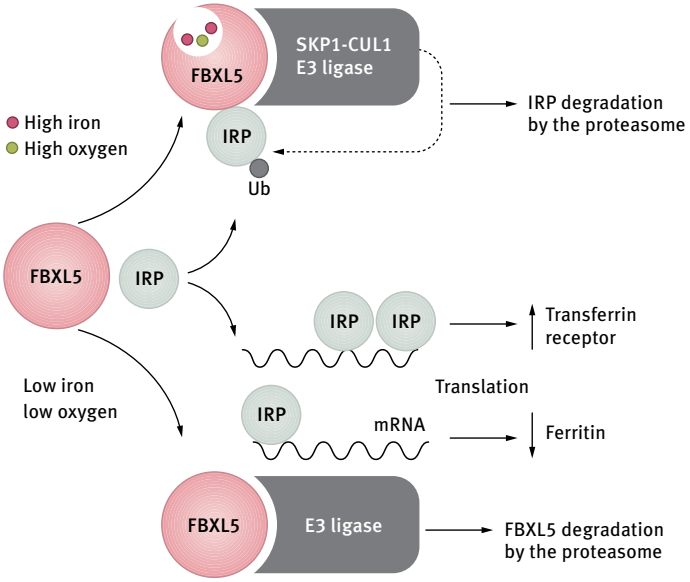

Fig. 8.3: Iron-dependent regulation of IRPs through regulation of their degradation. In addition to the Fe-S switch of IRP1, IRP2, which is highly homologous to IRP1, does not contain an Fe-S cluster but rather is degraded by the proteasome when cells are iron-rich, because the protein FBXL5 contains an iron-binding site and targets IRP2 for degradation when cells are iron rich [46, 47]. Figure from [49].

The lability of the Fe-S cluster allows IRE binding activity of IRP1 to be activated even when cells are otherwise iron replete, potentially leading to iron overload when cells are oxidatively stressed.

Although the two IRPs appear to be expressed in most or all cell types, expression levels of IRP1 are highest in the kidney and brown fat, whereas IRP2 expression is highest in the central nervous system [50, 51]. The differences in relative distribution among tissues may account for the fact that animals engineered to lack *IRP2* develop neurodegeneration [52–54] and anemia [55, 56], whereas animals that lack IRP1 develop polycythemia [57–59] and pulmonary hypertension [57]. Animals cannot develop beyond the blastocyst stage when both *IRP*s are deleted, illustrating the physiological significance and partial redundancy of this important posttranscriptional regulatory system [60].

Since the IRE was initially characterized in transcripts of ferritin H and L chains and TFR1, numerous transcripts that contain IREs at the 5′ end have been discovered that mediate translational repression, including ALAS2, which encodes a heme biosynthetic enzyme [61, 62], mitochondrial aconitase [63, 64], the iron exporter ferroportin [65–67], and HIF2α [68]. Interestingly, cells that need to evade suppression of ferroportin synthesis by IRPs for physiological reasons synthesize a ferroportin transcript that lacks a IRE, using a different promoter [69, 70]. Several other transcripts that contain IREs of unknown significance have been identified using a search program for IREs [71], including several transcripts that contain IREs in the 3′UTR [72], and by sequencing mRNAs that bind to IRPs [73]. Physiological relevance of the IRE in regulation of HIF2α expression was recently demonstrated when animals that lacked IRP1 developed high erythropoietin levels and polycythemia [57–59]. The roles of IRP1 and IRP2 in physiology have been extensively characterized in animal models, and their overlapping functions and association with differing phenotypes have been synthesized in several thorough reviews [74–76].

8.4 Identification of the mammalian cysteine desulfurase and two scaffold proteins: implications for compartmentalization of the process

In the 1990s, the sequencing of the human genome was not yet completed, but a database of short sequences from cloned human genes, known as expressed sequence tags (ESTs), was available and was used to search for human homologues to bacterial Fe-S biogenesis genes [77]. Remarkably, a human homologue of bacterial NifS was identified as having approximately 60% sequence homology to a bacterial cysteine desulfurase. Complete cloning and characterization of human NFS1 revealed that it encoded a major mitochondrial isoform that contained a mitochondrial targeting

sequence and also a minor isoform that lacked the mitochondrial targeting sequence and localized to the cytosolic/nuclear compartment of mammalian cells [78]. Using similar techniques, the major Fe-S scaffold protein, ISCU, was cloned, and alternative splicing provided a mechanism for generating both mitochondrial and cytosolic/nuclear isoforms [79]. Human NFU1, which is homologous to a portion of bacterial IscU, also encoded two isoforms through alternative splicing and was shown to bind a [4Fe-4S] cluster [80]. Function of the cytosolic form of ISCU was demonstrated by reducing the expression of the cytosolic isoform, but not the mitochondrial isoform [81]. These experiments suggested that a parallel machinery for nascent Fe-S assembly existed in the cytosolic/nuclear compartments of mammalian cells, but researchers working on *Saccharomyces cerevisiae* disputed this point because they found no evidence for cytosolic or nuclear isoforms of these proteins involved in early Fe-S assembly [82]. However, a nuclear isoform of NFS1 is present and necessary in *S. cerevisiae* [83] [84], and its required partner, ISD11, is also present in the nucleus and cytosol of mammalian cells [85]. Moreover, the co-chaperone, HSC20, is readily found in mammalian cytosolic lysates [86], again raising the question of whether Fe-S synthesis can be initiated in the cytosol and nucleus of mammalian cells. Extensive evidence supports that there is a parallel system for synthesis of nascent Fe-S clusters in the cytosol of mammalian cells (reviewed in [87]).

There are also numerous mammalian homologues of proteins identified in *S. cerevisiae* as important in cytosolic Fe-S synthesis, referred to as the CIA machinery, for *c*ytosolic *i*ron sulfur *a*ssembly. Recently, these proteins were recognized as important for Fe-S biogenesis in enzymes involved in mammalian DNA metabolism and maintenance [88, 89] (discussed further in chapters by Gari and by Lill and Wohlschlegel) and for Fe-S acquisition by IRP1 [90].

8.5 Sequential steps in Fe-S biogenesis – an initial Fe-S assembly process on a scaffold, followed by Fe-S transfer to recipient proteins, aided by a chaperone-cochaperone system

Based on biochemical and structural characterization of bacterial proteins [91, 92], a model for synthesis of nascent Fe-S clusters emerged in which Nfs1 dimerizes and the scaffold protein, IscU, binds to each end of the complex. In eukaryotes, Isd11 is an obligate binding partner of Nfs1, and a ternary complex has been identified in mammalian cells composed of NFS1, ISD11, and ISCU [93, 94] that works in concert with frataxin (FXN) to synthesize nascent clusters on ISCU. FXN was initially identified as the disease gene in the human disease Friedreich's ataxia in 1996 [95], but its function was completely unknown until 1997, when experiments in *S. cerevisiae* tied it to mitochondrial iron metabolism [96]. Subsequently, experiments have demonstrated that FXN is important in early Fe-S synthesis, where it may function as an

iron sequestration protein [97], as an iron carrier [98], or as an allosteric modifier [99] of the complex. Recent studies suggest that this tetrameric complex can generate [4Fe-4S] clusters that can ligate directly to mitochondrial aconitase [100] (Fig. 8.4).

After the initial cluster is synthesized on ISCU, a cochaperone known as HSC20 binds holo-ISCU and forms a complex with the chaperone protein, HSPA9 (also known as HSC70, HSCA, or mortalin), an ATPase that is activated by the HPD tripeptide of ISCU [101, 102]. Activation of HSPA9 may generate a conformational change that releases the Fe-S cluster from ISCU, allowing it to bind to recipient proteins or to intermediate scaffold-type carrier proteins. The sequence LPPVK of ISCU interacts with HSPA9, binding ISCU to the chaperone in bacterial [101] and *S. cerevisiae* model systems [103], where the critical motif of Isu was identified as the tripeptide, PVK.

Once ISCU, with its nascent cluster, binds to the chaperone-cochaperone complex through independent contacts with HSC20 and HSPA9, the cluster is transferred to recipient proteins, but few details were known about how Fe-S clusters are acquired by recipient proteins until recent work revealed that HSC20 binds LYR tripeptide motifs in recipient proteins such as succinate dehydrogenase subunit B (SDHB) to the Fe-S transfer complex, composed of HSC20, holo-ISCU, and HSPA9 [104, 105]. Notably, though some proteins such as zinc fingers could readily accommodate binding of a Fe-S cluster through their available cysteine ligands, mammalian cells appear to be able to specifically transfer Fe-S clusters to proteins that need Fe-S clusters for function by directly binding recipient proteins (reviewed in [106] and in Maio and Rouault, chapter 9, volume 2). Secondary scaffold proteins are also likely to be involved in ferrying Fe-S clusters from the basic Fe-S synthesis complexes to specific subsets of recipient proteins. Monothiol glutaredoxins have been proposed to function as secondary scaffolds in bacteria [107], and mutations in human glutaredoxin 5 disrupt Fe-S biogenesis and cause sideroblastic anemia [108].

Several recently described human diseases underscore the importance of various steps of Fe-S biogenesis. Mutations of ISD11, also known as LYRM4, cause severe impairments of mitochondrial oxidative phosphorylation in infants, as might be expected when initial Fe-S complex formation is compromised [109]. Abnormal splicing of ISCU causes skeletal myopathy [110, 111], and a missense mutation at this locus in combination with the abnormal splicing allele causes cardiac and skeletal disease [112]. Reduced expression of FXN due to heterochromatin formation on an expanded trinucleotide repeat leads to abnormal Fe-S protein functions in neurons and cardiomyocytes of patients and in animal models [113]. Mutations in NFU1 and BOLA3 cause defective function of proteins that require lipoic acid modification for function, including the E2 component of the pyruvate dehydrogenase complex, α keto-glutarate dehydrogenase, branched-chain keto acid dehydrogenase (BCKDH), and the H protein of the glycine cleavage system [114, 115]. Accordingly, infants with mutations in these genes had lactic acidosis along with elevated levels of glycine and the branched-chain amino acids, leucine, valine, and isoleucine. The clinical symptoms imply that NFU1 and BOLA3 are important for delivery of the Fe-S cluster to lipoic acid synthase (see chapter by Lanz and Booker), perhaps by functioning as secondary scaffolds.

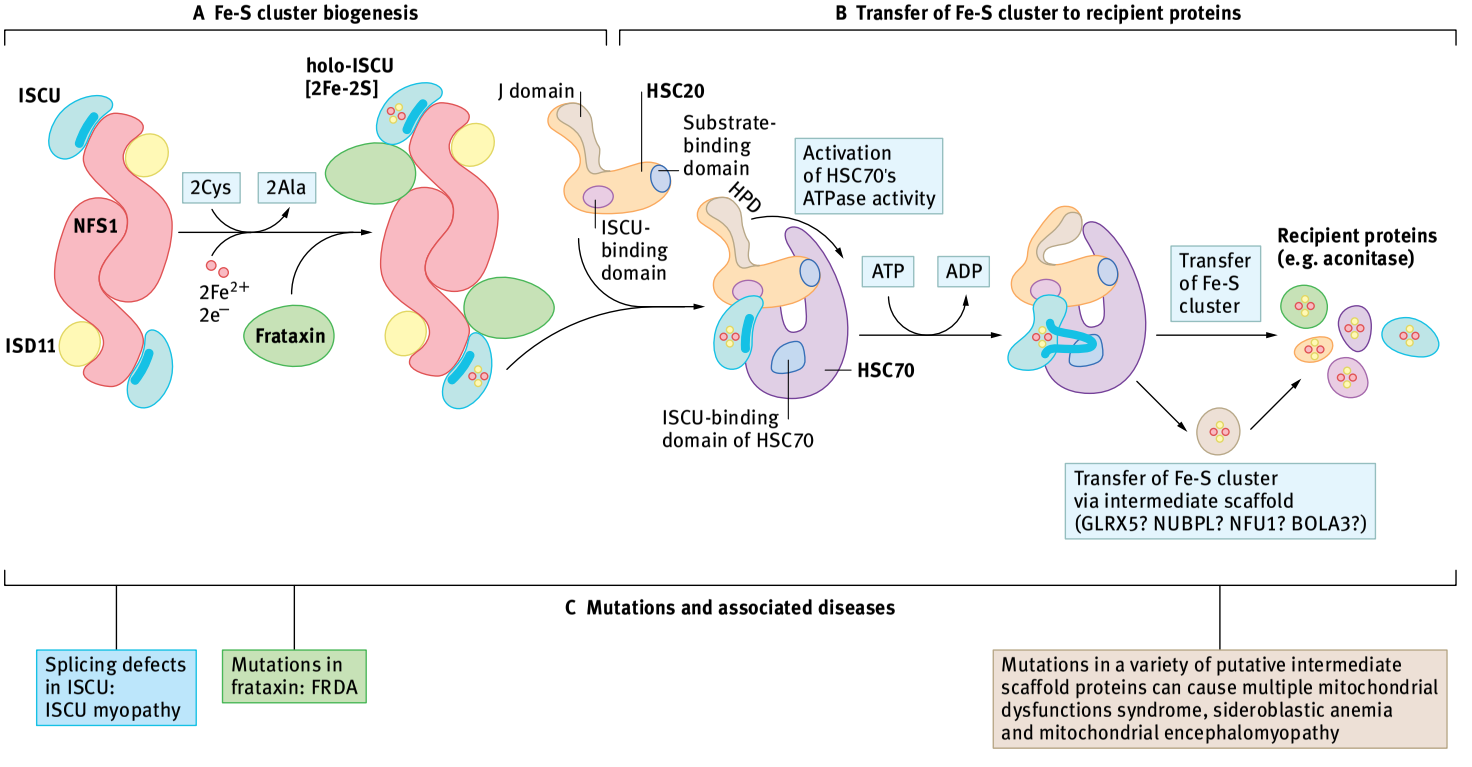

Fig. 8.4: A model for mammalian Fe-S biogenesis, based on the crystal structure of the Nfs1-IscU complex in bacteria [91, 92] and proposed roles of FXN [100, 116]. The first stage (A) of Fe-S synthesis depends on head-to-tail dimerization of the cysteine desulfurase, NFS1; in eukaryotes, each NFS1 monomer binds in an obligate manner to a small associated protein, ISD11, and to the Fe-S scaffold protein, ISCU. Nascent [2Fe-2S] clusters form on ISCU, aided in an unknown manner by transient FXN binding. (B) A co-chaperone, HSC20, binds holo-ISCU and forms a complex with the chaperone HSC70 (as labeled in the figure), also known as HSPA9 or mortalin, an ATPase that is activated by the HPD tripeptide of ISCU. Activation may generate a conformational change that facilitates release of the Fe-S cluster from ISCU, allowing it to bind to recipient proteins or to intermediate scaffold-type carrier proteins (see text and Maio and Rouault chapter). Mutations of various Fe-S biogenesis proteins cause specific diseases. Figure from [117], with permission.

Other candidates for secondary scaffolds include IBA57 [118] and glutaredoxin 5 [108]. Absence of glutaredoxin 5 was identified as a cause of sideroblastic anemia, a disease in which the mitochondria of immature red cells become markedly iron loaded, and too few mature red cells are produced. Thus, human diseases can highlight specific roles of Fe-S assembly proteins at various points in the pathway.

8.6 Mitochondrial iron overload in response to defects in Fe-S biogenesis raises important questions about how mitochondrial iron homeostasis is regulated

In Friedreich's ataxia [113], ISCU myopathy [110], and glutaredoxin 5 deficiency [119], abnormal mitochondrial iron accumulation occurs in affected tissues. The same phenotype has been observed in *S. cerevisiae* resulting from loss of Fe-S biogenesis proteins such as Nfs1 [120], FXN [96], and others (see chapter by Pain and Dancis). The fact that mitochondrial iron overload occurs (Fig. 8.5), sometimes at the expense of cytosolic iron [121], suggests that intact Fe-S biogenesis is required for maintenance of mitochondrial iron homeostasis. In skeletal muscle from humans with ISCU deficiency, expression of the mitochondrial iron importer, mitoferrin, increases [1]. Fe-S clusters have previously been shown to have regulatory function in bacteria [122] and the regulatory role of the Fe-S cluster of IRP1 was discussed earlier in this chapter. The occurrence of mitochondrial iron overload as a consequence of problems with Fe-S biogenesis hints that a Fe-S protein is involved in regulating mitochondrial iron

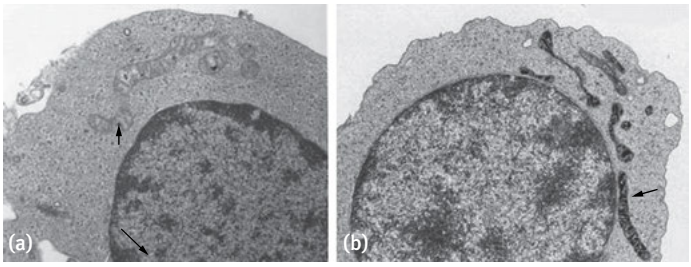

Fig. 8.5: Mitochondrial iron overload occurs in human and animal models when functions of some proteins involved in Fe-S biogenesis are impaired. Electron micrograph of mitochondrial iron overload in developing erythroblasts from the early stages (A) to advanced (B) in patients with sideroblastic anemia. Sideroblastic anemia is a term for anemias in which mitochondria show severe iron overload in the mitochondria of the developing red cell, which may be observed with the Prussian blue stain for iron, or by electron microscopy, where iron appears as black deposits. In A, a patient with mild disease has a small black iron deposit in a mitochondrion (small arrow) located near the nucleus (large arrow). In B, perinuclear mitochondria are loaded with black iron precipitates in a patient with advanced disease. Mitochondrial cristae are still visible as white band-like lines in the mitochondria (an arrow points to one iron-laden rod-shaped mitochondrion that is loaded with black iron deposits) (figures courtesy of Dr. M. Djaldetti).

homeostasis, perhaps by transcriptionally remodeling the cell to increase mitochondrial iron uptake and decrease mitochondrial iron export. In the past, researchers have postulated that iron may have no dedicated mitochondrial exporter and may exit the mitochondrial matrix in the form of heme or a Fe-S cluster. Thus far, neither a mitochondrial iron exporter nor a heme exporter has yet been discovered. However, mutations in an inner mitochondrial membrane transporter known as ABCB7 in humans, or Atm1 in the *S. cerevisiae* homologue, lead to mitochondrial accumulation. In humans, mutations cause a disease known as X-linked sideroblastic anemia with ataxia because the mutations are on the X chromosome, and males are typically affected [123]. Molecular dissection of other rare diseases in humans may lead to specific insights into the Fe-S biogenesis pathway, particularly in the downstream steps through which recipient proteins acquire their Fe-S clusters.

8.7 Perspectives and future directions

Much of the progress made in identifying the main genes involved in mammalian Fe-S biogenesis exploited the homology of mammalian to bacterial genes and built on biochemical and spectroscopic studies of bacterial processes. However, there are several issues that have not yet been resolved by studies in bacterial model systems. The problem of the role of FXN remains unresolved, even though bacteria express FXN. In addition, it is not yet known how the Fe-S biogenesis machinery specifically targets recipient proteins. Moreover, studies in bacteria cannot tackle the question of how eukaryotic cells coordinate Fe-S biogenesis in multiple compartments. If bacteria regulate Fe-S biogenesis by regulating transcription of the ISC operon (see chapter by Mettert et al.), what regulates eukaryotic Fe-S biogenesis? Some progress was made when it was recognized that ISCU expression was repressed during hypoxia by micro-RNA-mediated repression [124], which suppressed mitochondrial respiration. Other regulatory inputs must also govern the Fe-S biogenesis pathway, and mechanisms that coordinate mitochondrial and cytosolic/nuclear Fe-S biogenesis need to be elucidated. It is not clear whether mammalian cytosolic/nuclear FeS biogenesis requires a product of mitochondrial Fe-S biogenesis, as has been asserted for *S. cerevisiae*, or whether *de novo* Fe-S biogenesis can occur in the cytosol and/or nucleus using cytosolic isoforms of NFS1, ISCU, NFU1, and HSC20. In addition, regulatory mechanisms may have evolved that do not exist in less complex eukaryotes such as *S. cerevisiae*. As an illustration, it is noteworthy that the IRE-IRP regulatory system does not exist in *S. cerevisiae*. Studies performed in mammalian cells will likely be important in resolving numerous questions, because the strong protein-protein interactions characteristic of mammalian cells may facilitate biochemical identification of critical protein complexes. In addition, the excellent phenotyping associated with rare human diseases may lead to other unexpected insights into the Fe-S biogenesis pathway.

References

[1] Crooks DR, Natarajan TG, Jeong SY, et al. Elevated FGF21 secretion, PGC-1alpha and ketogenic enzyme expression are hallmarks of iron-sulfur cluster depletion in human skeletal muscle. Hum Mol Genet 2014;23:24–39.
[2] Beinert H, Sands RH. Studies on succinic and DPNH dehydrogenase preparations by paramagnetic resonance (EPR) spectroscopy. Biochem Biophys Res Commun 1960;3:41–6.
[3] Zheng L, Cash VL, Flint DH, Dean DR. Assembly of iron-sulfur clusters. Identification of an iscSUA-hscBA-fdx gene cluster from Azotobacter vinelandii. J Biol Chem 1998;273:13264–72.
[4] Leibold EA, Aziz N, Brown AJ, Munro HN. Conservation in rat liver of light and heavy subunit sequences of mammalian ferritin. Presence of unique octopeptide in the light subunit. J Biol Chem 1984;259:4327–34.
[5] Theil EC. Ferritin: at the crossroads of iron and oxygen metabolism. J Nutr 2003;133:1549S–53S.
[6] Kuhn LC, McClelland A, Ruddle FH. Gene transfer, expression, and molecular cloning of the human transferrin receptor gene. Cell 1984;37:95–103.
[7] Rouault TA, Hentze MW, Dancis A, Caughman W, Harford JB, Klausner RD. Influence of altered transcription on the translational control of human ferritin expression. Proc Natl Acad Sci USA 1987;84:6335–9.
[8] Zahringer J, Baliga BS, Munro HN. Relative abundance of specific messenger-RNA species in the free mRNP fraction of rat liver. FEBS Lett 1979;108:317–20.
[9] Hentze MW, Caughman SW, Rouault TA et al. Identification of the iron-responsive element for the translational regulation of human ferritin mRNA. Science 1987;238:1570–3.
[10] Rouault TA, Hentze MW, Caughman SW, Harford JB, Klausner RD. Binding of a cytosolic protein to the iron-responsive element of human ferritin messenger RNA. Science 1988;241:1207–10.
[11] Leibold EA, Munro HN. Cytoplasmic protein binds in vitro to a highly conserved sequence in the 5′ untranslated region of ferritin heavy- and light-subunit mRNAs. Proc Natl Acad Sci USA 1988;85:2171–5.
[12] Casey JL, Hentze MW, Koeller DM et al. Iron-responsive elements: regulatory RNA sequences that control mRNA levels and translation. Science 1988;240:924–8.
[13] Binder R, Horowitz JA, Basilion JP, Koeller DM, Klausner RD, Harford JB. Evidence that the pathway of transferrin receptor mRNA degradation involves an endonucleolytic cleavage within the 3′ UTR and does not involve poly(A) tail shortening. EMBO J 1994;13:1969–80.
[14] Rouault TA, Tang CK, Kaptain S et al. Cloning of the cDNA encoding an RNA regulatory protein – the human iron-responsive element-binding protein. Proc Natl Acad Sci USA 1990;87:7958–62.
[15] Yu Y, Radisky E, Leibold EA. The iron-responsive element binding protein. Purification, cloning, and regulation in rat liver. J Biol Chem 1992;267:19005–10.
[16] Patino MM, Walden WE. Cloning of a functional cDNA for the rabbit ferritin mRNA repressor protein. Demonstration of a tissue-specific pattern of expression. J Biol Chem 1992;267: 19011–6.
[17] Mullner EW, Rothenberger S, Muller AM, Kuhn LC. In vivo and in vitro modulation of the mRNA-binding activity of iron-regulatory factor. Tissue distribution and effects of cell proliferation, iron levels and redox state. Eur J Biochem 1992;208:597–605.
[18] Rouault TA, Stout CD, Kaptain S, Harford JB, Klausner RD. Structural relationship between an iron-regulated RNA-binding protein (IRE-BP) and aconitase: functional implications. Cell 1991;64:881–3.
[19] Eanes RZ, Kun E. Separation and characterization of aconitate hydratase isoenzymes from pig tissues. Biochim Biophys Acta 1971;227:204–10.
[20] Shows TB, Brown JA. Mapping AK1, ACONs, and AK3 to chromosome 9 in man employing and X/9 translocation and somatic cell hybrids. Cytogenet Cell Genet 1977;19:26–37.

[21] Kaptain S, Downey WE, Tang C et al. A regulated RNA binding protein also possesses aconitase activity. Proc Natl Acad Sci USA 1991;88:10109–13.
[22] Haile DJ, Rouault TA, Harford JB et al. Cellular regulation of the iron-responsive element binding protein: disassembly of the cubane iron-sulfur cluster results in high-affinity RNA binding. Proc Natl Acad Sci USA 1992;89:11735–9.
[23] Beinert H, Kennedy MC. Aconitase, a two-faced protein: enzyme and iron regulatory factor. FASEB J 1993;7:1442–9.
[24] Kennedy MC, Mende-Mueller L, Blondin GA, Beinert H. Purification and characterization of cytosolic aconitase from beef liver and its relationship to the iron-responsive element binding protein. Proc Natl Acad Sci USA 1992;89:11730–4.
[25] Weiss G, Goossen B, Doppler W et al. Translational regulation via iron-responsive elements by the nitric oxide/NO-synthase pathway. EMBO J 1993;12:3651–7.
[26] Drapier JC, Hirling H, Wietzerbin J, Kaldy P, Kuhn LC. Reciprocal modulation of aconitase activity and RNA-binding activity of iron regulatory factor by nitric oxide. Adv Exp Med Biol 1994;356:141–8.
[27] Tang CK, Chin J, Harford JB, Klausner RD, Rouault TA. Iron regulates the activity of the iron-responsive element binding protein without changing its rate of synthesis or degradation. J Biol Chem 1992;267:24466–70.
[28] Robbins AH, Stout CD. Structure of activated aconitase: formation of the [4Fe-4S] cluster in the crystal. Proc Natl Acad Sci USA 1989;86:3639–43.
[29] Philpott CC, Haile D, Rouault TA, Klausner RD. Modification of a free Fe-S cluster cysteine residue in the active iron-responsive element-binding protein prevents RNA binding. J Biol Chem 1993;268:17655–8.
[30] Philpott CC, Klausner RD, Rouault TA. The bifunctional iron-responsive element binding protein/cytosolic aconitase: the role of active-site residues in ligand binding and regulation. Proc Natl Acad Sci USA 1994;91:7321–5.
[31] Basilion JP, Rouault TA, Massinople CM, Klausner RD, Burgess WH. The iron-responsive element-binding protein: localization of the RNA-binding site to the aconitase active-site cleft. Proc Natl Acad Sci USA 1994;91:574–8.
[32] Hirling H, Henderson BR, Kuhn LC. Mutational analysis of the [4Fe-4S]-cluster converting iron regulatory factor from its RNA-binding form to cytoplasmic aconitase. EMBO J 1994;13:453–61.
[33] Dupuy J, Volbeda A, Carpentier P, Darnault C, Moulis JM, Fontecilla-Camps JC. Crystal structure of human iron regulatory protein 1 as cytosolic aconitase. Structure 2006;14:129–39.
[34] Walden WE, Selezneva AI, Dupuy J et al. Structure of dual function iron regulatory protein 1 complexed with ferritin IRE-RNA. Science 2006;314:1903–8.
[35] Rouault TA. The role of iron regulatory proteins in mammalian iron homeostasis and disease. Nat Chem Biol 2006;2:406–14.
[36] Addess KJ, Basilion JP, Klausner RD, Rouault TA, Pardi A. Structure and dynamics of the iron responsive element RNA: implications for binding of the RNA by iron regulatory binding proteins. J Mol Biol 1997;274(1):72–83.
[37] Rouault TA. Biochemistry. If the RNA fits, use it. Science 2006;314:1886–7.
[38] Eisenstein RS. Iron regulatory proteins and the molecular control of mammalian iron metabolism. Annu Rev Nutr 2000;20:627–62.
[39] Venkateswara Rao P, Holm RH. Synthetic analogues of the active sites of iron-sulfur proteins. Chem Rev 2004;104:527–59.
[40] Zheng L, White RH, Cash VL, Jack RF, Dean DR. Cysteine desulfurase activity indicates a role for NIFS in metallocluster biosynthesis. Proc Natl Acad Sci USA 1993;90:2754–8.
[41] Samaniego F, Chin J, Iwai K, Rouault TA, Klausner RD. Molecular characterization of a second iron-responsive element binding protein, iron regulatory protein 2. Structure, function, and post-translational regulation. J Biol Chem 1994;269:30904–10.

[42] Guo B, Yu Y, Leibold EA. Iron regulates cytoplasmic levels of a novel iron-responsive element-binding protein without aconitase activity. J Biol Chem 1994;269:24252–60.
[43] Kim HY, Klausner RD, Rouault TA. Translational repressor activity is equivalent and is quantitatively predicted by in vitro RNA binding for two iron-responsive element-binding proteins, IRP1 and IRP2. J Biol Chem 1995;270:4983–6.
[44] Guo B, Phillips JD, Yu Y, Leibold EA. Iron regulates the intracellular degradation of iron regulatory protein 2 by the proteasome. J Biol Chem 1995;270:21645–51.
[45] Iwai K, Klausner RD, Rouault TA. Requirements for iron-regulated degradation of the RNA binding protein, iron regulatory protein 2. EMBO J 1995;14:5350–7.
[46] Salahudeen AA, Thompson JW, Ruiz JC et al. An E3 ligase possessing an iron responsive hemerythrin domain is a regulator of iron homeostasis. Science 2009;326:722–6.
[47] Vashisht AA, Zumbrennen KB, Huang X et al. Control of iron homeostasis by an iron-regulated ubiquitin ligase. Science 2009;326:718–21.
[48] Zhang Z. Evolution by gene duplication: an update. Trends Ecol Evol 2003;18:292–8.
[49] Rouault TA. Cell biology. An ancient gauge for iron. Science 2009;326:676–7.
[50] Meyron-Holtz EG, Ghosh MC, Iwai K et al. Genetic ablations of iron regulatory proteins 1 and 2 reveal why iron regulatory protein 2 dominates iron homeostasis. EMBO J 2004;23:386–95.
[51] Meyron-Holtz EG, Ghosh MC, Rouault TA. Mammalian tissue oxygen levels modulate iron-regulatory protein activities in vivo. Science 2004;306:2087–90.
[52] LaVaute T, Smith S, Cooperman S, et al. Targeted deletion of the gene encoding iron regulatory protein-2 causes misregulation of iron metabolism and neurodegenerative disease in mice. Nat Genet 2001;27:209–14.
[53] Galy B, Holter SM, Klopstock T et al. Iron homeostasis in the brain: complete iron regulatory protein 2 deficiency without symptomatic neurodegeneration in the mouse. Nat Genet 2006;38:967–9; discussion 969.
[54] Jeong SY, Crooks DR, Wilson-Ollivierre H et al. Iron insufficiency compromises motor neurons and their mitochondrial function in Irp2-null mice. PLoS One 2011;6:e25404.
[55] Cooperman SS, Meyron-Holtz EG, Olivierre-Wilson H, Ghosh MC, McConnell JP, Rouault TA. Microcytic anemia, erythropoietic protoporphyria, and neurodegeneration in mice with targeted deletion of iron-regulatory protein 2. Blood 2005;106:1084–91.
[56] Galy B, Ferring D, Minana B, et al. Altered body iron distribution and microcytosis in mice deficient in iron regulatory protein 2 (IRP2). Blood 2005;106:2580–2589.
[57] Ghosh MC, Zhang DL, Jeong SY et al. Deletion of iron regulatory protein 1 causes polycythemia and pulmonary hypertension in mice through translational derepression of HIF2alpha. Cell Metab 2013;17:271–81.
[58] Anderson SA, Nizzi CP, Chang YI et al. The IRP1-HIF-2alpha axis coordinates iron and oxygen sensing with erythropoiesis and iron absorption. Cell Metab 2013;17:282–290.
[59] Wilkinson N, Pantopoulos K. IRP1 regulates erythropoiesis and systemic iron homeostasis by controlling HIF2alpha mRNA translation. Blood 2013;122:1658–1668.
[60] Smith SR, Ghosh MC, Ollivierre-Wilson H, Hang Tong W, Rouault TA. Complete loss of iron regulatory proteins 1 and 2 prevents viability of murine zygotes beyond the blastocyst stage of embryonic development. Blood Cells Mol Dis 2006;36:283–287.
[61] Cox TC, Bawden MJ, Martin A, May BK. Human erythroid 5-aminolevulinate synthase: promoter analysis and identification of an iron-responsive element in the mRNA. EMBO J 1991;10:1891–902.
[62] Gray NK, Hentze MW. Iron regulatory protein prevents binding of the 43S translation pre-initiation complex to ferritin and eALAS mRNAs. EMBO J 1994;13:3882–91.
[63] Kim HY, LaVaute T, Iwai K, Klausner RD, Rouault TA. Identification of a conserved and functional iron-responsive element in the 5′-untranslated region of mammalian mitochondrial aconitase. J Biol Chem 1996;271:24226–30.

[64] Schalinske KL, Chen OS, Eisenstein RS. Iron differentially stimulates translation of mitochondrial aconitase and ferritin mRNAs in mammalian cells. Implications for iron regulatory proteins as regulators of mitochondrial citrate utilization. J Biol Chem 1998;273:3740–6.
[65] Abboud S, Haile DJ. A novel mammalian iron-regulated protein involved in intracellular iron metabolism. J Biol Chem 2000;275:19906–12.
[66] McKie AT, Marciani P, Rolfs A et al. A novel duodenal iron-regulated transporter, IREG1, implicated in the basolateral transfer of iron to the circulation. Mol Cell 2000;5:299–309.
[67] Donovan A, Brownlie A, Zhou Y et al. Positional cloning of zebrafish ferroportin 1 identifies a conserved vertebrate iron exporter. Nature 2000;403:776–81.
[68] Sanchez M, Galy B, Muckenthaler MU, Hentze MW. Iron-regulatory proteins limit hypoxia-inducible factor-2alpha expression in iron deficiency. Nat Struct Mol Biol 2007;14:420–6.
[69] Zhang DL, Hughes RM, Ollivierre-Wilson H, Ghosh MC, Rouault TA. A ferroportin transcript that lacks an iron-responsive element enables duodenal and erythroid precursor cells to evade translational repression. Cell Metab 2009;9:461–73.
[70] Zhang DL, Senecal T, Ghosh MC, Ollivierre-Wilson H, Tu T, Rouault TA. Hepcidin regulates ferroportin expression and intracellular iron homeostasis of erythroblasts. Blood 2011;118:2868–77.
[71] Campillos M, Cases I, Hentze MW, Sanchez M. SIREs: searching for iron-responsive elements. Nucleic Acids Res 2010;38, W360–7.
[72] Hentze MW, Muckenthaler MU, Galy B, Camaschella C. Two to tango: regulation of Mammalian iron metabolism. Cell 2010;142:24–38.
[73] Sanchez M, Galy B, Schwanhaeusser B et al. Iron regulatory protein-1 and -2: transcriptome-wide definition of binding mRNAs and shaping of the cellular proteome by iron regulatory proteins. Blood 2011;118:e168–79.
[74] Wilkinson N, Pantopoulos K. The IRP/IRE system in vivo: insights from mouse models. Front Pharmacol 2014;5:176.
[75] Ghosh MC, Zhang DL, Rouault TA. Iron misregulation and neurodegenerative disease in mouse models that lack iron regulatory proteins. Neurobiol Dis 2015;81:66–75.
[76] Kühn LC. Iron regulatory proteins and their role in controlling iron metabolism. Metallomics 2015;7:232–43.
[77] Adams MD, Soares MB, Kerlavage AR, Fields C, Venter JC. Rapid cDNA sequencing (expressed sequence tags) from a directionally cloned human infant brain cDNA library. Nat Genet 1993;4:373–80.
[78] Land T, Rouault TA. Targeting of a human iron-sulfur cluster assembly enzyme, nifs, to different subcellular compartments is regulated through alternative AUG utilization. Mol Cell 1998;2:807–15.
[79] Tong WH, Rouault T. Distinct iron-sulfur cluster assembly complexes exist in the cytosol and mitochondria of human cells. EMBO J 2000;19:5692–700.
[80] Tong WH, Jameson GN, Huynh BH, Rouault TA. Subcellular compartmentalization of human Nfu, an iron-sulfur cluster scaffold protein, and its ability to assemble a [4Fe-4S] cluster. Proc Natl Acad Sci USA 2003;100:9762–7.
[81] Tong WH, Rouault TA. Functions of mitochondrial ISCU and cytosolic ISCU in mammalian iron-sulfur cluster biogenesis and iron homeostasis. Cell Metab 2006;3:199–210.
[82] Lill R, Muhlenhoff U. Maturation of iron-sulfur proteins in eukaryotes: mechanisms, connected processes, and diseases. Annu Rev Biochem 2008;77:669–700.
[83] Nakai Y, Nakai M, Hayashi H, Kagamiyama H. Nuclear localization of yeast Nfs1p is required for cell survival. J Biol Chem 2001;276:8314–20.
[84] Nakai Y, Nakai M, Lill R, Suzuki T, Hayashi H. Thio modification of yeast cytosolic tRNA is an iron-sulfur protein-dependent pathway. Mol Cell Biol 2007;27:2841–7.

[85] Shi Y, Ghosh MC, Tong WH, Rouault TA. Human ISD11 is essential for both iron-sulfur cluster assembly and maintenance of normal cellular iron homeostasis. Hum Mol Genet 2009;18:3014–25.
[86] Uhrigshardt H, Singh A, Kovtunovych G, Ghosh M, Rouault TA. Characterization of the human HSC20, an unusual DnaJ type III protein, involved in iron-sulfur cluster biogenesis. Hum Mol Genet 2010;19:3816–34.
[87] Rouault TA. Mammalian iron-sulphur proteins: novel insights into biogenesis and function. Nat Rev Mol Cell Biol 2015;16:45–55.
[88] Stehling O, Vashisht AA, Mascarenhas J et al. MMS19 assembles iron-sulfur proteins required for DNA metabolism and genomic integrity. Science 2012;337:195–9.
[89] Gari K, Leon Ortiz AM, Borel V, Flynn H, Skehel JM, Boulton SJ. MMS19 links cytoplasmic iron-sulfur cluster assembly to DNA metabolism. Science 2012;337:243–5.
[90] Stehling O, Mascarenhas J, Vashisht AA et al. Human CIA2A-FAM96A and CIA2B-FAM96B integrate iron homeostasis and maturation of different subsets of cytosolic-nuclear iron-sulfur proteins. Cell Metab 2013;18:187–98.
[91] Shi R, Proteau A, Villarroya M et al. Structural basis for Fe-S cluster assembly and tRNA thiolation mediated by IscS protein-protein interactions. PLoS Biol 2010;8:e1000354.
[92] Marinoni EN, de Oliveira JS, Nicolet Y et al. (IscS-IscU)2 complex structures provide insights into Fe2S2 biogenesis and transfer. Angew Chem Int Ed Engl 2012;51:5439–42.
[93] Schmucker S, Martelli A, Colin F et al. Mammalian frataxin: an essential function for cellular viability through an interaction with a preformed ISCU/NFS1/ISD11 iron-sulfur assembly complex. PLoS One 2011;6:e16199.
[94] Bridwell-Rabb J, Winn AM, Barondeau DP. Structure-function analysis of Friedreich's ataxia mutants reveals determinants for frataxin binding and activation of the Fe-S assembly complex. Biochemistry 2011;5:155–64.
[95] Campuzano V, Montermini L, Molto MD et al. Friedreich's ataxia: autosomal recessive disease caused by an intronic GAA triplet repeat expansion. Science 1996;271:1423–7.
[96] Babcock M, de Silva D, Oaks R et al. Regulation of mitochondrial iron accumulation by Yfh1p, a putative homolog of frataxin. Science 1997;276:1709–12.
[97] Vaubel RA, Isaya G. Iron-sulfur cluster synthesis, iron homeostasis and oxidative stress in Friedreich ataxia. Mol Cell Neurosci 2013;55:50–61.
[98] Cook JD, Kondapalli KC, Rawat S et al. Molecular details of the yeast frataxin-Isu1 interaction during mitochondrial Fe-S cluster assembly. Biochemistry 2010;49:8756–65.
[99] Tsai CL, Barondeau DP. Human frataxin is an allosteric switch that activates the Fe-S cluster biosynthetic complex. Biochemistry 2010;49:9132–9.
[100] Colin F, Martelli A, Clemancey M et al. Mammalian frataxin controls sulfur production and iron entry during de novo Fe4S4 cluster assembly. J Am Chem Soc 2013;135:733–40.
[101] Vickery LE, Cupp-Vickery JR. Molecular chaperones HscA/Ssq1 and HscB/Jac1 and their roles in iron-sulfur protein maturation. Crit Rev Biochem Mol Biol 2007;42:95–111.
[102] Kampinga HH, Craig EA. The HSP70 chaperone machinery: J proteins as drivers of functional specificity. Nat Rev Mol Cell Biol 2010;11:579–92.
[103] Dutkiewicz R, Schilke B, Cheng S, Knieszner H, Craig EA, Marszalek J. Sequence-specific interaction between mitochondrial Fe-S scaffold protein Isu and Hsp70 Ssq1 is essential for their in vivo function. J Biol Chem 2004;279:29167–74.
[104] Maio N, Rouault TA. Iron-sulfur cluster biogenesis in mammalian cells: new insights into the molecular mechanisms of cluster delivery. Biochim Biophys Acta 2015;1853:1493–512.
[105] Maio N, Ghezzi D, Verrigni D, et al. Disease-causing SDHAF1 mutations impair transfer of Fe-S clusters to SDHB. Cell Metab 2016;23:292–302.
[106] Maio N, Rouault TA. Mammalian Fe-S proteins: definition of a consensus motif recognized by the co-chaperone HSC20. Metallomics 2016;8:1032–46.

[107] Shakamuri P, Zhang B, Johnson MK. Monothiol glutaredoxins function in storing and transporting [Fe2S2] clusters assembled on IscU scaffold proteins. J Am Chem Soc 2012;134:15213–6.
[108] Ye H, Jeong SY, Ghosh MC, et al. Glutaredoxin 5 deficiency causes sideroblastic anemia by specifically impairing heme biosynthesis and depleting cytosolic iron in human erythroblasts. J Clin Invest 2010;120:1749–61.
[109] Lim SC, Friemel M, Marum JE, et al. Mutations in LYRM4, encoding iron-sulfur cluster biogenesis factor ISD11, cause deficiency of multiple respiratory chain complexes. Hum Mol Genet 2013;22:4460–73.
[110] Mochel F, Knight MA, Tong WH et al. Splice mutation in the iron-sulfur cluster scaffold protein ISCU causes myopathy with exercise intolerance. Am J Hum Genet 2008;82:652–60.
[111] Olsson A, Lind L, Thornell LE, Holmberg M. Myopathy with lactic acidosis is linked to chromosome 12q23.3-24.11 and caused by an intron mutation in the ISCU gene resulting in a splicing defect. Hum Mol Genet 2008;17:1666–72.
[112] Kollberg G, Tulinius M, Melberg A et al. Clinical manifestation and a new ISCU mutation in iron-sulphur cluster deficiency myopathy. Brain 2009;132:2170–9.
[113] Perdomini M, Hick A, Puccio H, Pook MA. Animal and cellular models of Friedreich ataxia. J Neurochem 2013;126 Suppl 1:65–79.
[114] Cameron JM, Janer A, Levandovskiy V, et al. Mutations in iron-sulfur cluster scaffold genes nfu1 and bola3 cause a fatal deficiency of multiple respiratory chain and 2-oxoacid dehydrogenase enzymes. Am J Hum Genet 2011;89:486–95.
[115] Navarro-Sastre A, Tort F, Stehling O, et al. A fatal mitochondrial disease is associated with defective NFU1 function in the maturation of a subset of mitochondrial Fe-S proteins. Am J Hum Genet 2011;89:656–67.
[116] Pastore A, Puccio H. Frataxin: a protein in search for a function. J Neurochem 2013;126 Suppl 1:43–52.
[117] Rouault TA. Biogenesis of iron-sulfur clusters in mammalian cells: new insights and relevance to human disease. Dis Model Mech 2012;5:155–64.
[118] Ajit Bolar N, Vanlander AV, Wilbrecht C, et al. Mutation of the iron-sulfur cluster assembly gene IBA57 causes severe myopathy and encephalopathy. Hum Mol Genet 2013;22:2590–602.
[119] Ye H, Rouault TA. Human iron-sulfur cluster assembly, cellular iron homeostasis, and disease. Biochemistry 2010;49:4945–56.
[120] Li J, Kogan M, Knight SA, Pain D, Dancis A. Yeast mitochondrial protein, Nfs1p, coordinately regulates iron-sulfur cluster proteins, cellular iron uptake, and iron distribution. J Biol Chem 1999;274:33025–34.
[121] Li K, Besse EK, Ha D, Kovtunovych G, Rouault TA. Iron-dependent regulation of frataxin expression: implications for treatment of Friedreich ataxia. Hum Mol Genet 2008;17:2265–73.
[122] Kiley PJ, Beinert H. The role of Fe-S proteins in sensing and regulation in bacteria. Curr Opin Microbiol 2003;6:181–5.
[123] Allikmets R, Raskind WH, Hutchinson A, Schueck ND, Dean M, Koeller DM. Mutation of a putative mitochondrial iron transporter gene (ABC7) in X-linked sideroblastic anemia and ataxia (XLSA/A). Hum Mol Genet 1999;8:743–9.
[124] Chan SY, Zhang YY, Hemann C, Mahoney CE, Zweier JL, Loscalzo J. MicroRNA-210 controls mitochondrial metabolism during hypoxia by repressing the iron-sulfur cluster assembly proteins ISCU1/2. Cell Metab 2009;10:273–84.

9 Delivery of iron-sulfur clusters to recipient proteins: the role of chaperone and cochaperone proteins

Nunziata Maio and Tracey A. Rouault

9.1 Introduction

The general pathway of iron-sulfur (Fe-S) cluster biogenesis has been uncovered over the years by a combination of genetic and biochemical studies, and the components of the assembly machinery were found to be broadly distributed in all kingdoms of life and to share common features, such as the use of a cysteine desulfurase to provide inorganic sulfur, the central role of scaffold proteins for Fe-S cluster assembly, and a highly conserved transfer system, which consists of an heat shock 70 kDa protein (HSP70) chaperone and a J-protein cochaperone, that interacts with scaffold proteins to facilitate Fe-S cluster delivery to recipient proteins. In this chapter, we discuss the role of the chaperone/cochaperone system in Fe-S cluster biogenesis in mammalian cells and discuss advances in understanding how the transfer complex efficiently engages recipient Fe-S target proteins to deliver a cluster.

9.2 A specialized chaperone-cochaperone system ensures efficient Fe-S cluster delivery

HSP70s are ubiquitous molecular chaperones that function in all major cellular compartments, participating in diverse cellular processes, including protein folding, degradation, translocation across membranes, and oligomeric assembly [1, 2]. All these activities depend on the ability of HSP70s to bind reversibly to short, unfolded segments of polypeptide chains. Most HSP70s are able to interact with a broad range of protein substrates, and recognition of these clients is determined by the intrinsic specificity of their binding partners, the HSP40 (heat shock 40 kDa proteins) molecular chaperones, also known as cochaperones [3]. Cochaperones or J-proteins invariably contain the so-called J-domain, which was named after the initially characterized DnaJ protein of *Escherichia coli*. The J-domain consists of a conserved ~70-amino-acid signature region, which contains a histidine, proline, and aspartic acid tripeptide (HPD) in a loop between the two main helices (II and III) that stimulates the ATPase activity of HSP70 chaperones [3]. In fact, despite their remarkable functional diversity, HSP70s have high sequence identity and common fundamental structural features [4, 5]. All HSP70s possess a highly conserved N-terminal nucleotide binding domain (NBD), which displays weak ATPase activity, and a C-terminal domain, which

DOI 10.1515/9783110479850-009

forms the substrate binding domain (SBD), where client proteins bind (Fig. 9.1) [6]. Molecular chaperones engage in a transient interaction with client proteins, which is regulated by the ATP binding and hydrolysis activities of the NBD. A conformational change generated upon hydrolysis of ATP stabilizes HSP70's interaction with the substrate protein, while facilitating the multiple cellular processes in which HSP70s are involved. Exchange of ADP for ATP promotes client release and completes the binding cycle (Fig. 9.2). HSP70s require a J-protein and, almost always, a nucleotide exchange factor (NEF) as key components that regulate their binding to client proteins and control the interaction with nucleotides (ATP or ADP). J-proteins or cochaperones, in addition to assisting in substrate delivery, stimulate the HSP70 ATPase activity, thereby stabilizing formation of the HSP70-substrate complex and facilitating selective substrate trapping [6].

Most HSP70s display broad substrate specificity proportional to the variety of proteins that they have to recognize, and prokaryotes were initially thought to have a single HSP70, named DnaK, that served both stress-related and housekeeping

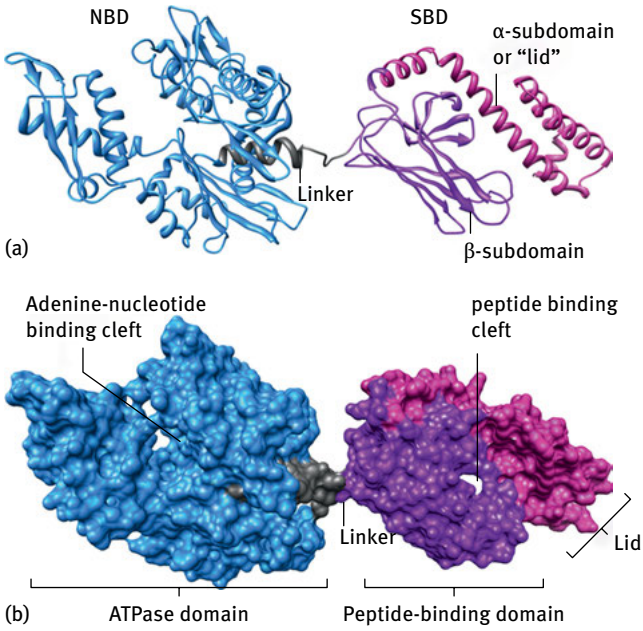

Fig. 9.1: Structure of a typical HSP70 chaperone, DnaK, the housekeeping HSP70 of *E. coli*, with ADP bound to the nucleotide-binding domain (protein data bank code: 2KHO). The ATPase domain of DnaK, which is also known as nucleotide-binding domain (NBD), and the peptide-binding domain, which is also known as substrate-binding domain (SBD), are connected by a short, flexible, hydrophobic linker. The NBD and the SBD dock when the chaperone is bound to ATP, which is the conformation that exhibits low affinity for the substrate, due to the shortening of the linker, which causes displacement of the lid (also known as α-subdomain) in the SBD and allows easy access and egress of the client protein from the cleft. (a) and (b) are the ribbon and surface representations, respectively, of DnaK of *E. coli* (created from PDB structures using the UCSF ChimeraX program).

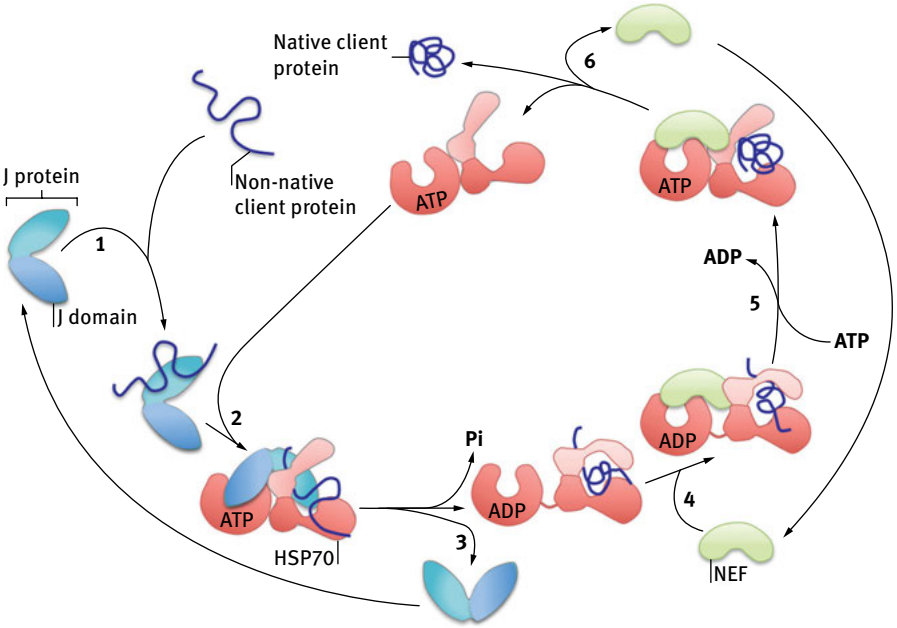

Fig. 9.2: ATPase cycle of the chaperone core machinery. (1) The J-protein, also known as cochaperone, binds to a subset of unfolded (non-native) substrate proteins (clients) and interacts with the HSP70 in the ATP-bound state through its J-domain (2). The client can then interact with the peptide-binding cleft, which is in the open conformation (2). ATP hydrolysis is simultaneously stimulated by both the J-domain of the cochaperone and the client and causes a conformational change in the HSP70 that closes the lid of the SBD over the cleft and stabilizes the interaction with the client. (3) The J-protein leaves the complex. A NEF, which exhibits high affinity for the ADP-bound state of the chaperone, binds to the HSP70-client complex (4) and exchanges ADP with ATP in the NBD (5). The client, which has folded into the native conformation driven by the energy provided by hydrolysis of ATP, is finally released (6).

functions [7]. However, in 1994, a gene encoding a novel HSP70 was identified in *E. coli* and designated *HscA* (*heat shock cognate A*) [8, 9]. The gene was located within the *isc* (Fe-S cluster) operon, immediately upstream of the *fdx* gene encoding a [Fe_2-S_2]-ferredoxin [10] and downstream of a gene, named *HscB*, encoding a novel J-protein [9]. The predicted HscA protein (also known as Hsc66, because it had a molecular weight of 66 KDa) exhibited 40% sequence identity to DnaK. Initial studies on the general biochemical properties of *E. coli* HscA and HscB revealed that the basal ATPase activity of HscA was stimulated fourfold to sixfold by HscB [11, 12], but not from DnaJ, the cochaperone for DnaK, indicating a lack of cross-talk between the two chaperone systems. Despite the evidence that HscA exhibited general chaperone activity *in vitro*, due to its ability to suppress protein aggregation [12], the endogenous physiological substrate for the HscA/HscB system remained unknown until completion of the genome sequencing of *E. coli* revealed that the chaperone/cochaperone system was encoded by a region of the genome, now known as *isc* operon,

that exhibited similarity to the *nif* operon involved in biogenesis of Fe-S clusters of nitrogenase (see the chapter by P.C. Dos Santos and D.R. Dean) [13, 14]. The *isc* genes were found to be essential for cell growth. Further investigations demonstrated a general housekeeping role of the *isc* components in the assembly and/or repair of Fe-S proteins [15, 16]. Inactivation of *HscA* or *HscB* reduced activities of Fe-S enzymes, such as glutamate synthase and succinate dehydrogenase (SDH), and significantly decreased the overall cell proliferation rates [17]. Parallel studies in the yeast *Saccharomyces cerevisiae* revealed the presence of *isc*- and *hsc*-like genes [18], suggesting a high degree of evolutionary conservation of the Fe-S biogenesis machinery. Experimental evidence that these genes encoded components of the Fe-S cluster assembly pathway came from the characterization of mutants that suppressed oxidative damage in yeast strains in which superoxide dismutase 1 was deleted [19]. Suppressor mutations were identified in two genes encoding a mitochondrial HSP70 and a J-type co-chaperone, respectively. The HSP70 protein was designated as Ssq1, and the cochaperone, which was predicted to be targeted to the mitochondrial compartment, was named Jac1 (J-type accessory chaperone). Both *Jac1* and *Ssq1* mutant strains exhibited impaired mitochondrial respiration and reduced activities of SDH and aconitase, a metabolic defect that had previously been reported for *Nfs1* mutants, which were unable to mobilize sulfur for the initial assembly of the cluster. Subsequent work by several groups confirmed that Ssq1 and Jac1 were essential for Fe-S cluster biogenesis in yeast [20–24].

The first experimental evidence for a specific molecular interaction of the chaperone/cochaperone system with a critical component of the Fe-S assembly pathway, the main scaffold protein IscU, came in 2000 from studies carried out by Hoff and colleagues on the effects of bacterial *isc* components on the ATPase activity of HscA [25]. IscU was found to stimulate HscA's ATPase activity approximately eightfold above the basal level. The cochaperone HscB synergistically activated HscA's activity up to 400-fold and enhanced IscU binding to the ATP-bound form of HscA [25]. Interestingly, IscU and/or HscB were unable to stimulate DnaK's ATPase activity, and DnaJ did not increase binding of IscU to HscA, suggesting that HscA formed a complex with HscB and that the main scaffold protein IscU might serve as a substrate for this chaperone complex. The substrate specificity of HscA and the selective nature of the interaction between HscA and IscU were studied in more detail by screening a library of peptides for their ability to bind HscA and, subsequently, by testing peptides that covered the entire IscU sequence [26, 27]. HscA was found to bind the residues between amino acids 99 and 103 of IscU, which contained the sequence Leu-Pro-Pro-Val-Lys. The LPPVK sequence is conserved among IscU proteins from bacteria to humans (Fig. 9.3), suggesting that the mechanism of chaperone recognition and binding has been conserved during evolution. Importantly, the cochaperone HscB was found to enhance the binding affinity of IscU to HscA [27], consistent with its role in targeting IscU to the HscA-ATP complex.

Studies of the yeast chaperone/cochaperone/scaffold complex (Ssq1/Jac1/Isu1) provided results similar to those of the bacterial HscA/HscB/IscU system [28] and offered additional insights into the mechanism of chaperone-scaffold interactions.

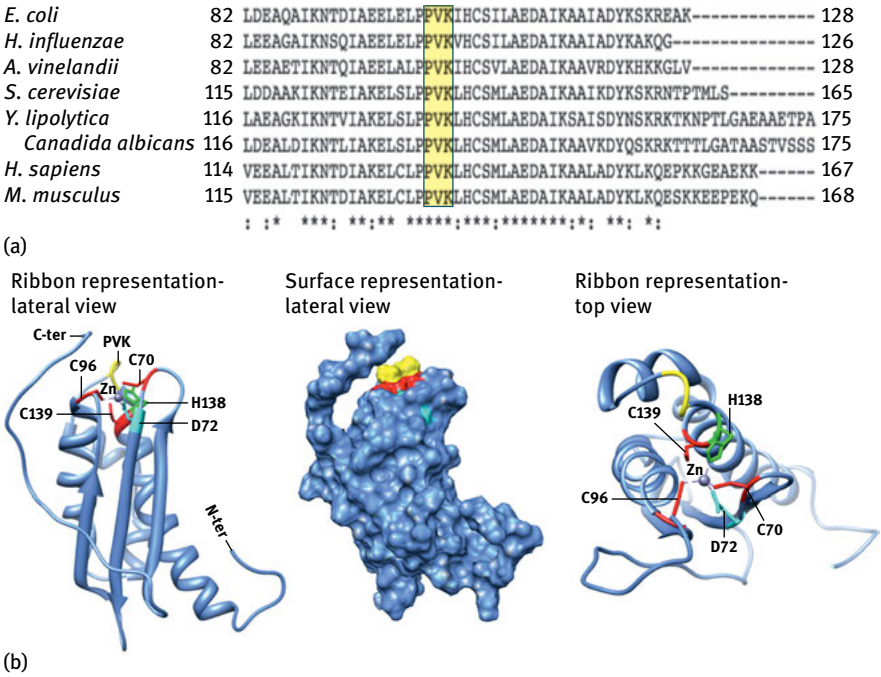

Fig. 9.3: ISCU scaffold proteins from bacteria to human contain a highly conserved PVK motif that is enclosed in the substrate-binding cleft of the HSP70 chaperone during the transfer step of Fe-S cluster biogenesis. In (a), the multiple sequence alignment of the main scaffold proteins ISCU from different organisms, ranging from bacteria, to yeast, to human, shows the highly conserved PVK tripeptide that is bound by chaperone proteins to facilitate Fe-S cluster transfer to recipients. In (b), the ribbon and surface representations of mammalian ISCU from *M. musculus* crystallized with zinc (PDB: 1WFZ) show in yellow the PVK motif, in red the cysteines, and in green the histidine that coordinate the cluster *in vivo*. In cyan, a crucial aspartate residue that is important for allowing labile coordination of the cluster on the main scaffold protein ISCU is highlighted. Substitution of this aspartate into alanine in multiple organisms causes stabilization of the cluster on ISCU and impairs its transfer to downstream recipients.

Ssq1 and Jac1 were found to act as partners in binding the scaffold protein Isu [28]. More importantly, Isu was targeted to Ssq1 in a Jac1-dependent manner, and both Jac1 and Isu were required for efficient stimulation of Ssq1 ATPase activity [28]. Interestingly, mitochondria of most eukaryotes, including the yeast *Schizosaccharomyces pombe*, contain a single multifunctional HSP70 [3, 29, 30], which is homologous to mitochondrial Ssc1 of *S. cerevisiae* [31], that performs the dual task of housekeeping molecular chaperone (participating in protein translocation across the inner mitochondrial membrane and protein folding) and of specialized HSP70 for Fe-S cluster biogenesis. Only a subset of fungi, including *S. cerevisiae* and *Candida albicans*, contains a highly specialized mitochondrial HSP70, named Ssq1, that arose through gene duplication about 300 million years ago [32] and that is unique in that it exhibits binding to a single protein substrate Isu1 [33].

9.3 Transfer of Fe-S clusters to recipient proteins: the ATPase cycle

Genetic and biochemical studies have clearly demonstrated that hydrolysis of ATP is essential for the chaperone activity of all the HSP70 proteins tested so far, and the rates of hydrolysis are very low under basal conditions [6]. ATP hydrolysis triggers the closing of the α-subdomain, also known as lid, in the SDB upon the substrate, which locks the substrate into position. In a thermodynamically coupled fashion, substrates activate the HSP70 ATPase activity by typically 2–10-fold, a low level of stimulation that is insufficient to drive the functional cycle of HSP70 chaperones. Instead, cochaperones are required for the productive coupling of ATP hydrolysis with substrate association [3, 34, 35]. On the basis of the data collected in bacteria and yeast, a model for the mode of action of the chaperone/cochaperone system in Fe-S cluster biogenesis has been proposed [34, 36, 37] (see Fig. 9.6 for a schematic of the main steps). Accordingly, the cochaperone (HscB in bacteria and Jac1 in yeast) starts the functional cycle of the cognate system by rapidly binding to and transiently associating with the main substrate, the scaffold protein IscU, and with a recipient Fe-S apo-protein. IscU rapidly binds to the HSP70 protein (HscA or Ssq1, in bacteria or yeast, respectively) in a two-step process, which involves the transient interaction of the J-domain of the cochaperone with the NBD of the ATP-bound chaperone and the interaction of IscU with the SBD. The chaperone in the ATP-bound state is in an open conformation, exhibiting the substrate-binding cavity to the interaction with IscU. Through a short interdomain communication between the SBD and the NBD in the chaperone, the simultaneous association of the substrate and the interaction of the NBD with the J-domain of the cochaperone lowers the activation energy for the hydrolysis of ATP by the chaperone. Hydrolysis of ATP and the coupled conformational change in the SBD of HSP70 leads to a tighter interaction with the scaffold protein and represents the rate-limiting step in the overall cycle, which is usually more than 10^3-fold slower than release of the products ADP and phosphate [5]. Nevertheless, under physiological conditions, nucleotide dissociation is a crucial step for substrate release. Therefore, exchange of ADP with ATP, which requires the opening of the nucleotide binding cleft, is a limiting gait in the cycle, and it is accordingly highly regulated and subject to strong evolutionary variation. For HscA, the dissociation rates for ADP ± Pi are 700-fold higher than those of the housekeeping chaperone DnaK [38]. Therefore, in contrast to other HSP70 proteins, which are regulated at both ATP hydrolysis and ADP/ATP exchange rate, the HscA reaction cycle is regulated primarily at the hydrolysis step. Accordingly, HscA does not associate with NEFs to complete its cycle [39]. In contradistinction, Ssq1 of *S. cerevisiae* has a higher nucleotide binding affinity than HscA and a slower ADP/ATP exchange rate [28]. Therefore, Ssq1 must interact with the NEF Mge1 to maintain high steady state rates of ATP hydrolysis [28]. The structural basis for these strong kinetic differences in nucleotide dissociation between HSP70 homologs has been proposed to depend on the length of an exposed loop close to the NBD and in the character of the amino acid residues that line the interface of the interaction of the SBD with the client protein [5, 38]. HscA, which exhibits the fastest turnover rate, has the shortest loop and lacks a hydrophobic patch

(which consists of Leu257-Val59 in DnaK) and two putative salt bridges (Glu264-Arg56 and Glu267-Lys55 in DnaK) at the interface of the NBD [5]. The physiological significance of the differences in maximal ATPase activity rates between HscA and Ssq1 determined *in vitro* with respect to the role of the chaperones in Fe-S cluster biogenesis *in vivo* is not known.

The mechanism by which energy release by the chaperone system is coupled to Fe-S cluster transfer to recipient proteins remains undefined. A full understanding of the transfer step requires detailed structural information of the components of the transfer machinery. Moreover, structures of different conformational states of the Fe-S transfer complex (chaperone/cochaperone/scaffold protein) will be necessary to reveal the effects that the chaperone/cochaperone system has on the scaffold protein and its Fe-S cluster and how the process of Fe-S cluster transfer is regulated. The crystal structure of a region of the SBD of *E. coli* HscA (amino acid residues 390–543) bound to an IscU peptide (^{98}ELPPVKIHC^{106}) was determined to a resolution of 1.95 Å (Fig. 9.4) [40]. The IscU peptide extends into a hydrophobic cleft within the

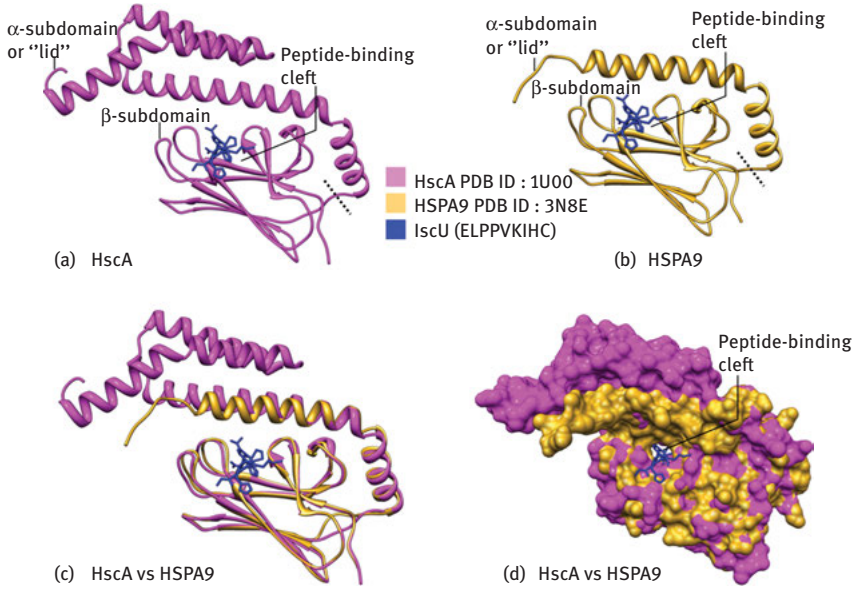

Fig. 9.4: Comparison of the crystal structures of the substrate-binding domains of HscA and HSPA9 in complex with the ELPPVKIHC peptide of IscU. (a) Structure of *E. coli* HscA (SBD)-ELPPVKIHC peptide complex (PDB ID: 1U00). The α-subdomain or "lid," which comprises residues 390–498 of HscA, and the β-subdomain (residues 506–609) constitute the NBD; the dotted line delineates the separation between the two subdomains. The IscU peptide is shown in blue. (b) Structure of the SDB of HSPA9 (PDB ID: 3N8E). The ELPPVKIHC peptide of IscU was docked to the peptide-binding cleft of the human chaperone. (c) Comparison of the crystal structures of the substrate-binding domains of HscA and HSPA9. The α- and β-subdomains of the SBDs of HscA and HSPA9 were aligned, and the ribbon diagrams of the two structures were superimposed. Color coding: HscA in magenta, HSPA9 in golden. (d) Superimposition of the surface diagrams of the SBDs of HscA and HSPA9 in complex with the ELPPVKIHC peptide of IscU (created from PDB structures using the UCSF ChimeraX program).

β-subdomain (Fig. 9.4), and a combination of nonpolar and hydrogen-bonding interactions appears to contribute to the binding affinity. The α-subdomain lies immediately above the binding cleft without making direct contacts with the peptide (Fig. 9.4). The central proline residue of the IscU peptide is completely buried within a hydrophobic pocket in the middle of the cleft. The tight interaction of this proline with the residues lining the substrate-binding cleft explains the crucial requirement of the highly conserved PVK motif in all ISCU scaffold proteins for binding to the chaperone [27, 41]. The peptide in the HscA(SBD)-ELPPVIHC complex appears to be trapped in place by the lid-like structure of the α-subdomain of HscA (Fig. 9.4). Transfer of Fe-S clusters from holo-ISCU to recipient proteins depends on conformational changes in both the scaffold and the recipient protein. Recent studies using solution NMR spectroscopy have provided insights into the mechanism of nucleotide-dependent interactions between the chaperone/cochaperone system and the scaffold protein IscU [42, 43]. IscU was found to interconvert between two alternative conformations, a more structured state (named S-conformation) that resembled the holo-protein IscU-[Fe_2-S_2] and bound preferentially the cochaperone HscB and a dynamically disordered form, which did not bind any metal and exhibited high affinity for HscA [42, 43]. Based on studies carried out by using purified components of the bacterial Fe-S transfer complex (HscA, HscB, and IscU) [44], a model has been proposed to describe the molecular mechanism by which modulation of the ATPase activity of the chaperone by the cochaperone is coupled to Fe-S cluster transfer from the scaffold protein IscU to recipient Fe-S apo-proteins. The cochaperone HscB binds to and delivers [Fe_2-S_2]-IscU (IscU in the S-conformation) to the SBD of HscA; together, IscU and HscB synergistically enhance HscA's ATPase activity nearly 1000-fold [25, 39]. The substrate-binding domain of HscA undergoes conformational change upon hydrolysis of ATP and encloses the PVK peptide of IscU, which is in close proximity to the cluster. The resulting conformational change may promote release of the [Fe_2-S_2] cluster from holo-IscU and transfer to the recipient protein [43–45].

9.4 The mammalian Fe-S transfer system

Advances in our understanding of mammalian Fe-S protein biogenesis have resulted from the biochemical characterization of the multimolecular complexes devoted to initial Fe-S cluster assembly in bacteria [46–49] and their counterparts in mammalian cells [50–52]. Likewise, transfer of a newly assembled cluster downstream of the main (or possibly sole) scaffold protein ISCU in mammalian cells relies on the activity of a chaperone/cochaperone system analogous to the bacterial and yeast complexes, which we have previously described [39, 53]. Mammalian cells lack an HSP70 chaperone specifically dedicated to Fe-S cluster biogenesis but rather, like most eukaryotes, employ a multifunctional mitochondrial HSP70, recently identified as HSPA9 in mammalian cells (also known as mortalin/PBP74/GRP75) [54, 55]. HSPA9 has been implicated in

several different processes, including the facilitation of protein import within mitochondria, together with the cochaperone DNAJC19 and the NEF BAP (also known as SIL1) [57], intracellular trafficking, stress response, hematopoiesis, control of cell proliferation, and tumor progression (reviewed in [58–61]). The absence of a chaperone that is solely dedicated to Fe-S cluster biogenesis in higher eukaryotes appears to warrant even greater participation of a specialized cochaperone to specify the function of the cognate HSP70. On the basis of its high sequence similarity to the bacterial and yeast cochaperones dedicated to Fe-S cluster biogenesis, the human DnaJ type III protein, HSC20, also referred to as DNAJC20 or HSCB, was predicted to be involved in the transfer of Fe-S clusters downstream of ISCU [62]. Further characterization of the human cochaperone established its role as an integral component of the Fe-S cluster transfer machinery [63]. HSC20 shares 34% and 29% overall identity with the bacterial and fungal orthologs, respectively [62, 63]. The high degree of sequence homology translates into a remarkable structural conservation of the J- and C-terminal domains of bacterial and human cochaperones dedicated to Fe-S cluster biogenesis [64] (Fig. 9.5). The crystal structures of HscB from *E. coli* [65], of Jac1 from *S. cerevisiae* [37], and of human HSC20 [64] revealed the presence of a conserved structural core that consists of two domains arranged in a L-shaped fold (Fig. 9.5). The N-terminal J-domain, which contains an invariant histidine, proline, aspartate (HPD) motif, is responsible for stimulating the ATPase activity of its HSP70 cognate chaperone [24, 55, 65, 66], whereas the C-terminus forms a three-helix bundle and is directly involved in binding the scaffold protein ISCU, with three highly conserved noncontiguous hydrophobic residues being of crucial importance for the HSC20-ISCU interaction [37, 55, 67]. The N-terminus of the human cochaperone shows distinctive features compared to the specialized DnaJ type III proteins of bacteria and fungi, in that it contains, downstream of the mitochondrial targeting sequence (residues 1–26 [54]), an additional domain, which harbors two CxxC modules (C41/C44 and C58/C61) that were found to coordinate a zinc ion *in vitro* [64] (Fig. 9.5). The physiological relevance of the unique N-terminal domain of HSC20 remains to be elucidated, though it may facilitate dimerization of the cochaperone. The C-terminal domains of cochaperones can selectively bind target substrates [68, 69], facilitate refolding of denatured proteins, and enhance cell viability [70, 71].

As previously discussed, cochaperones serve a dual function in Fe-S cluster biogenesis: they guide ISCU to the SBD of the HSP70 cognate chaperone, and they also activate the ATPase activity of the chaperone, thereby driving a conformational change that likely facilitates cluster release from ISCU and delivery to the final acceptor apoprotein or to intermediate carriers, which ultimately donate their clusters to specific recipients [39, 45] (Fig. 9.6). Recently, the mechanism by which recipient Fe-S proteins are selected by the transfer machinery from amongst the full complement of human proteins has been partially characterized [55]. Interestingly, clinical and biochemical investigations of several newly described human diseases caused by mutations in *NFU1*, *BOLA3*, *IBA57*, or *ISCA2* suggest that transfer of Fe-S clusters to secondary carriers that function downstream of the holo-ISCU/chaperone/cochaperone generates

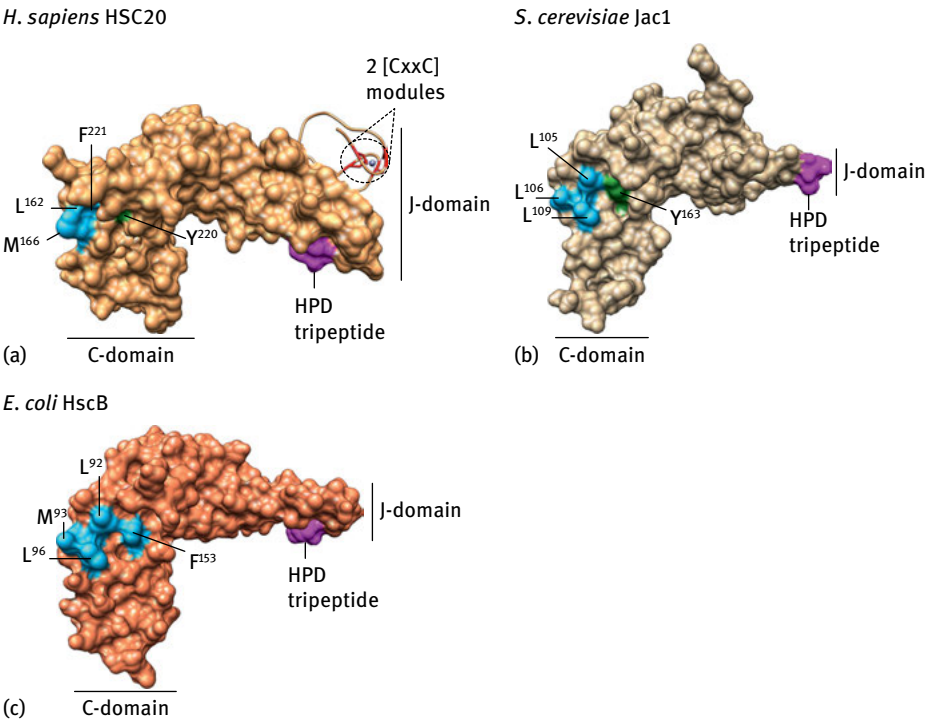

Fig. 9.5: 3D structures of cochaperones dedicated to Fe-S cluster biogenesis in *Homo sapiens* (HSC20, panel a, PDB ID: 3BVO), *S. cerevisiae* (Jac1, panel b, PDB ID: 3UO2), and *E. coli* (HscB, panel c, PDB ID: 1FPO). Conserved amino acid residues that interact with the main scaffold ISCU on the surface of the C-terminal domains of the cochaperones dedicated to Fe-S cluster biogenesis in human (a), yeast (b), and bacteria (c) are shown: in light blue are the hydrophobic amino acids (Leu, Met, and Phe) and in green the polar residues (Tyr). The His (H), Pro (P), Asp (D) tripeptide in the N-terminal domains (J-domains) of the cochaperones is shown in magenta. Two CxxC modules, which coordinate zinc in the crystal structure of human HSC20, are shown in red.

independent and specific delivery pathways to recipients that interact with distinct subsets of carriers. The distinctive phenotypes associated with the various disease gene mutations reveal our lack of knowledge about how discrete Fe-S proteins are targeted in order to incorporate their vital prosthetic groups [72–83]. Enhancing our understanding of the molecular mechanisms of Fe-S cluster assembly and delivery to recipient proteins might make it possible to target several human diseases associated with disruption of Fe-S clusters or loss of integrity of the Fe-S cluster biogenesis and repair processes. Friedreich's ataxia is the most prevalent form of hereditary ataxia in Caucasians, caused by deficiency of the protein frataxin, which is critical for initial biogenesis of Fe-S clusters. In addition, several rare human diseases have been linked to dysfunctional Fe-S cluster biogenesis and/or defects in Fe-S proteins (we refer the reader to the Chapter titled "Fe-S proteins and human diseases" from Wing-Hang Tong for an overview of the clinical, and biochemical aspects of diseases associated with defects in Fe-S proteins or in Fe-S cluster biogenesis).

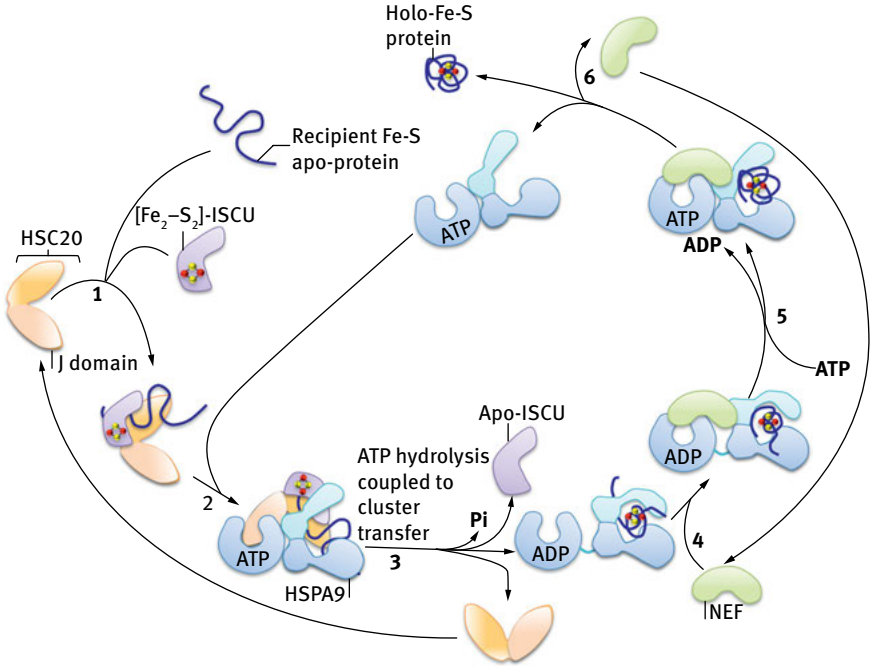

Fig. 9.6: Proposed schematic of the mode of action of the chaperone/cochaperone system in Fe-S cluster delivery to recipient proteins. The cochaperone HSC20 starts the functional cycle of the cognate system by associating with the scaffold protein ISCU, which is loaded with an Fe-S cluster, and with a recipient Fe-S apo-protein (1). (2) ISCU binds to the HSP70 chaperone (HSPA9 in mammalian cells) in a two-step process, which involves the transient interaction of the J-domain of HSC20 with the NBD of the ATP-bound state of HSPA9 and the interaction of ISCU with the SBD. ATP-bound HSPA9 is in the open conformation, which exhibits the substrate-binding cavity to allow the interaction with ISCU. (3) The simultaneous association of ISCU and the interaction of the NBD of HSPA9 with the J-domain of HSC20 lowers the activation energy for the hydrolysis of ATP. Hydrolysis of ATP and the coupled conformational change in the SBD of HSPA9 is proposed to facilitate cluster release from ISCU and transfer to the recipient protein. (4) A NEF, which exhibits high affinity for the ADP-bound state of the HSP70 chaperone, binds to the HSP70-client complex and exchanges ADP with ATP in the NBD (5). The client, which has folded into the native conformation driven by the energy provided by hydrolysis of ATP and has acquired its Fe-S cluster, is finally released (6).

9.5 Recent progress: identification of molecular features that guide selection of recipient Fe-S proteins by the Fe-S transfer complex

Recent studies were conducted to try to elucidate how Fe-S clusters are transferred from the initial scaffold protein, ISCU, to Fe-S clients, focusing on the human cochaperone HSC20, as the component of the Fe-S transfer machinery that guides the multifunctional HSP70 chaperone HSPA9 to function in Fe-S cluster delivery to recipient proteins [3, 37, 55, 57, 68–71, 84–86]. Importantly, there is only one highly conserved HSC20 homologue in the human genome [63], which also made HSC20 a good

candidate to use in a screening to identify potential target Fe-S proteins. HSC20 served as a bait in a stringent yeast two-hybrid (Y2H) screen, a method used to reveal direct molecular interactions between pairs of proteins, and several HSC20 binding partners were identified among the library of proteins [55]. Notably, multiple individual HSC20 interacting clones encoded SDH subunit b (SDHB), which is the Fe-S cluster containing subunit of complex II (CII). The interaction between HSC20 and SDHB was further validated *in vivo* in mammalian cells [55]. SDHB contains three clusters of different nuclearities: [Fe_2-S_2], [Fe_4-S_4], and [Fe_3-S_4] [87], which are deeply buried within the mature protein and that likely need to be inserted during folding. Assembly of CII is a multistep process that depends upon incorporation of several prosthetic groups, including flavin adenine dinucleotide, covalently attached to SDHA; three Fe-S clusters ligated by SDHB; and a heme b moiety bound by the SDHC/SDHD membrane anchor proteins [88].

The Y2H screen was also conducted in order to identify potential motifs present in recipient Fe-S proteins, which may act as a lure for binding of the cochaperone HSC20 and therefore function as molecular signatures that guide specific recruitment of the Fe-S transfer complex through direct binding to HSC20. In recent years, investigators have focused increasingly on molecular interactions mediated by compact modules that are typically less than 10 amino acid residues in length and are often found within intrinsically disordered regions of polypeptides. On average, binding motifs are six to seven amino acids in length, and only three to four core positions confer specificity [89]. Because the binding surface area is small, these motifs bind with low affinity and engage in interactions that are transient and readily modulated. It has been suggested that over one million such motifs are present in the human proteome and that they extend the functional capabilities of eukaryotes well beyond known structural domains [90], influencing protein processing, localization, degradation, and transient participation in multiprotein complexes. SDHB, which contains three Fe-S clusters, appeared to be the perfect candidate for identifying the potential motifs that mediate direct binding to the cochaperone HSC20. The primary sequence of SDHB was subdivided into multiple peptides, which were cloned into Y2H prey constructs to screen 50 to 100 subclones of varying sizes for their ability to interact with HSC20. Three independent binding sites for HSC20 were identified on SDHB, and two of these were iterations of a tripeptide motif, leucine, tyrosine, and arginine (the LYR motif). One SDHB peptide that interacted with HSC20 (residues 238–258 of SDHB) contained the distinctive motif, LYR, while the other (residues 35–52 of SDHB) contained a closely related sequence, IYR. Notably, the two native L(I)YR consensus sequences in SDHB are located in unstructured loops of the crystal structure (Fig. 9.7). One of the L(I)YR motifs appears in SDHB near the N-terminus, proximal to the first cysteines that ligate the [Fe_2-S_2] cluster, whereas the second is closer to the C-terminus and the cysteinyl ligands of the [Fe_4-S_4] and [Fe_3-S_4] clusters, in positions where binding of the chaperone-cochaperone transfer apparatus can guide release of the cluster from holo-ISCU

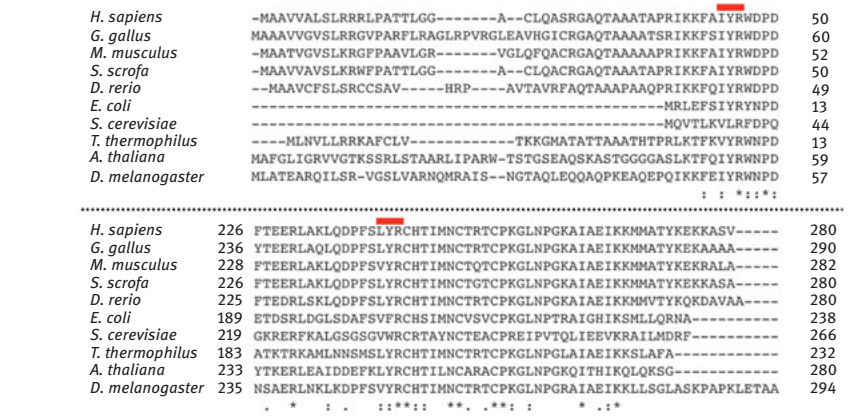

(a) Multiple sequence alignment of SDHB

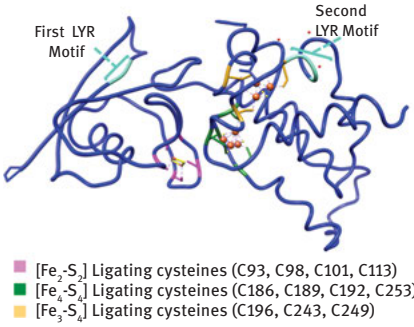

(b) 3D-structure of porcine SDHB

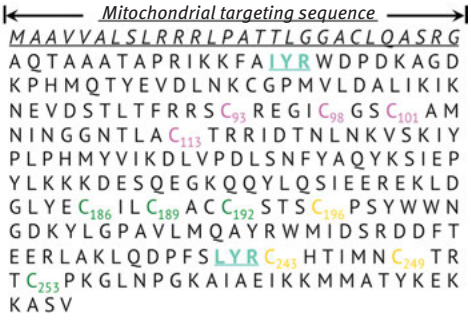

(c) Primary sequence of human SDHB

Fig. 9.7: SDHB contains two highly conserved LYR motifs that are essential for Fe-S cluster incorporation. (a) Multiple sequence alignment of the Fe-S subunit of complex II, SDHB. The two LYR motifs that engage the Fe-S transfer complex are highly conserved in human, yeast, plants, and bacteria. (b) Ribbon representation of the three-dimensional structure of porcine SDHB (PDB ID: 3SFD, 96% identical to human) and primary sequence of human SDHB (c). The two LYR motifs are shown in cyan. The cysteine residues that coordinate the [Fe_2-S_2] cluster are in magenta, and the ligands of [Fe_4-S_4] and of [Fe_3-S_4] clusters are shown in green and yellow, respectively.

into the distal Fe-S binding sites of SDHB (Fig. 9.7). Mutagenesis of the LYR or IYR tripeptide eliminated binding of motif-containing peptides to HSC20 [55]. Interestingly, the amino acid residues of the two L(I)YR motifs were highly conserved in SDHB throughout evolution, including bacteria and yeast [55] (Fig. 9.7). Homology searches indicated that the key features of this distinctive sequence, which mediated binding to HSC20, included having a hydrophobic residue in position 1, followed by an aromatic residue (Y or F) at position 2, and a positive residue, R or K, at position 3. Substitution of Arg46 into Gln in the IYR sequence was identified as a critical cause of renal cancer [91], and substitutions of the IYR, LYR, and cysteines important in ligating Fe-S clusters

were identified as frequent causal mutations in rare tumors such as paragangliomas and gastrointestinal stromal tumors [92]. The LYR motif family is an annotated family present only in eukaryotes (Conserved Domains Accession: cl05087) [93], which lists 11 proteins in humans characterized by having the LYR tripeptide close to their N-terminus. Members of the LYR family are SDHAF1 (LYRM8), an assembly factor involved in Fe-S cluster biogenesis for the SDH complex [94, 95]; ISD11 (LYRM4), a component of the initial Fe-S assembly complex [96]; LYRM7, a complex III assembly factor; and two subunits of respiratory chain complex I known as NDUFA6 and NDUFB9 (also annotated as LYRM6 and LYRM3, respectively) [97]. Several LYR motif proteins do not yet have a known function, such as LYRM2, LYRM5, and LYRM9, whereas others have been only partially characterized in yeast, such as ACN9 (acetate non-utilizing protein 9) [98] or FMC1 (formation of mitochondrial complexes protein 1) [99].

9.6 SDHAF1, a member of the LYR motif family, assists Fe-S cluster incorporation into SDHB

SDHAF1 (also known as LYRM8) was shown to be important for SDH activity and for assembly of the holo-complex in fibroblasts [94]. Homozygous mutations in *SDHAF1* cause a distinctive early-onset leukoencephalopathy in which accumulation of lactate and succinate in the white matter is associated with selective loss of SDH activity [94, 100, 101]; however, the molecular role of *SDHAF1* mutations in disease pathogenesis remained undefined for some time. A recent investigation used biochemical and functional approaches on cell lines derived from patients with *SDHAF1* mutations to characterize the role of this accessory factor in the assembly of Complex II [95]. SDHAF1 was shown to recruit the Fe-S transfer complex to the C-terminus of SDHB through direct binding of its N-terminal LYR motif to the cochaperone HSC20. The region L53-R65 of SDHAF1, enriched in arginine residues, was found to be involved in the interaction with SDHB at three binding sites containing multiple aromatic amino acids. Binding of SDHAF1 to SDHB and recruitment of the HSC20-HSPA9-holo-ISCU complex by its first LYR motif was shown to facilitate Fe-S cluster incorporation into SDHB [95]. *In vivo* iron radiolabeling of SDHB showed defective Fe-S cluster insertion into the protein synthesized in SDHAF1-deficient patient-derived cells. SDHB levels were drastically reduced in patient cells, where lack of functional SDHAF1 led to impaired biogenesis of SDHB, which was subsequently rapidly degraded by the mitochondrial protease, LONP1 [95].

9.7 Potential role of LYR motif proteins in Fe-S cluster biogenesis

The functional significance of the common LYR motif was completely unknown when the Pfam clan Complex1_LYR-like superfamily (CL0491) was built by P.C. Coggill [102].

Based on bioinformatics analyses, the motif was defined as a tripeptide in which the first position was generally an aliphatic hydrophobic amino acid such as isoleucine or leucine, the second was an aromatic amino acid such as tyrosine or phenylalanine, and the third was a positively charged arginine or lysine. In subsequent analyses, the tripeptide was observed to be frequently followed by a conserved phenylalanine separated from LYR by about 25 residues [97]. The LYR motif was present in several proteins selected in the Y2H screen as interacting partners of HSC20 (i.e. EPRS, HELZ, SPC25, GTF2E2, and ETFA), and also in LYRM7, the Rieske Fe-S protein chaperone of complex III [103] and an annotated member of the LYR family [97]. Overall, coimmunoprecipitation and Y2H studies indicated that LYR motifs present in known recipient Fe-S proteins (i.e. SDHB) or in accessory factors (i.e. SDHAF1, LYRM7) mediated an interaction with the cochaperone HSC20 and guided insertion of Fe-S clusters into the Fe-S subunit of respiratory chain complex II and, possibly, into complex III [55]. In fact, LYRM7, which has been characterized as a complex III assembly factor, binds UQCRFS1, the Rieske Fe-S protein of complex III [103], and engages the HSC20/HSPA9/ISCU complex [55, 56], suggesting that the LYRM7-HSC20 interaction might guide the insertion of the [Fe_2-S_2] cluster into UQCRFS1. LYR-containing subunits are present in mitochondrial complex I. The role of the complex I subunit LYRM6 (also known as NDUFA6 and as NB4M in the yeast *Yarrowia lipolytica*) has been recently characterized [104]. Chromosomal deletion of NB4M in *Y. lipolytica* or mutagenesis of the LYR tripeptide and of a conserved downstream phenylalanine into alanines caused loss of the [Fe_4-S_4] N2 cluster, which is the Fe-S center in the matrix protruding arm of complex I closest to the membrane, and totally abrogated the ubiquinone reductase activity of complex I, despite the fact that all the other central subunits of the complex were intact. This finding suggests that NB4M (NDUFA6) is required for proper incorporation of the N2 [Fe_4-S_4] center and for the function of complex I. Notably, NDUFS8, which ligates two [Fe_4-S_4] clusters, contains a conserved LYR motif in a noncanonical position, at its C-terminus. As only 14 of the 44 complex I subunits have a catalytic function, some of the accessory or supernumerary subunits may contribute to the assembly and stability of the complex, and the LYR-containing subunits may aid insertion of some of the Fe-S clusters.

A second consensus sequence, KKx(6-10)KK, was identified in the screening of the SDHB peptides that interacted with HSC20 through its C-terminal domain [55]. Interestingly, human glutaredoxin 5 (GLRX5) has a similar pattern of lysines at its C-terminus (K139K140(x10)K151K152) and was found to interact with HSC20 *in vivo* [55]. The yeast ortholog Grx5 interacts with Ssq1, the mitochondrial chaperone dedicated to Fe-S cluster biogenesis [105]. The LYR and KKx(6-10)KK consensus sequences constitute molecular signatures that are present in recipient Fe-S proteins or in accessory factors that assist Fe-S cluster biogenesis. These short motifs are binding sites for HSC20, which forms a complex with holo-ISCU (containing the intact [Fe_2-S_2] cluster) and the chaperone HSPA9. Upon hydrolysis of ATP, the nascent Fe-S cluster may directly transfer from ISCU into neighboring cysteinyl ligands in the primary unfolded peptide

sequence of the recipient protein, which can rapidly tether and protect the cluster while driving folding into the final tertiary structure.

9.8 Molecular features of peptides containing the LYR motif that affect binding to HSC20

The function of the LYR and KKx(6-10)KK motifs may be very dependent on their molecular context and structural location [55]. Other features may define which LYR proteins engage HSC20 and the transfer apparatus, and these features will likely be characterized as more LYR and Fe-S proteins are studied. Interestingly, there are two other examples in which a small peptide motif functions in the Fe-S transfer complex. The first is the well-known role of the tripeptide His, Pro, Asp (HPD) of HSC20 in activating the ATPase activity of its partner chaperone [24]. A second example is the role of the tripeptide Pro, Val, Lys (PVK) of ISCU in binding to the chaperone as part of the activation of the Fe-S transfer cycle [26, 40, 41]. Experimental work will be needed to establish what other features are required for LYR motif-containing proteins to engage in binding with the Fe-S transfer complex. Upon inspection of the two motifs in SDHB and of the LYR motifs in SDHAF1 and LYRM7 that mediate an interaction with HSC20 (as assessed by coimmunoprecipitation of endogenous human proteins), it appears that all four of these motifs are present in a peptide context in which a large hydrophobic residue, Phe, or two smaller hydrophobic amino acids, Val and Leu, are present just upstream of the LYR. Thus, it is possible that a small hydrophobic patch near the N-terminal side of LYR enhances binding to HSC20. A combination of informatics analyses and experimental tests will likely elucidate all the features of a functional LYR motif. In the years ahead, it will be interesting to see whether identification of LYR motifs through informatics can lead to discovery of unrecognized human Fe-S proteins [106].

9.9 Conclusions and future perspectives

Identification of novel Fe-S proteins at the core of ribosomal function and translation as well as of DNA metabolism has been made possible, during the last decades, by a combination of different approaches. Particularly, bioinformatics analyses have accelerated discoveries of Fe-S proteins based on homology studies [107]. An alternative approach was to identify specific motifs that are recognized by the Fe-S transfer machinery [55]. There are probably many more mammalian Fe-S proteins that have not been recognized thus far because of the instability of Fe-S clusters and the previous lack of identifying sequence elements. In addition, the characterization of the molecular basis of rare diseases may lead to other unexpected insights into the Fe-S cluster biogenesis pathway.

References

[1] Alderson TR, Kim JH, Markley JL. Dynamical Structures of Hsp70 and Hsp70-Hsp40 Complexes. Structure 2016;24:1014–30.
[2] Balchin D, Hayer-Hartl M, Hartl FU. In vivo aspects of protein folding and quality control. Science 2016;353:aac4354.
[3] Kampinga HH, Craig EA. The HSP70 chaperone machinery: J proteins as drivers of functional specificity. Nat Rev Mol Cell Biol 2010;11:579–92.
[4] Kominek J, Marszalek J, Neuveglise C, Craig EA, Williams BL. The complex evolutionary dynamics of Hsp70s: a genomic and functional perspective. Genome Biol Evol 2013;5:2460–77.
[5] Mayer MP. Hsp70 chaperone dynamics and molecular mechanism. Trends Biochem Sci 2013;38:507–14.
[6] Mayer MP, Bukau B. Hsp70 chaperones: cellular functions and molecular mechanism. Cell Mol Life Sci 2005;62:670–84.
[7] McKay DB. Structure and mechanism of 70-kDa heat-shock-related proteins. Adv Protein Chem 1993;44:67–98.
[8] Seaton BL, Vickery LE. A gene encoding a DnaK/hsp70 homolog in Escherichia coli. Proc Natl Acad Sci USA 1994;91:2066–70.
[9] Kawula TH, Lelivelt MJ. Mutations in a gene encoding a new Hsp70 suppress rapid DNA inversion and bgl activation, but not proU derepression, in hns-1 mutant Escherichia coli. J Bacteriol 1994;176:610–9.
[10] Ta DT, Seaton BL, Vickery LE. Localization of the ferredoxin (fdx) gene on the physical map of the Escherichia coli chromosome. J Bacteriol 1992;174:5760–1.
[11] Vickery LE, Silberg JJ, Ta DT. Hsc66 and Hsc20, a new heat shock cognate molecular chaperone system from Escherichia coli. Protein Sci 1997;6:1047–56.
[12] Silberg JJ, Hoff KG, Vickery LE. The Hsc66-Hsc20 chaperone system in Escherichia coli: chaperone activity and interactions with the DnaK-DnaJ-grpE system. J Bacteriol 1998;180:6617–24.
[13] Blattner FR, Plunkett G, 3rd, Bloch CA, et al. The complete genome sequence of Escherichia coli K-12. Science 1997;277:1453–62.
[14] Zheng L, Cash VL, Flint DH, Dean DR. Assembly of iron-sulfur clusters. Identification of an iscSUA-hscBA-fdx gene cluster from Azotobacter vinelandii. J Biol Chem 1998;273:13264–72.
[15] Takahashi Y, Nakamura M. Functional assignment of the ORF2-iscS-iscU-iscA-hscB-hscA-fdx-ORF3 gene cluster involved in the assembly of Fe-S clusters in Escherichia coli. J Biochem 1999;126:917–26.
[16] Nakamura M, Saeki K, Takahashi Y. Hyperproduction of recombinant ferredoxins in Escherichia coli by coexpression of the ORF1-ORF2-iscS-iscU-iscA-hscB-hs cA-fdx-ORF3 gene cluster. J Biochem 1999;126:10–8.
[17] Tokumoto U, Takahashi Y. Genetic analysis of the isc operon in Escherichia coli involved in the biogenesis of cellular iron-sulfur proteins. J Biochem 2001;130:63–71.
[18] Goffeau A, Barrell BG, Bussey H, et al. Life with 6000 genes. Science 1996;274:546, 63–7.
[19] Strain J, Lorenz CR, Bode J, et al. Suppressors of superoxide dismutase (SOD1) deficiency in Saccharomyces cerevisiae. Identification of proteins predicted to mediate iron-sulfur cluster assembly. J Biol Chem 1998;273:31138–44.
[20] Schilke B, Voisine C, Beinert H, Craig E. Evidence for a conserved system for iron metabolism in the mitochondria of Saccharomyces cerevisiae. Proc Natl Acad Sci USA 1999;96:10206–11.
[21] Garland SA, Hoff K, Vickery LE, Culotta VC. Saccharomyces cerevisiae ISU1 and ISU2: members of a well-conserved gene family for iron-sulfur cluster assembly. J Mol Biol 1999;294:897–907.
[22] Kim R, Saxena S, Gordon DM, Pain D, Dancis A. J-domain protein, Jac1p, of yeast mitochondria required for iron homeostasis and activity of Fe-S cluster proteins. J Biol Chem 2001;276:17524–32.

[23] Lutz T, Westermann B, Neupert W, Herrmann JM. The mitochondrial proteins Ssq1 and Jac1 are required for the assembly of iron sulfur clusters in mitochondria. J Mol Biol 2001;307:815–25.
[24] Voisine C, Cheng YC, Ohlson M, et al. Jac1, a mitochondrial J-type chaperone, is involved in the biogenesis of Fe/S clusters in Saccharomyces cerevisiae. Proc Natl Acad Sci USA 2001;98:1483–8.
[25] Hoff KG, Silberg JJ, Vickery LE. Interaction of the iron-sulfur cluster assembly protein IscU with the Hsc66/Hsc20 molecular chaperone system of Escherichia coli. Proc Natl Acad Sci USA 2000;97:7790–5.
[26] Hoff KG, Ta DT, Tapley TL, Silberg JJ, Vickery LE. Hsc66 substrate specificity is directed toward a discrete region of the iron-sulfur cluster template protein IscU. J Biol Chem 2002;277:27353–9.
[27] Hoff KG, Cupp-Vickery JR, Vickery LE. Contributions of the LPPVK motif of the iron-sulfur template protein IscU to interactions with the Hsc66-Hsc20 chaperone system. J Biol Chem 2003;278:37582–9.
[28] Dutkiewicz R, Schilke B, Knieszner H, Walter W, Craig EA, Marszalek J. Ssq1, a mitochondrial Hsp70 involved in iron-sulfur (Fe/S) center biogenesis. Similarities to and differences from its bacterial counterpart. J Biol Chem 2003;278:29719–27.
[29] Leustek T, Dalie B, Amir-Shapira D, Brot N, Weissbach H. A member of the Hsp70 family is localized in mitochondria and resembles Escherichia coli DnaK. Proc Natl Acad Sci USA 1989;86:7805–8.
[30] Mizzen LA, Chang C, Garrels JI, Welch WJ. Identification, characterization, and purification of two mammalian stress proteins present in mitochondria, grp 75, a member of the hsp 70 family and hsp 58, a homolog of the bacterial groEL protein. J Biol Chem 1989;264:20664–75.
[31] Craig EA, Kramer J, Shilling J, et al. SSC1, an essential member of the yeast HSP70 multigene family, encodes a mitochondrial protein. Mol Cell Biol 1989;9:3000–8.
[32] Taylor JW, Berbee ML. Dating divergences in the Fungal Tree of Life: review and new analyses. Mycologia 2006;98:838–49.
[33] Schilke B, Williams B, Knieszner H, et al. Evolution of mitochondrial chaperones utilized in Fe-S cluster biogenesis. Curr Biol 2006;16:1660–5.
[34] Karzai AW, McMacken R. A bipartite signaling mechanism involved in DnaJ-mediated activation of the Escherichia coli DnaK protein. J Biol Chem 1996;271:11236–46.
[35] Laufen T, Mayer MP, Beisel C, et al. Mechanism of regulation of hsp70 chaperones by DnaJ cochaperones. Proc Natl Acad Sci USA 1999;96:5452–7.
[36] Silberg JJ, Tapley TL, Hoff KG, Vickery LE. Regulation of the HscA ATPase reaction cycle by the co-chaperone HscB and the iron-sulfur cluster assembly protein IscU. J Biol Chem 2004;279:53924–31.
[37] Ciesielski SJ, Schilke BA, Osipiuk J, et al. Interaction of J-protein co-chaperone Jac1 with Fe-S scaffold Isu is indispensable in vivo and conserved in evolution. J Mol Biol 2012;417:1–12.
[38] Brehmer D, Rudiger S, Gassler CS, et al. Tuning of chaperone activity of Hsp70 proteins by modulation of nucleotide exchange. Nat Struct Biol 2001;8:427–32.
[39] Vickery LE, Cupp-Vickery JR. Molecular chaperones HscA/Ssq1 and HscB/Jac1 and their roles in iron-sulfur protein maturation. Crit Rev Biochem Mol Biol 2007;42:95–111.
[40] Cupp-Vickery JR, Peterson JC, Ta DT, Vickery LE. Crystal structure of the molecular chaperone HscA substrate binding domain complexed with the IscU recognition peptide ELPPVKIHC. J Mol Biol 2004;342:1265–78.
[41] Dutkiewicz R, Schilke B, Cheng S, Knieszner H, Craig EA, Marszalek J. Sequence-specific interaction between mitochondrial Fe-S scaffold protein Isu and Hsp70 Ssq1 is essential for their in vivo function. J Biol Chem 2004;279:29167–74.
[42] Kim JH, Tonelli M, Markley JL. Disordered form of the scaffold protein IscU is the substrate for iron-sulfur cluster assembly on cysteine desulfurase. Proc Natl Acad Sci USA 2012;109:454–9.

[43] Kim JH, Tonelli M, Frederick RO, Chow DC, Markley JL. Specialized Hsp70 chaperone (HscA) binds preferentially to the disordered form, whereas J-protein (HscB) binds preferentially to the structured form of the iron-sulfur cluster scaffold protein (IscU). J Biol Chem 2012;287:31406–13.
[44] Alderson TR, Kim JH, Cai K, Frederick RO, Tonelli M, Markley JL. The specialized Hsp70 (HscA) interdomain linker binds to its nucleotide-binding domain and stimulates ATP hydrolysis in both cis and trans configurations. Biochemistry 2014;53:7148–59.
[45] Bonomi F, Iametti S, Morleo A, Ta D, Vickery LE. Facilitated transfer of IscU-[2Fe2S] clusters by chaperone-mediated ligand exchange. Biochemistry 2011;50:9641–50.
[46] Shi R, Proteau A, Villarroya M, et al. Structural basis for Fe-S cluster assembly and tRNA thiolation mediated by IscS protein-protein interactions. PLoS Biol 2010;8:e1000354.
[47] Marinoni EN, de Oliveira JS, Nicolet Y, et al. (IscS-IscU) 2 complex structures provide insights into Fe2S2 biogenesis and transfer. Angew Chem Int Ed Engl 2012;51:5439–42.
[48] Kim JH, Frederick RO, Reinen NM, Troupis AT, Markley JL. [2Fe-2S]-ferredoxin binds directly to cysteine desulfurase and supplies an electron for iron-sulfur cluster assembly but is displaced by the scaffold protein or bacterial frataxin. J Am Chem Soc 2013;135:8117–20.
[49] Cai K, Frederick RO, Kim JH, Reinen NM, Tonelli M, Markley JL. Human mitochondrial chaperone (mtHSP70) and cysteine desulfurase (NFS1) bind preferentially to the disordered conformation, whereas co-chaperone (HSC20) binds to the structured conformation of the iron-sulfur cluster scaffold protein (ISCU). J Biol Chem 2013;288:28755–70.
[50] Prischi F, Konarev PV, Iannuzzi C, et al. Structural bases for the interaction of frataxin with the central components of iron-sulphur cluster assembly. Nat Commun 2010;1:95.
[51] Schmucker S, Martelli A, Colin F, et al. Mammalian frataxin: an essential function for cellular viability through an interaction with a preformed ISCU/NFS1/ISD11 iron-sulfur assembly complex. PloS One 2011;6:e16199.
[52] Bridwell-Rabb J, Fox NG, Tsai CL, Winn AM, Barondeau DP. Human frataxin activates Fe-S cluster biosynthesis by facilitating sulfur transfer chemistry. Biochemistry 2014;53:4904–13.
[53] Craig EA, Marszalek J. A specialized mitochondrial molecular chaperone system: a role in formation of Fe/S centers. Cell Mol Life Sci 2002;59:1658–65.
[54] Shan Y, Cortopassi G. HSC20 interacts with frataxin and is involved in iron-sulfur cluster biogenesis and iron homeostasis. Hum Mol Genet 2012;21:1457–69.
[55] Maio N, Singh A, Uhrigshardt H, Saxena N, Tong WH, Rouault TA. Cochaperone binding to LYR motifs confers specificity of iron sulfur cluster delivery. *Cell Metabol* 2014;19:445–57.
[56] Maio, N., Kim, K. S., Singh, A., and Rouault, T. A. (2017) A Single Adaptable Cochaperone-Scaffold Complex Delivers Nascent Iron-Sulfur Clusters to Mammalian Respiratory Chain Complexes I-III. *Cell Metab*. 25, 945–953:e946
[57] Chacinska A, Koehler CM, Milenkovic D, Lithgow T, Pfanner N. Importing mitochondrial proteins: machineries and mechanisms. Cell 2009;138:628–44.
[58] Wadhwa R, Taira K, Kaul SC. An Hsp70 family chaperone, mortalin/mthsp70/PBP74/Grp75: what, when, and where? Cell Stress Chaperones 2002;7:309–16.
[59] Kaul SC, Deocaris CC, Wadhwa R. Three faces of mortalin: a housekeeper, guardian and killer. Exp Gerontol 2007;42:263–74.
[60] Deocaris CC, Lu WJ, Kaul SC, Wadhwa R. Druggability of mortalin for cancer and neurodegenerative disorders. Curr Pharm Des 2013;19:418–29.
[61] Flachbartova Z, Kovacech B. Mortalin—a multipotent chaperone regulating cellular processes ranging from viral infection to neurodegeneration. Acta Virol 2013;57:3–15.
[62] Sun G, Gargus JJ, Ta DT, Vickery LE. Identification of a novel candidate gene in the iron-sulfur pathway implicated in ataxia-susceptibility: human gene encoding HscB, a J-type co-chaperone. J Hum Genet 2003;48:415–9.

[63] Uhrigshardt H, Singh A, Kovtunovych G, Ghosh M, Rouault TA. Characterization of the human HSC20, an unusual DnaJ type III protein, involved in iron-sulfur cluster biogenesis. Hum Mol Genet 2010;19:3816–34.
[64] Bitto E, Bingman CA, Bittova L, et al. Structure of human J-type co-chaperone HscB reveals a tetracysteine metal-binding domain. J Biol Chem 2008;283:30184–92.
[65] Cupp-Vickery JR, Vickery LE. Crystal structure of Hsc20, a J-type Co-chaperone from Escherichia coli. J Mol Biol 2000;304:835–45.
[66] Knieszner H, Schilke B, Dutkiewicz R, et al. Compensation for a defective interaction of the hsp70 ssq1 with the mitochondrial Fe-S cluster scaffold isu. J Biol Chem 2005;280:28966–72.
[67] Fuzery AK, Oh JJ, Ta DT, Vickery LE, Markley JL. Three hydrophobic amino acids in Escherichia coli HscB make the greatest contribution to the stability of the HscB-IscU complex. BMC Biochem2011;12:3.
[68] Perales-Calvo J, Muga A, Moro F. Role of DnaJ G/F-rich domain in conformational recognition and binding of protein substrates. J Biol Chem 2010;285:34231–9.
[69] Szabo A, Korszun R, Hartl FU, Flanagan J. A zinc finger-like domain of the molecular chaperone DnaJ is involved in binding to denatured protein substrates. EMBO J 1996;15:408–17.
[70] Lee S, Fan CY, Younger JM, Ren H, Cyr DM. Identification of essential residues in the type II Hsp40 Sis1 that function in polypeptide binding. J Biol Chem 2002;277:21675–82.
[71] Li J, Sha B. Structure-based mutagenesis studies of the peptide substrate binding fragment of type I heat-shock protein 40. Biochem J 2005;386:453–60.
[72] Maio N, Rouault TA. Iron-sulfur cluster biogenesis in mammalian cells: new insights into the molecular mechanisms of cluster delivery. Biochim Biophys Acta 2015;1853:1493–512.
[73] Cameron JM, Janer A, Levandovskiy V, et al. Mutations in iron-sulfur cluster scaffold genes NFU1 and BOLA3 cause a fatal deficiency of multiple respiratory chain and 2-oxoacid dehydrogenase enzymes. Am J Hum Genet 2011;89:486–95.
[74] Navarro-Sastre A, Tort F, Stehling O, et al. A fatal mitochondrial disease is associated with defective NFU1 function in the maturation of a subset of mitochondrial Fe-S proteins. Am J Hum Genet 2011;89:656–67.
[75] Ferrer-Cortes X, Font A, Bujan N, et al. Protein expression profiles in patients carrying NFU1 mutations. Contribution to the pathophysiology of the disease. J Inherit Metabol Dis 2013;36:841–7.
[76] Haack TB, Rolinski B, Haberberger B, et al. Homozygous missense mutation in BOLA3 causes multiple mitochondrial dysfunctions syndrome in two siblings. J Inherit Metabol Dis 2013;36:55–62.
[77] Nizon M, Boutron A, Boddaert N, et al. Leukoencephalopathy with cysts and hyperglycinemia may result from NFU1 deficiency. Mitochondrion 2014;15:59–64.
[78] Baker PR, 2nd, Friederich MW, Swanson MA, et al. Variant non ketotic hyperglycinemia is caused by mutations in LIAS, BOLA3 and the novel gene GLRX5. Brain 2014;137:366–79.
[79] Invernizzi F, Ardissone A, Lamantea E, et al. Cavitating leukoencephalopathy with multiple mitochondrial dysfunction syndrome and NFU1 mutations. Front Genet 2014;5:412.
[80] Tonduti D, Dorboz I, Imbard A, et al. New spastic paraplegia phenotype associated to mutation of NFU1. Orphanet J Rare Dis 2015;10:13.
[81] Ajit Bolar N, Vanlander AV, Wilbrecht C, et al. Mutation of the iron-sulfur cluster assembly gene IBA57 causes severe myopathy and encephalopathy. Hum Mol Genet 2013;22:2590–602.
[82] Lossos A, Stumpfig C, Stevanin G, et al. Fe/S protein assembly gene IBA57 mutation causes hereditary spastic paraplegia. Neurology 2015;84:659–67.
[83] Al-Hassnan ZN, Al-Dosary M, Alfadhel M, et al. ISCA2 mutation causes infantile neurodegenerative mitochondrial disorder. J Med Genet 2015;52:186–94.
[84] Daugaard M, Rohde M, Jaattela M. The heat shock protein 70 family: Highly homologous proteins with overlapping and distinct functions. FEBS Lett 2007;581:3702–10.
[85] Alderson TR, Kim JH, Markley JL. Dynamical structures of Hsp70 and Hsp70-Hsp40 complexes. Structure 2016.

[86] Pukszta S, Schilke B, Dutkiewicz R, et al. Co-evolution-driven switch of J-protein specificity towards an Hsp70 partner. EMBO Rep 2010;11:360–5.
[87] Singer TP, Johnson MK. The prosthetic groups of succinate dehydrogenase: 30 years from discovery to identification. FEBS Lett 1985;190:189–98.
[88] Hagerhall C, Hederstedt L. A structural model for the membrane-integral domain of succinate: quinone oxidoreductases. FEBS Lett 1996;389:25–31.
[89] Tompa P, Davey NE, Gibson TJ, Babu MM. A million peptide motifs for the molecular biologist. Mol Cell 2014;55:161–9.
[90] Babu MM, Kriwacki RW, Pappu RV. Structural biology. Versatility from protein disorder. Science 2012;337:1460–1.
[91] Ricketts C, Woodward ER, Killick P, et al. Germline SDHB mutations and familial renal cell carcinoma. J Natl Cancer Inst 2008;100:1260–2.
[92] Saxena N, Maio N, Crooks DR, et al. SDHB-deficient cancers: the role of mutations that impair iron sulfur cluster delivery. J Natl Cancer Inst 2016;108.
[93] Angerer H. Eukaryotic LYR Proteins interact with mitochondrial protein complexes. Biology (Basel) 2015;4:133–50.
[94] Ghezzi D, Goffrini P, Uziel G, et al. SDHAF1, encoding a LYR complex-II specific assembly factor, is mutated in SDH-defective infantile leukoencephalopathy. Nat Genet 2009;41:654–6.
[95] Maio N, Ghezzi D, Verrigni D, et al. Disease-causing SDHAF1 mutations impair transfer of Fe-S clusters to SDHB. Cell Metab 2016;23:292–302.
[96] Shi Y, Ghosh MC, Tong WH, Rouault TA. Human ISD11 is essential for both iron-sulfur cluster assembly and maintenance of normal cellular iron homeostasis. Hum Mol Genet 2009;18:3014–25.
[97] Angerer H. The superfamily of mitochondrial Complex1_LYR motif-containing (LYRM) proteins. Biochem Soc Trans 2013;41:1335–41.
[98] Dennis RA, McCammon MT. Acn9 is a novel protein of gluconeogenesis that is located in the mitochondrial intermembrane space. Eur J Biochem 1999;261:236–43.
[99] Lefebvre-Legendre L, Vaillier J, Benabdelhak H, Velours J, Slonimski PP, di Rago JP. Identification of a nuclear gene (FMC1) required for the assembly/stability of yeast mitochondrial F(1)-ATPase in heat stress conditions. J Biol Chem 2001;276:6789–96.
[100] Ohlenbusch A, Edvardson S, Skorpen J, et al. Leukoencephalopathy with accumulated succinate is indicative of SDHAF1 related complex II deficiency. Orphanet J Rare Dis 2012;7:69.
[101] Jain-Ghai S, Cameron JM, Al Maawali A, et al. Complex II deficiency—a case report and review of the literature. Am J Med Genet A 2013;161A:285–94.
[102] Punta M, Coggill PC, Eberhardt RY, et al. The Pfam protein families database. Nucleic Acids Res 2012;40:D290–301.
[103] Sanchez E, Lobo T, Fox JL, Zeviani M, Winge DR, Fernandez-Vizarra E. LYRM7/MZM1L is a UQCRFS1 chaperone involved in the last steps of mitochondrial complex III assembly in human cells. Biochim Biophys Acta 2013;1827:285–93.
[104] Angerer H, Radermacher M, Mankowska M, et al. The LYR protein subunit NB4M/NDUFA6 of mitochondrial complex I anchors an acyl carrier protein and is essential for catalytic activity. Proc Natl Acad Sci USA 2014;111:5207–12.
[105] Uzarska MA, Dutkiewicz R, Freibert SA, Lill R, Muhlenhoff U. The mitochondrial Hsp70 chaperone Ssq1 facilitates Fe/S cluster transfer from Isu1 to Grx5 by complex formation. Mol Biol Cell 2013;24:1830–41.
[106] Rouault TA. Iron-sulfur proteins hiding in plain sight. Nat Chem Biol 2015;11:442–5.
[107] Akiva E, Brown S, Almonacid DE, et al. The Structure-Function Linkage Database. Nucleic Acids Res 2014;42:D521–30.

10 Iron-sulfur proteins and human diseases

Wing Hang Tong

Abstract

Iron-sulfur (Fe-S) clusters are essential for numerous biological processes, including electron transfer in the mitochondrial respiratory chain, enzymatic catalysis in metabolic pathways, performing structural roles in DNA repair proteins, and sensing of intracellular iron levels and reactive oxygen species. Disruptions of Fe-S proteins and Fe-S cluster biogenesis proteins due to genetic defects or oxidative stress have been shown to cause human diseases with a variety of symptoms and distinctive tissue-specific manifestations. This chapter presents an overview of the clinical, biochemical and cellular aspects of the diseases associated with defects in Fe-S proteins or Fe-S cluster biogenesis and discusses current therapeutic approaches.

10.1 Introduction

Iron-sulfur (Fe-S) proteins constitute one of the most ubiquitous and functionally versatile classes of metalloproteins [1, 2]. More than 120 distinct types of proteins contain Fe-S clusters, and Fe-S proteins are involved in fundamental processes such as respiration, photosynthesis, intermediary metabolism, and nitrogen fixation. Fe-S clusters are essential for electron transfer processes in energy metabolism. Nicotinamide adenine dinucleotide (NADH):ubiquinone oxidoreductase (respiratory complex I) contains eight Fe-S clusters, and four additional Fe-S clusters are involved in electron transport in complexes II and III. A solvent exposed Fe-S cluster directly participates in substrate binding and acid-base catalysis in a family of dehydratases, which includes the mitochondrial aconitase in the tricarboxylic acid (TCA) cycle [3]. Fe-S clusters are essential components of diverse nucleic acid processing machineries including glycosylases, helicases, and primases [4]. Fanconi anemia group J protein (FANCJ) and Xeroderma pigmentosum group D protein (XPD) are Fe-S proteins involved in DNA repair and transcription [5, 6], whereas DNA polymerases have an essential Fe-S cluster binding domain that is important for accessory subunit recruitment and replisome stability [7, 8]. Fe-S clusters are also critical for the function of *S*-adenosyl-L-methionine (SAM)-dependent lipoic acid synthase (LIAS), both as the sulfur donor and in the generation of a catalytic 5′-deoxyadenosyl 5′-radical [9]. In addition, the sensitivities of Fe-S clusters to reactive oxygen species (ROS), reactive nitrogen species (RNS) and iron bioavailability provide cells with a sensitive mechanism to register oxidative stress and intracellular iron status and to regulate gene expressions accordingly [10]. For instance, the bifunctional iron regulatory protein-1/cytosolic aconitase (IRP1/ACO1) registers cytosolic iron levels through its labile Fe-S cluster. Reduced iron availability or

DOI 10.1515/9783110479850-010

oxidative stress limits Fe-S cluster assembly in IRP1, and IRP1 loses aconitase activity and binds to its mRNA targets and thereby regulates iron trafficking, intermediary metabolism, and heme biosynthesis (reviewed in [11–13]). Given the critical roles of Fe-S proteins in a wide range of cellular activities, disruption of Fe-S clusters or the Fe-S cluster assembly and repair processes, either as a result of genetic defects or oxidative stress, can affect basic cellular processes and result in human diseases.

10.2 Oxidative susceptibility of Fe-S proteins

Oxidative stress can cause damage to an array of cellular components and is linked to serious diseases in humans, including amyotrophic lateral sclerosis (ALS), Parkinson's disease, Huntington disease, cardiomyopathy, and cancer [14, 15]. Studies from bacterial to human model systems have shown that the reactivities of Fe-S clusters with O_2, ROS, and nitric oxide (NO) enable these metalloclusters to act as biosensors to O_2 levels and oxidative and nitrative stress [16] but also render Fe-S proteins the primary targets of oxidative damage [17, 18]. Early studies revealed that high oxygen levels block the ability of *Escherichia coli* to synthesize branched-chain amino acids [19], and studies from the Fridovich and Flint labs showed that superoxide (O_2^-) can inactivate the [4Fe-4S] family of dehydratases, including dihydroxyacid dehydratase, aconitase, and fumarase, which are key enzymes of the branched-chain amino acid metabolisms and TCA cycle in *E. coli* [20–22]. Studies in *Saccharomyces cerevisiae* showed that yeast deficient in cytosolic superoxide dismutase (CuZnSOD) and mitochondrial superoxide dismutase (MnSOD) exhibit deficiencies in [4Fe-4S]-dependent homoaconitase (which participates in lysine biosynthesis) and mitochondrial aconitase [23, 24]. Similarly, flies depleted of SOD exhibit loss of aconitase activities [25]. Rli1 in yeast (human ABCE1) is an essential and highly conserved protein that requires an Fe-S cluster for its functions in ribosome biogenesis and maturation [26], and Rli1 was shown to be an important target for inhibition of cell growth by ROS [27].

In mammals, Fe-S clusters in the respiratory complexes and mitochondrial aconitase (ACO2) are targets of oxidative damage during aging [18, 28–31]. C57BL/6J mice lacking MnSOD have reduced aconitase activity, suffer from dilated cardiomyopathy, and die within 10 days of birth [32, 33]. It has been suggested that the lipid accumulation observed in the livers of MnSOD-deficient mice resulted from oxidative damage to the Fe-S clusters in ACO2 and succinate dehydrogenase (SDH), which inhibited TCA cycle activity, allowing citrate to be diverted to lipid biosynthesis [34]. In addition to ROS, NO has been shown to inactivate respiratory complexes II and III through its reaction with the Fe-S clusters [35, 36], and electron paramagnetic resonance (EPR) studies of rat gastric tissue and human biopsy specimens revealed that dinitrosyl iron complexes were formed, indicating that Fe-S clusters are intracellular targets for NO that is generated from dietary nitrate [37]. Oxidative damages to ACO2 and respiratory complexes II and III have also been reported in the most affected regions in the brains of patients with Huntington disease [38, 39], and defects in mitochondrial energy metabolism leading to

increased susceptibility to excitotoxic injury is a potential mechanism contributing to the pathogenesis of Huntington disease [40, 41]. A genetic modifier screen in *Drosophila* identified aconitase as a dominant suppressor of PINK1 (PTEN-induced kinase 1), a mitochondrial kinase linked to early onset Parkinson's disease in humans, and it was suggested that increased O_2^- in *pink1* mutants led to the release of iron from the [4Fe-4S] cluster in ACO2, resulting in more oxidative stress and mitochondrial swelling [42]. In addition to damaging energy metabolism through the inactivation of aconitase and respiratory complexes, ROS and RNS can damage the Fe-S cluster in the heme biosynthetic enzyme ferrochelatase (FECH), leading to rapid degradation of the protein, and resulting in decreased heme biosynthesis [43, 44].

The molecular mechanisms of Fe-S cluster disassembly have been examined in a number of proteins, including dihydroxy-acid dehydratase, isopropylmalate isomerase, and fumarate and nitrate reduction regulatory protein (FNR) from *E. coli* and HydE from *Thermotoga maritima* [45–47]. O_2^--mediated inactivation of Fe-S-dependent dehydratases is thought to be initiated by oxidation of the solvent-exposed cluster, resulting in the formation of H_2O_2 and the release of Fe^{2+} from an unstable $[4Fe\text{-}4S]^{3+}$ intermediate [22] (Fig. 10.1A).

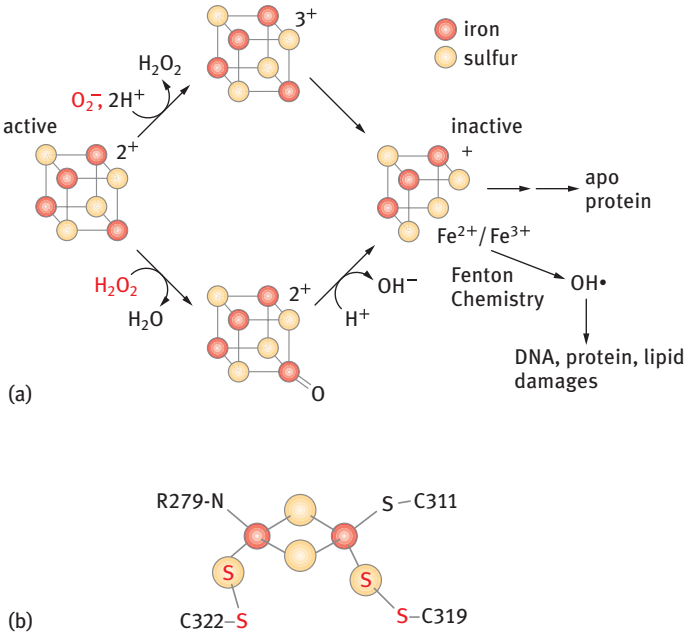

Fig. 10.1: Oxidative susceptibility of Fe-S clusters. (a) Superoxide (O_2^-) and hydrogen peroxide (H_2O_2) can directly oxidize the solvent-exposed catalytic iron atom of dehydratase Fe-S clusters, precipitating Fe^{3+} loss, and enzyme inactivation. O_2^- oxidizes the $[4Fe\text{-}4S]^{2+}$ cluster, generating H_2O_2 and an unstable $[4Fe\text{-}4S]^{3+}$ species. Subsequent release of Fe^{2+} generates a $[3Fe\text{-}4S]^+$ cluster [22]. Oxidation of the $[4Fe\text{-}4S]^{2+}$ cluster by H_2O_2 presumably generates a transient ferryl species, followed by release of Fe^{3+} [48]. (b) X-ray crystallography studies suggested that oxygen-induced degradation disassembly of the $[4Fe\text{-}4S]^{2+}$ cluster in the hydrogenase maturase HydE from *T. maritime* proceeds with retention of the bridging sulfides to generate $[2Fe\text{-}2S]^{2+}$ cluster-bound cysteine persulfides [47].

The resultant inactive enzyme containing a $[3Fe\text{-}4S]^{+}$ cluster can undergo further cluster disassembly or be reactivated *in vitro* and *in vivo* by reduction and remetallation. Similar to O_2^-, H_2O_2 can oxidize the catalytic iron atom of the dehydratase Fe-S cluster, generating a transient ferryl species that abstracts a second electron from the cluster, followed by the release of a Fe^{3+} to form a catalytically inactive $[3Fe\text{-}4S]^{+}$ form [48].

In the case of the O_2^--induced $[4Fe\text{-}4S]^{2+}$ to $[2Fe\text{-}2S]^{2+}$ cluster conversion in FNR, a metal-based oxidation mechanism was initially proposed that involved two one-electron oxidations of the cluster, followed by the release of one Fe^{3+}, one Fe^{2+}, and two S^{2-} to yield a $[2Fe\text{-}2S]^{2+}$ cluster [49]. Subsequently, a sulfur-based mechanism was proposed based on the data from Raman and ultraviolet (UV)-visible absorption/circular dichroism spectroscopies and mass spectrometry, which suggested that the cluster conversion proceeded with the retention of two sulfides as cysteine persulfide ligands [46]. X-ray crystallography studies of HydE from *T. maritima* also identified an [2Fe-2S] cluster bound by two cysteine persulfide residues [47] (Fig. 10.1B). The study suggested that cluster degradation starts with iron oxidation that leads to an intermediate [3Fe-4S] cluster with the formation of O_2^-, which reacts with one of the cysteine ligands to form a cysteine persulfenate, which is then converted to cysteine persulfide with the production of H_2O_2 and the release of a second Fe^{2+} ion. Subsequent oxidation of a second cysteine ligand generates a second cysteine persulfide. The differences in oxygen tolerance and mechanism of oxidative disassembly of the different Fe-S clusters may be determined by protein environments and cofactor geometries [50]. Interestingly, only iron and a source of electrons are required to promote the conversion of cysteine persulfide coordinated [2Fe-2S] back to the [4Fe-4S] form, therefore suggesting a repair mechanism that does not require the intervention of an Fe-S cluster biogenesis pathway [16].

10.2.1 Aconitases: targets of oxidative stress in disease and aging

Aconitase catalyzes the reversible isomerization of citrate, cis-aconitate, and isocitrate [3, 51]. Two aconitase isozymes are present in mammalian cells: the mitochondrial enzyme (ACO2) that functions in the TCA cycle and the bifunctional cytosolic enzyme (ACO1/IRP1) that also plays a role in the regulation of iron metabolism. Aconitase contains a $[4Fe\text{-}4S]^{2+}$ cluster that is essential for its activity; three of the Fe atoms in the cluster are ligated to three cysteines in the protein; a fourth catalytic Fe atom is uniquely free to ligate substrate and solvent molecules and act as a Lewis acid during the enzymatic reaction [3]. O_2^-, H_2O_2, and NO have been shown to react with the exposed catalytic Fe atom and initiate disassembly of the cluster [21, 52].

Given the key role of citrate in intermediary metabolism, inactivation of aconitases can have profound effects on many aspects of physiology [52]. Citrate is an

intermediate in major pathways of energy and intermediary metabolism. In the mitochondria, citrate is an intermediate in the TCA cycle, which is important for the generation of NADH and $FADH_2$ needed for oxidative phosphorylation. In the cytosol, citrate can be converted to acetyl-CoA, the building block for cholesterol and fatty acid biosynthesis in liver and adipose tissue. Citrate also has regulatory roles in glycolysis, fatty acid synthesis, and oxidation. Citrate is a negative regulator of the glycolytic enzyme phosphofructokinase [53, 54] and an allosteric activator of acetyl-CoA carboxylase, the enzyme that generates malonyl-CoA [55], a potent regulator of the partition between fatty acid biosynthesis and oxidation [56]. Decreased expression of a plasma membrane citrate transporter, Indy, in *Drosophila* and ceNAC-2 in *Caenorhabditis elegans* resulted in decreased lipid content and increased life span [57–59]. Thus, through its effects on malonyl-CoA production, glucose utilization, fatty acid synthesis, and oxidation, changes in aconitase activity can have profound impacts on obesity, insulin resistance, and diabetes [60, 61].

In addition to intermediary metabolism, citrate homeostasis is also important for many other biological processes. In the central nervous system and the retina, ACO1 is thought to be important for generating glutamate, the major excitatory neurotransmitter [62]. In cholinergic neurons, citrate can be used to generate acetyl-CoA for acetylcholine synthesis [63]. In the kidney, citrate is an inhibitor of kidney stone formation [64]. In prostate cells, zinc has been shown to be an inhibitor of ACO2 activity, and the downregulation of zinc transporters is thought to be an important factor in the metabolic transformation of normal citrate-secreting epithelial cells to malignant citrate-oxidizing cells in prostate cancer [65].

In addition, isocitate has been identified as a mediator of the erythroid response to iron restriction [66]. Erythropoiesis (the production of red blood cells) is regulated by the cytokine erythropoietin (EPO). In iron deficiency, erythroid progenitors lose responsiveness to EPO, resulting in hypoplastic anemia. *In vitro*, the aconitase inhibitor fluorocitrate blocked erythroid differentiation in a manner similar to iron deprivation [66], and infusion of an aconitase inhibitor sodium fluoroacetate in mice caused a rapid-onset hypoplastic anemia [67]. Administration of isocitrate abrogated the eythroid iron restriction response *in vitro* and reversed anemia progression in iron-deprived mice [66]. Taken together, these studies indicated that isocitrate production by ACO2 plays a key role in the regulation of erythropoiesis.

The importance of aconitases was illustrated by studies of animal models and human patients with aconitase deficiency. Oxidative inactivation of aconitase has been associated with decreased life span in flies [28]. Deletion of ACO2 in *Drosophila* was lethal, whereas RNA interference-generated ACO2-knockdown flies showed reduced locomotor activity, a shortened lifespan, and increased cell death in the developing brain [68]. In humans, aconitase deficiency causes infantile cerebellar-retinal disorder (MIM614559) [69, 70]. Homozygosity mapping with exome sequencing in eight patients with severe early-onset neurodegenerative degeneration identified a homozygous S112A mutation in ACO2 (Fig. 10.2).

These patients presented at 2–6 months of age with truncal hypotonia (low muscle tone), athetosis (repetitive involuntary, slow movements in the extremities), seizure disorder, and retinal abnormalities, culminating in profound psychomotor

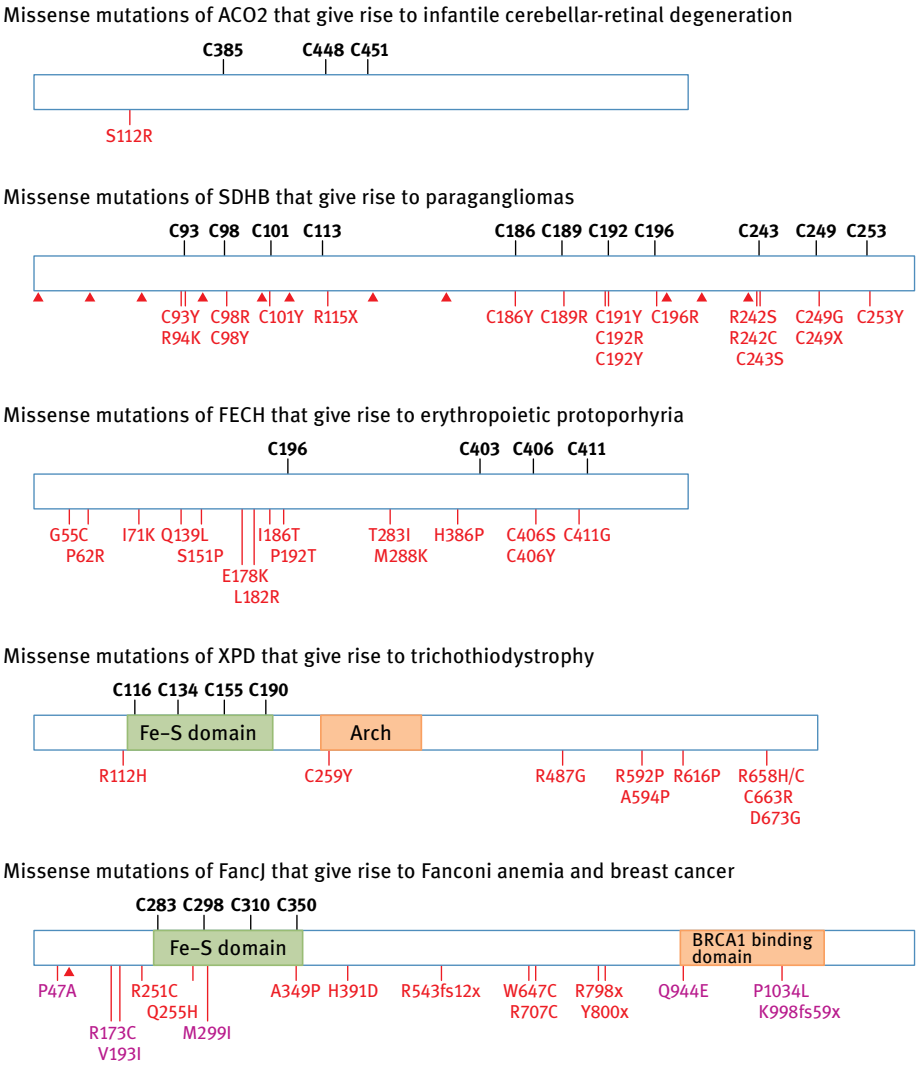

Fig. 10.2: Clinically relevant missense mutations in ACO2 [69], SDHB [131, 133–139], FECH [168, 169, 171], and XPD [607, 608] are indicated in red. The positions of frameshift mutations in SDHB are indicated by red arrowheads [133]. Mutations in FANCJ associated with Fanconi anemia are indicated in red, whereas those associated with breast cancers are indicated in pink [609]. Cysteine ligands of the Fe-S clusters are indicated in black.

retardation. Magnetic resonance imaging (MRI) showed progressive cerebral and cerebellar degeneration. One patient presented with peripheral demyelinating neuropathy. The mutant human ACO2 failed to complement a yeast aconitase deletion strain, indicating that this mutation inactivates the enzyme activity. Sadat *et al.* also described a 2-year-old patient who presented with milder neurodegenerative symptoms, including truncal ataxia, hypotonia, developmental delay, and hearing loss [71]. Whole exome sequencing and functional biochemical assays on patient fibroblasts revealed two missense variants in ACO2 (MIM100850) and showed that defects in cellular respiration and mtDNA depletion are dependent on a decrease in ACO2 activities.

Impairment of aconitase has also been identified in a cancer cell line derived from a patient with hereditary leiomyomatosis and renal cell cancer (HLRCC) [72] that is caused by germline mutations of the TCA cycle enzyme fumarate hydratase (FH) [73–75]. An FH-deficient HLRCC cell line, UOK262, exhibited decreased ACO1 activity, which may be a result of cellular iron limitation that is caused by decreased expression of the divalent metal transporter 1 DMT1 [72] and/or increased oxidative stress [76]. In addition, a proteomic-based screen in renal cysts from FH-deficient mice revealed that the three cysteine residues in ACO2 crucial for Fe-S cluster binding were succinated, suggesting that loss of FH activity resulted in accumulation of intracellular fumarate, which modified cysteine residues to form 2-succinocysteine [77]. *In vitro* experiments confirmed that increased succination by fumarate correlated with loss of ACO2 activity. Loss of aconitase activity may contribute to the dysregulation of cell metabolism that promotes oncogenesis [78].

Oxidative stress can also disrupt intracellular iron homeostasis *via* the disassembly of the Fe-S cluster in IRP1/ACO1 [79]. Given that iron is both essential for basic cellular processes, and toxic through its ability to generate ROS, systemic as well as intracellular iron status is tightly regulated by transcriptional and posttranscriptional mechanisms [80]. IRP1/ACO1 and IRP2 are RNA-binding proteins that play important roles in the posttranscriptional regulation of intracellular iron metabolism (reviewed in [11, 13]). IRP2 is regulated by iron- and oxygen-dependent protein degradation, whereas IRP1 regulation largely depends on the assembly and disassembly of its Fe-S cluster. When IRP1 contains an intact Fe-S cluster, it functions as a cytosolic aconitase; when it lacks the Fe-S cluster, it binds RNA stem-loop structures known as iron-responsive elements (IREs) that are present in a number of genes involved in iron metabolism. The IRE-binding activity of ACO1/IRP1 can be induced by O_2^-, H_2O_2, and NO [81–83] through oxidative disassembly of the Fe-S cluster, and activation of IRP1 by oxidative stress can disrupt iron homeostasis by stimulating iron uptake *via* transferrin receptor 1 (TfR1) and DMT1, reducing iron export *via* ferroportin, and suppressing the iron storage protein ferritin.

10.3 Diseases associated with genetic defects in Fe-S proteins

10.3.1 Mitochondrial respiratory complexes and human diseases

Greater than 70 polypeptides are organized in complexes I–IV of the mitochondrial respiratory chain. Each complex consists of multiple protein components that are associated with a variety of redox-active prosthetic groups, including flavins, Fe-S clusters, ubiquinone, cytochromes, and copper centers that make up the electron transport chain. Genetic defects or oxidative damages of respiratory complexes are associated with a range of clinical conditions (Tab. 10.1) [84–89], some of which have been shown to involve the Fe-S proteins in the respiratory complexes I–III. This section will focus on the diseases associated with the Fe-S protein SDHB in respiratory complex II.

Tab. 10.1: Diseases associated with Fe-S proteins.

Human protein	Function	Pathology
Complex I (NADH: ubiquinone oxidoreductase)	Respiration	Leigh syndrome, cardiomyopathy, encephalopathy, skeletal muscle myopathy [84, 85]
Complex II (succinate dehydrogenase)	Respiration	Encephalomyopathy, cardiomyopathy, skeletal muscle myopathy, Kearns-Sayre syndrome, optic defects, leukoencephalopathy, paraganglioma-pheochromocytoma syndrome, renal cell carcinoma, Carney-Stratakis syndrome [86]
Complex III (ubiquinone: cytochrome c oxidoreductase)	Respiration	Encephalopathy, hypoglycemia, Leigh syndrome, Leber hereditary optic neuropathy, Bjornstad syndrome, lactic acidosis, skeletal muscle myopathy, hepatic failure [87]
Electron transfer flavoprotein-ubiquinone oxidoreductase (ETFDH)	Fatty acid and amino acid oxidation	Multiple acyl-CoA dehydrogenation deficiency/type II glutaric acidemia [598]
Ferrochelatase (FECH)	Last step in heme biosynthesis	Erythropoietic protoporphyria: light-sensitive dermatitis [162]
Iron regulatory protein 1/cytosolic aconitase (IRP1/ACO1)	Sensing and regulation of cellular iron homeostasis	ACO1-/- mice develop polycythemia and pulmonary hypertension [599, 600]
Mitochondrial aconitase (ACO2)	TCA cycle	Infantile cerebellar-retinal disorder; hypotonia, athetosis, seizures, retinal abnormalities, psychomotor retardation [69–71]

Tab. 10.1 Continued

Human protein	Function	Pathology
Dihydropyrimidine dehydrogenase (DPYD)	Pyrimidine degradation	Thymine-uraciluria; convulsive disorder with motor and mental retardation [601]
Lipoic acid synthase (LIAS)	Biosynthesis of lipoic acid cofactor for PDH, OGDH, and glycine-cleavage system	Neonatal-onset encephalopathy, epilepsy, psychomotor retardation hypotonia, lactic acidosis, elevated glycine concentrations in plasma and urine [213]
Molybdenum cofactor synthesis 1 (MOCS1)	Biosynthesis of cofactor for aldehyde oxidase, xanthine dehydrogenase and sulfite oxidase	Molybdenum cofactor deficiency: neonatal seizures, fatal neurological abnormalities [218]
Xanthine dehydrogenase/ xanthine oxidase (XDH)	Oxidative metabolism of purines	Xanthinuria: renal failure and xanthine kidney stones [602]
Xeroderma pigmentosum group D (XPD)	DNA repair helicase	Xeroderma pigmentosum, trichothiodystrophy, Cockayne syndrome [174]
Fanconi anemia group J (FANCJ or BRIP1)	DNA repair helicase	Fanconi anemia, breast cancer [174]
RTEL1	Helicase, regulation of telomere length	Hoyeraal-Hreidarsson syndrome [603–605]
CHLR1	Helicase, sister chromatid cohesion, heterochromatin organization	Warsaw breakage syndrome [188, 189]
MutY homolog (MUTYH)	DNA repair glycosylase	Colorectal cancer [185]
DNA Polymerase delta subunit 1 (POLD1)	DNA replication and repair	Mandibular hypoplasia, deafness progeroid features and lipodystrophy (MDPL) syndrome, atypical Wener syndrome, early-onset colorectal cancer, endometrial cancer (reviewed in [232])

10.3.1.1 Diseases associated with complex II deficiencies

As complex II of the respiratory chain, SDH (succinate: ubiquinone oxidoreductase, EC 1.3.5.1) [90] is situated at the intersection of the TCA cycle and the mitochondrial respiratory chain, two pathways essential for energy production and anabolic processes. SDHA and SDHB encode the two catalytic subunits that project into the mitochondrial matrix, whereas SDHC and SDHD encode the membrane anchors in the mitochondrial inner membrane. The substrate succinate binds to the flavoprotein SDHA, and electrons from the oxidation of succinate to fumarate are channeled through three Fe-S clusters in SDHB to the ubiquinone site associated with SDHC and

SDHD. Major insights into the workings of human complex II have been provided by crystal structures, mutagenesis studies, and biophysical studies (EPR and magnetic circular dichroism [MCD] spectroscopies) of closely related enzymes in several species [91–96]. More recent studies also revealed a number of dedicated factors that assist the assembly of complex II by facilitating the delivery and insertion of the FAD and Fe-S cofactors and stabilizing assembly intermediates [97, 98].

Loss of complex II function leads to a range of clinical conditions [86, 98, 99, 100, 101]. Generally speaking, enzyme depletion and mutations in SDHA compromise TCA cycle activities and energy production, resulting in early-onset encephalopathy, whereas heterozygous mutations in SDHB, SDHC, and SDHD induce later-onset paraganglioma syndromes. Several biallelic SDHA mutations have been shown to cause Leigh syndrome, a rare severe neonatal neurological disorder [102]. Congenital complex II deficiencies due to inherited homozygous mutations of SDHA, SDHB, and the SDHAF1 assembly factor also lead to cardiomyopathy and infantile leukodystrophies (inflammation in the white matter of the brain). Heterozygous mutations/deletions of SDHB, SDHC, or SDHD result in increased risk for autosomal dominant tumor syndromes. These patients have a loss-of-function mutation in one of the germline copies of an SDH subunit gene. When the second, intact copy is somatically lost or mutated in particular tissues, tumors develop. SDHD mutations are associated with mostly benign paragangliomas and phaeochromocytomas, whereas SDHB mutations are associated with a higher proportion of malignant lesions and a greater risk of phaeochromocytoma [103]. Renal cell carcinoma (in patients with SDHB mutations) and gastrointestinal stromal tumors (GISTs) (in patients with SDHB, SDHC, and SDHD mutations) affect a minority of patients. Loss of complex II can promote tumorigenesis through several processes, including the activation of hypoxia inducible factor (HIF) as a result of succinate accumulation [104], the generation of ROS [105], the inhibition of histone demethylases [106], and the inhibition of EglN3-mediated apoptosis [107].

Cellular and animal models have provided valuable insights into the diseases associated with mutations in SDH. Homozygous deletion of SDHD in mice is embryonic lethal, underscoring the essential role of SDH in energy production [108, 109]. Several models of complex II mutations have increased ROS production and increased sensitivity to oxidative stress [110, 111]. Mutations in the ubiquinone-binding site in *S. cerevisiae* SDH promote O_2^- production [112]. Transgenic flies expressing a dominant-negative form of SDHC (I71E) [113] and a P-element insertion mutant with reduced expression of SDHB [114] exhibit hypersensitivity to oxygen, reduced lifespan, and age-related behavioral decay. Transgenic mice with a V69E mutation in SDHC have respiratory dysfunction, increased O_2^- levels in the mitochondria of their hearts and muscles, abnormal mitochondrial structures in muscles, decreased body weight and locomotion activity, and infertility [111]. Knockdown of SDHB in mammalian cells produce features of tumor phenotypes, with alterations in cellular proliferation and respiration, a metabolic shift to glycolysis, and changes in the expression levels of many genes involved in proliferation, adhesion, and the hypoxia pathway [115].

In addition to increasing oxidative stress, there is mounting evidence that points to the hyperactivation of the hypoxia-response pathway as a major cause of tumorigenesis in individuals with SDH mutations. Mammalian cells respond to changes in oxygen availability through a conserved pathway that is regulated by HIF [116]. HIF is a heterodimer composed of HIF-1α (or HIF-2α) and HIF-1β. In normoxia, HIF-1α and HIF-2α are hydroxylated at a proline residue by HIF prolyl hydroxylases (PHD1–3) and targeted for degradation by the proteasome [117, 118]. Pathological stabilization of HIFα can initiate the transcription of many genes, including those that encode vascular endothelial growth factor (VEGF), transforming growth factor, phosphoglycerate kinase, lactate dehydrogenase A, and EPO, thereby fueling tumorigenesis by promoting angiogenesis, proliferation, and changes in energy production [116, 119]. Mutations in *SDH* have been shown to induce the hypoxia-response pathway in tumors [120]. In particular, paragangliomas and extra-adrenal phaeochromocytoma from patients with the SDHD R22X mutation or R46Q SDHB mutation showed increased expression of VEGF [121, 122], whereas cells depleted of SDH using siRNA have increased succinate levels, overexpression of HIF-1α, and activation of HIF-1α target VEGF [75, 104]. Mass spectrometric analysis and *in vitro* assays confirmed that succinate can bind and inhibit PHD [123]. These studies indicate that accumulation of succinate due to SDH deficiency results in stabilization of HIF and that pseudohypoxia promotes tumorigenesis in patients with SDH deficiency.

10.3.1.2 Mutations in SDHB, an Fe-S protein, in paraganglioma-pheochromocytoma syndrome, renal cell carcinoma, Carney-Stratakis syndrome/GIST, and infantile leukoencephalopathy

10.3.1.2.1 Paraganglioma-pheochromocytoma syndrome

SDHB mutation carriers are prone to developing extra-adrenal paragangliomas, adrenal pheochromocytomas, or head and neck paragangliomas (Fig. 10.2) [124]. Paragangliomas are neuroendocrine neoplasms that originate from both the sympathetic and parasympathetic branches of the autonomic nervous system and may develop at various body sites, including the head, neck, thorax, and abdomen. Mutations of *SDHA*, *SDHB*, *SDHC*, *SDHD*, and SDH assembly factor 2 (*SDHAF2*) have been identified in familial head and neck paragangliomas [125–130]. A type of paraganglioma known as a pheochromocytoma develops in the adrenal glands, and mutations of *VHL*, *RET*, *NF1* (gene 17 neurofibromatosis type 1), *SDHB*, and *SDHD* are associated with familial pheochromocytoma. Around 20% of *SDHB* mutation carriers will develop metastatic disease [131, 132]. To date, more than 100 pathological genetic defects in *SDHB* have been reported in paraganglioma-pheochromocytoma syndrome (TCA cycle gene mutation database [133]), including mutations of 10 of the 11 cysteine ligands of the three Fe-S clusters in SDHB [131, 134–139]. In addition to mutations of the cysteine ligands, nonsense and frameshift mutations, deletions, or splicing defects can result

in the loss of one or more Fe-S cluster domains. Missense mutations close to the Fe-S binding sites can also potentially affect the binding and stability of the Fe-S clusters. For instance, paraganglioma patients have been reported to carry a c.281G>A mutation, which results in the substitution of a highly conserved R94 that is adjacent to a putative cysteine ligand for an Fe-S cluster in SDHB [140].

10.3.1.2.2 Renal cell carcinoma

Kidney cancer is a heterogeneous disorder, currently associated with mutations of 12 different genes (*VHL*, *MET*, *FLCN*, *TSC1*, *TSC2*, *TFE3*, *TFEB*, *MITF*, *FH*, *SDHB*, *SDHD,* and *PTEN*). A hereditary kidney cancer syndrome caused by *SDHB* mutation was initially reported by Vanharanta *et al.* [128] and was subsequently identified in individuals with or without a personal or family history of paraganglioma and/or pheochromocytoma [103, 141–145].

10.3.1.2.3 Carney-Stratakis syndrome/GIST

GISTs are rare mesenchymal tumors of the gastrointestinal tract, mostly associated with activating mutations in KIT (CD117) or platelet derived growth factor A (*PDFRA*) [146]. The Carney-Stratakis syndrome is a very rare subset of pediatric GIST, with a co-occurrence of GIST and familial paraganglioma, with characteristic decreased SDHB immunostaining [147]. Germline mutations in the *SDHB, SDHC*, and *SDHD* genes have been found in a number of these patients [148], although reduced SDHB protein levels have also been observed in GIST tumors without identifiable *SDH* mutations [149].

10.3.1.2.4 Infantile leukoencephalopathy

Leukoencephalopathies are a group of disorders characterized by degeneration of the white matter of the brain. The disorders arise during infancy or childhood, with progressive loss in body tone, movements, gait, speech, vision, hearing, and behavior, leading to premature death. A novel homozygous mutation in the *SDHB* gene (D48V) was recently observed in a specific infantile leukoencephalopathy [150]. The patient presented with hypotonia and leukodystrophy (degeneration of myelin) with elevated brain succinate levels. Patient fibroblasts showed decreased levels of fully assembled complex II and near-complete absence of the SDHB subunit. A muscle biopsy showed markedly reduced SDHB protein levels and complex II activity. This represents the first description of a homozygous SDHB mutation in any patient. Studies of the equivalent mutation in yeast showed only 50% reduction in SDH activity, consistent with the idea that only mutations with relatively mild effects on the catalytic functions of SDH can occur in a homozygous state.

10.3.2 FECH deficiency causes erythropoietic protoporhyria (MIM 177000)

FECH (E.C. 4.99.1.1) is the terminal enzyme of the heme biosynthetic pathway, catalyzing the insertion of Fe^{2+} into protoporphyrin IX (PPIX) to form heme [151]. Mammalian FECH contains a labile [2Fe-2S] cluster, similar to those found in 2Fe ferredoxins (FDXs), as judged by variable-temperature MCD, Mössbauer, and EPR

studies [152, 153]. However, no redox role has been found for the cluster in FECH. The cluster is essential for the function of human FECH [154], but the cluster does not participate directly in enzymatic catalysis, since FECHs in many organisms do not possess the cluster. The purified protein exhibited reduced stability under oxidative conditions [152, 155], and, in cultured cells, FECH is degraded during conditions of iron deficiency or oxidative stress [44, 156]. A set of pulse/chase experiments following the levels of the transcripts, newly-synthesized and steady-state levels of FECH protein demonstrated that iron limitation diminishes FECH levels by decreasing the stability of newly formed FECH protein [44]. FECH was also severely depleted in muscle biopsies and cultured myoblasts from patients with ISCU myopathy, a disease caused by deficiency of the scaffold protein ISCU that is essential for Fe-S cluster assembly [44]. Taken together, these data suggest that oxidative degradation of the Fe-S cluster or impaired Fe-S cluster assembly causes reduced maturation and destabilization of apo-FECH. Crystallographic studies revealed a stabilizing bridge formed by the Fe-S cluster between the three C-terminal cysteines and a fourth internal cysteine, suggesting that the cluster-ligating C-terminal region of the protein is important for folding of the mature enzyme and its protection from proteolysis [157, 158].

Erythropoietic protoporhyria (EPP) is an autosomal recessive disorder resulting from mutations in the FECH gene that reduce the activity of FECH, leading to the accumulation of the enzyme substrate PPIX. The disorder is characterized clinically by painful photosensitivity to visible light [159] and biochemically by the accumulation of PPIX in bone marrow reticulocytes, liver, bile, and skin [160–162]. In ~5% of the patients, protoporphyrin deposits cause liver disease that may progress to liver failure caused by biliary occlusions of crystalline protoporphyrin [163, 164]. Hemolysis and anemia are usually absent or mild. A mouse model for EPP harboring homozygous FECH M98K mutation exhibited low FECH activity (3%–6%), hemolytic anemia, photosensitivity, cholestasis, and severe hepatic dysfunction [165, 166].

EPP patients often show a 70%–95% loss in FECH activity [160, 164], which usually results from the inheritance of a nonfunctional mutated *FECH* allele together with a low-expressing wild-type *FECH* allele [167]. Exon deletions are a common cause of the nonfunctional *FECH* alleles [168, 169]. Individual deletions of exons 3 through 11 all resulted in proteins that failed to acquire the Fe-S cluster and lost enzyme activity [170]. It was suggested that with cluster ligands spanning the entire length of the protein, exon skipping may affect the ability of the protein to properly assume its native conformation with an intact Fe-S cluster. Subsequent studies revealed that three EPP patients had point mutations of the [2Fe-2S] cluster ligands, firmly establishing the importance of the Fe-S cluster in the stability and function of FECH (Fig. 10.2) [171].

10.3.3 DNA repair Fe-S proteins and human disorders

Many studies have indicated that the postmitotic neurons are particularly prone to accumulation of unrepaired DNA lesions, and deficiency in the repair of nuclear and

mitochondrial DNA damages has been linked to several neurodegenerative disorders [172, 173]. Nucleotide excision repair removes helix-distorting DNA damage, and deficiency in such repair is found in Xeroderma pigmentosum (XP) and Cockayne syndrome [174]. Mismatch repair corrects base mispair generated during replication and oxidative DNA damage and is linked to the trinucleotide repeat expansion in Huntington's disease [175]. Single-strand DNA breaks are associated with the neurodegenerative diseases, ataxia-oculomotor apraxia-1 [176] and spinocerebellar ataxia with axonal neuropathy [177]. Defects in homologous recombination and nonhomologous end-joining for repairing DNA double-strand breaks are associated with Ataxia telangiectasia [178]. Accumulation of oxidative mitochondrial DNA (mtDNA) damage has also been linked to the age-associated neurodegenerative disorders Alzheimer's disease [179] and ALS [180].

Fe-S clusters are present in DNA repair glycosylases of the EndoIII/MutY family [181], in the family 4 uracil DNA glycosylases [182], and in DNA helicases XPD and FANCJ [5, 6]. In MutY DNA glycosylase, the Fe-S cluster is thought to position a peptide loop that is important for DNA binding [183]. It has also been suggested that these DNA repair proteins detect DNA lesions through electron transfer *via* their Fe-S clusters [184]. Fe-S cluster DNA helicases, including XPD and FANCJ, unwind DNA and allow access to single-stranded DNA during DNA replication, repair, and recombination and RNA transcription. The observations that the Fe-S domain is found in a variety of helicases with different functions suggest that the role of the Fe-S cluster is not to detect specific forms of DNA damages. Structural studies of XPD and XPD homologues and characterization of Fe-S cluster site-directed mutants suggested that the integrity of the Fe-S domain is required for the proper folding and structural stability of the enzymes [5, 6].

Mutations in Fe-S cluster DNA repair enzymes have been shown to cause diseases in human patients and in animal models. MUTYH glycosylase is a component of a base excision repair system that protects the genome from oxidative damage. Bi-allelic germline mutations of *MUTYH* are linked to the mutation of cancer-related genes *APC* and *KRAS* in an autosomal-recessive colorectal cancer syndrome [185]. Mutations that affect the formation or stability of the Fe-S cluster in XPD and FANCJ have been implicated in trichothiodystrophy (TTD) and Fanconi anemia, respectively [5]. Other members of the XPD helicase family, RTEL (regular of telomere length) and ChlR1, also possess four conserved cysteine residues analogous to the cysteinyl ligands of the Fe-S clusters in XPD and FANCJ. RTEL1 mutations have been implicated in Hoyeraal-Hreidarsson syndrome, a severe form of dyskeratosis congenital, which is characterized by cerebellar hypoplasia, severe immunodeficiency, bone marrow failure, and predisposition to cancer [186] RTEL-knockout mice died during gestation, with defects in the nervous system, heart, vasculature, and extra-embryonic tissues as a result of telomere loss and genomic instability [187]. Biallelic mutations in the ChlR1 are associated with Warsaw breakage syndrome, which is characterized by microcephaly and prenatal and postnatal growth retardation [188, 189]. Human ChlR1 interacts with the

cohesin complex, and deletion of the mouse gene causes lethality due to defects in chromosome segregation, chromosome cohesion, and placental malformation [190].

10.3.3.1 Mutations in XPD in XP, TTD, and combined XP with Cockayne's syndrome

The XPD/Rad3 helicase family comprises a group of related superfamily 2 DNA helicases with a 5′ to 3′ directionality [191]. In eukaryotes, XPD functions as part of the transcription factor IIH (TFIIH) complex, which has a dual role in transcription initiation and nucleotide excision repair. Mutations in the *XPD* gene give rise to three different genetic conditions in humans – XP, TTD, and combined XP with Cockayne's syndrome (XP/CS) – with a wide spectrum of symptoms [192]. XP is characterized by extreme light sensitivity and highly elevated rates of skin cancer as a result of reduced repair of UV photoproducts in DNA. Mutations causing XP are thought to disrupt XPD helicase activity while preserving the role of TFIIH in transcription initiation. In contrast, TTD mutations cause developmental and growth abnormalities but typically do not result in elevated cancer rates. These symptoms are thought to arise due to defects in both nucleotide excision repair and DNA transcription initiation. Defective transcription probably prevents cells from becoming cancerous, explaining the distinction between XP and TTD. TTD mice exhibit many symptoms of premature aging, including osteoporosis and kyphosis, osteosclerosis, early greying, cachexia, infertility, and reduced life-span [193]. XP/CS is a rare disease characterized by segmental progeria (premature aging) in which both transcription and repair are defective. Four XPD mutations that give rise to XP/CS are known: G47R, G602D, R666W, and G675R [194]. Mouse models for XP/CS harboring the XPD G602D mutation exhibited cancer predisposition and symptoms of segmental progeria, including cachexia (loss of body mass) and progressive loss of germinal epithelium [195].

The presence of an Fe-S cluster in a DNA helicase was first demonstrated when the *XPD* homologue from *Sulfolobus acidocaldarius* was cloned and overexpressed in *E. coli* [5]. The Fe-S cluster binding domain is not important for the stability, binding of single-stranded DNA substrate, or ATPase activity of the enzyme but is essential for collaborating with the Arch domain for DNA strand displacement during helicase action [5, 196, 197]. The abolition of Fe-S cluster binding by mutagenesis of a conserved cysteine in yeast Rad3 resulted in loss of Rad3 activity and a severe UV-sensitive phenotype [5]. Structural, mutational, and biophysical studies suggested that the TTD mutation in XPD, R112H [198, 199], inactivates the helicase activity by disrupting the Fe-S cluster [5] (Fig. 10.2).

10.3.3.2 Mutations in FANCJ in Fanconi anemia

Fanconi anemia is a clinically and genetically heterogeneous disorder that causes genomic instability in about 1 in every 100,000 births [200, 201]. Biallelic mutations in Fanconi anemia genes lead to developmental abnormalities in major organs,

early-onset bone marrow failure, predisposition to acute myeloid leukemia (AML) and solid tumors, congenital abnormalities, and infertility. So far, 15 genes have been identified as mutated in patients, and many more interacting genes have been discovered [201]. These proteins work together in the repair of deleterious interstrand DNA crosslinks, and are important in maintaining genomic stability during DNA replication. On detection of a DNA crosslink, the core complex that comprises FANCA, FANCB, FANCC, FANCE, FANCF, FANCG, FANCL, and FANCM and accessory proteins, including FAAP20, FAAP24, and FAAP100 is activated and ubiquitinates the FANCI-FANCD2 complex, which then coordinates the action of downstream repair factors. SLX4 (also known as FANCP) interacts with multiple nucleases that make incisions at the site of DNA damage. FAN1 and SNM1A have a role in processing the crosslink after incision, whereas TLS polymerases (TLS Pol) are recruited to bypass the unhooked crosslink. The break is then repaired through homologous recombination by the Fanconi anemia proteins BRCA2, BRIP1, PALB2, and RAD51C. BRIP1 (also known as FANCJ) is implicated in homologous recombination but is also required at an earlier step for pathway activation.

Several clinically relevant mutations map close to the Fe-S cluster domain of FANCJ (Fig. 10.2) [5, 202]. FANCJ not only plays a role in DNA cross-link repair pathway [202–205] but also interacts with the breast cancer susceptibility protein BRCA1 and has a role in double-strand break repair [206]. A Fanconi anemia-associated mutation, A349P, reduced FANCJ enzyme activity, and A349 is positioned next to one of cysteine ligands (C350) of the Fe-S cluster in human FANCJ [202, 207]. Mutation of the equivalent residue in archaeal XPD (F136P) appeared to disrupt the hydrogen bond between the main-chain nitrogen and Fe ion ligand C137, resulting in the destabilization of the Fe-S cluster and a loss of helicase activity, suggesting that the A349P mutation of human FANCJ probably causes Fanconi's anemia by disrupting the Fe-S cluster binding domain [5]. The breast-cancer-associated M299I mutant has enhanced ATPase, helicase, and translocase activities [208], and M299 is positioned next to another cysteine ligand (C298) of the Fe-S cluster in human FANCJ (Fig. 10.2).

10.3.4 Diseases associated with genetic defects in radical S-adenosylmethionine enzymes

The radical SAM superfamily of enzymes contains [4Fe-4S] cluster cofactors that share the ability to catalyze a reductive cleavage of SAM to methionine and a high-energy 5-deoxyadenosyl radical (5′-dA•), which initiates catalysis of an array of complex and chemically challenging reactions by abstracting specific hydrogen atoms from enzyme-bound substrates [209]. Bioinformatics analysis and biochemical studies indicate that there are eight radical SAM enzymes in humans, and these metalloproteins are involved in the biosynthesis of the lipoyl and molybdopterin cofactors,

which are vital for cellular metabolism, modifications of tRNAs that are important for translation fidelity, and other reactions that have not been defined. Mutations or pathological conditions that damage or inhibit the assembly of the Fe-S clusters in these enzymes result in a variety of diseases (reviewed in [210]).

LIAS contains two [4Fe-4S] clusters, both essential for catalysis. One cluster is bound by cysteines in a canonical radical SAM Cx3Cx2C motif and participates in the reductive cleavage of SAM, whereas a second auxiliary cluster is used as a sacrificial source for the two sulfur atoms that are inserted at C6 and C8 of an octanoyl chain covalently attached to a specific lysine residue of a lipoyl carrier protein [211, 212]. LIAS catalyzes the formation of the covalently bound lipoyl cofactor in two enzymes that are essential for oxidiative metabolism, pyruvate dehydrogenase complex (PDHc) and α-ketoglutarate dehydrogenase complex, and three involved in amino acid metabolism pathways, branched-chain ketoacid dehydrogenase, 2-oxoadipate dehydrogenase, and glycine cleavage system. Deficiencies in LIAS are marked by neonatal-onset encephalopathy, epilepsy, psychomotor retardation hypotonia, lactic acidosis, and elevated glycine concentrations in plasma and urine [213, 214]. Four mutations in LIAS that result in reduced or nondetectable levels of lipoylated proteins and severe disease states have been reported [215, 216]. Defects in NFU1, a protein involved in Fe-S cluster biosynthesis, have also been implicated in inadequate lipoyl cofactor production, resulting in decreases in PDHc and GCS activities, lactate acidosis, elevated glycine levels, neurological impairment, respiratory failure, and shortened lifespan (see Section 10.4.6).

The radical SAM enzyme MOCS1 catalyzes the formation of cyclic pyranopterin monophosphate (cPMP) from 5′GTP in the first step of the biosynthetic pathway that generates molybodpterin, the precursor of molybdenum cofactor (MoCo) [217]. MoCo deficiency is a rare severe inherited inborn error (incidence below 1:100,000) that results in the pleiotropic loss of MoCo-dependent enzymatic activities, severe neurodegeneration in newborns, and early childhood death. MoCo deficiency (MIM 252150) is associated with the triple deficiency of sulfite oxidase (SO), xanthine oxidoreductase (XOR), and aldehyde oxidase (AO), due to the defective synthesis of the MoCo for all three enzymes [217, 218]. In particular, the enzyme SO catalyzes the oxidation of sulfite to sulfate, which protects the brain and other organs from elevated levels of toxic sulfite, which is formed upon degradation of sulfur-containing amino acids and sulfo-lipids, and the loss of SO activity leads to sulfite accumulation and sulfate deficiency, causing seizures, brain degradation, and loss of white matter in patients [219, 220]. XOR is the key enzyme of purine degradation, oxidizing hypoxanthine to xanthine and xanthine to uric acid in the cytosol. AO is a cytosolic enzyme that catalyzes the oxidation of a variety of aromatic and nonaromatic aldehydes to their corresponding carboxylic acids, but the physiological function of human AO remains unclear.

Among the key mutations leading to pathogenesis in MoCo-deficient patients, several are thought to diminish the ability of MOCS1 to ligate its Fe-S clusters [210]. A splice-site mutation, 418+1G→A, results in the exclusion of exon 2 that eliminates

two of the three cysteine residues comprising the canonical radical SAM Fe-S cluster binding motif, thereby rendering the enzyme inactive. Another splice-site mutation, 1102+1G→A, results in the omission of exon 8 and, therefore, loss of Cys329 and loss of the auxiliary [4Fe-4S] cluster. The G324R substitution is thought to cause conformational changes in the C-terminal region of the protein, resulting in the inability to ligate the auxiliary [4Fe-4S] cluster. A therapy for MoCo deficiency using cPMP has been developed [221].

Radical SAM enzymes that act on mammalian tRNAs include CDK5RAP1, CDKAL1, TYW1, and ELP3 [222]. Modifications of tRNAs are important for tRNA folding and stability and in maintaining high translational fidelity, and mutations in radical SAM-dependent tRNA modifying proteins have been associated with a number of human diseases [210]. CDK5RAP1 catalyzes 2-methylthio (ms^2) modification of four mitochondrial tRNAs. A decrease in ms^2 modification levels has been observed in patients who carry the A3243G mutations in their mtDNA and present with mitochondrial myopathy, encephalopathy, lactic acidosis, and stroke-like episodes (MELAS). Since Cdk5rap1 contains a highly oxidation-sensitive [4Fe-4S] cluster [223], Wei *et al.* suggested that oxidative stress that originated from mutant mitochondria oxidizes the [4Fe-4S] cluster and inactivates Cdk5rap1, resulting in the decrease in ms^2 modification level in MELAS patients [224].

ELP3 is the catalytic subunit of Elongator, a hexaheteromeric protein complex that was first identified by its association with an RNA polymerase II holoenzyme that engages in transcriptional elongation and later shown to be important for histone acetylation and transcription [225]. However, most Elongator complex is cytoplasmic, and subsequent data indicated a role of cytosolic ELP3 in tRNA modification, catalyzing the formation of 5-methoxycarbonylmethyl (mcm5) uridine in humans [226]. Greenwood *et al.* showed that the Fe-S cluster in ELP3 from *S. cerevisiae* is not necessary for histone acetyltransferase or RNA binding activities, but rather that an intact Fe-S cluster in ELP3 is required for Elongator integrity and for the association of the complex with its accessory factors [227]. In contrast, a more direct role for the Fe-S cluster in the modification of wobble position uridines of tRNA was supported by the studies of ELP3 from *Methanococcus internus* [228]. Assays using deuterium labeled acetyl-CoA resulted in deuterium enrichment in 5′-dA, indicating that the reaction occurs *via* a 5′-dA• intermediate.

Recent studies suggested that the Elongator complex plays crucial roles in nerve cell growth, cone motility, axon outgrowth, and guidance [229], and loss of Elongator complex is associated with a number of neurological disorders. The ELP1 subunit of Elongator is encoded by a gene that is mutated in patients suffering from the severe hereditary sensory and autonomic neurodevelopmental disorder familial dysautonomia (FD), and the amounts of ELP3 and Elongator complex are significantly reduced in fibroblasts from FD patients [229]. ALS, commonly known as Lou Gehrig disease, is an adult-onset progressive neurodegenerative disease. Rapid degeneration of motor neurons in the brain and spinal cord leads to spasticity, muscle

atrophy, and twitching, with survival time ranging from 3 to 5 years after symptoms appear. Studies on ALS patients showed that ELP3 expression levels were lower than in healthy individuals [230]. The authors suggested that lower expression levels of ELP3 may result in decreased transcription of heat shock protein 70 and diminished motor neuron protection. A subsequent study of a *Drosophia* model suggested that decreased acetylation of cytomatrix at the active zone-associated structural protein by ELP3 may lead to disruption of synaptic transmission regulation and the development of ALS and FD [231].

10.3.5 DNA polymerase delta 1 (POLD1) in mandibular hypoplasia, deafness, progeroid features, and lipodystrophy (MDPL) and cancer

The DNA polymerases are divided into seven families based on sequence homology and crystal structure analysis. Polδ, Polα, and Polε are members of Family B polymerases and are the main polymerases involved with nuclear DNA replication. The gene polymerase delta 1 (*POLD1*) encodes the large catalytic subunit of Polδ complex (reviewed in [232]). Binding of a [4Fe-4S] cluster in the yeast homologue of POLD1 in *S. cerevisiae* was shown to be essential for its interaction with other subunits in yeast Polδ [7] and the insertion of the Fe-S cluster is mediated by the CIA1-CIA2B/FAM96B-MMS19 complex [233, 234]. In addition to being essential for replication, Polδ is also important for DNA repair, including nucleotide excision repair, double-strand repair, base excision repair, and mismatch repair. Studies in the past decade have revealed that mutations in Polδ in mice and humans lead to genomic instability and tumorigenesis. Germline mutations in POLD1 have been found in patients with MDPL (MIM615381), a very rare disease characterized by a progressive lipodystrophy with loss of subcutaneous adipose tissue, mandibular hypoplasia, deafness, and progeria [232]. It has been speculated that these mutations lead to increased incidence of stalled replication forks, therefore increasing genomic instability, cell senescence, and cell death. Mutations in POLD1 have also been found in many human cancer cell lines and reported to be associated with oligo-adenomatous polyposis, early-onset colorectal cancer, and endometrial cancer (reviewed in [235]).

10.3.6 CDGSH iron sulfur domain (CISD) proteins

The CDGSH iron sulfur domain (CISD) proteins are a recently discovered class of [2Fe-2S] proteins (reviewed in [236]). CISD1 encodes the protein MitoNEET, named for its location in the outer mitochondrial membrane and for containing the amino acid sequence Asn-Glu-Glu-Thr (NEET), which shares a [**C**-X-C-X2-(S/T)-X3-P-X-C-**D**-**G**-(**S**/A/T)-H) domain with two human paralogues, CISD2 (also known as Miner1, NAF-1, ERIS, Noxp70) and CISD3 (Miner2). Crystal structures and biophysical studies of the soluble regions of

MitoNEET and CISD2/NAF-1 showed that these proteins are homodimers coordinating two redox-active [2Fe-2S] cluster with an unusual (Cys)3His1 coordination [237–242]. Unlike the FDX-type [2Fe-2S] clusters, where each Fe is bound to two cysteine sulfur atoms in a (Cys)2FeS2Fe(Cys)2 configuration, or Rieske-type, where one Fe ion is bound to two cysteine sulfur atoms and the other Fe is bound to the Nδ atoms of two histidine ligands in a (His)2FeS2Fe(Cys)2 configuation, CISD Fe-S clusters are unusual with a (Cys)(His)FeS2Fe(Cys)2 configuration. The His ligand is important for enabling cluster release and for tuning the redox potential [241, 243, 244].

MitoNEET was first identified as an interacting protein for pioglitazone, a member of the thiazolidinedione class of insulin-sensitizing drugs that are used extensively in the treatment of type 2 diabetes [245]. Subsequent studies showed that binding of pioglitazone stabilizes the protein against Fe-S cluster release [237]. In addition, cluster stability is controlled by the oxidation state: the reduced cluster is relatively stable, whereas the oxidized cluster is more labile [246]. The unusual coordination and cluster lability have prompted the suggestion that CISD proteins function as cluster assembly, storage, or shuttling agents [237]. It has been shown that mitoNEET is capable of transferring its Fe-S cluster to apo-acceptor proteins, including FDX [247, 248] and IRP1 [249], and both mitoNEET and CISD2 can transfer their 2Fe-2S clusters to apo-Anamorsin (also known as cytokine induced apoptosis inhibitor-1; CIAPIN-1) [250]. The observation of increased mitochondrial iron levels upon addition of purified NEET proteins to permeabilized cells was used to support the hypothesis that mitoNEET mediates the transfer of Fe-S cluster or iron into the mitochondria [236, 247]. However, the physiological relevance of these findings is still unclear.

CISD1 and CISD2 have been implicated in a diverse array of biological processes, including autophagy, apoptosis, aging, diabetes, and reactive oxygen homeostasis and are implicated in human diseases including cancer, diabetes, cystic fibrosis, Wolfram syndrome (WFS) 2, neurodegeneration, and muscle atrophy [245, 251–256]. WFS (MIM 222300) is an autosomal recessive disorder with severe neurodegeneration. Neurological and endocrine manifestations include juvenile-onset diabetes mellitus, optic atrophy, deafness, dementia, psychiatric illnesses, and renal-tract abnormalities. Patients with WFS2 have additional symptoms such as significant bleeding tendencies, as well as defective platelet aggregation with collagen. A single missense mutation was identified in CISD2 in three consanguineous families of Jordanian descent with WFS2 [252, 257]. A G to C change at nucleotide 109 disrupts mRNA splicing and eliminates exon 2, resulting in the introduction of a premature stop codon [252]. A second CISD2 mutation was reported in two sisters in an Italian family [258]. A G to A change at position 103 + 1 predicted the skipping of exon 1 in CISD2. Recent studies have also shown a link between CISD1 and CISD2 expression and proliferation of various cancer cells [255, 259]. CISD1 and CISD2 expressions were upregulated in human epithelial breast cancer cell lines, and knockdown of these proteins resulted in decreased cancer cell proliferation and decreased tumor growth [255]. CISD2 was also upregulated in cervical cancer cells and hepatocellular carcinoma cell lines

[260–262]. Overexpressing CISD2 promoted, while suppressing CISD2 expression inhibited, proliferation and tumorigenesis of liver and gastric cancer cells *in vivo*, suggesting a role for CISD2 in cancer progression [261, 262].

The exact roles of CISD proteins in diabetes, neurodegeneration, and cancer are still unclear. A screen to identify molecular markers for early neuronal development found the mRNA coding for CISD2 (Noxp70) was strongly expressed at embryonic day 15 [263]. CISD2 is located on the endoplasmic reticulum (ER) and the mitochondrial-associated membrane of the ER [264]. Notably, the main locus mutated in the majority of WFS patients encodes a transmembrane protein WFS1 that is located in the ER [265]. The exact function of WFS1 is unknown, but there is some evidence that it may play a role in Ca^{2+} homeostasis [266, 267]. Various studies have suggested that CISD2 is necessary for the control of Ca^{2+} homeostasis and the activation of autophagy through interaction with BCL-2 [254]. In the absence of CISD2, the autophagy-promoting Beclin1 complex dissociates from BCL-2, and autophagy is activated [256]. Knockout of CISD2 in mice led to impaired glucose tolerance, premature aging, severe neurodegeneration, blindness, muscle atrophy, and significantly shortened lifespan, suggesting that CISD2 is important for the maintenance of multiple organ systems, including the pancreas, skin, musculoskeletal, and nervous systems [253]. Fibroblasts from CISD2 knockout mice exhibit signs of ER stress, increased unfolded protein response, dysregulation of ER and mitochondrial Ca^{2+} homeostasis, and increased oxidative stress [264]. CISD2 has also been implicated in regulating iron homeostasis. Suppression of CISD2 resulted in increased expression of TfR1 at the cell surface, an increased uptake of transferrin-bound Fe into cells, and the activation of cellular stress pathways that are associated with HIF-1α, suggesting that CISD2 is involved in the metabolic regulation of breast cancer cells through its effects on cellular Fe ion distribution [268].

MitoNEET is localized on the outer mitochondrial membrane, and various studies have suggested that mitoNEET is a regulator of mitochondrial function. Mitochondria purified from the hearts of mice with a targeted disruption of the mitoNEET gene exhibited reduced state 3 (phosphorylating) respiration rate [269]. However, a subsequent study reported increased mitochondrial activity in the liver of mice harboring a shRNA knockdown construct for mitoNEET [270]. In the same study, Kusminski *et al*. also showed that overexpression of mitoNEET in adipocytes enhanced lipid uptake and storage, leading to massive obesity. Interestingly, overexpression of mitoNEET in adipose tissue also resulted in reduced mitochondrial iron levels, reduced mitochondrial membrane potential, and ROS damage, whereas reduced mitoNEET levels led to increased mitochondrial iron levels and glucose intolerance. Increased mitochondrial iron, together with a decrease in mitochondrial membrane potential, an increase in ROS accumulation in mitochondria, a decrease in aerobic respiration, and an increase in glycolysis, has also been observed in human epithelial breast cells with suppressed expression of mitoNEET and CISD2 proteins [255]. Taken together, these results suggest a role of mitoNEET

as a key factor in the regulation of iron content in the mitochondrial matrix, and a hypothesis was put forth that mitoNEET overexpression reduced mitochondrial iron and compromised mitochondrial function, thereby triggering a compensatory upregulation of PPARg and adiponectin, which induces adipogenesis, mitochondrial biogenesis, and enhanced lipid influx into the adipocytes [270].

10.4 Diseases associated with genetic defects in Fe-S cluster biogenesis

Fe-S cluster biogenesis is a complex biological process, involving more than 20 different proteins in eukaryotes [97, 271–275]. The basic components of this process were originally identified in bacterial *nif*, *isc*, and *suf* operons [2, 273], and analogous processes and protein homologues have been identified in yeast, plants, and animals. The process involves the assembly of nascent clusters from iron and sulfur atoms on scaffold proteins, followed by transfer of these nascent clusters to apo-target proteins directly or *via* intermediate carriers. In nonplant eukaryotes, Fe-S cluster biogenesis factors, including NFS1 (also known as ISCS), LYRM4/ISD11, ISCU (yeast Isu1 and Isu2), frataxin (FXN) (yeast Yfh1), FDX1 (yeast Yah1), FDX1L, and FDX reductase (FDXR) (Arh1), are thought to be important in the early steps of cluster assembly, whereas HSPA9 (yeast Ssq1), HSC20 (yeast Jac1), glutaredoxin 5 (GLRX5) (yeast Grx5), NFU1, BOLA3, ISCA (yeast Isa1 and Isa2), IBA57, ABCB7 (yeast Atm1), GFER (yeast Erv1), NUBPL/IND1, NUBP1 (yeast Nbp35), NUBP2 (yeast Cfd1), NARFL/IOP1 (yeast Nar1), CIAO1 (yeast Cia1), NDOR1 (yeast Tah18), CIAPIN1/anamorsin (yeast Dre2), MMS19, FAM96A/CIA2A, and FAM96B/CIA2B are involved in subsequent steps in which Fe-S clusters from the scaffold protein(s) are transferred and assembled on target apoproteins in different subcellular compartments.

The early steps of cluster assembly involves the abstraction of sulfur atoms from cysteine molecules by the cysteine desulfurase NFS1 [276–278], iron acquisition, and sulfur transfer to the scaffold protein ISCU [279–281], leading to the formation of [2Fe-2S] and [4Fe-4S] clusters [282–285]. LYRM4 (also known as ISD11) appears to be important for the stability and activity of NFS1 [286–289]. FXN is critical in this early stage of Fe-S cluster biogenesis, although the exact function of FXN has been elusive. Various roles have been proposed for FXN, including iron storage, iron chaperone, and allosteric factor [284, 290–294]. Redox proteins such as FDX and FDXR are thought to provide electrons for cluster assembly on scaffold proteins [295, 296], whereas the chaperone system comprising the heat shock 70-kDa protein HSPA9 (also known as GRP75 or mortalin), the DnaJ-like cochaperone HSC20, and the nucleotide exchange factor SIL1 (also known as BAP; yeast Mge1) utilizes energy derived from ATP hydrolysis to drive conformational changes in scaffold proteins to facilitate cluster transfer to intermediate carrier or final recipient proteins [297–304]. Yeast two hybrid (Y2H) and coimmunoprecipitation studies indicated that a conserved leucine-tyrosine-arginine

(LYR) motif that is present in SDHB, the SDH subunit that contains three Fe-S clusters, and in a SDH complex assembly factor SDHAF1 mediates an interaction with HSC20 and guides the insertion of Fe-S clusters into the Fe-S subunits of respiratory chain complex II and complex III, respectively [305, 306].

Additional Fe-S cluster biogenesis components are involved in guaranteeing the accurate and specific transfer of Fe-S clusters from the scaffold protein to target apoproteins. Homologues of the mitochondrial monothiol glutaredoxin GLRX5 have been implicated in Fe-S cluster biogenesis in yeast [307, 308], zebrafish [309], and humans [310], but its precise function is unclear. Chloroplast monothiol GLRXs were suggested to be scaffolds for the formation and delivery of [2Fe-2S] clusters [311], whereas yeast and mammalian GLRX5 were suggested to function in Fe-S cluster transfer [308, 312, 313]. Yeast Iba57 physically interacts with Isa1 and Isa2, and it was suggested that the complex of these three proteins functions to promote cluster transfer/assembly on a subset of Fe-S proteins including aconitase and radical SAM proteins [314, 315]. NFU1 was initially proposed to be an alternative scaffold protein [316–319]. However, more recent studies suggested that Nfu-type proteins can accept an Fe-S cluster from holo ISCU and serve as intermediate Fe-S cluster carriers to deliver Fe-S cluster to apo-targets [320–322]. The mitochondrial P-loop NTPase NUBPL/IND1 was initially proposed to serve as a specific scaffold or transfer protein for the assembly of the eight Fe-S clusters into complex I [323, 324], but more recent studies suggested that IND1 has a primary role in mitochondrial translation that indirectly affects the assembly of complex I [325]. The ABC transporter ABCB7 (yeast Atm1) in the inner mitochondrial membrane and sulphydryl oxidase GFER (yeast Erv1) in the intermembrane space [326], together with glutathione, have been described as an "export machinery" for Fe-S cluster biogenesis, although the identity of the transported compound(s) has remained unresolved [327].

Assembly and repair of Fe-S proteins in the cytosol and nucleus involves the extramitochondrial isoforms of NFS1 [277], ISCU [328], and NFU1 [317], as well as a number of additional proteins in the cytosolic Fe-S protein assembly (CIA) machinery. In yeast, the P-loop NTPases Cfd1 and Nbp35 form a heterotetrameric complex and can act as a scaffold or transfer proteins for cytosolic Fe-S cluster biogenesis [329–331]. Cfd1 and Nbp35 facilitate the assembly of two Fe-S clusters on the hydrogenase-like protein Nar1 [332, 333], which then assists the transfer of Fe-S clusters to target apoproteins by interacting with Cia1, a WD40 repeat protein [334, 335]. Electrons are transferred from NADPH *via* the FAD- and FMN-containing Tah18 to the Fe-S clusters of Dre2 [336–338], a process required for the assembly of cytosolic target proteins [337]. MMS19 functions as part of the CIA machinery that facilitates Fe-S cluster insertion into a specifi subset of apoproteins involved in methionine biosynthesis, DNA replication, DNA repair, and telomere maintenance [234]. In mammalian cells, the complex composed of FAM96B/CIA2B, CIA1, and MMS19 facilitates cluster assembly on cytosolic-nuclear Fe-S proteins including phosphoribosylpyrophosphate aminotranferase (GPAT), dihydropyrimidine dehydrogenase, and DNA polymerases,

whereas the complex composed of FAM96A/CIA2A, CIA1, and MMS19 facilitates Fe-S cluster assembly of IRP1 [233, 339, 340]. The functions of many of these cytosolic Fe-S cluster biogenesis factors appear to be conserved in plants and animals [233, 234, 337, 339–344]. More recently, additional proteins have been identified to have roles in Fe-S cluster biogenesis in specific proteins. Paul *et al.* identified two yeast proteins, Yae1 and Lto1, that interact with CIA1, FAM96A/CIA2A, and MMS19, as well as an essential cytosolic Fe-S protein, Rli [345]. Depletion of Yae1 or Lto1 in yeast resulted in defective Fe-S maturation of Rli1, but not other tested targets. These studies suggested that Yae1 binds to Rli1 and recruits it to the CIA machinery *via* interactions with a deca-GX3 motif on Lto1.

Given the essential roles of Fe-S clusters in electron transfer, enzyme catalysis, and sensing functions in many proteins, defects in Fe-S cluster biogenesis can disrupt many cellular process and cause human diseases [97, 346–348]. In *S. cerevisiae*, deletions of many genes involved in Fe-S cluster assembly, including *nfs1*, *isd11*, *jac1*, *yah1*, *arh1*, *cfd1*, *erv1*, *nbp35*, *nar1*, and *cia1*, are lethal. In addition, synthetic lethality was observed in pairwise combinations of several other Fe-S cluster assembly genes, including *isu1*, *isu2*, *nfu1*, *ssq1*, and *grx5* [349–351]. In vertebrates, deletions of the GLRX5 homologue in zebrafish and deletion of FXN, ABCB7, ISCU, NARFL, and MMS19 in mice are embryonic lethal [233, 309, 343, 352–354]. Depletion of mammalian Fe-S cluster assembly factors in cellular and animal models showed inactivation of many important proteins, including SDH, ACO1, ACO2, XOR and GPAT, and misregulation of proteins involved in iron metabolism [295, 328, 339, 355–358]. The following sections provide an overview of the human genetic defects associated with genes that encode proteins that have been implicated in various stages of Fe-S cluster biogenesis (Tab. 10.2) (Fig. 10.3).

10.4.1 A GAA trinucleotide repeat expansion in FXN is the major cause of the neurodegenerative disorder Friedreich ataxia

Friedreich ataxia (FRDA) (MIM 229300), an autosomal recessive neurodegenerative disorder caused by deficiency of FXN [359], is the most prevalent form of hereditary ataxia in Caucasians, occurring in about 1 in 50,000 individuals [360]. FXN deficiency leads to progressive spinocerebellar neurodegeneration associated with gait and limb ataxia, muscle weakness, as well as cardiomyopathy and diabetes [361–364]. Most of neurological manifestations result from the degeneration of the dorsal root ganglia and the posterior columns, followed by degeneration in the spinocerebellar tracts and the corticospinal tracts of the spinal cord [365]. Although cognitive functions remain largely intact during disease progression, patients develop communication difficulties due to dysarthria and vision and hearing loss. Cardiac failure is a frequent cause of death at a young age.

Expansion of an unstable GAA trinucleotide repeat in intron 1 of *FXN* is the most common causal mutation of FRDA [359]. Most FRDA individuals are homozygous for this

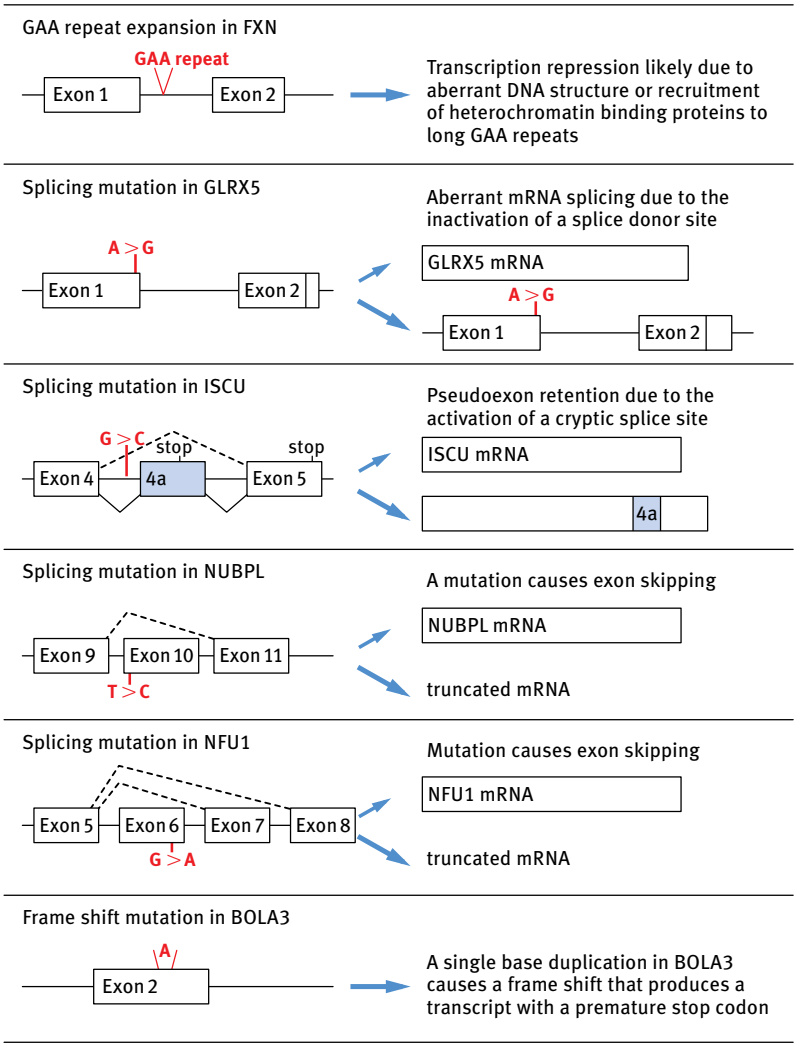

Fig. 10.3: In addition to missense mutations in FXN, ABCB7, GLRX5, ISCU, NUBPL, BOL3, and ISD11, dysfunction of Fe-S cluster biogenesis can also be the result of a variety of genetic defects, including trinucleotide repeat expansion, intron retention, pseudoexon retention, exon skipping, and frameshift, which lead to reduced production of the mRNA and/or protein products. In more than 98% of FRDA cases, the defect is a GAA repeat expansion in the first intron of the FXN gene. In one patient with GLRX5 deficiency, a homozygous silent mutation in exon 1 interferes with splicing and reduces the level of fully processed mature GLRX5 mRNA. In ISCU myopathy, a single G to C mutation in the fourth intron of ISCU activates a weak splice acceptor site, resulting in the increased production of an alternative splice form with a premature stop codon. In patients with NUBPL deficiency, a mutation in exon 10 of NUBPL results in exon skipping and production of a truncated transcript. In multiple mitochondrial dysfunctions syndrome 1, a homozygous missense mutation in exon 6 of NFU1 results in exon skipping and production of several truncated transcripts. In one of the patient with multiple mitochondrial dysfunctions syndrome 2, a single nucleotide duplication in exon 2 of BOLA3 causes a frameshift that produces a transcript with a premature stop codon.

Tab. 10.2: Diseases associated with Fe-S cluster biogenesis.

Human protein	Yeast homologue	Proposed function(s)	Pathology	Tissue(s) affected
Frataxin	Yfh1	Facilitate Fe-S cluster assembly in ISCU scaffold protein	Friedreich's ataxia [359, 413]	Dorsal root ganglia, cerebellum, and heart
ABCB7	Atm1	ABC transporter, mitochondrial export machinery component	X-linked sideroblastic anemia and cerebellar ataxia [433]	Central nervous system
GLRX5	Grx5	Monothiol glutaredoxins; Fe-S cluster transfer	Autosomal recessive pyridoxine-refractory sideroblastic anemia [310] Nonketotic hyperglycinemia with spastic paraplegia, spinal lesions, and optic atrophy [216]	Erythrocytes Spinal cord, optic nerve
ISCU	Isu1	Primary scaffold for Fe-S cluster assembly	Myopathy with lactic acidosis Cardiomyopathy [476, 498]	Skeletal muscle, heart
NUBPL	Ind1	A primary role in mitochondrial translation that indirectly affects the assembly of respiratory complex I	Childhood-onset mitochondrial encephalomyopathy and respiratory complex I deficiency [509, 511, 512]	Central nervous system, skeletal muscle
NFU1	Nfu1	Fe-S cluster transfer protein	Multiple mitochondrial dysfunctions syndrome 1 [517] [321]	Multisystem
BOLA3	Bola3	Fe-S cluster biogenesis in a subset of Fe-S proteins including lipoic acid synthase	Multiple mitochondrial dysfunctions syndrome 2, nonketotic hyperglycinemia with severe neurodegeneration, leukodystrophy, cardiomyopathy, and optic atrophy [216, 517, 530]	Central nervous system, heart, multisystem organ failure
IBA57	Iba57	Fe-S cluster biogenesis in a subset of Fe-S proteins including lipoic acid synthase	Multiple mitochondrial dysfunctions syndrome 2, fatal infantile leukodystrophy [543, 544]	Central nervous system, skeletal muscle
ISD11	Isd11	Important for cysteine desulfurase activity	Deficiencies of respiratory complexes [549]	Skeletal muscle, liver
NFS1	Nfs1	Cysteine desulfurase	Infantile complex II/III deficiency (IMC23D) [552]	Multisystem organ failure
FDX2	Yah1	Electron donor for Fe-S cluster biosynthesis	Mitochondrial muscle myopathy [606]	Skeletal muscle
HSPA9	Ssq1 Ssc1	Molecular chaperone	Sideroblastic anemia [556]	Erythrocytes

mutation, but 4% of the patients are compound heterozygous for the GAA expansion and a second inactivating mutation (nonsense, missense, deletions, insertions) [359, 366, 367]. Normal alleles have 5 to 30 repeats, whereas FRDA alleles have 70 to more than 1000 repeats. This GAA expansion leads to transcriptional silencing of *FXN* by inducing the formation of repressive heterochromatin of the locus, resulting in reduced expression of FXN (~5–30% of normal) (reviewed in [368]). Multiple factors contribute to FXN silencing in FRDA, including disrupted transcriptional elongation [369, 370] and epigenetic changes affecting chromatin remodeling and DNA methylation [371–373]. It has been suggested that the progressive pathology in the dorsal root ganglia may result from an age-dependent, tissue-specific increased expansion of the GAA triplet-repeat sequence [365]. Other disease mutations in *FXN* lead to the production of nonfunctional or partially functional proteins [374–377]. In addition, rare *FXN* isoforms that are specifically expressed in affected tissues have been shown to decrease more in FRDA patients than in healthy individuals, suggesting additional mechanisms for the tissue-specific pathology [378].

Despite intense investigations since the discovery of FXN, identification of the cellular function of FXN has so far remained elusive [379]. Early studies of endomyocardial biopsies of two FRDA patients revealed that activities of ACO2 and respiratory complexes I, II, and III were markedly decreased, providing the first hint of a role of FXN in the synthesis or stability of Fe-S proteins [380]. Disruption of the *FXN* homolog in *S. cerevisiae*, *yfh1*, resulted in a severe defect in respiration, deficiencies in multiple Fe-S-dependent enzymes, mitochondrial iron accumulation, and loss of mtDNA [380–382]. A role of FXN in Fe-S cluster biogenesis was further confirmed in yeast, *Drosophila*, and human cell lines depleted of FXN [383–389]. However, the exact function of FXN in Fe-S cluster biogenesis has remained a subject of debate. Extensive structural, complementation and biochemical studies on FXN in the last 15 years have yielded complex and contradictory results. *In vitro* studies of bacterial, yeast, or human FXN homologs showed a modest affinity of the proteins for iron (uM range) [390, 391]. Observation of an iron-dependent oligomerization of the recombinant Yfh1 led to a proposed role of FXN oligomers in mitochondrial iron storage [392], and *in vitro* reconstitution studies showed that the oligomeric forms of yeast and human FXN can provide iron for Fe-S cluster formation on the scaffold protein ISCU [393, 394]. However, the importance of FXN oligomerization in Fe-S cluster biogenesis is unclear since mutations of the acidic residues on the surface of Yfh1 abrogated iron-dependent oligomerization but showed no deleterious effects on Fe-S protein activities and iron homeostasis *in vivo* [395]. Other studies have suggested that FXN serves as an iron-binding chaperone protein that delivers Fe for Fe-S cluster assembly in the scaffold protein ISCU [290, 292, 396, 397]. It has also been suggested that FXN provides iron through direct protein-protein interactions with target Fe-S proteins, including ACO2 [398], FECH [399–401] and SDH [402], although the relevance of some of these interactions was under debate [403]. Other *in vitro* studies suggested that mammalian FXN interacts with a complex composed of NFS1, ISCU, and ISD11, acts as an allosteric factor that activates sulfur production

from cysteine [284, 293, 294], and controls iron entry during *de novo* Fe-S cluster assembly [284]. Interestingly, a point mutation in the yeast *isu1* gene (M107I) was found to restore many deficient functions in Yfh1-depleted yeast cells [404]: iron homeostasis and Fe-S cluster enzyme activities were improved, and cytochrome levels and heme synthesis were restored. It was suggested that the Isu1 mutation bypasses the putative allosteric activator Yfh1 by increasing exposure of a Fe-S cluster binding cysteine ligand and improving sulfur transfer from the cysteine desulfurase complex Nfs1-Isd11 to Isu1.

The effect of FXN depletion has been modeled in diverse systems, including *E. coli* [405], yeast [382, 406, 407], *C. elegans* [350, 408], *Drosophila* [386, 409], mice [410–412], and human cell lines [383, 385, 387, 388], and these cellular and animal models of FRDA have provided many insights into the pathophysiology of the disease (reviewed in [413]). Depletion of FXN homologs in yeast and *Drosophila* leads to Fe-S cluster deficiencies, mitochondrial iron accumulation, and increased sensitivity to oxidative stress [386, 406]. The complete knockout of *FXN* in mice leads to early embryonic lethality [352], whereas cardiac-specific and neuronal models of *FXN* deletion [410, 414] are viable and recapitulate most of the characteristic features of the disease, including progressive spinocerebellar and sensory ataxia and hypertrophic cardiomyopathy. More specifically, the cardiac-specific FRDA model revealed that a deficit in Fe-S clusters precedes cardiac dysfunction and mitochondrial iron accumulation [410], whereas the neuronal model showed that abnormal autophagy, with formation of lipofuscin and large vacuoles within large sensory neurons, might be involved in the neurodegeneration of the dorsal root ganglia [414]. Conditional models lacking FXN primarily in the pancreas were generated to model the pathophysiology of diabetes mellitus associated with FRDA [415], and these mice showed a progressive reduction in the number of pancreatic islets, resulting in an impaired insulin response to glucose and subsequent diabetes. In addition to the models of *FXN* deletion, several mouse models with GAA expansions in *FXN* have been generated to better mimic the human disease [411, 412]. These animal models are invaluable in revealing the molecular and cellular mechanisms associated with GAA-mediated silencing of the *FXN* gene *in vivo* and for the development of drugs to target FRDA pathology.

Notably, mitochondrial iron overload was observed in the hearts and brains of FRDA patients [416, 417] and heart-specific *FXN* deletion mouse models [410], and Yfh1-deficient yeast strains also develop profound mitochondrial iron overload [406]. These results suggest that Fe-S cluster biogenesis might be required for signaling information about the status of mitochondrial iron stores to the nucleus [418, 419]. In the absence of an appropriate signal, mitochondrial iron uptake might be upregulated [420], efflux might be diminished, and iron might accumulate as insoluble ferric phosphate nanoparticles in the mitochondrial matrix [421, 422] or within the iron sequestration protein, mitochondrial ferritin [388, 417]. Whether the mitochondrial iron overload might further cause mitochondrial damage *via* iron-catalyzed oxidation reactions and thereby contribute to FRDA pathology remains a subject of debate [409, 423–428].

10.4.2 Mutations in ABCB7 cause x-linked sideroblastic anemia with ataxia

The sideroblastic anemias are a heterogeneous group of acquired and heritable disorders, characterized by bone marrow ringed sideroblasts due to pathologic iron overload in the mitochondria of erythroid precursors [429–432]. The most common congenital sideroblastic anemia is the X-linked sideroblastic anemia (XLSA) caused by mutations in the erythroid-specific 5-aminolevulinate synthase gene (ALAS2), the first and rate-limiting enzyme in the mammalian heme biosynthetic pathway. Patients develop hepatic and systemic iron overload, but not ataxia. Other genetic defects found in congenital sideroblastic anemia include mutations in mitochondrial ATP-binding cassette transporter ABCB7 [433], high-affinity thiamine transporter SLC19A2 [434], RNA-modifying enzyme pseudouridine synthase 1 [435], GLRX5 [310], erythroid-specific mitochondrial transporter SLC25A38 [436], and deletions, duplications, and rearrangements of mtDNA [437].

Mutations in ABCB7 are associated with XLSA with ataxia, a rare form of congenital sideroblastic anemia with early-onset nonprogressive spinocerebellar ataxia, cerebellar hypoplasia, dysarthria, mild anemia, and elevated levels of protoporphyrin [433, 438–440]. Systemic iron overload is not detected. *ABCB7* has high sequence similarity to the yeast ABC transporter gene *ATM1* and ATM3 in *Arabidopsis*, whose protein product localizes to the inner mitochondrial membrane. Depletion of ABCB7 homologues in plants, mice, and human cell lines resulted in loss of ACO1 activity in the cytosol, but no significant changes in the activities of ACO2 and SDH in the mitochondria [353, 441, 442]. Moreover, deletion of yeast *ATM1* leads to mitochondrial iron accumulation [443, 444]. In mice, tissue-specific deletions of *ABCB7* in brain and bone marrow were lethal [353], whereas liver-specific deletion of *ABCB7* revealed changes in several proteins involved in cytosolic iron homeostasis, including activations of IRP1 and IRP2, increased IRP2 levels, and decreased expression of ferritin. Iron is essential for heme biosynthesis and red blood cell development [445, 446]. Thus, it appears that the anemia and the ataxia observed in XLSA-A may be related to disruption of intracellular iron homeostasis and damages caused by excess iron in the mitochondria in developing red blood cells and neural cells [447].

ABCB7 belongs to the family of B-type mitochondrial ABC transporters [448]. The crystal structures of the free and glutathione-bound forms of atm1, the yeast homologue of ABCB7 has been reported [449], but the substrate transported by ABCB7 remains unclear. Given its association with a form of anemia characterized by mitochondrial iron accumulation in erythroid precursors, ABCB7 was initially thought to be involved in transporting heme that is generated in the mitochondria to the cytosol for incorporation into hemoglobin, but *in vitro* studies in *S. cerevisiae* argued against heme export and iron import as possible functions of Atm1 [443, 450]. Instead, Kispal *et al.* observed that yeast depleted of *ATM1* contained no detectable activity of the cytosolic Fe-S enzyme isopropyl malate isomerase Leu1,

and proposed that Atm1 was involved in the export of Fe-S clusters generated by the mitochondrial Fe-S cluster assembly machinery into the cytosol for incorportation into extra-mitochondrial proteins [451, 452]. However, subsequent studies indicated that Atm1 is not required for exporting Fe-S clusters for incorporation into Leu1 [453], and the overexpression of an Atm1 homologue, Mdl1, which exports peptides out of mitochondrial matrix [454], can partially compensate for *ATM1* loss. Furthermore, Arabidopsis ATM3 can functionally complement a yeast Δ*atm1* mutant [455], but unlike yeast *atm1* mutants, mitochondria from *atm3* mutant plants do not accumulate significant amounts of iron [442]. These results and other studies have led to the suggestion that a sulfur-containing compound is exported to the cytosol by Atm1 [442, 456]. Transport studies using Arabidopsis ATM3 and yeast Atm1 in inside-out membrane vesicles showed that these proteins transport glutathione disulfide (GSSG) but not reduced glutathione [457]. In addition, glutathione trisulfide (GS-S-SH) was transported by Atm1 *in vitro*. A glutathione-conjugated [2Fe-2S] cluster has also been suggested as a candidate substrate [458]. It is noteworthy that Atm3 in Arabidopsis is required for the export of cPMP intermediate from the mitochondria into the cytosol for the biogenesis of MoCo [459]. Thus, Arabidopsis ATM3 may transport either a single compound or two distinct compounds for both Fe-S cluster and MoCo assembly machineries in the cytosol [442]. Neither deletion of *ATM1* in yeast nor *ATM3* in Arabidopsis is lethal, suggesting that either there is some low-level diffusion of the transported substrate(s) through the mitochondrial inner membrane or that the substrate(s) can be transported by other transporter(s).

10.4.3 Mutations in GLRX 5 cause an autosomal recessive pyridoxine-refractory sideroblastic anemia

A point mutation in *GLRX5* gene has been shown to be the genetic cause of an autosomal recessive pyridoxine-refractory sideroblastic anemia (MIM205950) [310]. The patient had mild anemia until midlife, when anemia worsened, and diabetes, splenomegaly, and cirrhosis were diagnosed. The anemia was worsened by blood transfusions but partially reversed by iron chelation therapy. DNA sequencing and RT-PCR experiments showed that a homozygous mutation in the penultimate nucleotide of exon 1 of GLRX5 interfered with splicing, resulting in drastically reduced mRNA levels. More recently, two heterozygous missense mutations in *GLRX5* were identified in a Chinese patient affected with sideroblastic anemia [460].

GLRXs were initially defined as thiol disulfide oxidoreductases that catalyze thiol-disulfide exchange reactions using reduced glutathione as the electron donor, but genome sequencing in recent years has shown that these proteins constitute a

complex family of proteins with diverse structural and functional properties [461, 462]. In yeast, three members of the subfamily of monothiol GLRXs – Grx3, Grx4, and Grx5 – have a conserved CGFS active site and have roles in iron homeostasis, facilitating Fe-S cluster biogenesis in the mitochondria (Grx5), or signaling intracellular iron status for the regulation of iron trafficking (Grx3 and Grx4). The CGFS active site is required for the coordination of a [2Fe-2S] cluster; CGFS GLRXs form $[2Fe\text{-}2S]^{2+}$-bridged homodimers with cysteine ligands provided by the two CGFS active sites and two glutathione molecules [311, 463–467].

The effects of GLRX5 depletion have been modeled in a number of studies. Yeast that lack Grx5 exhibit respiratory deficiency, iron accumulation, and reduction in mitochondrial aconitase and SDH activities, a loss of mtDNA and the absence of Rip1, the Fe-S Rieske protein in complex III [307, 468, 469]. Silencing of GLRX5 in human cells also resulted in reduced aconitase activities [470]. Depletion of Grx5 in yeast resulted in accumulation of ^{55}Fe on the scaffold protein Isu1, suggesting that Grx5 has a role in a step after the assembly of an Fe-S cluster on Isu1 [308]. Grx5 deficiency has also been shown to increase oxidative stress in yeast cells [471] and human osteoblasts [472]. In zebrafish, Grx5 mutations cause anemia as a result of IRP1-mediated translational repression of erythroid aminolevulinate synthase (ALAS2), the first enzyme in the heme biosynthetic pathway [309]. Human and zebrafish genomes contain two *ALAS* genes: the *ALAS2* transcript contains an IRE in its 5′UTR (5′ untranslated region) and is highly expressed in erythroid cells, whereas the *ALAS1* transcript is expressed in other tissues and lacks an IRE. In the GLRX5-deficient patient and in the zebrafish model, IRP1 becomes an active IRE binding protein that inhibits *ALAS2* translation and thereby blocks heme biosynthesis. It appeared that loss of mitochondrial GLRX5 resulted in mitochondrial iron overload and concomitant cytosolic iron depletion, which prevents *de novo* cytosolic cluster assembly in IRP1 and activates IRP1-mediated translational repression of *ALAS2*. These alterations may explain the sideroblastic anemia-associated phenotype resulting from the aberrant splicing of human *GLRX5* mRNA [310, 470].

Several roles have been proposed for GLRX5. One proposal is that the deglutathionylation activity of GLRXs might be important for repairing mixed disulfides between glutathione and Fe-S cluster assembly factors in the oxidizing environment of the mitochondrial matrix [351]. Other studies in plants have shown that a GLRX5 homologue is able to bind a [2Fe-2S] cluster and transfer the cluster to apo FDX *in vitro* and suggested that Grx5 may be a scaffold protein [311]. In yeast, depletion of Grx5 resulted in accumulation of ^{55}Fe on the scaffold protein Isu1, suggesting that Grx5 functions as an intermediate carrier in transferring Fe-S clusters from the scaffold proteins to dedicated apoproteins [308]. Spectroscopic evidence provided by circular dichroism spectroscopic studies of recombinant proteins from *Azotobacter vinelandii* showed a rapid, ATP-driven [2Fe-2S] cluster transfer from [2Fe-2S]-IscU to apo-Grx5 in the presence of chaperone proteins, HscA and HscB [312]. Phenotypic defects associated with the absence of Grx5 in yeast were suppressed by overexpression of the

HSPA9 homologue *SSQ1* [307], and yeast two-hybrid studies have indicated that Grx5 interacts with Ssq1 [473]. Defects in yeast lacking Grx5 were also suppressed by overexpression of *ISA2* [307]. This observation, together with yeast two-hybrid studies and bimolecular fluorescence complementation experiments showing physical interactions between Grx5 with Isa1 [468, 474] and Isa2 [468], led to the proposal that Grx5 functions with Isa type proteins in Fe-S cluster biogenesis.

10.4.4 Mutations in ISCU cause myopathy with lactic acidosis (MIM 255125)

ISCU is a scaffold protein on which nascent Fe-S clusters are assembled and from which the clusters are delivered to intermediate carriers or directly to target apoproteins [282, 284]. In mammalian cells, two splice isoforms of *ISCU* exist [328, 475]. These transcripts have different 5′UTRs and generate proteins that are localized to different subcellular compartments: ISCU1 is located in the cytosol and nucleus, whereas ISCU2 is located in the mitochondrial matrix. Human ISCU works in a complex with NFS1, ISD11, and FXN [293, 403]. Sulfur transfer from NFS1 and iron acquisition leads to assembly of [2Fe–2S] and/or [4Fe-4S] clusters in ISCU [282–284].

Because of its essential role in the very early steps in Fe-S cluster biogenesis, complete loss of ISCU homologues in *S. cerevisiae* and in mice is lethal [349, 354], and depletion of human ISCU has been shown to affect all Fe-S proteins that have been examined, including SDH, ACO1/IRP1, ACO2, FECH, GPAT, and LIAS) (as indicated by the decrease in lipolyated proteins) [44, 321, 328, 476]. Notably, ISCU has now been shown to be one of the mediators of the Pasteur effect, a metabolic shift in hypoxic cells resulting from the repression of TCA cycle, mitochondrial electron transport, and oxidative phosphorylation in favor of glycolysis [477–479]. This metabolic versatility of mammalian cells is essential for the maintenance of energy production and cell survival throughout a range of oxygen concentrations. Both ISCU1 and ISCU2 were found to be targets for repression by the microRNA-210 (miR-210) [480–483], which is specifically induced by HIF-1α during hypoxia [484, 485]. MiR-210 is upregulated and ISCU is downregulated in several clinical settings, including pregnancies complicated by preeclampsia, clear cell renal cancer, and head and neck paragangliomas [486–489]. By downregulating the expression of ISCU during hypoxia or in pseudohypoxia conditions, miR-210 decreases the activities of respiratory complex I and aconitases. These findings indicate that both miR-210 and ISCU are important factors in the regulation of mitochondrial respiration and metabolism during hypoxic stress and mitochondrial dysfunction in a variety of diseases [490, 491].

Deficiency in ISCU causes myopathy with lactic acidosis, a rare autosomal recessive hereditary disease found mainly in individuals of northern Swedish descent [492, 493]. Patients develop muscle weakness and experience severe activity-related muscle pain, associated with rhabdomyolysis (breakdown of skeletal muscle fibers

with leakage of muscle contents into the circulation) and myoglobinuria (reddish urine caused by excretion of myoglobin), followed by muscle regeneration and temporary resolution of these symptoms [492, 494]. Even minor exertion causes markedly increased heart rate and palpitations, dyspnea, muscle fatigue, and lactic acidosis [492, 495]. Physiological investigations of these patients during exercise showed impaired muscle oxidative phosphorylation and low maximal muscle oxygen extraction associated with exaggerated circulatory responses. Biochemical studies indicated a deficiency in SDH [496] and aconitase activities [476, 497], and the presence of iron-rich mitochondrial inclusions [476, 497] (Fig. 10.4). Modest deficiencies in respiratory complex I and the Rieske protein in complex III were also reported [497].

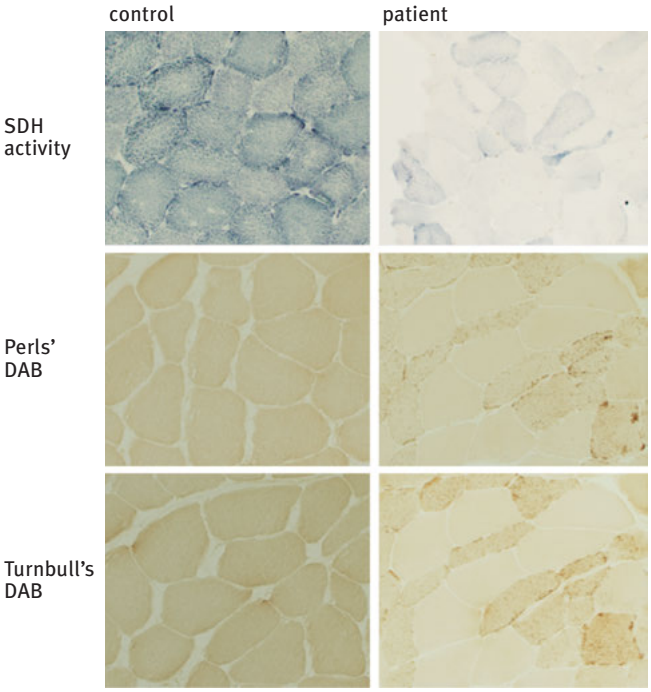

Fig. 10.4: Histochemistry indicated the loss of SDH activity and an increase in mitochondrial iron levels in the skeletal muscle of patients with ISCU myopathy. (A) Skeletal muscles from healthy individuals show robust SDH activity staining (blue), whereas patient muscles show very little SDH activity. (B) Perls' Prussian blue staining enhanced with 3, 3'-diaminobenzidine (Perls/DAB), a histochemical test for non-heme ferric iron, indicated iron overload (brown punctate stains) in the muscle fibers of patients with ISUC myopathy. The punctate distribution of the iron staining was consistent with the mitochondrial iron overload previously detected in ultrastructural studies of these patients. (C) Turnbull staining enhanced with DAB, a stain for non-heme ferrous iron, indicated an increase in ferrous iron in the skeletal muscle of ISCU myopathy patients. (Images courtesy of Karen Ayyad and Ron Haller, University of Texas Southwestern Medical Center and Veterans Administration North Texas Medical Center.)

Two independent studies revealed that the ISCU myopathy is caused by a homozygous intronic point mutation (g.7044 G>C) in intron 4 of *ISCU* gene that activates a cryptic splice site, resulting in the retention of a ~100 base pair fragment of intronic sequence [476, 498]. The incorporation of a premature translational stop codon in the aberrantly spliced ISCU mRNA gave rise to a truncated ISCU protein, and pulse-chase experiments in patient myoblasts demonstrated that the truncated ISCU protein is rapidly degraded [499]. Gene expression analysis on muscle biopsies from patients with the homozygous g.7044 G>C mutation revealed expression of the mitochondrial iron importer mitoferrin 2, suggesting that increased mitochondrial iron uptake may contribute to the mitochondrial iron overload seen in these patients [476, 497]. Gene expression analysis and biochemistry study also showed alterations of several key pathways involved in muscle fiber composition, fatty acid metabolism, and ketogenesis and induced expression of the starvation response hormone, FGF-21 [500], indicating a metabolic response to energy deprivation in the muscle tissue on the organismal level [501]. A third study reported a more severe progressive myopathy associated with hypertrophic cardiomyopathy that is caused by the g.7044 G>C mutation on one allele in combination with a heterozygous missense allele (c.149G>A) in *ISCU* exon 3 that converts a conserved Gly-50 residue to Glu (G50E) [502]. Biochemical characterization of G50E mutation showed that it compromises the ability of ISCU to interact with the sulfur donor NFS1 and with cochaperone HSC20 [503].

The g.7044 G>C mutation that underlies ISCU myopathy has the potential to cause aberrant splicing of ISCU in all cells and cause catastrophic loss of Fe-S cluster biogenesis in all tissues. Yet the patients with homozygous g.7044 G>C mutation all present with muscle-specific pathology. Several studies have attempted to identify the molecular features that may contribute to the tissue specificity and localized clinical phenotypes of ISCU myopathy. The ratio between aberrantly spliced to normal ISCU transcripts in patient muscle biopsies was markedly higher than those in patient myoblasts, fibroblasts, and heart tissue [354, 504]. Furthermore, Nordin *et al.* identified several muscle-specific cellular RNA-binding factors that facilitate the splicing of the mutant ISCU mRNA [505], suggesting that tissue-specific differences in RNA processing give rise to muscle-specific pathology and that disease will only manifest in tissues where the level of normal transcripts is below a certain threshold level. Interestingly, Crooks *et al.* showed that heterologous expression of the muscle-specific transcription factor MyoD1 decreased the amount of normal ISCU mRNA expressed in patient myoblasts, further suggesting that altered expression of RNA splicing factors during the process of terminal muscle differentiation enhances aberrant ISCU mRNA splicing [499]. In addition, they observed a decrease in ISCU protein levels in cells under oxidative stress and proposed that increased production of ROS during exercise may further contribute to a decrease in ISCU protein levels in the muscle tissue and to the phenotype of exercise-induced rhabdomyolysis in ISCU myopathy patients [499].

10.4.5 NUBPL mutations cause childhood-onset mitochondrial encephalomyopathy and respiratory complex I deficiency (MIM 252010)

Mitochondrial respiratory complex I (NADH:ubiquinone oxidoreductase; EC 1.6.5.3) is the main entry point to the mitochondrial respiratory chain and catalyzes the transfer of electrons from NADH to ubiquinone. Complex I is a large ~1-MDa macromolecule composed of 45 protein subunits encoded by both the nuclear and mitochondrial genomes. Defects in complex I activity are the most common type of mitochondrial disease [506], can present at a young age, and often result in multisystem disorders with a fatal outcome [84, 85]. The wide range of clinical manifestations include Leigh syndrome (an early-onset, fatal neurodegenerative disorder), dystonia, developmental delay, seizures, respiratory irregularities, cardiomyopathy, skeletal muscle myopathy, hypotonia, stroke, ataxia, lactic acidosis, and hepatopathy with renal tubulopathy. Mutations underlying human complex I deficiency have been identified in 19 of the subunits of the complex and 7 nuclear-encoded accessory factors that are required for the assembly, maturation or stability of complex I [507, 508].

A high-throughput sequencing project identified several mutations in NUBPL (also known as IND1) in an individual who presented at 2 years of age with developmental delay, leukodystrophy, elevated CSF lactate, and complex I deficiency [509]. The patient carried one *NUBPL* allele harboring a deletion that spans exons 1–4 and a second allele that harbors both a c.815-27T>C mutation that probably causes exon 10 skipping and a p.Gly56Arg missense mutation [509, 510]. Functional studies showed that the expression of wild-type NUBPL rescued complex I activity in fibroblasts from the patients, establishing NUBPL as the causal gene [509]. The c.815-27T>C branch-site mutation was subsequently found in six other cases, usually in combination with a null allele [511, 512]. RT-PCR and protein analysis indicated that the branch-site mutation led to a decrease in NUBPL1 mRNA and/or protein levels [510, 512, 513].

Deletion of the *IND1* in the respiratory yeast *Yarrowia lipolytica* carrying an alternative NADH dehydrogenase resulted in slower growth and strongly decreased complex I activity, whereas the activities of aconitase, SDH, and cytochrome bc1 complex were not affected, leading to the suggestion that Ind1 is specifically involved in the assembly/stability of complex I [323]. Knockdown of NUBPL in human HeLa cells caused decreases in several complex I subunits (NDUFS1, NDUFV1, NDUFS3, and NDUFA13), improper assembly of the peripheral arm of complex I, decreased complex I activity, and abnormal mitochondrial morphology [324]. Complex I contains 8 Fe-S clusters that are associated with five different subunits (NDUFS1, -S7, -S8, -V1, and -V2) [514]. NDUFS7 and -S8 assemble relatively early in the assembly pathway, and defects in these subunits usually do not result in accumulation of assembly intermediates. Kevelam *et al.* observed no accumulation of assembly intermediates of the peripheral arm in the patients and concluded that NUBPL is involved in early assembly of the Fe-S clusters [512]. NUBPL shows sequence similarity to Nbp35 and Cfd1 in yeast, which are P-loop NTPases that are involved in cytosolic

Fe-S protein maturation [515]. Recombinant NUBPL/IND1 binds a labile [4Fe-4S] cluster, as judged by UV-vis spectroscopies, and the Fe-S cluster could be transferred to an Fe-S apo-protein *in vitro* [324, 515]. These studies led to the proposal that Ind1 serves as a specific scaffold or transfer protein for the assembly of the Fe-S clusters in respiratory complex I. However, more recent studies designed to unravel primary from secondary phenotypes in *Arabidopsis IND1* mutants suggested that IND1 has a primary role in mitochondrial translation that indirectly but specifically affects the assembly of complex I [325].

10.4.6 Mutations in NFU1 cause multiple mitochondrial dysfunctions syndrome 1 (MIM 605711)

Multiple mitochondrial dysfunctions syndrome (MMDS), a fatal neonatal autosomal recessive disorder characterized by weakness, respiratory failure, developmental delay, and metabolic acidosis with elevated blood lactate levels, was first described in two families in 2001 [516]. Biochemical analysis indicated severe deficiencies of the pyruvate dehydrogenase (PDH) complex, oxoglutarate dehydrogenase (OGDH) complex (also known as α-ketoglutarate dehydrogenase complex), and complexes I, II, and III of the respiratory chain. Notably, mitochondrial aconitase activity is normal. Metabolite analysis performed on the patient urine samples revealed high levels of glycine, leucine, valine, and isoleucine, indicating abnormalities of the glycine-cleavage system and the branched-chain α-keto-acid dehydrogenase [516]. Using the technique of microcell-mediated chromosome transfer, the genetic defect in three patients in one family was mapped to chromosome 2p14–p13 [516] and subsequently mapped to NFU1 [317, 517], a gene with sequence homology to the C-terminal domain of *A. vinelandii* Fe-S cluster scaffold protein NifU. A homozygous missense mutation c.545G>A near the splice donor site of exon 6 in NFU1 causes abnormal mRNA splicing, leading to the production of several truncated transcripts and no detectable NFU1 protein product [517]. Transduction of fibroblast lines with retroviral vectors expressing the mitochondrial isoform of NFU1 restored respiratory chain function and oxoacid dehydrogenase complexes, confirming the pathogenicity of the NFU1 mutation. Immunostaining using lipoate antibodies indicated a severe reduction in lipoylated E2 proteins of the PDH and OGDH complexes [321, 517], suggesting that the loss of NFU1 might be specifically affecting the Fe-S enzyme LIAS [518].

A link between NFU1 defects and severe mitochondrial disorders was independently identified in individuals with fatal infantile encephalopathy, pulmonary hypertension, hyperglycemia, lactic acidosis, and decreased glycine cleavage system and PDH complex functions [321]. Nine of the individuals were homozygous for a G208C mutation in NFU1, and the tenth was compound heterozygous for a G208C mutation and a splice-site (c.545fl5G>A) mutation. G208 is highly conserved and is only one residue away from the Fe-S cluster binding motif. *In vitro* studies

confirmed that the G208C mutation of yeast Nfu1 leads to its functional impairment. Depletion or inactivation of NFU1 resulted in decreased SDHA and SDHB subunits of complex II and an assembly defect in complex II [321, 517, 519]. Interestingly, fibroblasts from NFU1 patients showed heterogeneous patterns of respiratory chain alterations, with isolated complex II deficiency in some patients [321] or combined deficiencies of complexes I, II, and III in others [517]. Other patients with an early-onset and rapidly fatal encephalopathy associated with NFU1 mutations have also been reported [520–522].

Several of the biochemical phenotypes observed in the NFU1 patients suggested that loss of NFU1 impaired LIAS function [321, 517]. Although the PDH complex, OGDH complex, and glycine cleavage system do not contain Fe-S clusters, these enzyme complexes all require a covalently linked lipoic acid moiety for their enzyme functions, and mutations in LIAS have been reported to impair PDH complex and glycine cleavage system activities [213]. Quantitative analysis for iron and sulfide on the *E. coli* LIAS, LipA, have shown that the active form of LipA contains two [4Fe-4S] clusters per polypeptide [523]. One of the Fe-S clusters binds SAM and is essential for the reductive cleavage of SAM to generate a methionine and a 5′-deoxyadenosyl 5′-radical (5′-dA•). The second Fe-S cluster is sacrificed during catalytic turnover as the source of the two sulfur atoms inserted into the substrate octanoic acid to form lipoic acid [9, 212]. Thus, the Fe-S cluster biogenesis pathway is important for the activities of lipoate-dependent enzymes, not only for the generation of 5′-dA• for the catalytic activity of LIAS but also as sulfur donors for the formation of lipoic acid.

A. vinelandii NifU consists of three distinct domains: the N-terminal ISCU-like domain, the central FDX-like domain, and the C-terminal NFU-like domain [524]. The NFU domain contains a CXXC motif, and proteins containing the NFU domain are present in bacteria, yeast, *Arabidopsis thaliana*, and humans [317, 319, 320, 322, 525, 526]. Depletion of NfuA in *E. coli* and in *A. vinelandii* resulted in increased sensitivity to oxidative stress [319]. In cyanobacteria, the NFU homolog is essential for viability [320, 527]. In *A. thaliana*, *Nfu2* gene disruption resulted in a dwarf phenotype, with impairment in the assembly of [4Fe-4S] and [2Fe-2S] FDX clusters, while Rieske and [3Fe-4S] glutamate synthase clusters were not affected [525, 526].

Early studies of Nfu homologues suggested that these proteins may serve as a scaffold for Fe-S cluster assembly. The protein containing Nfu domain in cyanobacterium *Synechocystis* PCC6803 was found by UV-visible spectroscopy to bind a [2Fe-2S] cluster and transfer it to apo-FDX [316, 525]. Mössbauer spectroscopic studies showed that nfuA from *Synechococcus* PCC7002 assembles and transfers [4Fe-Fs] clusters to apo-PsaC in photosystem I [318], whereas *E. coli* and *A. vinelandii* NfuA bind a [4Fe-4S] cluster, which is transferred to apo-aconitase [319, 320]. UV-visible spectral analysis suggested that *A. thaliana* NFU-like proteins are capable of binding a labile [2Fe-2S] cluster *in vitro* and transferring them to apo-FDX [528]. Mössbauer spectroscopy analysis indicated that human NFU1 is able to assemble a [4Fe-4S] cluster [317]. Liu *et al.* reported that human NFU forms a complex with the cysteine desulfurase NifS and

mediates persulfide bond cleavage of sulfur-loaded NifS persulfide and suggested that human NFU1 mediates sulfide delivery to ISCU in the final step of [2Fe-2S] cluster assembly [529]. However, a different model has been proposed, which suggests that Fe-S clusters initially formed on the IscU type of scaffolds are subsequently transferred to Nfu-type proteins. In this model, NfuA-type proteins serve as intermediate Fe-S cluster carriers to deliver Fe-S cluster to apo-targets [320]. In support of this proposal, siRNA-mediated depletion of ISCU resulted in marked decreases in the activity of SDH, mitochondrial and cytosolic aconitases, and cytosolic GPAT and decreases in the levels of lipoylated a-KGDH, PDH, and GCS, whereas depletion of NFU1 affected a subset of these proteins (lipoylated proteins and SDH) [321]. Furthermore, apo-NfuA in *E. coli* is able to accept a Fe-S cluster from holo ISCU or holo-SufBC2D, whereas no cluster transfer was observed between holo-NfuA and apo-ISCU or apo-SufBC2D, suggesting that NfuA is not a scaffold, but rather an Fe-S cluster carrier [322]. Taken together, these studies support the idea that NFU1 acts downstream of ISCU and may be involved in transferring newly synthesized Fe-S clusters from ISCU to specific apo-target proteins.

10.4.7 Mutations in BOLA3 cause MMDS 2 (MIM 614299)

A mutation in *BOLA3* was first described in an infant who developed epileptic seizures, dilated cardiomyopathy, encephalopathy, respiratory distress, hepatomegaly, and acidosis, with elevated levels of glycine in his serum and cerebrospinal fluid, and who subsequently died at 11 months of age [517]. Studies of patient skin fibroblasts showed elevated lactate-to-pyruvate ratios and decreased activities of the PDH complex, branched chain α-keto acid dehydrogenase, and mitochondrial respiratory chain complexes I and II. In contrast, the activity of ACO2 was normal. A single base-pair duplication c.123dupA was identified in exon 2 of *BOLA3*, which causes a frameshift that produces a premature stop codon in both isoforms of *BOLA3*. A second study soon followed, reporting the case of two siblings who presented with severe neonatal lactic acidosis, hypotonia, respiratory insufficiency, and intractable cardiomyopathy [530]. Both patients died within the first months of life due to multiorgan failure. Organic acids analyses of urine revealed elevated metabolites of the TCA cycle (succinate, fumarate, malate, aconitic acid, and citric acid), together with increased excretion of lactate and pyruvate. Assessment of skeletal muscle biopsies and fibroblasts showed combined deficiency of respiratory chain complexes I and II accompanied by a defect of the PDH complex. A decrease in complex IV activity was also observed in the muscle biopsy of one of the patients. Brain MRI indicated lesions in several areas in the brain. The identified homozygous missense mutation, c.200T>A I67N, is located in exon 3 and solely affects isoform I of *BOLA3*. In a 2014 study, three patients were shown to be homozygous for a truncating mutation c.136C>T p46X in exon 2 of BOLA3 isoform 1 [216].

The exact function of BOLA3 is still not fully understood. Because of the similar phenotypes of MMDS1 and MMDS2, BOLA3 has been proposed to function in concert with NFU1 for biogenesis of LIAS [517]. Mammalian cells have three BOLA homologues, denoted as BOLA1, BOLA2, and BOLA3. On the basis of functional genomics data, affinity purification, yeast two-hybrid studies, and structural characterizations, BOLA family members in yeast were postulated to act as reductases, interacting with the mono-thiol GLRX family that includes the cytosolic GRX3 and GRX4 and the mitochondrial [531]. Genetic studies in yeast demonstrate a crucial role for complexes between Grx3 and Grx4 with the BolA-like protein Fra2 in iron homeostasis, and that the Grx-BolA interaction is required for efficient iron-dependent inhibition of the Aft1 and Aft2 transcriptional activators [462, 532] (see also the chapter by C. Outten for in-depth discussion). Studies in zebrafish also indicated a crucial function of vertebrate Grx3 (PICOT) in iron homeostasis and hemoglobin maturation [533]. UV-visible absorption, CD, resonance Raman, EPR, ENDOR, Mossbauer, and EXAFS studies showed that yeast Fra2 forms a [2Fe-2S]-bridged heterodimeric complex with Grx3 or Grx4, with iron ligands provided by a cysteine from Grx3 or Grx4, a histidine from Fra2, and glutathione [467]. This complex plays a key role in iron regulation in *S. cerevisiae* [532, 534]. More recent studies have shown that BolA2 and Glrx3, the human homologues of Fra2 and Grx3, form a [2Fe-2S] chaperone complex that can transfer [2Fe-2S] cluster to CIAPIN *in vitro* [535, 536] and in the cytosol of human cells [537], suggesting that BolA2-Glrx5 function in the maturation of cytosolic Fe-S proteins. It has been suggested that BOLA3 possibly functions by interacting with GLRX5 and NFU1 in the mitochondria for the maturation of [4Fe-4S] proteins [538]. Melber *et al*. reported that Nfu1 and Bol3 in yeast function in the transfer of Fe-S clusters from the ISA1-ISA2-Iba57 complex to mitochondrial [4Fe-4S] client proteins [539].

10.4.8 IBA57 deficiency causes severe myopathy and encephalopathy

IBA57 was first identified as an Fe-S protein biogenesis factor in a genome-wide screen for yeast mutants that are auxotrophic for glutamate and lysine due to defects in mitochondrial aconitase and homoaconitase [314]. Depletion of yeast Iba57 results in diminished *de novo* Fe-S cluster formation on aconitase and homoaconitase, but not in FDX (Yah1) or isopropylmalate dehydratase (Leu1p). Depletion of Iba57 also resulted in loss of catalytic function of radical-SAM Fe-S protein biotin synthase and LIAS. In *E. coli*, suppression of an IBA57-related protein, YgfZ, resulted in deficiency in Fe-S proteins SDH and tRNA modification enzyme MiaB, but not aconitase [540]. In IBA57-depleted HeLa cells, catalytic activities of complex I and II were compromised, and steady-state levels of several Fe-S proteins, including subunits of complex I (NDUFA9, NDUFA13, NDUFB4, and NDUFS3), complex II (SDH), and complex IV (MT-CO2), were affected [541]. Notably, the activity of the [2Fe-2S] cluster-containing

complex III was not affected in these individuals, consistent with the suggestion that IBA57 is specific for [4Fe-4S] cluster formation [314, 541]. Yeast Iba57 physically interacts with the Fe-S cluster assembly proteins Isa1 and Isa2 [314], and *E. coli* YgfZ occurs in complexes with IscA-type proteins *in vivo* [542], suggesting that the complex of these three proteins forms the functional unit [314, 315].

Mutations in IBA57 were found in two siblings who became critically ill shortly after birth [543]. Patient 1 presented with severe hypotonia, absent primitive reflexes, microcephaly, dysmorphic features, hyperglycemia, and elevated lactate and glycine levels in serum and cerebrospinal fluid, but normal blood cell counts and hemoglobin and hematocrit measurements. Cerebral MRI showed cerebral atrophy. Patient 2 died shortly after birth due to hypoventilation and low cardiac activity. Biochemical studies revealed decreased catalytic activities of complexes I and II, whereas the activity of complex III was normal. Immunoblot analysis showed severely decreased levels of complexes I, II, and IV subunits in skeletal muscle, whereas levels of complexes III and V were unchanged. In addition, defects in ACO2 and the lipoate-containing enzymes, OGDH and PDH, were also found in these patients. Sequence analysis revealed a homozygous mutation, c.941A>C, resulting in a change of the residue G314 to a Pro. Analysis of mitochondrial extracts from skeletal muscle and cultured skin fibroblasts and IBA57-depleted HeLa cells indicated that the mutation resulted in a severe decrease in IBA57 protein due to proteolytic degradation. The lipoylated groups in PDH and OGDH were significantly decreased in cultured skin fibroblasts and skeletal muscle tissue of the patients. A second study reported a homozygous c.436C>T variant in IBA57 gene that converts a conserved Arg146 to Trp in an infant with multiple mitochondrial dysfunction syndrome and progressive leukodystrophy [544]. Biochemical studies of skeletal muscle isolated from the patient revealed deficiencies of complexes I and II and loss of protein lipoylation. These findings are consistent with the proposal that IBA57 is important for [4Fe-4S] cluster assembly in LIAS [314].

10.4.9 A mutation in ISD11 causes deficiencies of respiratory complexes

LYRM4 encodes the ISD11 protein that is essential for cell viability in yeast [286]. Yeast strains lacking Isd11 are deficient in aconitase and SDH activities [286, 287], and knockdown of ISD11 results in aconitase deficiency in human cell lines [288, 545], implicating an essential role of ISD11 in Fe-S cluster assembly. Pull-down and coimmunprecipitation experiments showed that ISD11 forms a complex with the cysteine desulfurase NFS1 in yeast and human cells [286, 287, 545]. In yeast without Isd11, it was initially reported that Nfs1 had normal desulfurase activity but was prone to aggregation and proteolytic degradation [286]. However, other studies suggested that Nfs1 by itself was inactive and that Isd11 is important for inducing an activating conformational change in Nfs1 [289]. In addition, Shi *et al.* showed that ISD11 depletion

in human cell lines activated the iron regulatory proteins IRP1 and IRP2, which led to upregulation of TfR1 and mitochondrial iron accumulation [288]. These results suggest that ISD11 is important in the biogenesis of Fe-S clusters, and loss of ISD11 disrupts normal mitochondrial and cytosolic iron homeostasis. In addition to sequestering the sulfur for Fe-S cluster biogenesis, Nfs1• ISD11 complex might be important for other biological pathways that require sulfur transfer, including the biogenesis pathways of biotin, thiamine, lipoic acid, molybdopterin, and sulfur containing bases in tRNA [546–548].

A homozygous mutation in LYRM4 was recently identified *via* massive parallel sequencing of >1,000 mitochondrial genes in two patients with deficiencies of the respiratory complexes containing Fe-S clusters [549]. Patient 1 had stridor (a high-pitched wheezing sound resulting from turbulent air flow in the upper airway), hypotonia, and lactic acidosis shortly after birth but improved later. Patient 2 had stridor, hepatomegaly, metabolic acidosis, severe ketosis, and died at 2 months of age. Postmortem muscle histology of patient 2 revealed reduced glycogen levels and increased lipid levels. Liver analysis showed steaosis (indicative of impairment of lipid metabolism), markedly reduced glycogen, and mildly increased iron levels. The mutation in *LYRM4* was predicted to cause a missense change affecting a highly conserved amino acid residue in ISD11, and ISD11 protein was undetectable in patient muscle and liver biopsies. Levels of complex I subunits NDUFB8 and NDUFS3, complex II subunit SDHB, complex III subunit UQCRFS1, and complex IV subunits COX2 and COX1 were reduced in both patients. Other Fe-S proteins, including ACO1, ACO2, and FECH, were also reduced in the patients.

10.4.10 Infantile mitochondrial complex II/III deficiency (IMC23D) caused by a missense mutation in NFS1

The cysteine desulfurase encoded by *NFS1* is essential in most organisms for providing sulfur for Fe-S cluster biogenesis [550]. In addition, NFS1 is important for the sulfuration of tRNAs [551] and for providing sulfur in the MoCo biosynthetic pathway that is essential for the function of SO, XOR, and AO [217, 548]. A mutation in *NFS1* gene (MIM 603485) has been shown to be the genetic cause of a fatal autosomal recessive disease in three children of healthy third cousins in an Old Order Mennonite community [552]. The patients presented with lactic acidemia, hypotonia, respiratory chain complex II and III deficiency, multisystem organ failure, and abnormal mitochondria. The first child was admitted at 7 months of age and died of cardiac failure 3 days postadmission. The second child was presented with respiratory failure, cyanosis, and elevated levels of lactate at 6 weeks of age and was treated with a mitochondrial cofactor therapy consisting of riboflavin, coenzyme Q10, thiamine, vitamin C, vitamin E, and vitamin K, which led to clinical and biochemical improvement. At 7 months, symptoms recurred and he died of cardiac failure. The third patient was treated with

a mitochondrial cofactor therapy from 6 months until about 11 years of age. He is generally healthy, with elevated levels of blood lactate, aspartate aminotransferase, and creatine kinase and mild developmental and gross motor delay. Exome sequencing and biochemical studies indicated that a c.215G>A mutation in these patients led to the substitution of Arg72 into Gln in NFS1 and a disruption of the NFS1-ISD11 complex. Notably, mutations in LYRM4, which encodes ISD11, also resulted in a disruption of the NFS1-ISD11 complex and leads to a clinical presentation similar to IMC23D [549]. The severe clinical outcome of NFS1 deficiency stresses the crucial importance of NFS1 for the biosynthesis of Fe-S clusters and for MoCo and tRNA modifications.

10.4.11 Mutations in HSPA9 in patients with congenital sideroblastic anemia and myelodysplastic syndrome

Human HSPA9 (HscA in bacteria, and Ssq1 in *S. cerevisiae*) encodes a heat uninducible member of the heat shock 70 protein family that has been documented by many names, including HSPA9B, mortalin, and GRP75 [553, 554]. HSP70 homologues use the energy released by the hydrolysis of ATP to drive conformational changes and refolding of target proteins [304, 554]. HSPA9 is mainly localized in the mitochondria but has also been found in other subcellular localizations including ER, Golgi apparatus, and cytosol, with binding partners including p53, FGF-1, IL-1 receptor type 1, GRP94, VDAC, NADH dehydrogenase, MPD, Mge1 Tim44, and Tim23. HSPA9 has been implicated in diverse molecular pathways including energy generation, stress response, and involvement in cancer, neurodegeneration, and EVEN-PLUS syndrome of congenital malformations and skeletal dysplasia [553, 555].

With respect to Fe-S cluster biogenesis, the HSPA9/HSC20 complex facilitates cluster transfer from the primary scaffold protein ISCU to recipient apoproteins or to intermediate carriers [305]. Genetic and functional analysis of patients from several families showed that germline incomplete loss of HSPA9 function results in a congenital sideroblastic anemia phenotype that reflects abnormal mitochondrial iron utilization by the erythroid precursors [556]. A large fraction of the patients carry HSPA9 loss-of-function alleles inherited in trans with a common coding single nucleotide polymorphism associated with reduced mRNA expression, resulting in pseudodominant inheritance in some families. HSPA9 deficiency in zebrafish resulted in anemia, dysplastic immature erythroblasts, accelerated apoptosis, and leukopenia, with accelerated apoptosis in erythroid cells consistent with ineffective hematopoiesis [557]. Knockdown of HSPA9 in primary human CD34+ cells delayed the maturation of erythroid precursors, and erythroid precursors were reduced in the mouse Hspa9 knockdown model [558]. These results make HSPA9 the second protein in the Fe-S cluster biogenesis pathway to be associated with sideroblastic anemia. In zebrafish, Grx5 mutations cause anemia as a result of IRP1-mediated translational repression of erythroid aminolevulinate synthase (ALAS2), the first enzyme in the heme biosynthetic pathway [309]. In the GLRX5-deficient patient

and in the zebrafish model, IRP1 becomes an active mRNA binding protein that inhibits *ALAS2* translation and thereby blocks heme biosynthesis. Studies of a zebrafish shiraz mutant and patients with sideroblastic anemia-associated mutations in GLRX5 showed that loss of GLRX5 resulted in mitochondrial iron overload and concomitant cytosolic iron depletion, which prevents *de novo* cytosolic cluster assembly in IRP1 and activates IRP1-mediated translational repression of *ALAS2*. Recent studies showed that HSPA9 depletion also increased IRP-RNA binding activities and decreased ALAS2 and FECH protein levels during erythroid differentiation of Murine Myeloid Erythroleukemia MEL cells [559]. These studies may explain the sideroblastic anemia-associated phenotype resulting from HSPA9 haploinsufficiency.

In addition to sideroblastic anemia, HSPA9 deficiency is associated with myelodysplastic syndromes (MDSs). MDSs are a heterogenous group of hematopoietic stem cell disorders. Progression to AML occurs in 30% of MDS patients, with mean survival rates of 6 months to 5 years [560]. MDS is characterized with peripheral blood cytopenias (reduction of blood cells) as a result of peripheral blood and bone marrow dysplasia and accelerated apoptotic death of multipotential hematopoietic progenitors and their progeny. Recurrent somatic mutations in genes involved in transcriptional regulation, signal transduction, epigenetic regulation, RNA splicing, and DNA damage response have been identified in MDS. Deletions at chromosome 5q32 are associated with more aggressive forms of MDS and HSPA9 is one of the genes in the 5q MDS deletion interval [561]. Loss of HSPA9 homologue in zebrafish closely recapitulates the ineffective hematopoiesis of the MDS including anemia, dysplasia, increased blood cell apoptosis, and multilineage cytopenia, suggesting that HSPA9 deficiency may contribute to MDS and AML pathogenesis [557].

10.5 Fe-S cluster biogenesis and iron homeostasis

Another important finding from the studies of genes involved in Fe-S cluster biogenesis is that Fe-S cluster biogenesis is important for the regulation of mitochondrial iron homeostasis [327, 418]. Many yeast strains that were depleted of Fe-S cluster biogenesis proteins (e.g. *yfh1*, *nfs1*, *isu1*, *isu2*, *isa1*, *isa2*, *nfu1*, *ssq1*, *jac1*, *yah1*) showed marked iron accumulation in their mitochondria [298, 349, 406, 562–564]. Disruption of intracellular iron homeostasis is also a prominent feature in human patients depleted of FXN, ABCB7, GLRX5, and ISCU [310, 417, 476] (Fig. 10.4) and in human cell lines depleted of ISCU, ABCB7, GLRX5, ISD11, and FDX *via* RNA silencing [288, 295, 328, 441, 470]. The increased mitochondrial iron uptake is facilitated by the mitochondrial iron transporters, mitoferrin 1 (MFRN1), the major importer of iron into mitochondria in erythroid cells and mitoferrin 2, which is mostly in nonerythroid cells [420, 565]. Disruption of the yeast mfrn orthologs, MRS3 and MRS4, caused defects in iron metabolism and in mitochondrial Fe-S cluster biogenesis [566, 567]. As mentioned in Section 10.3.2, most patients with EPP are heterozygous for a mutation in

FECH, the gene that encodes a [2Fe-2S] enzyme that inserts ferrous iron into PPIX for heme biosynthesis. Wang *et al.* reported that six patients with EPP had an abnormal transcript of MFRN1 that contained an insert of intron 2, resulting in a truncated MFRN1 protein that is retained in the cytosol [568]. Reduced MFRN1 expression can contribute to the EPP phenotype by causing a further reduction of FECH activity. In yeast, depletion of components of the mitochondrial Fe-S assembly systems induced strong transcriptional responses of many genes, and these alterations were very similar to the transcriptional profiles developed upon iron starvation, including many that are involved in cellular iron uptake [469, 569, 570]. In human cells, disruptions of Fe-S cluster biogenesis and mitochondrial iron homeostasis also activate iron regulatory proteins IRP1 and IRP2 [328, 339, 341, 358, 423], which triggers an increase in cellular iron uptake *via* TfR1 and a decrease in iron sequestration by ferritin. Together, these results suggest that an Fe-S protein might function as a sensor for mitochondrial iron status or in signaling the status of mitochondrial iron stores to the nucleus. In this scenario, dysfunction in Fe-S cluster biogenesis would be registered by the cell as mitochondrial iron deficiency, which triggers an increase in mitochondrial iron uptake *via* mitoferrin [420, 500], and iron accumulates in amorphous nanoparticles of ferric phosphate in the mitochondrial matrix [421, 422] or within mitochondrial ferritin [417]. In addition, cytosolic iron pools might become functionally depleted because of mitochondrial iron sequestration, which triggers the activation of IRP1 and IRP2, resulting in upregulation of iron import through TfR1, decrease in ferroportin-mediated iron export, and decreased iron sequestration by iron storage protein ferritin [420]. The aberrant upregulation of TfR1 and increase in mitochondrial iron uptake have the potential to engage the cell in a vicious cycle in which increased cellular iron uptake further exacerbates mitochondrial iron overload.

Interestingly, mitochondrial iron overload in cells with defects in Fe-S cluster biogenesis can cause increased oxidative stress not only directly *via* iron-catalyzed oxidation reactions [406, 571] but also by inactivating mitochondrial superoxide dismutase, MnSOD [572]. Although mitochondrial iron does not normally bind MnSOD, iron will misincorporate into *S. cerevisiae* MnSOD when mitochondrial iron homeostasis is disrupted in yeast mutants that have defects in the late stages of Fe-S cluster biogenesis (e.g. *grx5*, *ssq1*, and *atm1*). Iron binding inactivates the MnSOD enzyme, presumably by causing changes in the redox potential at the active site or by blocking substrate access.

10.6 Therapeutic strategies

A greater understanding of the physiological roles of Fe-S proteins and the process of Fe-S cluster biogenesis, together with technological advances in genetic diagnosis in recent years, has led to the discovery of disease-causing mutations in a number of Fe-S proteins and Fe-S cluster biogenesis factors and provided the opportunities to design more effective diagnostics and potential treatments for several devastating

diseases. Some therapeutic approaches target the specific disease mutation and disease symptoms. For instance, palliative treatments of FRDA patients typically consist of physical therapy and β-blockers, ACE-inhibitors, and surgery for cardiac symptoms [573]. In the case of patients with mutations in LYRM4/ISD11, the realization that the disease gene encodes a protein that is important for the enzymatic activity of a cysteine desulfurase led to the suggestion that providing a sulfur donor such as cysteine or N-acetyl cysteine may constitute a potential therapy [549]. Additional therapeutic approaches involve agents that aim to boost the expression levels of the disease genes [368]. In the case of FRDA, EPO has been shown to promote the translation of FXN [574, 575], and recombinant human EPO was found to increase FXN expression in FRDA patients [576]. A specific family of benzamide histone deacetylase inhibitors have been shown to mitigate FXN silencing in FRDA cells [577, 578] and showed promise in a pilot clinical study with FRDA patients [579]. In addition, there has been much interest in developing novel therapeutic applications such as cell or gene therapies for FRDA [580], and prevention and reversal of severe mitochondrial cardiomyopathy by gene therapy have been reported in an FRDA mouse model [581]. Interferon gamma-1β has been found to increase FXN expression in dorsal root ganglion neurons and improve sensorimotor performance in mouse FRDA models [582]. In addition, antisense oligonucleotides are being developed for neurological disorders, such as spinal muscular dystrophy and Huntington disease [583]. Recently, Li *et al*. showed that introducing anti-GAA duplex RNAs or single-stranded locked nucleic acids into FRDA patient cells restored FXN protein levels [584]. In the case of ISCU myopathy, *in vitro* studies have demonstrated that RNA modulating therapy with an antisense phosphorodiamidate morpholino oligonucleotide that specifically targets the aberrantly activated splice site in ISCU is able to restore the normal splicing pattern of ISCU [585]. An upregulation of normally spliced ISCU mRNA produced by blocking the cryptic splice site may thus be a therapeutic possibility for these patients. More recent studies using chemically advanced antisense oligomers demonstrated that blocking the point mutation site with a tightly binding antisense blocked abnormal splicing and restored ISCU function in myoblasts from patients with ISCU myopathy [586].

On the other hand, since mitochondrial iron overload and mitochondrial failure are common features in diseases associated with defects in Fe-S proteins and Fe-S cluster biogenesis, several common therapeutic strategies have emerged that involve administering antioxidants to reduce oxidative damages and iron chelators to decrease iron-mediated oxidative stress and attenuate iron overload [587, 588]. For instance, adenoviral delivery of the human SOD2 gene was shown to suppress the optic nerve degeneration in a mouse model of complex I deficiency [589], suggesting that antioxidant therapy may attenuate the disease process in patients with defective respiratory complexes. Patients with FRDA also have increased DNA damage [425] and lipid peroxidation [590], and much work has been done to evaluate the potential of antioxidants in preventing mitochondrial damage and preserving aerobic respiration.

Studies by the Schoumacher lab suggested that small molecule glutathione peroxidase mimetics have the potential to treat FRDA [591]. On the other hand, neither the administration of a MnSOD mimetic (MnTBAP) nor the overexpression of CuZnSOD improved the cardiomyopathy symptoms in a murine FRDA model [423]. Idebenone, a CoQ10 analog that can reduce intracellular ROS as well as shuttle electrons between damaged respiratory complex proteins, showed promise in animal models [428, 592] and early clinical studies [424–426] but failed the phase III clinical trial because it did not significantly improve cardiac outcomes in patients over a 6-month treatment period [427]. It has been suggested that antioxidants may prove to be more effective if given at an early stage of disease progression before significant neuronal and cardiomyocyte damage accumulates.

The consistent finding that dysregulation of iron homeostasis is a pathological hallmark of FRDA has led to efforts in testing iron chelators for use in the treatment of FRDA [587, 593]. Iron chelators, including deferoxamine and deferiprone, have been evaluated in *in vitro* models and in clinical trials, with mixed results. Although iron chelators reduced ROS damage to mitochondrial proteins and reduced iron buildup in the brain with improvements in neurological function in a number of studies [428, 594, 595], other studies indicated that iron chelation has the undesirable effects of reducing mRNA levels of and aconitase and in impairing aconitase function [358, 596]. A 6-month study showed little improvement in FRDA patients who were administered deferoprone over placebo, but the trial may have been too short to be conclusive [597].

Acknowledgments

I thank Drs. Karen Ayyad and Ron Haller for generously providing the SDH activity and iron stainings of skeletal muscle from patients with ISCU deficiency.

References

[1] Beinert H, Holm RH, Munck E. Iron-sulfur clusters: nature's modular, multipurpose structures. Science 1997;277:653–9.
[2] Johnson DC, Dean DR, Smith AD, Johnson MK. Structure, function, and formation of biological iron-sulfur clusters. Annu Rev Biochem 2005;74:247–81.
[3] Beinert H, Kennedy MC, Stout CD. Aconitase as iron-protein, enzyme, and iron-regulatory protein. Chem Rev 1996;96:2335–74.
[4] White MF, Dillingham MS. Iron-sulphur clusters in nucleic acid processing enzymes. Curr Opin Struct Biol 2012;22:94–100.
[5] Rudolf J, Makrantoni V, Ingledew WJ, Stark MJ, White MF. The DNA repair helicases XPD and FancJ have essential iron-sulfur domains. Mol Cell 2006;23:801–8.
[6] Wu Y, Brosh RM Jr. DNA helicase and helicase-nuclease enzymes with a conserved iron-sulfur cluster. Nucleic Acids Res 2012;40:4247–60.

[7] Netz DJ, Stith CM, Stumpfig M, Kopf G, Vogel D, Genau HM, Stodola JL, Lill R, Burgers PM, Pierik AJ. Eukaryotic DNA polymerases require an iron-sulfur cluster for the formation of active complexes. Nat Chem Biol 2012;8:125–32.
[8] Fuss JO, Tsai CL, Ishida JP, Tainer JA. Emerging critical roles of Fe-S clusters in DNA replication and repair. Biochim Biophys Acta 2015;1853:1253–71.
[9] Lanz ND, Booker SJ. Identification and function of auxiliary iron-sulfur clusters in radical SAM enzymes. Biochim Biophys Acta 2012;1824:1196–212.
[10] Mettert EL, Kiley PJ. Fe-S proteins that regulate gene expression. Biochim Biophys Acta 2015;1853:1284–93.
[11] Rouault TA. The role of iron regulatory proteins in mammalian iron homeostasis and disease. Nat Chem Biol 2006;2:406–14.
[12] Hentze MW, Muckenthaler MU, Galy B, Camaschella C. Two to tango: regulation of Mammalian iron metabolism. Cell 2010;142: 24–38.
[13] Anderson CP, Shen M, Eisenstein RS, Leibold EA. Mammalian iron metabolism and its control by iron regulatory proteins. Biochim Biophys Acta 2012;1823:1468–83.
[14] Roberts RA, Smith RA, Safe S, Szabo C, Tjalkens RB, Robertson FM. Toxicological and pathophysiological roles of reactive oxygen and nitrogen species. Toxicology 2010;276:85–94.
[15] Federico A, Cardaioli E, Da Pozzo P, Formichi P, Gallus GN, Radi E, Mitochondria, oxidative stress and neurodegeneration. J Neurol Sci 2012;322(1–2):254–62.
[16] Crack JC, Green J, Thomson AJ, Le Brun, NE. Iron-sulfur clusters as biological sensors: the chemistry of reactions with molecular oxygen and nitric oxide. Acc Chem Res 2014;47:3196–205.
[17] Imlay JA. Iron-sulphur clusters and the problem with oxygen. Mol Microbiol 2006;59:1073–82.
[18] Yarian CS, Toroser D, Sohal RS. Aconitase is the main functional target of aging in the citric acid cycle of kidney mitochondria from mice. Mech Ageing Dev 2006;127:79–84.
[19] Boehm DE, Vincent K, Brown OR. Oxygen and toxicity inhibition of amino acid biosynthesis. Nature 1976;262:418–20.
[20] Kuo CF, Mashino T, Fridovich I. alpha, beta-Dihydroxyisovalerate dehydratase. A superoxide-sensitive enzyme. J Biol Chem 1987;262:4724–7.
[21] Gardner PR, Fridovich I. Superoxide sensitivity of the Escherichia coli aconitase. J Biol Chem 1991;266(29):19328–33.
[22] Flint DH, Tuminello JF, Emptage MH. The inactivation of Fe-S cluster containing hydro-lyases by superoxide. J Biol Chem 1993;268(30):22369–76.
[23] Longo VD, Liou LL, Valentine JS, Gralla EB. Mitochondrial superoxide decreases yeast survival in stationary phase. Arch Biochem Biophys 1999;365(1):131–42.
[24] Wallace MA, Liou LL, Martins J, Clement MH, Bailey S, Longo VD, Valentine JS, Gralla EB. Superoxide inhibits 4Fe-4S cluster enzymes involved in amino acid biosynthesis. Cross-compartment protection by CuZn-superoxide dismutase. J Biol Chem 2004;279:32055–62.
[25] Missirlis F, Hu J, Kirby K, Hilliker AJ, Rouault TA, Phillips JP. Compartment-specific protection of iron-sulfur proteins by superoxide dismutase. J Biol Chem 2003;278(48):47365–9.
[26] Kispal G, Sipos K, Lange H, Fekete Z, Bedekovics T, Janaky T, Bassler J, Aguilar Netz DJ, Balk J, Rotte C, Lill R. Biogenesis of cytosolic ribosomes requires the essential iron-sulphur protein Rli1p and mitochondria. EMBO J 2005;24(3):589–98.
[27] Alhebshi A, Sideri TC, Holland SL, Avery SV. The essential iron-sulfur protein Rli1 is an important target accounting for inhibition of cell growth by reactive oxygen species. Mol Biol Cell 2012;23(18):3582–90.
[28] Yan LJ, Levine RL, Sohal RS. Oxidative damage during aging targets mitochondrial aconitase. Proc Natl Acad Sci USA 1997;94(21):11168–72.
[29] Van Remmen H, Richardson A. Oxidative damage to mitochondria and aging. Exp Gerontol 2001;36(7):957–68.

[30] Bulteau AL, Ikeda-Saito M, Szweda LI. Redox-dependent modulation of aconitase activity in intact mitochondria. Biochemistry 2003;42(50):14846–55.
[31] Delaval E, Perichon M, Friguet B. Age-related impairment of mitochondrial matrix aconitase and ATP-stimulated protease in rat liver and heart. Eur J Biochem 2004;271(22):4559–64.
[32] Li Y, Huang TT, Carlson EJ, Melov S, Ursell PC, Olson JL, Noble LJ, Yoshimura MP, Berger C, Chan PH, Wallace DC, Epstein CJ. Dilated cardiomyopathy and neonatal lethality in mutant mice lacking manganese superoxide dismutase. Nat Genet 1995;11:376–81.
[33] Huang TT, Carlson EJ, Kozy HM, Mantha S, Goodman SI, Ursell PC, Epstein CJ. Genetic modification of prenatal lethality and dilated cardiomyopathy in Mn superoxide dismutase mutant mice. Free Radic Biol Med 2001;31(9):1101–10.
[34] Armstrong JS, Whiteman M, Yang H, Jones DP. The redox regulation of intermediary metabolism by a superoxide-aconitase rheostat. Bioessays 2004;26:894–900.
[35] Welter R, Yu L, Yu CA. The effects of nitric oxide on electron transport complexes. Arch Biochem Biophys 1996;331(1):9–14.
[36] Tinberg CE, Tonzetich ZJ, Wang H, Do LH, Yoda Y, Cramer SP, Lippard SJ. Characterization of iron dinitrosyl species formed in the reaction of nitric oxide with a biological Rieske center. J Am Chem Soc 2010;132(51):18168–76.
[37] Asanuma K, Iijima K, Ara N, Koike T, Yoshitake J, Ohara S, Shimosegawa T, Yoshimura T. Fe-S cluster proteins are intracellular targets for nitric oxide generated luminally at the gastro-oesophageal junction. Nitric Oxide 2007;16(4):395–402.
[38] Tabrizi SJ, Cleeter MW, Xuereb J, Taanman JW, Cooper JM, Schapira AH. Biochemical abnormalities and excitotoxicity in Huntington's disease brain. Ann Neurol 1999;45(1):25–32.
[39] Sorolla MA, Reverter-Branchat G, Tamarit J, Ferrer I, Ros J, Cabiscol E. Proteomic and oxidative stress analysis in human brain samples of Huntington disease. Free Radic Biol Med 2008;45(5):667–78.
[40] Martin WR, Clark C, Ammann W, Stoessl AJ, Shtybel W, Hayden MR. Cortical glucose metabolism in Huntington's disease. Neurology 1992;42(1):223–9.
[41] Antonini A, Leenders KL, Spiegel R, Meier D, Vontobel P, Weigell-Weber M, Sanchez-Pernaute R, de Yebenez JG, Boesiger P, Weindl A, Maguire RP. Striatal glucose metabolism and dopamine D2 receptor binding in asymptomatic gene carriers and patients with Huntington's disease. Brain 1996;119 (Pt 6):2085–95.
[42] Esposito G, Vos M, Vilain S, Swerts J, De Sousa Valadas J, Van Meensel S, Schaap O, Verstreken P. Aconitase causes iron toxicity in Drosophila pink1 mutants. PLoS Genet 2013;9(4):e1003478.
[43] Sellers VM, Johnson MK, Dailey HA. Function of the [2FE-2S] cluster in mammalian ferrochelatase: a possible role as a nitric oxide sensor. Biochemistry 1996;35(8):2699–704.
[44] Crooks DR, Ghosh MC, Haller RG, Tong WH, Rouault TA. Posttranslational stability of the heme biosynthetic enzyme ferrochelatase is dependent on iron availability and intact iron-sulfur cluster assembly machinery. Blood 2010;115(4):860–9.
[45] Imlay JA. The molecular mechanisms and physiological consequences of oxidative stress: lessons from a model bacterium. Nat Rev Microbiol 2013;11(7):443–54.
[46] Zhang B, Crack JC, Subramanian S, Green J, Thomson AJ, Le Brun NE, Johnson MK. Reversible cycling between cysteine persulfide-ligated [2Fe-2S] and cysteine-ligated [4Fe-4S] clusters in the FNR regulatory protein. Proc Natl Acad Sci USA 2012;109(39):15734–9.
[47] Nicolet Y, Rohac R, Martin L, Fontecilla-Camps JC. X-ray snapshots of possible intermediates in the time course of synthesis and degradation of protein-bound Fe4S4 clusters. Proc Natl Acad Sci USA 2013;110(18):7188–92.
[48] Jang S, Imlay JA, Micromolar intracellular hydrogen peroxide disrupts metabolism by damaging iron-sulfur enzymes. J Biol Chem 2007;282(2):929–37.
[49] Crack JC, Jervis AJ, Gaskell AA, White GF, Green J, Thomson AJ, Le Brun NE. Signal perception by FNR: the role of the iron-sulfur cluster. Biochem Soc Trans 2008;36(Pt 6):1144–8.

[50] Bruska MK, Stiebritz MT, Reiher M. Analysis of differences in oxygen sensitivity of Fe-S clusters. Dalton transactions 2013;42(24):8729–35.
[51] Breusch FL. Citric acid in tissue metabolism. Physiol Chem 1937;250:262–80.
[52] Tong WH, Rouault TA. Metabolic regulation of citrate and iron by aconitases: role of iron-sulfur cluster biogenesis. Biometals 2007;20(3–4):549–64.
[53] Denton RM, Randle PJ. Citrate and the regulation of adipose-tissue phosphofructokinase. Biochem J 1966;100:420–3.
[54] Randle PJ. Regulatory interactions between lipids and carbohydrates: the glucose fatty acid cycle after 35 years. Diabetes Metab Rev 1998;14:263–83.
[55] Munday MR. Regulation of mammalian acetyl-CoA carboxylase. Biochem Soc Trans 2002;30:1059–64.
[56] Saha AK, Ruderman NB. Malonyl-CoA and AMP-activated protein kinase: an expanding partnership. Mol Cell Biochem 2003;253:65–70.
[57] Rogina B, Reenan RA, Nilsen SP, Helfand SL. Extended life-span conferred by cotransporter gene mutations in Drosophila. Science 2000;290:2137–40.
[58] Knauf F, Mohebbi N, Teichert C, Herold D, Rogina B, Helfand S, Gollasch M, Luft FC, Aronson PS. The life-extending gene Indy encodes an exchanger for Krebs-cycle intermediates. Biochem J 2006;397:25–9.
[59] Fei YJ, Liu JC, Inoue K, Zhuang L, Miyake K, Miyauchi S, Ganapathy V. Relevance of NAC-2, an Na+-coupled citrate transporter, to life span, body size and fat content in Caenorhabditis elegans. Biochem J 2004;379:191–8.
[60] Belfiore F, Iannello S. Insulin resistance in obesity: Metabolic mechanisms and measurement methods. Mol Gen Metab 1998;65:121–8.
[61] Wolfgang MJ, Lane MD. Control of energy homeostasis: role of enzymes and intermediates of fatty acid metabolism in the central nervous system. Annu Rev Nutr 2006;26:Epub ahead of print.
[62] McGahan MC, Harned J, Mukunnemkeril M, Goralska M, Fleisher L, Ferrell JB. Iron alters glutamate secretion by regulating cytosolic aconitase activity. Am J Physiol Cell Physiol 2005;288(5):C1117–24.
[63] Sterling GH, O'Neill JJ. Citrate as the precursor of the acetyl moiety of acetylcholine. J Neurochem 1978;31(2):525–30.
[64] Caudarella R, Vescini F, Buffa A, Stefoni S. Citrate and mineral metabolism: kidney stones and bone disease. Front Biosci 2003;8:s1084–106.
[65] Costello LC, Franklin RB. The clinical relevance of the metabolism of prostate cancer; zinc and tumor suppression: connecting the dots. Mol Cancer 2006;5:17.
[66] Bullock GC, Delehanty LL, Talbot AL, Gonias SL, Tong WH, Rouault TA, Dewar B, Macdonald JM, Chruma JJ, Goldfarb AN. Iron control of erythroid development by a novel aconitase-associated regulatory pathway. Blood 2010;116(1):97–108.
[67] Talbot AL, Bullock GC, Delehanty LL, Sattler M, Zhao ZJ, Goldfarb AN. Aconitase regulation of erythropoiesis correlates with a novel licensing function in erythropoietin-induced ERK signaling. PLoS One 2011;6(8):e23850.
[68] Cheng Z, Tsuda M, Kishita Y, Sato Y, Aigaki T. Impaired energy metabolism in a Drosophila model of mitochondrial aconitase deficiency. Biochem Biophys Res Commun 2013;433(1):145–50.
[69] Spiegel R, Pines O, Ta-Shma A, Burak E, Shaag A, Halvardson J, Edvardson S, Mahajna M, Zenvirt S, Saada A, Shalev S, Feuk L, Elpeleg O. Infantile cerebellar-retinal degeneration associated with a mutation in mitochondrial aconitase, ACO2. Am J Hum Genet 2012;90(3):518–23.
[70] Metodiev MD, Gerber S, Hubert L, Delahodde A, Chretien D, Gerard X, Amati-Bonneau P, Giacomotto MC, Boddaert N, Kaminska A, Desguerre I, Amiel J, Rio M, Kaplan J, Munnich A, Rotig A, Rozet JM, Besmond C. Mutations in the tricarboxylic acid cycle enzyme, aconitase 2,

cause either isolated or syndromic optic neuropathy with encephalopathy and cerebellar atrophy. J Med Genet 2014;51(12):834–8.
[71] Sadat R, Barca E, Masand R, Donti TR, Naini A, De Vivo DC, DiMauro S, Hanchard NA, Graham BH. Functional cellular analyses reveal energy metabolism defect and mitochondrial DNA depletion in a case of mitochondrial aconitase deficiency. Mol Genet Metab 2016;118(1):28–34.
[72] Tong WH, Sourbier C, Kovtunovych G, Jeong SY, Vira M, Ghosh M, Romero VV, Sougrat R, Vaulont S, Viollet B, Kim YS, Lee S, Trepel J, Srinivasan R, Bratslavsky G, Yang Y, Linehan WM, Rouault TA. The glycolytic shift in fumarate-hydratase-deficient kidney cancer lowers AMPK levels, increases anabolic propensities and lowers cellular iron levels. Cancer Cell 2011;20(3):315–27.
[73] Tomlinson IP, Alam NA, Rowan AJ, Barclay E, Jaeger EE, Kelsell D, Leigh I, Gorman P, Lamlum H, Rahman S, Roylance RR, Olpin S, Bevan S, Barker K, Hearle N, Houlston RS, Kiuru M, Lehtonen R, Karhu A, Vilkki S, Laiho P, Eklund C, Vierimaa O, Aittomaki K, Hietala M, Sistonen P, Paetau A, Salovaara R, Herva R, Launonen V, Aaltonen LA, Germline mutations in FH predispose to dominantly inherited uterine fibroids, skin leiomyomata and papillary renal cell cancer. Nat Genet 2002;30(4):406–10.
[74] Isaacs JS, Jung YJ, Mole DR, Lee S, Torres-Cabala C, Chung YL, Merino M, Trepel J, Zbar B, Toro J, Ratcliffe PJ, Linehan WM, Neckers L. HIF overexpression correlates with biallelic loss of fumarate hydratase in renal cancer: novel role of fumarate in regulation of HIF stability. Cancer Cell 2005;8(2):143–53.
[75] Pollard P, Wortham N, Barclay E, Alam A, Elia G, Manek S, Poulsom R, Tomlinson I. Evidence of increased microvessel density and activation of the hypoxia pathway in tumours from the hereditary leiomyomatosis and renal cell cancer syndrome. J Pathol 2005;205(1):41–9.
[76] Sudarshan S, Sourbier C, Kong HS, Block K, Valera Romero VA, Yang Y, Galindo C, Mollapour M, Scroggins B, Goode N, Lee MJ, Gourlay CW, Trepel J, Linehan WM, Neckers L. Fumarate hydratase deficiency in renal cancer induces glycolytic addiction and hypoxia-inducible transcription factor 1alpha stabilization by glucose-dependent generation of reactive oxygen species. Mol Cell Biol 2009;29(15):4080–90.
[77] Ternette N, Yang M, Laroyia M, Kitagawa M, O'Flaherty L, Wolhulter K, Igarashi K, Saito K, Kato K, Fischer R, Berquand A, Kessler BM, Lappin T, Frizzell N, Soga T, Adam J, Pollard PJ. Inhibition of mitochondrial aconitase by succination in fumarate hydratase deficiency. Cell Rep 2013;3(3):689–700.
[78] DeBerardinis RJ, Lum JJ, Hatzivassiliou G, Thompson CB. The biology of cancer: metabolic reprogramming fuels cell growth and proliferation. Cell Metab 2008;7(1):11–20.
[79] Galaris D, Pantopoulos K. Oxidative stress and iron homeostasis: mechanistic and health aspects. Crit Rev Clin Lab Sci 2008;45(1):1–23.
[80] Andrews NC. Forging a field: the golden age of iron biology. Blood 2008;112(2):219–30.
[81] Pantopoulos K, Hentze MW. Rapid responses to oxidative stress mediated by iron regulatory protein. EMBO J 1995;14:2917–24.
[82] Drapier JC, Hirling H, Wietzerbin J, Kaldy P, Kuhn LC. Biosynthesis of nitric oxide activates iron regulatory factor in macrophages. EMBO J 1993;12(9):3643–9.
[83] Weiss G, Goossen B, Doppler W, Fuchs D, Pantopoulos K, Werner-Felmayer G, Wachter H, Hentze MW. Translational regulation via iron-responsive elements by the nitric oxide/NO-synthase pathway. EMBO 1993;12(9):3651–7.
[84] Smeitink J, van den Heuvel L, DiMauro S. The genetics and pathology of oxidative phosphorylation. Nat Rev Genet 2001;2(5):342–52.
[85] Papa S, De Rasmo D. Complex I deficiencies in neurological disorders. Trends Mol Med 2013;19(1):61–9.
[86] Hoekstra AS, Bayley JP. The role of complex II in disease. Biochim Biophys Acta 2013;1827(5):543–51.

[87] Benit P, Lebon S, Rustin P. Respiratory-chain diseases related to complex III deficiency. Biochim. Biophys Acta 2009;1793(1):181–5.
[88] Pestronk A. Immune and inflammatory myopathies: pathology. Neuromuscular Disease Center. http://neuromuscular.wustl.edu/mitosyn.html-leigh. 2011.
[89] Koopman WJ, Distelmaier F, Smeitink JA, Willems PH. OXPHOS mutations and neurodegeneration. EMBO J 2013;32(1):9–29.
[90] Scheffler IE. Molecular genetics of succinate:quinone oxidoreductase in eukaryotes. Prog Nucleic Acid Res Mol Biol 1998;60:267–315.
[91] Kok JD, Muller JL, Slater EC. EPR studies on the respiratory chain of wild-type Saccharomyces cerevisiae and mutants with a deficiency in succinate dehydrogenase. Biochim Biophys Acta 1975;387(3):441–50.
[92] Ackrell BA, Kearney EB, Singer TP. Mammalian succinate dehydrogenase. Methods Enzymol 1978;53:466–83.
[93] Singer TP, Johnson MK. The prosthetic groups of succinate dehydrogenase: 30 years from discovery to identification. FEBS Lett 1985;190(2):189–98.
[94] Lemire BD, Oyedotun KS. The Saccharomyces cerevisiae mitochondrial succinate:ubiquinone oxidoreductase. Biochim Biophys Acta 2002;1553(1–2):102–16.
[95] Huang LS, Sun G, Cobessi D, Wang AC, Shen JT, Tung EY, Anderson VE, Berry EA. 3-nitropropionic acid is a suicide inhibitor of mitochondrial respiration that, upon oxidation by complex II, forms a covalent adduct with a catalytic base arginine in the active site of the enzyme. J Biol Chem 2006;281(9):5965–72.
[96] Zhou Q, Zhai Y, Lou J, Liu M, Pang X, Sun F. Thiabendazole inhibits ubiquinone reduction activity of mitochondrial respiratory complex II via a water molecule mediated binding feature. Protein Cell 2011;2(7):531–42.
[97] Maio N, Rouault TA. Iron-sulfur cluster biogenesis in mammalian cells: New insights into the molecular mechanisms of cluster delivery. Biochim Biophys Acta 2015;1853(6):1493–512.
[98] Van Vranken JG, Na U, Winge DR, Rutter J. Protein-mediated assembly of succinate dehydrogenase and its cofactors. Crit Rev Biochem Mol Biol 2015;50(2):168–80.
[99] Ackrell BA. Cytopathies involving mitochondrial complex II. Mol Aspects Med 2002;23(5):369–84.
[100] Briere JJ, Favier J, El Ghouzzi V, Djouadi F, Benit P, Gimenez AP, Rustin P. Succinate dehydrogenase deficiency in human. Cell Mol Life Sci 2005;62(19–20):2317–24.
[101] Gill AJ. Succinate dehydrogenase (SDH) and mitochondrial driven neoplasia. Pathology 2012;44(4):285–92.
[102] Bourgeron T, Rustin P, Chretien D, Birch-Machin M, Bourgeois M, Viegas-Pequignot E, Munnich A, Rotig A. Mutation of a nuclear succinate dehydrogenase gene results in mitochondrial respiratory chain deficiency. Nat Genet 1995;11(2):144–9.
[103] Neumann HP, Pawlu C, Peczkowska M, Bausch B, McWhinney SR, Muresan M, Buchta M, Franke G, Klisch J, Bley TA, Hoegerle S, Boedeker CC, Opocher G, Schipper J, Januszewicz A, Eng C. Distinct clinical features of paraganglioma syndromes associated with SDHB and SDHD gene mutations. JAMA 2004;292(8):943–51.
[104] Selak MA, Armour SM, MacKenzie ED, Boulahbel H, Watson DG, Mansfield KD, Pan Y, Simon MC, Thompson CB, Gottlieb E. Succinate links TCA cycle dysfunction to oncogenesis by inhibiting HIF-alpha prolyl hydroxylase. Cancer Cell 2005;7(1):77–85.
[105] Ishii T, Yasuda K, Akatsuka A, Hino O, Hartman PS, Ishii N. A mutation in the SDHC gene of complex II increases oxidative stress, resulting in apoptosis and tumorigenesis. Cancer Res 2005;65(1):203–9.
[106] Cervera AM, Bayley JP, Devilee P, McCreath KJ. Inhibition of succinate dehydrogenase dysregulates histone modification in mammalian cells. Mol Cancer 2009;8:89.
[107] Lee S, Nakamura E, Yang H, Wei W, Linggi MS, Sajan MP, Farese RV, Freeman RS, Carter BD, Kaelin WG Jr, Schlisio S. Neuronal apoptosis linked to EglN3 prolyl hydroxylase and

familial pheochromocytoma genes: developmental culling and cancer. Cancer Cell 2005;8(2):155–67.
[108] Piruat JI, Pintado CO, Ortega-Saenz P, Roche M, Lopez-Barneo J. The mitochondrial SDHD gene is required for early embryogenesis, and its partial deficiency results in persistent carotid body glomus cell activation with full responsiveness to hypoxia. Mol Cell Biol 2004;24(24):10933–40.
[109] Bayley JP, van Minderhout I, Hogendoorn PC, Cornelisse CJ, van der Wal A, Prins FA, Teppema L, Dahan A, Devilee P, Taschner PE. Sdhd and SDHD/H19 knockout mice do not develop paraganglioma or pheochromocytoma. PLoS One 2009;4(11):e7987.
[110] Turrens JF. Mitochondrial formation of reactive oxygen species. J Physiol 2003;552(Pt 2):335–44.
[111] Ishii T, Miyazawa M, Onouchi H, Yasuda K, Hartman PS, Ishii N. Model animals for the study of oxidative stress from complex II. Biochim Biophys Acta 2013;1827(5):588–97.
[112] Szeto SS, Reinke SN, Sykes BD, Lemire BD. Ubiquinone-binding site mutations in the Saccharomyces cerevisiae succinate dehydrogenase generate superoxide and lead to the accumulation of succinate. J Biol Chem 2007;282(37):27518–26.
[113] Tsuda M, Sugiura T, Ishii T, Ishii N, Aigaki T. A mev-1-like dominant-negative SdhC increases oxidative stress and reduces lifespan in Drosophila. Biochem Biophys Res Commun 2007;363(2):342–6.
[114] Walker DW, Hajek P, Muffat J, Knoepfle D, Cornelison S, Attardi G, Benzer S. Hypersensitivity to oxygen and shortened lifespan in a Drosophila mitochondrial complex II mutant. Proc Natl Acad Sci USA 2006;103(44):16382–7.
[115] Cervera AM, Apostolova N, Crespo FL, Mata M, McCreath KJ. Cells silenced for SDHB expression display characteristic features of the tumor phenotype. Cancer Res 2008;68(11):4058–67.
[116] Semenza GL. Hypoxia-inducible factors in physiology and medicine. Cell 2012;148(3):399–408.
[117] Bruick RK, McKnight SL. A conserved family of prolyl-4-hydroxylases that modify HIF. Science 2001;294(5545):1337–40.
[118] Epstein AC, Gleadle JM, McNeill LA, Hewitson KS, O'Rourke J, Mole DR, Mukherji M, Metzen E, Wilson MI, Dhanda A, Tian YM, Masson N, Hamilton DL, Jaakkola P, Barstead R, Hodgkin J, Maxwell PH, Pugh CW, Schofield CJ, Ratcliffe PJ. C. elegans EGL-9 and mammalian homologs define a family of dioxygenases that regulate HIF by prolyl hydroxylation. Cell 2001;107(1):43–54.
[119] Gordan JD, Simon MC. Hypoxia-inducible factors: central regulators of the tumor phenotype. Curr Opin Genet Dev 2007;17(1):71–7.
[120] Yang M, Soga T, Pollard PJ. Oncometabolites: linking altered metabolism with cancer. J Clin Invest 2013;123(9):3652–8.
[121] Gimenez-Roqueplo AP, Favier J, Rustin P, Mourad JJ, Plouin PF, Corvol P, Rotig A, Jeunemaitre X. The R22X mutation of the SDHD gene in hereditary paraganglioma abolishes the enzymatic activity of complex II in the mitochondrial respiratory chain and activates the hypoxia pathway. Am J Hum Genet 2001;69(6):1186–97.
[122] Gimenez-Roqueplo AP, Favier J, Rustin P, Rieubland C, Kerlan V, Plouin PF, Rotig A, Jeunemaitre X. Functional consequences of a SDHB gene mutation in an apparently sporadic pheochromocytoma. J Clin Endocrinol Metab 2002;87(10):4771–4.
[123] Hewitson KS, Lienard BM, McDonough MA, Clifton IJ, Butler D, Soares AS, Oldham NJ, McNeill LA, Schofield CJ. Structural and mechanistic studies on the inhibition of the hypoxia-inducible transcription factor hydroxylases by tricarboxylic acid cycle intermediates. J Biol Chem 2007;282(5):3293–301.
[124] Astuti D, Latif F, Dallol A, Dahia PL, Douglas F, George E, Skoldberg F, Husebye ES, Eng C, Maher ER. Gene mutations in the succinate dehydrogenase subunit SDHB cause susceptibility to familial pheochromocytoma and to familial paraganglioma. Am J Hum Genet 2001;69(1):49–54.
[125] Baysal BE, Ferrell RE, Willett-Brozick JE, Lawrence EC, Myssiorek D, Bosch A, van der Mey A, Taschner PE, Rubinstein WS, Myers EN, Richard CW, 3rd, Cornelisse CJ, Devilee P, Devlin B.

Mutations in SDHD, a mitochondrial complex II gene, in hereditary paraganglioma. Science 2000;287(5454):848–51.
[126] Niemann S, Muller U. Mutations in SDHC cause autosomal dominant paraganglioma, type 3. Nat Genet 2000;26(3):268–70.
[127] Astuti D, Douglas F, Lennard TW, Aligianis IA, Woodward ER, Evans DG, Eng C, Latif F, Maher ER. Germline SDHD mutation in familial phaeochromocytoma. Lancet 2001;357(9263):1181–2.
[128] Vanharanta S, Buchta M, McWhinney SR, Virta SK, Peczkowska M, Morrison CD, Lehtonen R, Januszewicz A, Jarvinen H, Juhola M, Mecklin JP, Pukkala E, Herva R, Kiuru M, Nupponen NN, Aaltonen LA, Neumann HP, Eng C. Early-onset renal cell carcinoma as a novel extraparaganglial component of SDHB-associated heritable paraganglioma. Am J Hum Genet 2004;74(1):153–9.
[129] Burnichon N, Briere JJ, Libe R, Vescovo L, Riviere J, Tissier F, Jouanno E, Jeunemaitre X, Benit P, Tzagoloff A, Rustin P, Bertherat J, Favier J, Gimenez-Roqueplo AP. SDHA is a tumor suppressor gene causing paraganglioma. Hum Mol Genet 2010;19(15):3011–20.
[130] Hao HX, Khalimonchuk O, Schraders M, Dephoure N, Bayley JP, Kunst H, Devilee P, Cremers CW, Schiffman JD, Bentz BG, Gygi SP, Winge DR, Kremer H, Rutter J. SDH5, a gene required for flavination of succinate dehydrogenase, is mutated in paraganglioma. Science 2009;325(5944):1139–42.
[131] Benn DE, Gimenez-Roqueplo AP, Reilly JR, Bertherat J, Burgess J, Byth K, Croxson M, Dahia PL, Elston M, Gimm O, Henley D, Herman P, Murday V, Niccoli-Sire P, Pasieka JL, Rohmer V, Tucker, K, Jeunemaitre X, Marsh DJ, Plouin PF, Robinson BG. Clinical presentation and penetrance of pheochromocytoma/paraganglioma syndromes. J Clin Endocrinol Metab 2006;91(3):827–36.
[132] Mannelli M, Castellano M, Schiavi F, Filetti S, Giacche M, Mori L, Pignataro V, Bernini G, Giache V, Bacca A, Biondi B, Corona G, Di Trapani G, Grossrubatscher E, Reimondo G, Arnaldi G, Giacchetti G, Veglio F, Loli P, Colao A, Ambrosio MR, Terzolo M, Letizia C, Ercolino T, Opocher G. Clinically guided genetic screening in a large cohort of Italian patients with pheochromocytomas and/or functional or nonfunctional paragangliomas. J Clin Endocrinol Metab 2009;94(5):1541–7.
[133] Bayley JP, Devilee P, Taschner PE. The SDH mutation database: an online resource for succinate dehydrogenase sequence variants involved in pheochromocytoma, paraganglioma and mitochondrial complex II deficiency. BMC Med Genet 2005;6:39.
[134] Cascon A, Pita G, Burnichon N, Landa I, Lopez-Jimenez E, Montero-Conde C, Leskela S, Leandro-Garcia LJ, Leton R, Rodriguez-Antona C, Diaz JA, Lopez-Vidriero E, Gonzalez-Neira A, Velasco A, Matias-Guiu X, Gimenez-Roqueplo AP, Robledo M. Genetics of pheochromocytoma and paraganglioma in Spanish patients. J Clin Endocrinol Metab 2009;94(5):1701–5.
[135] Neumann HP, Bausch B, McWhinney SR, Bender BU, Gimm O, Franke G, Schipper J, Klisch J, Altehoefer C, Zerres K, Januszewicz A, Eng C, Smith WM, Munk R, Manz T, Glaesker S, Apel TW, Treier M, Reineke M, Walz MK, Hoang-Vu C, Brauckhoff M, Klein-Franke A, Klose P, Schmidt H, Maier-Woelfle M, Peczkowska M, Szmigielski C, Eng C. Germ-line mutations in nonsyndromic pheochromocytoma. N Engl J Med 2002;346(19):1459–66.
[136] Lima J, Feijao T, Ferreira da Silva A, Pereira-Castro I, Fernandez-Ballester G, Maximo V, Herrero A, Serrano L, Sobrinho-Simoes M, Garcia-Rostan G. High frequency of germline succinate dehydrogenase mutations in sporadic cervical paragangliomas in northern Spain: mitochondrial succinate dehydrogenase structure-function relationships and clinical-pathological correlations. J Clin Endocrinol Metab 2007;92(12):4853–64.
[137] Burnichon N, Rohmer V, Amar L, Herman P, Leboulleux S, Darrouzet V, Niccoli P, Gaillard D, Chabrier G, Chabolle F, Coupier I, Thieblot P, Lecomte P, Bertherat J, Wion-Barbot N, Murat A, Venisse A, Plouin PF, Jeunemaitre X, Gimenez-Roqueplo AP. The succinate dehydrogenase genetic testing in a large prospective series of patients with paragangliomas. J Clin Endocrinol Metab 2009;94(8):2817–27.

[138] Korpershoek E, Petri BJ, van Nederveen FH, Dinjens WN, Verhofstad AA, de Herder WW, Schmid S, Perren A, Komminoth P, de Krijger RR. Candidate gene mutation analysis in bilateral adrenal pheochromocytoma and sympathetic paraganglioma. Endocr Relat Cancer 2007;14(2):453–62.
[139] Amar L, Baudin E, Burnichon N, Peyrard S, Silvera S, Bertherat J, Bertagna X, Schlumberger M, Jeunemaitre X, Gimenez-Roqueplo AP, Plouin PF. Succinate dehydrogenase B gene mutations predict survival in patients with malignant pheochromocytomas or paragangliomas. J Clin Endocrinol Metab 2007;92(10):3822–8.
[140] Bayley JP, van Minderhout I, Weiss MM, Jansen JC, Oomen PH, Menko FH, Pasini B, Ferrando B, Wong N, Alpert LC, Williams R, Blair E, Devilee P, Taschner PE. Mutation analysis of SDHB and SDHC: novel germline mutations in sporadic head and neck paraganglioma and familial paraganglioma and/or pheochromocytoma. BMC Med Genet 2006;7:1.
[141] Henderson A, Douglas F, Perros P, Morgan C, Maher ER. SDHB-associated renal oncocytoma suggests a broadening of the renal phenotype in hereditary paragangliomatosis. Fam Cancer 2009;8(3):257–60.
[142] Housley SL, Lindsay RS, Young B, McConachie M, Mechan D, Baty D, Christie L, Rahilly M, Qureshi K, Fleming S. Renal carcinoma with giant mitochondria associated with germ-line mutation and somatic loss of the succinate dehydrogenase B gene. Histopathology 2010;56(3):405–8.
[143] Gill AJ, Pachter NS, Clarkson A, Tucker KM, Winship IM, Benn DE, Robinson BG, Clifton-Bligh RJ. Renal tumors and hereditary pheochromocytoma-paraganglioma syndrome type 4. N Engl J Med 2011;364(9):885–6.
[144] Ricketts CJ, Shuch B, Vocke CD, Metwalli AR, Bratslavsky G, Middelton L, Yang Y, Wei MH, Pautler SE, Peterson J, Stolle CA, Zbar B, Merino MJ, Schmidt LS, Pinto PA, Srinivasan R, Pacak K, Linehan WM. Succinate dehydrogenase kidney cancer: an aggressive example of the Warburg effect in cancer. J Urol 2012;188(6):2063–71.
[145] Ricketts C, Woodward ER, Killick P, Morris MR, Astuti D, Latif F, Maher ER. Germline SDHB mutations and familial renal cell carcinoma. J Natl Cancer Inst 2008;100(17):1260–2.
[146] Miettinen M, Lasota J. Gastrointestinal stromal tumors – definition, clinical, histological, immunohistochemical, and molecular genetic features and differential diagnosis. Virchows Arch 2001;438(1):1–12.
[147] Gill AJ, Chou A, Vilain R, Clarkson A, Lui M, Jin R, Tobias V, Samra J, Goldstein D, Smith C, Sioson L, Parker N, Smith RC, Sywak M, Sidhu SB, Wyatt JM, Robinson BG, Eckstein RP, Benn DE, Clifton-Bligh RJ. Immunohistochemistry for SDHB divides gastrointestinal stromal tumors (GISTs) into 2 distinct types. Am J Surg Pathol 2010;34(5):636–44.
[148] Pasini B, McWhinney SR, Bei T, Matyakhina L, Stergiopoulos S, Muchow M, Boikos SA, Ferrando B, Pacak K, Assie G, Baudin E, Chompret A, Ellison JW, Briere JJ, Rustin P, Gimenez-Roqueplo AP, Eng C, Carney JA, Stratakis CA. Clinical and molecular genetics of patients with the Carney-Stratakis syndrome and germline mutations of the genes coding for the succinate dehydrogenase subunits SDHB, SDHC, and SDHD. Eur J Hum Genet 2008;16(1):79–88.
[149] Janeway KA, Kim SY, Lodish M, Nose V, Rustin P, Gaal J, Dahia PL, Liegl B, Ball ER, Raygada M, Lai AH, Kelly L, Hornick JL, O'Sullivan M, de Krijger RR, Dinjens WN, Demetri GD, Antonescu CR, Fletcher JA, Helman L, Stratakis CA. Defects in succinate dehydrogenase in gastrointestinal stromal tumors lacking KIT and PDGFRA mutations. Proc Natl Acad Sci USA 2011;108(1):314–8.
[150] Alston CL, Davison JE, Meloni F, van der Westhuizen FH, He L, Hornig-Do HT, Peet AC, Gissen P, Goffrini P, Ferrero I, Wassmer E, McFarland R, Taylor RW. Recessive germline SDHA and SDHB mutations causing leukodystrophy and isolated mitochondrial complex II deficiency. J Med Genet 2012;49(9):569–77.
[151] Dailey HA. Terminal steps of haem biosynthesis. Biochem Soc Trans 2002;30(4):590–5.

[152] Dailey HA, Finnegan MG, Johnson MK. Human ferrochelatase is an iron-sulfur protein. Biochemistry 1994;33(2):403–7.
[153] Ferreira GC, Franco R, Lloyd SG, Pereira AS, Moura I, Moura JJ, Huynh BH. Mammalian ferrochelatase, a new addition to the metalloenzyme family. J Biol Chem 1994;269(10):7062–5.
[154] Medlock AE, Dailey HA. Examination of the activity of carboxyl-terminal chimeric constructs of human and yeast ferrochelatases. Biochemistry 2000;39(25):7461–7.
[155] Furukawa T, Kohno H, Tokunaga R, Taketani S. Nitric oxide-mediated inactivation of mammalian ferrochelatase in vivo and in vitro: possible involvement of the iron-sulphur cluster of the enzyme. Biochem J 1995;310 (Pt 2):533–8.
[156] Taketani S, Adachi Y, Nakahashi Y. Regulation of the expression of human ferrochelatase by intracellular iron levels. Eur J Biochem 2000;267(15):4685–92.
[157] Crouse BR, Sellers VM, Finnegan MG, Dailey HA, Johnson MK. Site-directed mutagenesis and spectroscopic characterization of human ferrochelatase: identification of residues coordinating the [2Fe-2S] cluster. Biochemistry 1996;35(50):16222–9.
[158] Wu CK, Dailey HA, Rose JP, Burden A, Sellers VM, Wang BC. The 2.0 A structure of human ferrochelatase, the terminal enzyme of heme biosynthesis. Nat Struct Biol 2001;8(2):156–60.
[159] Peterka ES, Fusaro RM, Runge WJ, Jaffe MO, Watson CJ. Erythropoietic protoporphyria. I. Clinical and laboratory features in seven new cases. JAMA 1965;193:1036–42.
[160] Bonkowsky HL, Bloomer JR, Ebert PS, Mahoney, MJ. Heme synthetase deficiency in human protoporphyria. Demonstration of the defect in liver and cultured skin fibroblasts. J Clin Invest 1975;56(5):1139–48.
[161] Brenner DA, Didier JM, Frasier F, Christensen SR, Evans GA, Dailey HA. A molecular defect in human protoporphyria. Am J Hum Genet 1992;50(6):1203–10.
[162] Balwani M, Desnick RJ. The porphyrias: advances in diagnosis and treatment. Blood 2012;120(23):4496–504.
[163] Bloomer JR. Pathogenesis and therapy of liver disease in protoporphyria. Yale J Biol Med 1979;52(1):39–48.
[164] Bloomer J, Bruzzone C, Zhu L, Scarlett Y, Magness S, Brenner D. Molecular defects in ferrochelatase in patients with protoporphyria requiring liver transplantation. J Clin Invest 1998;102(1):107–14.
[165] Tutois S, Montagutelli X, Da Silva V, Jouault H, Rouyer-Fessard P, Leroy-Viard K, Guenet JL, Nordmann Y, Beuzard Y, Deybach JC. Erythropoietic protoporphyria in the house mouse. A recessive inherited ferrochelatase deficiency with anemia, photosensitivity, and liver disease. J Clin Invest 1991;88(5):1730–6.
[166] Boulechfar S, Lamoril J, Montagutelli X, Guenet JL, Deybach JC, Nordmann Y, Dailey H, Grandchamp B, de Verneuil H. Ferrochelatase structural mutant (Fechm1Pas) in the house mouse. Genomics 1993;16(3):645–8.
[167] Gouya L, Puy H, Lamoril J, Da Silva V, Grandchamp B, Nordmann Y, Deybach JC. Inheritance in erythropoietic protoporphyria: a common wild-type ferrochelatase allelic variant with low expression accounts for clinical manifestation. Blood 1999;93(6):2105–10.
[168] Nakahashi Y, Fujita H, Taketani S, Ishida N, Kappas A, Sassa S. The molecular defect of ferrochelatase in a patient with erythropoietic protoporphyria. Proc Natl Acad Sci USA 1992;89(1):281–5.
[169] Sarkany RP, Alexander GJ, Cox TM. Recessive inheritance of erythropoietic protoporphyria with liver failure. Lancet 1994;343(8910):1394–6.
[170] Sellers VM, Dailey HA. Expression, purification, and characterization of recombinant mammalian ferrochelatase. Methods Enzymol 1997;281:378–87.
[171] Schneider-Yin X, Gouya L, Dorsey M, Rufenacht U, Deybach JC, Ferreira GC. Mutations in the iron-sulfur cluster ligands of the human ferrochelatase lead to erythropoietic protoporphyria. Blood 2000;96(4):1545–9.

[172] McKinnon PJ. DNA repair deficiency and neurological disease. Nat Rev Neurosci 2009;10(2):100–12.
[173] Jeppesen DK, Bohr VA, Stevnsner T. DNA repair deficiency in neurodegeneration. Prog Neurobiol 2011;94(2):166–200.
[174] Suhasini AN, Brosh RM Jr. Disease-causing missense mutations in human DNA helicase disorders Mutat Res 2013;752(2):138–52.
[175] Kovtun IV, McMurray CT. Trinucleotide expansion in haploid germ cells by gap repair. Nat Genet 2001;27(4):407–11.
[176] Moreira MC, Barbot C, Tachi N, Kozuka N, Uchida E, Gibson T, Mendonca P, Costa M, Barros J, Yanagisawa T, Watanabe M, Ikeda Y, Aoki M, Nagata T, Coutinho P, Sequeiros J, Koenig M. The gene mutated in ataxia-ocular apraxia 1 encodes the new HIT/Zn-finger protein aprataxin. Nat Genet 2001;29(2):189–93.
[177] Takashima H, Boerkoel CF, John J, Saifi GM, Salih MA, Armstrong D, Mao Y, Quiocho FA, Roa BB, Nakagawa M, Stockton DW, Lupski JR. Mutation of TDP1, encoding a topoisomerase I-dependent DNA damage repair enzyme, in spinocerebellar ataxia with axonal neuropathy. Nat Genet 2002;32(2):267–72.
[178] Gatti RA, Becker-Catania S, Chun HH, Sun X, Mitui M, Lai CH, Khanlou N, Babaei M, Cheng R, Clark C, Huo Y, Udar NC, Iyer RK. The pathogenesis of ataxia-telangiectasia. Learning from a Rosetta Stone. Clin Rev Allergy Immunol 2001;20(1):87–108.
[179] Wang J, Xiong S, Xie C, Markesbery WR, Lovell MA. Increased oxidative damage in nuclear and mitochondrial DNA in Alzheimer's disease. J Neurochem 2005;93(4):953–62.
[180] Kikuchi H, Furuta A, Nishioka K, Suzuki SO, Nakabeppu Y, Iwaki T. Impairment of mitochondrial DNA repair enzymes against accumulation of 8-oxo-guanine in the spinal motor neurons of amyotrophic lateral sclerosis. Acta Neuropathol 2002;103(4):408–14.
[181] Kuo CF, McRee DE, Fisher CL, O'Handley SF, Cunningham RP, Tainer JA, Atomic structure of the DNA repair [4Fe-4S] enzyme endonuclease III. Science 1992;258(5081):434–40.
[182] Hinks JA, Evans MC, De Miguel Y, Sartori AA, Jiricny J, Pearl LH. An iron-sulfur cluster in the family 4 uracil-DNA glycosylases. J Biol Chem 2002;277(19):16936–40.
[183] Thayer MM, Ahern H, Xing D, Cunningham RP, Tainer JA. Novel DNA binding motifs in the DNA repair enzyme endonuclease III crystal structure. EMBO J 1995;14(16):4108–20.
[184] Arnold AR, Grodick MA, Barton JK. DNA Charge Transport: from Chemical Principles to the Cell. Cell Chem Biol 2016;23(1):183–97.
[185] Mazzei F, Viel A, Bignami M. Role of MUTYH in human cancer. Mutat Res 2013;743–744:33–43.
[186] Vannier JB, Sarek G, Boulton SJ. RTEL1: functions of a disease-associated helicase. Trends Cell Biol 2014;24(7):416–25.
[187] Ding H, Schertzer M, Wu X, Gertsenstein M, Selig S, Kammori M, Pourvali R, Poon S, Vulto I, Chavez E, Tam PP, Nagy A, Lansdorp PM. Regulation of murine telomere length by Rtel: an essential gene encoding a helicase-like protein. Cell 2004;117(7):873–86.
[188] van der Lelij P, Chrzanowska KH, Godthelp BC, Rooimans MA, Oostra AB, Stumm M, Zdzienicka MZ, Joenje H, de Winter JP. Warsaw breakage syndrome, a cohesinopathy associated with mutations in the XPD helicase family member DDX11/ChlR1. Am J Hum Genet 2010;86(2):262–6.
[189] Bharti SK, Khan I, Banerjee T, Sommers JA, Wu Y, Brosh RM Jr. Molecular functions and cellular roles of the ChlR1 (DDX11) helicase defective in the rare cohesinopathy Warsaw breakage syndrome. Cell Mol Life Sci 2014;71(14):2625–39.
[190] Inoue A, Li T, Roby SK, Valentine MB, Inoue M, Boyd K, Kidd VJ, Lahti JM. Loss of ChlR1 helicase in mouse causes lethality due to the accumulation of aneuploid cells generated by cohesion defects and placental malformation. Cell Cycle 2007;6(13):1646–54.

[191] White MF. Structure, function and evolution of the XPD family of iron-sulfur-containing 5′-->3′ DNA helicases. Biochem Soc Trans 2009;37(Pt 3):547–51.
[192] Lehmann AR. DNA repair-deficient diseases, xeroderma pigmentosum, Cockayne syndrome and trichothiodystrophy. Biochimie 2003;85(11):1101–11.
[193] de Boer J, Andressoo JO, de Wit J, Huijmans J, Beems RB, van Steeg H, Weeda G, van der Horst GT, van Leeuwen W, Themmen AP, Meradji M, Hoeijmakers JH. Premature aging in mice deficient in DNA repair and transcription. Science 2002;296(5571):1276–9.
[194] Theron T, Fousteri MI, Volker M, Harries LW, Botta E, Stefanini M, Fujimoto M, Andressoo JO, Mitchell J, Jaspers NG, McDaniel LD, Mullenders LH, Lehmann AR. Transcription-associated breaks in xeroderma pigmentosum group D cells from patients with combined features of xeroderma pigmentosum and Cockayne syndrome. Mol Cell Biol 2005;25(18):8368–78.
[195] Andressoo JO, Mitchell JR, de Wit J, Hoogstraten D, Volker M, Toussaint W, Speksnijder E, Beems RB, van Steeg H, Jans J, de Zeeuw CI, Jaspers NG, Raams A, Lehmann AR, Vermeulen W, Hoeijmakers JH, van der Horst GT. An Xpd mouse model for the combined xeroderma pigmentosum/Cockayne syndrome exhibiting both cancer predisposition and segmental progeria. Cancer Cell 2006;10(2):121–32.
[196] Pugh RA, Honda M, Leesley H, Thomas A, Lin Y, Nilges MJ, Cann IK, Spies M. The iron-containing domain is essential in Rad3 helicases for coupling of ATP hydrolysis to DNA translocation and for targeting the helicase to the single-stranded DNA-double-stranded DNA junction. J Biol Chem 2008;283(3):1732–43.
[197] Fan L, Fuss JO, Cheng QJ, Arvai AS, Hammel M, Roberts VA, Cooper PK, Tainer JA. XPD helicase structures and activities: insights into the cancer and aging phenotypes from XPD mutations. Cell 2008;133(5):789–800.
[198] Dubaele S, Proietti De Santis L, Bienstock RJ, Keriel A, Stefanini M, Van Houten B, Egly JM. Basal transcription defect discriminates between xeroderma pigmentosum and trichothiodystrophy in XPD patients. Mol Cell 2003;11(6):1635–46.
[199] Botta E, Nardo T, Lehmann AR, Egly JM, Pedrini AM, Stefanini M. Reduced level of the repair/transcription factor TFIIH in trichothiodystrophy. Hum Mol Genet 2002;11(23):2919–28.
[200] Andreassen PR, Ren K. Fanconi anemia proteins, DNA interstrand crosslink repair pathways, and cancer therapy. Curr. Cancer Drug Targets 2009;9(1):101–17.
[201] Kottemann MC, Smogorzewska A. Fanconi anaemia and the repair of Watson and Crick DNA crosslinks. Nature 2013;493(7432):356–63.
[202] Wu Y, Sommers JA, Suhasini AN, Leonard T, Deakyne JS, Mazin AV, Shin-Ya K, Kitao H, Brosh RM Jr. Fanconi anemia group J mutation abolishes its DNA repair function by uncoupling DNA translocation from helicase activity or disruption of protein-DNA complexes. Blood 2010;116(19):3780–91.
[203] Levitus M, Waisfisz Q, Godthelp BC, de Vries Y, Hussain S, Wiegant WW, Elghalbzouri-Maghrani E, Steltenpool J, Rooimans MA, Pals G, Arwert F, Mathew CG, Zdzienicka MZ, Hiom K, De Winter JP, Joenje H. The DNA helicase BRIP1 is defective in Fanconi anemia complementation group J Nat Genet 2005;37(9):934–5.
[204] Litman R, Peng M, Jin Z, Zhang F, Zhang J, Powell S, Andreassen PR, Cantor SB. BACH1 is critical for homologous recombination and appears to be the Fanconi anemia gene product FANCJ. Cancer Cell 2005;8(3):255–65.
[205] Schwab RA, Nieminuszczy J, Shin-ya K, Niedzwiedz W. FANCJ couples replication past natural fork barriers with maintenance of chromatin structure. J Cell Biol 2013;201(1):33–48.
[206] Cantor SB, Bell DW, Ganesan S, Kass EM, Drapkin R, Grossman S, Wahrer DC, Sgroi DC, Lane WS, Haber DA, Livingston DM. BACH1, a novel helicase-like protein, interacts directly with BRCA1 and contributes to its DNA repair function. Cell 2001;105(1):149–60.

[207] Levran O, Diotti R, Pujara K, Batish SD, Hanenberg H, Auerbach AD. Spectrum of sequence variations in the FANCA gene: an International Fanconi Anemia Registry (IFAR) study. Hum Mutat 2005;25(2):142–9.
[208] Gupta R, Sharma S, Doherty KM, Sommers JA, Cantor SB, Brosh RM Jr. Inhibition of BACH1 (FANCJ) helicase by backbone discontinuity is overcome by increased motor ATPase or length of loading strand. Nucleic Acids Res 2006;34(22):6673–83.
[209] Wang SC, Frey PA. S-adenosylmethionine as an oxidant: the radical SAM superfamily. Trends Biochem Sci 2007;32(3):101–10.
[210] Landgraf BJ, McCarthy EL, Booker SJ. Radical S-Adenosylmethionine Enzymes in Human Health and Disease. Annu Rev Biochem 2016;85:485–514.
[211] Cicchillo RM, Booker SJ. Mechanistic investigations of lipoic acid biosynthesis in *Escherichia coli*: both sulfur atoms in lipoic acid are contributed by the same lipoyl synthase polypeptide. J Am Chem Soc 2005;127(9):2860–1.
[212] McLaughlin MI, Lanz ND, Goldman PJ, Lee KH, Booker SJ, Drennan CL. Crystallographic snapshots of sulfur insertion by lipoyl synthase. Proc Natl Acad Sci USA 2016;113(34):9446–50.
[213] Mayr JA, Zimmermann FA, Fauth C, Bergheim C, Meierhofer D, Radmayr D, Zschocke J, Koch J, Sperl W. Lipoic acid synthetase deficiency causes neonatal-onset epilepsy, defective mitochondrial energy metabolism, and glycine elevation. Am J Hum Genet 2011;89(6):792–7.
[214] Mayr JA, Feichtinger RG, Tort F, Ribes A, Sperl W. Lipoic acid biosynthesis defects. J Inherit Metab Dis 2014;37(4):553–63.
[215] Tsurusaki Y, Tanaka R, Shimada S, Shimojima K, Shiina M, Nakashima M, Saitsu H, Miyake N, Ogata K, Yamamoto T, Matsumoto N. Novel compound heterozygous LIAS mutations cause glycine encephalopathy. J Hum Genet 2015;60(10):631–5.
[216] Baker PR, 2nd, Friederich MW, Swanson MA, Shaikh T, Bhattacharya K, Scharer GH, Aicher J, Creadon-Swindell G, Geiger E, MacLean KN, Lee WT, Deshpande C, Freckmann ML, Shih LY, Wasserstein M, Rasmussen MB, Lund AM, Procopis P, Cameron JM, Robinson BH, Brown GK, Brown RM, Compton AG, Dieckmann CL, Collard R, Coughlin CR, 2nd, Spector E, Wempe MF, Van Hove JL. Variant non ketotic hyperglycinemia is caused by mutations in LIAS, BOLA3 and the novel gene GLRX5. Brain 2014;137(Pt 2):366–79.
[217] Mendel RR, Leimkuhler S., The biosynthesis of the molybdenum cofactors. J Biol Inorg Chem 2015;20(2):337–47.
[218] Reiss J, Hahnewald R. Molybdenum cofactor deficiency: mutations in GPHN, MOCS1, and MOCS2. Hum Mutat 2011;32(1):10–8.
[219] Sass JO, Kishikawa M, Puttinger R, Reiss J, Erwa W, Shimizu A, Sperl W. Hypohomocysteinaemia and highly increased proportion of S-sulfonated plasma transthyretin in molybdenum cofactor deficiency. J Inherit Metab Dis 2003;26(1):80–2.
[220] Zhang X, Vincent AS, Halliwell B, Wong KP. A mechanism of sulfite neurotoxicity: direct inhibition of glutamate dehydrogenase. J Biol Chem 2004;279(41):43035–45.
[221] Veldman A, Santamaria-Araujo JA, Sollazzo S, Pitt J, Gianello R, Yaplito-Lee J, Wong F, Ramsden CA, Reiss J, Cook I, Fairweather J, Schwarz G. Successful treatment of molybdenum cofactor deficiency type A with cPMP. Pediatrics 2010;125(5):e1249–54.
[222] Kimura S, Suzuki T. Iron-sulfur proteins responsible for RNA modifications. Biochim Biophys Acta 2015;1853(6):1272–83.
[223] Arragain S, Handelman SK, Forouhar F, Wei FY, Tomizawa K, Hunt JF, Douki T, Fontecave M, Mulliez E, Atta M. Identification of eukaryotic and prokaryotic methylthiotransferase for biosynthesis of 2-methylthio-N6-threonylcarbamoyladenosine in tRNA. J Biol Chem 2010;285(37):28425–33.

[224] Wei FY, Zhou B, Suzuki T, Miyata K, Ujihara Y, Horiguchi H, Takahashi N, Xie P, Michiue H, Fujimura A, Kaitsuka T, Matsui H, Koga Y, Mohri S, Suzuki T, Oike Y, Tomizawa K. Cdk5rap1-mediated 2-methylthio modification of mitochondrial tRNAs governs protein translation and contributes to myopathy in mice and humans. Cell Metab 2015;21(3):428–42.
[225] Svejstrup JQ, Elongator complex: how many roles does it play? Curr Opin Cell Biol 2007;19(3):331–6.
[226] Karlsborn T, Tukenmez H, Mahmud AK, Xu F, Xu H, Bystrom AS. Elongator, a conserved complex required for wobble uridine modifications in eukaryotes. RNA Biol 2014;11(12):1519–28.
[227] Greenwood C, Selth LA, Dirac-Svejstrup AB, Svejstrup JQ. An iron-sulfur cluster domain in Elp3 important for the structural integrity of elongator. J Biol Chem 2009;284(1):141–9.
[228] Selvadurai K, Wang P, Seimetz J, Huang RH. Archaeal Elp3 catalyzes tRNA wobble uridine modification at C5 via a radical mechanism. Nat Chem Biol 2014;10(10):810–2.
[229] Close P, Hawkes N, Cornez I, Creppe C, Lambert CA, Rogister B, Siebenlist U, Merville MP, Slaugenhaupt SA, Bours V, Svejstrup JQ, Chariot A. Transcription impairment and cell migration defects in elongator-depleted cells: implication for familial dysautonomia. Mol Cell 2006;22(4):521–31.
[230] Simpson CL, Lemmens R, Miskiewicz K, Broom WJ, Hansen VK, van Vught PW, Landers JE, Sapp P, Van Den Bosch L, Knight J, Neale BM, Turner MR, Veldink JH, Ophoff RA, Tripathi VB, Beleza A, Shah MN, Proitsi P, Van Hoecke A, Carmeliet P, Horvitz HR, Leigh PN, Shaw CE, van den Berg LH, Sham PC, Powell JF, Verstreken P, Brown RH Jr., Robberecht W, Al-Chalabi A. Variants of the elongator protein 3 (ELP3) gene are associated with motor neuron degeneration. Hum Mol Genet 2009;18(3):472–81.
[231] Miskiewicz K, Jose LE, Bento-Abreu A, Fislage M, Taes I, Kasprowicz J, Swerts J, Sigrist S, Versees W, Robberecht W, Verstreken P. ELP3 controls active zone morphology by acetylating the ELKS family member Bruchpilot. Neuron 2011;72(5):776–88.
[232] Nicolas E, Golemis EA, Arora S. POLD1: central mediator of DNA replication and repair, and implication in cancer and other pathologies. Gene 2016;590(1):128–41.
[233] Gari K, Leon Ortiz AM, Borel V, Flynn H, Skehel JM, Boulton SJ. MMS19 links cytoplasmic iron-sulfur cluster assembly to DNA metabolism. Science 2012;337(6091):243–5.
[234] Stehling O, Vashisht AA, Mascarenhas J, Jonsson ZO, Sharma T, Netz DJ, Pierik AJ, Wohlschlegel JA, Lill R. MMS19 assembles iron-sulfur proteins required for DNA metabolism and genomic integrity. Science 2012;337(6091):195–9.
[235] Rayner E, van Gool IC, Palles C, Kearsey SE, Bosse T, Tomlinson I, Church DN. A panoply of errors: polymerase proofreading domain mutations in cancer. Nat Rev Cancer 2016;16(2):71–81.
[236] Tamir S, Paddock ML, Darash-Yahana-Baram M, Holt SH, Sohn YS, Agranat L, Michaeli D, Stofleth JT, Lipper CH, Morcos F, Cabantchik IZ, Onuchic JN, Jennings PA, Mittler R, Nechushtai R. Structure-function analysis of NEET proteins uncovers their role as key regulators of iron and ROS homeostasis in health and disease. Biochim Biophys Acta 2015;1853(6):1294–315.
[237] Paddock ML, Wiley SE, Axelrod HL, Cohen AE, Roy M, Abresch EC, Capraro D, Murphy AN, Nechushtai R, Dixon JE, Jennings PA. MitoNEET is a uniquely folded 2Fe 2S outer mitochondrial membrane protein stabilized by pioglitazone. Proc Natl Acad Sci USA 2007;104(36):14342–7.
[238] Lin J, Zhou T, Ye K, Wang J. Crystal structure of human mitoNEET reveals distinct groups of iron sulfur proteins. Proc Natl Acad Sci USA 2007;104(37):14640–5.
[239] Hou X, Liu R, Ross S, Smart EJ, Zhu H, Gong W. Crystallographic studies of human MitoNEET. J Biol Chem 2007;282(46):33242–6.
[240] Conlan AR, Paddock ML, Axelrod HL, Cohen AE, Abresch EC, Wiley S, Roy M, Nechushtai R, Jennings PA. The novel 2Fe-2S outer mitochondrial protein mitoNEET displays conformational

flexibility in its N-terminal cytoplasmic tethering domain. Acta Crystallogr Sect F Struct Biol Cryst Commun 2009;65(Pt 7):654–9.
[241] Tirrell TF, Paddock ML, Conlan AR, Smoll EJ Jr., Nechushtai R, Jennings PA, Kim JE. Resonance Raman studies of the (His)(Cys)3 2Fe-2S cluster of MitoNEET: comparison to the (Cys)4 mutant and implications of the effects ofon the labile metal center. Biochemistry 2009;48(22):4747–52.
[242] Dicus MM, Conlan A, Nechushtai R, Jennings PA, Paddock ML, Britt RD, Stoll S. Binding of histidine in the (Cys)3(His)1-coordinated [2Fe-2S] cluster of human mitoNEET. J Am Chem Soc 2010;132(6):2037–49.
[243] Wiley SE, Paddock ML, Abresch EC, Gross L, van der Geer P, Nechushtai R, Murphy AN, Jennings PA, Dixon JE. The outer mitochondrial membrane protein mitoNEET contains a novel redox-active 2Fe-2S cluster. J Biol Chem 2007;282(33):23745–9.
[244] Zuris JA, Ali SS, Yeh H, Nguyen TA, Nechushtai R, Paddock ML, Jennings PA. NADPH inhibits [2Fe-2S] cluster protein transfer from diabetes drug target MitoNEET to an apo-acceptor protein. J Biol Chem 2012;287(15):11649–55.
[245] Colca JR, McDonald WG, Waldon DJ, Leone JW, Lull JM, Bannow CA, Lund ET, Mathews WR. Identification of a novel mitochondrial protein ("mitoNEET") cross-linked specifically by a thiazolidinedione photoprobe. Am J Physiol Endocrinol Metab 2004;286(2):E252–60.
[246] Bak DW, Elliott SJ. Conserved hydrogen bonding networks of MitoNEET tune Fe-S cluster binding and structural stability. Biochemistry 2013;52(27):4687–96.
[247] Zuris JA, Harir Y, Conlan AR, Shvartsman M, Michaeli D, Tamir S, Paddock ML, Onuchic JN, Mittler R, Cabantchik ZI, Jennings PA, Nechushtai R. Facile transfer of [2Fe-2S] clusters from the diabetes drug target mitoNEET to an apo-acceptor protein. Proc Natl Acad Sci USA 2011;108(32):13047–52.
[248] Tamir S, Zuris JA, Agranat L, Lipper CH, Conlan AR, Michaeli D, Harir Y, Paddock ML, Mittler R, Cabantchik ZI, Jennings PA, Nechushtai R. Nutrient-deprivation autophagy factor-1 (NAF-1): biochemical properties of a novel cellular target for anti-diabetic drugs. PLoS One 2013;8(5):e61202.
[249] Ferecatu I, Goncalves S, Golinelli-Cohen MP, Clemancey M, Martelli A, Riquier S, Guittet E, Latour JM, Puccio H, Drapier JC, Lescop E, Bouton C. The diabetes drug target MitoNEET governs a novel trafficking pathway to rebuild an Fe-S cluster into cytosolic aconitase/iron regulatory protein 1. J Biol Chem 2014;289(41):28070–86.
[250] Lipper CH, Paddock ML, Onuchic JN, Mittler R, Nechushtai R, Jennings PA. Cancer-related NEET proteins transfer 2Fe-2S clusters to anamorsin, a protein required for cytosolic iron-sulfur cluster biogenesis. PLoS One 2015;10(10):e0139699.
[251] Taminelli GL, Sotomayor V, Valdivieso AG, Teiber ML, Marin MC, Santa-Coloma TA. CISD1 codifies a mitochondrial protein upregulated by the CFTR channel. Biochem Biophys Res Commun 2008;365(4):856–62.
[252] Amr S, Heisey C, Zhang M, Xia XJ, Shows KH, Ajlouni K, Pandya A, Satin LS, El-Shanti H, Shiang R. A homozygous mutation in a novel zinc-finger protein, ERIS, is responsible for Wolfram syndrome 2. Am J Hum Genet 2007;81(4):673–83.
[253] Chen YF, Kao CH, Chen YT, Wang CH, Wu CY, Tsai CY, Liu FC, Yang CW, Wei YH, Hsu MT, Tsai SF, Tsai TF. Cisd2 deficiency drives premature aging and causes mitochondria-mediated defects in mice. Genes Dev 2009;23(10):1183–94.
[254] Chang NC, Nguyen M, Shore GC. BCL2-CISD2: An ER complex at the nexus of autophagy and calcium homeostasis? Autophagy 2012;8(5):856–7.
[255] Sohn YS, Tamir S, Song L, Michaeli D, Matouk I, Conlan AR, Harir Y, Holt SH, Shulaev V, Paddock ML, Hochberg A, Cabanchick IZ, Onuchic JN, Jennings PA, Nechushtai R, Mittler R. NAF-1 and mitoNEET are central to human breast cancer proliferation by maintaining mitochondrial homeostasis and promoting tumor growth. Proc Natl Acad Sci USA 2013;110(36):14676–81.
[256] Chang NC, Nguyen M, Germain M, Shore GC. Antagonism of Beclin 1-dependent autophagy by BCL-2 at the endoplasmic reticulum requires NAF-1. EMBO 2010;29(3):606–18.

[257] El-Shanti H, Lidral AC, Jarrah N, Druhan L, Ajlouni K. Homozygosity mapping identifies an additional locus for Wolfram syndrome on chromosome 4q. Am J Hum Genet 2000;66(4):1229–36.
[258] Rondinelli M, Novara F, Calcaterra V, Zuffardi O, Genovese S. Wolfram syndrome 2: a novel CISD2 mutation identified in Italian siblings. Acta Diabetol 2015;52(1):175–8.
[259] Salem AF, Whitaker-Menezes D, Howell A, Sotgia F, Lisanti MP. Mitochondrial biogenesis in epithelial cancer cells promotes breast cancer tumor growth and confers autophagy resistance. Cell Cycle 2012;11(22):4174–80.
[260] Liu L, Xia M, Wang J, Zhang W, Zhang Y, He M. CISD2 expression is a novel marker correlating with pelvic lymph node metastasis and prognosis in patients with early-stage cervical cancer. Med Oncol 2014;31(9):183.
[261] Chen B, Shen S, Wu J, Hua Y, Kuang M, Li S, Peng B. CISD2 associated with proliferation indicates negative prognosis in patients with hepatocellular carcinoma. Int J Clin Exp Pathol 2015;8(10):13725–38.
[262] Wang L, Ouyang F, Liu X, Wu S, Wu HM, Xu Y, Wang B, Zhu J, Xu X, Zhang L. Overexpressed CISD2 has prognostic value in human gastric cancer and promotes gastric cancer cell proliferation and tumorigenesis via AKT signaling pathway. Oncotarget 2016;7(4):3791–805.
[263] Boucquey M, De Plaen E, Locker M, Poliard A, Mouillet-Richard S, Boon T, Kellermann O. Noxp20 and Noxp70, two new markers of early neuronal differentiation, detected in teratocarcinoma-derived neuroectodermic precursor cells. J Neurochem 2006;99(2):657–69.
[264] Wiley SE, Andreyev AY, Divakaruni AS, Karisch R, Perkins G, Wall EA, van der Geer P, Chen YF, Tsai TF, Simon MI, Neel BG, Dixon JE, Murphy AN. Wolfram syndrome protein, Miner1, regulates sulphydryl redox status, the unfolded protein response, and Ca2+ homeostasis. EMBO Mol Med 2013;5(6):904–18.
[265] Inoue H, Tanizawa Y, Wasson J, Behn P, Kalidas K, Bernal-Mizrachi E, Mueckler M, Marshall H, Donis-Keller H, Crock P, Rogers D, Mikuni M, Kumashiro H, Higashi K, Sobue G, Oka Y, Permutt MA. A gene encoding a transmembrane protein is mutated in patients with diabetes mellitus and optic atrophy (Wolfram syndrome). Nat Genet 1998;20(2):143–8.
[266] Osman AA, Saito M, Makepeace C, Permutt MA, Schlesinger P, Mueckler M. Wolframin expression induces novel ion channel activity in endoplasmic reticulum membranes and increases intracellular calcium. J Biol Chem 2003;278(52):52755–62.
[267] Lu S, Kanekura K, Hara T, Mahadevan J, Spears LD, Oslowski CM, Martinez R, Yamazaki-Inoue M, Toyoda M, Neilson A, Blanner P, Brown CM, Semenkovich CF, Marshall BA, Hershey T, Umezawa A, Greer PA, Urano F. A calcium-dependent protease as a potential therapeutic target for Wolfram syndrome. Proc Natl Acad Sci USA 2014;111(49):E5292–301.
[268] Holt SH, Darash-Yahana M, Sohn YS, Song L, Karmi O, Tamir S, Michaeli D, Luo Y, Paddock ML, Jennings PA, Onuchic JN, Azad RK, Pikarsky E, Cabantchik IZ, Nechushtai R, Mittler R. Activation of apoptosis in NAF-1-deficient human epithelial breast cancer cells. J.Cell Sci 2016;129(1): 155–65.
[269] Wiley SE, Murphy AN, Ross SA, van der Geer P, Dixon JE. MitoNEET is an iron-containing outer mitochondrial membrane protein that regulates oxidative capacity. Proc Natl Acad Sci USA 2007;104(13):5318–23.
[270] Kusminski CM, Holland WL, Sun K, Park J, Spurgin SB, Lin Y, Askew GR, Simcox JA, McClain DA, Li C, Scherer PE. MitoNEET-driven alterations in adipocyte mitochondrial activity reveal a crucial adaptive process that preserves insulin sensitivity in obesity. Nat Med 2012;18(10):1539–49.
[271] Balk J, Pilon M. Ancient and essential: the assembly of iron-sulfur clusters in plants. Trends Plant Sci 2011;16(4):218–26.
[272] Py B, Barras F. Building Fe-S proteins: bacterial strategies. Nat Rev Microbiol 2010;8(6):436–46.
[273] Peters JW, Broderick JB. Emerging paradigms for complex iron-sulfur cofactor assembly and insertion. Annu Rev Biochem 2012;81:429–50.

[274] Lill R, Dutkiewicz R, Freibert SA, Heidenreich T, Mascarenhas J, Netz DJ, Paul VD, Pierik AJ, Richter N, Stumpfig M, Srinivasan V, Stehling O, Muhlenhoff. The role of mitochondria and the CIA machinery in the maturation of cytosolic and nuclear iron-sulfur proteins. Eur J Cell Biol 2015;94(7–9):280–91.
[275] Barupala DP, Dzul SP, Riggs-Gelasco PJ, Stemmler TL. Synthesis, delivery and regulation of eukaryotic heme and Fe-S cluster cofactors. Arch Biochem Biophys 2016;592:60–75.
[276] Zheng L, White RH, Cash VL, Jack RF, Dean DR. Cysteine desulfurase activity indicates a role for NIFS in metallocluster biosynthesis. Proc Natl Acad Sci USA 1993;90:2754–8.
[277] Land T, Rouault TA. Targeting of a human iron-sulfur cluster assembly enzyme, nifs, to different subcellular compartments is regulated through alternative AUG utilization. Mol Cell 1998;2:807–15.
[278] Biederbick A, Stehling O, Rosser R, Niggemeyer B, Nakai Y, Elsasser HP, Lill R. Role of human mitochondrial Nfs1 in cytosolic iron-sulfur protein biogenesis and iron regulation. Mol Cell Biol 2006;26(15):5675–87.
[279] Urbina HD, Silberg JJ, Hoff KG, Vickery LE. Transfer of sulfur from IscS to IscU during Fe/S cluster assembly. J Biol Chem 2001;276:44521–6.
[280] Smith AD, Agar JN, Johnson KA, Frazzon J, Amster IJ, Dean DR, Johnson MK. Sulfur transfer from IscS to IscU: the first step in iron-sulfur cluster biosynthesis. J Am Chem Soc 2001;123(44):11103–4.
[281] Shi R, Proteau A, Villarroya M, Moukadiri I, Zhang L, Trempe JF, Matte A, Armengod ME, Cygler M. Structural basis for Fe-S cluster assembly and tRNA thiolation mediated by IscS protein-protein interactions. PLoS Biol 2010;8(4):e1000354.
[282] Agar JN, Krebs C, Frazzon J, Huynh BH, Dean DR, Johnson MK. IscU as a scaffold for iron-sulfur cluster biosynthesis: sequential assembly of [2Fe-2S] and [4Fe-4S] clusters in IscU. Biochemistry 2000;39(27):7856–62.
[283] Marinoni EN, de Oliveira JS, Nicolet Y, Raulfs EC, Amara P, Dean DR, Fontecilla-Camps JC. (IscS-IscU)2 complex structures provide insights into Fe2S2 biogenesis and transfer. Angew Chem Int Ed Engl 2012;51(22):5439–42.
[284] Colin F, Martelli A, Clemancey M, Latour JM, Gambarelli S, Zeppieri L, Birck C, Page A, Puccio H, Ollagnier de Choudens S. Mammalian frataxin controls sulfur production and iron entry during de novo Fe4S4 cluster assembly. J Am Chem Soc 2013;135(2):733–40.
[285] Fox NG, Chakrabarti M, McCormick SP, Lindahl PA, Barondeau DP. The human iron-sulfur assembly complex catalyzes the synthesis of [2Fe-2S] clusters on ISCU2 that can be transferred to acceptor molecules. Biochemistry 2015;54(25):3871–9.
[286] Adam AC, Bornhovd C, Prokisch H, Neupert W, Hell K. The Nfs1 interacting protein Isd11 has an essential role in Fe/S cluster biogenesis in mitochondria. EMBO J 2006;25(1):174–83.
[287] Wiedemann N, Urzica E, Guiard B, Muller H, Lohaus C, Meyer HE, Ryan MT, Meisinger C, Muhlenhoff U, Lill R, Pfanner N. Essential role of Isd11 in mitochondrial iron-sulfur cluster synthesis on Isu scaffold proteins. EMBO J 2006;25(1):184–95.
[288] Shi Y, Ghosh MC, Tong WH, Rouault TA. Human ISD11 is essential for both iron-sulfur cluster assembly and maintenance of normal cellular iron homeostasis. Hum Mol Genet 2009;18(16):3014–25.
[289] Pandey A, Golla R, Yoon H, Dancis A, Pain D. Persulfide formation on mitochondrial cysteine desulfurase: enzyme activation by a eukaryote-specific interacting protein and Fe-S cluster synthesis. Biochem J 2012;448(2):171–87.
[290] Gerber J, Muhlenhoff U, and Lill R. An interaction between frataxin and Isu1/Nfs1 that is crucial for Fe/S cluster synthesis on Isu1. EMBO Rep 2003;4(9):906–11.
[291] Gakh O, Park S, Liu G, Macomber L, Imlay JA, Ferreira GC, Isaya G. Mitochondrial iron detoxification is a primary function of frataxin that limits oxidative damage and preserves cell longevity. Hum Mol Genet 2006;15(3):467–79.

[292] Cook JD, Kondapalli KC, Rawat S, Childs WC, Murugesan Y, Dancis A, Stemmler TL. Molecular details of the yeast frataxin-Isu1 interaction during mitochondrial Fe-S cluster assembly. Biochemistry 2010;49(40):8756–65.
[293] Tsai CL, Barondeau DP. Human frataxin is an allosteric switch that activates the Fe-S cluster biosynthetic complex. Biochemistry 2010;49(43):9132–9.
[294] Fox NG, Das D, Chakrabarti M, Lindahl PA, Barondeau DP. Frataxin accelerates [2Fe-2S] cluster formation on the human Fe-S assembly complex. Biochemistry 2015;54(25):3880–9.
[295] Sheftel AD, Stehling O, Pierik AJ, Elsasser HP, Muhlenhoff U, Webert H, Hobler A, Hannemann F, Bernhardt R, Lill R, Humans possess two mitochondrial ferredoxins, Fdx1 and Fdx2, with distinct roles in steroidogenesis, heme, and Fe/S cluster biosynthesis. Proc Natl Acad Sci USA 2010;107(26):11775–80.
[296] Shi Y, Ghosh M, Kovtunovych G, Crooks DR, Rouault TA. Both human ferredoxins 1 and 2 and ferredoxin reductase are important for iron-sulfur cluster biogenesis. Biochim Biophys Acta 2012;1823(2):484–92.
[297] Hoff KG, Silberg JJ, Vickery LE. Interaction of the iron-sulfur cluster assembly protein IscU with the Hsc66/Hsc20 molecular chaperone system of Escherichia coli. Proc Natl Acad Sci USA 2000;97(14):7790–5.
[298] Voisine C, Cheng YC, Ohlson M, Schilke B, Hoff K, Beinert H, Marszalek J, Craig EA. Jac1, a mitochondrial J-type chaperone, is involved in the biogenesis of Fe/S clusters in Saccharomyces cerevisiae. Proc Natl Acad Sci USA 2001;98(4):1483–8.
[299] Chandramouli K, Johnson MK. HscA and HscB stimulate [2Fe-2S] cluster transfer from IscU to apoferredoxin in an ATP-dependent reaction. Biochemistry 2006;45(37):11087–95.
[300] Andrew AJ, Dutkiewicz R, Knieszner H, Craig EA, Marszalek J. Characterization of the interaction between the J-protein Jac1p and the scaffold for Fe-S cluster biogenesis, Isu1p. J Biol Chem 2006;281(21):14580–7.
[301] Schilke B, Williams B, Knieszner H, Pukszta S, D'Silva P, Craig EA, Marszalek J. Evolution of mitochondrial chaperones utilized in Fe-S cluster biogenesis. Curr Biol 2006;16(16):1660–5.
[302] Bonomi F, Iametti S, Morleo A, Ta D, Vickery LE. Studies on the mechanism of catalysis of iron-sulfur cluster transfer from IscU[2Fe2S] by HscA/HscB chaperones. Biochemistry 2008;47(48):12795–801.
[303] Uhrigshardt H, Singh A, Kovtunovych G, Ghosh M, Rouault TA. Characterization of the human HSC20, an unusual DnaJ type III protein, involved in iron-sulfur cluster biogenesis. Hum Mol Genet2010;19(19):3816–34.
[304] Kampinga HH, Craig EA. The HSP70 chaperone machinery: J proteins as drivers of functional specificity. Nat Rev Mol Cell Biol 2010;11(8):579–92.
[305] Maio N, Singh A, Uhrigshardt H, Saxena N, Tong WH, Rouault TA. Cochaperone binding to LYR motifs confers specificity of iron sulfur cluster delivery. Cell Metab 2014;19(3):445–57.
[306] Maio N, Ghezzi D, Verrigni D, Rizza T, Bertini E, Martinelli D, Zeviani M, Singh A, Carrozzo R, Rouault TA. Disease-causing SDHAF1 mutations impair transfer of Fe-S clusters to SDHB. Cell Metab 2016;23(2):292–302.
[307] Rodriguez-Manzaneque MT, Tamarit J, Belli G, Ros J, Herrero E. Grx5 is a mitochondrial glutaredoxin required for the activity of iron/sulfur enzymes. Mol Biol Cell 2002;13(4): 1109–21.
[308] Muhlenhoff U, Gerber J, Richhardt N, Lill R. Components involved in assembly and dislocation of iron-sulfur clusters on the scaffold protein Isu1p. EMBO J 2003;22(18):4815–25.
[309] Wingert RA, Galloway JL, Barut B, Foott H, Fraenkel P, Axe JL, Weber GJ, Dooley K, Davidson AJ, Schmid B, Paw BH, Shaw GC, Kingsley P, Palis J, Schubert H, Chen O, Kaplan J, Zon LI. Deficiency of glutaredoxin 5 reveals Fe-S clusters are required for vertebrate haem synthesis. Nature 2005;436(7053):1035–9.

[310] Camaschella C, Campanella A, De Falco L, Boschetto L, Merlini R, Silvestri L, Levi S, Iolascon A. The human counterpart of zebrafish shiraz shows sideroblastic-like microcytic anemia and iron overload. Blood 2007;110(4):1353–8.
[311] Bandyopadhyay S, Gama F, Molina-Navarro MM, Gualberto JM, Claxton R, Naik SG, Huynh BH, Herrero E, Jacquot JP, Johnson MK, Rouhier N. Chloroplast monothiol glutaredoxins as scaffold proteins for the assembly and delivery of [2Fe-2S] clusters. EMBO J 2008;27(7):1122–33.
[312] Shakamuri P, Zhang B, Johnson MK. Monothiol glutaredoxins function in storing and transporting [Fe2S2] clusters assembled on IscU scaffold proteins. J Am Chem Soc 2012;134(37):15213–6.
[313] Brancaccio D, Gallo A, Mikolajczyk M, Zovo K, Palumaa P, Novellino E, Piccioli M, Ciofi-Baffoni S, Banci L. Formation of [4Fe-4S] clusters in the mitochondrial iron-sulfur cluster assembly machinery. J Am Chem Soc 2014;136(46):16240–50.
[314] Gelling C, Dawes IW, Richhardt N, Lill R, Muhlenhoff U. Mitochondrial Iba57p is required for Fe/S cluster formation on aconitase and activation of radical SAM enzymes. Mol Cell Biol 2008;28(5):1851–61.
[315] Muhlenhoff U, Richter N, Pines O, Pierik AJ, Lill R. Specialized function of yeast Isa1 and Isa2 proteins in the maturation of mitochondrial [4Fe-4S] proteins. J Biol Chem 2011;286(48):41205–16.
[316] Nishio K, Nakai M. Transfer of iron-sulfur cluster from NifU to apoferredoxin. J Biol Chem 2000;275(30):22615–8.
[317] Tong WH, Jameson GN, Huynh BH, Rouault TA. Subcellular compartmentalization of human Nfu, an iron-sulfur cluster scaffold protein, and its ability to assemble a [4Fe-4S] cluster. Proc Natl Acad Sci USA 2003;100(17):9762–7.
[318] Jin Z, Heinnickel M, Krebs C, Shen G, Golbeck JH, Bryant DA. Biogenesis of iron-sulfur clusters in photosystem I: holo-NfuA from the cyanobacterium Synechococcus sp. PCC 7002 rapidly and efficiently transfers [4Fe-4S] clusters to apo-PsaC in vitro. J Biol Chem 2008;283(42):28426–35.
[319] Angelini S, Gerez C, Ollagnier-de Choudens S, Sanakis Y, Fontecave M, Barras F, Py B. NfuA, a new factor required for maturing Fe/S proteins in Escherichia coli under oxidative stress and iron starvation conditions. J Biol Chem 2008;283(20):14084–91.
[320] Bandyopadhyay S, Naik SG, O'Carroll IP, Huynh BH, Dean DR, Johnson MK, Dos Santos PC. A proposed role for the Azotobacter vinelandii NfuA protein as an intermediate iron-sulfur cluster carrier. J Biol Chem 2008;283(20):14092–9.
[321] Navarro-Sastre A, Tort F, Stehling O, Uzarska MA, Arranz JA, Del Toro M, Labayru MT, Landa J, Font A, Garcia-Villoria J, Merinero B, Ugarte M, Gutierrez-Solana LG, Campistol J, Garcia-Cazorla A, Vaquerizo J, Riudor E, Briones P, Elpeleg O, Ribes A, Lill R. A fatal mitochondrial disease is associated with defective NFU1 function in the maturation of a subset of mitochondrial Fe-S proteins. Am J Hum Genet 2011;89(5):656–67.
[322] Py B, Gerez C, Angelini S, Planel R, Vinella D, Loiseau L, Talla E, Brochier-Armanet C, Garcia Serres R, Latour JM, Ollagnier-de Choudens S, Fontecave M, Barras F. Molecular organization, biochemical function, cellular role and evolution of NfuA, an atypical Fe-S carrier. Mol Microbiol 2012;86(1):155–71.
[323] Bych K, Kerscher S, Netz DJ, Pierik AJ, Zwicker K, Huynen MA, Lill R, Brandt U, Balk J. The iron-sulphur protein Ind1 is required for effective complex I assembly. EMBO J 2008;27(12):1736–46.
[324] Sheftel AD, Stehling O, Pierik AJ, Netz DJ, Kerscher S, Elsasser HP, Wittig I, Balk J, Brandt U, Lill R. Human ind1, an iron-sulfur cluster assembly factor for respiratory complex I. Mol Cell Biol 2009;29(22):6059–73.

[325] Wydro M, Balk J. Iron, sulfur, and protein biogenesis – insights from complex I assembly in Arabidopsis. in 7th International Conference on Iron-Sulfur Cluster Biogenesis and Regulation. 2013. Columbia, South Carolina, USA.
[326] Mesecke N, Terziyska N, Kozany C, Baumann F, Neupert W, Hell K, Herrmann JM. A disulfide relay system in the intermembrane space of mitochondria that mediates protein import. Cell 2005;121(7):1059–69.
[327] Lill R, Hoffmann B, Molik S, Pierik AJ, Rietzschel N, Stehling O, Uzarska MA, Webert H, Wilbrecht C, Muhlenhoff U. The role of mitochondria in cellular iron-sulfur protein biogenesis and iron metabolism. Biochim Biophys Acta 2012;1823(9):1491–508.
[328] Tong WH, Rouault TA. Functions of mitochondrial ISCU and cytosolic ISCU in mammalian iron-sulfur cluster biogenesis and iron homeostasis. Cell Metab 2006;3(3):199–210.
[329] Roy A, Solodovnikova N, Nicholson T, Antholine W, Walden WE. A novel eukaryotic factor for cytosolic Fe-S cluster assembly. EMBO J 2003;22(18):4826–35.
[330] Netz DJ, Pierik AJ, Stumpfig M, Muhlenhoff U, Lill R. The Cfd1-Nbp35 complex acts as a scaffold for iron-sulfur protein assembly in the yeast cytosol. Nat Chem Biol 2007;3(5):278–86.
[331] Hausmann A, Aguilar Netz DJ, Balk J, Pierik AJ, Muhlenhoff U, Lill R. The eukaryotic P loop NTPase Nbp35: an essential component of the cytosolic and nuclear iron-sulfur protein assembly machinery. Proc Natl Acad Sci USA 2005;102(9):3266–71.
[332] Balk J, Pierik AJ, Netz DJ, Muhlenhoff U, Lill R. The hydrogenase-like Nar1p is essential for maturation of cytosolic and nuclear iron-sulphur proteins. EMBO J 2004;23(10):2105–15.
[333] Urzica E, Pierik AJ, Muhlenhoff U, Lill R. Crucial role of conserved cysteine residues in the assembly of two iron-sulfur clusters on the CIA protein Nar1. Biochemistry 2009;48(22):4946–58.
[334] Balk J, Aguilar Netz DJ, Tepper K, Pierik AJ, Lill R. The essential WD40 protein Cia1 is involved in a late step of cytosolic and nuclear iron-sulfur protein assembly. Mol Cell Biol 2005;25(24):10833–41.
[335] Srinivasan V, Netz DJ, Webert H, Mascarenhas J, Pierik AJ, Michel H, Lill R. Structure of the yeast WD40 domain protein Cia1, a component acting late in iron-sulfur protein biogenesis. Structure 2007;15(10):1246–57.
[336] Zhang Y, Lyver ER, Nakamaru-Ogiso E, Yoon H, Amutha B, Lee DW, Bi E, Ohnishi T, Daldal F, Pain D, Dancis A. Dre2, a conserved eukaryotic Fe/S cluster protein, functions in cytosolic Fe/S protein biogenesis. Mol Cell Biol 2008;28(18):5569–82.
[337] Netz DJ, Stumpfig M, Dore C, Muhlenhoff U, Pierik AJ, Lill R. Tah18 transfers electrons to Dre2 in cytosolic iron-sulfur protein biogenesis. Nat Chem Biol 2010;6(10):758–65.
[338] Netz DJ, Genau HM, Weiler BD, Bill E, Pierik AJ, Lill R. The conserved protein Dre2 uses essential [2Fe-2S] and [4Fe-4S] clusters for its function in cytosolic iron-sulfur protein assembly. Biochem J 2016;473(14):2073–85.
[339] Stehling O, Mascarenhas J, Vashisht AA, Sheftel AD, Niggemeyer B, Rosser R, Pierik AJ, Wohlschlegel JA, Lill R. Human CIA2A-FAM96A and CIA2B-FAM96B integrate iron homeostasis and maturation of different subsets of cytosolic-nuclear iron-sulfur proteins. Cell Metab 2013.
[340] van Wietmarschen N, Moradian A, Morin GB, Lansdorp PM, Uringa EJ. The mammalian proteins MMS19, MIP18, and ANT2 are involved in cytoplasmic iron-sulfur cluster protein assembly. J Biol Chem 2012;287(52):43351–8.
[341] Stehling O, Netz DJ, Niggemeyer B, Rosser R, Eisenstein RS, Puccio H, Pierik AJ, Lill R. Human Nbp35 is essential for both cytosolic iron-sulfur protein assembly and iron homeostasis. Mol Cell Biol 2008;28(17):5517–28.
[342] Seki M, Takeda Y, Iwai K, Tanaka K. IOP1 protein is an external component of the human cytosolic iron-sulfur cluster assembly (CIA) machinery and functions in the MMS19 protein-dependent CIA pathway. J Biol Chem 2013;288(23):16680–9.

[343] Song D, Lee FS. Mouse knock-out of IOP1 protein reveals its essential role in mammalian cytosolic iron-sulfur protein biogenesis. J Biol Chem 2011;286(18):15797–805.
[344] Nakamura M, Buzas DM, Kato A, Fujita M, Kurata N, Kinoshita T. The role of Arabidopsis thaliana NAR1, a cytosolic iron-sulfur cluster assembly component, in gametophytic gene expression and oxidative stress responses in vegetative tissue. New Phytol 2013;199(4):925–35.
[345] Paul VD, Muhlenhoff U, Stumpfig M, Seebacher J, Kugler KG, Renicke C, Taxis C, Gavin AC, Pierik AJ, Lill R. The deca-GX3 proteins Yae1-Lto1 function as adaptors recruiting the ABC protein Rli1 for iron-sulfur cluster insertion. Elife 2015;4:e08231.
[346] Stehling O, Wilbrecht C, Lill R. Mitochondrial iron-sulfur protein biogenesis and human disease. Biochimie 2014;100:61–77.
[347] Beilschmidt LK, Puccio HM. Mammalian Fe-S cluster biogenesis and its implication in disease. Biochimie 2014;100:48–60.
[348] Pain D, Dancis A. Roles of Fe-S proteins: from cofactor synthesis to iron homeostasis to protein synthesis. Curr Opin Genet Dev 2016;38:45–51.
[349] Schilke B, Voisine C, Beinert H, Craig E. Evidence for a conserved system for iron metabolism in the mitochondria of Saccharomyces cerevisiae. Proc Natl Acad Sci USA 1999;96(18):10206–11.
[350] Vazquez-Manrique RP, Gonzalez-Cabo P, Ros S, Aziz H, Baylis HA, Palau F. Reduction of Caenorhabditis elegans frataxin increases sensitivity to oxidative stress, reduces lifespan, and causes lethality in a mitochondrial complex II mutant. FASEB J 2006;20(1):172–4.
[351] Herrero E, de la Torre-Ruiz MA. Monothiol glutaredoxins: a common domain for multiple functions. Cell Mol Life Sci 2007;64(12):1518–30.
[352] Cossee M, Puccio H, Gansmuller A, Koutnikova H, Dierich A, LeMeur M, Fischbeck K, Dolle P, Koenig M. Inactivation of the Friedreich ataxia mouse gene leads to early embryonic lethality without iron accumulation. Hum Mol Genet 2000;9(8):1219–26.
[353] Pondarre C, Antiochos BB, Campagna DR, Clarke SL, Greer EL, Deck KM, McDonald A, Han AP, Medlock A, Kutok JL, Anderson SA, Eisenstein RS, Fleming MD. The mitochondrial ATP-binding cassette transporter Abcb7 is essential in mice and participates in cytosolic iron-sulfur cluster biogenesis. Hum Mol Genet 2006;15(6):953–64.
[354] Nordin A, Larsson E, Thornell LE, Holmberg M. Tissue-specific splicing of ISCU results in a skeletal muscle phenotype in myopathy with lactic acidosis, while complete loss of ISCU results in early embryonic death in mice. Hum Genet 2011;129(4):371–8.
[355] Fosset C, Chauveau MJ, Guillon B, Canal F, Drapier JC, Bouton C. RNA silencing of mitochondrial m-Nfs1 reduces Fe-S enzyme activity both in mitochondria and cytosol of mammalian cells. J Biol Chem 2006;281(35):25398–406.
[356] Martelli A, Wattenhofer-Donze M, Schmucker S, Bouvet S, Reutenauer L, Puccio H. Frataxin is essential for extramitochondrial Fe-S cluster proteins in mammalian tissues. Hum Mol Genet 2007;16(22):2651–8.
[357] Song D, Lee FS. A role for IOP1 in mammalian cytosolic iron-sulfur protein biogenesis. J Biol Chem 2008;283(14):9231–8.
[358] Li K, Besse EK, Ha D, Kovtunovych G, Rouault TA. Iron-dependent regulation of frataxin expression: implications for treatment of Friedreich ataxia. Hum Mol Genet 2008;17(15):2265–73.
[359] Campuzano V, Montermini L, Molto MD, Pianese L, Cossee M, Cavalcanti F, Monros E, Rodius F, Duclos F, Monticelli A, Zara F, Cañizares J, Koutnikova H, Bidichandani S, Gellera C, Brice A, Trouillas P, De Michele G, Filla A, De Frutos R, Palau F, Patel PI, Di Donato S, Mandel J-L, Cocozza S, Koenig M, Pandolfo M. Friedreich's ataxia: autosomal recessive disease caused by an intronic GAA triplet repeat expansion. Science 1996;271(5254):1423–7.
[360] Cossee M, Schmitt M, Campuzano V, Reutenauer L, Moutou C, Mandel JL, Koenig M. Evolution of the Friedreich's ataxia trinucleotide repeat expansion: founder effect and premutations. Proc Natl Acad Sci USA 1997;94(14):7452–7.

[361] Harding AE. Friedreich's ataxia: a clinical and genetic study of 90 families with an analysis of early diagnostic criteria and intrafamilial clustering of clinical features. Brain 1981;104(3):589–620.
[362] Pandolfo M, Pastore A. The pathogenesis of Friedreich ataxia and the structure and function of frataxin. J Neurol 2009;256 Suppl 1:9–17.
[363] Koeppen AH. Friedreich's ataxia: pathology, pathogenesis, and molecular genetics. J Neurol Sci 2011;303(1–2):1–12.
[364] Puccio H, Anheim M, Tranchant C. Pathophysiogical and therapeutic progress in Friedreich ataxia. Rev Neurol (Paris) 2014;170(5):355–65.
[365] De Biase I, Rasmussen A, Endres D, Al-Mahdawi S, Monticelli A, Cocozza S, Pook M, Bidichandani SI. Progressive GAA expansions in dorsal root ganglia of Friedreich's ataxia patients. Ann Neurol 2007;61(1):55–60.
[366] Cossee M, Durr A, Schmitt M, Dahl N, Trouillas P, Allinson P, Kostrzewa M, Nivelon-Chevallier A, Gustavson KH, Kohlschutter A, Muller U, Mandel JL, Brice A, Koenig M, Cavalcanti F, Tammaro, A, De Michele G, Filla A, Cocozza S, Labuda M, Montermini L, Poirier J, Pandolfo M. Friedreich's ataxia: point mutations and clinical presentation of compound heterozygotes. Ann Neurol 1999;45(2):200–6.
[367] Gellera C, Castellotti B, Mariotti C, Mineri R, Seveso V, Didonato S, Taroni F. Frataxin gene point mutations in Italian Friedreich ataxia patients. Neurogenetics 2007;8(4):289–99.
[368] Gottesfeld JM. Small molecules affecting transcription in Friedreich ataxia. Pharmacol 2007;116(2):236–48.
[369] Punga T, Buhler M. Long intronic GAA repeats causing Friedreich ataxia impede transcription elongation. EMBO Mol Med 2010;2(4):120–9.
[370] Kumari D, Biacsi RE, Usdin K. Repeat expansion affects both transcription initiation and elongation in Friedreich ataxia cells. J Biol Chem 2011;286(6):4209–15.
[371] Greene E, Mahishi L, Entezam A, Kumari D, Usdin K. Repeat-induced epigenetic changes in intron 1 of the frataxin gene and its consequences in Friedreich ataxia. Nucleic Acids Res 2007;35(10):3383–90.
[372] Al-Mahdawi S, Pinto RM, Ismail O, Varshney D, Lymperi S, Sandi C, Trabzuni D, Pook M. The Friedreich ataxia GAA repeat expansion mutation induces comparable epigenetic changes in human and transgenic mouse brain and heart tissues. Hum Mol Genet 2008;17(5):735–46.
[373] Castaldo I, Pinelli M, Monticelli A, Acquaviva F, Giacchetti M, Filla A, Sacchetti S, Keller S, Avvedimento VE, Chiariotti L, Cocozza S. DNA methylation in intron 1 of the frataxin gene is related to GAA repeat length and age of onset in Friedreich ataxia patients. J Med Genet 2008;45(12):808–12.
[374] Correia AR, Pastore C, Adinolfi S, Pastore A, Gomes CM. Dynamics, stability and iron-binding activity of frataxin clinical mutants. FEBS J 2008;275(14):3680–90.
[375] Bridwell-Rabb J, Winn AM, Barondeau DP. Structure-function analysis of Friedreich's ataxia mutants reveals determinants of frataxin binding and activation of the Fe-S assembly complex. Biochemistry 2011;50(33):7265–74.
[376] Tsai CL, Bridwell-Rabb J, Barondeau DP. Friedreich's ataxia variants I154F and W155R diminish frataxin-based activation of the iron-sulfur cluster assembly complex. Biochemistry 2011;50(29):6478–87.
[377] Faggianelli N, Puglisi R, Veneziano L, Romano S, Frontali M, Vannocci T, Fortuni S, Testi R, Pastore A. Analyzing the effects of a G137V mutation in the FXN gene. Front Mol Neurosci 2015;8:66.
[378] Xia H, Cao Y, Dai X, Marelja Z, Zhou D, Mo R, Al-Mahdawi S, Pook MA, Leimkuhler S, Rouault TA, Li K. Novel frataxin isoforms may contribute to the pathological mechanism of Friedreich ataxia. PLoS One 2012;7(10):e47847.
[379] Pastore A, Puccio H. Frataxin: a protein in search for a function. J Neurochem 2013;126 Suppl 1:43–52.

[380] Rotig A, de Lonlay P, Chretien D, Foury F, Koenig M, Sidi D, Munnich A, Rustin, P. Aconitase and mitochondrial iron-sulphur protein deficiency in Friedreich ataxia. Nat Genet 1997;17(2):215–7.
[381] Koutnikova H, Campuzano V, Foury F, Dolle P, Cazzalini O, Koenig M. Studies of human, mouse and yeast homologues indicate a mitochondrial function for frataxin. Nat Genet 1997;16(4):345–51.
[382] Babcock M, de Silva D, Oaks R, Davis-Kaplan S, Jiralerspong S, Montermini L, Pandolfo M, Kaplan J. Regulation of mitochondrial iron accumulation by Yfh1p, a putative homolog of frataxin. Science 1997;276(5319):1709–12.
[383] Santos MM, Ohshima K, Pandolfo M. Frataxin deficiency enhances apoptosis in cells differentiating into neuroectoderm. Hum Mol Genet 2001;10(18):1935–44.
[384] Muhlenhoff U, Richhardt N, Ristow M, Kispal G, Lill R. The yeast frataxin homolog Yfh1p plays a specific role in the maturation of cellular Fe/S proteins. Hum Mol Genet 2002;11(17):2025–36.
[385] Stehling O, Elsasser HP, Bruckel B, Muhlenhoff U, Lill R. Iron-sulfur protein maturation in human cells: evidence for a function of frataxin. Hum Mol Genet 2004;13(23):3007–15.
[386] Anderson PR, Kirby K, Hilliker AJ, Phillips JP. RNAi-mediated suppression of the mitochondrial iron chaperone, frataxin, in Drosophila. Hum Mol Genet 2005;14(22):3397–405.
[387] Napoli E, Morin D, Bernhardt R, Buckpitt A, Cortopassi G. Hemin rescues adrenodoxin, heme a and cytochrome oxidase activity in frataxin-deficient oligodendroglioma cells. Biochim Biophys Acta 2007;1772(7):773–80.
[388] Zanella I, Derosas M, Corrado M, Cocco E, Cavadini P, Biasiotto G, Poli M, Verardi R, Arosio P. The effects of frataxin silencing in HeLa cells are rescued by the expression of human mitochondrial ferritin. Biochim Biophys Acta, 2008;1782(2):90–8.
[389] Lu C, Schoenfeld R, Shan Y, Tsai HJ, Hammock B, Cortopassi G. Frataxin deficiency induces Schwann cell inflammation and death. Biochim Biophys Acta 2009;1792(11):1052–61.
[390] Nair M, Adinolfi S, Pastore C, Kelly G, Temussi P, Pastore A. Solution structure of the bacterial frataxin ortholog, CyaY: mapping the iron binding sites. Structure 2004;12(11):2037–48.
[391] Cook JD, Bencze KZ, Jankovic AD, Crater AK, Busch CN, Bradley PB, Stemmler AJ, Spaller MR, Stemmler TL. Monomeric yeast frataxin is an iron-binding protein. Biochemistry 2006;45(25):7767–77.
[392] Adamec J, Rusnak F, Owen WG, Naylor S, Benson LM, Gacy AM, Isaya G. Iron-dependent self-assembly of recombinant yeast frataxin: implications for Friedreich ataxia. Am J Hum Genet 2000;67(3):549–62.
[393] Li H, Gakh O, Smith DYt, Isaya G. Oligomeric yeast frataxin drives assembly of core machinery for mitochondrial iron-sulfur cluster synthesis. J Biol Chem 2009;284(33):21971–80.
[394] Gakh O, Bedekovics T, Duncan SF, Smith DYt, Berkholz DS, Isaya G. Normal and Friedreich ataxia cells express different isoforms of frataxin with complementary roles in iron-sulfur cluster assembly. J Biol Chem 2010;285(49):38486–501.
[395] Aloria K, Schilke B, Andrew A, Craig EA. Iron-induced oligomerization of yeast frataxin homologue Yfh1 is dispensable in vivo. EMBO Rep 2004;5(11):1096–101.
[396] Layer G, Ollagnier-de Choudens S, Sanakis Y, Fontecave M. Iron-sulfur cluster biosynthesis: characterization of Escherichia coli CYaY as an iron donor for the assembly of [2Fe-2S] clusters in the scaffold IscU. J Biol Chem 2006;281(24):16256–63.
[397] Bencze KZ, Kondapalli KC, Cook JD, McMahon S, Millan-Pacheco C, Pastor N, Stemmler TL. The structure and function of frataxin. Crit Rev Biochem Mol Biol 2006;41(5):269–91.
[398] Bulteau AL, O'Neill HA, Kennedy MC, Ikeda-Saito M, Isaya G, Szweda LI. Frataxin acts as an iron chaperone protein to modulate mitochondrial aconitase activity. Science 2004;305(5681):242–5.
[399] He Y, Alam SL, Proteasa SV, Zhang Y, Lesuisse E, Dancis A, Stemmler TL. Yeast frataxin solution structure, iron binding, and ferrochelatase interaction. Biochemistry 2004;43(51):16254–62.
[400] Yoon T, Cowan JA. Frataxin-mediated iron delivery to ferrochelatase in the final step of heme biosynthesis. J Biol Chem 2004;279(25):25943–6.

[401] Soderberg C, Gillam ME, Ahlgren EC, Hunter GA, Gakh O, Isaya G, Ferreira GC, Al-Karadaghi S. The Structure of the complex between yeast frataxin and ferrochelatase: characterization and pre-steady state reaction of ferrous iron delivery and heme synthesis. J Biol Chem 2016;291(22):11887–98.
[402] Gonzalez-Cabo P, Vazquez-Manrique RP, Garcia-Gimeno MA, Sanz P, Palau F. Frataxin interacts functionally with mitochondrial electron transport chain proteins. Hum Mol Genet 2005;14(15):2091–8.
[403] Schmucker S, Martelli A, Colin F, Page A, Wattenhofer-Donze M, Reutenauer L, Puccio H. Mammalian frataxin: an essential function for cellular viability through an interaction with a preformed ISCU/NFS1/ISD11 iron-sulfur assembly complex. PLoS One 2011;6(1):e16199.
[404] Yoon H, Knight SA, Pandey A, Pain J, Zhang Y, Pain D, Dancis. A, Frataxin-bypassing Isu1: characterization of the bypass activity in cells and mitochondria. Biochem J 2014;459(1):71–81.
[405] Li DS, Ohshima K, Jiralerspong S, Bojanowski MW, Pandolfo M. Knock-out of the cyaY gene in *Escherichia coli* does not affect cellular iron content and sensitivity to oxidants. FEBS Lett 1999;456(1):13–6.
[406] Foury F, Cazzalini O. Deletion of the yeast homologue of the human gene associated with Friedreich's ataxia elicits iron accumulation in mitochondria. FEBS Lett 1997;411(2–3):373–7.
[407] Wilson RB, Roof DM. Respiratory deficiency due to loss of mitochondrial DNA in yeast lacking the frataxin homologue. Nat Genet 1997;16(4):352–7.
[408] Zarse K, Schulz TJ, Birringer M, Ristow M. Impaired respiration is positively correlated with decreased life span in Caenorhabditis elegans models of Friedreich ataxia. FASEB J 2007;21(4):1271–5.
[409] Llorens JV, Navarro JA, Martinez-Sebastian MJ, Baylies MK, Schneuwly S, Botella JA, Molto MD. Causative role of oxidative stress in a Drosophila model of Friedreich ataxia. FASEB 2007;21(2):333–44.
[410] Puccio H, Simon D, Cossee M, Criqui-Filipe P, Tiziano F, Melki J, Hindelang C, Matyas R, Rustin P, Koenig M. Mouse models for Friedreich ataxia exhibit cardiomyopathy, sensory nerve defect and Fe-S enzyme deficiency followed by intramitochondrial iron deposits. Nat Genet 2001;27(2):181–6.
[411] Miranda CJ, Santos MM, Ohshima K, Smith J, Li L, Bunting M, Cossee M, Koenig M, Sequeiros J, Kaplan J, Pandolfo M. Frataxin knockin mouse. FEBS Lett 2002;512(1–3):291–7.
[412] Al-Mahdawi S, Pinto RM, Varshney D, Lawrence L, Lowrie MB, Hughes S, Webster Z, Blake J, Cooper JM, King R, Pook MA. GAA repeat expansion mutation mouse models of Friedreich ataxia exhibit oxidative stress leading to progressive neuronal and cardiac pathology. Genomics 2006;88(5):580–90.
[413] Martelli A, Napierala M, Puccio H. Understanding the genetic and molecular pathogenesis of Friedreich's ataxia through animal and cellular models. Dis Model Mech 2012;5(2):165–76.
[414] Simon D, Seznec H, Gansmuller A, Carelle N, Weber P, Metzger D, Rustin P, Koenig M, Puccio H. Friedreich ataxia mouse models with progressive cerebellar and sensory ataxia reveal autophagic neurodegeneration in dorsal root ganglia. J Neurochem 2004;24(8):1987–95.
[415] Ristow M, Mulder H, Pomplun D, Schulz TJ, Muller-Schmehl K, Krause A, Fex M, Puccio H, Muller J, Isken F, Spranger J, Muller-Wieland D, Magnuson MA, Mohlig M, Koenig M, Pfeiffer AF. Frataxin deficiency in pancreatic islets causes diabetes due to loss of beta cell mass. J Clin Invest 2003;112(4):527–34.
[416] Lamarche JB, Cote M, Lemieux B. The cardiomyopathy of Friedreich's ataxia morphological observations in 3 cases. Can J Neurol Sci 1980;7(4):389–96.
[417] Michael S, Petrocine SV, Qian J, Lamarche JB, Knutson MD, Garrick MD, Koeppen AH. Iron and iron-responsive proteins in the cardiomyopathy of Friedreich's ataxia. Cerebellum 2006;5(4):257–67.

[418] Rouault TA, Tong WH. Iron-sulphur cluster biogenesis and mitochondrial iron homeostasis. Nat Rev Mol Cel Biol 2005;6(4):345–51.
[419] Richardson DR, Huang ML, Whitnall M, Becker EM, Ponka P, Suryo Rahmanto Y. The ins and outs of mitochondrial iron-loading: the metabolic defect in Friedreich's ataxia. J Mol Med (Berl), 2010;88(4):323–9.
[420] Huang ML, Becker EM, Whitnall M, Suryo Rahmanto Y, Ponka P, Richardson DR. Elucidation of the mechanism of mitochondrial iron loading in Friedreich's ataxia by analysis of a mouse mutant. Proc Natl Acad Sci USA 2009;106(38):16381–6.
[421] Lesuisse E, Santos R, Matzanke BF, Knight SA, Camadro JM, Dancis A. Iron use for haeme synthesis is under control of the yeast frataxin homologue (Yfh1). Hum Mol Genet 2003;12(8):879–89.
[422] Miao R, Martinho M, Morales JG, Kim H, Ellis EA, Lill R, Hendrich MP, Munck E, Lindahl PA. EPR and Mossbauer spectroscopy of intact mitochondria isolated from Yah1p-depleted Saccharomyces cerevisiae. Biochemistry 2008;47(37):9888–99.
[423] Seznec H, Simon D, Bouton C, Reutenauer L, Hertzog A, Golik P, Procaccio V, Patel M, Drapier JC, Koenig M, Puccio H. Friedreich ataxia: the oxidative stress paradox. Hum Mol Genet 2005;14(4):463–74.
[424] Rustin P, von Kleist-Retzow JC, Chantrel-Groussard K, Sidi D, Munnich A, Rotig A. Effect of idebenone on cardiomyopathy in Friedreich's ataxia: a preliminary study. Lancet 1999;354(9177):477–9.
[425] Schulz JB, Dehmer T, Schols L, Mende H, Hardt C, Vorgerd M, Burk K, Matson W, Dichgans J, Beal MF, Bogdanov MB. Oxidative stress in patients with Friedreich ataxia. Neurology 2000;55(11):1719–21.
[426] Di Prospero NA, Baker A, Jeffries N, Fischbeck KH. Neurological effects of high-dose idebenone in patients with Friedreich's ataxia: a randomised, placebo-controlled trial. Lancet Neurol 2007;6(10):878–86.
[427] Lagedrost SJ, Sutton MS, Cohen MS, Satou GM, Kaufman BD, Perlman SL, Rummey C, Meier T, Lynch DR. Idebenone in Friedreich ataxia cardiomyopathy-results from a 6-month phase III study (IONIA). Am Heart J 2011;161(3):639–45 e1.
[428] Soriano S, Llorens JV, Blanco-Sobero L, Gutierrez L, Calap-Quintana P, Morales MP, Molto MD, Martinez-Sebastian MJ. Deferiprone and idebenone rescue frataxin depletion phenotypes in a Drosophila model of Friedreich's ataxia. Gene 2013;521(2):274–81.
[429] Fleming MD. The genetics of inherited sideroblastic anemias. Semin Hematol 2002;39(4):270–81.
[430] Camaschella C. Recent advances in the understanding of inherited sideroblastic anaemia. Br J Haematol 2008;143(1):27–38.
[431] Sheftel AD, Richardson DR, Prchal J, Ponka P. Mitochondrial iron metabolism and sideroblastic anemia. Acta Haematol 2009;122(2–3):120–33.
[432] Harigae H, Furuyama K. Hereditary sideroblastic anemia: pathophysiology and gene mutations. Int J Hematol 2010;92(3):425–31.
[433] Allikmets R, Raskind WH, Hutchinson A, Schueck ND, Dean M, Koeller DM. Mutation of a putative mitochondrial iron transporter gene (ABC7) in X-linked sideroblastic anemia and ataxia (XLSA/A). Hum Mol Genet 1999;8(5):743–9.
[434] Neufeld EJ, Fleming JC, Tartaglini E, Steinkamp MP. Thiamine-responsive megaloblastic anemia syndrome: a disorder of high-affinity thiamine transport. Blood Cells Mol Dis 2001;27(1):135–8.
[435] Bykhovskaya Y, Casas K, Mengesha E, Inbal A, Fischel-Ghodsian N. Missense mutation in pseudouridine synthase 1 (PUS1) causes mitochondrial myopathy and sideroblastic anemia (MLASA). Am J Hum Genet 2004;74(6):1303–8.
[436] Guernsey DL, Jiang H, Campagna DR, Evans SC, Ferguson M, Kellogg MD, Lachance M, Matsuoka M, Nightingale M, Rideout A, Saint-Amant L, Schmidt PJ, Orr A, Bottomley SS, Fleming MD, Ludman M, Dyack S, Fernandez CV, Samuels ME. Mutations in mitochondrial carrier family

gene SLC25A38 cause nonsyndromic autosomal recessive congenital sideroblastic anemia. Nat Genet 2009;41(6):651–3.
[437] Camaschella C. Hereditary sideroblastic anemias: pathophysiology, diagnosis, and treatment. Semin Hematol 2009;46(4):371–7.
[438] Bekri S, Kispal G, Lange H, Fitzsimons E, Tolmie J, Lill R, Bishop DF. Human ABC7 transporter: gene structure and mutation causing X-linked sideroblastic anemia with ataxia with disruption of cytosolic iron-sulfur protein maturation. Blood 2000;96(9):3256–64.
[439] Hellier KD, Hatchwell E, Duncombe AS, Kew J, Hammans SR. X-linked sideroblastic anaemia with ataxia: another mitochondrial disease? J Neurol Neurosurg Psychiatry 2001;70(1):65–9.
[440] D'Hooghe M, Selleslag D, Mortier G, Van Coster R, Vermeersch P, Billiet J, Bekri S. X-linked sideroblastic anemia and ataxia: a new family with identification of a fourth ABCB7 gene mutation. Eur J Paediatr Neurol 2012;16(6):730–5.
[441] Cavadini P, Biasiotto G, Poli M, Levi S, Verardi R, Zanella I, Derosas M, Ingrassia R, Corrado M, Arosio P. RNA silencing of the mitochondrial ABCB7 transporter in HeLa cells causes an iron-deficient phenotype with mitochondrial iron overload. Blood 2007;109(8):3552–9.
[442] Bernard DG, Cheng Y, Zhao Y, Balk J. An allelic mutant series of ATM3 reveals its key role in the biogenesis of cytosolic iron-sulfur proteins in Arabidopsis. Plant Physiol 2009;151(2):590–602.
[443] Kispal G, Csere P, Guiard B, Lill R. The ABC transporter Atm1p is required for mitochondrial iron homeostasis. FEBS Lett 1997;418(3):346–50.
[444] Miao R, Kim H, Koppolu UM, Ellis EA, Scott RA, Lindahl PA. Biophysical characterization of the iron in mitochondria from Atm1p-depleted Saccharomyces cerevisiae. Biochemistry 2009;48(40):9556–68.
[445] Fleming RE, Feng Q, Britton RS. Knockout mouse models of iron homeostasis. Annu Rev Nutr 2011;31:117–37.
[446] Chung J, Chen C, Paw BH. Heme metabolism and erythropoiesis. Curr Opin Hematol 2012;19(3):156–62.
[447] Napier I, Ponka P, Richardson DR. Iron trafficking in the mitochondrion: novel pathways revealed by disease. Blood 2005;105(5):1867–74.
[448] Schaedler TA, Faust B, Shintre CA, Carpenter EP, Srinivasan V, van Veen HW, Balk J. Structures and functions of mitochondrial ABC transporters. Biochem Soc Trans 2015;43(5):943–51.
[449] Srinivasan V, Pierik AJ, Lill R. Crystal structures of nucleotide-free and glutathione-bound mitochondrial ABC transporter Atm1. Science 2014;343(6175):1137–40.
[450] Leighton J, Schatz G. An ABC transporter in the mitochondrial inner membrane is required for normal growth of yeast. EMBO J 1995;14(1):188–95.
[451] Kispal G, Csere P, Prohl C, Lill R. The mitochondrial proteins Atm1p and Nfs1p are essential for biogenesis of cytosolic Fe/S proteins. EMBO J 1999;18(14):3981–9.
[452] Lill R, Muhlenhoff U. Iron-sulfur-protein biogenesis in eukaryotes. Trends Biochem Sci 2005;30:133–41.
[453] Bedekovics T, Li H, Gajdos GB, Isaya G. Leucine biosynthesis regulates cytoplasmic iron-sulfur enzyme biogenesis in an Atm1p-independent manner. J Biol Chem 2011;286(47):40878–88.
[454] Chloupkova M, LeBard LS, Koeller DM. MDL1 is a high copy suppressor of ATM1: evidence for a role in resistance to oxidative stress. J Mol Biol 2003;331(1):155–65.
[455] Chen S, Sanchez-Fernandez R, Lyver ER, Dancis A, Rea PA. Functional characterization of AtATM1, AtATM2, and AtATM3, a subfamily of Arabidopsis half-molecule ATP-binding cassette transporters implicated in iron homeostasis. J Biol Chem 2007;282(29):21561–71.
[456] Lill R. Function and biogenesis of iron-sulphur proteins. Nature 2009;460(7257):831–8.
[457] Schaedler TA, Thornton JD, Kruse I, Schwarzlander M, Meyer AJ, van Veen HW, Balk J. A conserved mitochondrial ATP-binding cassette transporter exports glutathione polysulfide for cytosolic metal cofactor assembly. J Biol Chem 2014;289(34):23264–74.

[458] Li J, Cowan JA. Glutathione-coordinated [2Fe-2S] cluster: a viable physiological substrate for mitochondrial ABCB7 transport. Chem Commun (Camb) 2015;51(12):2253–5.
[459] Teschner J, Lachmann N, Schulze J, Geisler M, Selbach K, Santamaria-Araujo J, Balk J, Mendel RR, Bittner F. A novel role for Arabidopsis mitochondrial ABC transporter ATM3 in molybdenum cofactor biosynthesis. Plant Cell 2010;22(2):468–80.
[460] Liu G, Guo S, Han B, Nie G. Novel heterozygous missense mutations in GLRX5 gene of a Chinese patient affected by sideroblastic anemia, in Fifth Congress of the International BioIron Society, Binennial Wolrd Meeting 2013;London, United Kingdom.
[461] Herrero E, Belli G, Casa C. Structural and functional diversity of glutaredoxins in yeast. Curr Protein Pept Sci 2010;11(8):659–68.
[462] Li H, Outten CE. Monothiol CGFS glutaredoxins and BolA-like proteins: [2Fe-2S] binding partners in iron homeostasis. Biochemistry 2012;51(22):4377–89.
[463] Johansson C, Roos AK, Montano SJ, Sengupta R, Filippakopoulos P, Guo K, von Delft F, Holmgren A, Oppermann U, Kavanagh KL. The crystal structure of human GLRX5: iron-sulfur cluster co-ordination, tetrameric assembly and monomer activity. Biochem J 2011;433(2):303–11.
[464] Picciocchi A, Saguez C, Boussac A, Cassier-Chauvat C, Chauvat F. CGFS-type monothiol glutaredoxins from the cyanobacterium Synechocystis PCC6803 and other evolutionary distant model organisms possess a glutathione-ligated [2Fe-2S] cluster. Biochemistry 2007;46(51):15018–26.
[465] Iwema T, Picciocchi A, Traore DA, Ferrer JL, Chauvat F, Jacquamet L. Structural basis for delivery of the intact [Fe2S2] cluster by monothiol glutaredoxin. Biochemistry 2009;48(26):6041–3.
[466] Haunhorst P, Berndt C, Eitner S, Godoy JR, Lillig CH. Characterization of the human monothiol glutaredoxin 3 (PICOT) as iron-sulfur protein. Biochem Biophys Res Commun 2010;394(2):372–6.
[467] Li H, Mapolelo DT, Dingra NN, Naik SG, Lees NS, Hoffman BM, Riggs-Gelasco PJ, Huynh BH, Johnson MK, Outten CE. The yeast iron regulatory proteins Grx3/4 and Fra2 form heterodimeric complexes containing a [2Fe-2S] cluster with cysteinyl and histidyl ligation. Biochemistry 2009;48(40):9569–81.
[468] Kim KD, Chung WH, Kim HJ, Lee KC, Roe JH. Monothiol glutaredoxin Grx5 interacts with Fe-S scaffold proteins Isa1 and Isa2 and supports Fe-S assembly and DNA integrity in mitochondria of fission yeast. Biochem Biophys Res Commun 2010;392(3):467–72.
[469] Belli G, Molina MM, Garcia-Martinez J, Perez-Ortin JE, Herrero E. Saccharomyces cerevisiae glutaredoxin 5-deficient cells subjected to continuous oxidizing conditions are affected in the expression of specific sets of genes. J Biol Chem 2004;279(13):12386–95.
[470] Ye H, Jeong SY, Ghosh MC, Kovtunovych G, Silvestri L, Ortillo D, Uchida N, Tisdale J, Camaschella C, Rouault TA. Glutaredoxin 5 deficiency causes sideroblastic anemia by specifically impairing heme biosynthesis and depleting cytosolic iron in human erythroblasts. J Clin Invest 2010;120(5):1749–61.
[471] Rodriguez-Manzaneque MT, Ros J, Cabiscol E, Sorribas A, Herrero E. Grx5 glutaredoxin plays a central role in protection against protein oxidative damage in Saccharomyces cerevisiae. Mol Cell Biol 1999;19(12):8180–90.
[472] Linares GR, Xing W, Govoni KE, Chen ST, Mohan S. Glutaredoxin 5 regulates osteoblast apoptosis by protecting against oxidative stress. Bone 2009;44(5):795–804.
[473] Uzarska MA, Dutkiewicz R, Freibert SA, Lill R, Muhlenhoff U. The mitochondrial Hsp70 chaperone Ssq1 facilitates Fe/S cluster transfer from Isu1 to Grx5 by complex formation. Mol Biol Cell 2013;24(12):1830–41.
[474] Vilella F, Alves R, Rodriguez-Manzaneque MT, Belli G, Swaminathan S, Sunnerhagen P, Herrero E. Evolution and cellular function of monothiol glutaredoxins: involvement in iron-sulphur cluster assembly. Comp Funct Genomics 2004;5(4):328–41.

[475] Tong W-H, Rouault T. Distinct iron-sulfur cluster assembly complexes exist in the cytosol and mitochondria of human cells. EMBO J 2000;19(21):5692–700.
[476] Mochel F, Knight MA, Tong WH, Hernandez D, Ayyad K, Taivassalo T, Andersen PM, Singleton A, Rouault TA, Fischbeck KH, Haller RG. Splice mutation in the iron-sulfur cluster scaffold protein ISCU causes myopathy with exercise intolerance. Am J Hum Genet 2008;82(3):652–60.
[477] Racker E. History of the Pasteur effect and its pathobiology. Mol Cell Biochem 1974;5(1–2):17–23.
[478] Aisenberg AC, Potter VR. Studies on the Pasteur effect. II. Specific mechanisms. J Biol Chem 1957;224(2):1115–27.
[479] Aisenberg AC, Reinafarje B, Potter VR. Studies on the Pasteur effect. I General observations. J Biol Chem 1957;224(2):1099–113.
[480] Chan SY, Zhang YY, Hemann C, Mahoney CE, Zweier JL, Loscalzo J. MicroRNA-210 controls mitochondrial metabolism during hypoxia by repressing the iron-sulfur cluster assembly proteins ISCU1/2. Cell Metab 2009;10(4):273–84.
[481] Fasanaro P, Greco S, Lorenzi M, Pescatori M, Brioschi M, Kulshreshtha R, Banfi C, Stubbs A, Calin GA, Ivan M, Capogrossi MC, Martelli F. An integrated approach for experimental target identification of hypoxia-induced miR-210. J Biol Chem 2009;284(50):35134–43.
[482] Favaro E, Ramachandran A, McCormick R, Gee H, Blancher C, Crosby M, Devlin C, Blick C, Buffa F, Li JL, Vojnovic B, Pires das Neves R, Glazer P, Iborra F, Ivan M, Ragoussis J, Harris AL. MicroRNA-210 regulates mitochondrial free radical response to hypoxia and Krebs cycle in cancer cells by targeting iron sulfur cluster protein ISCU. PLoS One 2010;5(4):e10345.
[483] Chen Z, Li Y, Zhang H, Huang P, Luthra R. Hypoxia-regulated microRNA-210 modulates mitochondrial function and decreases ISCU and COX10 expression. Oncogene 2010;29(30):4362–8.
[484] Kulshreshtha R, Ferracin M, Wojcik SE, Garzon R, Alder H, Agosto-Perez FJ, Davuluri R, Liu CG, Croce CM, Negrini M, Calin GA, Ivan M. A microRNA signature of hypoxia. Mol Cell Biol 2007;27(5):1859–67.
[485] Camps C, Buffa FM, Colella S, Moore J, Sotiriou C, Sheldon H, Harris AL, Gleadle JM, Ragoussis J. hsa-miR-210 Is induced by hypoxia and is an independent prognostic factor in breast cancer. Clin Cancer Res 2008;14(5):1340–8.
[486] Lee DC, Romero R, Kim JS, Tarca AL, Montenegro D, Pineles BL, Kim E, Lee J, Kim SY, Draghici S, Mittal P, Kusanovic JP, Chaiworapongsa T, Hassan SS, Kim CJ. miR-210 targets iron-sulfur cluster scaffold homologue in human trophoblast cell lines: siderosis of interstitial trophoblasts as a novel pathology of preterm preeclampsia and small-for-gestational-age pregnancies. Am J Pathol 2011;179(2):590–602.
[487] Muralimanoharan S, Maloyan A, Mele J, Guo C, Myatt LG, Myatt L. MIR-210 modulates mitochondrial respiration in placenta with preeclampsia. Placenta 2012;33(10):816–23.
[488] Merlo A, de Quiros SB, Secades P, Zambrano I, Balbin M, Astudillo A, Scola B, Aristegui M, Suarez C, Chiara MD. Identification of a signaling axis HIF-1alpha/microRNA-210/ISCU independent of SDH mutation that defines a subgroup of head and neck paragangliomas. J Clin Endocrinol Metab 2012;97(11):E2194–200.
[489] McCormick RI, Blick C, Ragoussis J, Schoedel J, Mole DR, Young AC, Selby PJ, Banks RE, Harris AL. miR-210 is a target of hypoxia-inducible factors 1 and 2 in renal cancer, regulates ISCU and correlates with good prognosis. Br J Cancer 2013;108(5):1133–42.
[490] Huang X, Le QT, Giaccia AJ. MiR-210 – micromanager of the hypoxia pathway. Trends Mol Med 2010;16(5):230–7.
[491] Devlin C, Greco S, Martelli F, Ivan M. miR-210: More than a silent player in hypoxia. IUBMB Life 2011;63(2):94–100.

[492] Larsson LE, Linderholm H, Mueller R, Ringqvist T, Soernaes R. Hereditary metabolic myopathy with paroxysmal myoglobinuria due to abnormal glycolysis. J Neurol Neurosurg Psychiatry 1964;27:361–80.
[493] Linderholm H, Muller R, Ringqvist T, Sornas R. Hereditary abnormal muscle metabolism with hyperkinetic circulation during exercise. Acta Med Scand 1969;185(3):153–66.
[494] Kollberg G, Melberg A, Holme E, Oldfors A. Transient restoration of succinate dehydrogenase activity after rhabdomyolysis in iron-sulphur cluster deficiency myopathy. Neuromuscul Disord 2011;21(2):115–20.
[495] Drugge U, Holmberg M, Holmgren G, Almay BG, Linderholm H. Hereditary myopathy with lactic acidosis, succinate dehydrogenase and aconitase deficiency in northern Sweden: a genealogical study. J Med Genet 1995;32(5):344–7.
[496] Linderholm H, Essen-Gustavsson B, Thornell LE. Low succinate dehydrogenase (SDH) activity in a patient with a hereditary myopathy with paroxysmal myoglobinuria. J Intern Med 1990;228(1):43–52.
[497] Haller RG, Henriksson KG, Jorfeldt L, Hultman E, Wibom R, Sahlin K, Areskog NH, Gunder M, Ayyad K, Blomqvist CG, et al. Deficiency of skeletal muscle succinate dehydrogenase and aconitase. Pathophysiology of exercise in a novel human muscle oxidative defect. J Clin Invest 1991;88(4):1197–206.
[498] Olsson A, Lind L, Thornell LE, Holmberg M. Myopathy with lactic acidosis is linked to chromosome 12q23.3-24.11 and caused by an intron mutation in the ISCU gene resulting in a splicing defect. Hum Mol Genet 2008;17(11):1666–72.
[499] Crooks DR, Jeong SY, Tong WH, Ghosh MC, Olivierre H, Haller RG, Rouault TA. Tissue specificity of a human mitochondrial disease: differentiation-enhanced mis-splicing of the Fe-S scaffold gene ISCU renders patient cells more sensitive to oxidative stress in ISCU myopathy. J Biol Chem 2012;287(48):40119–30.
[500] Crooks DR, Natarajan TG, Jeong SY, Chen C, Park SY, Huang H, Ghosh MC, Tong WH, Haller RG, Wu C, Rouault TA. Elevated FGF21 secretion, PGC-1alpha and ketogenic enzyme expression are hallmarks of iron-sulfur cluster depletion in human skeletal muscle. Hum Mol Genet 2013.
[501] Reitman ML. FGF21: a missing link in the biology of fasting. Cell Metab 2007;5(6):405–7.
[502] Kollberg G, Tulinius M, Melberg A, Darin N, Andersen O, Holmgren D, Oldfors A, Holme E. Clinical manifestation and a new ISCU mutation in iron-sulphur cluster deficiency myopathy. Brain 2009;132(Pt 8):2170–9.
[503] Saha PP, Kumar SK, Srivastava S, Sinha D, Pareek G, D'Silva P. The presence of multiple cellular defects associated with a novel G50E iron-sulfur cluster scaffold protein (ISCU) mutation leads to development of mitochondrial myopathy. J Biol Chem 2014;289(15):10359–77.
[504] Sanaker PS, Toompuu M, Hogan VE, He L, Tzoulis C, Chrzanowska-Lightowlers ZM, Taylor RW, Bindoff LA. Differences in RNA processing underlie the tissue specific phenotype of ISCU myopathy. Biochim Biophys Acta 2010;1802(6):539–44.
[505] Nordin A, Larsson E, Holmberg M. The defective splicing caused by the ISCU intron mutation in patients with myopathy with lactic acidosis is repressed by PTBP1 but can be derepressed by IGF2BP1. Hum Mutat 2012;33(3):467–70.
[506] Skladal D, Halliday J, Thorburn DR. Minimum birth prevalence of mitochondrial respiratory chain disorders in children. Brain 2003;126(Pt 8):1905–12.
[507] Distelmaier F, Koopman WJ, van den Heuvel LP, Rodenburg RJ, Mayatepek E, Willems PH, Smeitink JA. Mitochondrial complex I deficiency: from organelle dysfunction to clinical disease. Brain 2009;132(Pt 4):833–42.
[508] Lazarou M, Thorburn DR, Ryan MT, McKenzie M. Assembly of mitochondrial complex I and defects in disease. Biochim Biophys Acta 2009;1793(1):78–88.
[509] Calvo SE, Tucker EJ, Compton AG, Kirby DM, Crawford G, Burtt NP, Rivas M, Guiducci C, Bruno DL, Goldberger OA. Redman MC, Wiltshire E, Wilson CJ, Altshuler D, Gabriel SB, Daly MJ, Thorburn DR,

Mootha VK. High-throughput, pooled sequencing identifies mutations in NUBPL and FOXRED1 in human complex I deficiency. Nat Genet 2010;42(10):851–8.
[510] Tucker EJ, Mimaki M, Compton AG, McKenzie M, Ryan MT, Thorburn DR. Next-generation sequencing in molecular diagnosis: NUBPL mutations highlight the challenges of variant detection and interpretation. Hum Mutat 2012;33(2):411–8.
[511] Tenisch EV, Lebre AS, Grevent D, de Lonlay P, Rio M, Zilbovicius M, Funalot B, Desguerre I, Brunelle F, Rotig A, Munnich A, Boddaert N. Massive and exclusive pontocerebellar damage in mitochondrial disease and NUBPL mutations. Neurology 2012;79(4):391.
[512] Kevelam SH, Rodenburg RJ, Wolf NI, Ferreira P, Lunsing RJ, Nijtmans LG, Mitchell A, Arroyo HA, Rating D, Vanderver A, van Berkel CG, Abbink TE, Heutink P, van der Knaap MS. NUBPL mutations in patients with complex I deficiency and a distinct MRI pattern. Neurology 2013;80(17):1577–83.
[513] Wydro MM, Balk J. Insights into the pathogenic character of a common NUBPL branch-site mutation associated with mitochondrial disease and complex I deficiency using a yeast model. Dis Model Mech 2013.
[514] Sazanov LA, Hinchliffe P. Structure of the hydrophilic domain of respiratory complex I from Thermus thermophilus. Science 2006;311(5766):1430–6.
[515] Bych K, Netz DJ, Vigani G, Bill E, Lill R, Pierik AJ, Balk J. The essential cytosolic iron-sulfur protein Nbp35 acts without Cfd1 partner in the green lineage. J Biol Chem 2008;283(51):35797–804.
[516] Seyda A, Newbold RF, Hudson TJ, Verner A, MacKay N, Winter S, Feigenbaum A, Malaney S, Gonzalez-Halphen D, Cuthbert AP, Robinson BH. A novel syndrome affecting multiple mitochondrial functions, located by microcell-mediated transfer to chromosome 2p14-2p13. Am J Hum Genet 2001;68(2):386–96.
[517] Cameron JM, Janer A, Levandovskiy V, Mackay N, Rouault TA, Tong WH, Ogilvie I, Shoubridge EA, Robinson BH. Mutations in iron-sulfur cluster scaffold genes nfu1 and bola3 cause a fatal deficiency of multiple respiratory chain and 2-oxoacid dehydrogenase enzymes. Am J Hum Genet 2011;89(4):486–95.
[518] Schonauer MS, Kastaniotis AJ, Kursu VA, Hiltunen JK, Dieckmann CL. Lipoic acid synthesis and attachment in yeast mitochondria. J Biol Chem 2009;284(35):23234–42.
[519] Ferrer-Cortes X, Font A, Bujan N, Navarro-Sastre A, Matalonga L, Arranz JA, Riudor E, Del Toro M, Garcia-Cazorla A, Campistol J, Briones P, Ribes A, Tort F. Protein expression profiles in patients carrying NFU1 mutations. Contribution to the pathophysiology of the disease. J Inherit Metab Dis 2012.
[520] Invernizzi F, Ardissone A, Lamantea E, Garavaglia B, Zeviani M, Farina L, Ghezzi D, Moroni I. Cavitating leukoencephalopathy with multiple mitochondrial dysfunction syndrome and NFU1 mutations. Front Genet 2014;5:412.
[521] Nizon M, Boutron A, Boddaert N, Slama A, Delpech H, Sardet C, Brassier A, Habarou F, Delahodde A, Correia I, Ottolenghi C, de Lonlay P. Leukoencephalopathy with cysts and hyperglycinemia may result from NFU1 deficiency. Mitochondrion 2014;15:59–64.
[522] Ahting U, Mayr JA, Vanlander AV, Hardy SA, Santra S, Makowski C, Alston CL, Zimmermann FA, Abela L, Plecko B, Rohrbach M, Spranger S, Seneca S, Rolinski B, Hagendorff A, Hempel M, Sperl W, Meitinger T, Smet J, Taylor RW, Van Coster R, Freisinger P, Prokisch H, Haack TB. Clinical, biochemical, and genetic spectrum of seven patients with NFU1 deficiency. Front Genet 2015;6:123.
[523] Cicchillo RM, Lee KH, Baleanu-Gogonea C, Nesbitt NM, Krebs C, Booker SJ. *Escherichia coli* lipoyl synthase binds two distinct [4Fe-4S] clusters per polypeptide. Biochemistry 2004;43(37):11770–81.
[524] Dos Santos PC, Smith AD, Frazzon J, Cash VL, Johnson MK, Dean DR. Iron-sulfur cluster assembly: NifU-directed activation of the nitrogenase Fe protein. J Biol Chem 2004;279(19):19705–11.

[525] Yabe T, Morimoto K, Kikuchi S, Nishio K, Terashima I, Nakai M. The Arabidopsis chloroplastic NifU-like protein CnfU, which can act as an iron-sulfur cluster scaffold protein, is required for biogenesis of ferredoxin and photosystem I. Plant Cell 2004;16(4):993–1007.
[526] Touraine B, Boutin JP, Marion-Poll A, Briat JF, Peltier G, Lobreaux S. Nfu2: a scaffold protein required for [4Fe-4S] and ferredoxin iron-sulphur cluster assembly in Arabidopsis chloroplasts. Plant J 2004;40(1):101–11.
[527] Balasubramanian R, Shen G, Bryant DA, Golbeck JH. Regulatory roles for IscA and SufA in iron homeostasis and redox stress responses in the cyanobacterium Synechococcus sp. strain PCC 7002. J Bacteriol 2006;188(9):3182–91.
[528] Leon S, Touraine B, Ribot C, Briat JF, Lobreaux S. Iron-sulphur cluster assembly in plants: distinct NFU proteins in mitochondria and plastids from Arabidopsis thaliana. Biochem J 2003;371:823–30.
[529] Liu Y, Cowan JA. Iron sulfur cluster biosynthesis. Human NFU mediates sulfide delivery to ISU in the final step of [2Fe-2S] cluster assembly. Chem Commun (Camb), 2007(30):3192–4.
[530] Haack TB, Rolinski B, Haberberger B, Zimmermann F, Schum J, Strecker V, Graf E, Athing U, Hoppen T, Wittig I, Sperl W, Freisinger P, Mayr JA, Strom TM, Meitinger T, Prokisch H. Homozygous missense mutation in BOLA3 causes multiple mitochondrial dysfunctions syndrome in two siblings. J Inherit Metab Dis 2013;36(1):55–62.
[531] Huynen MA, Spronk CA, Gabaldon T, Snel B. Combining data from genomes, Y2H and 3D structure indicates that BolA is a reductase interacting with a glutaredoxin. FEBS Lett 2005;579(3):591–6.
[532] Kumanovics A, Chen OS, Li L, Bagley D, Adkins EM, Lin H, Dingra NN, Outten CE, Keller G, Winge D, Ward DM, Kaplan J. Identification of FRA1 and FRA2 as genes involved in regulating the yeast iron regulon in response to decreased mitochondrial iron-sulfur cluster synthesis. J Biol Chem 2008;283(16):10276–86.
[533] Haunhorst P, Hanschmann EM, Brautigam L, Stehling O, Hoffmann B, Muhlenhoff U, Lill R, Berndt C, Lillig CH. Crucial function of vertebrate glutaredoxin 3 (PICOT) in iron homeostasis and hemoglobin maturation. Mol Biol Cell 2013;24(12):1895–903.
[534] Li H, Mapolelo DT, Dingra NN, Keller G, Riggs-Gelasco PJ, Winge DR, Johnson MK, Outten CE. Histidine 103 in Fra2 is an iron-sulfur cluster ligand in the [2Fe-2S] Fra2-Grx3 complex and is required for in vivo iron signaling in yeast. J Biol Chem 2011;286(1):867–76.
[535] Banci L, Camponeschi F, Ciofi-Baffoni S, Muzzioli R. Elucidating the molecular function of human BOLA2 in GRX3-dependent anamorsin maturation pathway. J Am Chem Soc 2015;137(51):16133–43.
[536] Banci L, Ciofi-Baffoni S, Gajda K, Muzzioli R, Peruzzini R, Winkelmann J. N-terminal domains mediate [2Fe-2S] cluster transfer from glutaredoxin-3 to anamorsin. Nat Chem Biol 2015;11(10):772–8.
[537] Frey AG, Palenchar DJ, Wildemann JD, Philpott CC. A Glutaredoxin-BolA complex serves as an iron-sulfur cluster chaperone for the cytosolic cluster assembly machinery. J Biol Chem 2016.
[538] Uzarska MA, Nasta V, Weiler BD, Spantgar F, Ciofi-Baffoni S, Saviello MR, Gonnelli L, Muhlenhoff U, Banci L, Lill R. Mitochondrial Bol1 and Bol3 function as assembly factors for specific iron-sulfur proteins. Elife 2016;5.
[539] Melber A, Na U, Vashisht A, Weiler BD, Lill R, Wohlschlegel JA, Winge DR. Role of Nfu1 and Bol3 in iron-sulfur cluster transfer to mitochondrial clients. Elife 2016;5.
[540] Waller JC, Alvarez S, Naponelli V, Lara-Nunez A, Blaby IK, Da Silva V, Ziemak MJ, Vickers TJ, Beverley SM, Edison AS, Rocca JR, Gregory JF, 3rd, de Crecy-Lagard V, Hanson AD. A role for tetrahydrofolates in the metabolism of iron-sulfur clusters in all domains of life. Proc Natl Acad Sci USA 2010;107(23):10412–7.

[541] Sheftel AD, Wilbrecht C, Stehling O, Niggemeyer B, Elsasser HP, Muhlenhoff U, Lill R. The human mitochondrial ISCA1, ISCA2, and IBA57 proteins are required for [4Fe-4S] protein maturation. Mol. Cell Biol 2012;23(7):1157–66.
[542] Hu P, Janga SC, Babu M, Diaz-Mejia JJ, Butland G, Yang W, Pogoutse O, Guo X, Phanse S, Wong P, Chandran S, Christopoulos C, Nazarians-Armavil A, Nasseri NK, Musso G, Ali M, Nazemof N, Eroukova V, Golshani A, Paccanaro A, Greenblatt JF, Moreno-Hagelsieb G, Emili A. Global functional atlas of Escherichia coli encompassing previously uncharacterized proteins. PLoS Biol 2009;7(4):e96.
[543] Ajit Bolar N, Vanlander AV, Wilbrecht C, Van der Aa N, Smet J, De Paepe B, Vandeweyer G, Kooy F, Eyskens F, De Latter E, Delanghe G, Govaert P, Leroy JG, Loeys B, Lill R, Van Laer L, Van Coster R. Mutation of the iron-sulfur cluster assembly gene IBA57 causes severe myopathy and encephalopathy. Hum Mol Genet 2013;22(13):2590–602.
[544] Debray FG, Stumpfig C, Vanlander AV, Dideberg V, Josse C, Caberg JH, Boemer F, Bours V, Stevens R, Seneca S, Smet J, Lill R, van Coster, R. Mutation of the iron-sulfur cluster assembly gene IBA57 causes fatal infantile leukodystrophy. J Inherit Metab Dis 2015;38(6):1147–53.
[545] Shan Y, Napoli E, Cortopassi G. Mitochondrial frataxin interacts with ISD11 of the NFS1/ISCU complex and multiple mitochondrial chaperones. Hum Mol Genet 2007;16(8):929–41.
[546] Marquet A. Enzymology of carbon-sulfur bond formation. Curr Opin Chem Biol 2001;5(5):541–9.
[547] Mueller EG. Trafficking in persulfides: delivering sulfur in biosynthetic pathways. Nat Chem Biol 2006;2(4):185–94.
[548] Marelja Z, Stocklein W, Nimtz M, Leimkuhler S. A novel role for human Nfs1 in the cytoplasm: Nfs1 acts as a sulfur donor for MOCS3, a protein involved in molybdenum cofactor biosynthesis. J Biol Chem 2008;283(37):25178–85.
[549] Lim SC, Friemel M, Marum JE, Tucker EJ, Bruno DL, Riley LG, Christodoulou J, Kirk EP, Boneh A, Degennaro C, Springer M, Mootha VK, Rouault TA, Leimkuhler S, Thorburn DR, Compton AG. Mutations in LYRM4, encoding iron-sulfur cluster biogenesis factor ISD11, cause deficiency of multiple respiratory chain complexes. Hum Mol Genet 2013.
[550] Pandey A, Pain J, Ghosh AK, Dancis A, Pain D. Fe-S cluster biogenesis in isolated mammalian mitochondria: coordinated use of persulfide sulfur and iron and requirements for GTP, NADH, and ATP. J Biol Chem 2015;290(1):640–57.
[551] Shigi N. Biosynthesis and functions of sulfur modifications in tRNA. Front Genet 2014;5:67.
[552] Farhan SM, Wang J, Robinson JF, Lahiry P, Siu VM, Prasad C, Kronick JB, Ramsay DA, Rupar CA, Hegele RA. Exome sequencing identifies NFS1 deficiency in a novel Fe-S cluster disease, infantile mitochondrial complex II/III deficiency. Mol Genet Genomic Med 2014;2(1):73–80.
[553] Flachbartova Z, Kovacech B. Mortalin – a multipotent chaperone regulating cellular processes ranging from viral infection to neurodegeneration. Acta Virol 2013;57(1):3–15.
[554] Radons J. The human HSP70 family of chaperones: where do we stand? Cell Stress Chaperones 2016;21(3):379–404.
[555] Royer-Bertrand B, Castillo-Taucher S, Moreno-Salinas R, Cho TJ, Chae JH, Choi M, Kim OH, Dikoglu E, Campos-Xavier B, Girardi E, Superti-Furga G, Bonafe L, Rivolta C, Unger S, Superti-Furga A. Mutations in the heat-shock protein A9 (HSPA9) gene cause the EVEN-PLUS syndrome of congenital malformations and skeletal dysplasia. Sci Rep 2015;5:17154.
[556] Schmitz-Abe K, Ciesielski SJ, Schmidt PJ, Campagna DR, Rahimov F, Schilke BA, Cuijpers M, Rieneck K, Lausen B, Linenberger ML, Sendamarai AK, Guo C, Hofmann I, Newburger PE, Matthews D, Shimamura A, Snijders PJ, Towne MC, Niemeyer CM, Watson HG, Dziegiel MH, Heeney MM, May A, Bottomley SS, Swinkels DW, Markianos K, Craig EA, Fleming MD. Congenital sideroblastic anemia due to mutations in the mitochondrial HSP70 homologue HSPA9. Blood 2015;126(25):2734–8.

[557] Craven SE, French D, Ye W, de Sauvage F, Rosenthal A. Loss of Hspa9b in zebrafish recapitulates the ineffective hematopoiesis of the myelodysplastic syndrome. Blood 2005;105(9):3528–34.
[558] Chen TH, Kambal A, Krysiak K, Walshauser MA, Raju G, Tibbitts JF, Walter MJ. Knockdown of Hspa9, a del(5q31.2) gene, results in a decrease in hematopoietic progenitors in mice. Blood 2011;117(5):1530–9.
[559] Shan Y, Cortopassi, G. Mitochondrial Hspa9/Mortalin regulates erythroid differentiation via iron-sulfur cluster assembly. Mitochondrion 2016;26:94–103.
[560] Gangat N, Patnaik MM, Tefferi A. Myelodysplastic syndromes: Contemporary review and how we treat. Am J Hematol 2016;91(1):76–89.
[561] Horrigan SK, Arbieva ZH, Xie HY, Kravarusic J, Fulton NC, Naik H, Le TT, Westbrook CA. Delineation of a minimal interval and identification of 9 candidates for a tumor suppressor gene in malignant myeloid disorders on 5q31. Blood 2000;95(7):2372–7.
[562] Li J, Kogan M, Knight SAB, Pain D, Dancis A. Yeast mitochondrial protein, Nfs1p, coordinately regulates iron-sulfur cluster proteins, cellular iron uptake, and iron distribution. J Biol Chem 1999;274(46):33025–34.
[563] Jensen LT, Culotta VC. Role of Saccharomyces cerevisiae ISA1 and ISA2 in iron homeostasis. Mol Cell Biol 2000;20(11):3918–27.
[564] Lange H, Kaut A, Kispal G, Lill R. A mitochondrial ferredoxin is essential for biogenesis of cellular iron-sulfur proteins. Proc Natl Acad Sci USA 2000;97(3):1050–5.
[565] Foury F, Roganti T. Deletion of the mitochondrial carrier genes MRS3 and MRS4 suppresses mitochondrial iron accumulation in a yeast frataxin-deficient strain. J Biol Chem 2002;277(27):24475–83.
[566] Muhlenhoff U, Stadler JA, Richhardt N, Seubert A, Eickhorst T, Schweyen RJ, Lill R, Wiesenberger G. A specific role of the yeast mitochondrial carriers MRS3/4p in mitochondrial iron acquisition under iron-limiting conditions. J Biol Chem 2003;278(42):40612–20.
[567] Zhang Y, Lyver ER, Knight SA, Lesuisse E, Dancis A. Frataxin and mitochondrial carrier proteins, Mrs3p and Mrs4p, cooperate in providing iron for heme synthesis. J Biol Chem 2005;280(20):19794–807.
[568] Wang Y, Langer NB, Shaw GC, Yang G, Li L, Kaplan J, Paw BH, Bloomer JR, Abnormal mitoferrin-1 expression in patients with erythropoietic protoporphyria. Exp Hematol 2011;39(7):784–94.
[569] Foury F, Talibi D. Mitochondrial control of iron homeostasis. A genome wide analysis of gene expression in a yeast frataxin-deficient strain. J Biol Chem 2001;276(11):7762–8.
[570] Hausmann A, Samans B, Lill R, Muhlenhoff U. Cellular and mitochondrial remodeling upon defects in iron-sulfur protein biogenesis. J Biol Chem 2008;283(13):8318–30.
[571] Anderson PR, Kirby K, Orr WC, Hilliker AJ, Phillips JP. Hydrogen peroxide scavenging rescues frataxin deficiency in a Drosophila model of Friedreich's ataxia. Proc Natl Acad Sci USA 2008;105(2):611–6.
[572] Naranuntarat A, Jensen LT, Pazicni S, Penner-Hahn JE, Culotta VC. The interaction of mitochondrial iron with manganese superoxide dismutase. J Biol Chem 2009;284(34):22633–40.
[573] Pandolfo M. Friedreich ataxia: the clinical picture. J Neurol 2009;256 Suppl 1:3–8.
[574] Sturm B, Stupphann D, Kaun C, Boesch S, Schranzhofer M, Wojta J, Goldenberg H, Scheiber-Mojdehkar B. Recombinant human erythropoietin: effects on frataxin expression in vitro. Eur J Clin Invest 2005;35(11):711–7.
[575] Acquaviva F, Castaldo I, Filla A, Giacchetti M, Marmolino D, Monticelli A, Pinelli M, Sacca F, Cocozza S. Recombinant human erythropoietin increases frataxin protein expression without increasing mRNA expression. Cerebellum 2008;7(3):360–5.
[576] Nachbauer W, Hering S, Seifert M, Steinkellner H, Sturm B, Scheiber-Mojdehkar B, Reindl M, Strasak A, Poewe W, Weiss G, Boesch S. Effects of erythropoietin on frataxin levels and mitochondrial function in Friedreich ataxia – a dose-response trial. Cerebellum 2011;10(4):763–9.

[577] Herman D, Jenssen K, Burnett R, Soragni E, Perlman SL, Gottesfeld JM. Histone deacetylase inhibitors reverse gene silencing in Friedreich's ataxia. Nat Chem Biol 2006;2(10):551–8.
[578] Codazzi F, Hu A, Rai M, Salerno Scarzella F, Mangiameli E, Pelizzoni I, Grohovaz F, Pandolfo M. Friedreich ataxia induced pluripotent stem cell-derived neurons show a cellular phenotype that is corrected by a benzamide HDAC inhibitor. Hum Mol Genet 2016.
[579] Soragni E, Miao W, Iudicello M, Jacoby D, De Mercanti S, Clerico M, Longo F, Piga A, Ku S, Campau E, Du J, Penalver P, Rai M, Madara JC, Nazor K, O'Connor M, Maximov A, Loring JF, Pandolfo M, Durelli L, Gottesfeld JM, Rusche JR. Epigenetic therapy for Friedreich ataxia. Ann Neurol 2014;76(4):489–508.
[580] Evans-Galea MV, Pebay A, Dottori M, Corben LA, Ong SH, Lockhart PJ, Delatycki MB. Cell and gene therapy for Friedreich ataxia: progress to date. Hum Gene Ther 2014;25(8):684–93.
[581] Perdomini M, Belbellaa B, Monassier L, Reutenauer L, Messaddeq N, Cartier N, Crystal RG, Aubourg P, Puccio H. Prevention and reversal of severe mitochondrial cardiomyopathy by gene therapy in a mouse model of Friedreich's ataxia. Nat Med 2014;20(5):542–7.
[582] Tomassini B, Arcuri G, Fortuni S, Sandi C, Ezzatizadeh V, Casali C, Condo I, Malisan F, Al-Mahdawi S, Pook M, Testi R. Interferon gamma upregulates frataxin and corrects the functional deficits in a Friedreich ataxia model. Hum Mol Genet 2012;21(13):2855–61.
[583] Corey DR. Synthetic nucleic acids and treatment of neurological diseases. JAMA Neurol 2016.
[584] Li L, Matsui M, Corey DR. Activating frataxin expression by repeat-targeted nucleic acids. Nat Commun 2016;7:10606.
[585] Kollberg G, Holme E. Antisense oligonucleotide therapeutics for iron-sulphur cluster deficiency myopathy. Neuromuscul Disord 2009;19(12):833–6.
[586] Holmes-Hampton GP, Crooks DR, Haller RG, Guo S, Freier SM, Monia BP, Rouault TA. Use of antisense oligonucleotides to correct the splicing error in ISCU myopathy patient cell lines. Hum Mol Genet 2016. E. published Oct.
[587] Richardson TE, Kelly HN, Yu AE, Simpkins JW. Therapeutic strategies in Friedreich's ataxia. Brain Res 2013;1514:91–7.
[588] Kearney M, Orrell RW, Fahey M, Brassington R, Pandolfo M. Pharmacological treatments for Friedreich ataxia. Cochrane Database Syst Rev 2016(8):CD007791.
[589] Qi X, Lewin AS, Sun L, Hauswirth WW, Guy J. SOD2 gene transfer protects against optic neuropathy induced by deficiency of complex I Ann. Neurol 2004;56(2):182–91.
[590] Emond M, Lepage G, Vanasse M, Pandolfo M. Increased levels of plasma malondialdehyde in Friedreich ataxia. Neurology 2000;55(11):1752–3.
[591] Jauslin ML, Wirth T, Meier T, Schoumacher F. A cellular model for Friedreich Ataxia reveals small-molecule glutathione peroxidase mimetics as novel treatment strategy. Hum Mol Genet 2002;11(24):3055–63.
[592] Seznec H, Simon D, Monassier L, Criqui-Filipe P, Gansmuller A, Rustin P, Koenig M, Puccio H. Idebenone delays the onset of cardiac functional alteration without correction of Fe-S enzymes deficit in a mouse model for Friedreich ataxia. Hum Mol Genet 2004;13(10):1017–24.
[593] Kakhlon O, Breuer W, Munnich A, Cabantchik ZI. Iron redistribution as a therapeutic strategy for treating diseases of localized iron accumulation. Can J Physiol Pharmacol 2010;88(3):187–96.
[594] Boddaert N, Le Quan Sang KH, Rotig A, Leroy-Willig A, Gallet S, Brunelle F, Sidi D, Thalabard JC, Munnich A, Cabantchik ZI. Selective iron chelation in Friedreich ataxia: biologic and clinical implications. Blood 2007;110(1):401–8.
[595] Kakhlon O, Manning H, Breuer W, Melamed-Book N, Lu C, Cortopassi G, Munnich A, Cabantchik ZI. Cell functions impaired by frataxin deficiency are restored by drug-mediated iron relocation. Blood 2008;112(13):5219–27.
[596] Goncalves S, Paupe V, Dassa EP, Rustin P. Deferiprone targets aconitase: implication for Friedreich's ataxia treatment. BMC Neurol 2008;8:20.

[597] Pandolfo M, Arpa J, Delatycki MB, Le Quan Sang KH, Mariotti C, Munnich A, Sanz-Gallego I, Tai G, Tarnopolsky MA, Taroni F, Spino M, Tricta F. Deferiprone in Friedreich ataxia: a 6-month randomized controlled trial. Ann Neurol 2014;76(4):509–21.
[598] Olsen RK, Olpin SE, Andresen BS, Miedzybrodzka ZH, Pourfarzam M, Merinero B, Frerman FE, Beresford MW, Dean JC, Cornelius N, Andersen O, Oldfors A, Holme E, Gregersen N, Turnbull DM, Morris AA. ETFDH mutations as a major cause of riboflavin-responsive multiple acyl-CoA dehydrogenation deficiency. Brain 2007;130(Pt 8):2045–54.
[599] Ghosh MC, Zhang DL, Jeong SY, Kovtunovych G, Ollivierre-Wilson H, Noguchi A, Tu T, Senecal T, Robinson G, Crooks DR, Tong WH, Ramaswamy K, Singh A, Graham BB, Tuder RM, Yu ZX, Eckhaus M, Lee J, Springer DA, Rouault TA. Deletion of iron regulatory protein 1 causes polycythemia and pulmonary hypertension in mice through translational derepression of HIF2alpha. Cell Metab 2013;17(2):271–81.
[600] Anderson SA, Nizzi CP, Chang YI, Deck KM, Schmidt PJ, Galy B, Damnernsawad A, Broman AT, Kendziorski C, Hentze MW, Fleming MD, Zhang J, Eisenstein RS. The IRP1-HIF-2alpha axis coordinates iron and oxygen sensing with erythropoiesis and iron absorption. Cell Metab 2013;17(2):282–90.
[601] Van Kuilenburg AB, Vreken P, Abeling NG, Bakker HD, Meinsma R, Van Lenthe H, De Abreu RA, Smeitink JA, Kayserili H, Apak MY, Christensen E, Holopainen I, Pulkki K, Riva D, Botteon G, Holme E, Tulinius M, Kleijer WJ, Beemer FA, Duran M, Niezen-Koning KE, Smit GP, Jakobs C, Smit LM, Van Gennip AH, et al. Genotype and phenotype in patients with dihydropyrimidine dehydrogenase deficiency. Hum Genet 1999;104(1):1–9.
[602] Ichida K, Amaya Y, Okamoto K, Nishino T. Mutations associated with functional disorder of xanthine oxidoreductase and hereditary xanthinuria in humans. Int J Mol Sci 2012;13(11):15475–95.
[603] Ballew BJ, Joseph V, De S, Sarek G, Vannier JB, Stracker T, Schrader KA, Small TN, O'Reilly R, Manschreck C, Harlan Fleischut MM, Zhang L, Sullivan J, Stratton K, Yeager M, Jacobs K, Giri N, Alter BP, Boland J, Burdett L, Offit K, Boulton SJ, Savage SA, Petrini JH. A recessive founder mutation in regulator of telomere elongation helicase 1, RTEL1, underlies severe immunodeficiency and features of Hoyeraal Hreidarsson syndrome. PLoS Genet 2013;9(8):e1003695.
[604] Deng Z, Glousker G, Molczan A, Fox AJ, Lamm N, Dheekollu J, Weizman OE, Schertzer M, Wang Z, Vladimirova O, Schug J, Aker M, Londono-Vallejo A, Kaestner KH, Lieberman PM, Tzfati Y. Inherited mutations in the helicase RTEL1 cause telomere dysfunction and Hoyeraal-Hreidarsson syndrome. Proc Natl Acad Sci USA 2013;110(36):E3408–16.
[605] Le Guen T, Jullien L, Touzot F, Schertzer M, Gaillard L, Perderiset M, Carpentier W, Nitschke P, Picard C, Couillault G, Soulier J, Fischer A, Callebaut I, Jabado N, Londono-Vallejo A, de Villartay JP, Revy P. Human RTEL1 deficiency causes Hoyeraal-Hreidarsson syndrome with short telomeres and genome instability. Hum Mol Genet 2013;22(16):3239–49.
[606] Spiegel R, Saada A, Halvardson J, Soiferman D, Shaag A, Edvardson S, Horovitz Y, Khayat M, Shalev SA, Feuk L, Elpeleg O. Deleterious mutation in FDX1L gene is associated with a novel mitochondrial muscle myopathy. Eur J Hum Genet 2014;22(7):902–6.
[607] Broughton BC, Steingrimsdottir H, Weber CA, Lehmann AR. Mutations in the xeroderma pigmentosum group D DNA repair/transcription gene in patients with trichothiodystrophy. Nat Genet 1994;7(2):189–94.
[608] Botta E, Nardo T, Broughton BC, Marinoni S, Lehmann AR, Stefanini M. Analysis of mutations in the XPD gene in Italian patients with trichothiodystrophy: site of mutation correlates with repair deficiency, but gene dosage appears to determine clinical severity. Am J Hum Genet 1998;63(4):1036–48.
[609] Cantor SB, Guillemette S. Hereditary breast cancer and the BRCA1-associated FANCJ/BACH1/BRIP1. Future Oncol 2011;7(2):253–61.

11 Friedreich ataxia

Simon A.B. Knight and Robert B. Wilson

Abstract: Friedreich ataxia (FRDA) is an autosomal recessive neurodegenerative and cardiodegenerative disorder caused by decreased expression and/or function of the protein frataxin. Frataxin is involved in iron-sulfur cluster (ISC) biogenesis. Decreased expression of frataxin is associated with decreased ISC biogenesis, mitochondrial iron accumulation, and increased oxidative stress, all of which contribute to mitochondrial dysfunction. Frataxin binds iron and may chaperone iron for ISC biogenesis in the mitochondrial matrix. Frataxin also interacts with multiple proteins in the ISC-biogenesis complex and regulates ISC biogenesis in part through the activation of the cysteine desulfurase. Because decreased frataxin affects cytosolic ISC biogenesis as well as mitochondrial ISC biogenesis, the pathogenesis of FRDA undoubtedly results from decreased activities of both mitochondrial and cytosolic ISC proteins.

11.1 Introduction

Friedreich ataxia (FRDA) is an autosomal recessive neurodegenerative and cardiodegenerative disorder, with a prevalence of approximately 1 in 40,000 in European populations. (Recent reviews include those by Koeppen and Mazurkiewicz [1], Collins [2], and Gomes and Santos [3].) FRDA is characterized by progressive ataxia of all four limbs, dysarthria, areflexia, sensory loss, and muscle fatigability. As first described by Nicholaus Friedreich in the mid-1800s, the neurological signs and symptoms are largely secondary to degeneration of the large sensory neurons of the dorsal root ganglia and spinocerebellar tracts. Skeletal deformities and cardiomyopathy are found in most patients, impaired glucose tolerance, and diabetes mellitus are found in ~30% of patients, and reduced visual acuity and hearing loss are occasionally seen [4]. Onset of symptoms usually occurs around puberty and most patients are confined to a wheelchair by their late 20s. Myocardial failure and/or arrhythmias are the most common cause of premature death. Currently, there are no approved drugs to treat FRDA and the resultant disability, prolong the life of an FRDA patient, or cure the disorder.

DOI 10.1515/9783110479850-011

11.2 Clinical presentation and genetics

11.2.1 Signs and symptoms

Typical cases of FRDA include the clinical features enumerated by Harding [5]: (1) autosomal recessive inheritance, (2) onset before 25 years, (3) progressive limb and gait ataxia, (4) absent tendon reflexes in the legs, and (5) electrophysiologic evidence of axonal sensory neuropathy, followed within 5 years of onset by (6) dysarthria, (7) areflexia of all four limbs, (8) distal loss of position and vibration sense, (9) extensor plantar responses, and (10) pyramidal weakness of the legs. However, the clinical features of FRDA may be quite variable, even within the same sibship. This variability includes age of onset, rate of progression, and severity and extent of disease. In the context of an overall FRDA-like phenotype, atypical cases lack one or more of the Harding criteria: late-onset FRDA [6, 7], with onset after 25 years, and FRDA with retained reflexes [8], in which tendon reflexes in the legs are preserved, tend to cluster in families but may also occur in association with typical FRDA. The identification of the disease gene and its most common mutation, an expansion of an intronic GAA triplet repeat sequence, has allowed genotype-phenotype correlations to be made (see below).

11.2.2 Identification of the disease gene

Campuzano and colleagues identified the FRDA disease gene, *FXN (frataxin)*, on chromosome 9q13 [9]. Initial characterization of *FXN* revealed strong homologies with open reading frames in the lower eukaryotes *Caenorhabditis elegans (C. elegans)* and *Saccharomyces cerevisiae (S. cerevisiae)* [9]. Most individuals with FRDA (~97%) have expansions of a GAA repeat in the first intron of both FRDA alleles [9]. Normal alleles have 36 or fewer GAA repeats, while disease alleles have from approximately 100 to more than 1,700 repeats [10], although most commonly ~600–900 repeats. The GAA-repeat expansions transcriptionally silence *FXN* through heterochromatization, decreasing expression of the encoded protein, frataxin, to ~5%–30% of normal [11, 12]. The *FXN* allele with the smaller of the two GAA-repeat expansions expresses most of the residual frataxin; consistent with this, the size of the smaller expansion correlates inversely with age of onset and directly with rate of disease progression [4]. Individuals with FRDA have also been identified (~3%) who carry one allele with a trinucleotide repeat expansion and one allele with a point mutation [9, 13]; the clinical presentation of such individuals is often atypical [13]. A complete knockout of the murine frataxin gene causes embryonic lethality, indicating that at least some frataxin function is necessary for survival [14].

11.2.3 Mitochondrial dysfunction

Mitochondrial dysfunction had long been suspected of contributing to the pathophysiology of FRDA [15]. The known mitochondrial diseases and FRDA share a number of clinical manifestations, including ataxia, skeletal myopathy, cardiomyopathy, diabetes mellitus, and sensorineural hearing loss and optic neuropathy [4, 16]. Using phosphorus magnetic resonance spectroscopy, Lodi and colleagues found a decrease in the maximum rate of ATP production in skeletal muscle *in vivo* that correlated inversely with the size of the smaller GAA-repeat expansion [17]. The same group reported similar findings in cardiac muscle *in vivo* [18]. Using near-infrared spectroscopy, Lynch and colleagues found a prolonged deoxygenation recovery time in skeletal muscle *in vivo*, also consistent with mitochondrial dysfunction [19].

11.3 Iron metabolism and dysregulation

11.3.1 Mitochondrial iron accumulation

The connection between FRDA and iron metabolism was made in studies of the yeast frataxin homologue (Yfh1p). Both Yfh1p and frataxin localize to the mitochondrial matrix, at or near the inner mitochondrial membrane [20–23]. Frataxin can substitute for Yfh1p in yeast [24, 25], indicating that the two proteins are functional as well as structural homologues. Yeast lacking Yfh1p exhibit impaired mitochondrial respiration, sensitivity to oxidative stress, and decreased activities of mitochondrial iron-sulfur cluster (ISC) enzymes [22, 24, 26–28], indicating an important role in mitochondrial function. The myocardium of patients with FRDA exhibits decreased activities of mitochondrial ISC enzymes – including respiratory complexes I, II, and III – as well as impaired mitochondrial bioenergetics [18, 29, 30].

Perhaps the most striking observation is that yeast lacking Yfh1p constitutively up-regulate cellular iron uptake and accumulate mitochondrial iron to approximately 10 times the normal concentration [22], such that the iron deposits are readily visible in electron micrographs. Reexpression of Yfh1p in yeast lacking the protein reversed the mitochondrial iron accumulation over time [27]. Cardiomyocytes of individuals with FRDA exhibit stainable iron deposits [30, 31], and cells and tissues from individuals with FRDA accumulate mitochondrial iron [32–34]. However, serum iron and ferritin concentrations in individuals with FRDA are within normal limits, with means below the 50th percentile for each reference range, suggesting that, unlike hemochromatosis, FRDA is not a disease of total body iron overload [35]; rather, FRDA seems to include a component of intracellular iron maldistribution, with mitochondrial iron accumulation in the form of biologically unavailable ferric phosphate nanoparticles [36–38].

11.3.2 Oxidative stress

Ferrous iron can generate toxic reactive oxygen species by reducing hydrogen peroxide to the hydroxyl radical (the Fenton reaction) [39]. Consistent with the observation that iron accumulates in the mitochondria of individuals with FRDA, primary FRDA fibroblasts are sensitive to oxidative stress [33]. The evidence for oxidative stress in FRDA is the subject of a review by Armstrong and colleagues [40]. That there should be oxidative stress in FRDA, and that it might be difficult to measure directly, is unsurprising. A certain level of physiologic reactive oxygen species is present normally, which can obscure low-level signals from a relatively small number of affected disease cells and cells with extremes of oxidative stress often die by apoptosis. Having said this, although the differences from normal control individuals were small, Schulz *et al.* found increased urinary 8-hydroxy-2-deoxyguanosine (8-OHdG), a marker of oxidative DNA damage, in individuals with FRDA [41], and Emond *et al.* found increased plasma malondialdehyde, a marker of lipid peroxidation, in individuals with FRDA [42].

11.3.3 ISC biogenesis

Frataxin is involved in ISC biogenesis. In a database-driven study of 56 available genomes, Huynen and colleagues identified two genes, *hscA* and *hscB*, with identical phylogenetic distributions to *FXN*; both *hscA* and *hscB* encode chaperone proteins important for ISC biogenesis, which suggested a role for frataxin in this process [43]. Muhlenhoff and colleagues found that Yfh1p depletion decreased ISC biogenesis for mitochondrial and cytosolic ISC proteins *in vivo*, as well as *in vitro* using mitochondrial extracts [44]. Conversely, the import of pmol amounts of Yfh1p to intact mitochondria, isolated from yeast lacking *Yfh1*, restored biosynthesis of ISCs [45]. Collectively, these results indicate that Yfh1p is able to make mitochondrial iron available for ISCs and that mitochondrial iron accumulation is a secondary defect; in fact, mutation or depletion of any of the mitochondrial ISC biogenesis proteins is associated with mitochondrial iron accumulation. Using a conditional knockout approach, Puccio and colleagues generated striated-muscle frataxin-deficient mice and neuron/cardiac frataxin-deficient mice [46]; time-dependent mitochondrial iron accumulation occurred, but only after decreases in the activities of ISC enzymes were evident, again consistent with a primary role for Yfh1p and frataxin in ISC assembly.

Muhlenhoff and colleagues found that regulated Yfh1p depletion decreased ISC biogenesis on the scaffold protein Isu1p (Iron-sulfur cluster scaffold protein 1) [47], and several groups found that Yfh1p interacts directly with Isu1p [48–50], which suggested an important role for Yfh1p in this initial step. Gerber and colleagues found that Yfh1p also interacts directly with Nfs1p (Nitrogen fixation 1 homolog), the cysteine desulfurase that provides the sulfur for ISC biogenesis [48]. Biophysical experiments using recombinant mammalian proteins suggest that frataxin is part of a homodimeric complex, with each subunit consisting of Nfs1:Isd11 (Iron-sulfur

cluster desulferase interacting protein):Iscu (Iron-sulfur cluster scaffold protein U): Fxn with 1:2:1:1 stoichiometry [51, 52]. Higher-ordered complexes have also been proposed, consisting of as many as 24 copies of each protein; however, the physiological relevance of these structures awaits confirmation [53]. Although important for ISC biogenesis, Yfh1p is not absolutely required since yeast lacking Yfh1p completely are viable, whereas complete loss of ISC-biogenesis capability is generally lethal.

To distinguish primary from secondary consequences of frataxin depletion in human cells, Stehling and colleagues used RNAi in HeLa cells to regulate frataxin expression [54]; frataxin depletion decreased the activities of the ISC enzymes aconitase and succinate dehydrogenase, without affecting non-ISC enzyme activities, cellular iron uptake, cellular iron content, or mitochondrial iron accumulation, suggesting, as in yeast, a primary role in ISC biogenesis. Bulteau and colleagues found that frataxin interacted directly with aconitase in a citrate-dependent fashion and decreased aconitase inactivation by oxidative stress; the interaction protected the ISC of aconitase from disassembly – and thereby protected aconitase from irreversible inactivation and possibly degradation – and promoted enzyme reactivation [55, 56]. As noted above, Rotig *et al.* found that the myocardium of individuals with FRDA exhibited decreased activities of mitochondrial ISC enzymes, including respiratory complexes I, II, and III, and both cytosolic and mitochondrial aconitases [29].

11.3.4 Precise function of frataxin

There are two primary hypotheses for the precise function of frataxin in ISC biogenesis: (1) frataxin chaperones iron into the nascent ISC complex and (2) frataxin regulates the ISC-assembly complex. These two hypotheses are not mutually exclusive and there are data to support both. The structures of frataxin from humans, yeast (Yfh1p), and bacteria (CyaA) are highly conserved, with a platform of beta sheets, two parallel alpha helices in a separate plane, a hydrophobic core, and a negatively charged groove, between the alpha helices, comprising a patch of acidic residues from the beta sheet and one of the alpha helices [57–60]. Frataxin proteins bind iron *in vitro*, with numbers raging from two to six atoms of iron per frataxin molecule depending on species [49, 58, 61–66]; the affinity (Kd) is only in the low micromolar range and on the surface of the protein, *via* carboxylic amino acids, rather than *via* cysteines and histidines [67], as is more typical for iron-binding proteins. The low binding affinity of frataxin for iron tends to rule against the protein acting as a chaperone for iron in the manner that copper is delivered to recipient proteins by copper chaperone proteins, which have high affinity for copper [68]. However, Gerber and colleagues showed that the Yfh1p interaction with Isu1p and Nfs1p is iron dependent [48]; Yoon and Cowan showed that human frataxin can transfer iron to ISCU [49]; and Layer and colleagues showed that CyaY, the bacterial frataxin homolog, can provide iron for ISC biogenesis [69]. These data are all consistent with the hypothesis that frataxin is the iron donor for ISC biogenesis.

The other, not necessarily mutually exclusive, role for frataxin is as a regulator of ISC assembly. Mammalian frataxin interacts with a preformed complex of NFS1, ISCU, and ISD11 [51, 70], an interaction that increases cysteine desulfurase activity. Cysteine is the sole source of sulfur for ISCs. Using a two-step approach with recombinant yeast proteins and a 35S-Cys radiolabel, Pandey and colleagues demonstrated that Yfh1p specifically stimulated the binding of cysteine to Nfs1p by exposing the substrate binding site [71]. In contrast to this, Parent and colleagues used an engineered maleimide peptide to monitor the formation and reduction of the ISC intermediate persulfide on Nfs1p; these experiments revealed that rather than increase cysteine binding to Nfs1p, frataxin enhanced the transfer of the persulfide intermediate to the scaffold protein ICSU [72]. The mechanism may be a combination of the two: an acceleration of both the persulfide intermediate formation on Nfs1p and the transfer of the sulfur to ISCU [73].

Much of the pioneering work on ISC biosynthesis was performed in bacteria which possess the frataxin ortholog CyaY. Unfortunately, the bacterial system is unlikely to be of use in solving how eukaryotic frataxin stimulates Nfs1p activity, for in the bacteria CyaY *inhibits* IscS (cysteine desulfurase) activity [74–76]. Remarkably, this difference in the regulatory wiring of frataxin can be resolved by a single amino acid change in the scaffold protein (Isu1, eukaryotes; IscU, bacteria). Simply changing the methionine at position 141 in yeast Iscu1p to an isoleucine that is present in the bacterial ortholog at this position bypasses the requirement for Yfh1p. Conversely, changing the corresponding bacterial IscU isoleucine to a methionine removes the inhibitory function of bacterial CyaY on Fe-S cluster synthesis to a dependence [77, 78]. Together, these studies underscore the modulatory role that frataxin plays in ISC biosynthesis, a role that is evolutionarily conserved but wired according to an organism's need. Moving up the evolutionary ladder, Bridwell and colleagues and Tsai and colleagues studied disease-associated missense mutations in human frataxin and found mutations that primarily affected frataxin binding to the ISCU-NFS1-ISD11 complex, that primarily affected frataxin activation of NFS1, or that affected both; significantly, all of these mutations lead to a similar phenotype, mediated by decreased ISC biogenesis [79, 80].

11.3.5 Cellular consequences of frataxin deficiency

FRDA is a progressive disorder. As first demonstrated in mice bearing heart- and liver-restricted deletions of frataxin, the initial defect is in the synthesis of ISCs [46, 81]. This is followed by altered cellular iron metabolism, mitochondrial dysfunction, and eventually mitochondrial iron accumulation [81]. The key regulators of cellular iron metabolism in mammalian cells are IRP1 and IRP2 (Iron regulatory proteins 1 and 2). Knockout studies in mice have shown that IRP1 and IRP2 have both specific and overlapping functions in maintaining cellular iron homeostasis [82, 83]. IRP1 and IRP2 regulate iron-uptake (transferrin receptor [TFR], ferroportin) and iron-storage genes (ferritin) posttranscriptionally by binding to iron responsive elements (IREs) present in these genes. Under normal conditions, IRP1 exists as a cytosolic aconitase, but

in conditions of low cellular iron, the ISC cofactor is lost, allowing the apo-IRP1 to bind the 3′ UTR IRE of TFR and 5′ UTR of ferritin mRNA to increase iron transport and decrease iron storage, respectively. Deletion of frataxin also activates IRP1. HeLa cells depleted of frataxin by siRNA knockdown exhibited increased binding of IRP1 to the ferritin IRE in RNA electrophoretic mobility shift assays [54]. Similar results were obtained using primary human FRDA fibroblasts [36] and cardiomyocytes from conditional knockout mice [84]. Despite the activation of IRE binding by murine IRP1, the conditional-knockout-mice cardiomyocytes, which lacked murine frataxin completely, exhibited normal expression of ferritin subunits and the TFR early in the disease process and exhibited increased ferritin-light-chain expression and decreased transferrin-receptor expression later in the disease process, presumably in response to the trend toward mitochondrial iron accumulation [84]. These results suggested that IRP1 was partially if not completely dispensable for the regulation of ferritin and the TFR, which was consistent with the finding that IRP2, and not IRP1, is the contributor to iron regulation in normal murine physiology [85]. However lack of frataxin is not a normal condition, and Martelli and colleagues therefore constructed a double knock-out mouse completely lacking IRP1 and with a liver-specific deletion of frataxin [86]. Despite the role of IRP1 in triggering an increase in cellular iron (that could potentially exacerbate mitochondrial iron accumulation), deletion of IRP1 in the context of a lack of frataxin proved to be deleterious. Analysis of mitochondrial function, and ISC and heme biosysnthesis, indicated that IRP1 was important in maintaining mitochondrial iron supply for these processes. As the authors pointed out, this questions the concept of withholding iron from FRDA cells as a beneficial practice [86].

Cytosolic ISC biogenesis, which exists in mammalian cells but not in yeast, requires both mitochondrial and cytosolic machineries [87, 88]. Cytosolic isoforms of the core components (NFS1, ISD11, and ISCU), as well as other proteins involved in the process, have been identified [89]. However, a mitochondrially derived sulfur/iron intermediate is also required that is exported by the ABC transporter ABCB7 [90, 91]. The nature of this compound is not known, although a glutathione coordinated 2Fe-2S complex has been proposed [92]. There is some evidence for the existence of extra-mitochondrially located frataxin that might interact directly with cytoplasmic aconitase/IRP1 [93–95], but this awaits confirmation. What is clear is that the number of identified mitochondrial and extramitochondrial ISC-dependent proteins has increased [96] and that the pathogenesis of FRDA undoubtedly results from the decreased activities of many of these.

11.4 Summary

Underlying the neurodegenerative and cardiodegenerative disorder FRDA is decreased expression and/or function of the protein frataxin. Frataxin plays a direct role in ISC biogenesis. Frataxin interacts with multiple proteins in the ISC-biogenesis complex and regulates ISC biogenesis. Both intramitochondrial and

extramitochondrial ISCs are affected in FRDA; hence, the cellular consequences, and the signs and symptoms of the disorder, derive from decreased function of multiple ISCs, particularly in sensory neurons and the heart.

References

[1] Koeppen AH, Mazurkiewicz JE. Friedreich ataxia: neuropathology revised. J Neuropathol Exp Neurol 2013;72:78–90.
[2] Collins A. Clinical neurogenetics: Friedreich ataxia. Neurol Clin 2013;31:1095–120.
[3] Gomes CM, Santos R. Neurodegeneration in Friedreich's ataxia: from defective frataxin to oxidative stress. Oxid Med Cell Longev 2013;2013:487534.
[4] Durr A, Cossee M, Agid Y, et al. Clinical and genetic abnormalities in patients with Friedreich's ataxia. New Engl J Med 1996;335:1169–75.
[5] Harding AE. Friedreich's Ataxia: A clinical and genetic study of 90 families with an analysis of early diagnostic criteria and intrafamilial clustering of clinical features. Brain 1981;104:589–620.
[6] Klockgether T, Chamberlain S, Wullner U, et al. Late-onset Friedreich's ataxia. Molecular genetics, clinical neurophysiology, and magnetic resonance imaging. Arch Neurol 1993;50:803–6.
[7] De Michele G, Filla A, Cavalcanti F, et al. Late onset Friedreich's disease: clinical features and mapping of mutation to the FRDA locus. J Neurol Neurosurg Psychiatry 1994;57:977–9.
[8] Palau F, De Michele G, Vilchez JJ, et al. Early-onset ataxia with cardiomyopathy and retained tendon reflexes maps to the Friedreich's ataxia locus on chromosome 9q. Ann Neurol 1995;37:359–62.
[9] Campuzano V, Montermini L, Molto MD, et al. Friedreich's ataxia: autosomal recessive disease caused by an intronic GAA triplet repeat expansion [see comments]. Science 1996;271:1423–7.
[10] Pandolfo M. Molecular pathogenesis of Friedreich's ataxia. Neurol Rev 1999;56:1201–8.
[11] Gottesfeld JM. Small molecules affecting transcription in Friedreich ataxia. Pharmacol Ther 2007;116:236–48.
[12] Schmucker S, Puccio H. Understanding the molecular mechanisms of Friedreich's ataxia to develop therapeutic approaches. Hum Mol Genet 2010;19:R103–10.
[13] Cossee M, Durr A, Schmitt M, et al. Friedreich's ataxia: point mutations and clinical presentation of compound heterozygotes. Ann Neurol 1999;45:200–6.
[14] Cossee M, Puccio H, Gansmuller A, et al. Inactivation of the Friedreich ataxia mouse gene leads to early embryonic lethality without iron accumulation. Hum Mol Genet 2000;9:1219–26.
[15] Barbeau A. Friedreich's ataxia 1980 an overview of the pathophysiology. Can J Neurol Sci 1980;7:455–68.
[16] Johns DR. Mitochondrial DNA and disease. New Engl J Med 1995;333:638–44.
[17] Lodi R, Cooper JM, Bradley JL, et al. Deficit of in vivo mitochondrial ATP production in patients with Friedreich ataxia. Proc Nat Acad Sci USA 1999;96:11492–5.
[18] Lodi R, Hart PE, Rajagopalan B, et al. Antioxidant treatment improves in vivo cardiac and skeletal muscle bioenergetics in patients with Friedreich's ataxia. Ann Neurol 2001;49:590–6.
[19] Lynch DR, Lech G, Farmer JM, et al. Near-infrared muscle spectroscopy in patients with Friedreich's ataxia. Muscle Nerve 2002;25:664–73.
[20] Campuzano V, Montermini L, Lutz Y, et al. Frataxin is reduced in Friedreich ataxia patients and is associated with mitochondrial membranes. Hum Mol Genet 1997;6:1771–80.
[21] Koutnikova H, Campuzano V, Foury F, Dolle P, Cazzalini O, Koenig M. Studies of human, mouse, and yeast homologues indicate a mitochondrial function for frataxin. Nat Genet 1997;16:345–51.

[22] Babcock M, de Silva D, Oaks R, et al. Regulation of mitochondrial iron accumulation by Yfh1p, a putative homolog of Frataxin. Science 1997;276:1709–12.
[23] Priller J, Scherzer CR, Faber PW, MacDonald ME, Young AB. Frataxin gene of Friedreich's Ataxia is targeted to mitochondria. Ann Neurol 1997;42:265–9.
[24] Wilson RB, Roof DM. Respiratory deficiency due to loss of mitochondrial DNA in yeast lacking the frataxin homologue. Nat Genet 1997;16:352–7.
[25] Cavadini P, Gellera C, Patel PI, Isaya G. Human frataxin maintains mitochondrial iron homeostasis in Saccharomyces cerevisiae. Hum Mol Gen 2000;9:2523–30.
[26] Foury F, Cazzalini O. Deletion of the yeast homologue of the human gene associated with Friedreich's ataxia elicits iron accumulation in mitochondria. FEBS Lett 1997;411:373–7.
[27] Radisky DC, Babcock MC, Kaplan JK. The yeast frataxin homologue mediates mitochondrial iron efflux: evidence for a mitochondrial iron cycle. J Biol Chem 1999;274:4497–9.
[28] Foury F. Low iron concentration and aconitase deficiency in a yeast frataxin homologue deficient strain. FEBS Lett 1999;456:281–4.
[29] Rotig A, de Lonlay P, Chretien D, et al. Aconitase and mitochondrial iron-sulphur protein deficiency in Friedreich's ataxia. Nat Genet 1997;17:215–7.
[30] Bradley JL, Blake JC, Chamberlain S, Thomas PK, Cooper JM, Schapira AH. Clinical, biochemical and molecular genetic correlations in Friedreich's ataxia. Hum Mol Genet 2000;9:275–82.
[31] LaMarche JB, Cote M, Lemieux B. The cardiomyopathy of Friedreich's ataxia morphological observations in 3 cases. Can J Neurol Sci 1980;7:389–96.
[32] Delatycki MB, Camakaris J, Brooks H, et al. Direct evidence that mitochondrial iron accumulation occurs in Friedreich ataxia. Ann Neurol 1999;45:673–5.
[33] Wong A, Yang J, Cavadini P, et al. The Friedreich's ataxia mutation confers cellular sensitivity to oxidant stress which is rescued by chelators of iron and calcium and inhibitors of apoptosis. Hum Mol Genet 1999;8:425–30.
[34] Calmels N, Schmucker S, Wattenhofer-Donze M, et al. The first cellular models based on frataxin missense mutations that reproduce spontaneously the defects associated with Friedreich ataxia. PLoS One 2009;4:e6379.
[35] Wilson RB, Lynch DR, Fischbeck KH. Normal serum iron and ferritin concentrations in patients with Friedreich's Ataxia. Ann Neurol 1998;44:132–4.
[36] Lobmayr L, Brooks DG, Wilson RB. Increased IRP1 activity in Friedreich ataxia. Gene 2005;354:157–61.
[37] Kakhlon O, Manning H, Breuer W, et al. Cell functions impaired by frataxin deficiency are restored by drug-mediated iron relocation. Blood 2008;112:5219–27.
[38] Lesuisse E, Santos R, Matzanke BF, Knight SA, Camadro JM, Dancis A. Iron use for haeme synthesis is under control of the yeast frataxin homologue (Yfh1). Hum Mol Genet 2003;12:879–89.
[39] Horton AA, Fairhurst S. Lipid peroxidation and mechanisms of toxicity. CRC Crit Rev Toxicol 1987;18:27–79.
[40] Armstrong JS, Khdour O, Hecht SM. Does oxidative stress contribute to the pathology of Friedreich's ataxia? A radical question. FASEB J 2010;24:2152–63.
[41] Schulz JB, Dehmer T, Schols L, et al. Oxidative stress in patients with Friedreich ataxia. [see comments]. Neurology 2000;55:1719–21.
[42] Emond M, Lepage G, Vanasse M, Pandolfo M. Increased levels of plasma malondialdehyde in Friedreich ataxia [see comments]. Neurology 2000;55:1752–3.
[43] Huynen MA, Snel B, Bork P, Gibson TJ. The phylogenetic distribution of frataxin indicates a role in iron-sulfur cluster protein assembly. Hum Mol Genet 2001;10:2463–8.
[44] Muhlenhoff U, Richhardt N, Ristow M, Kispal G, Lill R. The yeast frataxin homolog Yfh1p plays a specific role in the maturation of cellular Fe/S proteins. Hum Mol Genet 2002;11:2025–36.
[45] Stemmler TL, Lesuisse E, Pain D, Dancis A. Frataxin and mitochondrial FeS cluster biogenesis. J Biol Chem 2010;285:26737–43.

[46] Puccio H, Simon D, Cossee M, et al. Mouse models for Friedreich ataxia exhibit cardiomyopathy, sensory nerve defect and Fe-S enzyme deficiency followed by intramitochondrial iron deposits. Nat Genet 2001;27:181–6.
[47] Muhlenhoff U, Gerber J, Richhardt N, Lill R. Components involved in assembly and dislocation of iron-sulfur clusters on the scaffold protein Isu1p. EMBO J 2003;22:4815–25.
[48] Gerber J, Muhlenhoff U, Lill R. An interaction between frataxin and Isu1/Nfs1 that is crucial for Fe/S cluster synthesis on Isu1. EMBO Rep 2003;4:906–11.
[49] Yoon T, Cowan JA. Iron-sulfur cluster biosynthesis. Characterization of frataxin as an iron donor for assembly of [2Fe-2S] clusters in ISU-type proteins. J Am Chem Soc 2003;125:6078–84.
[50] Ramazzotti A, Vanmansart V, Foury F. Mitochondrial functional interactions between frataxin and Isu1p, the iron-sulfur cluster scaffold protein, in Saccharomyces cerevisiae. FEBS Lett 2004;557:215–20.
[51] Schmucker S, Martelli A, Colin F, et al. Mammalian frataxin: an essential function for cellular viability through an interaction with a preformed ISCU/NFS1/ISD11 iron-sulfur assembly complex. PLoS One 2011;6:e16199.
[52] Colin F, Martelli A, Clemancey M, et al. Mammalian frataxin controls sulfur production and iron entry during de novo Fe4S4 cluster assembly. J Am Chem Soc 2013;135:733–40.
[53] Gakh O, Ranatunga W, Smith DYt, et al. Architecture of the human mitochondrial iron-sulfur cluster assembly machinery. J Biol Chem 2016;291:21296–321.
[54] Stehling O, Elsasser HP, Bruckel B, Muhlenhoff U, Lill R. Iron-sulfur protein maturation in human cells: evidence for a function of frataxin. Hum Mol Genet 2004;13:3007–15.
[55] Bulteau AL, O'Neill HA, Kennedy MC, Ikeda-Saito M, Isaya G, Szweda LI. Frataxin acts as an iron chaperone protein to modulate mitochondrial aconitase activity. Science 2004;305:242–5.
[56] Bulteau AL, Lundberg KC, Ikeda-Saito M, Isaya G, Szweda LI. Reversible redox-dependent modulation of mitochondrial aconitase and proteolytic activity during in vivo cardiac ischemia/reperfusion. Proc Natl Acad Sci USA 2005;102:5987–91.
[57] Dhe-Paganon S, Shigeta R, Chi YI, Ristow M, Shoelson SE. Crystal structure of human frataxin. J Biol Chem 2000;275:30753–6.
[58] He Y, Alam SL, Proteasa SV, et al. Yeast frataxin solution structure, iron binding, and ferrochelatase interaction. Biochemistry 2004;43:16254–62.
[59] Cho SJ, Lee MG, Yang JK, Lee JY, Song HK, Suh SW. Crystal structure of Escherichia coli CyaY protein reveals a previously unidentified fold for the evolutionarily conserved frataxin family. Proc Natl Acad Sci USA 2000;97:8932–7.
[60] Musco G, Stier G, Kolmerer B, et al. Towards a structural understanding of Friedreich's ataxia: the solution structure of frataxin. Structure 2000;8:695–707.
[61] Adamec J, Rusnak F, Owen WG, et al. Iron-dependent self-assembly of recombinant yeast frataxin: implications for Friedreich Ataxia. Am J Hum Genet 2000;67:549–62.
[62] Patel PI, Isaya G. Friedreich ataxia: from GAA triplet-repeat expansion to frataxin deficiency. Am J Hum Genet 2001;69:15–24.
[63] Cavadini P, O'Neill HA, Benada O, Isaya G. Assembly and iron-binding properties of human frataxin, the protein deficient in Friedreich ataxia. Hum Mol Genet 2002;11:217–27.
[64] Adinolfi S, Trifuoggi M, Politou AS, Martin S, Pastore A. A structural approach to understanding the iron-binding properties of phylogenetically different frataxins. Hum Mol Genet 2002;11:1865–77.
[65] Bou-Abdallah F, Adinolfi S, Pastore A, Laue TM, Dennis Chasteen N. Iron binding and oxidation kinetics in frataxin CyaY of *Escherichia coli*. J Mol Biol 2004;341:605–15.
[66] Kondapalli KC, Kok NM, Dancis A, Stemmler TL. Drosophila frataxin: an iron chaperone during cellular Fe-S cluster bioassembly. Biochemistry 2008;47:6917–27.

[67] Pastore C, Franzese M, Sica F, Temussi P, Pastore A. Understanding the binding properties of an unusual metal-binding protein – a study of bacterial frataxin. FEBS J 2007;274:4199–210.
[68] O'Halloran TV, Culotta VC. Metallochaperones, an intracellular shuttle service for metal ions. J Biol Chem 2000;275:25057–60.
[69] Layer G, Ollagnier-de Choudens S, Sanakis Y, Fontecave M. Iron-sulfur cluster biosynthesis: characterization of Escherichia coli CYaY as an iron donor for the assembly of [2Fe-2S] clusters in the scaffold IscU. J Biol Chem 2006;281:16256–63.
[70] Tsai CL, Barondeau DP. Human frataxin is an allosteric switch that activates the Fe-S cluster biosynthetic complex. Biochemistry 2010;49:9132–9.
[71] Pandey A, Gordon DM, Pain J, Stemmler TL, Dancis A, Pain D. Frataxin directly stimulates mitochondrial cysteine desulfurase by exposing substrate-binding sites, and a mutant Fe-S cluster scaffold protein with frataxin-bypassing ability acts similarly. J Biol Chem 2013;288:36773–86.
[72] Parent A, Elduque X, Cornu D, et al. Mammalian frataxin directly enhances sulfur transfer of NFS1 persulfide to both ISCU and free thiols. Nat Commun 2015;6:5686.
[73] Bridwell-Rabb J, Fox NG, Tsai CL, Winn AM, Barondeau DP. Human frataxin activates Fe-S cluster biosynthesis by facilitating sulfur transfer chemistry. Biochemistry 2014;53:4904–13.
[74] Iannuzzi C, Adinolfi S, Howes BD, et al. The role of CyaY in iron sulfur cluster assembly on the E. coli IscU scaffold protein. PLoS One 2011;6:e21992.
[75] Adinolfi S, Iannuzzi C, Prischi F, et al. Bacterial frataxin CyaY is the gatekeeper of iron-sulfur cluster formation catalyzed by IscS. Nat Struct Mol Biol 2009;16:390–6.
[76] Bridwell-Rabb J, Iannuzzi C, Pastore A, Barondeau DP. Effector role reversal during evolution: the case of frataxin in Fe-S cluster biosynthesis. Biochemistry 2012;51:2506–14.
[77] Yoon H, Knight SA, Pandey A, et al. Turning Saccharomyces cerevisiae into a Frataxin-Independent Organism. PLoS Genet 2015;11:e1005135.
[78] Roche B, Agrebi R, Huguenot A, Ollagnier de Choudens S, Barras F, Py B. Turning *Escherichia* coli into a frataxin-dependent organism. PLoS Genet 2015;11:e1005134.
[79] Bridwell-Rabb J, Winn AM, Barondeau DP. Structure-function analysis of Friedreich's ataxia mutants reveals determinants of frataxin binding and activation of the Fe-S assembly complex. Biochemistry 2011;50:7265–74.
[80] Tsai CL, Bridwell-Rabb J, Barondeau DP. Friedreich's ataxia variants I154F and W155R diminish frataxin-based activation of the iron-sulfur cluster assembly complex. Biochemistry 2011;50:6478–87.
[81] Martelli A, Napierala M, Puccio H. Understanding the genetic and molecular pathogenesis of Friedreich's ataxia through animal and cellular models. Dis Model Mech 2012;5:165–76.
[82] Anderson SA, Nizzi CP, Chang YI, et al. The IRP1-HIF-2alpha axis coordinates iron and oxygen sensing with erythropoiesis and iron absorption. Cell Metab 2013;17:282–90.
[83] Galy B, Ferring D, Minana B, et al. Altered body iron distribution and microcytosis in mice deficient in iron regulatory protein 2 (IRP2). Blood 2005;106:2580–9.
[84] Seznec H, Simon D, Bouton C, et al. Friedreich ataxia: the oxidative stress paradox. Hum Mol Genet 2005;14:463–74.
[85] Meyron-Holtz EG, Ghosh MC, Iwai K, et al. Genetic ablations of iron regulatory proteins 1 and 2 reveal why iron regulatory protein 2 dominates iron homeostasis. EMBO J 2004;23:386–95.
[86] Martelli A, Schmucker S, Reutenauer L, et al. Iron regulatory protein 1 sustains mitochondrial iron loading and function in frataxin deficiency. Cell Metab 2015;21:311–22.
[87] Rouault TA, Tong WH. Iron-sulfur cluster biogenesis and human disease. Trends Genet 2008;24:398–407.
[88] Maio N, Rouault TA. Iron-sulfur cluster biogenesis in mammalian cells: new insights into the molecular mechanisms of cluster delivery. Biochim Biophys Acta 2015;1853:1493–512.

[89] Netz DJ, Mascarenhas J, Stehling O, Pierik AJ, Lill R. Maturation of cytosolic and nuclear iron-sulfur proteins. Trends Cell Biol 2014;24:303–12.
[90] Kispal G, Csere P, Prohl C, Lill R. The mitochondrial proteins Atm1p and Nfs1p are essential for biogenesis of cytosolic Fe/S proteins. EMBO J 1999;18:3981–9.
[91] Lill R, Dutkiewicz R, Freibert SA, et al. The role of mitochondria and the CIA machinery in the maturation of cytosolic and nuclear iron-sulfur proteins. Eur J Cell Biol 2015;94:280–91.
[92] Li J, Cowan JA. Glutathione-coordinated [2Fe-2S] cluster: a viable physiological substrate for mitochondrial ABCB7 transport. Chem Commun (Camb) 2015;51:2253–5.
[93] Acquaviva F, De Biase I, Nezi L, et al. Extra-mitochondrial localisation of frataxin and its association with IscU1 during enterocyte-like differentiation of the human colon adenocarcinoma cell line Caco-2. J Cell Sci 2005;118:3917–24.
[94] Condo I, Ventura N, Malisan F, Tomassini B, Testi R. A pool of extramitochondrial frataxin that promotes cell survival. J Biol Chem 2006;281:16750–6.
[95] Condo I, Malisan F, Guccini I, Serio D, Rufini A, Testi R. Molecular control of the cytosolic aconitase/IRP1 switch by extramitochondrial frataxin. Hum Mol Genet 2010;19:1221–9.
[96] Paul VD, Lill R. Biogenesis of cytosolic and nuclear iron-sulfur proteins and their role in genome stability. Biochim Biophys Acta 2015;1853:1528–39.

12 Connecting the biosynthesis of the molybdenum cofactor, Fe-S clusters, and tRNA thiolation in humans

Silke Leimkühler

12.1 Introduction

The thiolation of biomolecules is a complex process that involves the activation of sulfur. The L-cysteine desulfurase NFS1 is the main sulfur-mobilizing protein that provides the sulfur from L-cysteine to several important biomolecules in the cell such as iron-sulfur (Fe-S) clusters, molybdopterin (MPT), and thionucleosides of tRNA. Various biomolecules mediate the transfer of sulfur from NFS1 to various biomolecules using different interaction partners. A direct connection among the sulfur-containing molecules, Fe-S clusters, thiolated tRNA, and the molybdenum cofactor (Moco) has been identified. The biosynthesis of Moco in humans originates in mitochondria, which is also the main compartment for Fe-S cluster biosynthesis. The first step of Moco biosynthesis involves the conversion of 5′GTP to cyclic pyranopterin monophosphate (cPMP), a reaction catalyzed by an Fe-S cluster containing protein. After transfer of cPMP to the cytosol, cPMP is converted to MPT by insertion of two sulfur atoms. The sulfur for this reaction is provided by the L-cysteine desulfurase NFS1 in the cytosol. Further sulfur transfer is mediated by the rhodanese-like protein, MOCS3, which forms a persulfide group on its active site cysteine. MOCS3 in humans directly connects Moco biosynthesis and tRNA thiolation in the cytosol by interacting with two proteins, URM1 and MOCS2A. A thiocarboxylate intermediate is formed on URM1 and MOCS2A, from which sulfur is further transferred to the target molecules, tRNA and cPMP, respectively. This review will dissect the sulfur transfer pathway in humans for both tRNA and Moco and their connection to Fe-S cluster biosynthesis and will explore how these reactions occur in the different compartments in the cell.

Sulfur is an essential element to all living organisms, and the presence of sulfur in cofactors was discovered more than a century ago [1]. The trafficking and delivery of sulfur to cofactors and nucleosides is a highly regulated process that occurs by complex sulfur relay systems involving numerous proteins in reactions that remain incompletely understood [2, 3]. In the last few years, several studies of sulfur transfer pathways in the cell concluded that the major enzymes involved in mobilization of sulfur are L-cysteine desulfurases and rhodanese homology domain proteins [3, 4]. These enzymes catalyze the formation of a persulfide group (R-S-S$^-$)] on specific conserved cysteine residues, which serves as a sulfur donor for the biosynthesis of sulfur-containing cofactors such as Fe-S clusters, thiamine, biotin, lipoic acid, and MPT and for thiomodification of tRNA [3]. In eukaryotes, only Fe-S clusters, the Moco, and thionucleosides in tRNA can be synthesized *de novo* (Fig. 12.1) [5–7]. The chemistry

DOI 10.1515/9783110479850-012

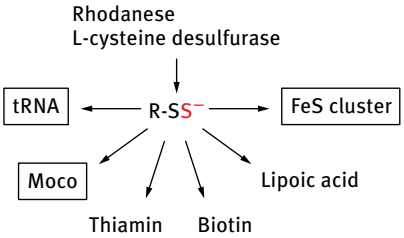

Fig. 12.1: Sulfur transfer to sulfur-containing biomolecules *via* protein-bound persulfide. A protein-bound persulfide group can be either formed on a rhodanese-like protein or on an L-cysteine desulfurase. The persulfide sulfur is further transferred by involvement of different proteins for the formation of sulfur-containing cofactors such as Moco, thiamine, biotin, lipoic acid, Fe-S clusters and for the thiolation of tRNA. Sulfur-containing molecules synthesized in humans are boxed.

of persulfide groups involves three oxidation states: S^0 (sulfane), S^{1-} (persulfide), or S^{2-} (sulfide) [1]. The terminal sulfur of the persulfide group can serve as a nucleophile to form a disulfide bond (R-S-S-R) with an electrophile [8]. The persulfide is usually generated by L-cysteine desulfurases that use L-cysteine as their sulfur source [3, 4].

L-cysteine desulfurases are pyridoxal-phosphate-containing homodimers, which decompose L-cysteine to L-alanine and sulfane sulfur *via* the formation of an enzyme-bound persulfide intermediate [9]. Further, the persulfide sulfur can be transferred in a relay mechanism to other proteins containing conserved cysteine residues, including the family of rhodanese-like proteins or other sulfur-transferring proteins [4]. The persulfide sulfur from the L-cysteine desulfurase is further incorporated either directly or *via* sulfur relay systems into the biosynthetic pathways of several sulfur-containing biofactors, thus providing an elegant mechanism for making sulfur atoms available without releasing them in solution [3, 8]. Many of the sulfur-relay proteins are highly conserved across species, e.g. the L-cysteine desulfurase that initiates the sulfur transfer step, the enzyme IscS from *Escherichia coli*, shares 60% amino acid sequence identity with its human homologue, NFS1 [3]. In this chapter, we focus on the connections between the pathways for the biosynthesis of three sulfur-containing biofactors in humans: Fe-S clusters, Moco, and thiolated tRNAs.

Fe-S clusters, which are thought to be among the earliest catalysts in the evolution of biomolecules, serve as electron carriers in redox reactions, regulatory sensors, stabilizers of protein structure, and chemical catalysts [1]. The mitochondria constitute the main compartment for the biosynthesis of Fe-S clusters in humans. However, Fe-S cluster biosynthesis also occurs in the cytosol, and some protein components of the pathway have also been identified in the nucleus [5]. The main proteins required for Fe-S cluster biosynthesis in mitochondria are NFS1, ISD11, ISCU, and FXN, which form the quaternary core complex [10–12]. After the synthesis of the Fe-S clusters on ISCU, the cluster can be transferred to acceptor proteins within the mitochondria [13]. Among these proteins is the MOCS1A protein, which is involved in the first step of Moco biosynthesis [14]. MOCS1A contains two [4Fe-4S] clusters.

Moco is a tricyclic pyranopterin containing a unique dithiolene group to which the molybdenum atom is coordinated [15]. Moco biosynthesis first starts with the conversion from 5′-GTP to cPMP, a reaction that is catalyzed by MOCS1A and MOCS1B in mitochondria (Fig. 12.2) [14]. All further steps for the formation of Moco from cPMP are localized in the cytosol and do not require Fe-S-containing proteins [6, 16]. However, it is believed that the sulfur for the dithiolene group originates from L-cysteine, which is mobilized by NFS1 in the cytosol [17, 18]. Thus, NFS1 would mobilize the sulfur for both pathways, Moco biosynthesis and Fe-S cluster biosynthesis, although mobilization of sulfur for Moco synthesis occurs in the cytosolic compartment. The direct insertion of two sulfur atoms into cPMP for the formation of MPT is catalyzed by the proteins MOCS2A, MOCS2B, and MOCS3 [19, 20]. The dithiolene group acts as a backbone for the ligation of the molybdenum atom in Moco. MOCS3 belongs to the class of rhodanese-like proteins, which accepts the sulfur from NFS1 and transfers the activated sulfur in a relay system to various acceptor proteins [17]. MOCS3 is not only involved in Moco biosynthesis because besides interacting with MOCS2A, it also interacts with URM1, which acts as a sulfur acceptor protein that is involved in the thiolation of some tRNAs [21]. Thus, Moco biosynthesis and tRNA thiolation are connected and share the same sulfur delivery pathway composed of NFS1 and MOCS3.

The wobble bases of tRNAs contain two thiouridines, 5-methoxycarbonylmethyl-2-thiouridine ($mcm^5s^2U_{34}$) in cytoplasmic tRNAs and 5-taurinomethyl-2-thiouridine ($\tau m^5s^2U_{34}$) in mitochondrial tRNAs [22]. More than five proteins are involved in the insertion of the sulfur group in mcm^5s^2U in humans in the cytosol: NFS1, URM1, MOCS3, CTU1, and CTU2 [7, 21]. For the thiolation of tRNA, thiomodification of uridine in the 2 position is known to ensure accurate deciphering of the genetic code and stabilization of tRNA structure [22, 23].

In this chapter, we will describe the biosynthesis of each biomolecule with respect to the different compartments with a focus on mitochondria, cytosol, and the nucleus. This chapter will mainly focus on Moco biosynthesis and tRNA thiomodification because mammalian Fe-S cluster biosynthesis is described in detail in other chapters.

12.2 Pathways for the formation of Moco and thiolated tRNAs in humans

12.2.1 Moco biosynthesis in mammals

In all organisms including humans, Moco is synthesized by a conserved biosynthetic pathway that can be divided into three steps, according to the stable biosynthetic intermediates that can be isolated and were first studied in *E. coli* (Fig. 12.2) [24]: the synthesis of cPMP [25], conversion of cPMP into MPT by introduction of two sulfur atoms [26], and insertion of molybdate to form Moco [27]. Moco is present in five enzymes in humans, sulfite oxidase (SUOX), xanthine oxidoreductase (XOR),

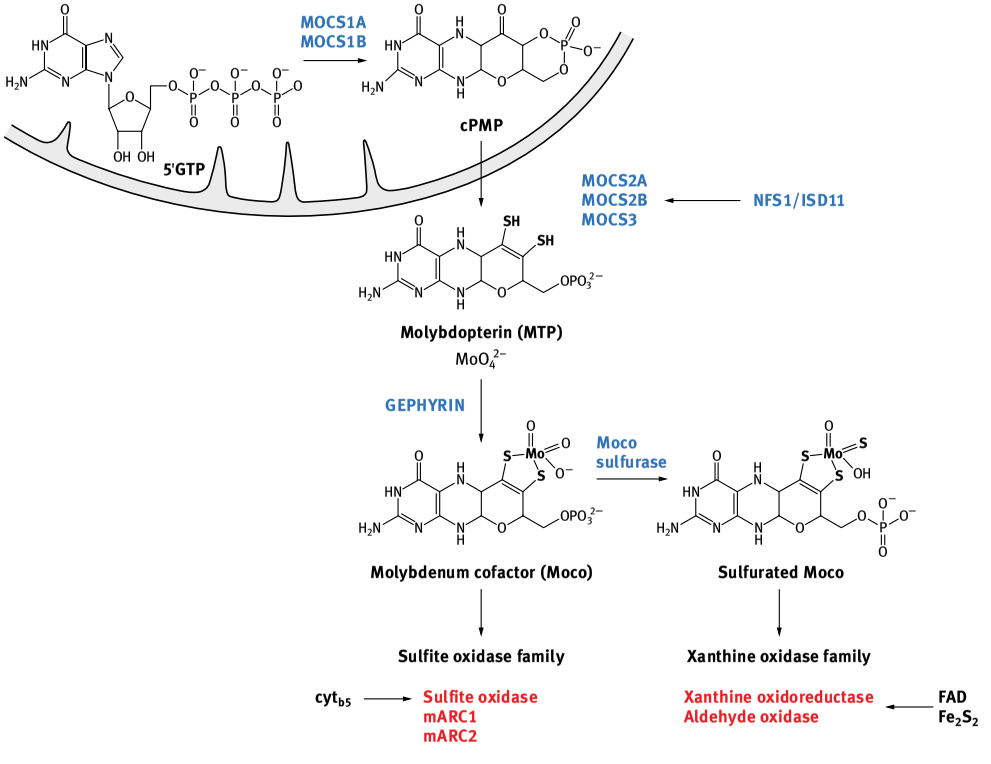

Fig. 12.2: The biosynthesis of Moco. Shown is a scheme of the biosynthetic pathway for Moco biosynthesis in humans. The proteins involved in the reactions are colored in blue. Moco can be modified by the replacement of one oxo ligand by a sulfido ligand, forming the mono-oxo Moco. The molybdenum-containing enzymes are divided into different families (xanthine oxidase and sulfite oxidase families in humans) according to their active-site structures.

aldehyde oxidase (AOX1), and two mitochondrial amidoxime-reducing components, mARC1 and mARC2 [6, 28]. SUOX is the only one of the five molybdoenzymes that is essential for humans [29, 30].

Six proteins that directly catalyze Moco biosynthesis have been identified in humans: MOCS1A, MOCS1B, MOCS2A, MOCS2B, MOCS3, and GPHN (gephyrin) [6]. Genes and the encoded proteins were named in humans as MOCS (molybdenum cofactor synthesis) [31–33].

12.2.1.1 Conversion of 5′-GTP to cPMP

The biosynthesis of Moco starts from 5′-GTP, which results in the formation of cPMP, the first stable intermediate of Moco biosynthesis [25] (Fig. 12.3). cPMP is an oxygen-sensitive 6-alkyl pterin with a cyclic phosphate group at the C2′ and C4′ atoms [34, 35]. The *MOCS1* locus encodes two proteins, MOCS1A and MOCS1B, which are involved in the conversion of 5′-GTP into cPMP [36]. MOCS1A belongs to the superfamily of *S*-adenosylmethionine (SAM)-dependent radical enzymes [14]. Members of this family catalyze the formation of protein and/or substrate radicals by reductive cleavage of SAM by a [4Fe-4S] cluster [37]. MOCS1A is a protein containing two oxygen-sensitive Fe-S clusters, each of which is coordinated by only three cysteine residues. The N-terminal [4Fe-4S] cluster, present in all radical SAM proteins, binds SAM and carries out the reductive cleavage of SAM to generate the 5′-deoxyadenosyl radical, which subsequently initiates the transformation of 5′-GTP bound through the C-terminal [4Fe-4S] cluster [14].

The mechanism of conversion of 5′-GTP to cPMP has been best studied using the bacterial proteins MoaA and MoaC [38, 39], but it has been shown that the human proteins catalyze the reaction in the same manner [40]. As shown in Fig. 12.3, formation of cPMP from GTP involves several steps including H-abstraction by the 5′-deoxyadenosyl radical of MOCS1A (MoaA) from the 3′ position of the ribose, attack of the C8 in the guanine ring by the C3′ radical, and formation of a (8*S*)-3′,8-cyclo-7,8-dihydroguanosine 5′-triphosphate (3′,8-cH$_2$GTP) intermediate, which further serves as a substrate for MOCS1B (MoaC) [40]. The additional reducing equivalents required for this step might be provided by the C-terminal [4Fe-4S] cluster in MOCS1A (MoaA). The reaction of MOCS1A (MoaC) is suggested to occur *via* general acid/base catalysis, converting 3′,8-cH$_2$GTP to cPMP, including pyrophosphate cleavage and formation of the cyclic phosphate group [40].

12.2.1.2 Conversion of cPMP to MPT

The next step involves the conversion of cPMP to MPT in which two sulfur atoms are incorporated in the C1′ and C2′ positions of cPMP [34] (Fig. 12.4). This reaction is catalyzed by MPT synthase, a protein consisting of two small (~10 kDa) and two large subunits (~21 kDa), encoded by *MOCS2A* and *MOCS2B*, respectively [41]. It was shown

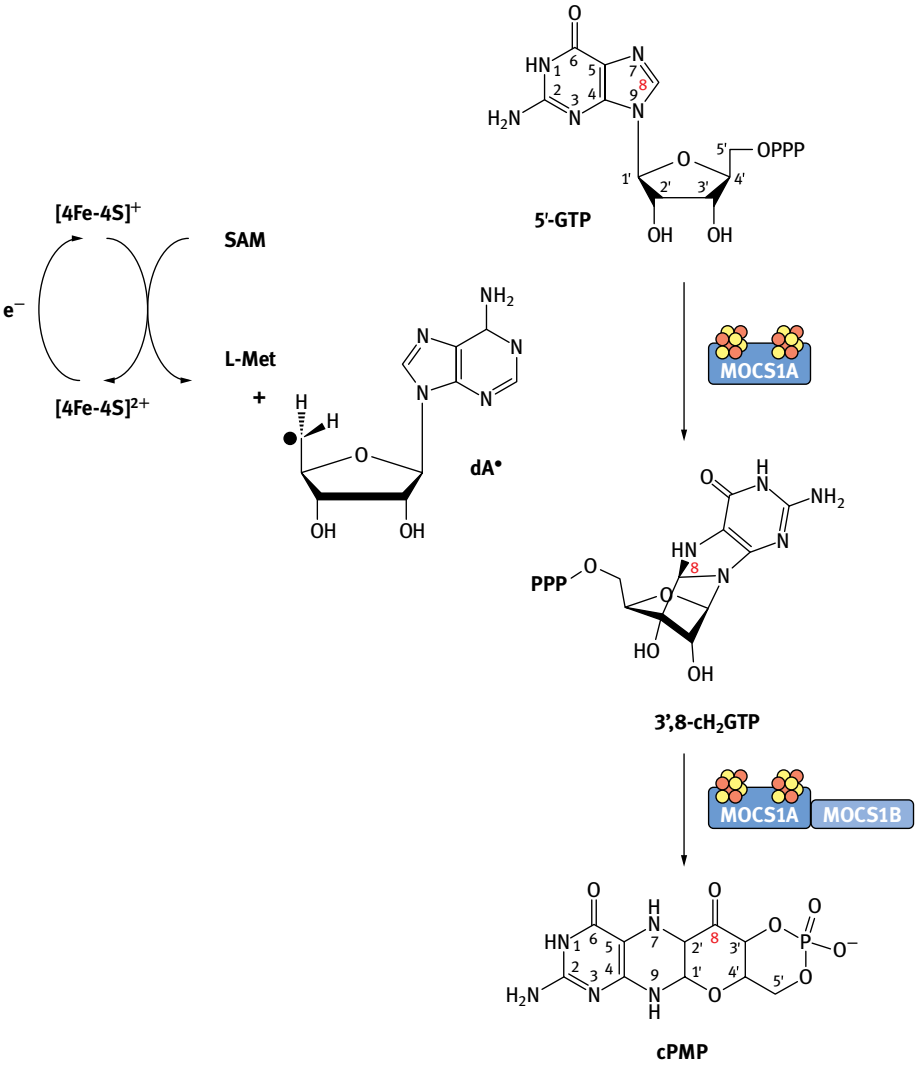

Fig. 12.3: Synthesis of cPMP from 5′-GTP. All carbon atoms of the 5′-GTP are found within cPMP. The C8 atom from the guanine ring is inserted between the C2′ and the C3′ atoms of the ribose. This reaction is catalyzed by the MOCS1A protein, a SAM-dependent enzyme. The MOCS1A/MOCS1B fusion protein cleaves the pyrophosphate group of the cyclic intermediate. cPMP is shown in the tetrahydropyrano form with a keto group at the C1′ position.

that MPT synthase carries the sulfur in form of a thiocarboxylate at the C-terminal glycine of MOCS2A [20, 42]. The central dimer is formed by two MOCS2B subunits containing one MOCS2A at each end, as revealed by the crystal structure of the bacterial homologues [43]. It was shown for the *E. coli* proteins that the two MOCS2A/MOCS2B dimers act independently. Thus, for the insertion of two sulfurs into cPMP,

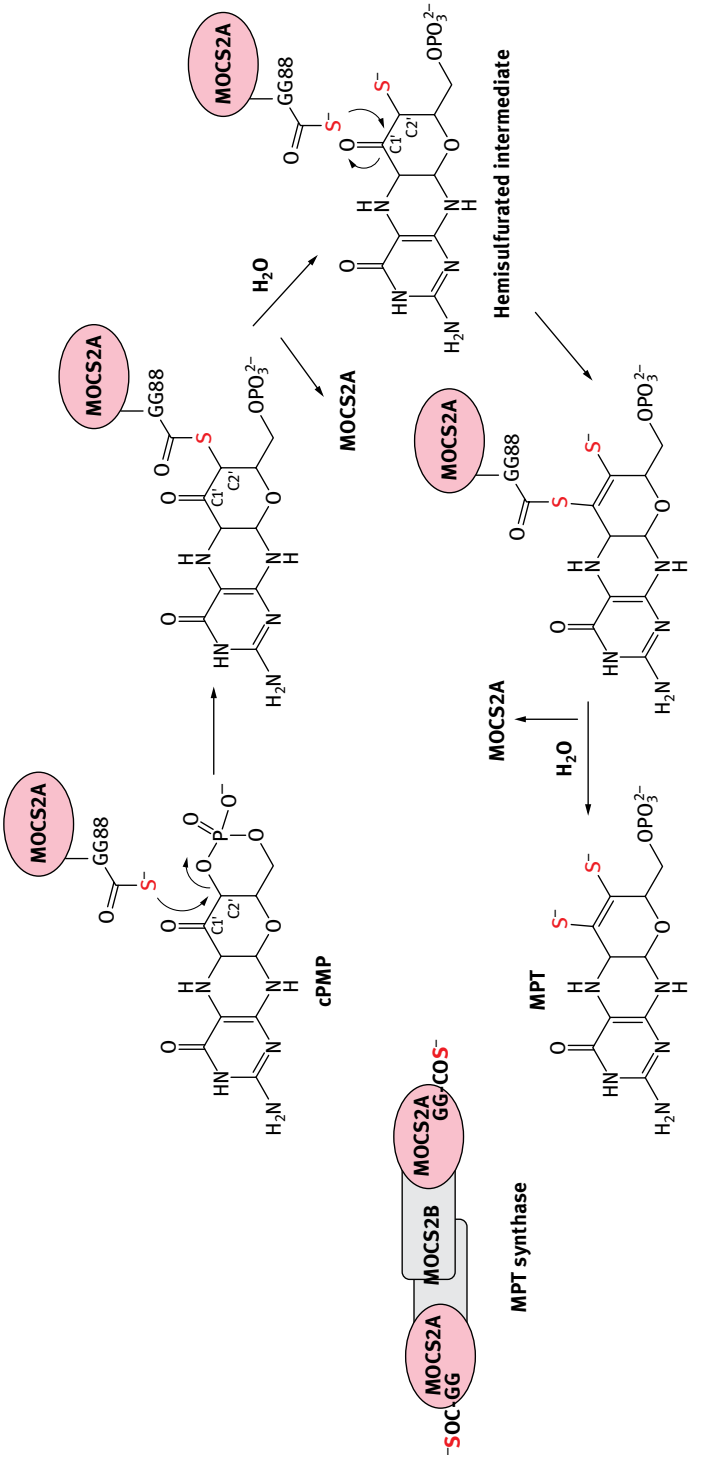

Fig. 12.4: The biosynthesis of MPT from cPMP. In the MPT synthase mechanism, the initial attack, and transfer of the first thiocarboxylated MOCS2A sulfur atom occurs at the C2′ position, coupled to the hydrolysis of the cPMP cyclic phosphate. An intermediate is formed in which the MOCS2A C-terminus is covalently linked to the substrate *via* a thioester linkage that is subsequently hydrolyzed by a water molecule to generate a hemi-sulfurated intermediate at C2′. Opening of the cyclic phosphate shifts the location of the intermediate within the complex to a position where C1′ becomes more accessible. A new MOCS2A thiocarboxylate attacks the C1,' resulting again in a second covalent intermediate that is converted to MPT *via* the elimination of a water molecule and hydrolysis of the thioester intermediate. On the left side, the MPT synthase tetramer is shown. During the reaction, cPMP remains bound to the MOCS2B molecule. The mechanism was adapted from the one proposed for the *E. coli* proteins [44].

two MOCS2A proteins are required at each end of the MPT synthase tetramer [45]. The first sulfur is added by one MOCS2A molecule at the C2′ position of cPMP (Fig. 12.4), a reaction that is coupled to the hydrolysis of the cPMP cyclic phosphate [44]. During the course of this reaction, a hemi-sulfurated intermediate is formed in which the MOCS2A C-terminus is covalently linked to the substrate *via* a thioester linkage, which subsequently is hydrolyzed by a water molecule. After transfer of its thiocarboxylate sulfur to cPMP, the first MOCS2A subunit dissociates from the MPT synthase complex [44, 45]. During the reaction of the first sulfur transfer, the opening of the cyclic phosphate is proposed to shift the location of the intermediate within the protein so that the C1′ position now becomes more accessible to attack by the second MOCS2A thiocarboxylate (Fig. 12.4). This results in a second covalent intermediate that is converted to MPT *via* the elimination of a water molecule and hydrolysis of the thioester intermediate. During the reaction, cPMP and the hemisulfurated intermediate remain bound to one MOCS2B subunit [31]. This reaction has been mainly revealed by studies with the homologous proteins MoaD and MoaE from *E. coli*; however, the same reaction can be catalyzed by hybrid complexes formed between the bacterial and the mammalian proteins, indicating that conservation of the reaction components is high among species [20].

The regeneration of sulfur at the C-terminal glycine of MOCS2A is catalyzed by MOCS3 [46] and resembles the first step of the ubiquitin-dependent protein degradation system [47] (Fig. 12.5). It was shown that the N-terminal domain of MOCS3 has homologies to E1-like proteins and activates the C-terminus of MOCS2A (which has a ubiquitin-like β-grasp fold) by addition of AMP forming an activated acyl-adenylate group on Gly88, the last amino acid of a highly conserved double glycine motif [19]. In the second reaction, the MOCS2A acyl-adenylate is converted to a thiocarboxylate by sulfur transfer from a persulfide present at the C-terminal rhodanese-like domain (RLD) of MOCS3 [31, 48]. In this reaction, the deprotonated persulfide group of RLD-C412 serves as a nucleophile at the activated MOCS2A-adenylate to form a disulfide intermediate (Fig. 12.5). Reductive cleavage of the disulfide bond could then occur by attack of another thiol group, e.g. the conserved MOCS3-C239 to form a disulfide bond with C412, and in turn, thiocarboxylated MOCS2A is generated and released [48]. The disulfide bond could be reduced by a thioredoxin system *in vivo*. The sulfur donor for the generation of the persulfide on C412 of MOCS3 was shown to be the L-cysteine desulfurase NFS1 in the cytosol [17, 18]. Here, the sulfur is transferred in a sulfur relay system from the NFS1 persulfide *via* the MOCS3 persulfide to MOCS2A and further to cPMP, resulting in the formation of MPT in the cytosol.

12.2.1.3 Insertion of molybdate into MPT and further modification of Moco

After synthesis of the dithiolene moiety in MPT, the chemical backbone is built for binding and coordination of the molybdenum atom. In humans, the *GPHN* gene encodes a two-domain protein known as gephyrin, which consists of an N-terminal

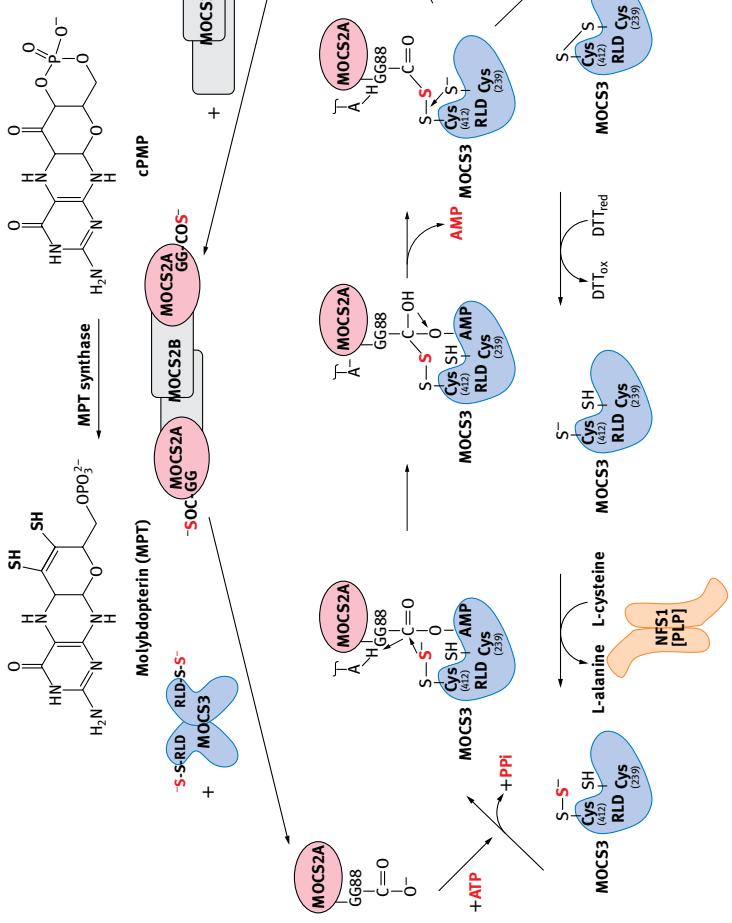

Fig. 12.5: Formation of the thiocarboxylate group on MOCS2A. cPMP is converted to MPT by the transfer of two sulfur groups from the C-terminal thiocarboxylate of the MOCS2A subunit of MPT synthase. Regeneration of the MOCS2A-SH sulfur occurs in a MOCS2A/MOCS3 complex. Here, adenylated MOCS2A is formed by attachment of an AMP moiety at the N-terminal E1-like domain of MOCS3. MOCS2A-AMP is then sulfurated by a protein-bound persulfide on Cys412 from the C-terminal RLD. Likely, an MOCS3-MOCS2A disulfide intermediate is formed during the reaction, which is further cleaved by reductive cleavage (e.g. MOCS3-Cys239). The disulfide bond formed between MOCS3-Cys412 and MOCS3-Cys239 is likely reduced by the thioredoxin system *in vivo* (*in vitro* reduction by DTT is shown). The sulfur donor for the persulfide group on MOCS3-Cys412 is NFS1, which acquires the sulfur from L-cysteine. After formation of the thiocarboxylate group, MOCS2A-SH dissociates from the MOCS3 dimer and reassociates with MOCS2B, forming the active MPT synthase.

domain that binds MPT and forms an MPT-AMP intermediate and a C-terminal domain that inserts the molybdate anion and splits the AMP from the activated MPT-AMP intermediate in a molybdate and Mg^{2+}-dependent manner [49, 50]. This reaction leads to the formation of Moco [31] (Fig. 12.6). Apart from the Moco biosynthesis, GPHN is also involved in synaptic anchoring of inhibitory ligand-gated ion channels [51]. Alternative splicing has been proposed to contribute to functional diversity of gephyrin proteins within the cell [52].

The completed Moco can be directly inserted into SUOX or mARC1 and mARC2 [28]. For XOR (also known as XDH) and AOX1, Moco is further modified by an exchange of the equatorial oxygen ligand by sulfur, forming the sulfurated or mono-oxo form of Moco [53, 54] (Fig. 12.2). This reaction is carried out by a Moco sulfurase, MOCOS (also known as HMCS) in humans, a two-domain protein with a N-terminal L-cysteine desulfurase domain and a C-terminal Moco binding (MOSC) domain [28, 55, 56]. L-Cysteine is the sulfur source in this reaction [57]. The Moco likely gets sulfurated while bound to the MOCOS protein and is then inserted into XOR and AOX1 [58, 59].

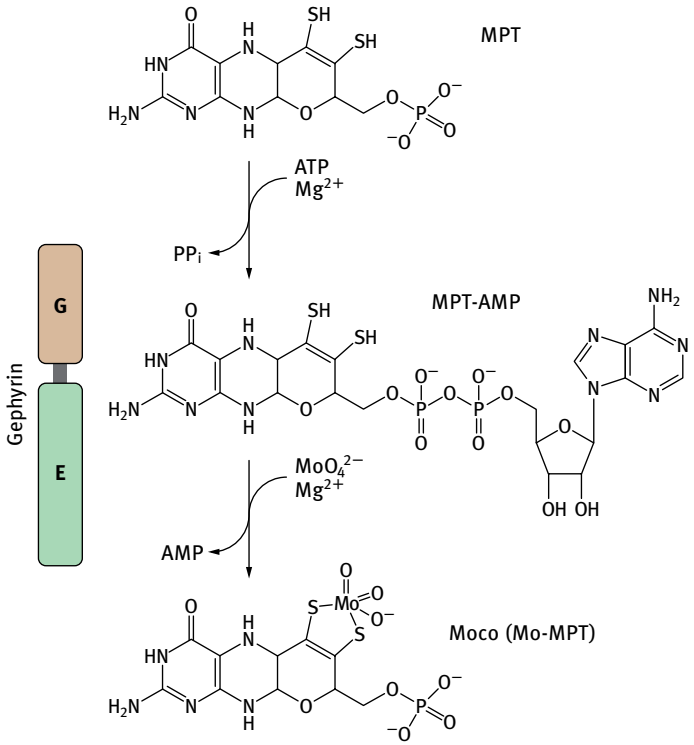

Fig. 12.6: Insertion of molybdate into MPT. The gephyrin protein catalyzes the specific incorporation of molybdenum into MPT in a multistep reaction with an adenylated MPT intermediate (MPT-AMP). While the N-terminal G-domain forms the MPT-adenylate intermediate, the C-terminal E-domain mediates molybdenum ligation to MPT at low concentrations of MoO_4^{2-} in a Mg^{2+}-dependent manner.

12.2.1.4 Finishing Moco biosynthesis: maturation and insertion into complex molybdoenzymes

After insertion of the molybdenum atom into MPT, the completed Moco can be either directly inserted into SUOX or mARC1 and mARC2 or is further modified by an exchange of the equatorial oxygen ligand by sulfur, forming the sulfurated or mono-oxo form of Moco present in AOX1 or XOR [28]. The basis of the structures of their molybdenum centers divides the molybdoenzymes into three distinct families, two of which are present in eukaryotes (Fig. 12.2): the xanthine oxidase family, the sulfite oxidase family, and the dimethylsulfoxide (DMSO) reductase family (not shown) [54]. The xanthine oxidase family is characterized by an MPT-$Mo^{VI}OS(OH)$ core in the oxidized state, with one MPT equivalent coordinated to the metal and no additional ligand from the polypeptide chain. The sulfido-group is cyanide labile. Enzymes of the sulfite oxidase family coordinate a single equivalent of the pterin cofactor with an MPT-$Mo^{VI}O_2$ core in its oxidized state and usually an additional cysteine ligand, which is provided by the polypeptide chain of the enzyme. The DMSO-reductase family is exclusively found in Bacteria and Archaea, and all members have two equivalents of the pterin cofactor bound to the metal. The molybdenum coordination sphere is usually characterized by an MPT_2-$Mo^{VI}S(X)$ core. The sixth ligand, X, can be a serine, a cysteine, a selenocysteine, or a hydroxide and/or water molecule (not shown).

All molybdoenzymes in eukaryotes are oxidoreductases that catalyze substrate hydroxylation or transfer an oxo group and two electrons from the substrate. The electrons are further transferred from the MoIV, which accepted two electrons from the substrate, and these electrons are donated in single one-electron steps to an electron acceptor such as FAD or cytochromes through an intramolecular pathway that can additionally be mediated by Fe-S clusters [28, 54]. The mechanism of Moco insertion into SUOX is not well understood [60], and little is known so far about how the cytochrome is inserted into the protein in the intermembrane space in humans. Insertion of the mature Moco for members of the xanthine oxidase family is now fairly well understood and has been studied in prokaryotes and eukaryotes [61, 62]. The final step in maturation of the molybdenum center is the incorporation of the catalytically essential sulfur as ligand to the molybdenum atom. The protein involved in the sulfuration binds the Moco and inserts the mature cofactor into the XOR or AOX1 apo-protein after its sulfuration [58, 63, 64]. It was shown that insertion of the molybdenum center occurs after incorporation of both the two [2FeS] clusters and FAD in a protein that is already largely folded into its final three-dimensional structure and assembled as a dimer [65].

SUOX is the only molybdoenzyme that is essential for humans. SUOX is a protein that is located in the intermembrane space of mitochondria in mammals [66]. It catalyzes the terminal step in the catabolism of the sulfur-containing amino acids cysteine and methionine. Electrons derived from sulfite oxidation to sulfate are transferred from Moco *via* the cyt_{b5} cofactor in SUOX to the final electron acceptor cytochrome *c* [67]. A mutation in the gene for SUOX leads to isolated SUOX deficiency, an inherited

sulfur metabolic disorder in humans that results in profound birth defects, severe neonatal neurological problems, and early death, and no effective therapies are known [31]. It has been suggested that the pathology associated with SUOX deficiency is due to the toxic buildup of sulfite in the developing brain [68–71]. Excess sulfite can react with disulfide bonds to form sulfonated Cys residues that distort protein structures [30]. In addition, the lack of sulfate in the brain may interfere with the production of sulfatides, lipid sulfate esters found in the white matter of the brain that are a component of myelin. SUOX is synthesized as a pre-protein with a mitochondrial targeting sequence that localizes to the mitochondrial intermembrane space after processing [60]. Subsequently, insertion of Moco, insertion of the cyt_{b5} and dimerization occurs in the intermembrane space [60].

Recent investigations of the aerobic reduction of amidoxime structures led to the discovery of a previously unknown molybdenum-containing enzyme system [28, 72]. It was named "mitochondrial amidoxime-reducing component" (mARC) because, initially, *N*-reduction of amidoxime structures was studied with this enzyme purified from mammalian liver mitochondria. The human genome harbors two mARC genes, referred to as *hmARC1* and *hmARC2*, which are organized in a tandem arrangement on chromosome 1 (designated as *MOSC1* and *MOSC2* in the databases) [73]. The two enzymes form the catalytic part of a three-component enzyme system, consisting of mARC, heme/cytochrome b_5, and NADH/FAD-dependent cytochrome b_5 reductase. It was shown that the mARC proteins are associated with the outer mitochondrial membrane [74]. However, nothing is known about the targeting, assembly, and cofactor insertion of the protein complex. Additionally, although many N-hydroxylated compounds have been found to serve as substrates for native and recombinant mARC proteins, the physiological substrates and physiological functions of mARC proteins remain unknown [28].

In contrast to SUOX and mARC1 and mARC2, XOR and AOX1 are cytosolic enzymes. XOR generally is involved in the later stages of purine catabolism, catalyzing the oxidation of hypoxanthine to xanthine and of xanthine to uric acid, which is finally excreted in the urine [75]. XOR and AOX1 belong to the class of molybdoflavoenzymes, containing in addition to Moco, two distinct [2Fe-2S] centers and FAD as catalytically acting units [76, 77]. XOR in mammals is synthesized as the dehydrogenase form (XDH, EC 1.17.1.4) but can be converted to the oxidase form (XO, EC 1.1.3.22) either reversibly by oxidation of sulfhydryl residues of the protein molecule or irreversibly by proteolysis [78]. XDH shows a preference for NAD^+ reduction at the FAD reaction site, whereas XO exclusively uses dioxygen as its terminal electron acceptor, leading to the formation of superoxide and hydrogen peroxide [79]. The enzyme has been implicated in diseases characterized by oxygen radical-induced tissue damage, such as post-ischemic reperfusion injury [80]. The oxidation of xanthine takes place at the molybdenum center and the electrons thus introduced are rapidly distributed in one-electron transfer reactions to the Fe-S centers and finally to FAD according to their relative redox potentials [54]. The reoxidation of the reduced enzyme by either NAD^+ or molecular oxygen occurs through the FAD cofactor [81].

Although the biochemical function of XOR is well established, the biochemical and physiological functions of AOX1 are still largely obscure. Only limited information is available about the physiological substrates of AOX1 or about the role of this enzyme in the mammalian organism [77]. It has been shown that the enzyme is located in the cytosol and is involved in the metabolism of drugs and xenobiotics of toxicological importance, and AOX1 metabolizes N-heterocyclic compounds and aldehydes of pharmacological relevance [77]. Single monogenic AOX1 deficits have not been described yet in mammalia; absence of a phenotype is perhaps not surprising because genetic deficiencies in the downstream Moco sulfurase (*MCSF*) gene are not associated with pathophysiological consequences [28]. It is likely that AOX1 serves to detoxify exogenously derived unphysiological compounds of wide structural diversity in animals, and it is believed that the absence of AOX1 produces symptoms in animals after high intake of such xenobiotics.

Although Moco is inserted into XOR and AOX1 in the cytosol by the MCSF after the insertion of the terminal sulfido ligand, nothing is known so far about which proteins are involved in Fe-S cluster insertion or FAD insertion in the cytosol. However, the presence of two [2Fe-2S] clusters in XOR and AOX1 directly link the activity of these two enzymes to the cytosolic iron-sulfur cluster assembly (CIA) machinery for Fe-S cluster biosynthesis. It still remains to be elucidated which proteins are directly involved in [2Fe-2S] cluster biosynthesis and insertion for cytosolic molybdo-flavoenzymes in mammals.

12.2.2 The role of tRNA thiolation in the cell

Post-transcriptional RNA modifications are a characteristic structural feature of RNA molecules. The diverse modifications have been shown to play critical roles in biogenesis, metabolism, structural stability, and function of RNA molecules [23]. More than 100 different RNA modifications have been reported to date [22, 82]. These post-transcriptional modifications are required for several functions in translation including codon recognition, maintenance of reading frame, stabilization of tertiary structure and directing the specificity of the codons recognition by the ribosome. Base modifications at the wobble positions in anticodon loops of tRNA have been shown to play important roles in deciphering genetic codes, which include the precise codon-anticodon interactions at the ribosomal A-site. In particular, the wobble bases of tRNAs for Glu, Gln and Lys are modified, and sulfurated to form 5-methyl-2-thiouridine derivatives (xm^5s^2U), such as 5-taurinomethyl-2-thiouridine (τm^5s^2U) in mammalian mitochondrial tRNAs, and 5-methoxycarbonylmethyl-2-thiouridine (mcm^5s^2U) in eukaryotic cytoplasmic tRNAs [22]. The result of these thio modifications is that the conformation of xm^5s^2U is trapped in the C3′-*endo* form of the ribose because the large van der Waals' radius of the 2-thio group causes a steric clash with its 2′-OH group [22, 83]. This conformational rigidity causes preferential pairing of the xm^5s^2U-modified bases with purines and prevents misreading of codons ending in pyrimidines [83–85].

Recently, it was shown that this 2-thio group of mcm^5s^2U is required for efficient codon recognition on the ribosome [86]. Lack of the xm^5s^2U modification in the mutant mitochondrial $tRNA^{Lys}$ from individuals with myoclonus epilepsy associated with ragged-red fibers (MERRFs) results in a marked defect in all mitochondrial translation [87]. For the thiolation and formation of the mcm^5s^2U in the cytoplasm of eukaryotes, the biosynthesis of the 5-methoxycarbonylmethyl group of the uracil ring is required for efficient 2-thiouridine formation in the cytoplasm [7]. In humans it was shown that the proteins MOCS3, URM1, CTU1, and CTU2 are essential for the biogenesis of the 2-thiouridine group in cytoplasmic tRNAs Lys, Gln, and Glu (Fig. 12.7) [88]. The URM1 protein (ubiquitin-related modifier) was shown to have a ubiquitin-like β-grasp-fold

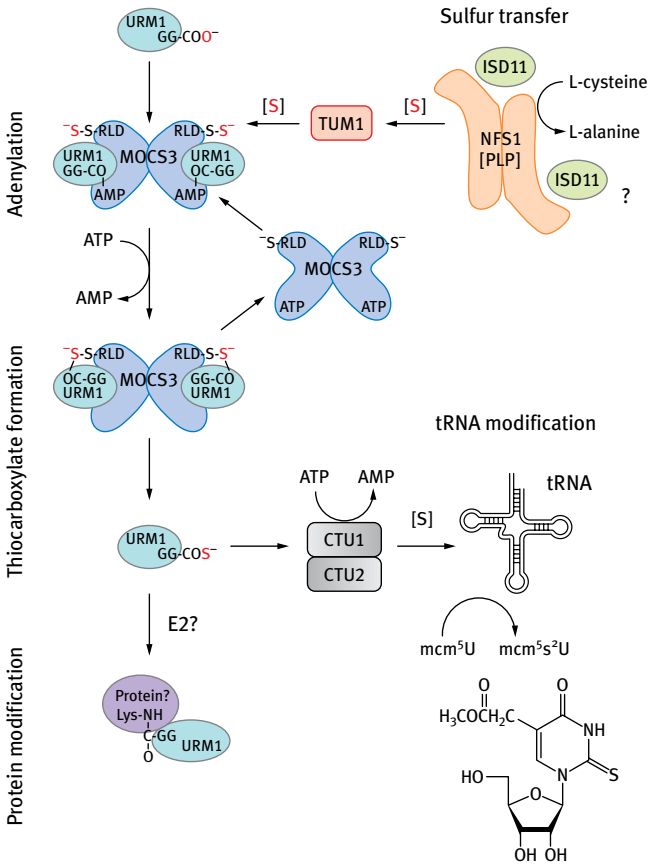

Fig. 12.7: Proposed mechanism of 5-methoxycarbonylmethyl-2-thiouridine ($mcm^5s^2U^{34}$) in humans. MOCS3 activates URM1 in the presence of ATP by formation of an acyl-adenylate bond. URM1 is further transferred to a persulfide group on Cys412 of MOCS3-RLD, forming a disulfide bond. URM1-thiocarboxylate is released and transfers the sulfur further onto uridine 34 on the lysine tRNA, helped by the CTU1 and CTU2 proteins under ATP consumption. URM1 was also shown to be conjugated to target proteins *via* a lysine-isopeptide bond, showing that it is a dual-function protein.

and contains a conserved C-terminal double-glycine motif on which a thiocarboxylate group is formed for direct sulfur tranfer to mcm^5U_{34} in tRNA [89–92]. The sulfur is transferred to URM1 *via* MOCS3, which was originally recognized for its role in Moco biosynthesis (see Section 12.2.1.2) [21]. MOCS3 activates URM1 in the presence of ATP by formation of an acyl-adenylate bond. URM1 is further transferred to a persulfide group on Cys412 of MOCS3-RLD, forming a disulfide bond (Fig. 12.7). The disulfide bond can be cleaved by C239 of MOCS3, which releases thiocarboxylated URM1. URM1-thiocarboxylate further transfers the sulfur onto uridine 34 of the tRNA, aided by the CTU1 and CTU2 proteins and ATP consumption [21]. As described Section 12.2.1.2, NFS1 was shown to be the protein that supplies sulfur to MOCS3, which links tRNA modification to the sulfur supplied by L-cysteine desulfurases [17]. Additionally and in contrast to MOCS2A, URM1 was also shown to be conjugated to target protein *via* a lysine-isopeptide bond, revealing that it is a dual-function protein [88]. Among the targets for urmylation are the components of the tRNA thiolation machinery itself (CTU1 and CTU2) and a deubiquitinating-enzyme (USP15) and, in addition, proteins involved in nuclear transport such as the cellular apoptosis susceptibility protein, CAS, which promotes the shuttling of proteins between cytosol and nucleus [88]. However, the role of the protein urmylation is not completely clear to date and might only occur under certain conditions in the cell such as oxidative stress.

12.3 The connection between sulfur-containing biomolecules and their distribution in different compartments in the cell

12.3.1 Sulfur transfer in mitochondria

Mitochondria are the main compartment for Fe-S cluster biosynthesis [93]. The initial phase of mitochondrial Fe-S cluster biosynthesis in mammals is accomplished by a multimeric protein complex in which a dimer of the L-cysteine desulfurase NFS1 in conjunction with its stabilizing protein ISD11 builds the core for the interaction of two monomers of ISCU and two FXN (frataxin) monomers (Fig. 12.8) [11, 94]. The ISCU protein provides the scaffold for building the Fe-S clusters from sulfur, delivered by NFS1 and iron from an unknown iron donor. FXN might function as an iron donor or act as a regulator for the formation of Fe-S clusters depending on the iron availability in the cell [95]. After the formation of [2Fe-2S] clusters and [4Fe-4S] clusters, the clusters are transferred to target proteins with the help of co-chaperones and chaperones such as HSC20 and HSPA9 [5, 13].

In addition to Fe-S cluster biosynthesis, mitochondria are the compartment for the first step of Moco biosynthesis, namely the conversion of 5′-GTP to cPMP, catalyzed by MOCS1A and MOCS1B as described above (Fig. 12.8) [14]. The *MOCS1* locus encodes two proteins, MOCS1A and MOCS1B [36]. An unusual bicistronic transcript of the *MOCS1* locus was identified, with open reading frames for both *MOCS1A* and

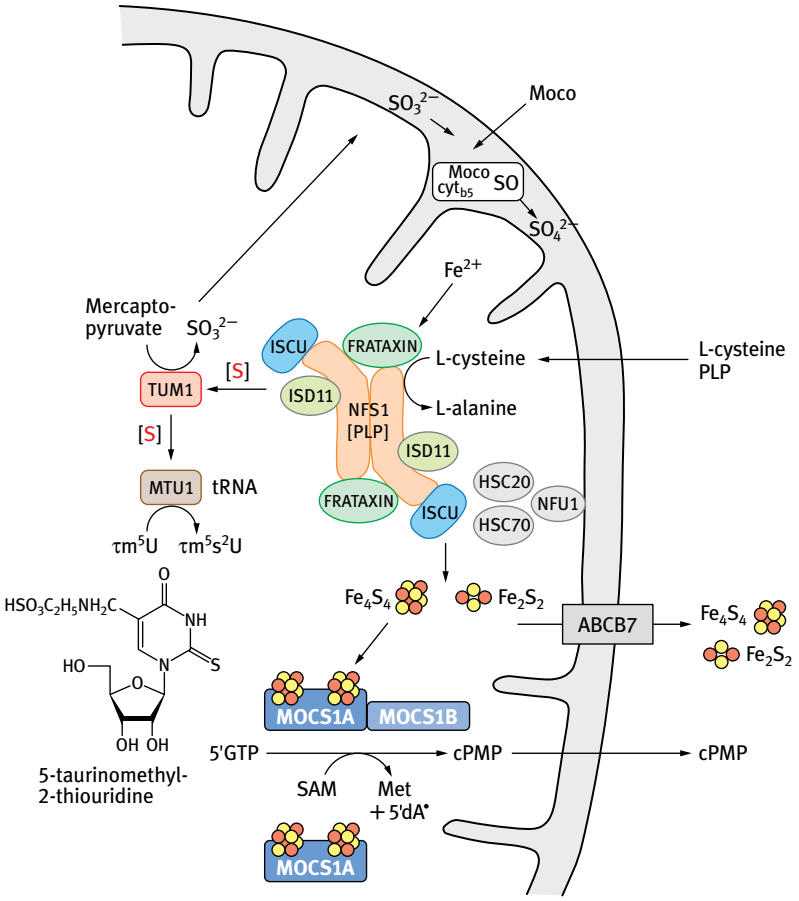

Fig. 12.8: Localization and role of proteins in mitochondria. Shown is the localization of proteins involved in Fe-S cluster biosynthesis, Moco biosynthesis, and tRNA thiolation and their connection in the mitochondrion. Human SUOX is localized in the intermembrane space of mitochondria. Shown are also compounds that need to be imported or exported to mitochondria.

MOCS1B in a single transcript, separated by a stop codon [96]. Splice variants of the *MOCS1* locus were identified that bypass the termination codon of *MOCS1A*, resulting in a new two-domain protein fusing MOCS1A and MOCS1B [97]. No evidence was found for the expression of MOCS1B from the bicistronic *MOCS1A-MOCS1B* splice-type I cDNA, indicating that MOCS1B is only expressed as a fusion with MOCS1A, whereas MOCS1A is also expressed as a separate protein [98]. Both proteins contain a mitochondrial targeting sequence for the translocation to mitochondria. The reaction catalyzed by MOCS1A and MOCS1B (in the MOCS1A-MOCS1B fusion) is described in detail Section 12.2.1.1. MOCS1A contains two [4Fe-4S] clusters that are directly involved in SAM cleavage and 5′-GTP binding and are therefore essential for the reaction [14]. The presence of these two Fe-S clusters directly links the first step of Moco

biosynthesis to Fe-S cluster biosynthesis in mitochondria (Fig. 12.8). Thus, mutations in genes for Fe-S cluster biosynthesis would also result in a decrease of Moco biosynthesis in mammals and impaired cPMP production in mitochondria. After biosynthesis of cPMP from 5′-GTP in a reaction requiring reducing equivalents and SAM, cPMP has to be transported to the cytosol, where it is further modified.

The transporter involved in exporting cPMP to the cytosol was identified in plants to be ATM3 (a homologue of human ABCB7) [99]; however, cPMP has been additionally proposed to pass through the membrane without specific transport proteins due to its hydrophobic nature [25]. Thus, it remains unclear how cPMP is specifically transported to the cytosol in humans. Surprisingly, ABCB7 is also suggested to transport an essential molecule for Fe-S cluster biosynthesis in the cytosol [100]. This would present essential functions for the mitochondria in both cytosolic Fe-S cluster and Moco biosynthesis.

However, the mitochondria are also a compartment in which tRNAs are thiolated [101]. Thiolated tRNAs in mitochondria were identified to contain a 5-taurinomethyl-2-thiouridine (τm^5s^2U) modification in tRNAs for Lys, Glu, and Gln [87]. Mitochondrial tRNAs are transcribed from mitochondrial DNA, and taurine is transported into mitochondria, where the specific modification of uridine 34 at the wobble position occurs. The proteins MSS1 and MTO1 in humans have been shown to be involved in the τm^5U modification in mitochondrial tRNA in humans. Further, the mitochondrial tRNA specific 2-thiouridylase, MTU1, is involved transferring sulfur to form the τm^5s^2U tRNAs [101]. The sulfur donor for MTU1 is the NFS1/ISD11 complex that thus links tRNA thiolation and Fe-S cluster biosynthesis in mitochondria (Fig. 12.8) [23]. The NFS1/ISD11 complex transfers sulfur to MTU1 either directly or through an additional sulfur relay protein. This sulfur relay protein was shown in yeast to be the rhodanese-like protein, Tum1p [7]. TUM1 is also found in the mitochondria of humans, but its direct involvement in tRNA thiolation in humans still needs to be elucidated [102]. Lack of post-transcriptional modifications at the wobble positions of mitochondrial tRNAs for Leu and Lys has been associated with mitochondrial encephalomyopathy, lactic acidosis, and stroke-like episodes and myoclonic epilepsy with ragged-red fibers [103–106].

12.3.2 Sulfur transfer in the cytosol

Recently, several reports suggested that the mitochondria are not the sole compartment where Fe-S cluster biosynthesis is initiated [5]. Thus far, it has been proposed for yeast that the mitochondrial transporter Atm1 exports either fully formed Fe-S clusters or a special form of sulfur that is required for cytosolic Fe-S cluster biosynthesis [100, 107]. In *Saccharomyces cerevisiae*, export of a "sulfur compound" from mitochondria has been proposed to contribute to cytosolic Fe-S cluster assembly (CIA) *via* proteins known as Tah18 and Dre2 [108]. It was proposed that a cluster is transferred from Dre2 to other members of the CIA pathway [109]. The mammalian homologues of

Tah18 and Dre2 are NDOR1 and CIAPIN1, respectively, and they work with the NUBP1, NUBP2, NARFL, and CIAO1 proteins of the CIA pathway (Fig. 12.9) [110]. Because, in addition to these proteins, other proteins of the initial Fe-S cluster core complex have been identified in the cytosol (NFS1, ISCU, FXN, and HSC20), it is possible that the Fe-S clusters are also *de novo* formed in the cytosol [5]. However, although these proteins are present in the cytosol, their involvement in cytosolic Fe-S cluster biosynthesis still has to be proven.

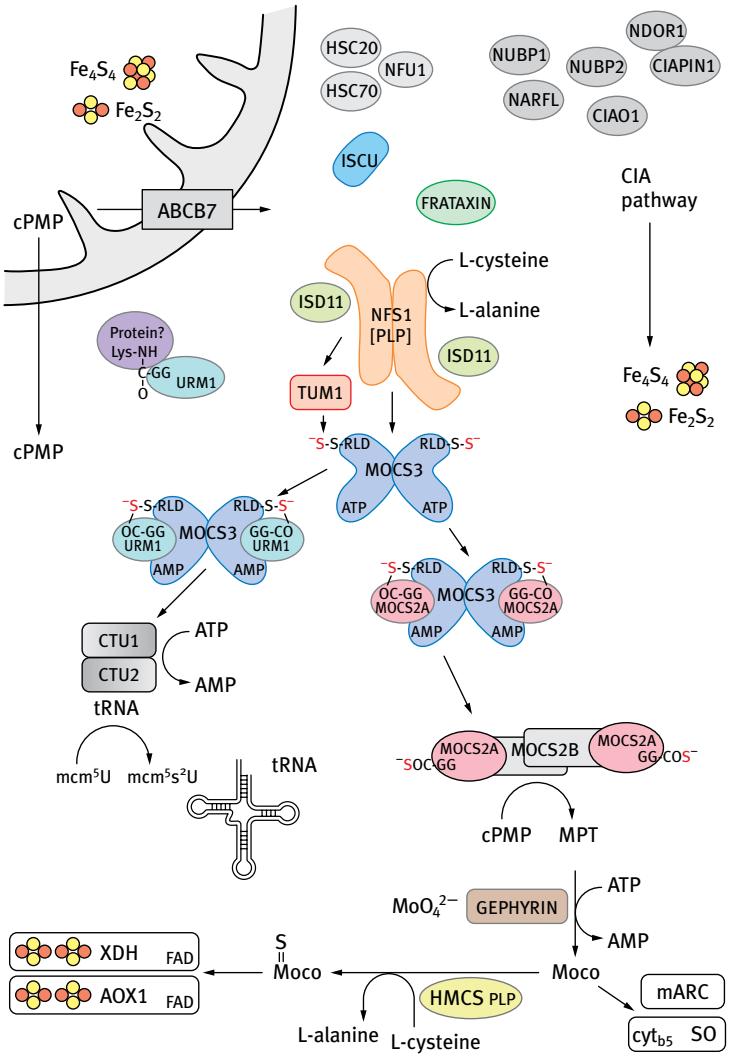

Fig. 12.9: Localization and role of proteins in the cytosol. Shown is the localization of proteins involved in Fe-S cluster biosynthesis, Moco biosynthesis, and tRNA thiolation and their connection in the cytosol. The enzymes in which synthesized Moco is inserted are shown schematically.

It has been reported that small amounts of NFS1 are present in the cytosol, where NFS1 interacts with MOCS3 [17]. Thus, cytosolic NFS1 is an important sulfur supplier for both Moco biosynthesis and tRNA thiolation [22]. The interaction of NFS1 and MOCS3 was revealed using Förster resonance energy transfer and a split EGFP system. The colocalization of NFS1 and MOCS3 in the cytosol was additionally confirmed by immunodetection of fractionated cells and localization studies using confocal fluorescence microscopy [17]. However, although the role of NFS1 in the cytosol for sulfur transfer to MOCS3 seems to be established, the involvement of ISD11 in this reaction still remains unclear. Thus far, ISD11 was described as a stabilizing factor of NFS1 in eukaryotes that is essential for its activity in Fe-S cluster formation in mitochondria [111]. In the absence of ISD11, NFS1 is prone to aggregation and Fe-S clusters cannot be formed [18, 112]. However, localization studies showed that ISD11 mainly is located in mitochondria and the nucleus in human cells [111]. Thus, the role of ISD11 and its involvement in the interaction of NFS1 and MOCS3 in the cytosol still needs to be investigated. It is possible that MOCS3 might replace the role of ISD11 as a stabilizing protein to NFS1 in the cytosol. This also might imply that cytosolic NFS1 is only involved in Moco biosynthesis and tRNA thiolation in conjunction with MOCS3, whereas in the absence of ISD11, it has no role in Fe-S cluster biosynthesis.

For Moco biosynthesis, cPMP is transferred from mitochondria to the cytosol, where two sulfur molecules are inserted to build the dithiolene group of MPT [99]. In this reaction, the MPT synthase composed of MOCS2A and MOCS2B is directly involved (see Section 12.2.1.2) [20]. In humans, the *MOCS2* locus encodes the two subunits of MPT synthase, MOCS2A and MOCS2B in a bicistronic transcript, from overlapping reading frames [42]. *In vitro* translation and mutagenesis experiments demonstrated that *MOCS2A* and *MOCS2B* are translated independently, from two alternative *MOCS2* splice forms, I and III, which contain different first exons in alternative transcripts [113]. The sulfur-relay system for Moco biosynthesis for the formation of the dithiolene moiety in MPT was shown to consist of the NFS1-C239 persulfide, the MOCS3-C412 persulfide, and the MOCS2A-G88 thiocarboxylate [17–20] (Fig. 12.9).

In a similar manner, the sulfur relay for tRNA thiolation in the cytosol is linked directly to Moco biosynthesis by the MOCS3 protein, which interacts with URM1 and forms the thiocarboxylate group on URM1-G101 (Fig. 12.9) [21, 92]. The interaction between MOCS3 and URM1 was revealed using Förster resonance energy transfer, in addition to functional *in vitro* studies for tRNA thiolation [21]. Here, MOCS3 is the E1-like protein of URM1 activating the C-terminal Gly88 under ATP consumption. The C-terminus of URM1 is first activated as an acyl-adenylate intermediate (-COAMP) and then thiocarboxylated (-COSH) by the persulfide group on the C-terminal RLD of MOCS3-C412, which originates from the NFS1-C239 persulfide [18]. The activated URM1-thiocarboxylate can be utilized in subsequent reactions for 2-thiouridine formation, mediated by a heterodimeric complex consisting of CTU1 and CTU2 in humans [21, 88].

In the cytosolic pathway for tRNA thiolation in yeast, the involvement of the mercaptopyruvate sulfur-tranferase Tum1p was shown [7]. Tum1p is a rhodanese-like

protein with two RLDs, which was shown to be localized in the mitochondria and the cytosol [114]. An *in vitro* sulfur transfer experiment revealed that Tum1p stimulates the L-cysteine desulfurase activity of Nfs1p and accepts the sulfur from this protein [7]. Thus, Tum1p may function as a mediator between Nfs1p and its sulfur acceptor proteins, adding another protein component to the sulfur relay system. It has been suggested for yeast that the sulfur moiety in mitochondria is transferred from Nfs1 to the relay protein Tum1p. Because, in yeast, Nfs1p has not been revealed to reside in the cytosol so far, it has been suggested that Tum1 may function as a sulfur shuttle between the mitochondrial and the cytosolic compartments due to the dual localization of Tum1p. However, the proposed retrograde transfer of sulfur-loaded Tum1p after its interaction with Nfs1p from mitochondria to the cytosol occurs has not been observed and remains only speculative [22]. In humans, TUM1 was also shown to be localized in the cytosol and in mitochondria [114]. However, its involvement in tRNA thiolation and its interaction with cytosolic or mitochondrial NFS1 has not yet been reported, and its role in the sulfur-relay system between NFS1 and MOCS3 in the human cytosol remains to be elucidated. Because NFS1 is able to directly interact with MOCS3 in the cytosol, the role of TUM1 might be restricted to conditions of sulfur starvation or oxidative stress, by enhancing the activity of NFS1 or making the sulfur-tranfer process more specific.

For yeast mcm^5s^2U formation (in cytoplasmic tRNAs), it was shown that components of the CIA apparatus for cytoplasmic (Fe-S) protein assembly and the scaffold proteins for the mitochondrial ISC machinery are required, which indicates that cytoplasmic 2-thiouridine formation essentially requires a protein containing an (Fe-S) cluster in yeast [22, 87]. The Fe-S containing protein has not been identified so far. Because, in humans, the proteins NFS1, MOCS3, URM1, CTU1, and CTU2 are sufficient for the formation of the s^2U in mcm^5U-modified tRNAs, CTU1 and CTU2 would be the only candidates for being Fe-S-containing proteins. The requirement and nature of Fe-S clusters in tRNA thiolation in humans needs to be investigated in the future.

12.3.3 Role of NFS1, ISD11, URM1, and MOCS2A in the nucleus

In addition to the localization of NFS1 in mitochondria and the cytosol, NFS1 was also detected in the nucleus [17, 111]. However, its function of this compartment still needs to be revealed. Recent studies also showed that ISD11 is additionally detected in the nucleus, but it is not clear yet whether both proteins interact in this cellular compartment (Fig. 12.10) [17].

For yeast Nfs1p, a small but significant portion was identified to be localized to the nucleus and was shown to play an unknown essential role in cell viability that depended on its role as a L-cysteine desulfurase [115]. It has been suggested that the role of Nfs1p in the nucleus might be the synthesis Fe-S clusters for nuclear Fe-S proteins.

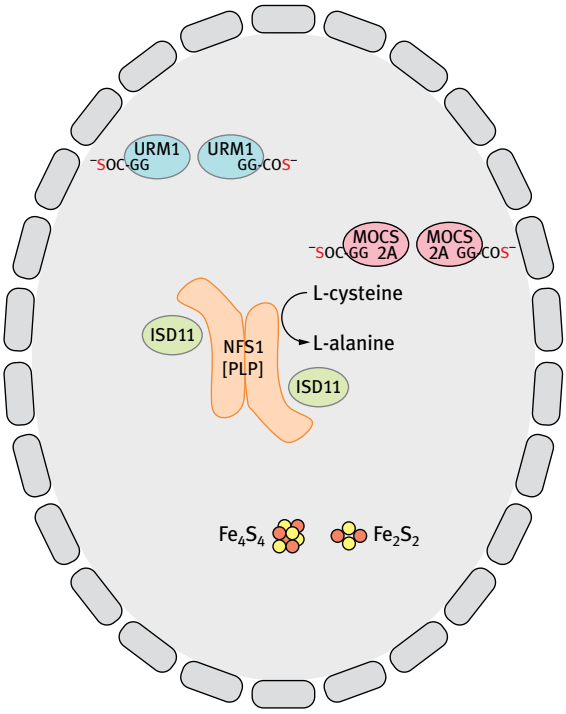

Fig. 12.10: Localization and role of proteins in the nucleus. Shown is the localization of proteins with a role in Fe-S cluster biosynthesis, Moco biosynthesis, and tRNA thiolation in the nucleus. The roles of NFS1, ISD11, URM1, and MOCS2A in the nucleus are not yet clear to date.

Another function might also be an involvement in the repair or maintenance of pre-assembled Fe-S clusters or the thiolation of nuclear tRNAs [115]. However, the role of Nfs1 in the nucleus remains unclear so far. Additionally, it is not known whether a similar phenotype exists for cell viability in human NFS1.

Additionally, URM1 and MOCS2A were identified in the nucleus (Fig. 12.10) [19, 21], where their specific functions remain unclear. For URM1, van der Veen *et al.* [88] identified targets of urmylation in response to oxidative stress in humans, among which were proteins involved in nuclear transport such as CAS, a protein involved in the shuttling between cytosol and nucleus. The role of the nucleocytoplasmic shuttling factor CAS as a target of urmylation would link the nuclear transport to oxidative stress, which is in good agreement with the observation that nuclear import is impaired upon oxidant treatment [116]. Speculation on the influence of urmylation on the arrest of nuclear transport is underlined by similar phenotypes of CAS depletion [117] and URM1 silencing [118], which both result in the arrest in G2/M phase. Thus, a contribution of URM1 to the control of global processes such as nuclear transport, cytokinesis, and cell cycle progression is possible. The role of MOCS2A in the nucleus has not been studied so far. In total, several proteins involved in cytoplasmic

Fe-S cluster formation, Moco biosynthesis and tRNA thiolation were also identified to be located in the nucleus, namely NFS1, ISD11, URM1, and MOCS2A, although their functions still remain unclear in this compartment.

Acknowledgments

The author thanks all current and former members of their research groups in addition to collaboration partners who were involved in this work over the past years and decades. The work was mainly supported by continuous grants of the Deutsche Forschungsgemeinschaft to S.L. Special thanks goes to Mita Mullick Chowdhury for critical reading of the manuscript.

References

[1] Beinert H. A tribute to sulfur. Eur J Biochem 2000;267:5657–64.
[2] Kessler D. Enzymatic activation of sulfur for incorporation into biomolecules in prokaryotes. FEMS Microbiol Rev 2006;30:825–40.
[3] Hidese R, Mihara H, Esaki N. Bacterial cysteine desulfurases: versatile key players in biosynthetic pathways of sulfur-containing biofactors. Applied Microbiol Biotechnol 2011;91:47–61.
[4] Bordo D, Bork P. The rhodanese/Cdc25 phosphatase superfamily. EMBO Rep 2002;3:741–746.
[5] Rouault TA. Biogenesis of iron-sulfur clusters in mammalian cells: new insights and relevance to human disease. Dis Models Mech 2012;5:155–64.
[6] Mendel RR, Kruse T. Cell biology of molybdenum in plants and humans. Biochim Biophys Acta 2012;1823:1568–79.
[7] Noma A, Sakaguchi Y, Suzuki T. Mechanistic characterization of the sulfur-relay system for eukaryotic 2-thiouridine biogenesis at tRNA wobble positions. Nucleic Acids Res 2009;37:1335–52.
[8] Mueller EG. Trafficking in persulfides: delivering sulfur in biosynthetic pathways. Nat Chem Biol 2006;2:185–94.
[9] Zheng L, White RH, Cash VL, Dean DR. Mechanism for the desulfurization of L-cysteine catalyzed by the nifS gene product. Biochemistry 1994;33:4714–20.
[10] Tsai CL, Barondeau DP. Human frataxin is an allosteric switch that activates the Fe-S cluster biosynthetic complex. Biochemistry 2010;49:9132–9.
[11] Bridwell-Rabb J, Winn AM, Barondeau DP. Structure-function analysis of Friedreich's ataxia mutants reveals determinants of frataxin binding and activation of the Fe-S assembly complex. Biochemistry 2011;50:7265–74.
[12] Schmucker S, Martelli A, Colin F, et al. Mammalian frataxin: an essential function for cellular viability through an interaction with a preformed ISCU/NFS1/ISD11 iron-sulfur assembly complex. PloS One 2011;6:e16199.
[13] Uhrigshardt H, Singh A, Kovtunovych G, Ghosh M, Rouault TA. Characterization of the human HSC20, an unusual DnaJ type III protein, involved in iron-sulfur cluster biogenesis. Hum Mol Genet 2010;19:3816–34.
[14] Hanzelmann P, Hernandez HL, Menzel C, et al. Characterization of MOCS1A, an oxygen-sensitive iron-sulfur protein involved in human molybdenum cofactor biosynthesis. J Biol Chem 2004;279:34721–32.
[15] Johnson JL, Rajagopalan KV. Structural and metabolic relationship between the molybdenum cofactor and urothione. Proc Natl Acad Sci USA 1982;79:6856–6860.

[16] Schwarz G, Mendel RR, Ribbe MW. Molybdenum cofactors, enzymes and pathways. Nature 2009;460:839–47.
[17] Marelja Z, Mullick Chowdhury M, Dosche C, et al. The L-cysteine desulfurase NFS1 is localized in the cytosol where it provides the sulfur for molybdenum cofactor biosynthesis in humans. PloS One 2013;8:e60869.
[18] Marelja Z, Stocklein W, Nimtz M, Leimkuhler S. A novel role for human Nfs1 in the cytoplasm: Nfs1 acts as a sulfur donor for MOCS3, a protein involved in molybdenum cofactor biosynthesis. J Biol Chem 2008;283:25178–85.
[19] Matthies A, Rajagopalan KV, Mendel RR, Leimkuhler S. Evidence for the physiological role of a rhodanese-like protein for the biosynthesis of the molybdenum cofactor in humans. Proc Natl Acad Sci USA 2004;101:5946–51.
[20] Leimkuhler S, Freuer A, Araujo JA, Rajagopalan KV, Mendel RR. Mechanistic studies of human molybdopterin synthase reaction and characterization of mutants identified in group B patients of molybdenum cofactor deficiency. J Biol Chem 2003;278:26127–34.
[21] Chowdhury MM, Dosche C, Lohmannsroben HG, Leimkuhler S. Dual role of the molybdenum cofactor biosynthesis protein MOCS3 in tRNA thiolation and molybdenum cofactor biosynthesis in humans. J Biol Chem 2012;287:17297–307.
[22] Noma A, Shigi N, Suzuki T. Biogenesis and functions of thio-compounds in transfer RNA: Comparison of bacterial and eukaryotic thiolation machineries. In: Grosjean H, ed. DNA and RNA modification enzymes: structure, mechanism, function and evolution. Landes Bioscience; 2009:392–405.
[23] El Yacoubi B, Bailly M, de Crecy-Lagard V. Biosynthesis and function of posttranscriptional modifications of transfer RNAs. Annu Rev Genet 2012;46:69–95.
[24] Rajagopalan KV. Biosynthesis of the molybdenum cofactor. In: Neidhardt FC, ed. Escherichia coli and Salmonella. Cellular and molecular biology. Washington (DC): ASM Press; 1996:674–9.
[25] Wuebbens MM, Rajagopalan KV. Structural characterization of a molybdopterin precursor. J Biol Chem 1993;268:13493–13498.
[26] Pitterle DM, Johnson JL, Rajagopalan KV. In vitro synthesis of molybdopterin from precursor Z using purified converting factor. Role of protein-bound sulfur in formation of the dithiolene. J Biol Chem 1993;268:13506–13509.
[27] Joshi MS, Johnson JL, Rajagopalan KV. Molybdenum cofactor biosynthesis in Escherichia coli mod and mog mutants. J Bacteriol 1996;178:4310–4312.
[28] Hille R, Nishino T, Bittner F. Molybdenum enzymes in higher organisms. Coord Chem Rev 2011;255:1179–1205.
[29] Duran M, Beemer FA, van der Heiden C, et al. Combined deficiency of xanthine oxidase and sulphite oxidase: a defect of molybdenum metabolism or transport? J Inherit Metab Dis 1978;1:175–178.
[30] Duran M, de Bree PK, de Klerk JBC, Dorland L, Berger R. Molybdenum cofactor deficiency: clinical presentation and laboratory diagnosis. Int Pediatr 1996;11:334–338.
[31] Mendel RR, Schwarz G. Molybdenum cofactor biosynthesis in plants and humans. Coord Chem Rev 2011;255:1145–1158.
[32] Reiss J, Cohen N, Dorche C, et al. Mutations in a polycistronic nuclear gene associated with molybdenum cofactor deficiency. Nat Genet 1998;20:51–53.
[33] Reiss J. Genetics of molybdenum cofactor deficiency. Hum Genet 2000;106:157–163.
[34] Leimkühler S, Wuebbens M, Rajagopalan KV. The history of the discovery of the molybdenum cofactor and novel aspects of its biosynthesis in bacteria. Coord Chem Rev 2011;255:1129–1144.
[35] Santamaria-Araujo JA, Fischer B, Otte T, et al. The tetrahydropyranopterin structure of the sulfur- and metal-free molybdenum cofactor precursor. J Biol Chem 2004;279:15994–9.
[36] Reiss J, Christensen E, Kurlemann G, Zabot M-T, Dorche C. Genomic structure and mutational spectrum of the bicistronic MOCS1 gene defective in molybdenum cofactor deficiency type A. Hum Genet 1998;103:639–644.

[37] Sofia HJ, Chen G, Hetzler BG, Reyes-Spindola JF, Miller NE. Radical SAM, a novel protein superfamily linking unresolved steps in familiar biosynthetic pathways with radical mechanisms: functional characterization using new analysis and information visualization methods. Nucleic Acids Res 2001;29:1097–1106.
[38] Hanzelmann P, Schindelin H. Crystal structure of the S-adenosylmethionine-dependent enzyme MoaA and its implications for molybdenum cofactor deficiency in humans. Proc Natl Acad Sci USA 2004;101:12870–5.
[39] Hanzelmann P, Schindelin H. Binding of 5′-GTP to the C-terminal FeS cluster of the radical S-adenosylmethionine enzyme MoaA provides insights into its mechanism. Proc Natl Acad Sci USA 2006;103:6829–34.
[40] Hover BM, Loksztejn A, Ribeiro AA, Yokoyama K. Identification of a cyclic nucleotide as a cryptic intermediate in molybdenum cofactor biosynthesis. J Am Chem Soc 2013;135:7019–32.
[41] Stallmeyer B, Drugeon G, Reiss J, Haenni AL, Mendel RR. Human molybdopterin synthase gene: identification of a bicistronic transcript with overlapping reading frames. Am J Hum Genet 1999;64:698–705.
[42] Gutzke G, Fischer B, Mendel RR, Schwarz G. Thiocarboxylation of molybdopterin synthase provides evidence for the mechanism of dithiolene formation in metal-binding pterins. J Biol Chem 2001;276:36268–36274.
[43] Rudolph MJ, Wuebbens MM, Rajagopalan KV, Schindelin H. Crystal structure of molybdopterin synthase and its evolutionary relationship to ubiquitin activation. Nat Struct Biol 2001;8:42–6.
[44] Daniels JN, Wuebbens MM, Rajagopalan KV, Schindelin H. Crystal structure of a molybdopterin synthase-precursor Z complex: insight into its sulfur transfer mechanism and its role in molybdenum cofactor deficiency. Biochemistry 2008;47:615–26.
[45] Wuebbens MM, Rajagopalan KV. Mechanistic and mutational studies of Escherichia coli molybdopterin synthase clarify the final step of molybdopterin biosynthesis. J Biol Chem 2003;278:14523–14532.
[46] Stallmeyer B, Coyne KE, Wuebbens MM, Johnson JL, Rajagopalan KV, Mendel RR. The cDNA sequence of MOCS3, human molybdopterin synthase sulfurylase. GenBank accession number AF102544; 1998.
[47] Lake MW, Wuebbens MM, Rajagopalan KV, Schindelin H. Mechanism of ubiquitin activation revealed by the structure of a bacterial MoeB-MoaD complex. Nature 2001;414:325–9.
[48] Matthies A, Nimtz M, Leimkuhler S. Molybdenum cofactor biosynthesis in humans: identification of a persulfide group in the rhodanese-like domain of MOCS3 by mass spectrometry. Biochemistry 2005;44:7912–20.
[49] Stallmeyer B, Schwarz G, Schulze J, et al. The neurotransmitter receptor-anchoring protein gephyrin reconstitutes molybdenum cofactor biosynthesis in bacteria, plants, and mammalian cells. Proc Natl Acad Sci USA 1999;96:1333–1338.
[50] Belaidi AA, Schwarz G. Metal insertion into the molybdenum cofactor: product-substrate channelling demonstrates the functional origin of domain fusion in gephyrin. Biochem J 2013;450:149–57.
[51] Schwarz G. Molybdenum cofactor biosynthesis and deficiency. Cell Mol Life Sci 2005;62:2792–810.
[52] Herweg J, Schwarz G. Splice-specific glycine receptor binding, folding, and phosphorylation of the scaffolding protein gephyrin. J Biol Chem 2012;287:12645–56.
[53] Wahl RC, Rajagopalan KV. Evidence for the inorganic nature of the cyanolyzable sulfur of molybdenum hydroxylases. J Biol Chem 1982;257:1354–1359.
[54] Hille R. The mononuclear molybdenum enzymes. Chem Rev 1996;96:2757–2816.
[55] Anantharaman V, Aravind L. MOSC domains: ancient, predicted sulfur-carrier domains, present in diverse metal-sulfur cluster biosynthesis proteins including molybdenum cofactor sulfurases. FEMS Microbiol Lett 2002;207:55–61.

[56] Peretz H, Naamati MS, Levartovsky D, et al. Identification and characterization of the first mutation (Arg776Cys) in the C-terminal domain of the Human Molybdenum Cofactor Sulfurase (HMCS) associated with type II classical xanthinuria. Mol Genet Metab 2007;91:23–9.
[57] Bittner F, Oreb M, Mendel RR. ABA3 is a molybdenum cofactor sulfurase required for activation of aldehyde oxidase and xanthine dehydrogenase in Arabidopsis thaliana. J Biol Chem 2001;276:40381–4.
[58] Wollers S, Heidenreich T, Zarepour M, et al. Binding of sulfurated molybdenum cofactor to the C-terminal domain of ABA3 from Arabidopsis thaliana provides insight into the mechanism of molybdenum cofactor sulfuration. J Biol Chem 2008;283:9642–50.
[59] Lehrke M, Rump S, Heidenreich T, Wissing J, Mendel RR, Bittner F. Identification of persulfide-binding and disulfide-forming cysteine residues in the NifS-like domain of the molybdenum cofactor sulfurase ABA3 by cysteine-scanning mutagenesis. Biochem J 2012;441:823–32.
[60] Klein JM, Schwarz G. Cofactor-dependent maturation of mammalian sulfite oxidase links two mitochondrial import pathways. J Cell Sci 2012;125:4876–85.
[61] Neumann M, Leimkuhler S. The role of system-specific molecular chaperones in the maturation of molybdoenzymes in bacteria. Biochem Res Int 2011;2011:850–924.
[62] Hille R. The molybdenum oxotransferases and related enzymes. Dalton transactions 2013;42:3029–42.
[63] Neumann M, Stocklein W, Leimkuhler S. Transfer of the molybdenum cofactor synthesized by Rhodobacter capsulatus MoeA to XdhC and MobA. J Biol Chem 2007;282:28493–500.
[64] Neumann M, Stocklein W, Walburger A, Magalon A, Leimkuhler S. Identification of a Rhodobacter capsulatus L-cysteine desulfurase that sulfurates the molybdenum cofactor when bound to XdhC and before its insertion into xanthine dehydrogenase. Biochemistry 2007;46:9586–95.
[65] Schumann S, Saggu M, Moller N, et al. The mechanism of assembly and cofactor insertion into Rhodobacter capsulatus xanthine dehydrogenase. J Biol Chem 2008;283:16602–11.
[66] Kisker C, Schindelin H, Pacheco A, et al. Molecular basis of sulfite oxidase deficiency from the structure of sulfite oxidase. Cell 1997;91:973–983.
[67] Feng C, Kedia RV, Hazzard JT, Hurley JK, Tollin G, Enemark JH. Effect of solution viscosity on intramolecular electron transfer in sulfite oxidase. Biochemistry 2002;41:5816–21.
[68] Johnson JL, Coyne KE, Rajagopalan KV, et al. Molybdopterin synthase mutations in a mild case of molybdenum cofactor deficiency. Am J Med Genet 2001;104:169–73.
[69] Johnson JL, Duran M. Molybdenum cofactor deficiency and isolated sulfite oxidase deficiency. In: Scriver CR, Beaudet AL, Sly WS, Valle D, Childs B, Vogelstein B, eds. The metabolic and molecular bases of inherited disease. 8th edn. New York: McGraw-Hill; 2001:3163–77.
[70] Johnson JL, Garrett RM, Rajagopalan KV. The biochemistry of molybdenum cofactor deficiency and isolated sulfite oxidase deficiency. Int Pediatr 1997;12:22–26.
[71] Johnson JL, Rajagopalan KV. Human sulfite oxidase deficiency. Characterization of the molecular defect in a multicomponent system. J Clin Invest 1976;58:551–556.
[72] Gruenewald S, Wahl B, Bittner F, et al. The fourth molybdenum containing enzyme mARC: cloning and involvement in the activation of N-hydroxylated prodrugs. J Med Chem 2008;51:8173–7.
[73] Wahl B, Reichmann D, Niks D, et al. Biochemical and spectroscopic characterization of the human mitochondrial amidoxime reducing components hmARC-1 and hmARC-2 suggests the existence of a new molybdenum enzyme family in eukaryotes. J Biol Chem 2010;285:37847–59.
[74] Havemeyer A, Grunewald S, Wahl B, et al. Reduction of N-hydroxy-sulfonamides, including N-hydroxy-valdecoxib, by the molybdenum-containing enzyme mARC. Drug Metab Dispos 2010;38:1917–21.
[75] Harrison R. Physiological roles of xanthine oxidoreductase. Drug Metab Rev 2004;36:363–75.

[76] Garattini E, Fratelli M, Terao M. Mammalian aldehyde oxidases: genetics, evolution and biochemistry. Cell Mol Life Sci 2008;65:1019–48.
[77] Garattini E, Mendel R, Romao MJ, Wright R, Terao M. Mammalian molybdo-flavoenzymes, an expanding family of proteins: structure, genetics, regulation, function and pathophysiology. Biochem J 2003;372:15–32.
[78] Nishino T, Okamoto K, Kawaguchi Y, et al. Mechanism of the conversion of xanthine dehydrogenase to xanthine oxidase: identification of the two cysteine disulfide bonds and crystal structure of a non-convertible rat liver xanthine dehydrogenase mutant. J Biol Chem 2005;280:24888–94.
[79] Nishino T. The conversion of xanthine dehydrogenase to xanthine oxidase and the role of the enzyme in reperfusion injury. J Biochem (Tokyo) 1994;116:1–6.
[80] McCord JM. Oxygen-derived free radicals in postischemic tissue injury. N Engl J Med 1985;312:159–163.
[81] Komai H, Massey V, Palmer G. The preparation and properties of deflavo xanthine oxidase. J Biol Chem 1969;244:1692–700.
[82] Rozenski J, Crain PF, McCloskey JA. The RNA modification database: 1999 update. Nucleic Acids Res 1999;27:196–7.
[83] Yokoyama S, Watanabe T, Murao K, et al. Molecular mechanism of codon recognition by tRNA species with modified uridine in the first position of the anticodon. Proc Natl Acad Sci USA 1985;82:4905–9.
[84] Agris PF, Soll D, Seno T. Biological function of 2-thiouridine in Escherichia coli glutamic acid transfer ribonucleic acid. Biochemistry 1973;12:4331–7.
[85] Durant PC, Bajji AC, Sundaram M, Kumar RK, Davis DR. Structural effects of hypermodified nucleosides in the Escherichia coli and human tRNALys anticodon loop the effect of nucleosides s2U, mcm5U, mcm5s2U, mnm5s2U, t6A, and ms2t6A. Biochemistry 2005;44:8078–89.
[86] Rezgui VA, Tyagi K, Ranjan N, et al. tRNA tKUUU, tQUUG, and tEUUC wobble position modifications fine-tune protein translation by promoting ribosome A-site binding. Proc Natl Acad Sci USA 2013;110:12289–94.
[87] Suzuki T. Biosynthesis and function of tRNA wobble modifications. Top Curr Genet 2005;12:23–69.
[88] Van der Veen AG, Schorpp K, Schlieker C, et al. Role of the ubiquitin-like protein Urm1 as a noncanonical lysine-directed protein modifier. Proc Natl Acad Sci USA 2011;108:1763–70.
[89] Leidel S, Pedrioli PG, Bucher T, et al. Ubiquitin-related modifier Urm1 acts as a sulphur carrier in thiolation of eukaryotic transfer RNA. Nature 2009;458:228–32.
[90] Pedrioli PG, Leidel S, Hofmann K. Urm1 at the crossroad of modifications. In: “Protein modifications: beyond the usual suspects” review series. EMBO Rep 2008;9:1196–202.
[91] Xu J, Zhang J, Wang L, et al. Solution structure of Urm1 and its implications for the origin of protein modifiers. Proc Natl Acad Sci USA 2006;103:11625–30.
[92] Schmitz J, Chowdhury MM, Hanzelmann P, et al. The sulfurtransferase activity of Uba4 presents a link between ubiquitin-like protein conjugation and activation of sulfur carrier proteins. Biochemistry 2008;47:6479–89.
[93] Lill R, Muhlenhoff U. Iron-sulfur protein biogenesis in eukaryotes: components and mechanisms. Annu Rev Cell Dev Biol 2006;22:457–86.
[94] Colin F, Martelli A, Clemancey M, et al. Mammalian frataxin controls sulfur production and iron entry during de novo Fe4S4 cluster assembly. J Am Chem Soc 2013;135:733–40.
[95] Pastore A, Puccio H. Frataxin: a protein in search for a function. J Neurochem 2013;126:43–52.
[96] Gross-Hard S, Reiss J. The bicistronic MOCS1 gene has alternative start codons on two mutually exclusive exons. Mol Genet Metab 2002;76:340–343.
[97] Gray TA, Nicholls RD. Diverse splicing mechanisms fuse the evolutionarily conserved bicistronic MOCS1A and MOCS1B open reading frames. RNA 2000;6:928–936.

[98] Hänzelmann P, Schwarz G, Mendel RR. Functionality of alternative splice forms of the first enzymes involved in human molybdenum cofactor biosynthesis. J Biol Chem 2002;277:18303–18312.
[99] Teschner J, Lachmann N, Schulze J, et al. A novel role for Arabidopsis mitochondrial ABC transporter ATM3 in molybdenum cofactor biosynthesis. Plant Cell 2010;22:468–80.
[100] Hausmann A, Samans B, Lill R, Muhlenhoff U. Cellular and mitochondrial remodeling upon defects in iron-sulfur protein biogenesis. J Biol Chem 2008;283:8318–30.
[101] Sasarman F, Antonicka H, Horvath R, Shoubridge EA. The 2-thiouridylase function of the human MTU1 (TRMU) enzyme is dispensable for mitochondrial translation. Hum Mol Genet 2011;20: 4634–43.
[102] Yadav PK, Yamada K, Chiku T, Koutmos M, Banerjee R. Structure and kinetic analysis of H2S production by human mercaptopyruvate sulfurtransferase. J Biol Chem 2013;288:20002–13.
[103] James AM, Wei YH, Pang CY, Murphy MP. Altered mitochondrial function in fibroblasts containing MELAS or MERRF mitochondrial DNA mutations. Biochem J 1996;318:401–7.
[104] Antonicka H, Floryk D, Klement P, et al. Defective kinetics of cytochrome c oxidase and alteration of mitochondrial membrane potential in fibroblasts and cytoplasmic hybrid cells with the mutation for myoclonus epilepsy with ragged-red fibres ("MERRF") at position 8344 nt. Biochem J 1999;342:537–44.
[105] Boczonadi V, Smith PM, Pyle A, et al. Altered 2-thiouridylation impairs mitochondrial translation in reversible infantile respiratory chain deficiency. Hum Mol Genet 2013;22:4602–15.
[106] Gaignard P, Gonzales E, Ackermann O, et al. Mitochondrial infantile liver disease due to TRMU gene mutations: three new cases. JIMD Rep 2013;11:117–23.
[107] Lill R, Dutkiewicz R, Elsasser HP, et al. Mechanisms of iron-sulfur protein maturation in mitochondria, cytosol and nucleus of eukaryotes. Biochim Biophys Acta 2006;1763:652–67.
[108] Netz DJ, Stumpfig M, Dore C, Muhlenhoff U, Pierik AJ, Lill R. Tah18 transfers electrons to Dre2 in cytosolic iron-sulfur protein biogenesis. Nature Chem Biol 2010;6:758–65.
[109] Sharma AK, Pallesen LJ, Spang RJ, Walden WE. Cytosolic iron-sulfur cluster assembly (CIA) system: factors, mechanism, and relevance to cellular iron regulation. J Biol Chem 2010;285:26745–51.
[110] Stehling O, Netz DJ, Niggemeyer B, et al. Human Nbp35 is essential for both cytosolic iron-sulfur protein assembly and iron homeostasis. Mol Cell Biol 2008;28:5517–28.
[111] Shi Y, Ghosh MC, Tong WH, Rouault TA. Human ISD11 is essential for both iron-sulfur cluster assembly and maintenance of normal cellular iron homeostasis. Hum Mol Genet 2009;18: 3014–25.
[112] Wiedemann N, Urzica E, Guiard B, et al. Essential role of Isd11 in mitochondrial iron-sulfur cluster synthesis on Isu scaffold proteins. EMBO J 2006;25:184–95.
[113] Hahnewald R, Leimkuhler S, Vilaseca A, Acquaviva-Bourdain C, Lenz U, Reiss J. A novel MOCS2 mutation reveals coordinated expression of the small and large subunit of molybdopterin synthase. Mol Genet Metab 2006;89:210–3.
[114] Nagahara N, Ito T, Kitamura H, Nishino T. Tissue and subcellular distribution of mercaptopyruvate sulfurtransferase in the rat: confocal laser fluorescence and immunoelectron microscopic studies combined with biochemical analysis. Histochem Cell Biol 1998;110:243–50.
[115] Nakai Y, Nakai M, Hayashi H, Kagamiyama H. Nuclear localization of yeast Nfs1p is required for cell survival. J Biol Chem 2001;276:8314–20.
[116] Kodiha M, Tran D, Morogan A, Qian C, Stochaj U. Dissecting the signaling events that impact classical nuclear import and target nuclear transport factors. PloS One 2009;4:e8420.
[117] Ogryzko VV, Brinkmann E, Howard BH, Pastan I, Brinkmann U. Antisense inhibition of CAS, the human homologue of the yeast chromosome segregation gene CSE1, interferes with mitosis in HeLa cells. Biochemistry 1997;36:9493–500.
[118] Schlieker CD, Van der Veen AG, Damon JR, Spooner E, Ploegh HL. A functional proteomics approach links the ubiquitin-related modifier Urm1 to a tRNA modification pathway. Proc Natl Acad Sci USA 2008;105:18255–60.

13 Iron-sulphur proteins and genome stability

Kerstin Gari

Summary

The blueprint of each cell – be it a single bacterium or part of a multicellular organism, such as man – is encoded in its genome. For a cell to remain functional throughout its life cycle, its genetic program has to remain accurate, and hence, its genome has to be protected from damage. Such damage can be the result of exogenous factors, such as ultraviolet light, or endogenous factors, such as oxidative stress. Moreover, the ability of a cell to replicate its genome and divide into two identical daughter cells is a naturally complicated process that can pose a problem to genome integrity. Not surprisingly, a huge number of proteins work together to faithfully replicate DNA and to detect, signal, and repair DNA damage. Failure to do so results in genome instability, one of the hallmarks of cancer.

For a long time, it appeared that iron-sulphur (FeS) proteins are relatively rare in the processes of DNA replication and repair. Given that upon FeS cluster oxidation, free iron atoms can generate dangerous reactive oxygen species, this notion seemed rather intuitive. Over the last years, however, a surprisingly high number of proteins involved in DNA replication and repair have been identified to bind to an FeS cluster. In many cases, the function of the FeS cluster has remained elusive so far.

In this chapter, an overview of FeS proteins in DNA metabolism will be given and the potential role of the FeS cluster in these proteins will be discussed. The major focus will be on eukaryotic proteins, with some examples from the prokaryotic world.

13.1 The importance of genome stability

The maintenance of genome stability is essential for cellular function, and the consequences of genome instability are most dramatically exemplified in human cancer. As a common characteristic trait, tumor cells generally display gross chromosomal rearrangements and genetic mutations.

In recent years, it has become clear that genome instability is not a secondary effect of aberrant cellular behavior but rather one of the causes of tumor development. In the oncogene-induced DNA damage model (Fig. 13.1) it has been suggested that in early cancerous lesions, the activation of oncogenes leads to perturbed DNA replication due to the stalling and collapsing of DNA replication forks [1–5]. As a consequence of such DNA replication stress, the DNA damage checkpoint is activated, which involves a multitude of factors that decide to either repair the damage or (if it is beyond repair) to induce cell cycle arrest, apoptosis, or senescence. This response to DNA replication stress acts as a barrier to tumorigenesis and is dependent on a functional copy of the tumor suppressor gene *p53*.

DOI 10.1515/9783110479850-013

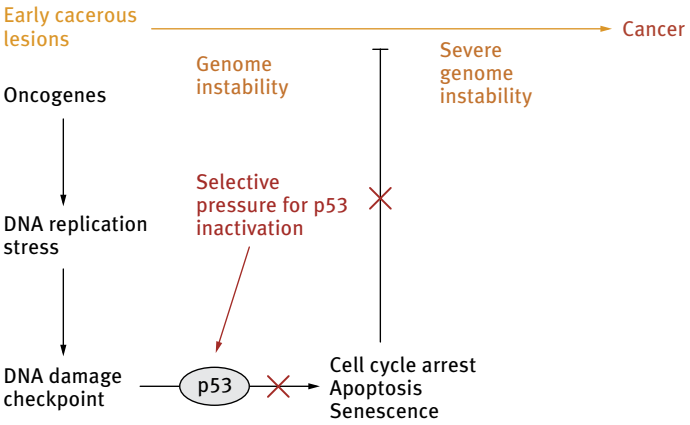

Fig. 13.1: Oncogene-induced DNA damage model.

This could be the end of the story of cancer if it was not for the adaptiveness of cancer cells. Instead, this initial tumorigenesis barrier creates selective pressure toward the inactivation of p53, which in turn allows full tumor development. Loss of heterozygosity (LOH), i.e. the loss of one of the two alleles of a gene, is one of the dangerous consequences of uncontrolled genome instability.

13.2 Link between iron-sulphur cluster biogenesis and genome stability

In 2008, Veatch and colleagues showed that LOH in yeast can also be caused by the loss of mitochondrial DNA [6]. They further demonstrated that nuclear genome instability did not occur as a consequence of dysfunctional cellular respiration but rather due to a defect in FeS cluster biogenesis. Based on their findings, they proposed that impaired FeS protein maturation might compromise the function of nuclear FeS proteins that function in DNA replication and repair, such as DNA primase [7], the helicase Rad3 [8], and the glycosylase Ntg2 [9]. Their hypothesis was based on the fact that maturation of nuclear FeS proteins – while primarily taking place in the cytoplasm – also depends on the mitochondrial iron-sulphur cluster (ISC) machinery [10].

While it is still controversial whether the ISC machinery is active both in mitochondria and the cytoplasm or whether an FeS cluster precursor is produced in mitochondria and then exported into the cytoplasm [11], it is well established that the subsequent maturation of nuclear FeS proteins is carried out in the cytoplasm by the cytoplasmic iron-sulphur assembly (CIA) machinery. In an early step, an FeS cluster is transiently assembled on a scaffold complex composed of the NTPases NBP35 and CFD1 [12, 13]. The loosely bound cluster is then transferred to FeS apoproteins, a process that requires the function of the WD40 repeat protein CIAO1 and the iron-only hydrogenase-like protein IOP1 [14–16].

Recently, two studies have found a molecular explanation for the link between FeS cluster biogenesis and proteins involved in DNA metabolism, as had been previously proposed [6].

Coming from either the FeS field, or the genome stability field, both studies identified the cytoplasmic HEAT-repeat protein MMS19 as a component of the CIA machinery that physically interacts with multiple FeS proteins involved in DNA metabolism [17, 18]. They further showed that MMS19 is required for FeS cluster transfer to FeS apoproteins and that in the absence of MMS19, the stability of multiple FeS proteins involved in DNA replication and repair is affected. As a consequence, both yeast and human cells depleted of MMS19 showed an altered response to agents that cause DNA damage or DNA replication stress. Moreover, *Mms19* knockout mice displayed early embryonic lethality, presumably because Mms19 deficiency has pleiotropic effects on multiple proteins involved in DNA metabolism [17].

The MMS19 interacting protein MIP18 was later shown to contribute substantially to FeS protein recognition by binding to the FeS cluster binding domain within apoproteins [19]. Interestingly, MIP18 had originally been identified in a proteome-wide screen for factors that contain hyperreactive cysteines [20], a feature that is commonly found in FeS biogenesis proteins. Future studies will therefore have to address whether MIP18 plays a direct role in FeS cluster transfer by transiently binding to an FeS cluster and handing it over to apoproteins.

Collectively, these data suggest that MMS19 and MIP18 physically and functionally link FeS cluster biogenesis to DNA replication and repair (Fig. 13.2).

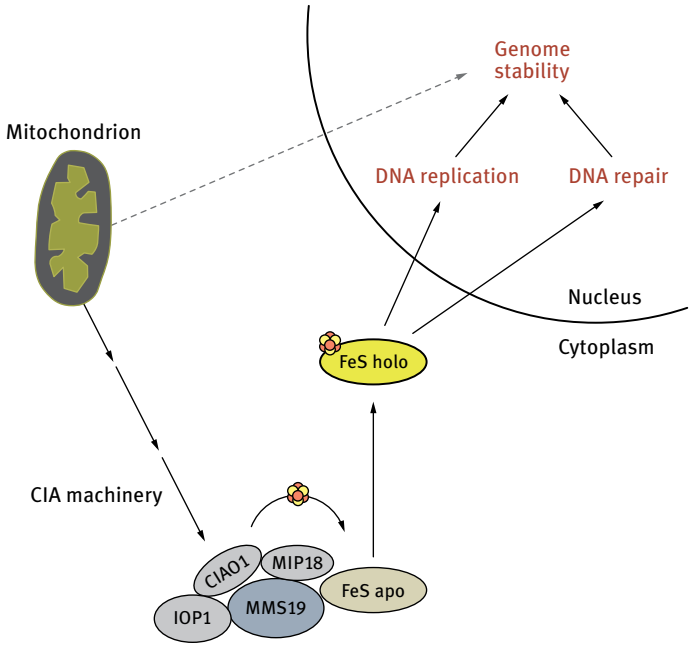

Fig. 13.2: MMS19 and MIP18 link FeS cluster biogenesis to DNA metabolism.

13.3 FeS proteins in DNA replication

DNA replication is a highly regulated process that involves the concerted action of a considerable number of proteins. Essentially, however, it requires unwinding of the parental DNA strands by a helicase activity and synthesis of the two daughter strands by the replicative DNA polymerases alpha, delta, and epsilon [21, 22].

Two complications arise from the intrinsic properties of DNA polymerases and the antiparallel nature of DNA: First, all DNA polymerases have a 5′-3′ polarity, which implies that one of the two DNA strands can be elongated in a continuous manner (the leading strand), whereas the other strand has to be synthesized in a discontinuous manner (the lagging strand).

The second complication stems from the fact that DNA polymerases can only synthesize DNA by extension of an existing nucleotide primer. DNA replication therefore relies on the activity of a complex formed of DNA primase and DNA polymerase alpha (Pol α) that can carry out the *de novo* synthesis of a short chimeric RNA-DNA primer on the parental template [23]. Following primer synthesis, the leading strand template will then be primarily replicated by DNA polymerase epsilon (Pol ε), whereas lagging strand synthesis is carried out by DNA polymerase delta (Pol δ) [24–26].

Due to its discontinuous mode of replication, initiation by DNA primase and Pol α has to take place multiple times during synthesis of the lagging strand. The switch between initial synthesis and processive replication requires the replication clamp proliferating cell nuclear antigen (PCNA) that displaces DNA primase-Pol α from the DNA template and loads Pol δ onto it [22, 27].

The stretches of replicated DNA that are created due to this discontinuous mode of replication are referred to as Okazaki fragments. When Pol δ reaches a downstream Okazaki fragment, it displaces a few nucleotides of the RNA primer and creates a 5′-single stranded flap structure [22]. Flap endonuclease 1 (FEN1) is required to cleave this short flap at the junction between double-stranded and single-stranded DNA and to create a structure that can be sealed by DNA ligase I [28, 29].

It is believed that Pol δ usually displays only limited strand displacement synthesis and that the resulting short flaps are readily cleaved by FEN1 [30]. However, in case longer flaps are created – at least in yeast – the activity of the helicase/nuclease DNA2 is required for Okazaki fragment maturation [29, 31, 32]. To date, however, it is unclear whether DNA2 can cleave such long flaps as the sole nuclease [33] or whether FEN1 and DNA2 functionally work together to sequentially cleave the flap [34–36] (Fig. 13.3).

In recent years, it has turned out that DNA polymerases alpha, delta, and epsilon [37], as well as DNA primase [7, 38] and DNA2 [39, 40], are all FeS proteins. Whereas it should be kept in mind that DNA replication in this paragraph was considerably simplified and more factors are involved, the number of FeS proteins in the very heart of the DNA replication machinery is nevertheless astonishing. Given that upon FeS cluster oxidation, free iron atoms can generate dangerous reactive oxygen species (ROS) *via* Fenton chemistry, having FeS clusters in DNA polymerases seems like putting the fox

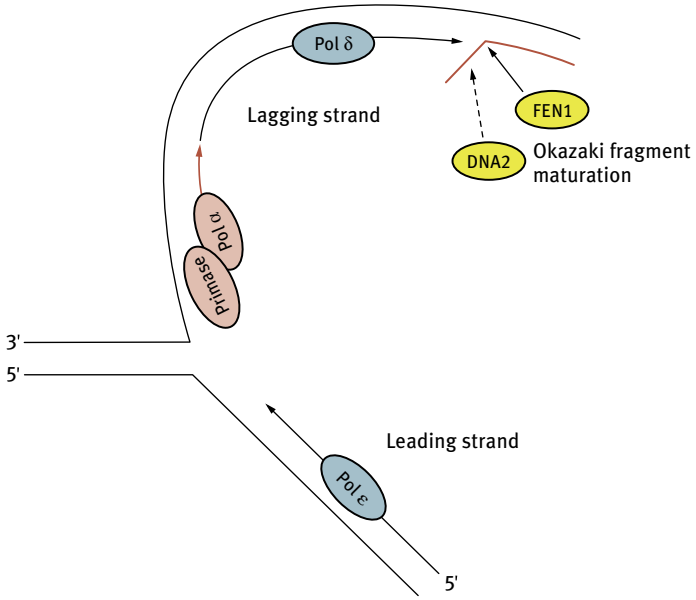

Fig. 13.3: DNA replication.

in charge of the henhouse. Unless, of course, FeS clusters in these enzymes carry out – as yet, unclear – functions that cannot be achieved with alternative co-factors.

13.3.1 DNA primase and DNA polymerase alpha

DNA primase and Pol α form an evolutionarily conserved complex that couples two activities crucial for replication initiation: first, the *de novo* synthesis of a 8–13-nucleotide-long RNA primer by the DNA-dependent RNA polymerase DNA primase; and second, the subsequent primer extension by a few dNTPs by Pol α [23].

DNA primase is composed of a small (PRI1) and a large (PRI2) subunit, both of which are required for viability in yeast [41]. Although PRI1 carries the catalytic activity, PRI2 seems to be required for efficient primer initiation and elongation [42] and possibly hand-off of the RNA primer to Pol α [43]. In 2007, two groups reported that the C-terminal domain of PRI2 in human [38], as well as yeast and Archaea [7], contains a $[4Fe\text{-}4S]^{2+}$ cluster. Klinge and colleagues further showed that FeS cluster binding is required for efficient RNA primer synthesis in yeast [7].

Resolution of the crystal structure of the C-terminal part of PRI2 later showed that the FeS cluster is located at the interface of two largely independent helical folds [44]. Interestingly, the overall architecture of PRI2 has a striking similarity to the active site of DNA photolyases. Given that photolyases recognise ultraviolet (UV)-induced cyclobutane-pyrimidine dimers, an interesting possibility is that the large subunit of

DNA primase might play a similar role and recognize the two initial ribonucleotides during primer synthesis [44]. Whether this is the case and which role the FeS cluster plays in this scenario – if any – need to be further investigated.

Like DNA primase, Pol α is composed of two subunits: the catalytic subunit (POLA1) and the regulatory B subunit (POLA2) [23]. Interaction between the two subunits is likely mediated by the C-terminal domain of the catalytic subunit [45]. For a long time, this function was assigned to a putative zinc finger motif in this domain, a notion that was supported by structural analysis that suggested the presence of a Zn^{2+} ion at the binding interface of POLA1 to POLA2 [46]. As discussed in more depth in the next paragraph, however, a recent study has demonstrated that the C-terminal domain of POLA1 does not contain a zinc finger module but rather an FeS cluster binding motif [37].

13.3.2 DNA polymerases delta and epsilon

Pol δ and ε – like Pol α – belong to the class B family of DNA polymerases [47]. They are multisubunit proteins composed of a catalytic subunit, a regulatory B subunit, and (at least in human) two accessory subunits [48].

The catalytic subunits are evolutionarily conserved and contain two cysteine-rich motifs (CysA and CysB) in their C-terminal domains. For a long time, the CysA and B motifs were believed to be zinc finger modules [49]. The CysB motif, in particular, had been well studied and shown to mediate interaction with the regulatory B subunit [50].

Intrigued by the fact that *pol3-13*, a yeast mutant strain with a single point mutation (cysteine to serine) in the CysB motif of Pol δ, displays synthetic lethality with multiple members of the CIA machinery, Netz *et al.* recently challenged the assumption that CysB was a zinc finger module and set out to investigate the possibility that it could be an FeS cluster binding motif [37].

Using ^{55}Fe incorporation assays, they could indeed show that Pol-δ and Pol-α, Pol-ε, and the translesion DNA polymerase ζ are FeS proteins [37]. UV-visible and EPR spectroscopy, together with site-directed mutagenesis, confirmed the presence of a $[4Fe\text{-}4S]^{2+}$ cluster that is coordinated by the cysteines of the CysB motif. Upon protein purification, the FeS cluster in the Pol δ holo-complex was mildly sensitive to oxidation, which could be exacerbated by addition of the oxidizing agent ferricyanide. In contrast, the cluster was insensitive to reduction by dithionite.

Further biochemical analysis showed that FeS cluster binding by CysB is required for Pol δ holo-complex formation, whereas the CysA motif – which seems to represent a *bona fide* zinc finger – confers binding of Pol δ to PCNA and allows processive DNA replication [37].

The finding that all replicative DNA polymerases in yeast and (given their evolutionary conservation) presumably in all eukaryotes are FeS proteins was surprising considering that this family had been studied rather extensively. The structural

analysis of Pol α in particular, which showed the presence of a Zn^{2+} ion in the interaction domain of the catalytic subunit with the regulatory B subunit [46], seemed a rather convincing argument for the presence of a zinc finger module in this family of DNA polymerases. On the other hand, it has to be kept in mind that in this study, Pol α had been overexpressed and purified from *Escherichia coli*. Presumably for lack of interaction with the bacterial FeS assembly system, a Zn^{2+} ion was incorporated into Pol α – an erroneous but seemingly successful attempt to produce a stable protein. Whether replacement of the FeS cluster with a Zn^{2+} ion could also happen *in vivo* cannot be categorically excluded from the results presented by Netz and colleagues. However, two recent studies showed that the protein levels of Pol δ in the absence of the late-acting CIA component MMS19 are severely reduced, strongly reinforcing the idea that the stability of Pol δ depends on the presence of an FeS cluster [17, 18].

The question of why all replicative DNA polymerases contain an FeS cluster has remained unanswered so far. It is particularly surprising since – at least in the case of Pol α – the FeS cluster can be replaced by a Zn^{2+} ion without losing the overall structure of the protein. One would assume that there was a selective pressure against FeS clusters in favor of safer structural elements in proteins whose function it is to replicate the genome as faithfully as possible. The fact that this is visibly not the case and that the FeS cluster is a common element of all replicative polymerases points toward a specific function of FeS clusters that cannot be performed by other cofactors. Since FeS clusters are intrinsically sensitive to the surrounding redox conditions, oxidative stress-induced decomposition of the FeS cluster might be a unique way of regulating DNA polymerases in response to suboptimal conditions of DNA replication.

13.3.3 DNA2

DNA2 is a multifunctional protein that – apart from Okazaki fragment maturation – has been implicated in a variety of processes related to DNA metabolism: repair of DNA double-strand breaks [51, 52], telomere maintenance [53], prevention of replication fork reversal [54], and mitochondrial DNA replication and repair [55].

From a biochemical point of view, DNA2 is a particularly interesting protein since it has both helicase (5′-3′) and endonuclease activity [56, 57]. Whereas its primary function in Okazaki fragment maturation depends on its endonuclease activity [57, 58], its helicase activity seems to facilitate flap cleavage [59].

In 2009, Yeeles and colleagues reported that a bacterial helicase/nuclease complex, *Bacillus subtilis* AddA/AddB, carries a $[4Fe\text{-}4S]^{2+}$ cluster in its nuclease domain [39]. By sequence comparison, they suggested that this might also be true for the nuclease domain of the related eukaryotic DNA2.

Interestingly, the four cysteines required for FeS cluster binding in AddAB are not clustered together but instead flank the nuclease domain AddB on either side; the first cysteine is located on the N-terminal side of the nuclease domain, whereas

the other three cysteines are found in close proximity to each other in the C-terminal portion of the nuclease domain. Due to this unusual arrangement, the FeS cluster might act as an "iron staple" that is required to pin back and stabilize the nuclease domain. In turn, impaired FeS cluster binding results in loss of structural integrity of the nuclease domain and compromised binding to DNA ends [39].

It is noteworthy that FeS cluster binding is a highly conserved feature of AddB family proteins with the exception of lactic acid bacteria that have supposedly replaced the FeS cluster with an alternative metal cofactor [39]. Since lactic acid bacteria thrive in iron-poor environments, it is not unusual for them to replace iron-containing with alternative cofactors [60]. Does this in turn mean that the FeS cluster in AddAB and DNA2 has an exclusively structural function? It does seem so, but more studies are required to address this question.

Recently, a study from the Campbell lab has formally proven that yeast Dna2 indeed is an FeS protein. As suggested, it binds to an FeS cluster *via* the proposed FeS cluster binding motif that spans its N-terminal nuclease domain [40]. In the absence of an FeS cluster, Dna2's nuclease activity is severely compromised. In contrast to AddAB, however, the presence of an FeS cluster did not prove to be essential for DNA binding, nor did it seem to influence the overall structure of DNA2, as suggested by limited protease digestion experiments with wild-type and FeS cluster binding mutant proteins. Unexpectedly, however, loss of the FeS cluster clearly reduced the ATPase activity of Dna2, despite the fact that the ATPase domain is located far away from the FeS cluster binding site in the C-terminal helicase domain of the protein. This might suggest that the FeS cluster functionally couples helicase and endonuclease activities [40].

In a recent biochemical study from the Cejka lab, it was shown for yeast Dna2 that its nuclease activity autoinhibits its helicase activity [61]. A nuclease-dead version of Dna2 in turn displayed significantly increased helicase activity, suggesting that in a wild-type situation, Dna2's strong endonuclease activity prevails and cleaves potential helicase substrates before unwinding can occur [61]. These findings open the possibility that the dual activity of Dna2 might be highly regulated *in vivo* and – depending on the cellular context – nuclease activity or helicase activity could prevail. Needless to say that it is tempting to speculate whether the redox state of the FeS cluster plays a role in this regulation.

13.4 FeS proteins in DNA repair

In contrast to DNA replication, a role for FeS clusters in the processes of DNA repair and genome maintenance has been appreciated for many years. However, for a long time, their contribution seemed to be limited to a subset of DNA repair proteins: DNA glycosylases. More recently, the members of the Rad3 family of helicases have joined the club, underlining the fact that FeS clusters are not limited to a specific pathway but play a more general role in DNA repair.

13.4.1 DNA glycosylases

13.4.1.1 ROS and DNA damage

Oxidative DNA damage caused by ROS is a major threat to genome stability. ROS are either generated endogenously, e.g. as by-products of mitochondrial respiration, or by exogenous factors, such as xenobiotics or ionizing radiation [62, 63]. ROS include hydroxyl radicals ($OH^{\bullet}$), superoxide radicals ($O_2^{\bullet-}$), and nonradical species, such as hydrogen peroxide (H_2O_2), all of which can cause oxidative damage to DNA [64]. A common ROS-induced lesion is the oxidation of guanine to 8-oxoguanine (^{8}OG). During DNA replication adenine instead of cytosine is incorporated opposite of ^{8}OG, which leads to the formation of ^{8}OG:A mispairs that – when left unrepaired – cause G:C to T:A transversion mutations [65].

13.4.1.2 Base excision repair and DNA glycosylases

DNA base oxidations or other chemical alterations, such as nonenzymatic methylations, interfere with DNA replication and transcription when left unrepaired. The evolutionary conserved base excision repair (BER) pathway has an important role in recognizing and removing altered bases [66–68].

BER is initiated when a DNA glycosylase recognizes a damaged base and cleaves the *N*-glycosylic bond that links the base to the DNA backbone. The resulting abasic site is subsequently cleaved by either the intrinsic apurinic/apyrimidinic (AP) lyase activity of the DNA glycosylase itself (in case of bifunctional glycosylases) or, alternatively, by an AP endonuclease (in case of monofunctional glycosylases), thereby creating a single-stranded break. Further steps include cleaning of the break-flanking region, filling of the resulting gap by a DNA polymerase, and sealing of the remaining nick by a DNA ligase [68].

In human cells, 11 DNA glycosylases are known to date, 5 of which are required for the recognition and excision of oxidized bases [68]. The specificity of DNA glycosylases for various forms of base damage depends on the size and structure of their base binding pocket; however, given that the amount of base damage variations largely exceeds the number of glycosylases, their specificities do not seem to be very stringent.

13.4.1.3 Endo III and MutY

E. coli endonuclease III (Endo III) was the first glycosylase to be reported to bind to an FeS cluster [69]. Despite its misleading name, Endo III is not a nuclease, but a bifunctional glycosylase with intrinsic AP lyase activity; it is required for the excision of a variety of oxidized pyrimidine bases [70]. Later on, the human counterpart of Endo III, NTH1, was also shown to bind to an FeS cluster [71, 72].

Another example of an FeS glycosylase is MutY [73]. Like Endo III, it is a bifunctional glycosylase that is highly conserved from *E. coli* to human (MUTYH). However, unlike Endo III, it displays specificity for ^{8}OG:A mispairs [74].

Both Endo III and MutY were shown to bind to a $[4Fe\text{-}4S]^{2+}$ cluster that – under physiological conditions – can neither be oxidized nor reduced [69]. At first, this led to the assumption that the redox state of the FeS cluster is unlikely to have any influence on protein function [75] and that the cluster must have a purely structural role. This proved to be wrong since the FeS cluster does not contribute significantly to the overall structure of the protein but is instead required for DNA binding and enzymatic activity [76].

Interestingly, when Endo III and MutY are bound to DNA, they become redox-active and the redox potential of their FeS clusters is shifted toward the oxidized $[4Fe\text{-}4S]^{3+}$ state [77]. At the same time, oxidized glycosylases seem to have a higher affinity for DNA [78], suggesting that DNA binding could be modulated by the redox state of the FeS cluster.

13.4.1.4 Damage detection by DNA-mediated charge transfer

Double-stranded DNA has been shown to allow the transport of electric charge over distances of around 200 Å due to the π-stacking of its aromatic base pairs [79, 80]. DNA-mediated charge transfer is very sensitive to disruptions in the π-stack, and DNA molecules with mismatches or lesions, such as oxidized bases, are impaired for charge transfer [81]. While numerous *in vitro* studies leave no doubt about the ability of DNA to mediate charge transfer, evidence that this is of importance *in vivo* is rather rare [82], and the physiological relevance of it is subject to debate.

From a theoretical point of view, however, DNA-mediated charge transfer could be an elegant explanation as to how DNA repair proteins manage to scan the enormous length of the genome for oxidative damage in a timely fashion [77, 78, 83, 84]. The fact that charge transfer can take place only through perfectly π-stacked DNA could give redox-active proteins a means to distinguish between intact and damaged DNA.

In a model put forward by the Barton lab (Fig. 13.4), a glycosylase (MutY or Endo III) binds to DNA, which leads to the oxidation of its FeS cluster and tighter binding to DNA [77]. The electron that is released upon FeS cluster oxidation could then travel along the DNA *via* charge transfer and reduce another glycosylase that is distantly bound. The reduced glycosylase would then have less affinity for the DNA substrate and dissociate. However, if a DNA lesion, such as an oxidized base, is present between the two proteins, charge transport would be interrupted, leaving the second protein in its oxidized state and tightly bound to DNA. As a consequence, DNA glycosylases would accumulate close to the site of DNA damage, thereby facilitating DNA damage signaling and repair.

An overall environment of oxidative stress could further facilitate the initial binding of glycosylases to DNA since guanine radicals can directly oxidize the FeS cluster in MutY (and possibly other FeS glycosylases), which in turn increases their affinity for DNA [85]. Given that guanine radicals are generated early during physiological oxidative stress conditions [86], FeS cluster oxidation could be a means to force accumulation of MutY (and possibly other BER factors) on damaged DNA.

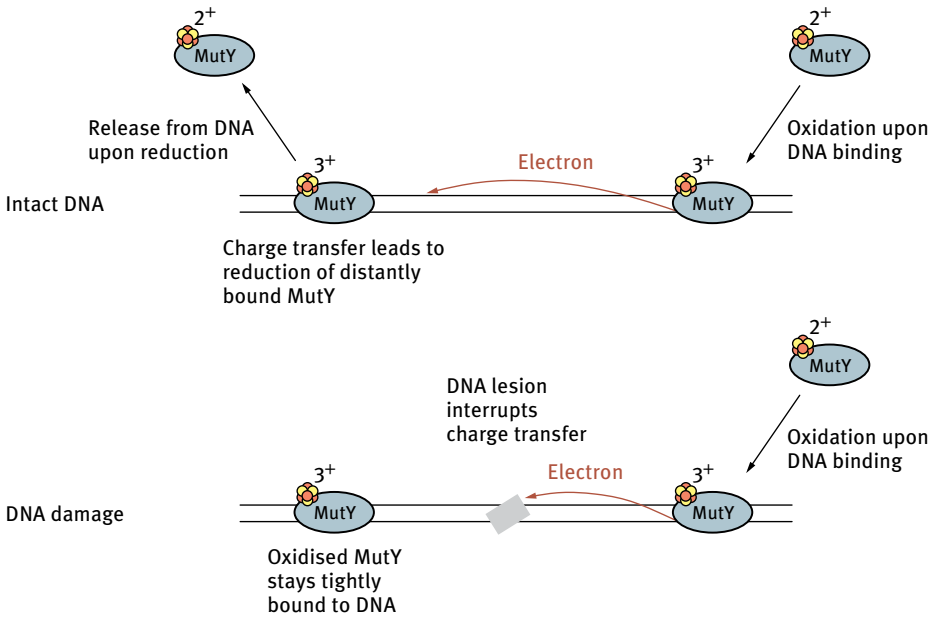

Fig. 13.4: DNA damage detection by charge transfer.

In favor of such a model of damage detection are two recent studies that show that DNA-mediated charge transfer is required for MutY and Endo III to locate DNA damage and to cluster in the vicinity [84]. Interestingly, cooperativity between MutY and Endo III was observed in this process, which was dependent on the ability of the proteins to mediate charge transfer [87]. However attractive this model is, further studies are required to decide whether DNA-mediated charge transfer has any physiological relevance in DNA damage detection.

13.4.2 The Rad3 family of helicases

13.4.2.1 A conserved family of helicases with links to human disease

Saccharomyces cerevisiae Rad3 is the founding member of a superfamily 2 of helicases that, apart from its human homologue XPD, also includes RTEL1, FANCJ, and ChlR1, all of which have been linked to human disease [88, 89]. As a common feature, they all possess 5′-3′ helicase activity but have preferences for different DNA substrates, which presumably explains their functions in different pathways essential for the maintenance of genome stability.

RTEL1 (regulator of telomere length protein 1) does not seem to have classical DNA unwinding activity but is instead able to dismantle DNA recombination intermediates, so-called D-loop structures, in which a third strand invades the DNA duplex

[90]. This anti-recombinogenic function is required to limit meiotic recombination [91], to maintain the integrity of telomeres [92], and to counteract the accumulation of toxic recombination intermediates during DNA repair [90].

SNP variations in *RTEL1* have been associated with high-grade glioma susceptibility [93], and more recently, *RTEL1* mutations have been found in several Hoyeraal-Hreidarsson syndrome patients, a severe form of dyskeratosis congenita caused by dysfunctional telomeres [94].

FANCJ is defective in a subgroup of patients suffering from Fanconi anemia (FA), a genome instability disorder that confers an elevated cancer risk [95, 96]. FANCJ was originally identified as an interaction partner of the breast cancer susceptibility protein BRCA1 [97]; mutations in *FANCJ* have later been detected in breast and ovarian cancer [98–100], suggesting a role for FANCJ as a tumor suppressor.

From a biochemical point of view, FANCJ can bind to and unwind branched DNA molecules *in vitro* [101]. A combination of biochemical and *in vivo* data, however, suggests that FANCJ's main role is the unwinding of G-quadruplex (G4) DNA [102–104]. G4 DNA are secondary structures that are stabilized by Hoogsteen base pairing; they can form in guanine-rich regions of the genome and represent an obstacle for the DNA replication machinery [105].

ChlR1 preferentially unwinds branched DNA molecules with a 5′ single-stranded region [106, 107]. It interacts with various components of the DNA replication machinery [108] and seems to play an important role in sister chromatid cohesion during DNA replication, which is a prerequisite for normal chromosome segregation [109–113].

The gene coding for ChlR1, *DDX11*, is mutated in Warsaw breakage syndrome (WABS) [114], an extremely rare disorder characterized by congenital abnormalities and – on a cellular level – defects in sister chromatid cohesion.

XPD functions in both transcription initiation and nucleotide excision repair (NER), a DNA repair pathway specialized in the removal damaged nucleotides, as e.g. caused by UV light [115]. XPD's 5′-3′ helicase activity has been shown to be essential for NER but dispensable for transcription initiation [116].

Surprisingly, mutations in *XPD* give rise to three symptomatically distinct human disorders: the eponymous xeroderma pigmentosum (XP), Cockayne's syndrome, and trichothiodystrophy (TTD) [117]. These multiple syndromes can be explained with the fact that depending on the mutation either transcription alone, NER alone or both pathways are affected. XP patients e.g. are extremely light-sensitive and at a high risk of developing skin cancer due to a defective NER pathway [117].

13.4.2.2 The FeS cluster in XPD

In eukaryotes, XPD is integral part of the multi-subunit transcription factor II H (TFIIH) complex and is required for its stability [118, 119]. A homologue of XPD is also found in Archaea; in contrast to eukaryotes, however, archaeal XPD is active as a monomer, which makes it an interesting and amenable protein to study. In 2006, a

study from the White lab found that *Sulfolobus acidocaldarius* XPD (sacXPD) binds to a $[4Fe\text{-}4S]^{2+}$ cluster that is sensitive to oxidation [8]. Sequence alignment showed that the cluster-binding cysteines are highly conserved across all Rad3-like helicases and located in the HD1 helicase domain between the Walker A and B box motifs (Fig. 13.5; cysteines highlighted in yellow) [8].

Analysis of FeS cluster binding mutants further demonstrated that the FeS cluster is dispensable for ATPase activity and the overall stability of sacXPD. In contrast, helicase activity is severely impaired in these mutants, suggesting that the FeS cluster is required to couple ATPase activity to DNA unwinding [8].

Our understanding of the FeS cluster binding region within XPD has been significantly furthered by the structural analysis of XPD from three archaeal organisms (*S. acidocaldarius* [120], *Sulfolobus tokodaii* [121], and *Thermoplasma acidophilum* [122]). All three reports are in agreement with XPD being composed of four domains: two canonical RecA-like helicase domains (HD1 and HD2) and two accessory domain inserted into HD1 (the FeS domain and an arch-shaped domain) [120–122]. Binding of an FeS cluster is required for the stability of the FeS and arch domains [120]. Together with a later study of *T. acidophilum* XPD in complex with DNA [123], these structural data suggest that the HD1, arch, and FeS domains together form a channel that can accommodate single-stranded DNA and that DNA unwinding occurs by threading single-stranded DNA through this channel.

In addition to these structural studies, much has been learned from a number of single-molecule studies that take advantage of the fact that FeS clusters can act as intrinsic quenchers of fluorescently labeled DNA substrates [124–126]. Taken together, in the current model, the FeS domain is thought to recognize the junction between single- and double-stranded DNA and to act as a wedge or ploughshare for the separation of DNA strands.

A possible extension to this model comes from a recent study, in which Mathieu and colleagues generated rationally designed mutant versions of XPD with amino acid replacements in the FeS cluster binding pocket [127]. These mutants retained helicase activity but could not distinguish between damaged and undamaged nucleotides anymore, suggesting the exciting possibility that the FeS domain could play a role in the recognition of damaged nucleotides during strand unwinding.

```
Rad3        102     DFRGLGLTSRKNLCLHPEVSKERKGTVVDEKCRRMTNGQAKRKLEED---PEANV---E-LCEYHENLYNIEVEDY----
XPD         103     PFLGLALSSRKNLCIHPEVTPLRFGKDVDGKCHSLTASYVRAQYQHD-----TSL---P-HCRFYEEFDAHGREVP----
RTEL1       136     ----CVLGSREQLCIHPEVKKQESNHLQIHLCRKKVAS--------------------R-SCHFYNNVEEKSLEQE----
FANCJ       270     GVPMTILSSRDHTCVHPEVVGNFNR---NEKCMELLD-----------------GKNGK-SCYFYHGVHKISDQHTLQTF
Chlr1       254     DVRLVSLGSRQNLCVNEDVKSLGSVQLINDRCVDMQRSRHEKKKGAEEEKPKRRRQEKQAACPFYNHEQMGLLRDE----

Rad3        171     ----LPKGVFSFEKLLKYCEEKTLCPYFIVRRMISLCNIIIYSYHYLLDPKIAERVSNEVSKDSIVIFDEAH
XPD         170     ----LPAGIYNLDDLKALGRRQGWCPYFLARYSILHANVVVYSYHYLLDPKIADLVSKELARKAVVVFDEAH
RTEL1       187     ----LASPILDIEDLVKSGSKHRVCPYYLSRNLKQQADIIFMPYNYLLDAKSRRAHNIDL-KGTVVIFDEAH
FANCJ       329     QGMC---KAWDIEELVSLGKKLKACPYYTARELIQDADIIFCPYNYLLDAQIRESMDLNL-KEQVVILDEAH
Chlr1       330     ----ALAEVKDMEQLLALGKEARACPYYGSRLAIPAAQLVVLPYQMLLHAATRQAAGIRL-QDQVVIIDEAH
```

Fig. 13.5: Rad3 family of helicases.

13.4.2.3 Mutations in the FeS cluster binding region of XPD, FANCJ, and ChlR1

Interestingly, a number of clinically relevant mutations in *XPD*, *FANCJ*, and *DDX11* are located in the FeS cluster binding region (Fig. 13.5; mutations marked in red).

Arginine to histidine replacement in XPD (R112H XPD) is common in TTD patients [128]. R112H XPD does not stably integrate an FeS cluster and displays completely abolished helicase activity [8, 128]. The aforementioned structural analysis of archaeal XPD homologues indicated that the corresponding R112 residues (R88 in *T. acidophilum* and K84 in *S. acidocaldarius*) are located in close proximity to the FeS cluster, enabling them to contribute to the stabilization of the FeS domain [120, 122].

Remarkably, the corresponding amino acid exchange in ChlR1 is also found in WABS patients, and biochemical analysis of R263Q ChlR1 showed that – as in XPD – this arginine residue is essential for helicase function [129].

In the case of FANCJ, a proline to alanine substitution (A349P FANCJ) is found right next to one of the coordinating cysteine residues in the FeS cluster binding domain in some FA patients [96]. Similar to the mutations in XPD and ChlR1, this exchange abolishes FeS cluster binding and results in uncoupling of ATP hydrolysis from translocase activity [8, 130]. Moreover, two further mutations in the FeS cluster-binding domain of FANCJ are associated with an increased breast cancer risk: alleles coding for M299I FANCJ [131] and L340F FANCJ [132]. Surprisingly, M299I FANCJ seems to display increased ATPase and helicase activities [133], suggesting that not only a nonfunctional FANCJ version but also a hyperactive one can be deleterious to the cell. As for L340F FANCJ, no biochemical analysis has been performed yet; interestingly, however, the mutated leucine residue is highly conserved across all family members, suggesting that it is important for the functionality of this domain.

Taken together, these findings are in agreement with the FeS cluster being essential for helicase activity and underline the significance of FeS cluster binding *in vivo*.

13.4.2.4 Possible functions of the FeS cluster in Rad3-like helicases

Future studies have to show which role exactly the FeS cluster plays in the different Rad3-like helicases. Using the FeS cluster binding pocket for the recognition of damaged nucleotides, as suggested for XPD [127], certainly is an exciting possibility. However, taking into consideration that FANCJ, RTEL1, and ChlR1 have no specificity for damaged bases, but rather display a preference for unusual DNA structures, it seems unlikely that damage recognition is a general feature of FeS clusters in these helicases.

Another attractive hypothesis is that the redox sensitivity of FeS clusters could be used to modulate the biochemical activities of FeS repair proteins in response to altered redox conditions in the cell. For example, *in vitro* studies with DinG, the closest homologue of Rad3-like helicases in *E. coli*, have shown that reduction of its $[4Fe\text{-}4S]^{2+}$ cluster to the $[4Fe\text{-}4S]^{1+}$ state leads to a reversible switch-off of its helicase activity [134]. On the other hand, the FeS cluster is stable in the $[4Fe\text{-}4S]^{2+}$ state under oxidizing conditions, suggesting the possibility that DinG is in an inactive ($[4Fe\text{-}4S]^{1+}$)

state under normal conditions but can become activated ($[4Fe\text{-}4S]^{2+}$) under conditions of oxidative stress. However, whether this redox-regulation mechanism plays a role *in vivo* is not clear yet.

Studies from the Barton lab suggest that – at least in theory – a similar mechanism could regulate XPD. They could show that sacXPD has a physiologically relevant redox potential when bound to DNA (~80 mV versus the normal hydrogen electrode), which increases with ATP hydrolysis [135]. Importantly, the redox signal depends on the DNA substrate, raising the possibility that the ATPase and helicase activities of XPD could be regulated *via* the redox state of its FeS cluster and that regulation would depend on the DNA substrate encountered.

Taking the idea of redox-signaling between XPD and DNA a step further, it is also conceivable that DNA-mediated charge transport is used by XPD to screen for DNA lesions or alterations, in a similar way as had been suggested for DNA glycosylases. Indeed, as for MutY and Endo III, location of XPD to damaged sites seems to depend on charge transfer [136]. Moreover, in the same study, charge transfer-mediated signaling occurred between XPD and other FeS proteins, suggesting a potential communication between multiple FeS repair proteins during their search for DNA damage [136]. Future studies will have to address whether long-distance screening of DNA and possibly communication between different repair factors by DNA-mediated charge transport has *in vivo* significance or whether it is merely an attractive hypothesis.

13.5 Outlook

The significance of FeS clusters in DNA replication and repair proteins is far from being clear. In some cases, their role might be purely structural. However, given their potentially dangerous nature for the integrity of DNA, it seems likely that they have functions beyond a structural role. Their redox-sensitivity certainly makes FeS clusters very interesting cofactors that could be used to modulate biochemical activities, react to conditions of oxidative stress, recognize DNA damage or screen the DNA for lesions or abnormal structures. Further studies – both *in vitro* and *in vivo* – will be needed to address the role of FeS clusters in DNA replication and repair and decipher their importance for the maintenance of genome stability.

References

[1] Bartkova J, Rezaei N, Liontos M, et al. Oncogene-induced senescence is part of the tumorigenesis barrier imposed by DNA damage checkpoints. Nature 2006;444:633–7.
[2] Bartkova J, Horejsí Z, Koed K, et al. DNA damage response as a candidate anti-cancer barrier in early human tumorigenesis. Nature 2005;434:864–70.
[3] Halazonetis TD, Gorgoulis VG, Bartek J. An oncogene-induced DNA damage model for cancer development. Science 2008;319:1352–5.

[4] Gorgoulis VG, Vassiliou L-VF, Karakaidos P, et al. Activation of the DNA damage checkpoint and genomic instability in human precancerous lesions. Nature 2005;434:907–13.
[5] Di Micco R, Fumagalli M, Cicalese A, et al. Oncogene-induced senescence is a DNA damage response triggered by DNA hyper-replication. Nature 2006;444:638–42.
[6] Veatch JR, McMurray MA, Nelson ZW and Gottschling DE. Mitochondrial dysfunction leads to nuclear genome instability via an iron-sulfur cluster defect. Cell 2009;137:1247–1258.
[7] Klinge S, Hirst J, Maman JD, Krude T, Pellegrini L. An iron-sulfur domain of the eukaryotic primase is essential for RNA primer synthesis. Nat Struct Mol Biol 2007;14:875–7.
[8] Rudolf J, Makrantoni V, Ingledew WJ, Stark MJ, White MF. The DNA repair helicases XPD and FancJ have essential iron-sulfur domains. Mol Cell 2006;23:801–8.
[9] Alseth I, Eide L, Pirovano M, Rognes T, Seeberg E, Bjørås M. The Saccharomyces cerevisiae homologues of endonuclease III from Escherichia coli, Ntg1 and Ntg2, are both required for efficient repair of spontaneous and induced oxidative DNA damage in yeast. Mol Cell Biol 1999;19:3779–87.
[10] Lill R. Function and biogenesis of iron-sulphur proteins. Nature 2009;460:831–8.
[11] Rouault TA. Biogenesis of iron-sulfur clusters in mammalian cells: new insights and relevance to human disease. Dis Model Mech 2012;5:155–64.
[12] Netz DJA, Pierik AJ, Stümpfig M, Mühlenhoff U, Lill R. The Cfd1-Nbp35 complex acts as a scaffold for iron-sulfur protein assembly in the yeast cytosol. Nat Chem Biol 2007;3:278–86.
[13] Netz DJ, Pierik AJ, Stumpfig M, et al. A bridging [4Fe-4S] cluster and nucleotide binding are essential for function of the Cfd1-Nbp35 complex as a scaffold in iron-sulfur protein maturation. J Biol Chem 2012;287:12365–78.
[14] Balk J, Aguilar Netz DJ, Tepper K, Pierik AJ, Lill R. The essential WD40 protein Cia1 is involved in a late step of cytosolic and nuclear iron-sulfur protein assembly. Mol Cell Biol 25;2005: 10833–41.
[15] Balk J, Pierik AJ, Aguilar Netz DJ, Mühlenhoff U, Lill R. The hydrogenase-like Nar1p is essential for maturation of cytosolic and nuclear iron-sulphur proteins. EMBO J 2004;23:2105–15.
[16] Song D, Lee FS. A role for IOP1 in mammalian cytosolic iron-sulfur protein biogenesis. J Biol Chem 2008;283:9231–8.
[17] Gari K, León Ortiz AM, Borel V, Flynn H, Skehel JM, Boulton SJ. MMS19 links cytoplasmic iron-sulfur cluster assembly to DNA metabolism. Science 2012;337:243–5.
[18] Stehling O, Vashisht AA, Mascarenhas J, et al. MMS19 assembles iron-sulfur proteins required for DNA metabolism and genomic integrity. Science 2012;337:195–9.
[19] van Wietmarschen N, Moradian A, Morin GB, Lansdorp PM, Uringa EJ. The mammalian proteins MMS19, MIP18, and ANT2 are involved in cytoplasmic iron-sulfur cluster protein assembly. J Biol Chem 2012;287:43351–8.
[20] Weerapana E, Wang C, Simon GM et al. Quantitative reactivity profiling predicts functional cysteines in proteomes. Nature 2010;468:790–5.
[21] Kunkel TA and Burgers PM. Dividing the workload at a eukaryotic replication fork. Trends Cell Biol 2008;18:521–527.
[22] Burgers PM. Polymerase dynamics at the eukaryotic DNA replication fork. J Biol Chem 2009;284:4041–4045.
[23] Pellegrini L. The Pol alpha-Primase complex. Subcell Biochem 2012;62:157–169.
[24] Larrea AA, Lujan SA, Nick McElhinny SA et al. Genome-wide model for the normal eukaryotic DNA replication fork. Proc Natl Acad Sci USA 2010;107:17674–17679.
[25] Pursell ZF, Isoz I, Lundstrom EB, Johansson E and Kunkel TA. Yeast DNA polymerase epsilon participates in leading-strand DNA replication. Science 2007;317:127–130.
[26] Miyabe I, Kunkel TA and Carr AM. The major roles of DNA polymerases epsilon and delta at the eukaryotic replication fork are evolutionarily conserved. PLoS Genet 2011;7:e1002407.

[27] Moldovan G-L, Pfander B and Jentsch S. PCNA, the maestro of the replication fork. Cell 2007;129:665–679.
[28] Liu Y, Kao HI and Bambara RA. Flap endonuclease 1: a central component of DNA metabolism. Annu Rev Biochem 2004;73:589–615.
[29] Zheng L and Shen B. Okazaki fragment maturation: nucleases take centre stage. J Mol Cell Biol 2011;3:23–30.
[30] Stith CM, Sterling J, Resnick MA, Gordenin DA and Burgers PM. Flexibility of eukaryotic Okazaki fragment maturation through regulated strand displacement synthesis. J Biol Chem 2008;283:34129–34140.
[31] Budd ME and Campbell JL. A yeast gene required for DNA replication encodes a protein with homology to DNA helicases. Proc Natl Acad Sci USA 1995;92:7642–7646.
[32] Bae SH and Seo YS. Characterization of the enzymatic properties of the yeast Dna2 helicase/endonuclease suggests a new model for Okazaki fragment processing. J Biol Chem 2000;275:38022–38031.
[33] Levikova M and Cejka P. The Saccharomyces cerevisiae Dna2 can function as a sole nuclease in the processing of Okazaki fragments in DNA replication. in *Nucleic Acids Research* Vol. 43, 2015;7888–7897.
[34] Kim JH, Kim HD, Ryu GH, Kim DH, Hurwitz J and Seo YS. Isolation of human Dna2 endonuclease and characterization of its enzymatic properties. Nucleic Acids Res 2006;34:1854–1864.
[35] Ayyagari R, Gomes XV, Gordenin DA and Burgers PM. Okazaki fragment maturation in yeast. I. Distribution of functions between FEN1 AND DNA2. J Biol Chem 2003;278:1618–1625.
[36] Masuda-Sasa T, Imamura O and Campbell JL. Biochemical analysis of human Dna2. Nucleic Acids Res 2006;34:1865–1875.
[37] Netz DJA, Stith CM, Stümpfig M et al. Eukaryotic DNA polymerases require an iron-sulfur cluster for the formation of active complexes. Nat Chem Biol 2012;8:125–132.
[38] Weiner BE, Huang H, Dattilo BM, Nilges MJ, Fanning E and Chazin WJ. An iron-sulfur cluster in the C-terminal domain of the p58 subunit of human DNA primase. J Biol Chem 2007;282:33444–33451.
[39] Yeeles JTP, Cammack R and Dillingham MS. An iron-sulfur cluster is essential for the binding of broken DNA by AddAB-type helicase-nucleases. J Biol Chem 2009;284:7746–7755.
[40] Pokharel S and Campbell JL. Cross talk between the nuclease and helicase activities of Dna2: role of an essential iron-sulfur cluster domain. Nucleic Acids Res 2012;40:7821–7830.
[41] Foiani M, Santocanale C, Plevani P and Lucchini G. A single essential gene, PRI2, encodes the large subunit of DNA primase in Saccharomyces cerevisiae. Mol Cell Biol 1989;9:3081–3087.
[42] Zerbe LK and Kuchta RD. The p58 subunit of human DNA primase is important for primer initiation, elongation, and counting. Biochemistry 2002;41:4891–4900.
[43] Agarkar VB, Babayeva ND, Pavlov YI and Tahirov TH. Crystal structure of the C-terminal domain of human DNA primase large subunit: implications for the mechanism of the primase-polymerase alpha switch. Cell Cycle 2011;10:926–931.
[44] Sauguet L, Klinge S, Perera RL, Maman JD and Pellegrini L. Shared active site architecture between the large subunit of eukaryotic primase and DNA photolyase. PloS ONE 2010;5:e10083.
[45] Mizuno T, Yamagishi K, Miyazawa H and Hanaoka F. Molecular architecture of the mouse DNA polymerase alpha-primase complex. Mol Cell Biol 1999;19:7886–7896.
[46] Klinge S, Nunez-Ramirez R, Llorca O and Pellegrini L. 3D architecture of DNA Pol alpha reveals the functional core of multi-subunit replicative polymerases. EMBO J 2009;28:1978–1987.
[47] Burgers PM, Koonin EV, Bruford E et al. Eukaryotic DNA polymerases: proposal for a revised nomenclature. J Biol Chem 2001;276:43487–43490.
[48] Johansson E and Macneill SA. The eukaryotic replicative DNA polymerases take shape. Trends Biochem Sci 2010;35:339–347.

[49] Krishna SS, Majumdar I and Grishin NV. Structural classification of zinc fingers: survey and summary. Nucleic Acids Res 2003;31:532–550.
[50] Sanchez Garcia J, Ciufo LF, Yang X, Kearsey SE and MacNeill SA. The C-terminal zinc finger of the catalytic subunit of DNA polymerase delta is responsible for direct interaction with the B-subunit. Nucleic Acids Res 2004;32:3005–3016.
[51] Zhu Z, Chung WH, Shim EY, Lee SE and Ira G. Sgs1 helicase and two nucleases Dna2 and Exo1 resect DNA double-strand break ends. Cell 2008;134:981–994.
[52] Cejka P, Cannavo E, Polaczek P et al. DNA end resection by Dna2-Sgs1-RPA and its stimulation by Top3-Rmi1 and Mre11-Rad50-Xrs2. Nature 2010;467:112–116.
[53] Lin W, Sampathi S, Dai H et al. Mammalian DNA2 helicase/nuclease cleaves G-quadruplex DNA and is required for telomere integrity. EMBO J 2013;32:1425–1439.
[54] Hu J, Sun L, Shen F et al. The intra-S phase checkpoint targets Dna2 to prevent stalled replication forks from reversing. Cell 2012;149:1221–1232.
[55] Zheng L, Zhou M, Guo Z et al. Human DNA2 is a mitochondrial nuclease/helicase for efficient processing of DNA replication and repair intermediates. Mol Cell 2008;32:325–336.
[56] Bae SH, Choi E, Lee KH, Park JS, Lee SH and Seo YS. Dna2 of Saccharomyces cerevisiae possesses a single-stranded DNA-specific endonuclease activity that is able to act on double-stranded DNA in the presence of ATP. J Biol Chem 1998;273:26880–26890.
[57] Budd ME, Choe WC and Campbell JL. DNA2 encodes a DNA helicase essential for replication of eukaryotic chromosomes. J Biol Chem 1995;270:26766–26769.
[58] Lee KH, Kim DW, Bae SH et al. The endonuclease activity of the yeast Dna2 enzyme is essential in vivo. Nucleic Acids Res 2000;28:2873–2881.
[59] Bae SH, Kim DW, Kim J et al. Coupling of DNA helicase and endonuclease activities of yeast Dna2 facilitates Okazaki fragment processing. J Biol Chem 2002;277:26632–26641.
[60] Gostick DO, Green J, Irvine AS, Gasson MJ and Guest JR. A novel regulatory switch mediated by the FNR-like protein of Lactobacillus casei. Microbiology 1998;144 (Pt 3):705–717.
[61] Levikova M, Klaue D, Seidel R and Cejka P. Nuclease activity of Saccharomyces cerevisiae Dna2 inhibits its potent DNA helicase activity. Proc Natl Acad Sci USA 2013;110:E1992–2001.
[62] Lindahl T. Instability and decay of the primary structure of DNA. Nature 1993;362:709–715.
[63] Mitra S, Boldogh I, Izumi T and Hazra TK. Complexities of the DNA base excision repair pathway for repair of oxidative DNA damage. Environ Mol Mutagen 2001;38:180–190.
[64] Dizdaroglu M, Jaruga P, Birincioglu M and Rodriguez H. Free radical-induced damage to DNA: mechanisms and measurement. Free Radic Biol Med 2002;32:1102–1115.
[65] Shibutani S, Takeshita M and Grollman AP. Insertion of specific bases during DNA synthesis past the oxidation-damaged base 8-oxodG. Nature 1991;349:431–434.
[66] Lindahl T. Repair of intrinsic DNA lesions. Mutat Res 1990;238:305–311.
[67] Dianov G and Lindahl T. Reconstitution of the DNA base excision-repair pathway. Curr Biol 1994;4:1069–1076.
[68] Dianov GL and Hubscher U. Mammalian base excision repair: the forgotten archangel. Nucleic Acids Res 2013;41:3483–3490.
[69] Cunningham RP, Asahara H, Bank JF et al. Endonuclease III is an iron-sulfur protein. Biochemistry 1989;28:4450–4455.
[70] Asahara H, Wistort PM, Bank JF, Bakerian RH and Cunningham RP. Purification and characterization of Escherichia coli endonuclease III from the cloned nth gene. Biochemistry 1989;28:4444–4449.
[71] Aspinwall R, Rothwell DG, Roldan-Arjona T et al. Cloning and characterization of a functional human homolog of Escherichia coli endonuclease III. Proc Natl Acad Sci USA 1997;94:109–114.
[72] Ikeda S, Biswas T, Roy R et al. Purification and characterization of human NTH1, a homolog of Escherichia coli endonuclease III. Direct identification of Lys-212 as the active nucleophilic residue. J Biol Chem 1998;273:21585–21593.

[73] Michaels ML, Pham L, Nghiem Y, Cruz C and Miller JH. MutY, an adenine glycosylase active on G-A mispairs, has homology to endonuclease III. Nucleic Acids Res 1990;18:3841–3845.
[74] Tsai-Wu JJ, Liu HF and Lu AL. Escherichia coli MutY protein has both N-glycosylase and apurinic/apyrimidinic endonuclease activities on A.C and A.G mispairs. Proc Natl Acad Sci USA 1992;89:8779–8783.
[75] Fu W, O'Handley S, Cunningham RP and Johnson MK. The role of the iron-sulfur cluster in Escherichia coli endonuclease III. A resonance Raman study. J Biol Chem 1992;267:16135–16137.
[76] Porello SL, Cannon MJ and David SS. A substrate recognition role for the [4Fe-4S]2+ cluster of the DNA repair glycosylase MutY. Biochemistry 1998;37:6465–6475.
[77] Boon EM, Livingston AL, Chmiel NH, David SS and Barton JK. DNA-mediated charge transport for DNA repair. Proc Natl Acad Sci USA 2003;100:12543–12547.
[78] Boal AK, Yavin E, Lukianova OA, O'Shea VL, David SS and Barton JK. DNA-bound redox activity of DNA repair glycosylases containing [4Fe-4S] clusters. Biochemistry 2005;44:8397–8407.
[79] Kelley SO and Barton JK. Electron transfer between bases in double helical DNA. Science 1999;283:375–381.
[80] Nunez ME, Hall DB and Barton JK. Long-range oxidative damage to DNA: effects of distance and sequence. Chem Biol 1999;6:85–97.
[81] Boon EM, Ceres DM, Drummond TG, Hill MG and Barton JK. Mutation detection by electrocatalysis at DNA-modified electrodes. Nat Biotechnol 2000;18:1096–1100.
[82] Nunez ME, Holmquist GP and Barton JK. Evidence for DNA charge transport in the nucleus. Biochemistry 2001;40:12465–12471.
[83] Boal AK, Yavin E and Barton JK. DNA repair glycosylases with a [4Fe-4S] cluster: a redox cofactor for DNA-mediated charge transport? J Inorg Biochem 2007;101:1913–1921.
[84] Boal AK, Genereux JC, Sontz PA, Gralnick JA, Newman DK and Barton JK. Redox signaling between DNA repair proteins for efficient lesion detection. Proc Natl Acad Sci USA 2009;106:15237–15242.
[85] Yavin E, Boal AK, Stemp ED et al. Protein-DNA charge transport: redox activation of a DNA repair protein by guanine radical. Proc Natl Acad Sci USA 2005;102:3546–3551.
[86] Cadet J, Bellon S, Berger M et al. Recent aspects of oxidative DNA damage: guanine lesions, measurement and substrate specificity of DNA repair glycosylases. Biol Chem 2002;383:933–943.
[87] Romano CA, Sontz PA and Barton JK. Mutants of the base excision repair glycosylase, endonuclease III: DNA charge transport as a first step in lesion detection. Biochemistry 2011;50:6133–6145.
[88] White MF. Structure, function and evolution of the XPD family of iron-sulfur-containing 5′-3′ DNA helicases. Biochem Soc Trans 2009;37:547–551.
[89] Wu Y, Suhasini AN and Brosh RM. Welcome the family of FANCJ-like helicases to the block of genome stability maintenance proteins. Cell Mol Life Sci 2009;66:1209–1222.
[90] Barber LJ, Youds JL, Ward JD et al. RTEL1 maintains genomic stability by suppressing homologous recombination. Cell 2008;135:261–271.
[91] Youds JL, Mets DG, McIlwraith MJ et al. RTEL-1 enforces meiotic crossover interference and homeostasis. Science 2010;327:1254–1258.
[92] Vannier JB, Pavicic-Kaltenbrunner V, Petalcorin MI, Ding H and Boulton SJ. RTEL1 dismantles T loops and counteracts telomeric G4-DNA to maintain telomere integrity. Cell 2012;149:795–806.
[93] Wrensch M, Jenkins RB, Chang JS et al. Variants in the CDKN2B and RTEL1 regions are associated with high-grade glioma susceptibility. Nat Genet 2009;41:905–908.
[94] Le Guen T, Jullien L, Touzot F et al. Human RTEL1 deficiency causes Hoyeraal-Hreidarsson syndrome with short telomeres and genome instability. Hum Mol Genet 2013;22:3239–3249.

[95] Levitus M, Waisfisz Q, Godthelp BC et al. The DNA helicase BRIP1 is defective in Fanconi anemia complementation group J. Nat Genet 2005;37:934–935.
[96] Levran O, Attwooll C, Henry RT et al. The BRCA1-interacting helicase BRIP1 is deficient in Fanconi anemia. Nat Genet 2005;37:931–933.
[97] Cantor SB, Bell DW, Ganesan S et al. BACH1, a novel helicase-like protein, interacts directly with BRCA1 and contributes to its DNA repair function. Cell 2001;105:149–160.
[98] Cantor S, Drapkin R, Zhang F et al. The BRCA1-associated protein BACH1 is a DNA helicase targeted by clinically relevant inactivating mutations. Proc Natl Acad Sci USA 2004;101:2357–2362.
[99] Seal S, Thompson D, Renwick A et al. Truncating mutations in the Fanconi anemia J gene BRIP1 are low-penetrance breast cancer susceptibility alleles. Nat Genet 2006;38:1239–1241.
[100] Rafnar T, Gudbjartsson DF, Sulem P et al. Mutations in BRIP1 confer high risk of ovarian cancer. Nat Genet 2011;43:1104–1107.
[101] Gupta R, Sharma S, Sommers JA, Jin Z, Cantor SB and Brosh RM, Jr. Analysis of the DNA substrate specificity of the human BACH1 helicase associated with breast cancer. J Biol Chem 2005;280:25450–25460.
[102] Kruisselbrink E, Guryev V, Brouwer K, Pontier DB, Cuppen E and Tijsterman M. Mutagenic capacity of endogenous G4 DNA underlies genome instability in FANCJ-defective C. elegans. Curr Biol 2008;18:900–905.
[103] Wu Y, Shin-ya K and Brosh RM, Jr. FANCJ helicase defective in Fanconia anemia and breast cancer unwinds G-quadruplex DNA to defend genomic stability. Mol Cell Biol 2008;28:4116–4128.
[104] Maizels N. Genomic stability: FANCJ-dependent G4 DNA repair. Curr Biol 2008;18:R613–614.
[105] Maizels N. Dynamic roles for G4 DNA in the biology of eukaryotic cells. Nat Struct Mol Biol 2006;13:1055–1059.
[106] Hirota Y and Lahti JM. Characterization of the enzymatic activity of hChlR1, a novel human DNA helicase. Nucleic Acids Res 2000;28:917–924.
[107] Wu Y, Sommers JA, Khan I, de Winter JP and Brosh RM, Jr. Biochemical characterization of Warsaw breakage syndrome helicase. J Biol Chem 2012;287:1007–1021.
[108] Farina A, Shin JH, Kim DH et al. Studies with the human cohesin establishment factor, ChlR1. Association of ChlR1 with Ctf18-RFC and Fen1. J Biol Chem 2008;283:20925–20936.
[109] Petronczki M, Chwalla B, Siomos MF et al. Sister-chromatid cohesion mediated by the alternative RF-CCtf18/Dcc1/Ctf8, the helicase Chl1 and the polymerase-alpha-associated protein Ctf4 is essential for chromatid disjunction during meiosis II. J Cell Sci 2004;117:3547–3559.
[110] Skibbens RV. Chl1p, a DNA helicase-like protein in budding yeast, functions in sister-chromatid cohesion. Genetics 2004;166:33–42.
[111] Mayer ML, Pot I, Chang M et al. Identification of protein complexes required for efficient sister chromatid cohesion. Mol Biol Cell 2004;15:1736–1745.
[112] Inoue A, Li T, Roby SK et al. Loss of ChlR1 helicase in mouse causes lethality due to the accumulation of aneuploid cells generated by cohesion defects and placental malformation. Cell Cycle 2007;6:1646–1654.
[113] Parish JL, Rosa J, Wang X, Lahti JM, Doxsey SJ and Androphy EJ. The DNA helicase ChlR1 is required for sister chromatid cohesion in mammalian cells. J Cell Sci 2006;119:4857–4865.
[114] van der Lelij P, Chrzanowska KH, Godthelp BC et al. Warsaw breakage syndrome, a cohesinopathy associated with mutations in the XPD helicase family member DDX11/ChlR1. Am J Hum Genet 2010;86:262–266.
[115] Kuper J and Kisker C. Damage recognition in nucleotide excision DNA repair. Curr Opin Struct Biol 2012;22:88–93.

[116] Winkler GS, Araujo SJ, Fiedler U et al. TFIIH with inactive XPD helicase functions in transcription initiation but is defective in DNA repair. J Biol Chem 2000;275:4258–4266.
[117] Lehmann AR. The xeroderma pigmentosum group D (XPD) gene: one gene, two functions, three diseases. Genes Dev 2001;15:15–23.
[118] Laine JP, Mocquet V and Egly JM. TFIIH enzymatic activities in transcription and nucleotide excision repair. Methods Enzymol 2006;408:246–263.
[119] Egly JM and Coin F. A history of TFIIH: two decades of molecular biology on a pivotal transcription/repair factor. DNA Repair 2011;10:714–721.
[120] Fan L, Fuss JO, Cheng QJ et al. XPD helicase structures and activities: insights into the cancer and aging phenotypes from XPD mutations. Cell 2008;133:789–800.
[121] Liu H, Rudolf J, Johnson KA et al. Structure of the DNA repair helicase XPD. Cell 2008;133:801–812.
[122] Wolski SC, Kuper J, Hanzelmann P et al. Crystal structure of the FeS cluster-containing nucleotide excision repair helicase XPD. PLoS Biol 2008;6:e149.
[123] Kuper J, Wolski SC, Michels G and Kisker C. Functional and structural studies of the nucleotide excision repair helicase XPD suggest a polarity for DNA translocation. EMBO J 2012;31:494–502.
[124] Pugh RA, Honda M, Leesley H et al. The iron-containing domain is essential in Rad3 helicases for coupling of ATP hydrolysis to DNA translocation and for targeting the helicase to the single-stranded DNA-double-stranded DNA junction. J Biol Chem 2008;283:1732–1743.
[125] Pugh RA, Honda M and Spies M. Ensemble and single-molecule fluorescence-based assays to monitor DNA binding, translocation, and unwinding by iron-sulfur cluster containing helicases. Methods 2010;51:313–321.
[126] Pugh RA, Wu CG and Spies M. Regulation of translocation polarity by helicase domain 1 in SF2B helicases. EMBO J 2012;31:503–514.
[127] Mathieu N, Kaczmarek N, Rüthemann P, Luch A and Naegeli H. DNA quality control by a lesion sensor pocket of the xeroderma pigmentosum group D helicase subunit of TFIIH. Curr Biol 2013;23:204–212.
[128] Dubaele S, Proietti De Santis L, Bienstock RJ et al. Basal transcription defect discriminates between xeroderma pigmentosum and trichothiodystrophy in XPD patients. Mol Cell 2003;11:1635–1646.
[129] Capo-Chichi JM, Bharti SK, Sommers JA et al. Identification and biochemical characterization of a novel mutation in DDX11 causing Warsaw breakage syndrome. Hum Mutat 2013;34:103–107.
[130] Wu Y, Sommers JA, Suhasini AN et al. Fanconi anemia group J mutation abolishes its DNA repair function by uncoupling DNA translocation from helicase activity or disruption of protein-DNA complexes. Blood 2010;116:3780–3791.
[131] Cantor SB et al. BACH1, a novel helicase-like protein, interacts directly with BRCA1 and contributes to its DNA repair function. in *Cell* Vol. 105, 2001;149–160.
[132] Kim H et al. Analysis of BRIP1 Variants Among Korean Patients with BRCA1/2 Mutation-Negative High-Risk Breast Cancer. in *Cancer Res Treat* (2016).
[133] Gupta R et al. Inhibition of BACH1 (FANCJ) helicase by backbone discontinuity is overcome by increased motor ATPase or length of loading strand. in *Nucleic Acids Research* Vol. 34, 2006;6673–6683.
[134] Ren B, Duan X and Ding H. Redox control of the DNA damage-inducible protein DinG helicase activity via its iron-sulfur cluster. J Biol Chem 2009;284:4829–4835.
[135] Mui TP, Fuss JO, Ishida JP, Tainer JA and Barton JK. ATP-stimulated, DNA-mediated redox signaling by XPD, a DNA repair and transcription helicase. J Am Chem Soc 2011;133:16378–16381.
[136] Sontz PA, Mui TP, Fuss JO, Tainer JA and Barton JK. DNA charge transport as a first step in coordinating the detection of lesions by repair proteins. Proc Natl Acad Sci USA 2012;109:1856–1861.

14 Eukaryotic iron-sulfur protein biogenesis and its role in maintaining genomic integrity

Roland Lill, Marta A. Uzarska and James Wohlschlegel

14.1 Introduction

The biogenesis of iron-sulfur (Fe-S) proteins in eukaryotes is a complex biosynthetic process. Failure to assemble Fe-S clusters and insert them into apo-proteins is incompatible with life and in humans can lead to various neurological, hematological, and metabolic diseases. Fe-S protein biogenesis is initiated by the mitochondrial iron-sulfur cluster (ISC) assembly machinery which is involved in the biogenesis of all cellular Fe-S proteins including those located in the cytosol and nucleus. Maturation of the latter proteins additionally requires the cytosolic iron-sulfur protein assembly (CIA) machinery and a still unknown sulfur-containing molecule exported from mitochondria. The essential character of the biosynthetic process is explained by the function of Fe-S proteins involved in cytosolic protein translation and in numerous steps of nuclear DNA metabolism including DNA synthesis and repair, chromosome segregation, and telomere length regulation. Many of these latter Fe-S proteins have been linked to diseases such as various forms of cancer as well as ageing. Here, we first provide an overview of the components and molecular mechanisms of the ISC and CIA machineries required for Fe-S protein assembly. In a second part, we explain the intimate molecular links of this essential process to DNA maintenance and chromosome instability.

Fe-S clusters are ancient protein cofactors that function as electron carriers, catalysts in chemical reactions, regulatory sensors, or sulfur donors (see other chapters in this book). In the (non-plant) eukaryotic cell, known Fe-S proteins are localized in the mitochondria, cytosol, and nucleus where they participate in a large number of biochemical reactions (Fig. 14.1). In the model organism *Saccharomyces cerevisiae*, Fe-S proteins perform functions in energy production (respiratory complexes II and III, mitochondrial aconitase), amino acid metabolism (e.g. ketoacid hydratases Leu1 and Ilv3 or a subunit of sulfite reductase, Ecm17), cofactor biosynthesis (lipoate and biotin synthase), and in protein synthesis (Rli1 involved in translation termination) (Fig. 14.1a). In the yeast nucleus, several Fe-S proteins have been identified that perform functions in DNA synthesis (replicative DNA polymerases, primase subunit Pri2) and various aspects of DNA repair (DNA helicase Rad3 and the glycosylase Ntg2). Additionally, a conspicuous number of the Fe-S protein biogenesis components (Yah1, Grx5, Dre2, Cfd1, Nbp35, and Nar1) depend on Fe-S clusters themselves, i.e. they are both components and targets of the biogenesis systems. Mammalian cells lack some of the biosynthetic Fe-S proteins of yeast (e.g. biotin synthase or Fe-S proteins involved in amino acid synthesis) yet contain additional Fe-S proteins not present in yeast

DOI 10.1515/9783110479850-014

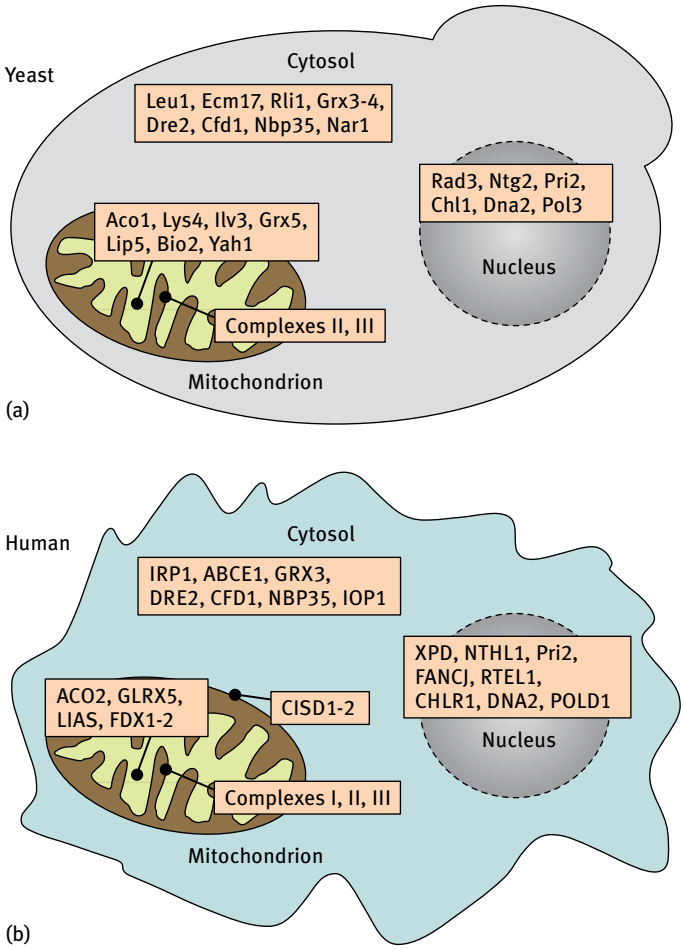

Fig. 14.1: Important Fe/S proteins in *S. cerevisiae* and mammalian cells. In (non-green) eukaryotes, Fe/S proteins are localized in mitochondria, cytosol, and nucleus. The figure presents a selection of the Fe/S protein inventory of (a) *S. cerevisiae* and (b) human cells. Some Fe/S proteins are present in only one of these organisms. Examples of mitochondrial Fe/S proteins (human names in parenthesis): Aco1 (ACO2), aconitase; Lys4, homoaconitase; Ilv3, dihydroxyacid dehydratase; Grx5 (GLRX5), monothiol glutaredoxin; Lip5 (LIAS), lipoate synthase; Bio2, biotin synthase; Yah1 (FDX1-FDX2), ferredoxin (adrenodoxin); respiratory complexes II and III. Cytosolic Fe/S proteins: Leu1, isopropylmalate isomerase; Ecm17, subunit of sulfite reductase; Rli1 (ABCE1), ABC protein involved in ribosome function; Grx3-Grx4 (GRX3), monothiol glutaredoxins; Dre2, Cfd1, Nbp35, and Nar1 (IOP1), CIA components. Nuclear Fe/S proteins: Rad3 (XPD), ATP-dependent DNA helicase; Ntg2 (NTHL1), DNA repair protein *N*-glycosylase, Pri2, primase subunit; Chl1 (CHLR1), DNA helicase; Dna2, ATP-dependent nuclease and helicase; Pol3 (POLD1), DNA polymerase δ subunit. Additionally, human cells possess a few Fe/S proteins that are not present in yeast, such as respiratory complex I, members of the mitoNEET (CISD) family attached to the mitochondrial outer membrane, IRP1 (cytosolic aconitase), FANCJ (DNA repair helicase mutated in Fanconi anemia), and RTEL1 (helicase involved in telomere stability).

(Fig. 14.1b). These include respiratory complex I with 8 Fe-S clusters, members of the mitoNEET (CISD) family in mitochondria and possibly the endoplasmic reticulum, and cytosolic aconitase, also known as iron regulatory protein 1 (IRP1), which uses its Fe-S cluster for sensing the intracellular iron status. The mammalian nucleus harbors, in addition to the aforementioned replicative DNA polymerases, a number of ATP-dependent DNA helicases with rather diverse functions in various aspects of DNA metabolism such as nucleotide excision repair (NER), telomere length regulation and chromosome segregation [xeroderma pigmentosum complementation group D (XPD), Fanconi anemia complement group J (FANCJ), regulator of telomere elongation 1 (RTEL1), and CHLR1]. A number of these factors have been implicated in human disease such as xeroderma pigmentosum, Fanconi anemia, and trichothiodystrophy. It is clear from this list of Fe-S proteins that knowledge of their assembly pathways in the living cell is not only of basic scientific interest but also has important medical implications.

The biogenesis of cellular Fe-S proteins is a complex process that requires the coordinated function of some 30 proteins in mitochondria and cytosol. The mitochondrial ISC assembly machinery was inherited from a similar system in bacteria yet is highly conserved from yeast to man (Fig. 14.2) [1–6]. The molecular mechanisms of the ISC assembly pathway have been worked out mainly in yeast and bacteria [7, 8] and can be divided into three main steps (Fig. 14.2a). First, a Fe-S cluster is synthesized *de novo* on a scaffold protein from iron and sulfur, which is released from cysteine by a desulfurase enzyme to form a persulfide group (-SSH) on the desulfurase. Second, the Fe-S cluster is released from the scaffold protein and transferred to proteins that transiently bind the cluster, and in a third step, insert the Fe-S cluster into different target apoproteins. Each of these steps requires the participation of several additional ISC proteins and low-molecular-mass cofactors, which will be explained in detail in Section 14.2.

Cytosolic and nuclear Fe-S proteins also require the mitochondrial ISC assembly system in both yeast and human cells [9–11]. Mitochondria export an as-yet unknown sulfur-containing molecule (X-S in Fig. 14.2) that is used by the CIA machinery for maturation. Both the ISC and CIA systems contain numerous constituents that are essential for the viability of yeast and human cells. Moreover, many diseases are linked to genetic mutations in various mitochondrial ISC components (Fig. 14.2b) [6, 12]. This demonstrates the importance of the overall biogenesis process for life. Moreover, because numerous essential Fe-S proteins with functions in protein synthesis, tRNA modification, and DNA replication and repair depend on the mitochondrial ISC system for maturation, the participation of the mitochondria in cellular Fe-S protein biosynthesis renders it essential for life [3, 4, 13]. This fact is impressively underlined by the discovery of mitosomes, i.e. mitochondria-derived organelles that, like mitochondria, possess a double membrane and import their proteins from the cytosol [14, 15]. However, during the evolution, the function of these organelles was drastically reduced by the loss of all classical mitochondrial functions including heme synthesis, citric acid cycle, oxidative phosphorylation, fatty acid oxidation, and mitochondrial

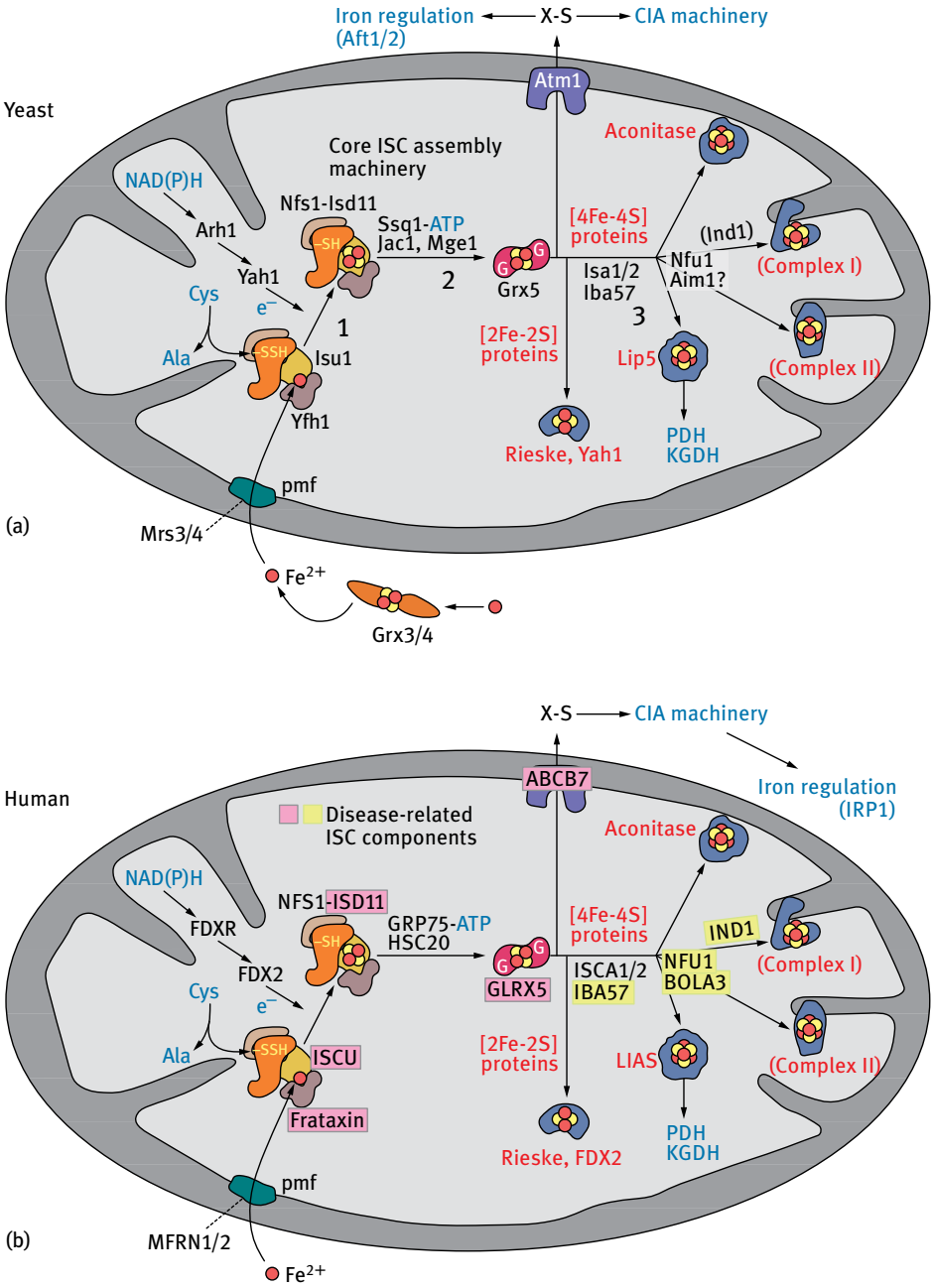

(*Figure Continued*)

(*Figure Continued*)

Fig. 14.2: The three steps of mitochondrial Fe/S protein assembly and diseases associated with this process. The components and mechanisms of mitochondrial Fe/S protein biogenesis are highly conserved from (a) yeast to (b) human cells. (a) In yeast, the glutaredoxins Grx3-Grx4 facilitate mitochondrial import of ferrous iron (red circle) from the cytosol *via* the inner membrane carriers Mrs3-Mrs4, which use the proton motive force (pmf) as a driving force for membrane transport. The biogenesis of mitochondrial Fe/S proteins is accomplished by the ISC assembly machinery in three major steps. First, a [2Fe-2S] cluster is synthesized on the scaffold protein Isu1, a step that requires the cysteine desulfurase complex Nfs1-Isd11 as a sulfur (yellow circle) donor and releases sulfur from cysteine *via* a Nfs1-bound persulfide intermediate (-SSH). This step further requires frataxin (yeast Yfh1), which undergoes an iron-dependent interaction with Isu1 and may serve as an iron donor and/or an allosteric regulator of the desulfurase enzyme. An electron (e^-) transfer chain consisting of NAD(P)H, ferredoxin reductase (Arh1) and ferredoxin (Yah1) is needed for Fe/S cluster assembly on Isu1. Second, the Isu1-bound Fe/S cluster is labilized by functional involvement of a dedicated chaperone system comprised of the ATP-dependent Hsp70 chaperone Ssq1, its co-chaperone Jac1, and the nucleotide exchange factor Mge1. Monothiol glutaredoxin Grx5 may receive the Fe/S cluster directly from Isu1 and binds it in a glutathione (G)-dependent fashion (see Fig. 14.3). The aforementioned proteins are involved in the biogenesis of all mitochondrial Fe/S proteins (including the [2Fe-2S] proteins Rieske and Yah1) and are termed core ISC assembly components. The ABC transporter Atm1 exports an unknown, sulfur-containing component (X-S) produced by the core ISC components for use in the maturation of cytosolic-nuclear Fe/S proteins by the CIA machinery (Fig. 14.4a) and for iron regulation by the Aft1-Aft2 transcription factors. In a third step, the generation of [4Fe-4S] clusters is catalyzed by Isa1-Isa2-Iba57 proteins. Further, specialized ISC targeting components (Nfu1, Aim1) assist the insertion of the Fe/S clusters into specific apo-proteins such as lipoate synthase (Lip5) and respiratory complex II (SDH), whereas Ind1 (not present in *S. cerevisiae* but in other fungi such as *Yarrowia*) is specific for complex I. The role of the BolA-like protein Aim1 is still hypothetical. Matured Lip5 produces lipoate for enzymes such as PDH and KGDH. (b) The human ISC assembly components use similar mechanisms as the yeast proteins. The function of the core ISC assembly components also impacts on cellular iron regulation *via* ABCB7- and CIA machinery-dependent maturation of IRP1 (see Fig. 14.4b). Defects in several of these mitochondrial components (highlighted in pink) lead to severe diseases with mitochondrial iron accumulation. In contrast, genetic defects in late-acting ISC components (highlighted in yellow) cause severe diseases that are not associated with alterations in cellular or mitochondrial iron levels. A variant erythropoietic protoporphyria is caused by dysfunctional mitoferrin 1 (MFRN1) in erythroid tissue. Cys, cysteine; Ala, alanine.

gene expression [16–18]. The only known process maintained in mitosomes is the Fe-S protein biosynthesis pathway, which likely has been maintained to support the maturation of extra-mitochondrial Fe-S proteins, as mitosomes do not contain any relevant Fe-S proteins themselves [15, 19, 20].

In this chapter, we will first summarize the molecular mechanisms of Fe-S protein biogenesis in eukaryotes. Then, we will provide an overview on the link between this pathway and the maintenance of genomic stability by several important Fe-S proteins. Other links of the Fe-S protein maturation process, e.g. to cellular iron regulation, and the diseases linked to Fe-S protein biogenesis will only be briefly discussed. These aspects are covered in other parts of this volume and have been comprehensively reviewed elsewhere [5, 6, 12, 21, 22].

14.2 Biogenesis of mitochondrial Fe-S proteins

14.2.1 Step 1: *De novo* Fe-S cluster assembly on the Isu1 scaffold protein

The ISC assembly machinery in yeast mitochondria consists of 17 known proteins, many of which are homologues of bacterial ISC factors [4, 5, 23] (Fig. 14.2a). Virtually all these ISC components are conserved in human cells (Fig. 14.2b), which, in addition, contains a specific maturation factor for respiratory complex I (IND1), which is present in all eukaryotes harboring this respiratory complex. In all eukaryotes, the ISC components are encoded in the nucleus and after their synthesis are imported into the mitochondrial matrix. For import, they use typical mitochondrial targeting sequences that are recognized by the TOM-TIM import machinery [24, 25].

Fe-S protein biogenesis starts with the *de novo* assembly of a Fe-S cluster on the scaffold protein Isu1 (yeast) or ISCU (human) (Fig. 14.2) [2, 26–28]. In yeast, a functionally redundant homologue termed Isu2 is present that arose by gene duplication. Isu1 scaffold proteins are highly conserved in bacteria and eukaryotes and contain three cysteine residues that are critical for Fe-S cluster synthesis. The sulfur is provided by the mitochondrial cysteine desulfurase Nfs1, which is required for all cellular Fe-S proteins [1, 9]. Nfs1 contains a conserved cysteine residue that is transiently converted to a persulfide following cysteine conversion to alanine and thus serves as a site for sulfur activation. Nfs1 tightly interacts with the small LYRM family protein Isd11. This protein is not necessary for desulfurase activity, yet essential for sulfur transfer from Nfs1 to Isu1 and Fe-S cluster formation on Isu1 [29–31].

The pathway by which iron is recruited by Isu1 is not fully understood. Iron import into the mitochondria is conducted *via* carrier proteins Mrs3 and Mrs4 (mitoferrin 1 and 2 in vertebrates) [32–35]. Recently, a minor role in mitochondrial iron import has been documented for the carrier Rim2, which co-imports iron and a pyrimidine nucleotide [36, 37]. In the matrix, the ISC protein frataxin (yeast Yfh1) has been implicated as an iron donor because it binds iron with micromolar affinities and forms an iron-stimulated complex with Isu1 and Nfs1/Isd11 [38–41]. Recent *in vitro* work on human frataxin suggests that it acts as an iron-dependent allosteric activator of Nfs1 desulfurase activity [42]. Additional experiments performed in yeast show that an Isu1 point mutation localized near one of the conserved cysteine residues is able to rescue the Fe-S protein biogenesis defect of *YFH1* deletion cells [43], showing that this function can be bypassed, at least in yeast. Although all these studies are consistent with a function of Yfh1 in Fe-S cluster synthesis on Isu1, its precise molecular function is not yet clear.

Another requirement for Fe-S cluster synthesis on Isu1 is the electron transfer from the [2Fe-2S] ferredoxin Yah1, which receives its electrons from the ferredoxin reductase Arh1 and NAD(P)H [27, 44–47] (Fig. 14.2a). It is not exactly known what this electron flow is used for. One possibility is the need for reduction of the sulfan sulfur (S^0) present in the cysteine to the sulfide (S^{2-}) present in the Fe-S cluster [4]. It has also been suggested to be needed for fusion of two [2Fe-2S] clusters into one [4Fe-4S] by

reductive coupling [48, 49]. However, as pointed out later, [4Fe-4S] cluster generation requires late-acting ISC proteins. Interestingly, Yah1 is also necessary for heme A and coenzyme Q biosynthesis [50, 51]. It is the only essential Fe-S protein of yeast mitochondria (besides the scaffold protein Isu1 itself) and requires the core ISC assembly machinery for its own maturation [52]. Human cells possess two distinct mitochondrial ferredoxins, which differ in their expression pattern. The classical adrenodoxin FDX1 is found in adrenal gland and kidney cells where the protein, together with mitochondrial cytochrome P450 proteins, is involved steroid hormone and vitamin D production [46]. In contrast, the only recently characterized FDX2 is ubiquitously expressed. As expected from this tissue-specific expression pattern, FDX2 was found to be specifically involved in Fe-S protein assembly and able to replace yeast Yah1, whereas FDX1 cannot. Moreover, FDX1 does not complement FDX2-depleted HeLa cells in their defect in Fe-S protein biogenesis. In contrast, another study found effects on Fe-S protein biogenesis upon RNAi depletion of both FDX1 and FDX2 [47]. Recent *in vitro* studies reconstituting *de novo* Fe-S cluster synthesis on Isu1 confirmed the specific function of FDX2, but not of FDX1 in this process (Webert *et al.*, unpublished data). Conversely, only FDX1 but not FDX2 was active in cytochrome P450-dependent cortisol biosynthesis [46]. RNAi depletion of the human ferredoxin reductase FDXR demonstrated its requirement for the biogenesis of Fe-S proteins [47].

In conclusion, the initial step of Fe-S cluster synthesis requires the concerted action of six ISC proteins, in addition to iron, cysteine, and NADPH, and leads to a transiently bound [2Fe-2S] cluster on the Isu1 scaffold (Fig. 14.2).

14.2.2 Step 2: Chaperone-dependent release of the Isu1-bound Fe-S cluster

In the second major step, the Fe-S cluster is released from the Isu1 scaffold and delivered to so-called Fe-S cluster transfer proteins [27, 53] (Fig. 14.2a). Fe-S cluster release from Isu1 is facilitated by a dedicated chaperone system consisting of the Hsp70 protein Ssq1, its co-chaperone J-type protein Jac1, and nucleotide exchange factor Mge1 [54, 55]. Studies performed on these chaperones and their bacterial homologs [56, 57] gave insights into how they function within the ISC assembly pathway. The mechanistic model for the dedicated chaperone function in Fe-S protein biogenesis was derived from chaperones that function in protein folding [54] with Isu1 serving as a specific client protein of the Ssq1 chaperone. According to the current model (Fig. 14.3), the co-chaperone Jac1 recruits the holo-form of Isu1 and directs it to the ATP-bound form of Ssq1 [58, 59]. Both Jac1 and Isu1 stimulate the ATPase activity of Ssq1 thereby inducing a conformational change of the peptide-binding domain of Ssq1 to its closed state. This conformational change stabilizes the interaction between Ssq1 and the LPPVK motif of Isu1 [60, 61] and facilitates the removal of Jac1 from the complex. It is believed that Isu1 also undergoes a conformational change that results in its Fe-S cluster to be bound in a more labile fashion, thus facilitating its release from the scaffold protein [62, 63] (Fig. 14.3). To close the cycle and regenerate the

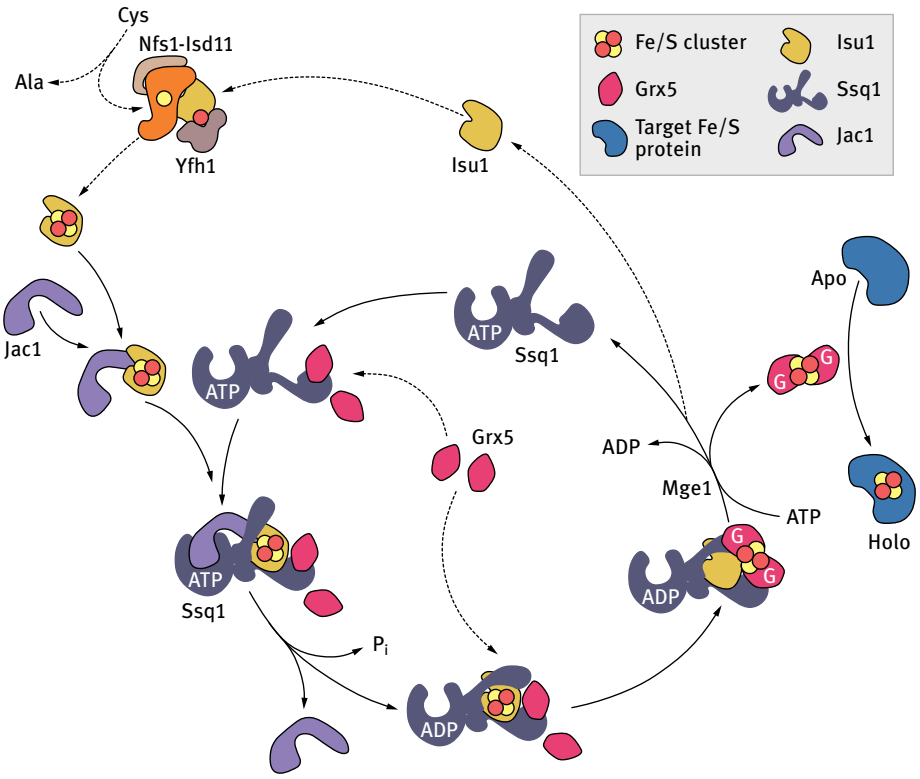

Fig. 14.3: The working cycle of the dedicated chaperone system in mitochondrial Fe/S protein biogenesis. The working cycle of ISC chaperone system is similar to that of the Hsp70 chaperones in protein folding [54]. After synthesis of the [2Fe-2S] cluster on the scaffold protein Isu1 (Fig. 14.2a), the co-chaperone Jac1 recruits holo-Isu1 and delivers it to the ATP-bound form of the Hsp70 chaperone Ssq1. ATP hydrolysis induced by Isu1 and Jac1 triggers a conformational change of the peptide-binding domain of Ssq1, thus tightly binding the LPPVK motif of Isu1. In turn, this is believed to induce a conformational change on Isu1 and weakens the binding of the Fe/S cluster to Isu1. Apo-Grx5 binds to Ssq1 at a site that does not overlap with that of Isu1. Eventually, this results in Fe/S cluster transfer from holo-Isu1 to Apo-Grx5. The exchange factor Mge1 facilitates ADP to ATP exchange, which triggers another conformational change in the peptide-binding domain of Ssq1 from the closed to an open state, thus leading to disassembly of the Ssq1-Isu1-holo-Grx5 complex. The Hsp70 reaction cycle can then resume with the binding of a new holo-Isu1-Jac1 complex to Ssq1-ATP. The Grx5-bound Fe/S cluster is finally transferred to target proteins (see Fig. 14.2a).

individual components, the nucleotide exchange factor Mge1 joins the complex to exchange ADP for ATP [64]. This induces another conformational change in Ssq1 that triggers disassembly of the entire protein complex and recycling of apo-Isu1 that can be used for another round of Fe-S cluster synthesis.

The Fe-S cluster released from Isu1 is then transferred toward apo-proteins, which likely involves transient binding to ISC transfer proteins. One of these proteins is the

monothiol glutaredoxin Grx5 or human GLRX5 (Fig. 14.2). The protein binds to Ssq1 at a site that does not overlap with that of Isu1 [65] (Fig. 14.3). Most avid binding of Grx5 is observed for the ADP-bound form of Ssq1, which is known to tightly associate with the holo-form of Isu1. Therefore, it was suggested that the vicinity of holo-Isu1 and apo-Grx5 on Ssq1 accelerates the transfer of the labilized Fe-S cluster to Grx5. Depletion of Grx5 in yeast causes a general cellular Fe-S protein defect and leads to Fe-S cluster accumulation on Isu1, similar to what was found for Ssq1 or Jac1 depletion [27, 66]. As a result, Grx5-depleted cells display an iron overload in mitochondria and develop a severe oxidative stress. A similar phenotype, together with an impaired heme synthesis, is seen in zebrafish and human cells [67–69]. Hence, the function of Grx5 seems to be conserved throughout evolution. This is supported by the observation that *GRX5* deletion in yeast can be complemented by most monothiol glutaredoxins from both prokaryotic and eukaryotic species [70, 71]. The fact that Grx5 is involved in the biogenesis of both [2Fe-2S] and [4Fe-4S] mitochondrial Fe-S proteins and is also required for maturation of cytosolic-nuclear Fe-S proteins demonstrated that it belongs to the core ISC assembly machinery [65], thus distinguishing it from late-acting ISC factors discussed in Section 14.2.3 (Fig. 14.2a).

In vitro experiments on monothiol glutaredoxins from different organisms demonstrated the coordination of an unusual, glutathione (GSH)-coordinated [2Fe-2S] cluster [72]. Cysteine mutagenesis studies and the structure of the *Escherichia coli* Grx4 homodimer documented that the Grx-bound [2Fe-2S] cluster is coordinated by two GSH molecules and the active-site cysteine residues of two Grx monomers [70, 73–76]. The active-site cysteine residue is necessary for Grx5's *in vivo* function because its substitution results in the same phenotype as that seen for the null mutant [77]. The Fe-S cluster is bound to Grx5 in a rather labile fashion, making it difficult to detect *in vivo* [65, 70]. Its assembly in yeast depends on the core ISC components such as Nfs1, Isu1, and Jac1. Kinetic studies *in vitro* indicated that it is possible to transfer the [2Fe-2S] cluster to a chloroplast apo-ferredoxin [70]. These data support the view that monothiol Grx5 binds a Fe-S cluster transiently to subsequently pass it on to other Fe-S cluster-coordinating ISC proteins or to recipient target proteins including [2Fe-2S] proteins (Fig. 14.2a). However, it has to be noted that alternative Grx5 functions are not yet excluded.

In conclusion, step 2 leads to the chaperone-assisted dissociation of the Isu1-bound [2Fe-2S] cluster and its transfer to acceptor proteins including Grx5 and [2Fe-2S] target proteins (Fig. 14.2).

14.2.3 Step 3: Late-acting ISC assembly proteins function in [4Fe-4S] cluster synthesis and in target-specific Fe-S cluster insertion

The core ISC assembly machinery discussed so far is sufficient for maturation of mitochondrial [2Fe-2S] cluster-containing proteins. In contrast, virtually all mitochondrial

[4Fe-4S] proteins require additional ISC assembly components for their maturation. The formation of [4Fe-4S] clusters in both yeast and human cells strongly depends on the A-type ISC proteins Isa1 and Isa2 (human ISCA1 and ISCA2, respectively) [52, 78–82]. The proteins form a complex and bind either a [2Fe-2S] cluster or iron, yet the functional role of these metal cofactors is unclear. Both proteins further interact with the potential folate-binding protein Iba57 [82, 83]. Depletion of all three proteins in either *S. cerevisiae* or in human cells leads to similar and severe mitochondrial phenotypes such respiratory deficiency, loss of mitochondrial DNA, and ultrastructural alterations of mitochondria. These phenotypes can be readily explained by the maturation defect of mitochondrial [4Fe-4S] proteins prevailing in these cells. In addition, the Isa- or Iba57-depleted cells display a severe diminution of cytochrome oxidase activity. This terminal respiratory complex lacks Fe-S clusters and hence should not be affected. To date, it is unclear why its activity strictly depends on Isa-Iba57 function.

Another late-acting factor is the P-loop NTPase Ind1 (also termed NUBPL1 in humans), which binds a [4Fe-4S] cluster at two conserved cysteine residues present on its C-terminus [84, 85]. The protein is related in sequence to the two CIA proteins Cfd1-Nbp35, which act as scaffolds for [4Fe-4S] cluster generation in the cytosol (see in Section 14.4). In contrast, Ind1 is present only in organisms containing respiratory complex I, which contains eight Fe-S clusters in eukaryotes. Studies performed in *Yarrowia lipolytica* and human cells showed that deficiency of Ind1 affects the assembly of respiratory complex I, in particular of its soluble, Fe-S cluster-containing arm. The Fe-S cluster present on Ind1 is dependent on the function of the core ISC assembly machinery [84]. Therefore, it was proposed that Ind1 serves late in the biogenesis pathway and may serve as a specific Fe-S cluster-targeting factor, which delivers the cofactor to the matrix-exposed arm of complex I. In that sense, Fe-S cluster binding would serve a similar role as Fe-S cluster binding to the Cfd1-Nbp35 complex.

Proteins containing the 70-amino acid long C-terminal region of *A. vinelandii* NifU protein are termed Nfu-like proteins. Although this conserved segment possesses a CXXC motif and is able to transiently bind a [4Fe-4S] cluster [86], its location and function in the mitochondrial ISC assembly pathway remained unclear for a long period of time. Because Nfu-like proteins can assemble [2Fe-2S] or [4Fe-4S] clusters and transfer them to other Fe-S proteins, it was proposed that they might serve a scaffold function in addition to Isu1 [7, 86]. Initial evidence that Nfu1 may be involved in Fe-S protein biosynthesis was obtained in a synthetic lethal screen in yeast where the deletion of *NFU1* and *SSQ1* was synthetic lethal [2]. However, Fe-S protein activities were only slightly affected. This defect was enhanced when double mutants were analyzed in which both *NFU1* and *ISU1* were deleted. In addition to the Fe-S protein defects, mitochondria accumulated iron similar to other depletion mutants in core ISC assembly proteins [5] (Fig. 14.2).

The first insights into Nfu1 function came from studies on two groups of patients carrying mutations in the *NFU1* gene [87, 88]. In one case, a non-sense mutation resulted in abnormal mRNA splicing and complete loss of the protein, whereas in the

other, a G→C point mutation led to a glycine to cysteine substitution next to the active site CXXC motif of NFU1. Affected individuals were born normally with no evident symptoms but quickly developed severe developmental retardation, brain abnormalities, and pulmonary hypertension before their deaths between 3 months and 1 year of age. The biochemical analyses of these patients showed normal aconitase activities but a massive decrease in complexes I and II [87, 88]. Additionally, strong defects in the lipoic acid-containing proteins pyruvate dehydrogenase (PDH) and α-ketoglutarate dehydrogenase (KGDH) were seen, together with hyperglycinemia and an increase in organic ketoacids. This phenotype was explained by a maturation defect in the Fe-S cluster containing-protein lipoate synthase [89] (Fig. 14.2). Because lipoate synthase activity was not routinely measured during Fe-S protein biogenesis studies, this phenotype was missed in most previous studies. RNAi depletion of NFU1 in human cell culture recapitulated the biochemical phenotype of the patients demonstrating a role of NFU1 in the assembly of complex Fe-S proteins (respiratory complexes I and II and lipoate synthase containing eight, three, and two Fe-S clusters, respectively) [5, 87, 88]. All these results indicate a function of Nfu1 not as an alternative scaffold protein but rather a role in the delivery of [4Fe-4S] clusters to dedicated target apoproteins. This idea is consistent with the finding that assembly of the Fe-S cluster transiently bound to Nfu1 requires the function of the core ISC components such as Nfs1, Isu1, and Grx5 [88]. It remains to be elucidated what the exact biochemical role of Nfu1 protein in Fe-S cluster biogenesis might be and how it coordinates its function with other components of the late part of the ISC assembly pathway.

Patients with a mutation in the *BOLA3* gene display a strikingly similar phenotype as the Canadian group of *NFU1* patients [87]. In those individuals, the *BOLA3* gene carries a frame shift mutation introducing a premature stop codon. The individuals died at a few months of age, and their cells displayed severe defects in the lipoic acid-containing proteins PDH and KGDH as well as respiratory complexes I and II, whereas mitochondrial Fe-S protein aconitase activities were unchanged. Another group of patients with a *BOLA3* mutation displayed the same phenotype, yet with an additional complex III deficiency [90]. Results of clinical and biochemical studies performed on these patients suggested that the BOLA3 protein may play an auxiliary role in the insertion of Fe-S clusters into specific target proteins such as lipoic acid synthase and the respiratory chain complexes I and II [87, 90]. Even though the participation of the BOLA3 protein in mitochondrial Fe-S protein biogenesis seems clear, its evolutionary conservation and its biochemical function remain to be unraveled.

BolA-like proteins are highly conserved throughout evolution and are, with few exceptions, present in all living organisms. BolA was first identified in bacteria that show a round or "bola" (Spanish for ball or sphere) morphology when *bolA* was overexpressed [91]. Eukaryotes from yeast to man possess three BolA-like proteins, two in the mitochondria, namely Yal044W/BOLA1 and Aim1/BOLA3, and one in the cytosol, termed Fra2/BOLA2. Not much is known about the yeast mitochondrial proteins. Deletion of *AIM1* (altered inheritance of mitochondria) in *S. cerevisiae* displayed elevated

frequency of mitochondrial genome loss [92]. A bioinformatics study combining genome sequences, physical interaction data and three-dimensional structures suggested that BolA proteins are reductases that might interact with glutaredoxins [93]. Although a direct interaction of Aim1/BOLA3 with Grx5/GLRX5 in mitochondria is uncertain, yeast Fra2 is known to form a complex with Grx3/4 in the cytosol and nucleus [94, 95]. These proteins are involved in cellular iron regulation, transmitting the iron status of the yeast cell to the transcription factors Aft1-Aft2 [5, 21, 22]. *In vitro* studies showed that Grx3/4 and Fra2 can form a heterodimeric complex bridged by a [2Fe-2S] cluster. This cluster is coordinated by the active-site cysteine of Grx3/4, GSH, and a histidine residue of Fra2. A similar complex was shown for the human proteins GRX3 and BOLA2 [96], implying that Grx-BolA interaction is conserved in higher eukaryotes, even though iron regulation in higher eukaryotes is not transcriptionally controlled. Overall, a role of BOLA3 in mitochondrial Fe-S protein biogenesis seems established, but where and how the protein functions in the pathway remains to be determined.

In conclusion, step 3 is needed for proteins carrying a [4Fe-4S] cluster and involves the Isa-Iba57-mediated generation of this cluster, which subsequently is inserted into target proteins with the help of dedicated ISC targeting factors.

14.3 The role of the mitochondrial ABC transporter Atm1 in the biogenesis of cytosolic and nuclear Fe-S proteins and in iron regulation

Biogenesis of extra-mitochondrial Fe-S proteins in yeast strictly depends on the mitochondrial ISC assembly machinery [1, 10]. This is particularly true for the cysteine desulfurase Nfs1, which is also localized in the cytosol and/or nucleus in yeast and man [97, 98]. Only mitochondrial versions of Nfs1 and Isu1 support the biogenesis of extra-mitochondrial Fe-S proteins. Moreover, the expression of Nfs1 or Isu1 in the cytosol does not rescue the Fe-S cluster assembly defects in that compartment [1, 9, 10, 99, 100], suggesting that mitochondria produce the sulfur moiety that is utilized for cytosolic and nuclear Fe-S cluster biogenesis. Cytosolic-nuclear Nfs1 is essential for cell viability in yeast, but its function remains elusive. It was suspected that cytosolic-nuclear Nfs1 might be involved in the thio-modification of certain cytosolic tRNAs. However, this speculation was experimentally refuted [101]. The current belief why mitochondria are required for extra-mitochondrial Fe-S protein assembly is that the core components of the ISC machinery produce a sulfur-containing component termed X-S (Fig. 14.2 and Fig. 14.4), which is utilized for cytosolic and nuclear Fe-S cluster production. The nature of this component is not presently known, but the ABC transporter Atm1 may be responsible for its export to the cytosol [1, 102, 103]. Atm1 might cooperate with the FAD-dependent sulfhydryl oxidase Erv1 of the intermembrane space and GSH in this export task [44, 104]. Depletion of both Erv1 and GSH

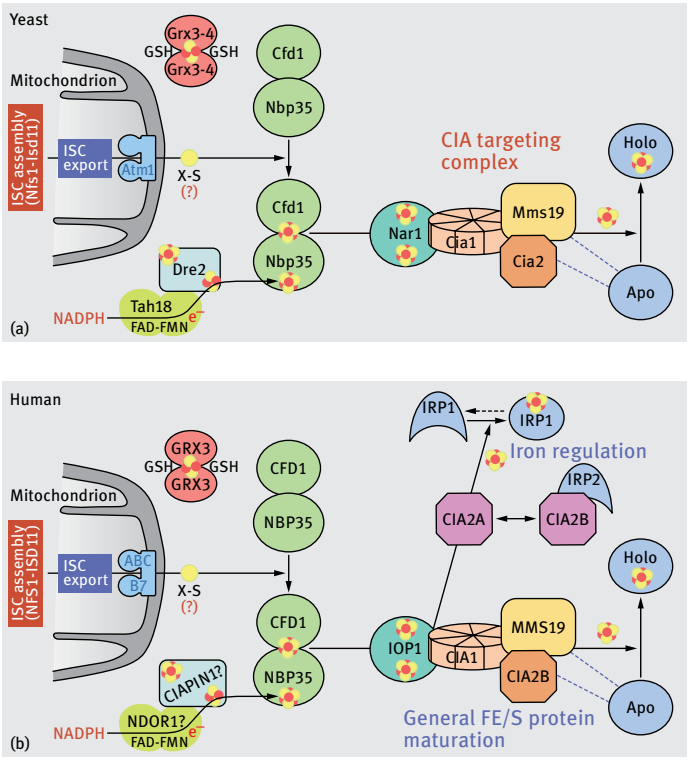

Fig. 14.4: The role of mitochondria and the CIA machinery in the maturation of cytosolic and nuclear Fe/S proteins. (a) In yeast, the CIA machinery encompasses eight known proteins. The assembly process can be dissected into two different steps. First, a bridging [4Fe-4S] cluster is assembled on the Cfd1-Nbp35 scaffold complex. This reaction requires a sulfur source (X-S) generated by the mitochondrial ISC assembly machinery and exported by the mitochondrial ABC transporter Atm1 (Fig. 14.2a). Generation of the functionally essential N-terminal Fe/S cluster of Nbp35 (bottom) depends on the flavoprotein Tah18 and the Fe/S protein Dre2, which serve as an NADPH-dependent electron transfer chain. Second, the bridging Fe/S cluster is released from Cfd1-Nbp35, a reaction mediated by the Fe/S protein Nar1 and the CIA-targeting complex Cia1-Cia2-Mms19. The latter three proteins interact with target (apo)proteins and assure specific Fe/S cluster insertion. Biogenesis further requires the cytosolic multidomain monothiol glutaredoxins Grx3-Grx4, which bind a GSH-coordinated, bridging [2Fe-2S] cluster, and may serve as an iron donor. (b) In humans, the components of the CIA machinery are structurally and functionally similar to those of yeast. As a major difference, humans possess two isoforms of Cia2. CIA2B is the functional orthologue of yeast Cia2 and is involved in the biogenesis of canonical cytosolic and nuclear Fe/S proteins. In contrast, CIA2A is specifically involved in the maturation of IRP1, a protein regulating cellular iron homeostasis in humans. Additionally, CIA2A tightly binds to IRP2, which does not contain a Fe/S cluster yet also plays a decisive role in cellular iron metabolism. Note that the role of some indicated (?) human CIA components has not been verified yet.

causes similar phenotypes as that of Atm1, namely cytosolic Fe-S proteins defects and an accumulation of iron in the mitochondria [1, 105]. Erv1 is known to introduce disulfide bridges into target proteins during their Mia40-dependent import into the intermembrane space [106], and hence, it is not excluded that the Erv1 function in Fe-S protein biogenesis is indirectly caused by a failure to generate disulfide bridges in this compartment.

14.4 The role of the CIA machinery in the biogenesis of cytosolic and nuclear Fe-S proteins

14.4.1 Step 1: The synthesis of a [4Fe-4S] on the scaffold complex Cfd1-Nbp35

As pointed out in Section 14.1, the cytosol and nucleus contain numerous Fe-S proteins with essential functions for life (Fig. 14.1). Their maturation depends on mitochondria and the CIA machinery, which comprises eight known yeast proteins that are conserved in eukaryotes [107, 108] (Fig. 14.4). Analogous to mitochondrial Fe-S protein biogenesis, the roles of individual CIA proteins can be attributed to functions that are formally similar to those performed by the mitochondrial ISC machinery [109–111]. First, a [4Fe-4S] cluster is transiently assembled on the P-loop NTPases Cfd1 and Nbp35, which serve as a scaffold complex. This step requires the core mitochondrial ISC assembly machinery including Nfs1-Isd11 for production of the sulfur donor (Fig. 14.4) [9, 99]. Cfd1-Nbp35 form a hetero-tetramer and bind the [4Fe-4S] cluster in a bridging manner [107, 110]. Mutation of the Walker motifs of Cfd1 or Nbp35 destroys the function of these proteins suggesting that NTP hydrolysis is required for Fe-S cluster assembly, but experimental proof for nucleotide binding or hydrolysis is still missing. In addition to its transient Fe-S cluster, Nbp35 contains another [4Fe-4S] cluster at its N-terminus that is more stably bound and essential for function [112]. Its assembly depends on electron transfer from the electron source NADPH to the flavin-containing oxidoreductase Tah18 and finally the Fe-S protein Dre2 [111, 113, 114] (Fig. 14.4a). The precise role of reduction in this early step of CIA function remains unclear. One possibility is the reduction of the sulfur moiety exported from mitochondria to sulfide, but other options are equally plausible.

In conclusion, the initial step of cytosolic-nuclear Fe-S protein maturation involves the synthesis of a [4Fe-4S] cluster on the Cfd1-Nbp35 scaffold, which requires a sulfur-containing product of mitochondria and electron input from the CIA electron transfer chain.

14.4.2 Step 2: Transfer of the [4Fe-4S] cluster to target apo-proteins

In the next step, the transiently bound, bridging [4Fe-4S] cluster on Cfd1-Nbp35 is transferred to apo-proteins. The CIA protein Nar1 interacts with Nbp35 and may

therefore be involved in Fe-S cluster mobilization [115, 116]. Nar1 shows similarity to iron-only hydrogenases and binds two [4Fe-4S] clusters that are assembled with the help of Cfd1-Nbp35 [117]. Because later-acting CIA factors are dispensable for the assembly of the two Nar1 Fe-S clusters, the protein may act as a mediator between early and late steps of the CIA biogenesis process (Fig. 14.4a). The recently identified CIA components Cia1, Cia2, and Mms19 form the so-called CIA-targeting complex [118–122], which facilitates both Fe-S cluster transfer and target-specific cluster insertion into the various polypeptide chains. These partial reactions involve the direct physical interaction of the CIA-targeting complex components with the target Fe-S proteins, which presumably are in their apo-forms (Fig. 14.4a, dotted lines). The direct contact between late-acting CIA and Fe-S proteins became most evident from systematic affinity pull-down experiments in human cells where the various CIA targeting factors interact with a large number of cytosolic and nuclear Fe-S proteins [120–124]. The list of interacting Fe-S proteins includes DNA polymerases and primases, ATP-dependent DNA helicases, DNA glycosylases, and the ABC protein ABCE1. Possibly, there are more Fe-S proteins hidden in this collection of CIA interactors. In yeast, the CIA association with target Fe-S proteins seem to be weaker or less stable. Both dedicated and systematic approaches have identified only few such interactions including the binding of Cia2 to the helicase-nuclease Dna2, and the interaction of Mms19 with the Fe-S helicase Rad3 [120] (Mascarenhas *et al.*, unpublished data). The precise molecular function of the late-acting CIA components remains to be determined.

In addition to the aforementioned CIA proteins, the cytosolic monothiol glutaredoxins Grx3-Grx4 (in humans termed Grx3 or PICOT) were also shown to be crucial for cytosolic and nuclear Fe-S protein biogenesis [125, 126]. Because these proteins are generally involved in intracellular iron trafficking and iron uptake regulation [5, 21, 22], they appear to play a more general function and hence are not considered as CIA proteins. For instance, these glutaredoxins are involved in the maturation of yeast di-iron proteins such as ribonucleotide reductase and participate in heme biosynthesis in zebrafish erythroid cells [125–127]. Thus, Grx3-Grx4 could potentially supply iron to some step of the biosynthesis reaction, but their precise role remains to be elucidated.

In conclusion, step 2 leads to dissociation of the [4Fe-4S] from Cfd1-Nbp35 and its CIA targeting complex-dependent incorporation into specific apo-proteins.

14.5 Specialized functions of the human CIA-targeting complex components

14.5.1 Dedicated biogenesis of cytosolic and nuclear Fe-S proteins

Although yeast cells have served as a primary model organism to identify and characterize the known constituents of the CIA machinery, the process seems to be conserved in all eukaryotes including man (Fig. 14.4). All eight known yeast CIA

proteins have a counterpart in human cells, and initial RNAi-mediated depletion studies have shown a function for human Nbp35 and IOP1 (yeast Nar1) in cytosolic and nuclear Fe-S protein biogenesis [116, 128]. Ongoing investigations also suggest conserved functions for CFD1 (O. Stehling, unpublished data). The *in vivo* functions of NDOR1 (human homologue of yeast Tah18) and CIAPIN1 (yeast Dre2) in human cells remain to be established. The (studied) human CIA proteins appear to be required for maturation of all analyzed cytosolic-nuclear [4Fe-4S] proteins. The members of the human equivalent of the yeast CIA-targeting complex (termed CIA1, CIA2B, and MMS19) were recently identified and functionally characterized by RNAi depletion technology and subsequent analysis of Fe-S protein function [120–122]. In contrast to yeast, the members of the human CIA-targeting complex exhibit a striking specificity for target apo-proteins. For instance, MMS19 is less important for GPAT maturation than the other CIA proteins, and CIA2B is not crucially required for DNA polymerase δ (POLD1) assembly [122]. It appears that the CIA-targeting complex members perform dedicated functions in the delivery of Fe-S clusters to specific apo-proteins. Several systematic proteomic screens identified numerous interaction partners of CIA1, CIA2B, and MMS19 proteins [120–124, 129–132]. These included a large number of cytosolic and nuclear Fe-S proteins that were mostly bound to both CIA1 and CIA2B.

Cia2 contains a C-terminal domain (CTD) of unknown function 59 (DUF59). A global study of proteins containing reactive cysteine residues identified a hyperreactive cysteine in yeast Cia2 (Cys161) and in one of the two human Cia2 homologues (Cys93 of CIA2B). Mutation of the corresponding cysteine residue was lethal in yeast and abolished the activity of the Fe-S protein Leu1 [119, 133]. Cia2 and CIA2B are general Fe-S protein maturation factors acting as part of the CIA-targeting complex in yeast and humans, respectively [122] (Mascarenhas *et al.*, unpublished data). In *Arabidopsis*, mutation of the three Cia2 homologues AE7 leads to lower activities of the [4Fe-4S] proteins cytosolic aconitase and nuclear glycosylase [134]. Hence, the function of this protein seems to be conserved in eukaryotes. The DUF59 domain is also present in the plastid Fe-S protein biogenesis factor HCF101 [135] as well as bacterial proteins, but their precise molecular role remains unresolved. Structural information has been obtained for three bacterial Cia2 (also termed SufT) homologues (see e.g. [136]). Additionally, an NMR structure and two different X-ray structures of CIA2A have been reported [137]. Thus far, the structural information has not provided any decisive functional insights.

In conclusion, the various components of the CIA-targeting complex undergo direct and specific interactions with client Fe-S proteins to assure their specific maturation.

14.5.2 The dual role of CIA2A in iron homeostasis

Human cells encode a second CIA2 homologue termed CIA2A, which forms a subcomplex with CIA1. Depletion of CIA2A does not elicit any defects in canonical

cytosolic and nuclear Fe-S proteins [122]. However, CIA2A is exclusively required for the maturation of the [4Fe-4S] protein IRP1, which is a key regulatory element of mammalian iron metabolism. In mammals, the major impact on cellular iron supply and distribution within the cell is mediated by IRP1 and IRP2 *via* complex post-transcriptional regulatory mechanisms (for comprehensive recent reviews see [138, 139]). IRP1 is a cytosolic aconitase whose activity depends on the [4Fe-4S] cluster. Upon iron starvation, IRP1 loses its Fe-S cluster, and its apo-form can bind to iron-responsive elements (IREs) of mRNAs, which encode proteins involved in iron trafficking (e.g. transferrin receptor), storage (ferritin), and utilization (mitochondrial aconitase and eALAS). IRP1 binding differentially regulates the efficiency of translation or mRNA stability [138, 139]. Accordingly, CIA2A (but not CIA2B or MMS19) depletion increases the IRE binding activity of IRP1. In turn, ferritin levels are diminished and the expression of the transferrin receptor is increased. Thus, CIA2A depletion mimics iron deficiency. Upon iron repletion, the equilibrium between the apo- and holo-forms of IRP1 is shifted back to the Fe-S cluster form in an assembly step that is dependent on CIA2A and all earlier-acting CIA proteins, but not CIA2B or MMS19 (Fig. 14.4b).

Surprisingly, there is a second important effect of CIA2A on cellular iron regulation. The protein tightly binds to IRP2 [122], which does not contain a Fe-S cluster but is regulated by iron-dependent degradation by the proteasome (Fig. 14.4b). The precise role of CIA2A in the mechanism of this IRP2 regulatory step is currently unknown. Under iron-replete conditions, IRP2 is degraded in an iron- and oxygen-dependent fashion by the E3 ubiquitin ligase FBXL5, which responds to iron and oxygen *via* its hemerythrin domain [139]. Upon iron depletion or under low oxygen concentrations, FBXL5 is destabilized and degraded, leading to increased levels of IRP2. The stabilizing effect of CIA2A binding to IRP2 introduces another unexpected level of iron regulation *via* the CIA machinery. Thus, the CIA2A branch of the CIA machinery, through the regulation of both IRP1 and IRP2, impacts on cellular iron homeostasis in multiple ways.

In conclusion, human CIA2A has a crucial function in cellular iron homeostasis as a dedicated CIA targeting factor for IRP1 maturation and as a stabilizer of IRP2.

14.6 Fe-S protein assembly and the maintenance of genomic stability

The conceptual framework for Fe-S cluster assembly that been established over the past 15 years has provided novel insights into the breadth of cellular processes that are directly impacted by Fe-S proteins. The remainder of this chapter will focus specifically on how the Fe-S biogenesis pathways described above directly influence multiple aspects of genome maintenance including DNA replication and repair. Evidence for the global involvement of Fe-S cluster assembly pathways in DNA metabolism

emerged from two converging discoveries: (1) proteins previously identified as DNA repair factors were actually central components of the Fe-S protein assembly machinery and (2) multiple enzymes involved in DNA metabolism require Fe-S clusters for activity. Both of these research arcs will be discussed further.

14.6.1 Late-acting CIA factors in DNA metabolism

The CIA-targeting complex component MMS19 was originally identified in two independent genetic screens in budding yeast as a gene required for methionine biosynthesis, NER, and RNA polymerase II transcription [140, 141]. Although its role in methionine biosynthesis remained largely unexplored, multiple follow-up studies focused on elucidating its role in transcription and DNA repair. Specifically, work in budding yeast showed that MMS19 was required for the function of the general transcription factor TFIIH and that the DNA repair and transcription defects observed in cell-free protein extracts derived from MMS19-deficient yeast strains could be complemented by the addition of purified TFIIH [142]. It was also demonstrated that while MMS19 was not itself a component of TFIIH, it was required for maintaining cellular levels of Rad3, the yeast homologue of XPD and a member of the TFIIH complex [143]. Studies of the human homologue of MMS19 were consistent with the work done in yeast and suggested an important role in DNA repair and transcription through regulation of TFIIH function [144, 145]. In both systems, however, the molecular mechanism by which MMS19 exerted its "regulatory" effects on Rad3 and TFIIH was elusive.

The first direct link between the CIA machinery and the DNA repair pathways was documented in 2012 [120, 121]. As described earlier, both articles reported the discovery that MMS19 was a late-acting factor of the CIA pathway and functioned as part of a CIA-targeting complex that physically links early CIA components to apo-protein targets (Fig. 14.4). Importantly, these studies provided multiple lines of evidence directly implicating the CIA-targeting complex in DNA repair pathways. First, the CIA-targeting complex was physically associated with a large number of DNA metabolic enzymes including DNA helicases (XPD, FANCJ, and RTEL1), the DNA glycosylase NTHL1, DNA polymerases (POLD1, POLA1, and POLE1), the nuclease DNA2, and the DNA primase PRI2 (Fig. 14.1b). Second, the depletion of MMS19 led to a variety of defects consistent with widespread deregulation of DNA metabolism including increased sensitivity to DNA damaging agents, destabilization of DNA polymerase δ, and inhibition of XPD incorporation into TFIIH. Together, these data established the central role for Fe-S protein assembly in regulating the integrity of multiple DNA metabolic pathways.

In addition to its major role in Fe-S cluster biogenesis, a recent study also implicated a protein complex consisting of MMS19, CIA2B (also known as FAM96B or MIP18),

CIA1 (also known as CIAO1), and XPD (denoted by the authors as MMXD and likely identical to the CIA targeting complex) in mitosis [146]. They demonstrated that MMXD localized to mitotic spindles and that depletion of MMS19, CIA2B, or XPD led to defects in spindle assembly and chromosome segregation as well as the accumulation of abnormal nuclei. These defects were also observed in fibroblasts derived from patients expressing XPD mutants that are known to give rise to xeroderma pigmentosum, Cockayne syndrome, and trichothiodystrophy suggesting that this mitotic role for MMXD may be of pathological relevance. Interestingly, these phenotypes cannot be readily traced to the reported function of individual Fe-S proteins, suggesting that this may be related to the general function of the CIA-targeting complex in the biogenesis of the bulk of cytosolic and nuclear Fe-S proteins.

14.6.2 XPD and the Rad3 family of DNA helicases

XPD is a Fe-S cluster-requiring DNA helicase that functions as a component of the general transcription complex TFIIH [147]. TFIIH is a highly conserved 10-subunit complex consisting of XPB, p63, p52, p44, p34, p8, XPD, CDK7, cyclin H, and MAT1 that is required for both transcription initiation and NER. XPD is thought to play at least two distinct roles in TFIIH function. First, it physically bridges the CDK-activating subcomplex (CDK7, cyclin H, and MAT1) to the rest of the TFIIH core complex. Second, XPD is a member of the superfamily 2 (SF2) class of helicases and possesses a 5′-3′ DNA helicase activity that unwinds the region surrounding the DNA lesion during NER. In a landmark finding in 2006, the White group used a combination of biochemical and spectroscopic approaches to identify a metal-binding site in archaeal XPD in which a [4Fe-4S] cluster was coordinated by four highly conserved cysteine ligands [148]. Multiple high-resolution structural studies subsequently verified the presence of a [4Fe-4S] domain that together with a novel “Arch” domain abuts the two helicase domains to form a channel through which they hypothesized ssDNA was extruded [149–151]. In this model, the [4Fe-4S] domain could potentially act as a “ploughshare” that is physically responsible for DNA strand separation. Considerable functional data have been reported that are consistent with this model including the observation that mutation of any of the conserved cysteine ligands leads to loss of [4Fe-4S] cluster binding and a concomitant loss of strand displacement activity without a detectable loss of ATPase activity [148, 152]. Together, these data established XPD as the first Fe-S cluster-dependent helicase to be characterized and provided a novel link between DNA repair and iron metabolism.

In addition to XPD, higher eukaryotes contain multiple SF2 XPD-like paralogues including FANCJ, RTEL1, and DDX11/CHLR1 [153, 154]. FANCJ is a downstream component of the Fanconi anemia pathway and is involved in responding to and repairing DNA interstrand cross-links. RTEL1 is involved in maintaining genome stability

by regulating telomere length and suppressing inappropriate homologous recombination. CHLR1 is required for sister chromatid cohesion and heterochromatin organization. The cysteine residues required for coordinating the Fe-S cluster are conserved across these paralogues, suggesting that Fe-S cluster binding is a conserved feature for this family of helicases. Moreover, direct experimental evidence that recombinant FANCJ co-purifies with Fe and that clinically relevant mutations in its Fe-S cluster domain reduce both Fe binding and helicase activity has been reported, thus highlighting the central role of the Fe-S domain across the entire helicase family [155].

14.6.3 Fe-S proteins involved in DNA replication

DNA replication requires the coordinated activities of a large number of cellular enzymes [156]. These enzymes include (but are not limited to) (1) DNA primase, the enzyme responsible for synthesizing the RNA primers that nucleate DNA synthesis, (2) multiple DNA polymerases that catalyze DNA template-dependent DNA synthesis, and (3) DNA2, a nuclease involved in Okazaki fragment processing that is essential for lagging strand replication. Interestingly, all of these factors have been shown to be Fe-S cluster proteins and are dependent on Fe-S cofactor binding for either structure stabilization or function.

Eukaryotic primases are heterodimeric enzymes consisting of large (Pri2) and small (Pri1) subunits [157]. Although RNA synthesis is carried out specifically by the Pri1 subunit, Pri2 is equally essential and is required for initiation, elongation, and regulation of primer length. Biochemical studies of the CTD of Pri2 showed that the purified protein was brownish in color and contained four conserved cysteine residues, suggesting that it contains an Fe-S cluster [158, 159]. The presence of the cluster was confirmed by EPR spectroscopy. Subsequent mutational and functional analyses demonstrated that the C-terminal Fe-S cluster domain is required for primase activity and plays a role in recognizing and binding the ss/dsDNA junction [158, 159].

Eukaryotic DNA replication depends on the coordinated activity of three DNA polymerase complexes – Pol-α, Pol-δ, and Pol-ε [160]. Pol-α forms a protein complex with DNA primase and is required for the initiation of DNA replication, whereas Pol-δ and Pol-ε are required for processive DNA elongation. The CTDs of Pol1, Pol2, and Pol3, i.e. the catalytic subunits of Pol-α, Pol-ε, and Pol-δ, respectively, each contain two cysteine-rich motifs termed CysA and CysB, which were previously thought to be Zn-binding sites. Although CysA is still believed to be a Zn-binding site, definitive evidence has recently emerged demonstrating that CysB actually binds an essential [4Fe-4S] cluster [161]. This includes data showing that the CTDs of Pol1, Pol2, and Pol3 from budding yeast co-purify with iron *in vivo* using ^{55}Fe-radiolabeling assays and spectroscopic data showing that recombinant versions of these CTDs contain [4Fe-4S] clusters after purification from *E. coli*. The exact molecular function of these Fe-S

clusters in Pol1, Pol2, and Pol3 remains unclear, although, at least for Pol3, it appears that Pol3 Fe-S cluster integrity is required for the assembly of the accessory subunits (Pol31-Pol32) of the Pol-δ complexes [161].

Dna2 is a multifunctional enzyme with distinct nuclease and helicase domains and plays essential roles in Okazaki fragment maturation during DNA replication, double-stranded DNA break repair, and telomere maintenance [156]. Embedded within the nuclease domain is a conserved four-cysteine motif ($CX_{248}CX_2CX_5C$), which has been shown to bind an Fe-S cluster using spectroscopic and mutational approaches [162]. Interestingly, mutation of any of the conserved cysteine residues to alanine impairs both nuclease and helicase activities without inhibiting its DNA-binding activity or causing gross structural rearrangements in the protein as assayed by protease sensitivity. Based on these findings, a role for DNA2's Fe-S cluster in mediating the dynamic conformational changes that are required for coupling the nuclease and helicase activities has been proposed.

14.6.4 DNA glycosylases as Fe-S proteins

Endonuclease III/MutY DNA glycosylases are a highly conserved family of DNA repair enzymes that play a key role in base excision repair (BER) [163]. They function by excising specific damaged bases from intact DNA helices, leaving an apurinic site that can be repaired by downstream enzymes in the BER pathway. *E. coli* endonuclease III, which catalyzes the removal of oxidatively damaged bases, was the first DNA repair enzyme demonstrated to require a Fe-S cluster for function [164]. Structural and functional studies have indicated that this Fe-S cluster plays both a structural role in positioning the DNA-binding residues of endonuclease III to facilitate DNA binding and a redox-mediated role in localizing the enzyme to sites of DNA damage *via* charge transport [165–167]. This charge transport function will be discussed in greater detail in Section 14.7. Unlike their *E. coli* counterparts, the human homologues of this family have not been extensively studied, although evidence demonstrating that they are Fe-S proteins has been reported [168].

14.7 Biochemical functions of Fe-S clusters in DNA metabolic enzymes

As the number of Fe-S proteins with roles in DNA metabolism has increased, understanding the molecular roles of their metal centers has become a major priority. For the majority of Fe-S proteins involved in DNA metabolism, the Fe-S cluster has been proposed to play a noncatalytic role in stabilizing the structure of the enzyme and potentially facilitating nucleic acid binding [169]. The major exception to this trend is a model developed by the Barton group in which the Fe-S clusters play a role in

a novel redox process known as DNA charge transport [170, 171]. The basic premise of this model is that DNA can effectively conduct an electric charge *via* overlapping π-orbitals of stacked aromatic nucleotide bases. This charge transport has two important features. First, it can efficiently occur over long molecular distances, making it a potential mechanism for long distance signaling across a large part of a chromosome. Second, it is extremely sensitive to perturbations in the integrity of the base pair stack such as those that occur as a consequence of exposure to DNA damaging agents. These characteristics led the Barton group to explore whether the DNA repair machinery can exploit these features to better facilitate the cellular response to DNA damage.

Initial studies from the Barton laboratory focused on the DNA glycosylases MutY and endonuclease III (EndoIII) from *E. coli*. These glycosylases both contain an evolutionarily conserved [4Fe-4S] cluster and are components of the BER pathway that functions in the repair of damaged or modified bases [165, 166, 172]. Through a series of elegant biochemical studies, they have established a model in which these enzymes monitor the integrity of the genome using their Fe-S clusters to signal to one another through DNA charge transport. Their proposed model is shown in Fig. 14.5 and is as follows. First, a reduced Fe-S cluster enzyme is weakly bound to DNA as it scans the genome. This enzyme can be activated by oxidation potentially as a result of oxidative stress or other DNA damaging agents. This increases its affinity for DNA by 1000-fold and "locks" it onto the DNA. Second, as the enzyme is oxidized, it releases an electron that is transported along "healthy" DNA until it reaches a second oxidized DNA-bound enzyme nearby. Third, reduction of the second enzyme signals the integrity of the intervening DNA sequence promoting its release from the undamaged DNA

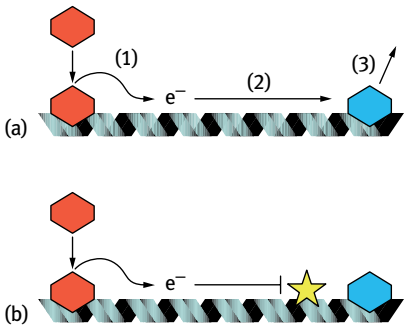

Fig. 14.5: DNA charge transport model for localization of Fe/S enzymes. (a) Step 1: Oxidation of a Fe/S DNA repair protein stabilizes its association with DNA. Step 2: If the surrounding DNA is undamaged, DNA charge transport occurs between the oxidized enzyme and the other nearby oxidized Fe/S DNA repair enzymes. Step 3: The reduction of DNA-bound Fe/S cluster proteins triggers their dissociation from the DNA and enables them to continue scanning the genome for lesions. (b) If the intervening DNA between two DNA-bound Fe/S enzymes contains damaged or mismatched bases that block DNA charge transport, then the Fe/S cluster enzymes remain bound in close proximity to the DNA lesion and facilitate their repair.

region. However, if these two DNA-bound enzymes are flanking a damaged base, then DNA charge transport is blocked and the oxidized DNA repair enzymes remain bound near the DNA lesion where they can initiate the repair process.

Although these charge transport studies were previously limited to these DNA glycosylases, more recent work has expanded the breadth of DNA repair enzymes that potentially function using DNA charge transport [173]. This includes work on the helicase XPD, which is essential for both transcription initiation and NER and contains a [4Fe-4S] cluster that possesses a physiologically relevant redox potential when bound to DNA. In atomic force microscopy experiments, it was shown that XPD redistributes to DNA lesions in a manner that is dependent on an intact Fe-S cluster and consistent with the DNA charge transport model for repair protein localization. It was also demonstrated that XPD could cooperate with EndoIII to localize to DNA lesions, raising the intriguing possibility that scanning the genome for different types of DNA damage could occur *via* coordinated DNA charge transport between different DNA repair pathways.

Despite strong *in vitro* evidence supporting this DNA charge transport model for DNA repair, *in vivo* data for this model remains sparse [165]. The strongest *in vivo* experiments supporting charge transport come from genetic experiments performed in *E. coli*. It was shown that MutY activity was partially lost in strains deficient for EndoIII. Importantly, this phenotype could be rescued by the introduction of a catalytically inactive EndoIII mutant, suggesting that EndoIII's ability to regulate MutY activity was independent of its own enzymatic activity. Because the mutant EndoIII retained its capacity for charge transport, the authors concluded that DNA-mediated signaling between MutY and EndoIII likely accounted for the cooperation found between the two enzymes.

14.8 Interplay among Fe-S proteins, genome stability, and tumorigenesis

During the multistep development of cancer, normal cells acquire new biological capabilities that enable their progression to a neoplastic state [174]. The acquisition of these capabilities is enabled by chance genomic alterations that give rise to heritable mutant phenotypes. To accelerate the accumulation of these mutations, cancer cells invariably disrupt critical cellular pathways that normally function to ensure proper maintenance of the genome. Tumor-associated genomic instability thus becomes an essential and enabling characteristic of tumor pathogenesis [175]. Although the contribution of iron metabolism and Fe-S protein assembly defects to promoting genome instability remains largely unclear, several lines of evidence suggest that they may play both positive and negative roles in this process.

The inability to assemble Fe-S clusters in proteins involved in DNA metabolism is likely to promote genomic instability in a multitude of ways. Fe-S proteins are essential components of a wide range of DNA repair pathways (NER, BER, telomere

maintenance, DNA interstrand cross-link repair, DNA double-strand break repair) that are collectively required to respond to a broad spectrum of DNA lesions including base modifications, UV-induced thymidine dimers, DNA interstrand cross-links, and DNA strand breaks [169, 176]. From the tumorigenesis point of view, this strong dependency of DNA repair on proper Fe-S protein assembly makes it an attractive target whereby inactivation of a single pathway (Fe-S protein assembly) can broadly disrupt the majority of the cellular DNA repair pathways and strongly promote genomic instability. As described earlier, many DNA replication factors are Fe-S proteins including DNA polymerase, DNA primases, and nucleases involved in Okazaki fragment maturation such as DNA2. Thus, inhibition of Fe-S protein maturation would also lead to misregulation and/or inactivation of these replication factors, resulting in profound impacts on genomic integrity. Successful DNA replication requires that the entire nuclear genome be replicated once and only once. Previous studies have shown that misregulation of DNA replication factors is sufficient to cause either over-replication or under-replication of specific genomic regions and thus directly breach genomic integrity mechanisms [177].

Although intriguing, this proposed model of how inhibiting Fe-S protein biogenesis may induce genomic instability through the disruption of key DNA repair and replication pathways remains largely speculative. The strongest evidence for a physiological relevance of this connection comes from work by the Gottschling group exploring aging in budding yeast [178, 179]. They demonstrated that yeast undergo an age-dependent increase in genomic instability, specifically increased loss of heterozygosity (LOH), that particularly is induced by mitochondrial dysfunction [178, 180]. Specifically, their studies showed that an age-associated or chemically induced loss of mtDNA decreased the mitochondrial membrane potential and an increased frequency of nuclear LOH. This loss of mitochondrial function correlated with a transcriptional signature that was similar to iron starvation, suggesting the cellular iron metabolism was disrupted [179]. As Fe-S protein biogenesis is central for cellular iron regulation (see in Section 14.5), they hypothesized that the increased nuclear LOH resulted from a Fe-S protein assembly defect during the "crisis" stemming from the loss of mtDNA. Further credence to this model came from the observation that conditional inactivation of the CIA factor Nar1 led to increased nuclear LOH [179]. Interestingly, it also been shown that human cultured cell lines that have lost their mtDNA exhibit a decreased capacity for the repair of oxidatively damaged DNA and an increase in their nuclear mutation rates, suggesting that the role of mitochondria in maintaining genomic integrity is highly conserved [181].

If defects in Fe-S cluster biogenesis can drive genomic instability, then it would also be expected that reduced Fe-S protein biogenesis would promote tumorigenesis. Although evidence in this regard is scarce, several key observations have been reported. First, mice in which the Fe-S cluster biogenesis protein frataxin gene has been knocked out in hepatocytes show a reduced life span, resulting from a dramatic increase in hepatic tumor incidence [182]. Second, a gene expression signature that includes ISCU, ISCA1, and CIAO1 is effective at stratifying breast cancer patients based

on metastasis-free long-term survival [183]. Third, mutations that specifically disrupt the assembly of Fe-S clusters in XPD and FANCJ give rise to xeroderma pigmentosum and Fanconi anemia, two syndromes that are characterized by a predisposition to cancer [148, 155].

Additional indirect evidence that may support a connection between Fe-S protein biogenesis and tumorigenesis comes from broader work looking at the role of excess iron in tumorigenesis. Both animal and population studies have clearly established a link between cancer susceptibility and excess iron resulting from either high dietary intake or genetic disorders such as hemochromatosis, which lead to iron overload and deposition in liver, heart, and endocrine organs [184, 185]. The mechanism by which iron overload promotes tumorigenesis results, at least in part, from the ability of iron to generate reactive oxygen species *via* the Fenton reaction, which in turn leads to oxidative damage of cellular macromolecules. These high levels of oxidative stress can also impact Fe-S cluster metabolism and the downstream genome stability pathways through multiple mechanisms. First, the Fe-S clusters of DNA repair holoenzymes can be directly damaged by oxidation, leading to their inactivation [6, 186]. Second, oxidative stress can also lead to mitochondrial dysfunction and reduced Fe-S cluster biogenesis [12, 187]. Together, these two mechanisms may offer a plausible route by which excess iron can disrupt Fe-S cluster-dependent genomic stability pathways and thereby promote tumor-associated genome stability.

14.9 Summary

It is essential to emphasize that although the connection between Fe-S protein biogenesis and genome stability and tumorigenesis may be reasonable based on existing data, this issue remains highly speculative. Genetic data indicating that components of the Fe-S cluster machinery pathway are either mutated or inactivated during the course of tumorigenesis are completely lacking. Similarly, a systematic analysis of the integrity of the Fe-S protein assembly pathways or the activity of Fe-S proteins in primary tumors has not been reported. Additional work in this area is clearly needed to establish the pathological relevance of these pathways with respect to cancer.

To better understand the role of Fe-S protein assembly in tumorigenesis, it will also be necessary to focus on how substrate specificity and prioritization is determined by the biogenesis machinery. Considering that different subsets of Fe-S proteins are essential for cell proliferation, viability, and genome maintenance, it will be interesting to see what cellular mechanisms might be available for the differential maturation of different sets of Fe-S substrates. For example, precancerous cells would benefit from maintaining those Fe-S proteins necessary for growth and proliferation, while blocking the biogenesis of Fe-S proteins required for genome stability. It is not clear, however, to what extent this type of differential regulation is possible

and whether cellular mechanisms even exist for prioritizing the maturation of one set of Fe-S proteins over another. Bacterial systems contain an alternate Fe-S cluster assembly pathway known as the SUF system that is activated in cells undergoing physiological stress or iron deprivation. This system may provide a potential paradigm for how cells might regulate Fe-S cluster assembly of a distinct group of client apo-proteins under defined physiological conditions [8, 188]. Examples of specialized Fe-S protein assembly pathways in eukaryotes are provided by the dedicated maturation of IRP1 *via* CIA2A (instead of CIA2B; Fig. 14.4b) and the MMS19-independent maturation of GPAT [120, 122]. Understanding the global regulation of the Fe-S protein assembly pathways and how the integrity of the genome stability pathways can be influenced by altering the flux of Fe-S clusters to specific substrates will be a crucial step in providing the conceptual framework necessary for elucidating how these pathways might be co-opted in the context of tumorigenesis.

A major impetus for elucidating the complex relationships governing Fe-S cluster assembly and genome stability is to assess whether these pathways may offer a novel avenue for therapeutic intervention in the context of cancer. One therapeutic strategy could entail the development of small molecule activators of Fe-S protein assembly capable of stimulating the maturation of Fe-S cluster-dependent DNA repair enzymes and thereby promote genome stability pathways. Alternatively, pharmacological inhibition of Fe-S protein biogenesis could lead to inactivation of genome stability pathways and thus sensitize tumors to chemotherapy. Preliminary studies looking at how the inhibition of Fe-S protein assembly could interfere with cell proliferation in the context of tumorigenesis could be performed using iron-chelating agents such as deferoxamine, whose anti-tumor activity is already being examined clinically [189].

Acknowledgments

We thank the members of our groups for excellent work and stimulating discussions. R.L. acknowledges generous support from Deutsche Forschungsgemeinschaft (SFB 593, SFB 987, and GRK 1216), von Behring-Röntgen Stiftung, LOEWE program of state Hessen, and Max-Planck Gesellschaft.

References

[1] Kispal G, Csere P, Prohl C, Lill R. The mitochondrial proteins Atm1p and Nfs1p are required for biogenesis of cytosolic Fe/S proteins. EMBO J 1999;18:3981–9.
[2] Schilke B, Voisine C, Beinert H, Craig E. Evidence for a conserved system for iron metabolism in the mitochondria of Saccharomyces cerevisiae. Proc Natl Acad Sci USA 1999;96:10206–11.
[3] Lill R, Mühlenhoff U. Maturation of iron-sulfur proteins in eukaryotes: mechanisms, connected processes, and diseases. Annu Rev Biochem 2008;77:669–700.
[4] Lill R. Function and biogenesis iron-sulphur proteins. Nature 2009;460:831–8.

[5] Lill R, Hoffmann B, Molik S, et al. The role of mitochondria in cellular iron-sulfur protein biogenesis and iron metabolism. Biochim Biophys Acta 2012;1823:1491–508.
[6] Rouault TA. Biogenesis of iron-sulfur clusters in mammalian cells: new insights and relevance to human disease. Dis Model Mech 2012;5:155–64.
[7] Johnson DC, Dean DR, Smith AD, Johnson MK. Structure, function and formation of biological iron-sulfur clusters. Annu Rev Biochem 2005;74:247–81.
[8] Py B, Barras F. Building Fe-S proteins: bacterial strategies. Nat Rev Microbiol 2010;8:436–46.
[9] Biederbick A, Stehling O, Rösser R, et al. Role of human mitochondrial Nfs1 in cytosolic iron-sulfur protein biogenesis and iron regulation. Mol Cell Biol 2006;26:5675–87.
[10] Gerber J, Neumann K, Prohl C, Mühlenhoff U, Lill R. The yeast scaffold proteins Isu1p and Isu2p are required inside mitochondria for maturation of cytosolic Fe/S proteins. Mol Cell Biol 2004;24:4848–57.
[11] Fosset C, Chauveau MJ, Guillon B, Canal F, Drapier JC, Bouton C. RNA silencing of mitochondrial m-Nfs1 reduces Fe-S enzyme activity both in mitochondria and cytosol of mammalian cells. J Biol Chem 2006;281:25398–406.
[12] Stehling O, Lill R. The role of mitochondria in cellular iron-sulfur protein biogenesis: mechanisms, connected processes, and diseases. Cold Spring Harb Perspect Biol 2013;5:a011312.
[13] Lill R, Mühlenhoff U. Iron-sulfur protein biogenesis in eukaryotes: components and mechanisms. Annu Rev Cell Dev Biol 2006;22:457–86.
[14] Embley TM, Martin W. Eukaryotic evolution, changes and challenges. Nature 2006;440:623–30.
[15] Molik S, Lill R. Role of mitosomes in cellular iron-sulfur protein biogenesis. J Endocyt Cell Res 2012;23:77–85.
[16] Shiflett AM, Johnson PJ. Mitochondrion-related organelles in eukaryotic protists. Annu Rev Microbiol 2010;64:409–29.
[17] van der Giezen M, Tovar J. Degenerate mitochondria. EMBO Rep 2005;6:525–30.
[18] Hjort K, Goldberg AV, Tsaousis AD, Hirt RP, Embley TM. Diversity and reductive evolution of mitochondria among microbial eukaryotes. Philos Trans R Soc Lond B Biol Sci 2010;365: 713–27.
[19] Goldberg AV, Molik S, Tsaousis AD, et al. Localization and functionality of microsporidian iron-sulphur cluster assembly proteins. Nature 2008;452:624–8.
[20] Tovar J, Leon-Avila G, Sanchez LB, et al. Mitochondrial remnant organelles of Giardia function in iron-sulphur protein maturation. Nature 2003;426:172–6.
[21] Li H, Outten CE. Monothiol CGFS glutaredoxins and BolA-like proteins: [2Fe-2S] binding partners in iron homeostasis. Biochemistry 2012;51:4377–89.
[22] Philpott CC, Leidgens S, Frey AG. Metabolic remodeling in iron-deficient fungi. Biochim Biophys Acta 2012;1823:1509–20.
[23] Rawat S, Stemmler TL. Key players and their role during mitochondrial iron-sulfur cluster biosynthesis. Chemistry 2011;17:746–53.
[24] Neupert W, Herrmann JM. Translocation of proteins into mitochondria. Annu Rev Biochem 2007;76:723–49.
[25] Schmidt O, Pfanner N, Meisinger C. Mitochondrial protein import: from proteomics to functional mechanisms. Nat Rev Mol Cell Biol 2010;11:655–67.
[26] Garland SA, Hoff K, Vickery LE, Culotta VC. Saccharomyces cerevisiae ISU1 and ISU2: members of a well-conserved gene family for iron-sulfur cluster assembly. J Mol Biol 1999;294:897–907.
[27] Mühlenhoff U, Gerber J, Richhardt N, Lill R. Components involved in assembly and dislocation of iron-sulfur clusters on the scaffold protein Isu1p. EMBO J 2003;22:4815–25.
[28] Tong WH, Rouault TA. Functions of mitochondrial ISCU and cytosolic ISCU in mammalian iron-sulfur cluster biogenesis and iron homeostasis. Cell Metab 2006;3:199–210.

[29] Adam AC, Bornhövd C, Prokisch H, Neupert W, Hell K. The Nfs1 interacting protein Isd11 has an essential role in Fe/S cluster biogenesis in mitochondria. EMBO J 2006;25:174–83.
[30] Wiedemann N, Urzica E, Guiard B, et al. Essential role of Isd11 in iron-sulfur cluster synthesis on Isu scaffold proteins. EMBO J 2006;25:184–95.
[31] Shi Y, Ghosh MC, Tong WH, Rouault TA. Human ISD11 is essential for both iron-sulfur cluster assembly and maintenance of normal cellular iron homeostasis. Hum Mol Genet 2009;18:3014–25.
[32] Foury F, Roganti T. Deletion of the mitochondrial carrier genes MRS3 and MRS4 suppresses mitochondrial iron accumulation in a yeast frataxin-deficient strain. J Biol Chem 2002;277:24475–83.
[33] Mühlenhoff U, Stadler J, Richhardt N, et al. A specific role of the yeast mitochondrial carriers Mrs3/4p in mitochondrial iron acquisition under iron-limiting conditions. J Biol Chem 2003;278:40612–20.
[34] Zhang Y, Lyver ER, Knight SA, Pain D, Lesuisse E, Dancis A. Mrs3p, Mrs4p, and frataxin provide iron for Fe-S cluster synthesis in mitochondria. J Biol Chem 2006;281:22493–502.
[35] Shaw GC, Cope JJ, Li L, et al. Mitoferrin is essential for erythroid iron assimilation. Nature 2006;440:96–100.
[36] Yoon H, Zhang Y, Pain J, et al. Rim2, a pyrimidine nucleotide exchanger, is needed for iron utilization in mitochondria. Biochem J 2011;440:137–46.
[37] Froschauer EM, Rietzschel N, Hassler MR, et al. The mitochondrial carrier Rim2 co-imports pyrimidine nucleotides and iron. Biochem J 2013;455:57–65.
[38] Gerber J, Mühlenhoff U, Lill R. An interaction between frataxin and Isu1/Nfs1 that is crucial for Fe/S cluster synthesis on Isu1. EMBO Rep 2003;4:906–11.
[39] Schmucker S, Martelli A, Colin F, et al. Mammalian frataxin: an essential function for cellular viability through an interaction with a preformed ISCU/NFS1/ISD11 iron-sulfur assembly complex. PLoS One 2011;6:e16199.
[40] Stemmler TL, Lesuisse E, Pain D, Dancis A. Frataxin and mitochondrial FeS cluster biogenesis. J Biol Chem 2010;285:26737–43.
[41] Stehling O, Elsässer HP, Brückel B, Mühlenhoff U, Lill R. Iron-sulfur protein maturation in human cells: evidence for a function of frataxin. Hum Mol Genet 2004;13:3007–15.
[42] Tsai CL, Barondeau DP. Human frataxin is an allosteric switch that activates the Fe-S cluster biosynthetic complex. Biochemistry 2010;49:9132–9.
[43] Yoon H, Golla R, Lesuisse E, et al. Mutation in the Fe-S scaffold protein Isu bypasses frataxin deletion. Biochem J 2012;441:473–80.
[44] Lange H, Kaut A, Kispal G, Lill R. A mitochondrial ferredoxin is essential for biogenesis of cellular iron-sulfur proteins. Proc Natl Acad Sci USA 2000;97:1050–5.
[45] Li J, Saxena S, Pain D, Dancis A. Adrenodoxin reductase homolog (Arh1p) of yeast mitochondria required for iron homeostasis. J Biol Chem 2001;276:1503–9.
[46] Sheftel AD, Stehling O, Pierik AJ, et al. Humans possess two mitochondrial ferredoxins, Fdx1 and Fdx2, with distinct roles in steroidogenesis, heme, and Fe/S cluster biosynthesis. Proc Natl Acad Sci USA 2010;107:11775–80.
[47] Shi Y, Ghosh M, Kovtunovych G, Crooks DR, Rouault TA. Both human ferredoxins 1 and 2 and ferredoxin reductase are important for iron-sulfur cluster biogenesis. Biochim Biophys Acta 2012;1823:484–92.
[48] Chandramouli K, Unciuleac MC, Naik S, Dean DR, Huynh BH, Johnson MK. Formation and properties of [4Fe-4S] clusters on the IscU scaffold protein. Biochemistry 2007;46:6804–11.
[49] Unciuleac MC, Chandramouli K, Naik S, et al. In vitro activation of apo-aconitase using a [4Fe-4S] cluster-loaded form of the IscU [Fe-S] cluster scaffolding protein. Biochemistry 2007;46:6812–21.

[50] Barros MH, Nobrega FG, Tzagoloff A. Mitochondrial ferredoxin is required for heme A synthesis in Saccharomyces cerevisiae. J Biol Chem 2002;277:9997–10002.
[51] Pierrel F, Hamelin O, Douki T, et al. Involvement of mitochondrial ferredoxin and para-aminobenzoic acid in yeast coenzyme Q biosynthesis. Chem Biol 2010;17:449–59.
[52] Mühlenhoff U, Richter N, Pines O, Pierik AJ, Lill R. Specialized function of yeast Isa1 and Isa2 proteins in the maturation of mitochondrial [4Fe-4S] proteins. J Biol Chem 2011;286:41205–16.
[53] Dutkiewicz R, Marszalek J, Schilke B, Craig EA, Lill R, Mühlenhoff U. The Hsp70 chaperone Ssq1p is dispensable for iron-sulfur cluster formation on the scaffold protein Isu1p. J Biol Chem 2006;281:7801–8.
[54] Kampinga HH, Craig EA. The HSP70 chaperone machinery: J proteins as drivers of functional specificity. Nat Rev Mol Cell Biol 2010;11:579–92.
[55] Uhrigshardt H, Singh A, Kovtunovych G, Ghosh M, Rouault TA. Characterization of the human HSC20, an unusual DnaJ type III protein, involved in iron-sulfur cluster biogenesis. Hum Mol Genet 2010;19:3816–34.
[56] Vickery LE, Cupp-Vickery JR. Molecular chaperones HscA/Ssq1 and HscB/Jac1 and their roles in iron-sulfur protein maturation. Crit Rev Biochem Mol Biol 2007;42:95–111.
[57] Silberg JJ, Tapley TL, Hoff KG, Vickery LE. Regulation of the HscA ATPase reaction cycle by the co-chaperone HscB and the iron-sulfur cluster assembly protein IscU. J Biol Chem 2004;279:53924–31.
[58] Knieszner H, Schilke B, Dutkiewicz R, et al. Compensation for a defective interaction of the Hsp70 Ssq1 with the mitochondrial Fe-S cluster scaffold Isu. J Biol Chem 2005;280:28966–72.
[59] Ciesielski SJ, Schilke BA, Osipiuk J, et al. Interaction of J-protein co-chaperone Jac1 with Fe-S scaffold Isu is indispensable in vivo and conserved in evolution. J Mol Biol 2012;417:1–12.
[60] Dutkiewicz R, Schilke B, Cheng S, Knieszner H, Craig EA, Marszalek J. Sequence-specific interaction between mitochondrial Fe-S scaffold protein Isu and Hsp70 Ssq1 is essential for their in vivo function. J Biol Chem 2004;279:29167–74.
[61] Hoff KG, Cupp-Vickery JR, Vickery LE. Contributions of the LPPVK motif of the iron-sulfur template protein IscU to interactions with the Hsc66-Hsc20 chaperone system. J Biol Chem 2003;278:37582–9.
[62] Bonomi F, Iametti S, Morleo A, Ta D, Vickery LE. Studies on the mechanism of catalysis of iron-sulfur cluster transfer from IscU[2Fe2S] by HscA/HscB chaperones. Biochemistry 2008;47:12795–801.
[63] Bonomi F, Iametti S, Morleo A, Ta D, Vickery LE. Facilitated transfer of IscU-[2Fe2S] clusters by chaperone-mediated ligand exchange. Biochemistry 2011;50:9641–50.
[64] Dutkiewicz R, Schilke B, Kneiszner H, Walter W, Craig EA, Marszalek J. Ssq1, a mitochondrial Hsp70 involved in iron-sulfur (Fe/S) center biogenesis: similarities to and differences from its bacterial counterpart. J Biol Chem 2003;278:29719–27.
[65] Uzarska MA, Dutkiewicz R, Freibert SA, Lill R, Mühlenhoff U. The mitochondrial Hsp70 chaperone Ssq1 facilitates Fe/S cluster transfer from Isu1 to Grx5 by complex formation. Mol Biol Cell 2013;24:1830–41.
[66] Rodriguez-Manzaneque MT, Tamarit J, Belli G, Ros J, Herrero E. Grx5 is a mitochondrial glutaredoxin required for the activity of iron/sulfur enzymes. Mol Biol Cell 2002;13:1109–21.
[67] Wingert RA, Galloway JL, Barut B, et al. Deficiency of glutaredoxin 5 reveals Fe-S clusters are required for vertebrate haem synthesis. Nature 2005;436:1035–9.
[68] Camaschella C, Campanella A, De Falco L, et al. The human counterpart of zebrafish shiraz shows sideroblastic-like microcytic anemia and iron overload. Blood 2007;110:1353–8.
[69] Ye H, Jeong SY, Ghosh MC, et al. Glutaredoxin 5 deficiency causes sideroblastic anemia by specifically impairing heme biosynthesis and depleting cytosolic iron in human erythroblasts. J Clin Invest 2010;120:1749–61.

[70] Bandyopadhyay S, Gama F, Molina-Navarro MM, et al. Chloroplast monothiol glutaredoxins as scaffold proteins for the assembly and delivery of [2Fe-2S] clusters. EMBO J 2008;27:1122–33.
[71] Molina-Navarro MM, Casas C, Piedrafita L, Belli G, Herrero E. Prokaryotic and eukaryotic monothiol glutaredoxins are able to perform the functions of Grx5 in the biogenesis of Fe/S clusters in yeast mitochondria. FEBS Lett 2006;580:2273–80.
[72] Herrero E, de la Torre-Ruiz MA. Monothiol glutaredoxins: a common domain for multiple functions. Cell Mol Life Sci 2007;64:1518–30.
[73] Iwema T, Picciocchi A, Traore DA, Ferrer JL, Chauvat F, Jacquamet L. Structural basis for delivery of the intact [Fe2S2] cluster by monothiol glutaredoxin. Biochemistry 2009;48:6041–3.
[74] Rouhier N, Unno H, Bandyopadhyay S, et al. Functional, structural, and spectroscopic characterization of a glutathione-ligated [2Fe-2S] cluster in poplar glutaredoxin C1. Proc Natl Acad Sci USA 2007;104:7379–84.
[75] Rada P, Smid O, Sutak R, et al. The monothiol single-domain glutaredoxin is conserved in the highly reduced mitochondria of Giardia intestinalis. Eukaryot Cell 2009;8:1584–91.
[76] Picciocchi A, Saguez C, Boussac A, Cassier-Chauvat C, Chauvat F. CGFS-type monothiol glutaredoxins from the cyanobacterium Synechocystis PCC6803 and other evolutionary distant model organisms possess a glutathione-ligated [2Fe-2S] cluster. Biochemistry 2007;46: 15018–26.
[77] Belli G, Polaina J, Tamarit J, et al. Structure-function analysis of yeast Grx5 monothiol glutaredoxin defines essential amino acids for the function of the protein. J Biol Chem 2002;277:37590–6.
[78] Jensen LT, Culotta VC. Role of Saccharomyces cerevisiae ISA1 and ISA2 in iron homeostasis. Mol Cell Biol 2000;20:3918–27.
[79] Kaut A, Lange H, Diekert K, Kispal G, Lill R. Isa1p Is a Component of the mitochondrial machinery for maturation of cellular iron-sulfur proteins and requires conserved cysteine residues for function. J Biol Chem 2000;275:15955–61.
[80] Pelzer W, Mühlenhoff U, Diekert K, Siegmund K, Kispal G, Lill R. Mitochondrial Isa2p plays a crucial role in the maturation of cellular iron-sulfur proteins. FEBS Lett 2000;476:134–9.
[81] Mühlenhoff U, Gerl MJ, Flauger B, et al. The ISC proteins Isa1 and Isa2 are required for the function but not for the de novo synthesis of the Fe/S clusters of biotin synthase in Saccharomyces cerevisiae. Eukaryot Cell 2007;6:495–504.
[82] Sheftel AD, Wilbrecht C, Stehling O, et al. The human mitochondrial ISCA1, ISCA2, and IBA57 proteins are required for [4Fe-4S] protein maturation. Mol Biol Cell 2012;23:1157–66.
[83] Gelling C, Dawes IW, Richhardt N, Lill R, Mühlenhoff U. Mitochondrial Iba57p is required for Fe/S cluster formation on aconitase and activation of radical SAM enzymes. Mol Cell Biol 2008;28:1851–61.
[84] Bych K, Kerscher S, Netz DJ, et al. The iron-sulphur protein Ind1 is required for effective complex I assembly. EMBO J 2008;27:1736–46.
[85] Sheftel AD, Stehling O, Pierik AJ, et al. Human Ind1, an iron-sulfur cluster assembly factor for respiratory complex I. Mol Cell Biol 2009;29:6059–73.
[86] Tong WH, Jameson GN, Huynh BH, Rouault TA. Subcellular compartmentalization of human Nfu, an iron-sulfur cluster scaffold protein, and its ability to assemble a [4Fe-4S] cluster. Proc Natl Acad Sci USA 2003;100:9762–7.
[87] Cameron JM, Janer A, Levandovskiy V, et al. Mutations in iron-sulfur cluster scaffold genes NFU1 and BOLA3 cause a fatal deficiency of multiple respiratory chain and 2-oxoacid dehydrogenase enzymes. Am J Hum Genet 2011;89:486–95.
[88] Navarro-Sastre A, Tort F, Stehling O, et al. A fatal mitochondrial disease is associated with defective NFU1 function in the maturation of a subset of mitochondrial Fe-S proteins. Am J Hum Genet 2011;89:656–67.

[89] Hiltunen JK, Autio KJ, Schonauer MS, Kursu VA, Dieckmann CL, Kastaniotis AJ. Mitochondrial fatty acid synthesis and respiration. Biochim Biophys Acta 2010;1797:1195–202.
[90] Haack TB, Rolinski B, Haberberger B, et al. Homozygous missense mutation in BOLA3 causes multiple mitochondrial dysfunctions syndrome in two siblings. J Inherit Metab Dis 2013;36:55–62.
[91] Aldea M, Garrido T, Hernandez-Chico C, Vicente M, Kushner SR. Induction of a growth-phase-dependent promoter triggers transcription of bolA, an Escherichia coli morphogene. EMBO J 1989;8:3923–31.
[92] Hess DC, Myers CL, Huttenhower C, et al. Computationally driven, quantitative experiments discover genes required for mitochondrial biogenesis. PLoS Genet 2009;5:e1000407.
[93] Huynen MA, Spronk CA, Gabaldon T, Snel B. Combining data from genomes, Y2H and 3D structure indicates that BolA is a reductase interacting with a glutaredoxin. FEBS Lett 2005;579:591–6.
[94] Kumanovics A, Chen O, Li L, et al. Identification of FRA1 and FRA2 as genes involved in regulating the yeast iron regulon in response to decreased mitochondrial iron-sulfur cluster synthesis. J Biol Chem 2008;283:10276–86.
[95] Li H, Mapolelo DT, Dingra NN, et al. The yeast iron regulatory proteins Grx3/4 and Fra2 form heterodimeric complexes containing a [2Fe-2S] cluster with cysteinyl and histidyl ligation. Biochemistry 2009;48:9569–81.
[96] Li H, Mapolelo DT, Randeniya S, Johnson MK, Outten CE. Human glutaredoxin 3 forms [2Fe-2S]-bridged complexes with human BolA2. Biochemistry 2012;51:1687–96.
[97] Land T, Rouault TA. Targeting of a human iron-sulfur cluster assembly enzyme, nifs, to different subcellular compartments is regulated through alternative AUG utilization. Mol Cell 1998;2:807–15.
[98] Nakai Y, Nakai M, Hayashi H, Kagamiyama H. Nuclear Localization of Yeast Nfs1p Is Required for Cell Survival. J Biol Chem 2001;276:8314–20.
[99] Mühlenhoff U, Balk J, Richhardt N, et al. Functional characterization of the eukaryotic cysteine desulfurase Nfs1p from Saccharomyces cerevisiae. J Biol Chem 2004;279:36906–15.
[100] Crooks DR, Jeong SY, Tong WH, et al. Tissue specificity of a human mitochondrial disease: differentiation-enhanced mis-splicing of the Fe-S scaffold gene ISCU renders patient cells more sensitive to oxidative stress in ISCU myopathy. J Biol Chem 2012;287:40119–30.
[101] Nakai Y, Nakai M, Lill R, Suzuki T, Hayashi H. Thio modification of yeast cytosolic tRNA is an iron-sulfur protein-dependent pathway. Mol Cell Biol 2007;27:2841–7.
[102] Pondarre C, Antiochos BB, Campagna DR, et al. The mitochondrial ATP-binding cassette transporter Abcb7 is essential in mice and participates in cytosolic iron-sulphur cluster biogenesis. Hum Mol Genet 2006;15:953–64.
[103] Cavadini P, Biasiotto G, Poli M, et al. RNA silencing of the mitochondrial ABCB7 transporter in HeLa cells causes an iron-deficient phenotype with mitochondrial iron overload. Blood 2007;109:3552–9.
[104] Sipos K, Lange H, Fekete Z, Ullmann P, Lill R, Kispal G. Maturation of cytosolic iron-sulfur proteins requires glutathione. J Biol Chem 2002;277:26944–9.
[105] Kispal G, Csere P, Guiard B, Lill R. The ABC transporter Atm1p is required for mitochondrial iron homeostasis. FEBS Lett 1997;418:346–50.
[106] Mesecke N, Terziyska N, Kozany C, et al. A disulfide relay system in the intermembrane space of mitochondria that mediates protein import. Cell 2005;121:1059–70.
[107] Sharma AK, Pallesen LJ, Spang RJ, Walden WE. Cytosolic iron-sulfur cluster assembly (CIA) system: factors, mechanism, and relevance to cellular iron regulation. J Biol Chem 2010;285:26745–51.
[108] Netz DJ, Pierik AJ, Macarenhas J, Stehling O, Lill R. Maturation of cytosolic and nuclear iron-sulfur proteins. Trends Cell Biol 2014;in press.

[109] Netz DJ, Pierik AJ, Stümpfig M, Mühlenhoff U, Lill R. The Cfd1-Nbp35 complex acts as a scaffold for iron-sulfur protein assembly in the yeast cytosol. Nat Chem Biol 2007;3:278–86.
[110] Netz DJ, Pierik AJ, Stuempfig M, et al. A bridging [4Fe-4S] cluster and nucleotide binding are essential for the function of the Cfd1-Nbp35 complex as a scaffold in iron-sulfur protein maturation. J Biol Chem 2012;287:12365–78.
[111] Netz DJ, Stumpfig M, Dore C, Mühlenhoff U, Pierik AJ, Lill R. Tah18 transfers electrons to Dre2 in cytosolic iron-sulfur protein biogenesis. Nat Chem Biol 2010;6:758–65.
[112] Pallesen LJ, Solodovnikova N, Sharma AK, Walden WE. Interaction with Cfd1 Increases the Kinetic Lability of FeS on the Nbp35 Scaffold. J Biol Chem 2013.
[113] Zhang Y, Lyver ER, Nakamaru-Ogiso E, et al. Dre2, a conserved eukaryotic Fe/S cluster protein, functions in cytosolic Fe/S protein biogenesis. Mol Cell Biol 2008;28:5569–82.
[114] Banci L, Bertini I, Calderone V, et al. Molecular view of an electron transfer process essential for iron-sulfur protein biogenesis. Proc Natl Acad Sci USA 2013;110:7136–41.
[115] Balk J, Pierik AJ, Aguilar Netz D, Mühlenhoff U, Lill R. The hydrogenase-like Nar1p is essential for maturation of cytosolic and nuclear iron-sulphur proteins. EMBO J 2004;23:2105–15.
[116] Song D, Lee FS. A role for IOP1 in mammalian cytosolic iron-sulfur protein biogenesis. J Biol Chem 2008;283:9231–8.
[117] Urzica E, Pierik AJ, Muhlenhoff U, Lill R. Crucial role of conserved cysteine residues in the assembly of two iron-sulfur clusters on the CIA protein Nar1. Biochemistry 2009;48:4946–58.
[118] Srinivasan V, Netz DJA, Webert H, et al. Structure of the yeast WD40 domain protein Cia1, a component acting late in iron-sulfur protein biogenesis. Structure 2007;15:1246–57.
[119] Weerapana E, Wang C, Simon GM, et al. Quantitative reactivity profiling predicts functional cysteines in proteomes. Nature 2010;468:790–5.
[120] Stehling O, Vashisht AA, Mascarenhas J, et al. MMS19 assembles iron-sulfur proteins required for DNA metabolism and genomic integrity. Science 2012;337:195–9.
[121] Gari K, Leon Ortiz AM, Borel V, Flynn H, Skehel JM, Boulton SJ. MMS19 links cytoplasmic iron-sulfur cluster assembly to DNA metabolism. Science 2012;337:243–5.
[122] Stehling O, Mascarenhas J, Vashisht AA, et al. Human CIA2A-FAM96A and CIA2B-FAM96B integrate iron homeostasis and maturation of different subsets of cytosolic-nuclear iron-sulfur proteins. Cell Metab 2013;18:187–98.
[123] van Wietmarschen N, Moradian A, Morin GB, Lansdorp PM, Uringa EJ. The mammalian proteins MMS19, MIP18, and ANT2 are involved in cytoplasmic iron-sulfur cluster protein assembly. J Biol Chem 2012;287:43351–8.
[124] Seki M, Takeda Y, Iwai K, Tanaka K. IOP1 protein is an external component of the human cytosolic iron-sulfur cluster assembly (CIA) machinery and functions in the MMS19 protein-dependent CIA pathway. J Biol Chem 2013;288:16680–9.
[125] Mühlenhoff U, Molik S, Godoy JR, et al. Cytosolic monothiol glutaredoxins function in intracellular iron sensing and trafficking via their bound iron-sulfur cluster. Cell Metab 2010;12:373–85.
[126] Haunhorst P, Hanschmann EM, Brautigam L, et al. Crucial function of vertebrate glutaredoxin 3 (PICOT) in iron homeostasis and hemoglobin maturation. Mol Biol Cell 2013;24:1895–903.
[127] Zhang Y, Liu L, Wu X, An X, Stubbe J, Huang M. Investigation of in vivo diferric tyrosyl radical formation in Saccharomyces cerevisiae Rnr2 protein: requirement of Rnr4 and contribution of Grx3/4 AND Dre2 proteins. J Biol Chem 2011;286:41499–509.
[128] Stehling O, Netz DJ, Niggemeyer B, et al. Human Nbp35 is essential for both cytosolic iron-sulfur protein assembly and iron homeostasis. Mol Cell Biol 2008;28:5517–28.
[129] Krogan NJ, Cagney G, Yu H, et al. Global landscape of protein complexes in the yeast Saccharomyces cerevisiae. Nature 2006;440:637–43.

[130] Rual JF, Venkatesan K, Hao T, et al. Towards a proteome-scale map of the human protein-protein interaction network. Nature 2005;437:1173–8.
[131] Tarassov K, Messier V, Landry CR, et al. An in vivo map of the yeast protein interactome. Science 2008;320:1465–70.
[132] Collins SR, Kemmeren P, Zhao XC, et al. Toward a comprehensive atlas of the physical interactome of Saccharomyces cerevisiae. Mol Cell Proteomics 2007;6:439–50.
[133] Pace NJ, Weerapana E. Diverse functional roles of reactive cysteines. ACS Chem Biol 2013;8:283–96.
[134] Luo D, Bernard DG, Balk J, Hai H, Cui X. The DUF59 family gene AE7 acts in the cytosolic iron-sulfur cluster assembly pathway to maintain nuclear genome integrity in Arabidopsis. Plant Cell 2012;24:4135–48.
[135] Schwenkert S, Netz DJ, Frazzon J, et al. Chloroplast HCF101 is a scaffold protein for [4Fe-4S] cluster assembly. Biochem J 2010;425:207–14.
[136] Almeida MS, Herrmann T, Peti W, Wilson IA, Wüthrich K. NMR structure of the conserved hypothetical protein TM0487 from Thermotoga maritima: implications for 216 homologous DUF59 proteins. Protein Sci 2005;14:2880–6.
[137] Mas C, Chen KE, Brereton IM, Martin JL, Hill JM. Backbone resonance assignments of the monomeric DUF59 domain of human Fam96a. Biomol NMR Assign 2012.
[138] Anderson CP, Shen M, Eisenstein RS, Leibold EA. Mammalian iron metabolism and its control by iron regulatory proteins. Biochim Biophys Acta 2012;1823:1468–83.
[139] Thompson JW, Bruick RK. Protein degradation and iron homeostasis. Biochim Biophys Acta 2012;1823:1484–90.
[140] Prakash L, Prakash S. Three additional genes involved in pyrimidine dimer removal in Saccharomyces cerevisiae: RAD7, RAD14 and MMS19. Mol Gen Genet 1979;176:351–9.
[141] Thomas D, Barbey R, Henry D, Surdin-Kerjan Y. Physiological analysis of mutants of Saccharomyces cerevisiae impaired in sulphate assimilation. J Gen Microbiol 1992;138:2021–8.
[142] Lauder S, Bankmann M, Guzder SN, Sung P, Prakash L, Prakash S. Dual requirement for the yeast MMS19 gene in DNA repair and RNA polymerase II transcription. Mol Cell Biol 1996;16:6783–93.
[143] Kou H, Zhou Y, Gorospe RM, Wang Z. Mms19 protein functions in nucleotide excision repair by sustaining an adequate cellular concentration of the TFIIH component Rad3. Proc Natl Acad Sci USA 2008;105:15714–9.
[144] Queimado L, Rao M, Schultz RA, et al. Cloning the human and mouse MMS19 genes and functional complementation of a yeast mms19 deletion mutant. Nucleic Acids Res 2001;29:1884–91.
[145] Seroz T, Winkler GS, Auriol J, et al. Cloning of a human homolog of the yeast nucleotide excision repair gene MMS19 and interaction with transcription repair factor TFIIH via the XPB and XPD helicases. Nucleic Acids Res 2000;28:4506–13.
[146] Ito S, Tan LJ, Andoh D, et al. MMXD, a TFIIH-independent XPD-MMS19 protein complex involved in chromosome segregation. Mol Cell 2010;39:632–40.
[147] Compe E, Egly JM. TFIIH: when transcription met DNA repair. Nat Rev Mol Cell Biol 2012;13:343–54.
[148] Rudolf J, Makrantoni V, Ingledew WJ, Stark MJ, White MF. The DNA repair helicases XPD and FancJ have essential iron-sulfur domains. Mol Cell 2006;23:801–8.
[149] Fan L, Fuss JO, Cheng QJ, et al. XPD helicase structures and activities: insights into the cancer and aging phenotypes from XPD mutations. Cell 2008;133:789–800.
[150] Liu H, Rudolf J, Johnson KA, et al. Structure of the DNA repair helicase XPD. Cell 2008;133:801–12.
[151] Wolski SC, Kuper J, Hanzelmann P, et al. Crystal structure of the FeS cluster-containing nucleotide excision repair helicase XPD. PLoS Biol 2008;6:e149.

[152] Pugh RA, Honda M, Leesley H, et al. The Iron-containing Domain Is Essential in Rad3 Helicases for Coupling of ATP Hydrolysis to DNA Translocation and for Targeting the Helicase to the Single-stranded DNA-Double-stranded DNA Junction. J Biol Chem 2008;283:1732–43.
[153] White MF. Structure, function and evolution of the XPD family of iron-sulfur-containing 5′->3′ DNA helicases. Biochem Soc Trans 2009;37:547–51.
[154] Wu Y, Suhasini AN, Brosh RM Jr. Welcome the family of FANCJ-like helicases to the block of genome stability maintenance proteins. Cell Mol Life Sci 2009;66:1209–22.
[155] Wu Y, Sommers JA, Suhasini AN, et al. Fanconi anemia group J mutation abolishes its DNA repair function by uncoupling DNA translocation from helicase activity or disruption of protein-DNA complexes. Blood 2010;116:3780–91.
[156] Bell SP, Dutta A. DNA replication in eukaryotic cells. Annu Rev Biochem 2002;71:333–74.
[157] Arezi B, Kuchta RD. Eukaryotic DNA primase. Trends Biochem Sci 2000;25:572–6.
[158] Klinge S, Hirst J, Maman JD, Krude T, Pellegrini L. An iron-sulfur domain of the eukaryotic primase is essential for RNA primer synthesis. Nat Struct Mol Biol 2007;14:875–7.
[159] Weiner BE, Huang H, Dattilo BM, Nilges MJ, Fanning E, Chazin WJ. An iron-sulfur cluster in the C-terminal domain of the p58 subunit of human DNA primase. J Biol Chem 2007;282:33444–51.
[160] Kunkel TA, Burgers PM. Dividing the workload at a eukaryotic replication fork. Trends Cell Biol 2008;18:521–7.
[161] Netz DJ, Stith CM, Stumpfig M, et al. Eukaryotic DNA polymerases require an iron-sulfur cluster for the formation of active complexes. Nat Chem Biol 2012;8:125–32.
[162] Pokharel S, Campbell JL. Cross talk between the nuclease and helicase activities of Dna2: role of an essential iron-sulfur cluster domain. Nucleic Acids Res 2012;40:7821–30.
[163] Robertson AB, Klungland A, Rognes T, Leiros I. DNA repair in mammalian cells: Base excision repair: the long and short of it. Cell Mol Life Sci 2009;66:981–93.
[164] Cunningham RP, Asahara H, Bank JF, et al. Endonuclease III is an iron-sulfur protein. Biochemistry 1989;28:4450–5.
[165] Boal AK, Genereux JC, Sontz PA, Gralnick JA, Newman DK, Barton JK. Redox signaling between DNA repair proteins for efficient lesion detection. Proc Natl Acad Sci USA 2009;106:15237–42.
[166] Boal AK, Yavin E, Barton JK. DNA repair glycosylases with a [4Fe-4S] cluster: a redox cofactor for DNA-mediated charge transport? J Inorg Biochem 2007;101:1913–21.
[167] Kuo CF, McRee DE, Fisher CL, O'Handley SF, Cunningham RP, Tainer JA. Atomic structure of the DNA repair [4Fe-4S] enzyme endonuclease III. Science 1992;258:434–40.
[168] McGoldrick JP, Yeh YC, Solomon M, Essigmann JM, Lu AL. Characterization of a mammalian homolog of the Escherichia coli MutY mismatch repair protein. Mol Cell Biol 1995;15:989–96.
[169] White MF, Dillingham MS. Iron-sulphur clusters in nucleic acid processing enzymes. Current opinion in structural biology 2011.
[170] Genereux JC, Boal AK, Barton JK. DNA-mediated charge transport in redox sensing and signaling. J Am Chem Soc 2010;132:891–905.
[171] Sontz PA, Muren NB, Barton JK. DNA charge transport for sensing and signaling. Acc Chem Res 2012;45:1792–800.
[172] Romano CA, Sontz PA, Barton JK. Mutants of the base excision repair glycosylase, endonuclease III: DNA charge transport as a first step in lesion detection. Biochemistry 2011;50:6133–45.
[173] Sontz PA, Mui TP, Fuss JO, Tainer JA, Barton JK. DNA charge transport as a first step in coordinating the detection of lesions by repair proteins. Proc Natl Acad Sci USA 2012;109:1856–61.
[174] Hanahan D, Weinberg RA. Hallmarks of cancer: the next generation. Cell 2011;144:646–74.
[175] Cassidy LD, Venkitaraman AR. Genome instability mechanisms and the structure of cancer genomes. Curr Opin Genet Dev 2012;22:10–3.

[176] Wu Y, Brosh RM Jr. DNA helicase and helicase-nuclease enzymes with a conserved iron-sulfur cluster. Nucleic Acids Res 2012;40:4247–60.
[177] Hook SS, Lin JJ, Dutta A. Mechanisms to control rereplication and implications for cancer. Curr Opin Cell Biol 2007;19:663–71.
[178] McMurray MA, Gottschling DE. An age-induced switch to a hyper-recombinational state. Science 2003;301:1908–11.
[179] Veatch JR, McMurray MA, Nelson ZW, Gottschling DE. Mitochondrial dysfunction leads to nuclear genome instability via an iron-sulfur cluster defect. Cell 2009;137:1247–58.
[180] McMurray MA, Gottschling DE. Aging and genetic instability in yeast. Current opinion in microbiology 2004;7:673–9.
[181] Minocherhomji S, Tollefsbol TO, Singh KK. Mitochondrial regulation of epigenetics and its role in human diseases. Epigenetics 2012;7:326–34.
[182] Thierbach R, Schulz TJ, Isken F, et al. Targeted disruption of hepatic frataxin expression causes impaired mitochondrial function, decreased life span and tumor growth in mice. Hum Mol Genet 2005;14:3857–64.
[183] Miller LD, Coffman LG, Chou JW, et al. An iron regulatory gene signature predicts outcome in breast cancer. Cancer Res 2011;71:6728–37.
[184] Pra D, Franke SI, Henriques JA, Fenech M. Iron and genome stability: an update. Mutat Res 2012;733:92–9.
[185] Torti SV, Torti FM. Iron and cancer: more ore to be mined. Nat Rev Cancer 2013;13:342–55.
[186] Flint DH, Tuminello JF, Emptage MH. The inactivation of Fe-S cluster containing hydro-lyases by superoxide. J Biol Chem 1993;268:22369–76.
[187] Gao X, Campian JL, Qian M, Sun XF, Eaton JW. Mitochondrial DNA damage in iron overload. J Biol Chem 2009;284:4767–75.
[188] Ayala-Castro C, Saini A, Outten FW. Fe-S cluster assembly pathways in bacteria. Microbiol Mol Biol Rev 2008;72:110–25.
[189] Yu Y, Gutierrez E, Kovacevic Z, et al. Iron chelators for the treatment of cancer. Curr Med Chem 2012;19:2689–702.

15 DNA signaling by iron-sulfur cluster proteins

Phillip L. Bartels, Elizabeth O'Brien, and Jacqueline K. Barton

15.1 Introduction

The multimetal [4Fe-4S] clusters in mitochondrial and cytosolic proteins have long been known to serve critical functions ranging from electron transfer to catalysis [1]. In an exciting turn, the last three decades have expanded the known cellular distribution of [4Fe-4S] clusters to the nucleus, where they occur in DNA-processing enzymes throughout all domains of life [2–12]. Tab. 15.1 illustrates many of these new DNA processing enzymes containing [4Fe-4S] clusters. As is evident, the clusters are involved in all aspects of DNA processing. These enzymes are structurally and functionally diverse, acting in a range of pathways from base excision repair (BER) and nucleotide excision repair (NER) to DNA replication. In all of these proteins, the [4Fe-4S] cluster is noncatalytic, largely redox-inert in solution, and only secondarily involved in maintaining structural integrity. These features remained puzzling to researchers for years, but work in our laboratory has demonstrated that DNA binding activates these proteins toward redox chemistry and enables them to take advantage of a fundamental property of DNA: its ability to conduct charge through the base stack in a process known as DNA-mediated charge transport (DNA CT). DNA CT thus allows [4Fe-4S] proteins to signal to one another on a rapid timescale and across vast molecular distances through duplex DNA, facilitating the coordination of complex biological processes. The development of this model has already begun to provide insight into formerly mysterious mutations in the [4Fe-4S] domain. The importance of signaling among these proteins along with possible roles illuminated through mutations causing disease underscores the need for a better understanding of the chemistry of [4Fe-4S] clusters in DNA processing [8, 13, 14]. Here, we summarize results of research in our laboratory focused on elucidating the function of these clusters in DNA-binding proteins and our current understanding of their role in the cell.

15.2 DNA-mediated signaling in BER

The BER pathway involves the targeting and removal of damaged or misincorporated bases from DNA by one of several specialized DNA glycosylase enzymes [2]. The resulting abasic (AP) site is then exposed by an endonuclease that nicks the phosphate backbone, allowing the short gap to be filled in by a DNA polymerase and then sealed by a DNA ligaseJ+. Within this pathway, [4Fe-4S] clusters are present in several glycosylases of the helix-hairpin-helix family; the *Escherichia coli* enzymes endonuclease III (EndoIII) and MutY were the first well-characterized examples [3–6]. EndoIII is a bifunctional

DOI 10.1515/9783110479850-015

Tab. 15.1: Known DNA-processing [4Fe4S] proteins from the three domains of life.

Pathway	[4Fe4S] Proteins			Function
	Bacteria	Archaea	Eukarya	
Base excision repair (BER)	EndoIII, MutY	UDG, Mig	Ntg2, MUTYH, DME	DNA glycosylases that excise oxidized or misincorporated bases
Nucleotide excision repair (NER)	–	XPD	Rad3/XPD	Helicases that unwind DNA surrounding bulky lesions
DNA replication	–	–	DNA primase, DNA polymerase (Pol) α, δ, ε, ζ	RNA priming of ssDNA and 5′ to 3′ synthesis of primed DNA
Replication coupled repair	AddAB, DinG	–	Dna2, FANCJ, ExoV	Varied; helicases and nucleases that expose ssDNA for homologous recombination or, in the case of DinG, unwind R-loops
Telomere maintenance/ meiotic crossover	–	–	Rtel1, Chl1	Helicases that unwind specialized DNA structures
Transcription	–	RNA Polymerase	Elp3	Template-directed RNA synthesis

glycosylase responsible for excising oxidized pyrimidines and nicking the DNA backbone at the site of damage, while MutY is a monofunctional glycosylase that removes adenine mispaired with 8-oxoguanine. Homologues of both proteins are present in nearly all organisms, from bacteria to man, and the [4Fe-4S] domain is conserved throughout [4, 6]. Early studies on EndoIII by Cunningham showed the cluster to be largely insensitive to both oxidation and reduction, leading to the eventual assignment of a structural role [3, 15]. In the case of MutY, however, the cluster was found to be unnecessary for structural integrity, and a possible substrate-sensing role for the cluster was proposed instead [5]. However, this mechanism could not explain the role of the [4Fe-4S] cluster in proteins other than MutY, and recent work demonstrating full activity in the MutY homologues of anaerobic organisms that lack a cluster entirely provides a further argument against this possibility [16]. Amidst this perplexing situation, support for a functional role for the cluster arose, due to strict conservation of [4Fe-4S] clusters in these proteins despite the metabolic expense associated with cluster production and loading into target apoproteins [17].

Unexpectedly, the key to understanding the role of the cluster turned out to be a fundamental property of the DNA substrate itself: ground state B-form DNA can conduct charge due to the π-stacked arrangement of the aromatic base pairs, which have a similar spacing and arrangement to that of conductive graphite sheets [18]. This remarkable property was demonstrated in the ground state through electrochemical experiments where DNA containing a covalent alkane-thiol linker at one end was tethered to a gold electrode, and a redox-active intercalator appended to the

opposite end of the duplex served as an electron donor/acceptor upon the application of a potential (Fig. 15.1). Using cyclic voltammetry (CV) and square wave voltammetry (SQWV), rapid, long-range CT has been observed over distances up to 34 nm (100 bp of duplex DNA) with rates comparable to those measured in a 17-mer [19]. CT is efficient even with multiple breaks present in the phosphate backbone, but just a slight perturbation to base stacking, such as the presence of a CA mismatch (MM), has been shown to sharply attenuate CT yields (Fig. 15.2). Well-stacked base pairs are thus a requirement for DNA CT. The biological accessibility of DNA on this platform has been demonstrated by experiments measuring restriction enzyme activity electrochemically, so that proteins are able to recognize their cognate sequence and carry out reactions on the DNA duplex on the electrode. Overall, CT renders DNA an effective redox sensor of DNA integrity in cells, and this concept, combined with the propensity of biological systems to use all available resources at their disposal, led to a series of experiments designed to test the redox activity of DNA-bound [4Fe-4S] proteins.

To determine if otherwise redox-inert [4Fe-4S] proteins could become activated to carry out DNA CT upon binding the DNA polyanion, [4Fe-4S] proteins were added to DNA-modified gold electrodes, with the DNA-bound [4Fe-4S] enzyme taking the place of a redox probe (Fig. 15.1). In a revealing study, EndoIII and MutY from *E. coli* and Uracil DNA glycosylase (UDG) from *Archeoglobus fulgidus* were each incubated in buffered solution at physiological pH on DNA-modified electrodes and scanned

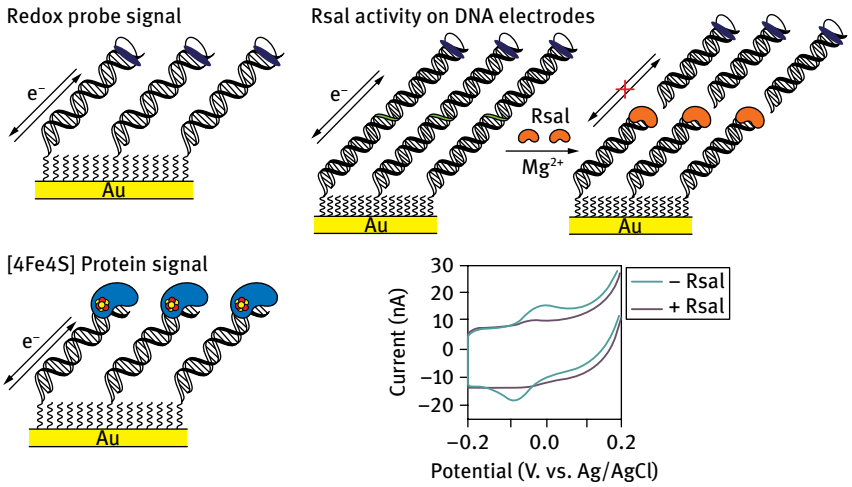

Fig. 15.1: Redox probe and protein electrochemistry on DNA-modified gold electrodes. DNA-intercalating redox probes, as well as DNA-bound [4Fe-4S] enzymes, can participate in DNA-mediated charge transport on this platform to produce a redox signal. (Left) The DNA on these gold electrodes is accessible to proteins, such as restriction enzyme RsaI, (Right) which is shown binding and cutting the duplex DNA substrate at its recognition site (green). The redox signal from the DNA-intercalating probe in this setup disappears after RsaI has been incubated on the surface and allowed to cut the DNA, removing the segment attached to the redox-active moiety. Cyclic voltammogram adapted from Ref. [19].

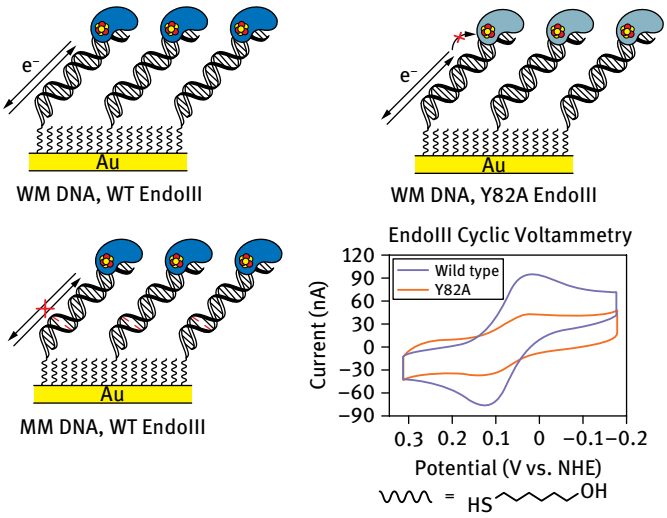

Fig. 15.2: Redox probe and protein electrochemistry on DNA-modified gold electrodes. When an enzyme containing a [4Fe-4S] cluster binds to DNA present in a self-assembled monolayer, electron transfer between the cluster and the electrode is highly efficient; if a mismatched base pair is incorporated into the DNA sequence, CT is disrupted and the signal is effectively shut off. Similarly, mutations in aromatic residues that form the CT pathway between the DNA and the cluster can also attenuate charge, as seen in the overlaid cyclic voltammograms of WT EndoIII and the Y82A mutant. Cyclic voltammogram adapted from Ref. [18].

by CV [20]. Remarkably, a reversible redox signal was observed for all three proteins and at quite similar potentials. DNA CT from the protein to electrode surface was severely attenuated both in the absence of DNA and when the DNA duplex contained an intervening abasic site proximal to the electrode surface, verifying that the signal was DNA mediated. Midpoint potentials ranging from 75 mV versus NHE (EndoIII) to 95 mV (MutY and UDG) placed all three enzymes at the lower end of the 100–300 mV range reported for high potential iron proteins (HiPIPs), and well above the –200 to –600 mV range expected for ferredoxins [21]. These electrochemical results, combined with data from EPR spectroscopy of native and chemically oxidized DNA-bound proteins, led to an assignment of the observed signal to the $[4Fe\text{-}4S]^{3+/2+}$ couple utilized by HiPIPs rather than the $[4Fe\text{-}4S]^{2+/1+}$ couple favored by ferredoxins.

To understand how this redox activation occurred, it was necessary to compare directly the redox potential of the [4Fe-4S] cluster in the presence and absence of DNA. The DNA-dissociated [4Fe-4S] enzymes were previously shown to be resistant to a change in cluster redox state even in the presence of powerful chemical oxidants [3]. This redox insensitivity suggested that the DNA-dissociated proteins have high reduction potentials outside the physiological range, requiring an electrode with a wider available potential window than gold. The 2V scanning window of highly oriented pyrolytic graphite satisfied this requirement, and it could furthermore be modified with DNA by appending a pyrene linker to the end of the duplex to form a noncovalent bond with the surface [22].

On the bare electrode, CV and SQWV revealed an irreversible signal for EndoIII with an oxidative peak centered at 250 mV versus NHE, just outside the physiologically relevant potential range. An irreversible $[4Fe\text{-}4S]^{2+/1+}$ reduction was also observed around –300 mV, supporting the initial assignment of the DNA-bound signal to the $[4Fe\text{-}4S]^{3+/2+}$ couple. In the presence of DNA, however, the $[4Fe\text{-}4S]^{3+/2+}$ couple underwent a shift in potential of ≥–200 mV and became much larger and more reversible; signal loss in the presence of an abasic site confirmed that this process was DNA mediated (Fig. 15.3). The potential shift, in turn, corresponded thermodynamically to an increase in DNA binding affinity of 3 orders of magnitude for the oxidized $[4Fe\text{-}4S]^{3+}$ form of the protein, relative to the reduced $[4Fe\text{-}4S]^{2+}$ form. The lack of significant conformational differences between the DNA-dissociated and DNA-bound structures of EndoIII and MutY [16, 23] suggested that this potential shift is due to the electrostatic effects resulting from binding to the polyanionic backbone of DNA; the DNA polyanion tunes the potential of the bound [4Fe-4S] cluster. More recent results examining EndoIII and MutY along with electrostatic mutants in electrochemistry experiments on graphite support that idea [24].

Overall, these electrochemical experiments revealed several critical details about the redox properties of [4Fe-4S] proteins in BER. First, DNA binding activated the proteins for redox activity under physiological conditions by negatively shifting the potential, and this negative shift meant that the oxidized form of the protein would necessarily bind DNA with a much greater affinity than the native, reduced form. Second, EndoIII, MutY, and UDG all displayed DNA-mediated redox signals centered around 85 mV *vs*. NHE and, thus, similar DNA-bound redox potentials for the cluster. With no other obvious redox partners, it was reasonable to consider whether these DNA-bound enzymes might be using DNA CT

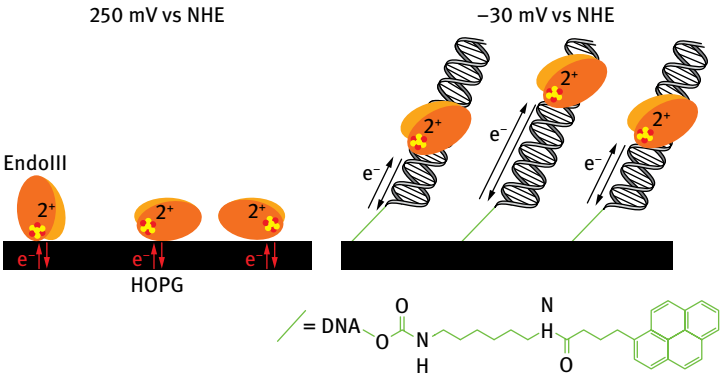

Fig. 15.3: EndoIII electrochemistry on a highly oriented pyrolytic graphite (HOPG) electrode in the presence and absence of DNA. When EndoIII was incubated in solution on HOPG, an irreversible signal with a potential of 250 mV vs NHE by square wave voltammetry was observed (left). Importantly, the $[4Fe\text{-}4S]^{2+/1+}$ couple could also be observed around –300 mV vs NHE, in agreement with the assignment of the high-potential couple to the $[4Fe\text{-}4S]^{3+/2+}$. In contrast, when a film of pyrene-modified DNA was present, the EndoIII signal was reversible and the potential shifted over 200 mV to –30 mV vs NHE (right). Due to the lack of significant conformational changes upon DNA binding, this effect was attributed primarily to the electrostatic effects associated with binding to the polyanionic DNA backbone.

to signal to each other. CT between even distant DNA-bound proteins is certainly temporally feasible, as DNA charge equilibration takes place on the nanosecond timescale [25], while proteins diffuse along DNA on the microsecond to millisecond timescale.

One clear partner for redox chemistry was the guanine radical. Under conditions of oxidative stress, guanine radicals are generated in the DNA duplex, and indeed, MutY recognizes and repairs 8-oxoguanine/A MMs, generated after the formation of oxidized guanine radicals in DNA. Guanine damage generated by long-range oxidation of guanine through DNA-mediated CT has been measured biochemically and occurs over long molecular distances [26, 27]. Monitoring guanine radical formation spectroscopically was used to determine rates of DNA CT; DNA CT occurs on the nanosecond timescale and is rate-limited by the base pair motions [25]. In fact, EPR and transient absorption spectroscopies were used to characterize DNA CT between the guanine radical and MutY, resulting in the formation of the oxidized $[4Fe\text{-}4S]^{3+}$ cluster [28]. We have also demonstrated that guanine radicals can, from a distance, transcriptionally activate SoxR, an iron-sulfur protein that acts as a sensor of oxidative stress in bacteria and activates a series of genes to respond to the stress [29] (Fig. 15.4). Thus, under conditions of oxidative stress, we can consider that the guanine radical can be a source for oxidation of the BER enzymes with [4Fe-4S] clusters by DNA CT and a means potentially to signal the need to activate necessary repair.

The fact that cellular DNA is not linear but wrapped around histones in chromatin brought up an important concern about the feasibility of long-range signaling *in vivo*, however: can DNA CT still occur in DNA wrapped around histones in a nucleosome core particle? This issue was addressed by an experiment that isolated DNA cleavage at sites of guanine oxidation in nucleosome-wrapped DNA using a rhodium photooxidant covalently tethered to one end of the DNA [30]. The occurrence of damage, even

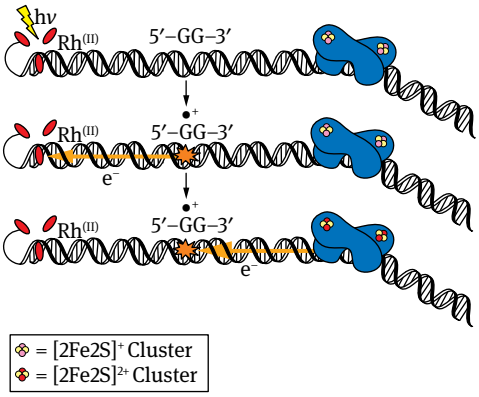

Fig. 15.4: Transcription factor SoxR, activated in response to oxidative stress in the cell, contains a [2Fe-2S] cluster, which is oxidized from the $[2Fe\text{-}2S]^{+}$ form to the $[2Fe\text{-}2S]^{2+}$ form when turned on for activity. Using a DNA-intercalating Rh (III) photooxidant, a guanine radical is generated at the 5′-position in a 5′-GG-3′ doublet. The guanine damage can be repaired at a distance by bound SoxR, through DNA CT. The guanine damage in turn oxidizes SoxR to the $[2Fe\text{-}2S]^{2+}$ form and turns on the oxidative stress response.

at sites distant from the photooxidant, demonstrated that the curvature of the DNA is unimportant as long as local π-stacking is unperturbed. The wrapping of DNA around histones produces very gradual curvature, not the kinking of DNA, which is known to interfere with DNA CT. Local π-stacking perturbations can arise from the binding of certain proteins, as has been shown with the transcription factor TATA binding protein, which kinks the DNA duplex at a sharp angle and effectively shuts off CT [31]. This is not, however, the typical binding mode of DNA-binding proteins; helix-turn-helix proteins do not interfere with DNA CT, and thus, many proteins that coat the DNA in the cell are not expected to affect long range signaling through DNA CT.

15.3 Assessing redox signaling by [4Fe-4S] proteins *in vitro* and *in vivo*

In addition to exploring chemically whether the [4Fe-4S] cluster of the repair proteins could be oxidized in a DNA-mediated reaction, we became interested in visualizing the process. To do so, an atomic force microscopy (AFM) assay was developed to assess the distribution of [4Fe-4S] proteins on DNA (Fig. 15.5 [32]). Specifically, this assay involved the addition of WT EndoIII to a mixture consisting of a 3.8-kb DNA substrate, either completely well matched (WM) or containing a single CA MM, and two smaller (2.2 and 1.6 kb) strands of WM DNA (from which the larger strand was composed). This solution was dried on a mica surface and imaged, with DNA-bound proteins distinguished by their greater height

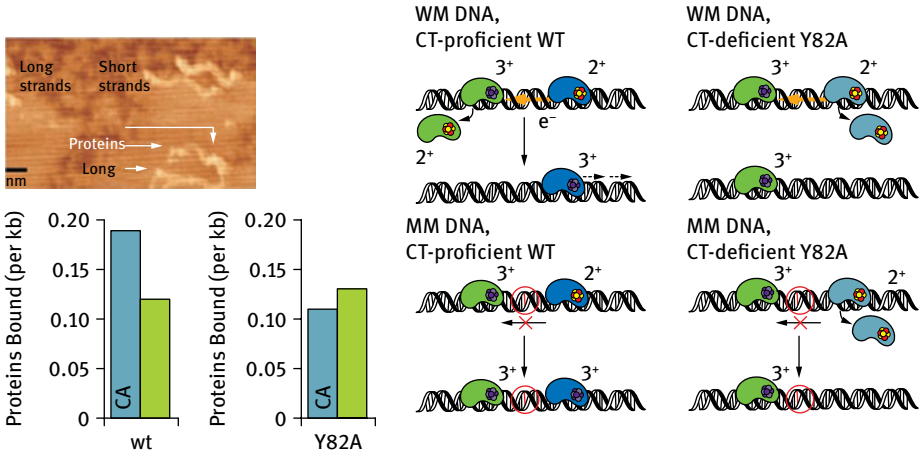

Fig. 15.5: Atomic force microscopy (AFM) assay to assess protein redistribution by CT. DNA-bound proteins can be visually distinguished by their relatively great height on the surface, as seen in a sample image on the top left. If CT signaling is occurring (middle), WT proteins like EndoIII preferentially bind to DNA containing a CA mismatch, leading to significantly more proteins bound to mismatched strands, as seen in the plot at bottom left. Conversely, when the assay is carried out with a CT-deficient mutant such as EndoIII Y82A (far right), no redistribution is observed (bottom left). Adapted from Ref. [32].

relative to DNA and free proteins, thereby providing a visual snapshot of the equilibrium binding distributions of proteins on the DNA. With respect to the distribution, it was predicted that redox signaling would cause tightly bound oxidized proteins to be trapped in the vicinity of a CT-attenuating MM, leading to an increase in binding density on MM DNA over WM DNA. The notion is that on the WM strand, there is extensive DNA-mediated CT between the DNA-bound proteins, facilitating the dissociation (with reduction) and reassociation (with oxidation) of proteins onto different strands. With an MM on the strand, DNA CT is inhibited, and thus little dissociation and redistribution occur, leading ultimately to proteins being bound preferentially on the mismatched versus fully matched duplexes. Importantly, a CA MM is not a substrate for EndoIII, so there is no intrinsic reason for the proteins to localize to this strand. Indeed, we found that EndoIII binding density ratios for WM versus MM DNA (proteins bound per kb on long DNA/proteins bound per kb on short DNA) averaged to 1.6 for mismatched long DNA, indicating a preference for mismatched strands. In control experiments where the long and short strands were both fully matched, the binding densities were always essentially the same.

Although EndoIII as purified is largely in the $[4Fe\text{-}4S]^{2+}$ oxidation state, enough $[4Fe\text{-}4S]^{3+}$ EndoIII must be present in a given sample to allow redistribution in the AFM assay. However, EndoIII and other BER proteins generally operate under conditions of oxidative stress in which one would expect a higher proportion of the proteins to be oxidized. To test conditions in which more oxidized $[4Fe\text{-}4S]^{3+}$ protein is initially present, EndoIII/DNA mixtures were incubated with hydrogen peroxide prior to AFM imaging [32]. Consistent with oxidative stress activating this process, oxidation resulted in an increase in the redistribution, with the binding density ratio on mismatched DNA increasing from 1.6 to 2.4. The protein is able to "find" the strand containing a single MM on a 3.8 kilobase duplex.

EndoIII mutants that were defective in carrying out DNA CT had been prepared and characterized, and it was of interest to see how these mutations would affect redistribution. Tyrosine and tryptophan residues are well known to facilitate electron transfer within proteins [33], and it was reasonable to consider that they might be involved in relaying electrons between DNA and the cluster in EndoIII. With this aim, a range of mutants were prepared and characterized in activity assays, and their CT properties were then investigated in electrochemical experiments and the AFM assay [34]. Independent mutation of several aromatic residues in EndoIII, including F30, Y55, Y70, and Y82, resulted in proteins with full catalytic activity and an identical midpoint potential but differing extents of CT deficiency relative to WT, as measured by the current signal height per cluster in a cyclic voltammogram on a DNA electrode. Interestingly, we could correlate directly the efficiency of DNA CT with redistribution in the AFM assay; those proteins that showed poor electrochemical signals on DNA electrodes, reflecting poor DNA CT, also showed low binding density ratios in the AFM assay, while those with high DNA CT efficiency showed high ratios for redistribution onto the mismatched strand. Thus, proteins with efficient DNA CT could more effectively find the mismatched strand.

But does this signaling occur within the cell? To see if these redox-based exchanges between [4Fe-4S] proteins occur in the cell, we took advantage of a genetic assay, our "helper function" assay designed to assess the effect of CT signaling on MutY activity

(Fig. 15.6 [32]). This assay used *E. coli* strain CC104, which has a cytosine swapped for an adenine in the *lacZ* Glu-461 codon, preventing β-galactosidase activity and

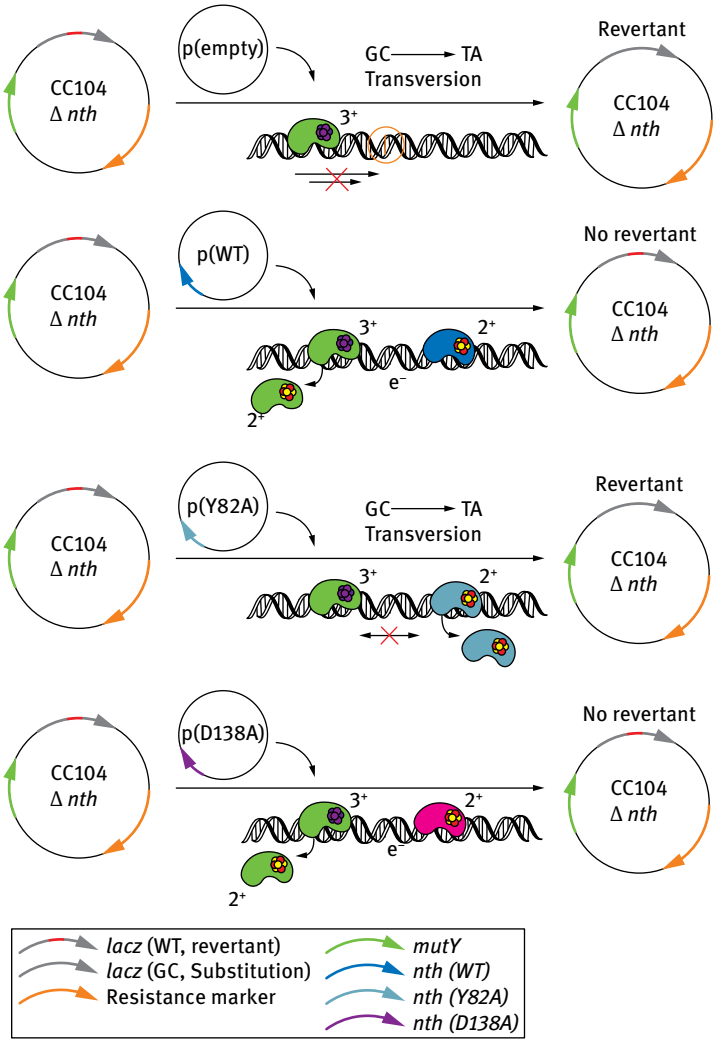

Fig. 15.6: *E. coli* helper function assay for MutY activity. The CC104 strain used in this assay contains a GC substitution in the *lacZ* gene, rendering the cells unable to metabolize lactose. Oxidative stress generates 8-oxoguanine, which is readily mispaired with adenine during replication; repair by enzymes that target 8-oxo G ultimately causes a GC → TA transversion, reverting the *lacZ* gene back to WT. MutY, however, excises adenine mispaired with 8-oxoG, so its activity prevents reversions. Remarkably, when EndoIII (nth) is knocked out and an empty plasmid is added in (top), revertants are observed, indicating an impairment in MutY activity. WT EndoIII restores the efficiency of MutY (top middle), while the CT-deficient mutant Y82A is unable to rescue MutY activity (bottom middle). In contrast, the CT-proficient, but catalytically defective, mutant EndoIII D138A has the same restorative effect on MutY activity as WT (bottom), confirming that DNA-mediated redox signaling is the primary factor responsible for this result.

inhibiting growth in media with lactose as the primary carbon source. Because MutY specifically removes adenine mispaired with oxo-guanine, lowered MutY activity in the CC104 strain results in CG → AT transversions that restore β-galactosidase activity and growth on lactose (*lac*$^+$). Numbers obtained could range from ~20 revertants per 10^9 plated cells in the background to over 300 revertants per 10^9 cells when MutY was knocked out. To see if cooperation or signaling with other [4Fe-4S] proteins might affect MutY activity, the EndoIII gene (*nth*) was knocked out in the CC104 strain; critically, EndoIII does not resolve A-oxoG mispairs, so it cannot function redundantly with MutY. Despite this, *nth*$^-$ cells showed an average of 54 *lac*$^+$ revertants, more than a twofold increase over background, indicating that EndoIII "helps" MutY find its targets. To verify that this effect was due to long range CT, CC104 *nth*$^-$ strains were complemented with plasmids encoding either CT-deficient EndoIII Y82A or catalytically inactive but CT-proficient D138A. Y82A was unable to restore background transversion rates, which were indistinguishable from uncomplemented *nth*$^-$; in contrast, D138A, despite its inability to carry out the glycosylase reaction, was able to help MutY and lower transversion rates to background levels. These genetic results provided a direct link between DNA CT and the observed ability of EndoIII to assist MutY in finding its targets.

These assays thus laid a foundation for considering how long-range signaling through DNA CT might indeed function for communication and cooperation among [4Fe-4S] cluster repair proteins within the cell. In our model, DNA repair proteins with [4Fe-4S] clusters use long-range redox signaling to communicate on DNA as a first step in locating their targets [32]. As illustrated in Fig. 15.7, a redox-inert repair protein in the native $[4Fe\text{-}4S]^{2+}$ oxidation state binds to DNA and becomes activated toward oxidation. If another distally bound protein is in the oxidized $[4Fe\text{-}4S]^{3+}$ state, the newly bound protein can reduce it at a distance via DNA CT; upon reduction, the binding affinity of the distal protein is lowered and the protein is free to diffuse to another region of the genome. When the intervening DNA between the two proteins is undamaged, this self-exchange reaction proceeds efficiently. However, if an MM or lesion is present between the proteins, CT is attenuated and the proteins can no longer communicate; both proteins then remain oxidized and bound to the DNA in the vicinity of the lesion, significantly reducing the range over which diffusion must occur and allowing repair of the entire genome on a biologically relevant time scale.

In addition to the novelty of the CT-based damage search, this model was particularly relevant because it presented a solution to the significant problem of how repair proteins manage to locate substrates on a time scale feasible for biological processes. Earlier models generally invoked some combination of one dimensional and three-dimensional diffusion along DNA to explain this problem [35], but these mechanisms alone have been estimated to take far too long (over twice the cell's doubling time) for low-copy number proteins like MutY to search the ~4.5-Mb *E. coli* genome [32]. If oxidative lesions were rare, this might not be a problem, but roughly 1,000 such lesions occur per doubling time [32], and the situation is no more favorable in other organisms [5]. However, when DNA-mediated CT scanning of the genome is factored into this process,

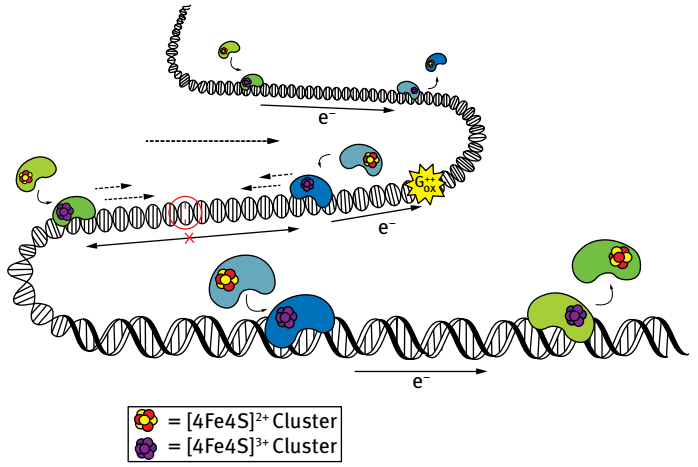

Fig. 15.7: A model for DNA-mediated redox signaling between repair proteins. Enzymes with the cluster in the native $[4Fe\text{-}4S]^{2+}$ form first bind DNA, causing the cluster to become activated toward oxidation. Oxidative stress initiates the damage search when highly reactive species such as the guanine radical cation are formed; these can oxidize DNA-bound proteins in their vicinity. Oxidation of the cluster to the $[4Fe\text{-}4S]^{3+}$ form leads to a 1,000-fold increase in DNA binding affinity, so oxidized proteins remain bound and diffuse along the DNA. When another [4Fe-4S] protein binds at a distant site, it can send an electron through the DNA base stack to reduce the oxidized protein. At this point, the reduced protein binds less tightly to DNA and diffuses away, while the newly oxidized protein continues the damage search. This process of redox exchange continues until a segment of DNA containing a lesion is approached. Since even subtle lesions can disrupt base stacking, CT is attenuated and any nearby oxidized proteins remain bound. Thus, DNA CT allows repair proteins to scan large sections of the genome and focus their time on areas containing damage.

the search time is significantly reduced even with short CT distances of ~200 bp, and substantially more so with longer CT distances [32]. Critically, this mechanism does not preclude diffusional search methods but instead simply provides a way for proteins to reach the vicinity of a lesion significantly more rapidly, and independent of the many other proteins associated with the DNA; once in the vicinity, diffusion over relatively short (~200 kb) distances would be used to locate and recognize the damaged base.

15.4 DNA CT in other repair pathways

In addition to BER, [4Fe-4S] proteins have also been found in NER pathways in archaea and, by homology, eukaryotes [8]. NER involves the removal of bulky lesions such as thymine dimers by exposing the damage through helicase-mediated unwinding of the surrounding ~25 nt of DNA, after which an endonuclease excises the segment and the resultant gap is filled in by a DNA polymerase [36]. In archaea and eukaryotes, DNA unwinding is dependent upon the ATP-stimulated activity of the [4Fe-4S] helicase enzyme XPD. Although XPD is itself part of the transcription factor IIH (TFIIH) complex,

it has nonetheless been isolated from the extremophile *Sulfolobus acidocaldarius* and structurally characterized. Upon incubation on a gold electrode modified with an appropriate DNA substrate (20-mer duplex with a 9-mer ssDNA overhang), a reversible, DNA-mediated signal centered at 80 mV *vs.* NHE is observed [37] This signal is comparable in both shape and potential to EndoIII and MutY, in line with predictions for the CT scanning model. In the case of XPD, however, the addition of ATP to stimulate DNA unwinding strongly enhances the current, while the nonhydrolysable analogue ATP γ-S does not. This signal enhancement indicates improved coupling of the cluster to the DNA during activity, a function that could be very important in coordinating with other proteins during NER, effectively "signaling" that the repair protein is functioning.

In humans, mutations in XPD are associated with several diseases, including xeroderma pigmentosum, Cockayne syndrome, and trichothiodystrophy [8]. The archaeal versions of two of these mutants, G34R and L325V, were characterized electrochemically; both were CT-deficient [37, 38]. To see if DNA-mediated signaling could occur between disparate pathways and proteins, *S. acidocaldarius* XPD and *E. coli* EndoIII were incubated together in the presence of DNA and imaged by AFM [38]. As with experiments involving only EndoIII, the presence of a CA MM resulted in an elevated DNA-binding density ratio; this effect was lost if WT EndoIII or XPD were incubated with a CT-deficient signaling partner, namely XPD L325V or EndoIII Y82A, respectively. Thus, XPD was able to help EndoIII localize to damaged DNA, but only if both proteins were CT-proficient. This experiment established two important general properties of CT between [4Fe-4S] proteins: first, that long-range signaling can occur between proteins in distinct pathways, and second, that the proteins do not even have to be from the same organism in order to communicate in this manner. What is critical is that they both bind DNA, have similar DNA-bound redox potentials, and are well coupled into the DNA helix to carry out DNA CT.

E. coli DinG is a superfamily 2 helicase with homology to XPD that also contains a [4Fe-4S] cluster [7], although DinG is primarily tasked with R-loop maturation rather than NER. R-loop maturation involves the helicase-mediated unwinding of RNA-DNA hybrids that result from collisions between transcription and replication machinery [39]. We found that DinG behaved similarly to XPD on DNA-modified Au electrodes, displaying a virtually identical midpoint potential, and the increase in current upon the addition of ATP was even more dramatic than for XPD [40]. Likewise, DinG showed a redistribution onto mismatched DNA in the AFM assay, both alone and in a mixture with WT EndoIII but not when combined with CT-deficient EndoIII Y82A. These assays supported the model developed for CT signaling in repair.

The real value in probing signaling by DinG, as an *E. coli* protein, was the ability to examine *in vivo* signaling in a bacterial system both with EndoIII and MutY. As an initial effort in elucidating signaling between pathways, the lac^+ helper function assay discussed above was employed to see if CT-active DinG could stimulate MutY activity in the same way as EndoIII. Remarkably, a DinG knockout did cause an increase in lac^+ reversions, despite the fact that DinG and MutY are active in distinct repair pathways. This result was in agreement with the *in vitro* AFM studies showing communication

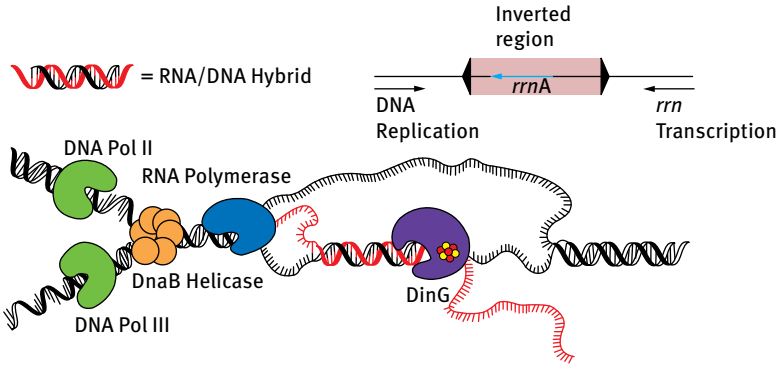

Fig. 15.8: *E. coli* inverted A assay for DinG activity. In this assay, the highly transcribed *rrn*A operon has been inverted to increase the rate of replication/transcription collisions, generating R-loops, which the [4Fe-4S] helicase DinG unwinds to resolve the stalled fork. Surprisingly, knocking out EndoIII prevented DinG from resolving R-loops, abolishing cell growth. As in the helper function assay (Fig. 15.6), both WT and the CT-proficient mutant D138A rescued this effect, while CT-deficient EndoIII Y82A did not. Overall, this indicates that CT signaling between EndoIII and DinG is important in helping DinG localize to collision sites.

between XPD and EndoIII but went further by demonstrating such communication *in vivo* within the same organism.

Importantly, we could ask also if EndoIII signaling was necessary for DinG activity. Here, we used the InvA *E. coli* strain to test the effect of EndoIII CT on DinG activity (Fig. 15.8 [41]). This assay relied upon the reversal of the frequently transcribed *rrnA* operon in *E. coli* to increase the frequency of replication/transcription collisions, causing stalled forks and generating R-loops; DinG correction of these R-loops was essential for cell survival. Indeed, cell growth was abolished when EndoIII was knocked out, and complementation with either WT or the enzymatically inactive, CT-proficient mutant EndoIII D138A restored survival. In contrast, complementation with the CT-deficient but enzymatically active EndoIII Y82A did not restore survival. Taken together, the MutY helper function and InvA strain survival assays showed that long-range signaling by DNA CT is critical to [4Fe-4S] enzymes in disparate pathways: DinG signals BER proteins in their search for damage, and the BER proteins, in turn, can facilitate R-loop resolution by DinG.

15.5 A role for CT in eukaryotic DNA replication?

In addition to BER and NER, conserved [4Fe-4S] clusters have been identified in eukaryotic replication proteins, including yeast and human DNA primase and the yeast B-family DNA polymerases (Pols) α, δ, ε, and ζ [9, 10] (Fig. 15.9). In DNA replication, a replication bubble is generated by two helicase complexes unwinding DNA in opposite directions, and new DNA strands are synthesized in the 5′ → 3′ direction by

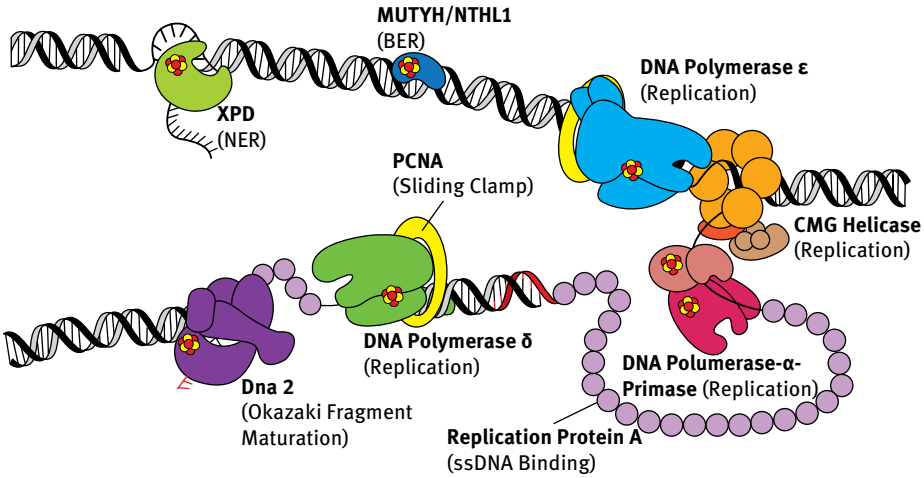

Fig. 15.9: DNA-binding eukaryotic enzymes containing [4Fe-4S] clusters are found both in replication and in repair pathways. The three polymerases (polymerase-α-primase, polymerase ε, and polymerase δ) responsible for copying genomic DNA from a parent template all contain a cluster. Polymerase-α-primase initiates replication through RNA/DNA primer synthesis; polymerase ε and polymerase δ then take over replication on the leading and lagging strand of the replication fork, respectively. Dna2 helicase-nuclease, instrumental in Okazaki fragment processing, also contains a [4Fe-4S] cluster in its nuclease domain. Repair enzymes, such as XPD helicase in the TFIIH complex (NER) and MUTYH/NTHL1 glycosylases (BER), search for and repair any mismatched/damaged bases on the nascent genomic DNA. This array of [4Fe-4S] enzymes in several pathways, with the ability to communicate with one another through DNA CT, suggests that redox signaling may play a larger role in coordinating the complex and dynamic process of eukaryotic replication.

DNA polymerases, which extend from a short (8–10 nucleotide) RNA primer generated by a primase enzyme [42]. The directionality of the polymerases necessitates that one strand, the leading strand, undergoes continuous synthesis in the direction of the fork, and the other, the lagging strand, be formed in discontinuous 120–150 nt Okazaki fragments. Under normal conditions, eukaryotic polymerases divide the task of DNA replication, with Pol α adding 10–20 nt of DNA to the RNA primer before ceding the leading strand to Pol ε and the lagging strand to Pol δ [43].

Replication presents an additional puzzle beyond DNA repair, as these proteins do not scan the genome, but instead associate in complexes at replication forks [44]. Faithful duplication of the genome requires a large amount of coordination among DNA-bound [4Fe-4S] proteins, which may be facilitated by DNA-mediated redox signaling. Work in our laboratory has indeed shown this to be the case for DNA primase and the lagging strand polymerase Pol δ [45]. Primase forms a complex with Pol α (Pol-Prim) *in vivo*, and together, these proteins form a 20–30-nt RNA-DNA hybrid primer. The means by which the RNA and DNA segment lengths are precisely controlled and the mechanism of the primase-Pol α handoff are currently poorly understood. In the case of DNA primase, oxidation of the cluster electrochemically results

in markedly enhanced DNA binding, and redox activity has been proposed to act as a switch mediating the hand-off from primase to Pol α. In this model, DNA-bound primase in the $[4Fe\text{-}4S]^{3+}$ state would synthesize an 8–10-nt RNA primer, at which point reduction of the oxidized primase by the [4Fe-4S] cluster of Pol α would terminate primer synthesis and facilitate the hand-off. Signaling between these particular proteins is a compelling possibility, given that primase and Pol α form a single complex flexible enough to position the [4Fe-4S] clusters in primase and Pol α for CT signaling.

Upon completion of the RNA-DNA hybrid primer by Pol-Prim, the primer end is handed off to the clamp loader complex, which attaches the circular sliding clamp PCNA to the primed end; PCNA is then bound by Pol ε on the leading strand and Pol δ on the lagging strand to synthesize long stretches of DNA in a processive manner [46]. Because the clamp loader does not contain a [4Fe-4S] cluster, the Pol δ cluster must have a purpose other than primer handoff. Preliminary work with Pol δ has shown that, while Pol δ is redox active on DNA, oxidation of the cluster leads to reversible stalling of DNA synthesis [45]. Such a stalling mechanism could provide a way for the cell to rapidly coordinate a response to replication stress, keeping proteins bound near the fork and allowing repair to be undertaken without the need to irreversibly dismantle the replication fork. Oxidative stress in particular is a frequent occurrence in cells, and it is certainly plausible that the polymerase could be oxidized either directly by species like guanine radicals or by other [4Fe-4S] proteins present at the fork; in any case, a fast-responding network of redox signaling in replication would be an advantage for the cell, complementing slower responses such as phosphorylation cascades [47].

15.6 DNA-binding [4Fe-4S] proteins in human disease

Many DNA processing proteins containing [4Fe-4S] clusters are known to be involved in human disease, with noncatalytic mutations near the cluster being surprisingly prevalent. These proteins include the human homologues of MutY and EndoIII (MUTYH and NTHL1, respectively) and XPD; poorly understood mutations in the [4Fe-4S] domain are also present in DNA primase and Pol δ. MUTYH is a critical player in colon cancer, specifically in MUTYH-associated polyposis [13]. Several poorly characterized mutations in residues near the cluster have recently been recognized. While difficult to understand from conventional perspectives, preliminary electrochemical studies have revealed at least one of these mutants to be more sensitive to oxygen-mediated cluster degradation [48]. Cluster degradation would be especially devastating from the perspective of a CT-based damage search, compromising not only MUTYH but also other repair proteins within the redox signaling network. Similarly, NTHL1 has been recognized as important in a variety of different cancers, although mutations in NTHL1 have not been studied to the extent that those in MUTYH have [14]. XPD

mutations are better known for their direct role in three major genetic disorders: trichothiodystrophy, Cockayne syndrome, and xeroderma pigmentosum. These disorders cause a photosensitivity phenotype that ultimately results in the development of cancer and/or accelerated aging. Cancer-relevant mutations in the [4Fe-4S] domain have also been reported in both DNA primase and Pol δ [49, 50]; however, mutations in replicative polymerases are relatively rare due to the essential nature of these enzymes, and those that have been studied generally occur in catalytic domains [51, 52]. From these examples, it is clear, however, that noncatalytic [4Fe-4S] clusters in DNA-processing enzymes are more relevant to disease than previously suspected. Some work has already implicated defective CT capabilities as important, but many questions remain to be answered.

15.7 Conclusions

Our understanding of the role of [4Fe-4S] clusters in DNA-processing enzymes has progressed from that of an unusually complex structural group to that of a critical element of rapid, long-range redox signaling along DNA. Considered from another perspective, the recognition of redox-signaling between [4Fe-4S] proteins has demonstrated the importance of DNA-mediated CT to biological systems. Indeed, DNA CT is crucial for the identification of lesions by low-copy number proteins like MutY, which would otherwise be unable to find their targets on a relevant timescale. Redox signaling by [4Fe-4S] clusters has moreover been shown to have utility in a wide range of repair pathways and has most recently been documented as critical in eukaryotic DNA replication. While these disparate proteins may all use CT for a slightly different purpose, the overarching pattern is clear: DNA CT provides a means of rapidly coordinating protein activities across the genome, especially under stress conditions. Although nuclear proteins utilize other search and signaling mechanisms, these are all limited by diffusion; in contrast, CT occurs on a uniquely rapid timescale, providing a first-step response to events such as oxidative stress. DNA CT serves as a sensor for the integrity of the genome and can expedite the cellular response to DNA damage, oxidative stress, and other insults to the genome. As more proteins involved in DNA processing that contain [4Fe-4S] clusters are identified, more critical roles for long-range DNA CT will emerge. Even now, however, it has become clear that long-range signaling by DNA CT offers a powerful means of genome-wide coordination and communication.

Acknowledgments

We are grateful to the NIH for their financial support of this research. We thank also all our coworkers and collaborators for their efforts in elucidating this chemistry.

References

[1] Beinert H, Holm RH, Münck E. Iron-sulfur clusters: nature's modular, multipurpose structures. Science 1997;277:653–9.
[2] Jacobs AL, Schär P. DNA glycosylases: in DNA repair and beyond. Chromosoma 2012;121:1–20.
[3] Cunningham RP, Asahara H, Bank JF, Scholes CP, Salerno JC, Surerus K, Münck E, McCracken J, Peisach J, Emptage MH. Endonuclease III is an iron-sulfur protein. Biochemistry 1989;28:4450–55.
[4] You HJ, Swanson RL, Doetsch PW. Saccharomyces cerevisiae possesses two functional homologues of Escherichia coli endonuclease III. Biochemistry 1998;37:6033–40.
[5] Markkanen E, Dorn J, Hübscher U. MUTYH DNA glycosylase: the rationale for removing undamaged bases from the DNA. Front Genet 2013;4:1–20.
[6] Porello SL, Cannon MJ, David SS. A substrate recognition role for the [4Fe-4S]$^{2+}$ cluster of the DNA repair glycosylase MutY. Biochemistry 1998;37:6465–75.
[7] Ren B, Duan X, Ding H. Redox Control of the DNA-damage inducible protein DinG helicase activity via its iron-sulfur cluster. J Biol Chem 2009;284:4829–35.
[8] Fan L, Fuss JO, Cheng QJ, Arvai AS, Hammel M, Roberts VA, Cooper PK, Tainer JA. XPD helicase structure and activities: insights into the cancer and aging phenotypes from XPD mutations. Cell 2008;133:789–800.
[9] a. Klinge S, Hirst J, Maman JD, Krude T, Pellegrini L. An iron-sulfur domain of the eukaryotic primase is essential for RNA primer synthesis. Nat Struct Mol Biol 2007;14:875–7. b. Weiner BE, Huang H, Dattilo BM, Nilges MJ, Fanning E, Chazin WJ. An iron-sulfur cluster in the C-terminal domain of the p58 subunit of human DNA primase. J Biol Chem 2007;282:33444–51.
[10] Netz DJA, Stith CM, Stümpfig M, Köpf G, Vogel D, Genau HM, Stodola JL, Lill R, Burgers PMJ, Pierik AJ. Eukaryotic DNA polymerases require an iron-sulfur cluster for the formation of active complexes. Nat Chem Biol 2012;8:125–32.
[11] Pokharel S, Campbell JS. Cross talk between the nuclease and helicase activities of Dna2: role of an essential iron-sulfur cluster domain. Nucleic Acids Res 2012;40:7821–30.
[12] Lessner FH, Jennings ME, Hirata A, Duin EC, Lessner DJ. Subunit D of RNA Polymerase from Methanosarcina acetivorans contains two oxygen-labile [4Fe-4S] clusters: implications for oxidant-dependent regulation of transcription. J Biol Chem 2012;287:18510–23.
[13] D'Agostino VG, Minoprio A, Torreri P, Marinoni I, Bossa C, Petrucci TC, Albertini AM, Ranzani GN, Bignami M, Mazzei F. Functional analysis of MUTYH mutated proteins associated with familial adenomatous polyposis. DNA Repair (Amst) 2010;9:700–7.
[14] Weren, R.D.A, Lightenberg, MJ, Kets CM, et al. A germline homozygous mutation in the base-excision repair gene NTHL1 causes adenomatous polyposis and colorectal cancer. Nat Genet 2015;47:668–71.
[15] Thayer MM, Ahern H, Xing D, Cunningham RP, Tainer JA. Novel DNA binding motifs in the DNA repair enzyme endonuclease III crystal structure. EMBO J 1995;14:4108–20.
[16] Transviña-Arenas CH, Lopez-Castillo LM, Sanchez-Sandoval E, Brieba LG. Dispensability of the [4Fe-4S] cluster in novel homologues of adenine glycosylase MutY. FEBS J 2016;283:521–40.
[17] Netz DJA, Mascarenhas J, Stehling O, Pierik AJ, Lill R. Maturation of cytosolic and nuclear iron-sulfur proteins. Trends Cell Biol. 2014;24:303–12.
[18] Arnold AR, Grodick MA, Barton JK. DNA charge transport: from chemical principles to the cell. Cell Chem Biol 2016;23:183–97.
[19] Slinker JD, Muren NB, Renfrew SE, Barton JK. DNA charge transport over 34 nm. Nat Chem 2011;3:228–33.
[20] Boal AK, Yavin E, Lukianova OA, O'Shea VL, David SS, Barton JK. DNA-bound redox activity of DNA repair glycosylases containing [4Fe-4S] clusters. Biochemistry 2005;44:8397–407.
[21] Backes G, Mino Y, Loehr TM, Meyer TE, Cusanovich MA, Sweeney WV, Adman ET, Sanders-Loehr J. The environment of Fe4S4 clusters in ferredoxins and high-potential iron proteins: new

information from x-ray crystallography and resonance Raman spectroscopy. J Am Chem Soc 1991;113:2055–64.
[22] Gorodetsky AA, Boal AK, Barton JK. Direct electrochemistry of Endonuclease III in the presence and absence of DNA. J Am Chem Soc 2006;128:12082–3.
[23] a. Fromme JC, Verdine GL. Structure of a trapped endonuclease III-DNA covalent intermediate. EMBO J 2003;22:3461–71. b. Guan Y, Manuel RC, Arvai AS, Parikh SS, Mol CD, Miller JH, Lloyd RS, Tainer JA. MutY catalytic core, mutant, and bound adenine structures define specificity for DNA repair enzyme superfamily. Nat Struct Biol 1998;5:1058–64. c. Woods RD, O'Shea VL, Chu A, Cao S, Richards JL, Horvath MP, David SS. Structure and stereochemistry of the base excision repair glycosylase MutY reveal a mechanism similar to retaining glycosylases. Nucleic Acids Res 2015;44:801–10.
[24] Bartels PL, Zhou A, Arnold AR, Chaffee N, Crespilho FN, David SS, Barton JK. Electrochemistry of the [4Fe4S] cluster in base excision repair proteins: tuning the redox potential with DNA. Langmuir 2017; 33:2523–2530.
[25] O'Neill MA, Becker H-C, Wan C, Barton JK, Zewail AH. Ultrafast dynamics in DNA-mediated electron transfer: base gating and the role of temperature. Angew Chem Int Ed Engl 2003;42:5896–900.
[26] Nunez ME, Hall DB, Barton JK. Long-range oxidative damage to DNA: effects of distance and sequence. Chem Biol (Oxford, UK) 1999;6:85–97.
[27] Hall DB, Holmlin RE, Barton JK. Oxidative DNA damage through long range electron transfer. Nature 1996;382:731–5.
[28] Yavin E, Boal AK, Stemp EDA, Boon EM, Livingston AL, O'Shea VL, David SS, Barton JK. Protein-DNA charge transport: redox activation of a DNA repair protein by a guanine radical. Proc Natl Acad Sci USA 2005;102:3546–51.
[29] Lee PE, Demple B, Barton JK. DNA-mediated redox signaling for transcriptional activation of SoxR. Proc Natl Acad Sci USA 2009;106:13164–8.
[30] Nunez ME, Noyes KT, Barton JK. Oxidative charge transport through DNA in nucleosome particles. Chem Biol 2002;9:403–15.
[31] Gorodetsky AA, Ebrahim A, Barton JK. Electrochemical detection of TATA binding protein at DNA-modified microelectrodes. J Am Chem Soc 2008;130:2924–5.
[32] Boal AK, Genereux JC, Sontz PA, Gralnick JA, Newman DK, Barton JK. Redox signaling between repair proteins for efficient lesion detection. Proc Natl Acad Sci USA 2009;106:15237–42.
[33] Winkler JR, Gray HB. Could tyrosine and tryptophan serve multiple roles in biological redox processes? Philos Trans A Math Phys Eng Sci 2015;373. doi:10.1098/RSTA.2014.0178
[34] Romano CA, Sontz PA, Barton JK. Mutants of the base excision repair glycosylase, endonuclease III: DNA charge transport as a first step in lesion detection. Biochemistry 2011;50:6133–45.
[35] Verdine GL, Bruner SD. How do DNA repair proteins locate damaged bases in the genome? Chem Biol 1997;4:329–34.
[36] Marteijn JA, Lans H, Vermeulen W, Hoeijmakers JHJ. Understanding nucleotide excision repair and its roles in cancer and aging. Nat Rev Mol Cell Biol 2014;15:465–81.
[37] Mui TP, Fuss JO, Ishida JP, Tainer JA, Barton JK. ATP-stimulated, DNA-mediated redox signaling by XPD, a DNA repair and transcription helicase. J Am Chem Soc 2011;133:16378–81.
[38] Sontz PA, Mui TP, Fuss JO, Tainer JA, Barton JK. DNA charge transport as a first step in coordinating the detection of lesions by repair proteins. Proc Natl Acad Sci USA 2012;109:1856–61.
[39] Voloshin ON, Camerini-Otero RD. The DinG protein from Escherichia coli is a structure-specific helicase. J Biol Chem 2007;282:18437–47.
[40] Grodick MA, Segal HM, Zwang TJ, Barton JK. DNA-mediated signaling by proteins with 4Fe-4S clusters is necessary for genomic integrity. J Am Chem Soc 2014;136:16470–8.

[41] Boubakri H, Langlois de Septenville A, Viguera E, Michel B. The helicases DinG, Rep, and UvrD cooperate to promote replication across transcription units in vivo. EMBO J 2010;29:145–57.
[42] Leman AR, Noguchi E. The replication fork: understanding the eukaryotic replication machinery and the challenges to genome duplication. Genes (Basel) 2013;4:1–32.
[43] Lujan SA, Williams JS, Kunkel TA. DNA polymerases divide the labor of genome replication. trends in cell biology 2016;26:640–654.
[44] Sun J, Shi Y, Georgescu RE, Yuan Z, Chait BT, Li H, O'Donnell ME. The architecture of a eukaryotic replisome. Nat Struct Mol Biol 2015;22:976–82.
[45] a. O'Brien E, Holt, ME, Thompson MK, Salay Le. Ehlinger AC, Chazin WJ, Barton JK, The [4Fe4S] cluster of human DNA primase functions as a redox switch using DNA charge transport. Science; 355: 813 b. Bartels PL, Stodola JL, Stith CM, Burgers PMJ, Barton JK. A redox role for the [4Fe4S] cluster of yeast DNA Polymerase δ. 2016 Unpublished manuscript.
[46] Georgescu RE, Schauer GD, Yao NY, Langston LD, Yurieva O, Zhang D, Finkelstein J, O'Donnell ME. Reconstitution of a eukaryotic replisome reveals suppression mechanisms that define leading/lagging strand operation. eLife 2015. doi: 10.7554/eLife.04988.
[47] Leroy C, Mann C, Marsolier M. Silent repair accounts for cell cycle specificity in the signaling of oxidative DNA lesions. EMBO J 2001;20:2896–906.
[48] Bartels PL, O'Brien E, Barton JK. 2016. Unpublished work in collaboration with McDonnell K, Chemler JA, Marvin M, Stern R, Raskin L, Sherman DH, Gruber S.
[49] Forbes SA, Bindal M, Bamford S, et al. COSMIC: mining complete cancer genomes in the Catalogue of Somatic Mutations in Cancer. Nucleic Acids Res 2011;39:D945–50.
[50] Ma X, Edmonson M, Yergeau D, et al. Rise and fall of subclones from diagnosis to relapse in pediatric B-acute lymphoblastic leukaemia. Nat Comm 2015. doi: 10.1038/ncomms7604.
[51] Fuss JO, Tsai C, Ishida JP, Tainer JA. Emerging critical roles of Fe-S clusters in DNA replication and repair. Biochim Biophys Acta 2015;1853:1253–71.
[52] Flohr T, Dai J, Büttner J, Popanda O, Hagmüller E, Thielmann HW. Detection of mutations in the DNA polymerase δ gene of human sporadic colorectal cancers and colon cancer cell lines. Int J Cancer 1999;80:919–29.

16 Iron-sulfur cluster assembly in plants

Hong Ye

16.1 Introduction

Iron is an essential micromineral nutrient. To overcome the insolubility of ferric iron in soil, plants reduce ferric iron to increase solubility or secrete chelators and absorb iron chelates to increase acquisition of iron (strategies I and II). The translocation, distribution, and delivery of iron throughout the whole plant involve a number of specific transporters and chelators. Inside the plant cell, iron is utilized to assemble heme and iron-sulfur (Fe-S) clusters. Fe-S cluster biosynthesis takes place separately in major subcellular compartments. It is mediated by the SUF system in plastids, by the ISC system in mitochondria, and by the CIA system in the cytosolic and nuclear compartments. As an essential pathway, the Fe-S cluster assembly machinery is highly conserved across the green lineage. In contrast to bacteria, plants lack the machinery for nitrogen fixation, but the legume plants often have a symbiotic relationship with nitrogen-fixing bacteria that use nitrogenase to assimilate nitrogen in specialized structures that surround their roots. The potential impact of the research on Fe-S protein biogenesis on agriculture will likely be quite significant.

16.2 Iron uptake, translocation, and distribution

Iron is an essential mineral nutrient for plants. Plants take up iron from soil, in addition to water and all other minerals. Iron contents in plants are variable; for instance, iron concentrations in major staple foods are 4.31 mg/100 g for rice and 0.27 mg/100 g for cassava (www.usda.gov), whereas the iron content in some other plants is 10 mg/100 g [1]. Despite the fact that iron concentration in soil is high compared with other minerals, most of the soil iron is in the form of insoluble ferric hydroxides and hence is not bioavailable. The solubility of iron depends on the pH of soil [2]. Iron in low-pH soil is more soluble and hence more bioavailable, whereas iron in high-pH soil is more insoluble and hence less bioavailable. Therefore, plants grown in basic soil often suffer iron deficiency, demonstrating dwarf size and chlorotic (yellowing of the leaves) symptoms.

To take up iron from soil at the roots, plants generally employ one of two different strategies, either strategy I or strategy II [1–6]. Dicotyledenous plants, for example, *Arabidopsis thaliana*, use strategy I and express ferric reductases and ferrous iron transporters on the cell membrane of roots. These plants also express a proton pump to acidify the root surface. The ferric reductase FRO2 reduces ferric iron into much more soluble ferrous iron in the root rhizosphere, the soil rich in plant exudates that surrounds the root [7, 8], and subsequently, ferrous iron is imported into root cells by the

DOI 10.1515/9783110479850-016

ferrous transporter, IRT1 [9–11]. Because of their central roles in iron uptake, the gene expression levels of IRT1 and FRO2 are highly inducible by iron deficiency. However, inside cells, free iron is toxic because it catalyzes the formation of reactive oxygen species (ROS) in the Haber-Weiss cycle; therefore, most iron is likely contained within chelated complexes in plants. An important intracellular chelator is nicotianamine (NA), a compound derived from methionine. The Fe-NA chelate is transported symplastically (through pores that allow cytoplasmic contacts between neighboring cells) through plasmodesmata (pores in the plant cell wall) toward the vasculature. At the boundary between the endodermis and the vasculature, iron is transported across the plasma membrane into the xylem, likely by the transporter ferroportin [1, 2]. The Fe-citrate chelate is translocated in the xylem from the root to the shoot driven by the force of transpiration. In leaves, iron is unloaded from the vasculature and transported into mesophyll cells by members of the Yellow Stripe-Like (YSL) family of transporters.

In contrast, monocots, which include the graminaceous plants, for example, rice (*Oryza sativa*), use strategy II for iron uptake [1, 2]. Rice plants secrete phytosiderophores of the mugineic acid (MA) family into the rhizosphere, which release insoluble ferric iron from soil particles to form an iron chelator complex. The resulting Fe-MA chelate is directly taken up into root cells by members of the YSL family of transporters. However, a recent study has shown that in addition to strategy II, rice is also able to take up ferrous iron through the IRT1 transporter [12]. The subsequent steps of translocation from root cells to vasculature and from vasculature to leaves are similar between strategy I and II plants.

In plant cells, iron is delivered into major organelles including chloroplasts, mitochondria, and vacuoles, where it is either stored or utilized for the synthesis of Fe-S clusters, heme, and nonheme iron proteins. Iron is imported into mitochondria by a mitoferrin-like transporter on the inner membrane [13]. To maintain iron homeostasis in the compartment, iron should be exportable. However, no potential mitochondrial iron exporter has yet been identified. Iron is imported into chloroplasts by PIC1 [14, 15], whereas iron may be exported from chloroplasts by the YSL4 and YSL6 transporters [16]. Chloroplasts are the major sink of iron in plant leaf cells, accommodating up to 80%–90% of total cellular iron in leaf cells. However, it is unknown whether the photosynthetic green organelle is important for the regulation of overall cellular iron homeostasis. Iron is used for the Fe-S cluster and heme synthesis in chloroplasts, and some iron is stored in ferritin, the iron storage protein of plants [17–19]. Unlike ferritin of mammalian cells, which is in the cytosol, the ferritin in plant cells is in chloroplasts/plastids [19]. To protect from toxicity, iron should be associated with some iron chaperone or chelated by chelators in plant cytosol, such as citrate, NA, and phytosiderophores. Potential iron chaperones in the cytosol of plant cells have not been identified. Some have proposed that PCBP family proteins are iron chaperones in eukaryotic cells [20], whereas others propose that the complex of monothiol glutaredoxin and glutathione bridging an Fe-S cluster facilitates iron delivery in cytosol and nuclei [21]. The excess iron in cytosol is delivered to the vacuole for storage, imported by the VIT1

transporter, and stored as ferric citrate [22, 23]; the vacuolar iron can be exported by NRAMP3/4 transporters [1].

More than 60 Fe-S proteins have been confirmed or estimated in *Arabidopsis* [24]. These proteins have various physiological functions. Fe-S proteins in plastids are involved in chlorophyll synthesis, nitrite reduction, sulfite reduction, redox homeostasis, and photosynthesis [25]. Fe-S proteins in mitochondria are involved in molybdenum cofactor (Moco) biosynthesis, electron transfer in complexes I and II, glutamate synthesis, and biotin synthesis. Fe-S proteins in cytosol and nuclei are involved in abscisic acid biosynthesis, ribosome assembly, DNA replication, and DNA repair.

16.3 Fe-S cluster assembly

Despite the simplicity in the structure of Fe-S clusters, the biological assembly of an Fe-S cluster is extremely complex [26–30]. Research on plant Fe-S cluster biosynthesis has mainly focused on the model plant, *A. thaliana*. To date, 42 genes have been identified in *Arabidopsis* with a proposed function in Fe-S assembly [24, 31, 32]. As listed in Tab. 16.1, all these genes are encoded in the nuclear genome, and the expressed proteins are targeted to chloroplasts, mitochondria, and cytosol, respectively. Because these compartments are physically separated by membranes, it is thought that Fe-S biosynthesis takes place independently in each of the subcellular compartments [25, 26, 33–35]. Due to the sequence similarity to their orthologues in bacteria, the Fe-S

Tab. 16.1: List of proteins that are involved in the Fe-S cluster assembly in plant cells.

	Protein name	Locus	Function	Reference
Plastid	NFS2	At1g08490	Cysteine desulfurase	Pilon-Smits *et al.* (2003)
	SUFE1	At4g26500	Activator of NFS2	Xu *et al.* (2006)
	SUFE2	At1g67810	Activator of NFS2	Murthy *et al.* (2007)
	SUFE3	At5g50210	Activator of NFS2	Murthy *et al.* (2007)
	SUFA	At1g10500	Cluster transfer	Abdel-Ghany *et al.* (2005) [53]
	NFU1	At4g01940	Scaffold	Léon *et al.* (2003) [48]
	NFU2	At5g49940	Scaffold	Touraine *et al.* (2004) [49]
	NFU3	At4g25910	Scaffold	Léon *et al.* (2003) [48]
	SUFB	At4g04770	Scaffold	Xu *et al.* (2005) [51]
	SUFC	At3g10670	Scaffold	Xu *et al.* (2006) [43]
	SUFD	At1g32500	Scaffold	Xu *et al.* (2005) [51]
	HCF101	At3g24430	4Fe-4S insertion	Schwenkert *et al.* (2010) [56]
	GRXS14	At3g54900	2Fe-2S transfer	Bandyopadhyay *et al.* (2008) [57]
	GRXS16	At2g38270	2Fe-2S transfer	Cheng *et al.* (2006) [58]

Tab. 16.1 (continued)

	Protein name	Locus	Function	Reference
Mitochondria	NFS1	At5g65720	Cysteine desulfurase	Frazzon *et al.* (2007) [60]
	ISD11	At5g61220	Interacting with NFS1	Heis *et al.* (2011) [62]
	ISU1	At4g22220	Scaffold	Frazzon *et al.* (2007) [60]
	ISU2	At3g01020	Scaffold	Léon *et al.* (2005) [74]
	ISU3	At4g04080	Scaffold	Frazzon *et al.* (2007) [60]
	ISA1	At2g16710	Cluster transfer	Uncharacterized
	ISA2	At2g36260	Cluster transfer	Uncharacterized
	ISA3	At5g03905	Cluster transfer	Uncharacterized
	NFU4	At3g20970	Scaffold	Léon *et al.* (2003) [48]
	NFU5	At1g51390	Scaffold	Léon *et al.* (2003) [48]
	ADX1	At4g21090	Electron transfer	Takubo *et al.* (2003) [75]
	ADX2	At4g05450	Electron transfer	Picciocchi *et al.* (2003) [76]
	ADXR	At4g32360	Electron transfer	Takubo *et al.* (2003) [75]
	FH	At4g03240	Iron donor	Busi *et al.* (2006) [67]
	HSCA1	At4g37910	HSP70-type chaperone	Xu *et al.* (2009) [77]
	HSCA2	At5g09590	HSP70-type chaperone	Uncharacterized
	HSCB	At5g06410	Co-chaperone	Xu *et al.* (2009) [77]
	INDL	At4g19540	Cluster transfer/ insertion	Bych *et al.* (2008) [81]
	IBA57	At4g12130	Cluster transfer	Waller *et al.* (2010) [78]
	GRXS15	At3g15660	Glutaredoxin	Bandyopadhyay *et al.* (2008) [57]
	ATM3	At5g58270	ABC transporter	Bernard *et al.* (2009) [86]
	ERV1	At1g49880	Sulfhydryl oxidase	Levitan *et al.* (2004) [90]
Cytosol	TAH18	At3g02280	Electron transfer	Varadarajan *et al.* (2010) [94]
	DRE2	At5g18400	Electron transfer	Varadarajan *et al.* (2010) [94]
	NBP35	At5g50960	Scaffold	Bych *et al.* (2008) [81]
	NAR1	At4g16440	[FeFe]-hydrogenase-like	Cavazza C.*et al.* (2008) [95]
	CIA1	At2g26060	WD40 protein	Srinivasan *et al.* (2007) [97]
	CIA2	At1g68310	DUF59 domain	Luo *et al.* (2012) [89]
	MMS19	At5g48120	Interacting with CIA	Stehling *et al.* (2012) [99]

The proposed function and subcellular localization for each protein is as indicated.

assembly machinery in chloroplasts/plastids is termed as SUF (mobilization of sulfur) system, whereas mitochondrial Fe-S assembly is termed as ISC (iron-sulfur cluster) system, and the Fe-S biosynthesis in cytosol is referred to as the CIA system (cytosolic iron-sulfur assembly).

16.3.1 SUF system in plastids

The chloroplast/plastid SUF machinery of *Arabidopsis* consists of at least 14 proteins (Fig. 16.1 and Tab. 16.1), which are NFS2, SUFE1, SUFE2, SUFE3, SUFA, NFU1, NFU2, NFU3, SUFB, SUFC, SUFD, HCF101, GRXS14, and GRXS16.

NFS2 (nitrogen fixation, S protein) is the cysteine desulfurase that provides sulfur for Fe-S cluster assembly [36–38]. In isolated form, NFS2 is a dual function enzyme,

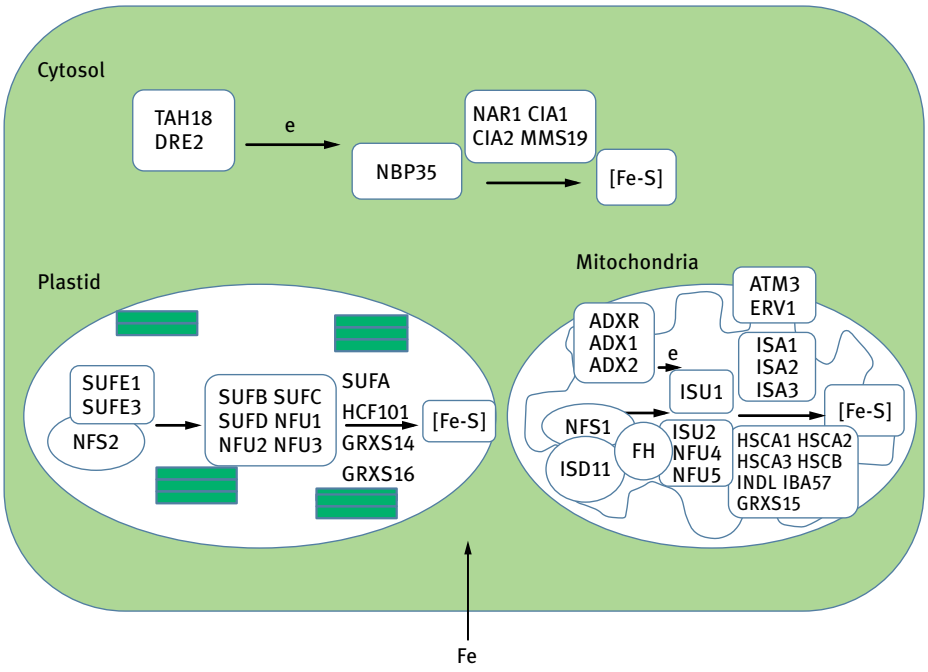

Fig. 16.1: Working model of the Fe-S cluster biosynthesis in a plant cell. About 40 genes have been confirmed or estimated to be involved in the Fe-S cluster assembly in plant cells. All these genes are nuclear genome encoded. The expressed proteins are translocated to plastids, mitochondria, and cytosol, where Fe-S clusters are assembled separately. The reaction is initiated by the donation of sulfur and iron, which are assembled into an Fe-S cluster on a major scaffold. Facilitated by multiple delivery or carrier proteins, the preassembled Fe-S cluster is delivered to target proteins, resulting in the maturation of Fe-S proteins. In each of the reactions, the arrows from left to right indicate the upstream to downstream steps in the Fe-S assembly pathway.

with both cysteine desulfurase (CysD) activity and selenocysteine lyase (SL) activity. The CysD activity catalyzes the removal of a sulfur from cysteine to produce sulfur and alanine, whereas its SL activity catalyzes the lysis of selenocysteine to produce selenide and alanine. The two enzymatic activities use the same core active site, but the CysD activity requires an additional cysteine residue that is not required for the SL activity. Homozygous, knockout deletions of NFS2 in plants by T-DNA insertion have not been reported, consistent with a crucial role of NFS2. RNAi knockdown plants of NFS2 exhibit severe phenotypes including chlorosis, chloroplast disorganization, leaf necrosis, and early death; concomitantly, various chloroplast Fe-S proteins are decreased in both abundance and activity. In contrast, mitochondrial Fe-S proteins and respiration remain unaffected, suggesting that Fe-S assembly is independent in mitochondria and chloroplasts [39]. Overexpression of NFS2 enhances selenium and sulfur accumulation in plants and increases tolerance to selenate exposure [36, 40], suggesting that NFS2 might be a part of a system to prevent selenium toxicity in plants. The physiological relevance of the SL enzyme activity may not be essential to plants because some plant species do not require any selenium. In contrast, the CysD activity is essential to plants. However, when measured *in vitro*, the CysD activity of NFS2 was much weaker than its SL activity [36, 38]. This observation suggested that an additional factor was required in planta for the CysD activity. The subsequent discovery that SUFE proteins strongly stimulated NFS2 provided a possible explanation for the assay results [41, 42]. The *Arabidopsis* genome encodes three SUFE genes, SUFE1, SUFE2, and SUFE3. As demonstrated by *in vitro* biochemical assays, each of the SUFE proteins can stimulate the CysD activity of the NFS2 protein 40- to 70-fold and increase Fe-S cluster assembly at least 20-fold. NFS2 and SUFE form a protein complex and together function as the cysteine desulfurase in plant chloroplasts/plastids [41, 42].

SUFE1 is a fusion protein with an N-terminal SUFE domain and a C-terminal BOLA domain [42, 43]. The SUFE domain is responsible for CysD-stimulating activity, whereas the function of the BOLA domain is currently unknown. Bioinformatics analysis and experimental results for BOLA-like proteins in other species have suggested that BOLA interacts with glutaredoxin [44–47]. Hence, it is very likely that the C-terminal BOLA domain of SUFE1 may interact with glutaredoxins in chloroplasts, such as GRXS14 and GRXS16. The SUFE domain of SUFE1 physically interacts with NFS2 to form a hetero-tetrameric complex, which increases NFS2 enzyme affinity for its substrate, cysteine, and increases Vmax 40-fold. T-DNA insertion knockout of SUFE1, a method for generating loss-of-function mutations in plants, is embryonic lethal, suggesting that the essential role of SUFE1 cannot be substituted by other SUFE paralogues. SUFE2 and SUFE3 share a SUFE domain with SUFE1. They also stimulate the CysD activity of NFS2 in a similar manner [41]. Because SUFE2, which consists solely of the SUFE region, is specifically expressed in flowers, especially in pollen, it is possible that SUFE2 may specifically enhance Fe-S cluster biosynthesis in pollen, the male gametophyte of flowering plants. SUFE3 is another fusion protein with an N-terminal SUFE domain and C-terminal NadA domain. NadA is a quinolinate synthase, required

for NAD biosynthesis, and it is a [4Fe-4S] protein. SUFE3 stimulates CysD activity and enhances Fe-S cluster assembly and delivery to the NadA domain of SUFE3. The resulting holo-SUFE3 is the NadA enzyme of plants, involved in a critical step of NAD biosynthesis. Knockout of SUFE3 in *Arabidopsis* is embryonic lethal.

NFU1, NFU2, and NFU3 (nitrogen fixation, U protein) are scaffold proteins [48–50]. Their protein sequences consist of an N-terminal NFU domain and a C-terminal B domain, whereas mitochondrial NFU4 and NFU5 proteins consist of an N-terminal N domain and a C-terminal NFU domain. These NFU proteins share a conserved CXXC motif in the NFU domain. They are capable of assembling Fe-S clusters and delivering them to target proteins. Plants in which NFU2 is inactivated exhibit a dwarf phenotype with pale-green leaves, decreased activity of [4Fe-4S] sulfite reductase, and drastically impaired photosystem I (PSI) and ferredoxin accumulation in chloroplasts [49, 50]. However, glutamate synthase and Rieske Fe-S proteins are not affected in the mutants, indicating that the NFU2 scaffold is responsible for a subset of target proteins. SUFB, SUFC, and SUFD form a complex and together function as a multimolecular scaffold [51, 52]. The SUFBCD complex can assemble Fe-S clusters *in vitro* and transfer them to target proteins. SUFC is the subunit that possesses ABC/ATPase activity. SUFC knockout mutant plants are embryonic lethal, and mutant embryos contain abnormal plastids with disorganized thylakoid structures, which are membrane-bound compartments inside chloroplasts. SUFA is an alternative scaffold that probably functions in the delivery of Fe-S clusters [53, 54]. In an *in vitro* reconstitution experiment, SUFA was able to acquire a transient [2Fe-2S] cluster. The holo-SUFA was stable and could be purified by chromatography. When incubated with ferredoxin, a target protein, SUFA could donate its [2Fe-2S] cluster to generate holo-ferredoxin [53].

HCF101 (high chlorophyll fluorescence 101) is an alternative scaffold that functions in Fe-S cluster targeting [55, 56]. It is specifically required for the biogenesis of [4Fe-4S] proteins, such as PSI and ferredoxin-thioredoxin reductase (FTR) in chloroplasts, but not for [2Fe-2S] proteins such as ferredoxin. In the HCF101-deficient mutant plants, both the activity and protein level of [4Fe-4S] proteins are reduced. HCF101 belongs to the [4Fe-4S] cluster-containing P-loop NTPase superfamily. HCF101 protein binds a [4Fe-4S] cluster through ligation to three HCF101-specific cysteine residues. The reconstituted cluster can be transferred from HCF101 to a [4Fe-4S] apo-protein [56]. GRXS14 and GRXS16 possess the canonical CGFS active site characteristic of monothiol glutaredoxins. They function as alternative scaffold proteins [57, 58] that can bind [2Fe-2S] clusters transiently, before rapidly and quantitatively transferring them to the apoprotein form of ferredoxin in chloroplasts. A recent structural and biochemical study has identified that the *Arabidopsis* GRXS16 is a two-domain protein [59]. Its N-terminal domain has DNA endonuclease activity, whereas the C-terminal GRX domain has redox activity and Fe-S cluster biosynthetic activity. GRXS16 may link Fe-S cluster assembly, iron homeostasis, the ROS response, and DNA metabolism in chloroplasts of higher plants. Moreover, these two plastid glutaredoxins, GRXS14 and GRXS16, are potential candidate proteins that physically interact with the BOLA domain of SUFE1 (Fig. 16.1).

16.3.2 ISC system in mitochondria

The mitochondrial ISC machinery of *Arabidopsis* consists of 22 proteins (Fig. 16.1, Tab. 16.1). They are NFS1, ISD11, ISU1, ISU2, ISU3, ISA1, ISA2, ISA3, NFU4, NFU5, ADX1, ADX2, ADXR, FH, HSCA1, HSCA2, HSCB, INDL, IBA57, GRXS15, ATM3, and ERV1.

NFS1 is the cysteine desulfurase [60, 61], and an accessory protein, ISD11, is required to stimulate the cysteine desulfurase activity of NFS1 enzyme [62]. The NFS1-ISD11 complex forms persulfide. It has been suggested that ISD11 induces a conformational change in NFS1 and brings the substrate and the active site cysteine in proximity to form persulfide. Hence, ISD11 could regulate cysteine desulfurase activity of NFS1 enzyme [63]. Frataxin (FH) is a potential iron donor for Fe-S cluster assembly [64–67]. Numerous studies have suggested that frataxin may function as an iron-binding chaperone for Fe-S cluster assembly, particularly in humans [68–72]. However, the function of the plant frataxin orthologue, FH, remains elusive and reports on FH roles are quite variable. Meanwhile, FH is thought to be an iron chaperone that delivers iron for Fe-S clusters. FH insertion mutant plants exhibit decreased activity of mitochondrial Fe-S proteins, such as aconitase and succinate dehydrogenase. In addition, FH mutant plants also manifest alteration in transcripts from the heme biosynthesis pathway, diminished total heme content, and deficient catalase activity. Thus, FH also plays a role in heme biosynthesis of higher plants [66]. FH is involved in energy conversion and oxidative phosphorylation, iron handling, and response to oxidative stress. FH may have other functions in different tissues and in different organisms [73].

ISU1 is the central scaffold protein in mitochondria. As paralogues to ISU1, ISU2 and ISU3 are alternative scaffolds [74]. Among all three ISU family proteins, ISU1 has the highest physiological importance. In agreement with this, ISU1 is constitutively expressed at constant levels, whereas ISU2 and ISU3 expression is minimal or nondetectable. None of the ISU1–ISU3 deletion mutant plants seem to be lethal, probably suggesting that ISU1–ISU3 functions are redundant [60]. It is possible that ISU1 is the central housekeeping scaffold in plants and is constantly expressed at high levels. In normal plant cells, expression of the other ISU paralogues is repressed. However, in the absence of ISU1, expression of the other ISU paralogues is induced, and the increased ISU2 and ISU3 proteins could substitute for the function of ISU1. Adrenodoxins ADX1 and ADX2 and adrenodoxin reductase, ADXR, together form the reducing system that provides electrons for *de novo* Fe-S cluster assembly in the central scaffold ISU1. In addition to Fe-S cluster assembly, the ADX-ADXR low-potential electron-transfer chain transfers electrons from NADH to cytochrome *c* [75] and also reconstitutes a functional plant biotin synthase complex [76]. The transcript levels of ADX and ADXR are high in flowers, whereas the protein level of ADXR is high in the leaf, stem, and flower. HSCA1/HSCA2 and HSCB are the chaperones and co-chaperone, respectively, that work together in the delivery of Fe-S clusters from the ISU1 scaffold to target apo-proteins [21]. The preassembled Fe-S cluster on ISU1 needs to be labilized by the dedicated chaperone system through sequential protein-protein interactions.

A recent study has reported that HSCA1 and HSCB are localized to both mitochondria and cytosol in *A. thaliana* [77]. It would be interesting to see whether some fraction of ISU1 is also localized in cytosol because ISU1 is the physiologically relevant partner for the chaperone system. HSCB is highly expressed in anthers, the part of the stamen where pollen is produced, and trichomes, cells that project from the surface of the epidermis. The HSCB insertion mutant shows reduced seed production, reduced wax production, which is needed to protect the plant surface in a terrestrial environment, inappropriate trichome development, and dramatically reduced activities of Fe-S enzymes including aconitase and succinate dehydrogenase [77].

GRXS15, a monothiol glutaredoxin in mitochondria, is an alternative scaffold. GRXS15 helps to transfer the Fe-S cluster from ISU1 to apo-proteins, likely *via* transient binding of the Fe-S cluster in a glutathione-GRXS15 complex [57]. NFU4 and NFU5 are alternative scaffolds, and their mitochondrial localization is confirmed [48]. Their function is likely to deliver Fe-S clusters to a subset of target apo-proteins, which remain to be identified. ISA1–ISA3 are putative Fe-S cluster delivery proteins, which are not yet characterized in plants. IBA57 is a tetrahydrofolate-binding protein. *In vivo* evidence indicates that IBA57 is required for the activity of MiaB, a [4Fe-4S]-containing tRNA modification enzyme [78]. The expression of IBA57 is high in flowers, long narrow seed-pods known as siliques, and seeds. Insertional mutagenesis of IBA57 is embryonic lethal. ISA1, ISA2, ISA3, and IBA57 may form a protein complex that functions in the targeting of [4Fe-4S] clusters to specific mitochondrial apo-proteins, including aconitase and radical SAM enzymes [79, 80]. INDL is an assembly factor that may be specific to complex I of mitochondria. INDL may bind and transfer a [4Fe-4S] cluster to acceptor Fe-S proteins in complex I [81]. The molecular details of INDL function remain to be characterized in plants.

ATM3 is an ABC transporter located in the inner membrane of mitochondria [82–85]. It is thought to export a substance from the matrix of mitochondria to cytosol, but molecular details on functions of this transporter and its substrate(s) are unknown so far. However, several lines of evidence have strongly indicated that ATM3 is not required for the Fe-S biosynthesis in mitochondria but is rather needed for Fe-S assembly in cytosol [86–88]. In the absence of ATM3, cytosolic Fe-S biosynthesis is defective. The substrate(s) exported by ATM3 are thought to be a component used for the Fe-S cluster assembly in cytosol, which, however, remains to be characterized. In addition to a function in the maturation of extramitochondrial Fe-S proteins, ATM3 has a crucial role in the molybdenum cofactor (Moco) biosynthesis. It has been observed that cyclic pyranopterin monophosphate (cPMP), an intermediate of Moco biosynthesis, accumulates in the mitochondria of ATM3 mutant plants (Moco synthesis is discussed in greater detail in Chapter 19 by Leimkühler in this volume). It is therefore reasonable to presume that ATM3 has a function in the export of cPMP from mitochondria to cytosol [87]. An ATM3 knockout mutant (*Sta1) Arabidopsis* demonstrates dwarfism and chlorosis phenotype. It also shows altered morphology of leaf and cell nuclei [88]. In a comprehensive study using an allelic mutant series of ATM3, the activity of a cytosolic

Fe-S protein aconitase was strongly decreased, whereas mitochondrial and plastid Fe-S proteins were not affected. In contrast to ATM3, orthologous mutants in yeast and mammals accumulate iron in mitochondria, whereas the plant ATM3 mutants do not display a dramatic iron homeostasis defect and do not accumulate iron in mitochondria [86]. The difference between plants and other eukaryotes concerning the effects of ATM3 mutation on cellular iron homeostasis may be because of the presence of chloroplasts in plant cells, the organelle known to be more important in acquiring cellular iron. Recently, mutagenesis of ATM3 was found to result in defective genome integrity in the plant, *A. thaliana* [89]. These data support that ATM3 function is required for the maturation of Fe-S proteins in cytosol and nuclei, many of which are the genome DNA repair enzymes. ERV1 is a redox-active and FAD-containing sulfhydryl oxidase. It is located in the intermembrane space of mitochondria. Similar to orthologues in yeast and animal cells, ERV1 is required for the maturation of Fe-S proteins in cytosol. *In vitro* assays with purified protein and artificial substrates demonstrate a preference of ERV1 for dithiols that have a defined space between the thiol groups, suggesting that their substrate is thioredoxin-like [90].

16.3.3 CIA system in cytosol

The cytosolic CIA machinery of *Arabidopsis* consists of seven proteins (Fig. 16.1 and Tab. 16.1), involving TAH18, DRE2, NBP35, NAR1, CIA1, CIA2, and MMS19. The nuclear genome of *Arabidopsis* encodes only two cysteine desulfurases, NFS1 and NFS2. They are localized in the mitochondria and plastids, respectively, led by the targeting peptide in each protein [36, 37, 60]. There is not an exclusively cytosolic cysteine desulfurase present in plants, which is also true for other eukaryotes. The sulfur source for the Fe-S cluster assembly in cytosol is not clear. However, the sulfur for Fe-S assembly in cytosol might be provided by two mechanisms. One possibility is that ATM3 may export the sulfur to the cytosol for Fe-S assembly. The second possible mechanism is to generate a cytosolic cysteine desulfurase by alternative initiation site utilization of the mitochondrial NFS1 mRNA, which is believed the case in humans [34, 91] but has never been reported in plants.

NBP35 is the scaffold for Fe-S cluster assembly in cytosol of plants [92]. It is constitutively expressed in planta. NBP35 binds a [4Fe-4S] cluster in the C terminus and a stable [4Fe-4S] cluster in the N terminus. Holo-NBP35 is able to transfer an Fe-S cluster to an apo-protein *in vitro*. NBP35 mutant plants show an arrest of embryo development [92]. NBP35-deficient *Arabidopsis* mutants are seedling lethal, suggesting an essential function [93]. TAH18 is a diflavin reductase, which is able to reduce cytochrome *c* *in vitro*. It forms a protein complex with DRE2, and these two proteins together provide electrons for Fe-S assembly on the NBP35 scaffold [94]. Loss of TAH18 function results in early embryonic lethality in plants. TAH18 also has possible roles in the control of cell death and chromosomal segregation in mitosis [94]. Consistently, the promoter of

TAH18 is activated during cell cycle progression, probably because many DNA replication and DNA repair proteins are Fe-S proteins, and increased expression of TAH18 is required to help synthesize more Fe-S clusters for the DNA metabolism proteins during cell cycle progression.

NAR1 is an [FeFe]-hydrogenase-like gene. The recombinant NAR1 protein coordinates two Fe-S clusters. NAR1 knockdown results in a dwarf phenotype under normoxia, but the phenotype is indistinguishable from wild type under hypoxic conditions. This result suggests that the exposure to low oxygen might alleviate the severity of the phenotype caused by NAR1 knockdown [95]. Another study reports that the expression of some hypoxia-responsive genes, including ferredoxin (Fdx5) and two [FeFe]-hydrogenases, HydA1 and HydA2, could be upregulated by hypoxia treatment in both NAR1 knockdown and wild-type plants. This result indicates that NAR1 is not involved in regulating the hypoxia response of green algae [96]. The activity of cytosolic Fe-S enzymes, including aldehyde oxidase and xanthine dehydrogenase, is decreased in NAR1 knockdown lines, whereas Fe-S protein activities in the chloroplast and mitochondria are unaffected. These results indicate that NAR1 is required for the activity of cytosolic Fe-S enzymes but not for Fe-S proteins in chloroplasts or mitochondria [96].

CIA1 is a WD40-repeat protein, an essential and conserved member of the Fe-S assembly CIA machinery. The structure of CIA1 protein folds into a β propeller with seven blades arranged around a central axis. The conserved top surface residue R127 performs a critical function in cytosolic Fe-S protein assembly [97]. CIA2, also named AE7, is a DUF59 family gene that acts in the CIA Fe-S cluster assembly pathway to maintain nuclear genome integrity [89]. CIA2 mutations result in lower activities of the cytosolic [4Fe-4S] enzyme aconitase and the nuclear [4Fe-4S] enzyme DNA glycosylase, ROS1. The severe CIA2 mutant allele is embryonic lethal, whereas the weaker CIA2 mutant alleles are viable but exhibit highly increased DNA damage, which results in cell cycle arrest through the DNA damage response pathway [89].

MMS19, a conserved HEAT repeat protein, is a component of the CIA pathway for Fe-S cluster assembly and is implicated in DNA repair. MMS19 is encoded in the genome of plants, for instance, in *Arabidopsis*, but it has not yet been fully characterized in plants. Studies on its orthologues in mammalian cells indicate that MMS19 is a member of the cytosolic Fe-S protein assembly (CIA) machinery [98–100]. MMS19 functions as part of the CIA-targeting complex that specifically facilitates Fe-S cluster insertion into apo-proteins involved in methionine biosynthesis, DNA replication, DNA repair, and telomere maintenance. However, MMS19 is not required for targeting Fe-S clusters to other cytosolic apo-proteins, such as aconitase/IRP1 and glutamine amidotransferase (GPAT) [99]. By co-immunoprecipitation and mass spectrometry analysis, 12 known Fe-S proteins have been identified in the MMS19 complex, including XPD, FANCJ, DNA polymerase D, DNA primase, and DNA2. Consistent with an essential role of MMS19 in DNA metabolism, MMS19 knockout is embryonically lethal in mice [100]. As in other eukaryotic cells, NAR1, CIA1, CIA2, and MMS19 proteins

form a stable complex in plant cells [89]. This protein complex may be termed as "CIA-targeting complex," which physically interacts with and transfers Fe-S clusters to various DNA metabolism Fe-S proteins.

16.4 Regulation of cellular iron homeostasis by Fe-S cluster biosynthesis

In mammals, cellular regulation of iron metabolism involves the cytosolic Fe-S protein IRP1, providing a tight link between Fe-S protein biogenesis and mitochondrial iron homeostasis [101, 102]. Similarly, cellular iron homeostasis in yeast cells is also tightly linked to mitochondrial ISC machinery [21, 28]. The mitochondrial inner membrane transporter ATM3 homologues export an unknown signal "X" into cytosol. The signal reflects iron status in mitochondria, and it affects CIA activity in cytosol. In the deficiency of signal "X," iron overaccumulates in mitochondria, and cellular iron homeostasis is impaired [33, 34].

Except for the plastid SUF system that is unique to plants, the mitochondrial ISC and cytosolic CIA machineries in plant cells are highly homologous to those in yeast and mammalian cells. However, to date, there is no strong evidence of an association between mitochondrial Fe-S assembly and cellular iron homeostasis in plants. Defects in mitochondrial ISC machinery or plant ATM3 do not cause iron accumulation in mitochondria of plant cells, although they decrease Fe-S protein activity in cytosol [86, 87]. The reason for nonaccumulation of iron in the mitochondria of ATM3 mutant plant cells may be because chloroplasts are also involved in cellular iron homeostasis or that the chloroplast rather than mitochondrion may develop iron homeostasis problems. Indeed, it has been reported in an ATM3 mutant (*Sta1*) plant that the mutant shows a chlorosis phenotype [88], a classical indication of iron deficiency in plants. Although chloroplasts have normal levels of iron, the mutant plant cells cannot properly utilize iron. The interplay among mitochondria ISC, plastids SUF, and cellular iron homeostasis in plants needs to be further elucidated.

16.5 Conservation of Fe-S cluster assembly genes across the green lineage

The green lineage is a diverse group of photosynthetic organisms, including unicellular green algae, mosses, ferns, and seed plants. The evolution has resulted in increasing levels of complexity, from the simplest green algae to the more complex higher plants. As an essential biological pathway, the Fe-S cluster biosynthetic pathway is conserved with the evolution of plants. Comparative genomic analysis of Fe-S cluster biosynthesis genes could reveal valuable information. To date, the genomes of over 40 plant and photosynthetic species have been sequenced, and

gene sequences are available in the Phytozome and NCBI databases. In this chapter, five representative plant and photosynthetic species have been selected for a comparison of Fe-S biosynthesis genes, including green algae (*Chlamydomonas reinhardtii*), rice (*O. sativa*), tomato (*Solanum lycopersicum), Arabidopsis* (*A. thaliana*), and soybean (*Glycine max*).

Among all Fe-S synthesis genes (Tab. 16.1), the majority are conserved in the five species compared and probably in all plants. Only eight genes are not conserved in all five species (Tab. 16.2), including SUFE2, NFU3, ISU2, ISU3, ISA2, NFU5, ADX2, and MMS19. Lack of conservation suggests that these genes are not essential for all plants. It may be that the losses of some non-conserved genes are compensated by paralogous genes. Indeed, except for SUFE2 and MMS19, all other non-conserved genes belong to a gene family, in which all members have similar functions and can compensate for each other. SUFE1–SUFE3 share the SUFE domain, but they are not in the same gene family. The presence or absence of a BOLA or NadA domain makes them work differently. MMS19 is the only gene without a paralogue that is not conserved in all five species. MMS19 is encoded in the genome of all four multicellular plants including monocots and dicots, but it is not present in the unicellular algae, *Chlamydomonas* (Tab. 16.2). MMS19 is a central component of the NAR1-CIA1-CIA2-MMS19 complex in mammalian cytosol required for targeting Fe-S clusters to apoproteins involved in DNA replication and DNA repair [89, 99, 100]. Hence, MMS19 may be essential for the maintenance of genome integrity in multicellular plants. Unicellular green algae may employ a MMS19-independent mechanism for DNA repair. Most of the nonconserved genes are scaffolds, including NFU3, ISU2, ISU3, ISA2, and NFU5. An Fe-S biosynthesis machinery typically contains multiple scaffolds for delivering the preassembled [Fe-S] clusters to various target proteins. The

Tab. 16.2: The Fe-S biosynthesis genes that are not conserved across green lineage using five species as examples.

	Chlamydomonas	**Rice**	**Tomato**	***Arabidopsis***	**Soybean**
Plastid					
SUFE2	–	–	+	+	+
NFU3	–	+	+	+	+
Mitochondria					
ISU2	–	+	+	+	+
ISU3	–	–	–	+	+
ISA2	–	+	+	+	+
NFU5	–	–	–	+	–
ADX2	–	+	+	+	+
Cytosol					
MMS19	–	+	+	+	+

–, Gene is not encoded in the genome of the specific species; +, gene is encoded in the species.

least important nonconserved gene is NFU5, as it is encoded only in the genome of *Arabidopsis* among the five species compared here (Tab. 16.2). NFU5 and all other four NFU genes have been identified and characterized in *Arabidopsis*. NFU5 is an alternative scaffold in mitochondria of *Arabidopsis*.

The SUFE2 gene is present in all three dicot plants but not in the monocot rice (Tab. 16.2). Interestingly, more systematic phylogenetic analysis reveals that the SUFE2 gene is encoded in genomes of the majority of dicot plants (>90% of sequenced dicot species). In contrast, it is not present in all six monocot plant genomes, including *Zea mays, Sorghum bicolor, O. sativa, Brachypodium distachyon, Setaria italica, Panicum virgatum*. It seems that SUFE2 is perhaps a dicot-specific gene. As SUFE2 expression is flower-specific and high in pollen, SUFE2 has been thought to specifically function in pollen Fe-S cluster biosynthesis [41]. Hence, it is speculated that SUFE2 may be important for Fe-S assembly in pollens of dicots, but it is not required for Fe-S assembly in pollens of monocots.

16.6 Potential significance to agriculture

Gene mutations in Fe-S cluster biosynthesis are known to cause many severe diseases and even death to humans [26, 33, 34]. The research on mammalian Fe-S biosynthesis is of great medical importance. Gene mutations in Fe-S biosynthesis do not necessarily cause diseases in plants, but the resulting severe phenotypes, such as dwarf, chlorosis, and even embryonic lethality, highlight that Fe-S cluster assembly is an essential and basic biological pathway. Research on plant Fe-S biosynthesis is of potential significance to agriculture, based on the following reasons. First, iron is an important mineral nutrient to humans, and iron deficiency causes anemia and disorders. The majority of the world's population acquires iron nutrition from plant foods (crops, grains, vegetables, fruits), and the iron contents in plant foods therefore affect human health. Further research on plant Fe-S cluster biosynthesis could help us to identify central gene(s) in regulating cellular iron metabolism, which could be used in genetic engineering to produce iron-fortified crops. Second, Fe-S proteins are involved in the assimilation of nitrogen, sulfur, molybdenum, and iron nutrition [24, 25, 31]. These minerals are components of fertilizers widely used in agriculture. The Fe-S protein biogenesis in crops would affect the efficiency in the uptake and utilization of mineral nutrients from fertilizers. Excellent gene alleles in the Fe-S protein biogenesis could be used as selection markers in molecular breeding to achieve high efficiency of crops in the uptake and utilization of mineral nutrients, and reduction in the use of fertilizers, which would be good for both agriculture and environmental protection. Third, toxic heavy metal pollution in soil is increasingly a problem to agriculture. Some of the Fe-S cluster assembly genes are already known to have functions in improving plant tolerance to heavy metals. For example, the overexpression of NFS2 in plants results in higher tolerance to toxic levels of selenium [40], whereas

increased expression of ATM3 increases the tolerance of plants to cadmium [103]. Better understanding of plant Fe-S cluster assembly could help us to develop strategies to reduce toxic heavy metal accumulation in our foods.

Acknowledgments

The author thanks Dr Marinus Pilon (Colorado State University) for the critical reading of the manuscript, and thanks also to Lu Qin and Xuejiao Liang for making the figure and tables. The work in the author's laboratory is supported by grants from 100-Talent Program of Chinese Academy of Sciences, National Basic Research Program of China (973 Program 2013CB127102), Foundation of Key Laboratory of Plant Resources Conservation, and Sustainable Utilization, South China Botanical Garden, Chinese Academy of Sciences.

References

[1] Palmer CM, Guerinot ML. Facing the challenges of Cu, Fe and Zn homeostasis in plants. Nat Chem Biol 2009;5:333–40.
[2] Kobayashi T, Nishizawa NK. Iron uptake, translocation, and regulation in higher plants. Annu Rev Plant Biol 2012;63:131–52.
[3] Morrissey J, Guerinot ML. Iron uptake and transport in plants: the good, the bad, and the ionome. Chem Rev 2009;109:4553–67.
[4] Jeong J, Guerinot ML. Homing in on iron homeostasis in plants. Trends Plant Sci 2009;14:280–5.
[5] Grotz N, Guerinot ML. Molecular aspects of Cu, Fe and Zn homeostasis in plants. Biochim Biophys Acta 2006;1763:595–608.
[6] Colangelo EP, Guerinot ML. Put the metal to the petal: metal uptake and transport throughout plants. Curr Opinion Plant Biol 2006;9:322–30.
[7] Connolly EL, Campbell NH, Grotz N, Prichard CL, Guerinot ML. Overexpression of the FRO2 ferric chelate reductase confers tolerance to growth on low iron and uncovers posttranscriptional control. Plant Physiol 2003;133:1102–10.
[8] Vasconcelos M, Eckert H, Arahana V, Graef G, Grusak MA, Clemente T. Molecular and phenotypic characterization of transgenic soybean expressing the Arabidopsis ferric chelate reductase gene, FRO2. Planta 2006;224:1116–28.
[9] Connolly EL, Fett JP, Guerinot ML. Expression of the IRT1 metal transporter is controlled by metals at the levels of transcript and protein accumulation. Plant Cell 2002;14:1347–57.
[10] Korshunova YO, Eide D, Clark WG, Guerinot ML, Pakrasi HB. The IRT1 protein from Arabidopsis thaliana is a metal transporter with a broad substrate range. Plant Mol Biol 1999;40:37–44.
[11] Vert G, Grotz N, Dedaldechamp F, et al. IRT1, an Arabidopsis transporter essential for iron uptake from the soil and for plant growth. Plant Cell 2002;14:1223–33.
[12] Ishimaru Y, Suzuki M, Tsukamoto T, et al. Rice plants take up iron as an Fe3+-phytosiderophore and as Fe2+. Plant J Cell Mol Biol 2006;45:335–46.
[13] Bashir K, Ishimaru Y, Shimo H, et al. The rice mitochondrial iron transporter is essential for plant growth. Nat Commun 2011;2:322.
[14] Duy D, Stube R, Wanner G, Philippar K. The chloroplast permease PIC1 regulates plant growth and development by directing homeostasis and transport of iron. Plant Physiol 2011;155:1709–22.

[15] Duy D, Wanner G, Meda AR, von Wiren N, Soll J, Philippar K. PIC1, an ancient permease in Arabidopsis chloroplasts, mediates iron transport. Plant Cell 2007;19:986–1006.
[16] Divol F, Couch D, Conejero G, Roschzttardtz H, Mari S, Curie C. The Arabidopsis yellow stripe like4 and 6 transporters control iron release from the chloroplast. Plant Cell 2013;25:1040–55.
[17] Briat JF. Plant ferritin and human iron deficiency. Nat Biotechnol 1999;17:621.
[18] Petit JM, van Wuytswinkel O, Briat JF, Lobreaux S. Characterization of an iron-dependent regulatory sequence involved in the transcriptional control of AtFer1 and ZmFer1 plant ferritin genes by iron. J Biol Chem 2001;276:5584–90.
[19] Briat JF, Duc C, Ravet K, Gaymard F. Ferritins and iron storage in plants. Biochim Biophys Acta 2010;1800:806–14.
[20] Leidgens S, Bullough KZ, Shi H, et al. Each member of the PCBP family exhibits iron chaperone activity toward ferritin. J Biol Chem 2013;288:17791–802.
[21] Lill R, Hoffmann B, Molik S, et al. The role of mitochondria in cellular iron-sulfur protein biogenesis and iron metabolism. Biochim Biophys Acta 2012;1823:1491–508.
[22] Kim SA, Punshon T, Lanzirotti A, et al. Localization of iron in Arabidopsis seed requires the vacuolar membrane transporter VIT1. Science 2006;314:1295–8.
[23] Zhang Y, Xu YH, Yi HY, Gong JM. Vacuolar membrane transporters OsVIT1 and OsVIT2 modulate iron translocation between flag leaves and seeds in rice. Plant J Cell Mol Biol 2012;72:400–10.
[24] Balk J, Pilon M. Ancient and essential: the assembly of iron-sulfur clusters in plants. Trends Plant Sci 2011;16:218–26.
[25] Ye H, Pilon M, Pilon-Smits EA. CpNifS-dependent iron-sulfur cluster biogenesis in chloroplasts. New Phytol 2006;171:285–92.
[26] Rouault TA, Tong WH. Iron-sulphur cluster biogenesis and mitochondrial iron homeostasis. Nat Rev Mol Cell Biol 2005;6:345–51.
[27] Johnson DC, Dean DR, Smith AD, Johnson MK. Structure, function, and formation of biological iron-sulfur clusters. Annu Rev Biochem 2005;74:247–81.
[28] Lill R, Muhlenhoff U. Maturation of iron-sulfur proteins in eukaryotes: mechanisms, connected processes, and diseases. Annu Rev Biochem 2008;77:669–700.
[29] Frazzon J, Dean DR. Formation of iron-sulfur clusters in bacteria: an emerging field in bioinorganic chemistry. Curr Opin Chem Biol 2003;7:166–73.
[30] Frazzon J, Fick JR, Dean DR. Biosynthesis of iron-sulphur clusters is a complex and highly conserved process. Biochem Soc Trans 2002;30:680–5.
[31] Balk J, Lobreaux S. Biogenesis of iron-sulfur proteins in plants. Trends Plant Sci 2005;10:324–31.
[32] Pilon M, Abdel-Ghany SE, Van Hoewyk D, Ye H, Pilon-Smits EA. Biogenesis of iron-sulfur cluster proteins in plastids. Genet Eng 2006;27:101–17.
[33] Ye H, Rouault TA. Human iron-sulfur cluster assembly, cellular iron homeostasis, and disease. Biochemistry 2010;49:4945–56.
[34] Rouault TA. Biogenesis of iron-sulfur clusters in mammalian cells: new insights and relevance to human disease. Dis Model Mech 2012;5:155–64.
[35] Xu XM, Moller SG. Iron-sulfur clusters: biogenesis, molecular mechanisms, and their functional significance. Antioxid Redox Signal 2011;15:271–307.
[36] Pilon-Smits EA, Garifullina GF, Abdel-Ghany S, et al. Characterization of a NifS-like chloroplast protein from Arabidopsis. Implications for its role in sulfur and selenium metabolism. Plant Physiol 2002;130:1309–18.
[37] Léon S, Touraine B, Briat JF, Lobreaux S. The AtNFS2 gene from Arabidopsis thaliana encodes a NifS-like plastidial cysteine desulphurase. Biochem J 2002;366:557–64.
[38] Ye H, Garifullina GF, Abdel-Ghany SE, Zhang L, Pilon-Smits EA, Pilon M. The chloroplast NifS-like protein of Arabidopsis thaliana is required for iron-sulfur cluster formation in ferredoxin. Planta 2005;220:602–8.

[39] Van Hoewyk D, Abdel-Ghany SE, Cohu CM, et al. Chloroplast iron-sulfur cluster protein maturation requires the essential cysteine desulfurase CpNifS. Proc Natl Acad Sci USA 2007;104:5686–91.
[40] Van Hoewyk D, Garifullina GF, Ackley AR, et al. Overexpression of AtCpNifS enhances selenium tolerance and accumulation in Arabidopsis. Plant Physiol 2005;139:1518–28.
[41] M NM, Ollagnier-de-Choudens S, Sanakis Y, et al. Characterization of Arabidopsis thaliana SufE2 and SufE3: functions in chloroplast iron-sulfur cluster assembly and Nad synthesis. J Biol Chem 2007;282:18254–64.
[42] Ye H, Abdel-Ghany SE, Anderson TD, Pilon-Smits EA, Pilon M. CpSufE activates the cysteine desulfurase CpNifS for chloroplastic Fe-S cluster formation. J Biol Chem 2006;281:8958–69.
[43] Xu XM, Moller SG. AtSufE is an essential activator of plastidic and mitochondrial desulfurases in Arabidopsis. EMBO J 2006;25:900–9.
[44] Willems P, Wanschers BF, Esseling J, et al. BOLA1 is an aerobic protein that prevents mitochondrial morphology changes induced by glutathione depletion. Antioxid Redox Signal 2013;18:129–38.
[45] Li H, Mapolelo DT, Randeniya S, Johnson MK, Outten CE. Human glutaredoxin 3 forms [2Fe-2S]-bridged complexes with human BolA2. Biochemistry 2012;51:1687–96.
[46] Couturier J, Jacquot JP, Rouhier N. Evolution and diversity of glutaredoxins in photosynthetic organisms. Cell Mol Life Sci 2009;66:2539–57.
[47] Huynen MA, Spronk CA, Gabaldon T, Snel B. Combining data from genomes, Y2H and 3D structure indicates that BolA is a reductase interacting with a glutaredoxin. FEBS Lett 2005;579:591–6.
[48] Léon S, Touraine B, Ribot C, Briat JF, Lobreaux S. Iron-sulphur cluster assembly in plants: distinct NFU proteins in mitochondria and plastids from Arabidopsis thaliana. Biochem J 2003;371:823–30.
[49] Touraine B, Boutin JP, Marion-Poll A, Briat JF, Peltier G, Lobreaux S. Nfu2: a scaffold protein required for [4Fe-4S] and ferredoxin iron-sulphur cluster assembly in Arabidopsis chloroplasts. Plant J Cell Mol Biol 2004;40:101–11.
[50] Yabe T, Morimoto K, Kikuchi S, Nishio K, Terashima I, Nakai M. The Arabidopsis chloroplastic NifU-like protein CnfU, which can act as an iron-sulfur cluster scaffold protein, is required for biogenesis of ferredoxin and photosystem I. Plant Cell 2004;16:993–1007.
[51] Xu XM, Adams S, Chua NH, Moller SG. AtNAP1 represents an atypical SufB protein in Arabidopsis plastids. J Biol Chem 2005;280:6648–54.
[52] Xu XM, Moller SG. AtNAP7 is a plastidic SufC-like ATP-binding cassette/ATPase essential for Arabidopsis embryogenesis. Proc Natl Acad Sci USA 2004;101:9143–8.
[53] Abdel-Ghany SE, Ye H, Garifullina GF, Zhang L, Pilon-Smits EA, Pilon M. Iron-sulfur cluster biogenesis in chloroplasts. Involvement of the scaffold protein CpIscA. Plant Physiol 2005;138:161–72.
[54] Yabe T, Nakai M. Arabidopsis AtIscA-I is affected by deficiency of Fe-S cluster biosynthetic scaffold AtCnfU-V. Biochem Biophys Res Commun 2006;340:1047–52.
[55] Lezhneva L, Amann K, Meurer J. The universally conserved HCF101 protein is involved in assembly of [4Fe-4S]-cluster-containing complexes in Arabidopsis thaliana chloroplasts. Plant J Cell Mol Biol 2004;37:174–85.
[56] Schwenkert S, Netz DJ, Frazzon J, et al. Chloroplast HCF101 is a scaffold protein for [4Fe-4S] cluster assembly. Biochem J 2010;425:207–14.
[57] Bandyopadhyay S, Gama F, Molina-Navarro MM, et al. Chloroplast monothiol glutaredoxins as scaffold proteins for the assembly and delivery of [2Fe-2S] clusters. EMBO J 2008;27:1122–33.
[58] Cheng NH, Liu JZ, Brock A, Nelson RS, Hirschi KD. AtGRXcp, an Arabidopsis chloroplastic glutaredoxin, is critical for protection against protein oxidative damage. J Biol Chem 2006;281:26280–8.

[59] Liu X, Liu S, Feng Y, et al. Structural insights into the N-terminal GIY-YIG endonuclease activity of Arabidopsis glutaredoxin AtGRXS16 in chloroplasts. Proc Natl Acad Sci USA 2013;110:9565–70.
[60] Frazzon AP, Ramirez MV, Warek U, et al. Functional analysis of Arabidopsis genes involved in mitochondrial iron-sulfur cluster assembly. Plant Mol Biol 2007;64:225–40.
[61] Turowski VR, Busi MV, Gomez-Casati DF. Structural and functional studies of the mitochondrial cysteine desulfurase from Arabidopsis thaliana. Mol Plant 2012;5:1001–10.
[62] Heis MD, Ditmer EM, de Oliveira LA, Frazzon AP, Margis R, Frazzon J. Differential expression of cysteine desulfurases in soybean. BMC Plant Biol 2011;11:166.
[63] Pandey A, Golla R, Yoon H, Dancis A, Pain D. Persulfide formation on mitochondrial cysteine desulfurase: enzyme activation by a eukaryote-specific interacting protein and Fe-S cluster synthesis. Biochem J 2012;448:171–87.
[64] Busi MV, Zabaleta EJ, Araya A, Gomez-Casati DF. Functional and molecular characterization of the frataxin homolog from Arabidopsis thaliana. FEBS Lett 2004;576:141–4.
[65] Maliandi MV, Busi MV, Clemente M, Zabaleta EJ, Araya A, Gomez-Casati DF. Expression and one-step purification of recombinant Arabidopsis thaliana frataxin homolog (AtFH). Protein Expr Purif 2007;51:157–61.
[66] Maliandi MV, Busi MV, Turowski VR, Leaden L, Araya A, Gomez-Casati DF. The mitochondrial protein frataxin is essential for heme biosynthesis in plants. FEBS J 2011;278:470–81.
[67] Busi MV, Maliandi MV, Valdez H, et al. Deficiency of Arabidopsis thaliana frataxin alters activity of mitochondrial Fe-S proteins and induces oxidative stress. Plant J Cell Mol Biol 2006;48:873–82.
[68] Stemmler TL, Lesuisse E, Pain D, Dancis A. Frataxin and mitochondrial FeS cluster biogenesis. J Biol Chem 2010;285:26737–43.
[69] Bencze KZ, Kondapalli KC, Cook JD, et al. The structure and function of frataxin. Crit Rev Biochem Mol Biol 2006;41:269–91.
[70] Wilson RB. Frataxin and frataxin deficiency in Friedreich's ataxia. J Neurol Sci 2003;207:103–5.
[71] Patel PI, Isaya G. Friedreich ataxia: from GAA triplet-repeat expansion to frataxin deficiency. Am J Hum Genet 2001;69:15–24.
[72] Palau F. Friedreich's ataxia and frataxin: molecular genetics, evolution and pathogenesis (Review). Int J Mol Med 2001;7:581–9.
[73] Busi MV, Gomez-Casati DF. Exploring frataxin function. IUBMB Life 2012;64:56–63.
[74] Léon S, Touraine B, Briat JF, Lobreaux S. Mitochondrial localization of Arabidopsis thaliana Isu Fe-S scaffold proteins. FEBS Lett 2005;579:1930–4.
[75] Takubo K, Morikawa T, Nonaka Y, et al. Identification and molecular characterization of mitochondrial ferredoxins and ferredoxin reductase from Arabidopsis. Plant Mol Biol 2003;52:817–30.
[76] Picciocchi A, Douce R, Alban C. The plant biotin synthase reaction. Identification and characterization of essential mitochondrial accessory protein components. J Biol Chem 2003;278:24966–75.
[77] Xu XM, Lin H, Latijnhouwers M, Moller SG. Dual localized AtHscB involved in iron sulfur protein biogenesis in Arabidopsis. PloS One 2009;4:e7662.
[78] Waller JC, Alvarez S, Naponelli V, et al. A role for tetrahydrofolates in the metabolism of iron-sulfur clusters in all domains of life. Proc Natl Acad Sci USA 2010;107:10412–7.
[79] Muhlenhoff U, Richter N, Pines O, Pierik AJ, Lill R. Specialized function of yeast Isa1 and Isa2 proteins in the maturation of mitochondrial [4Fe-4S] proteins. J Biol Chem 2011;286:41205–16.
[80] Gelling C, Dawes IW, Richhardt N, Lill R, Muhlenhoff U. Mitochondrial Iba57p is required for Fe/S cluster formation on aconitase and activation of radical SAM enzymes. Mol Cell Biol 2008;28:1851–61.

[81] Bych K, Kerscher S, Netz DJ, et al. The iron-sulphur protein Ind1 is required for effective complex I assembly. EMBO J 2008;27:1736–46.
[82] Chen S, Sanchez-Fernandez R, Lyver ER, Dancis A, Rea PA. Functional characterization of AtATM1, AtATM2, and AtATM3, a subfamily of Arabidopsis half-molecule ATP-binding cassette transporters implicated in iron homeostasis. J Biol Chem 2007;282:21561–71.
[83] Camaschella C. Hereditary sideroblastic anemias: pathophysiology, diagnosis, and treatment. Semin Hematol 2009;46:371–7.
[84] Lill R, Kispal G. Mitochondrial ABC transporters. Res Microbiol 2001;152:331–40.
[85] Shimada Y, Okuno S, Kawai A, et al. Cloning and chromosomal mapping of a novel ABC transporter gene (hABC7), a candidate for X-linked sideroblastic anemia with spinocerebellar ataxia. J Hum Genet 1998;43:115–22.
[86] Bernard DG, Cheng Y, Zhao Y, Balk J. An allelic mutant series of ATM3 reveals its key role in the biogenesis of cytosolic iron-sulfur proteins in Arabidopsis. Plant Physiol 2009;151:590–602.
[87] Teschner J, Lachmann N, Schulze J, et al. A novel role for Arabidopsis mitochondrial ABC transporter ATM3 in molybdenum cofactor biosynthesis. Plant Cell 2010;22:468–80.
[88] Kushnir S, Babiychuk E, Storozhenko S, et al. A mutation of the mitochondrial ABC transporter Sta1 leads to dwarfism and chlorosis in the Arabidopsis mutant starik. Plant Cell 2001;13:89–100.
[89] Luo D, Bernard DG, Balk J, Hai H, Cui X. The DUF59 family gene AE7 acts in the cytosolic iron-sulfur cluster assembly pathway to maintain nuclear genome integrity in Arabidopsis. Plant Cell 2012;24:4135–48.
[90] Levitan A, Danon A, Lisowsky T. Unique features of plant mitochondrial sulfhydryl oxidase. J Biol Chem 2004;279:20002–8.
[91] Land T, Rouault TA. Targeting of a human iron-sulfur cluster assembly enzyme, nifs, to different subcellular compartments is regulated through alternative AUG utilization. Mol Cell 1998;2:807–15.
[92] Bych K, Netz DJ, Vigani G, et al. The essential cytosolic iron-sulfur protein Nbp35 acts without Cfd1 partner in the green lineage. J Biol Chem 2008;283:35797–804.
[93] Kohbushi H, Nakai Y, Kikuchi S, Yabe T, Hori H, Nakai M. Arabidopsis cytosolic Nbp35 homodimer can assemble both [2Fe-2S] and [4Fe-4S] clusters in two distinct domains. Biochem Biophys Res Commun 2009;378:810–5.
[94] Varadarajan J, Guilleminot J, Saint-Jore-Dupas C, et al. ATR3 encodes a diflavin reductase essential for Arabidopsis embryo development. New Phytol 2010;187:67–82.
[95] Cavazza C, Martin L, Mondy S, Gaillard J, Ratet P, Fontecilla-Camps JC. The possible role of an [FeFe]-hydrogenase-like protein in the plant responses to changing atmospheric oxygen levels. J Inorg Biochem 2008;102:1359–65.
[96] Godman JE, Molnar A, Baulcombe DC, Balk J. RNA silencing of hydrogenase(-like) genes and investigation of their physiological roles in the green alga Chlamydomonas reinhardtii. Biochem J 2010;431:345–51.
[97] Srinivasan V, Netz DJ, Webert H, et al. Structure of the yeast WD40 domain protein Cia1, a component acting late in iron-sulfur protein biogenesis. Structure 2007;15:1246–57.
[98] Papatriantafyllou M. DNA Metabolism: MMS19: CIA agent for DNA-linked affairs. Nat Rev Mol Cell Biol 2012;13:538.
[99] Stehling O, Vashisht AA, Mascarenhas J, et al. MMS19 assembles iron-sulfur proteins required for DNA metabolism and genomic integrity. Science 2012;337:195–9.
[100] Gari K, Leon Ortiz AM, Borel V, Flynn H, Skehel JM, Boulton SJ. MMS19 links cytoplasmic iron-sulfur cluster assembly to DNA metabolism. Science 2012;337:243–5.
[101] Rouault TA. The role of iron regulatory proteins in mammalian iron homeostasis and disease. Nat Chem Biol 2006;2:406–14.

[102] Ghosh MC, Zhang DL, Jeong SY, et al. Deletion of iron regulatory protein 1 causes polycythemia and pulmonary hypertension in mice through translational derepression of HIF2alpha. Cell Metab 2013;17:271–81.
[103] Kim DY, Bovet L, Kushnir S, Noh EW, Martinoia E, Lee Y. AtATM3 is involved in heavy metal resistance in Arabidopsis. Plant Physiol 2006;140:922–32.

17 Origin and evolution of Fe-S proteins and enzymes

Eric S. Boyd, Gerrit J. Schut, Eric M. Shepard, Joan B. Broderick, Michael W. W. Adams and John W. Peters

17.1 Introduction

The strong relationship between the structure and reactivity of various Fe-S minerals and their derivatives and biological Fe-S clusters is beyond coincidental and provides insights into key aspects of the transition between the abiotic and the biotic earth. The near-universal occurrence and the functional diversity of Fe-S clusters in biology provide a strong basis for their essential role in biology and almost assuredly indicates that their use was a property of the Last Universal Common Ancestor (LUCA) ~3.5 to 3.8 billion years ago and of more primitive life forms. The parallels between biological Fe-S clusters and Fe-S mineral structure and reactivity is one of the main arguments in support of an "Fe-S world" theory for the origin of life. There is a great deal of merit in arguments supporting a central role for Fe-S moieties in the origin and evolution of life given their ubiquitous role and central importance in electron transfer reactions and energy conservation in all modes of extant life. However, in addition to Fe-S clusters, energy transformation reactions require nucleotide moieties, suggesting that the partnership between the "Fe-S world" and the "RNA world" was likely a very early protobiological event. This chapter brings together topics of Fe-S cluster structure, function, and biosynthesis, which have been emphasized in preceding chapters of this book, in the context of plausible pathways for their integration into biology as an important component of the origin and evolution of life.

17.2 Fe-S chemistry and the origin of life

A number of chemical properties inherent to Fe-S minerals and their derivatives compel us to think that they had a central role in the origin of life. Wächterhäuser's "Fe-S world" suggests that the first protocells could have existed where Fe-S compounds were not only at the heart of catalysis but could potentially function in heredity and compartmentalization [1, 2]. Others share the view that compartmentalization and even heredity may have been inorganic in nature, much in the same manner as the pioneers of the original "RNA world" theory suggested that the first generation of life involved RNA molecules with the combined roles of heredity and catalysis and energy metabolism [3, 4]. Many put the constraints for defining life as having the elements of a gene-encoded energy metabolism. Thus, both the "Fe-S world" and "RNA world" theories as they were originally drafted essentially suggest that the first life forms functioned with a single class of molecules. For biochemists

DOI 10.1515/9783110479850-017

working with various metalloenzymes, the idea that first-generation metabolism could function without mineral- or metal-mediated chemistry seems impractical and unlikely. Although it is easy to envision that nucleotides had a role in metabolism from the onset of life, there is no rational reason to suggest that they functioned in the absence of minerals or mineral-derived metals and metal clusters. Wächtershäuser championed the idea that life arose in and around hydrothermal systems *via* a metabolism-first scenario founded on the reductive citric acid cycle [5], an idea further explored by Russell and Hall [6]. A key feature of this theory is the notion that reactions are catalyzed by pyrite, or other metal sulfides, such as Ni-Fe-S phases. Russell and colleagues [7, 8] have more recently proposed a metabolism-first theory in which ensembles of molecules are contained in iron-sulfide "membranes" (proto-membranes). A common notion in metabolism-first theories is that mineral catalysts were gradually replaced with protein-based biocatalysts. To support this notion, it is often noted that the active metal centers in many proteins, cofactors, and pigments are in fact remnants of their mineral-based precursors [9–13].

Whatever the merits of the "Fe-S world," "RNA world," and "metabolism-first" theories for the origin of life, the strong relationship between the structure and the reactivity of Fe-S minerals and the biological Fe-S clusters associated with extant life is believed by many to be too strong to be purely coincidental. The implications of this compelling relationship are that one can envision a path from minerals to enzymes and that perhaps the earliest life forms lived vicariously through aspects of the reactivity of metals and minerals in their local environment. In this scenario, the selective pressure for the adaptation of metals in biology would be to refine their reactivity for specific functions and to release life from dependency on mineral surfaces, which would inherently lower the barrier for diversification into new ecological niches. The shared attributes of the abiotic and biotic world are invaluable for understanding potential mechanisms for the emergence of initial life and life's functional diversification over the past >3.8 billion years of evolution. A more detailed understanding of the commonalities and parallels between the structure and reactivity of Fe-S minerals and the active sites of Fe-S proteins and enzymes could contribute significantly to developing more advanced and rational theories for the origin of life that can be probed experimentally.

Fe-S clusters are well represented in both the abiotic [9] and biotic worlds [14, 15]. For example, Fe-S minerals, in particular pyrite (FeS_2) and pyrrhotite ($Fe_{1-x}S$), are common on earth, whereas troilite (FeS) is common in iron meteorites. Moreover, various proteins and enzymes that have well defined Fe-S clusters are found in nearly all life forms. In addition to the essential role of Fe-S clusters in biological electron transfer, complex Fe-S clusters are known to be at the catalytic sites of many enzymes, including carbon monoxide dehydrogenase, hydrogenase, and nitrogenase [16]. These enzymes catalyze the activation of gases that were important on the early earth and in present-day biology, namely, hydrogen, nitrogen, carbon monoxide, and carbon dioxide, reactions that are often characterized by high activation barriers [17–20].

Given the similarity of enzymatic Fe-S clusters and iron-sulfide minerals and their derivatives, it has been suggested that biocatalysis was preceded by mineral-based catalysis on the prebiotic earth, with emerging life recruiting and optimizing mineral-based catalysis over time [8, 13, 21, 22].

In some respects it is really not just the parallels that can be drawn between Fe-S minerals and biological Fe-S clusters that allow us to rationalize potential pathways connecting the two, but it is perhaps even more important to understand the differences. As the simplest example of an Fe-S mineral, pyrite consists of Fe and S arranged in a lattice of alternating disulfides (S_2) intermingled with bound octahedral Fe in what is best described as the 2^+ oxidation state. In contrast, the simplest biological Fe-S clusters contain Fe typically in the 2^+ or 3^+ oxidation state bound in a tetrahedral geometry to sulfide (S^{2-}) and thiolate sulfurs (Fig. 17.1). When thinking about these two types of Fe-S structures, one can envision a continuum in which mineral surfaces are transformed through time by fracture and weathering. Subsequent extraction of

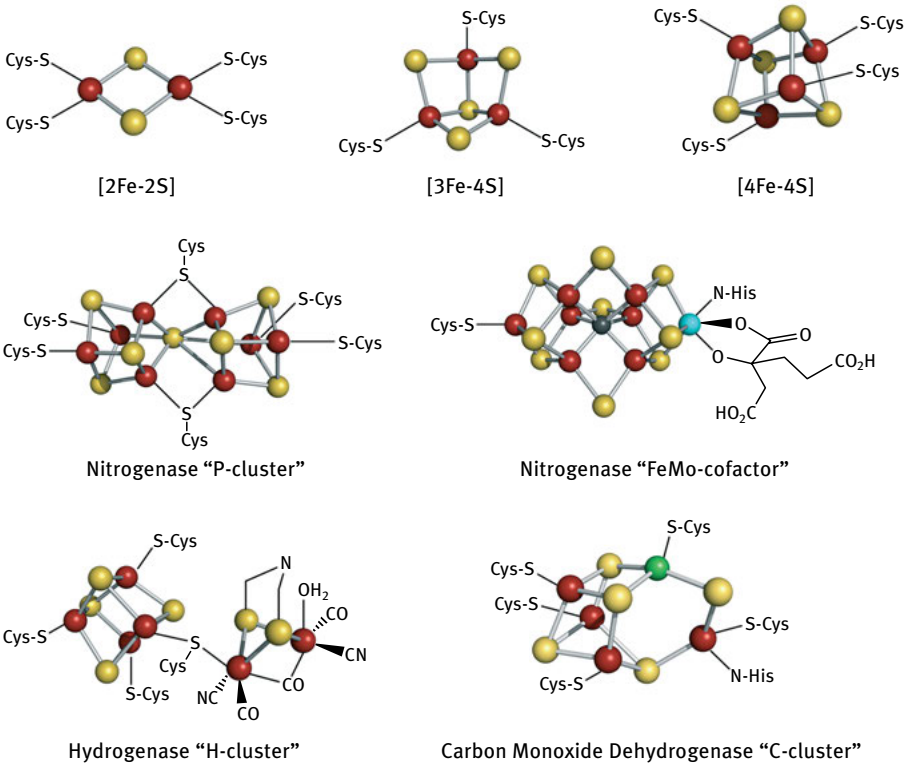

Fig. 17.1: Examples of simple (top) and more complex (middle and bottom) biological Fe-S clusters. Clusters are depicted in ball-and-stick fashion with ligands denoted by text. Color scheme: red, iron; yellow, sulfur; gray, carbon; cyan, molybdenum; green, nickel.

Fe ions and Fe-S fragments at these weathered surfaces by thiolate or carboxylate-based chelators would result in the liberation of protobiological Fe-S clusters. Fe-S clusters of this sort have been generated in mimetic inorganic synthesis and have been demonstrated to essentially self-assemble and remain stable under anaerobic conditions [23–25].

In biological settings, the reactions catalyzed by the complex Fe-S clusters associated with carbon monoxide dehydrogenase, acetyl-CoA synthase, hydrogenase, and nitrogenase, which all include the synthesis of small organic molecules and the redox dependent interconversion of small molecules, only act to provide additional enticement to invoke roles for Fe-S clusters in prebiotic chemistry and protobiology (Fig. 17.1). There is really no evidence of a step wise type progression that relates Fe-S mineral and biological moieties; however, the ability to envision such a hypothetical trajectory highlights the necessity for further examination of the properties and genesis of Fe-S clusters in the context of understanding the transition between abiotic and biotic earth and the origin of life.

17.3 The ubiquity and antiquity of biological Fe-S clusters

The previous chapters firmly establish the ubiquity of Fe-S clusters and their importance as essential components of living cells. In addition to the central role in general redox reactions and trafficking electrons, simple and more complex Fe-S clusters have key catalytic roles in a number of both catabolic and anabolic metabolic processes [17, 18, 26–28]. The aforementioned connections that can be used to relate Fe-S minerals in nature and Fe-S clusters in biology coupled with the selective advantages of reactions involving Fe-S proteins and enzymes lead one to generally accept that these functionalities are ancient, primordial and even likely predate coded proteins and the LUCA [29–31]. Although there are clear limitations of phylogenetic work, especially for addressing origin of life problems, there is a great deal that can be learned about rational evolutionary paths for proteins as well as assigning hypothetical biological functionalities that might be ancient or even primordial. A loose requirement for something to be considered ancient or predating the LUCA of extant life is ubiquity among organisms comprising the three domains of life. This property was one of the key motivating factors for the pioneering work of Carl Woese in establishing 16S/18S ribosomal RNA as a standard for defining taxonomic classifications and evolutionary relationships between organisms forming the three domains of life [32, 33]. The protein synthesis machinery, the ribosome, is conserved across all the domains of life in form and function and is one of a number of functionalities that was likely a property of LUCA.

In addition to the ribosome, other functionalities exist that are universal among organisms throughout all domains of life. Several Fe-S protein and enzyme families can be placed into this category and probably the most obvious examples are the

ferredoxins [34, 35] and the radical *S*-adenosylmethionine (SAM) enzymes [36, 37]. Both are large families that are involved in a variety of cellular functions, occur in all domains of life, and are universally present in deeply rooted organisms within each domain. As touched on throughout this book, ferredoxins are key components in electron transfer in a broad range of metabolic processes. They are widely and integrally distributed among both simple and complex metabolic pathways where they can exist as independent electron transfer functionalities or as domains associated with more complex redox enzymes. Examples of the latter include the numerous ferredoxin binding domains present in the N- and C-terminal domains of [FeFe]-hydrogenase. Moreover, ferredoxins are involved in a number of widely distributed components of energy metabolism including respiration and photosynthesis. Ferredoxins and ferredoxin-like domains of enzymes, especially those related to the 2-[4Fe-4S] ferredoxins, which are the most abundant, exist with a significant level of primary sequence and structural conservation and can be readily identified by the relative location of Cys residues in the primary sequence, or what is commonly referred to as Cys motifs. Motifs for binding [4Fe-4S] clusters that have been clearly conserved through all manner and form of extant life, are strongly suggestive of their antiquity and imply an origin that predates the Last Universal Common Ancestor (LUCA) of extant life.

The radical SAM enzyme family is defined by a conserved motif of Cys residues that are involved in binding a [4Fe-4S] cluster [36]. The Fe-S cluster in radical SAM enzymes is bound differently than in ferredoxins where four cysteine thiolates coordinate the Fe ions of the cluster. In radical SAM proteins, the motif is defined by just three cysteines that coordinate only three of the Fe ions of the [4Fe-4S] cluster, leaving one unique Fe site free to bind the co-substrate SAM (Fig. 17.2) [38, 39]. The reductive cleavage of SAM that occurs at this "site-differentiated" Fe ion is common to all radical SAM enzymes and the 5′-deoxyadenosyl radical product is associated with a large variety of radical reactions involving hydrogen atom abstraction. Although the reactions in which enzymes of the radical SAM family are involved are diverse, there are a couple of observations concerning the nature of the reactions and their evolutionary characteristics that would indicate a potentially primordial origin. Similar to ferredoxins, radical SAM enzymes are present and widely distributed through all domains of life and their functionalities are associated with processes often ascribed to primitive metabolisms (e.g. hydrogenotrophic methanogenesis), and as such are present in numerous deeply rooted lineages. It has been suggested that the radical SAM enzyme anaerobic ribonucleotide reductase, responsible for the conversion of ribonucleotides to deoxyribonucleotides, is more ancient than other forms of ribonucleotide reductases [40]. If true, this implies that DNA synthesis is dependent on Fe-S cluster chemistry or biochemistry, consistent with an origin for Fe-S cluster chemistry/biochemistry prior to the divergence from LUCA. Moreover, this observation may suggest that SAM-mediated Fe-S cluster chemistry/biochemistry predates encoded proteins, at least DNA-encoded proteins. The ferredoxins and radical SAM

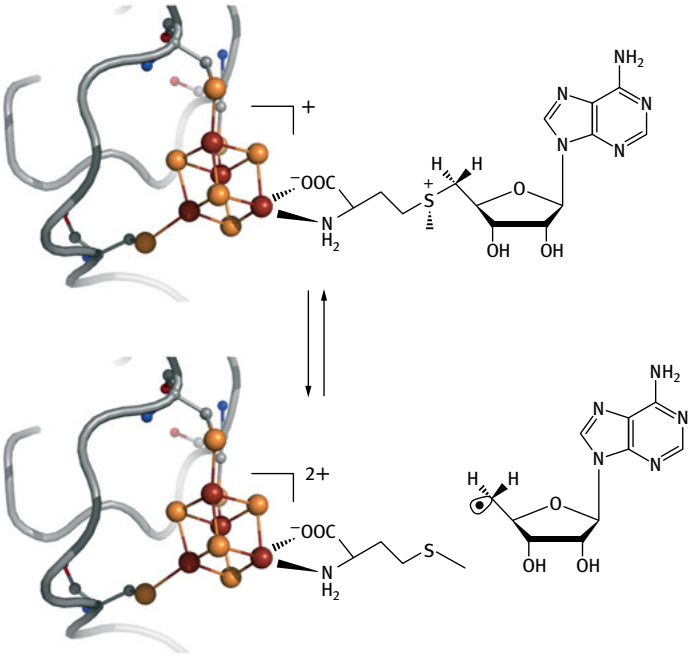

Fig. 17.2: Coordination of SAM to a site-differentiated [4Fe-4S] cluster followed by its reductive cleavage to L-methionine and the 5′-deoxyadenosyl radical species.

enzymes are just two specific examples of ancient Fe-S cluster proteins, but there are a number of other connections that can be drawn to suggest that Fe-S chemistry is as much of a hallmark of life as nucleotides and nucleic acids.

Increased application of phylogenetic and bioinformatic tools clearly point to the ubiquity of Fe-S clusters in early life and suggest a primitive origin for their use in biology that predates the proposed appearance of LUCA ~3.8 billion years ago. Although it is unclear what type of environment may have precipitated the emergence of life and which may have sustained early life, hydrothermal vents harbor a number of features that lead many to suggest these as potential originators of life [7, 41]. Most notable among these are the strong redox gradients present in these systems that are created by the merging of very reduced and hot (~350°C) hydrothermal fluids with lower temperature sea water, creating a suitable energetic driving force for the generation of mineral-based catalysts. As an example, the presence of elevated concentrations of iron and sulfide in these environments react spontaneously to form Fe-S clusters (nanoparticles) that can be further reduced by sulfide to generate Fe-S_2 and molecular H_2 [42]. Fe-S and Fe-S_2 produced through these anoxic abiotic reaction pathways under the sulfidic and ferruginous conditions present at hydrothermal vents may have catalyzed primitive reactions that were adapted and

refined by biology as protein catalysts, as outlined in detail in previous sections. However, the critical questions become how life met its Fe-S cluster requirements for enzyme-based catalysis as it diversified away from sulfidic and ferruginous environments and how the mechanisms that life employs to generate simple Fe-S clusters may have been impacted by the advent of oxygenic photosynthesis and the gradual oxidation of early earth environments.

Life's requirements for Fe-S clusters has led to the emergence of redundant mechanisms to control their synthesis, namely the iron-sulfur cluster (ISC), sulfur formation (SUF), the nitrogenase system (NIF), and the APB systems [43–45]. It has been suggested previously that the various systems can be categorized as those used for general housekeeping (ISC), those used under oxidative stress (SUF), and those used for the synthesis of Fe-S clusters associated with specific processes, e.g. NIF, nitrogenase. Although the evolutionary trajectory of these systems is complex and remains unclear to date, the presence of multiple pathways in some organisms speaks to the central role of Fe-S clusters in biology. Unlike ISC, which exhibits a wide distribution among bacteria and eukaryotes, the SUF system of Fe-S cluster assembly is present in anaerobic methanogens and several archaea, as well as bacteria, which may point to its primitive nature and origin prior to the origin of oxygenic photosynthesis. The near-universal occurrence of SUF in oxygenic cyanobacteria and other aerobes suggests that SUF proteins evolved mechanisms to deal with O_2, and these adaptations likely underpin the utility of this system in repairing Fe-S clusters during the oxidative stress response [43]. Further bioinformatic work is needed to tease apart the phylogenetic distribution and complex evolutionary history of the major Fe-S cluster assembly systems and to provide insight into the role of major geological events (e.g. rise of oxygen, nitrogen crisis) in their evolutionary history.

Among the components of the major Fe-S cluster assembly systems are several proteins that have shared evolutionary history and that are common among the different assembly systems [43]. Similarities between the homologues present challenges in delineating the taxonomic distribution of the major Fe-S cluster assembly systems, but at the same time provide opportunities to place the pathways in evolutionary time, relative to each other. Homologous copies of cysteine desulfurase (encoded by *nifS, iscS, sufS/E*) [46], which functions to abstract sulfide from cysteine for use as a sulfur source in Fe-S cluster synthesis [47], are often encoded by each of the three major systems. As an interesting side note, methanogens do not encode for a homologue of cysteine desulfurase and instead presumably derive sulfur for Fe-S cluster biosynthesis from sulfide, a phenotype that has been attributed to the distribution of methanogens primarily within ecological niches that are anoxic and rich in sulfide [48]. However, the availability of sulfide in the environment is unlikely to explain the absence of a recognizable cysteine desulfurase, as other physiological groups that do not inhabit sulfidic environments also lack homologues of cysteine desulfurases. Like cysteine desulfurase, U-type scaffold (IscU, NifU, and SufU) and A-type scaffold (NifA, IscA, and SufA) proteins are encoded by each system where they function as

platforms for Fe-S cluster synthesis [43]. These scaffolds harbor numerous cysteine-rich regions that coordinate cluster synthesis; the Fe-S clusters formed at these sites are often only bound transiently and are ultimately transferred to apoenzymes.

A critical challenge for all extant life is protecting redox-sensitive Fe-S clusters from oxidative damage due to molecular oxygen or oxygen radicals. This raises the central question as to what the response of Fe-S cluster assembly processes was to the origin of oxygenic photosynthesis and the gradual rise of oxygen. The rise of oxygen would have created at least two problems for biology. First, early oceans were reduced and replete with ferrous iron, which may have acted as the selective pressure leading to the emergence of and proliferation of Fe-dependent enzymes and proteins [49]. However, the gradual production of oxygen would eventually overcome the "buffering capacity" of the reduced ocean, due in part to the abundance of reduced iron [50]. Simultaneously, the once-abundant soluble Fe^{2+} pools in oceans gradually diminished as iron was oxidized and became less soluble, placing strong selection on the development of mechanisms for acquiring and sequestering iron, which may have been achieved through the use of chelators and perhaps scaffold proteins or ferritins, respectively. Second, once the sinks for oxygen had been overcome and oxygen began to accumulate in natural systems, biology would need to develop mechanisms to shield intracellular Fe-S clusters from coming into direct contact with oxygen, or retreat to anoxic niches where oxygen would not be freely available to destabilize Fe-S clusters. Accordingly, the Fe-S cluster assembly process is likely a sentinel system that accurately reflects selection in the face of oxygen-induced oxidative stress, a feature that should be clearly depicted in the evolutionary history of constituent proteins. Alternatively, it is possible that the redundant Fe-S cluster assembly processes evolved in response to the requirement for a stress-resistant cluster assembly pathway or quick production of Fe-S clusters in actively O_2 respiring cells, which would be evident in a taxonomic profiling of the distribution of the various Fe-S assembly systems. Further phylogenetic and taxonomic analysis of the distribution of SUF and ISC on taxonomic trees, especially during the emergence of cyanobacteria, would go a long way toward defining the role of oxygen in the evolution of biological Fe-S cluster assembly.

17.4 Early energy conversion

Electron transfer-linked ion pumping across an ion-impenetrable barrier likely represents the most ancient form of energy conservation. We propose that Fe-S minerals provided the raw materials that enabled Fe-S clusters to both function in the capacity to act as electron wires and to catalyze redox-linked reactions. Moreover, Fe-S clusters have potentially a third function in being able to couple electron transfer and proton translocation, thereby affecting the first form of biological energy conservation. A good example is the class of energy-conserving, membrane-bound [NiFe]-hydrogenase (MBH) found in hyperthermophilic

organisms. These grow at extreme temperatures and are thought by some to be the most ancient of extant microbes. These MBH enzymes catalyze the coupling of electron transfer from ferredoxin through a highly conserved Fe-S cluster to proton reduction (hydrogen gas production), and this is also coupled to thermodynamically unfavorable ion pumping [51]. Phylogenetic analyses of these enzymes demonstrated that this is a blueprint for ancestral energy-conserving mechanisms and that this mechanism of electron transfer through these Fe-S clusters is highly conserved and used throughout almost all present life forms [52]. In some cases the oxidation of simple one-carbon compounds, such as carbon monoxide, and formate, is coupled to H_2 production and energy conservation based on the MBH mechanism. This Fe-S-dependent MBH system also provided the framework for the evolution of modern-day oxygen-dependent respiratory systems that use NADH as the source of electrons and the Fe-S electron wire and ion-translocating mechanisms are without doubt evolutionarily related to those in the MBH-type systems. It is therefore clear that these types of Fe-S clusters are extremely well conserved throughout respiratory systems and that ancestral life performing some kind of respiration most likely contained homologues of these electron wire modules.

Recent new insights and the discovery of electron bifurcation mechanisms have reinforced the central role of Fe-S clusters in diverse and arguably ancient metabolic processes. Electron bifurcation refers to the mechanism by which endergonic and exergonic reactions are coupled in energy conservation transformations. The key component of bifurcating mechanisms is the essential and central role of a two-electron donor/acceptor group, which, for all characterized bifurcating mechanisms, is a flavin that allows the switching/splitting of electrons. Energy conservation by electron bifurcation was first proposed in 2008 [53], in which an exergonic reaction drives an endergonic reaction without the involvement of an ion gradient. In this case, the cytoplasmic enzyme complex butyryl-CoA dehydrogenase catalyzes the reduction of crotonyl-CoA (E_0' = –10 mV) to butyryl-CoA with NADH (E_0' = –320 mV) as the electron donor, and this is coupled to the endergonic reduction of ferredoxin (E_m = −410 mV). As a consequence of this pair of linked redox reactions, the oxidation of NADH can be coupled to H_2 production and consequently associates electron bifurcation and respiration processes. The flavin-containing systems characterized to date are butyryl-CoA dehydrogenase, bifurcating [FeFe]-hydrogenase, hydrogenase-heterodisulfide reductase, *trans*-hydrogenase (NfnAB), bifurcating NADP [FeFe]-hydrogenase/formate dehydrogenase complex, and caffeyl-CoA reductase [54]. By mixing or splitting high/low-potential electrons through the flavin, unfavorable redox reactions can be driven by simultaneous exergonic redox reactions. Electron bifurcation is also assumed to be an ancient energy-conserving mechanism. Indeed, flavins (including the methanogenic cofactor F_{420}, described in the following paragraph) can be considered remnants of an RNA world. In addition, flavins are often loosely associated with proteins and it can be argued that other, more simple redox active centers such as Fe-S clusters played their present-day role in an ancient bifurcation system. The

importance of Fe-S clusters in bifurcation systems is striking in the case of the [FeFe]-hydrogenase. That some of these enzymes have a bifurcation mechanism was first demonstrated with the [FeFe]-hydrogenase of the hyperthermophilic bacterium *Thermotoga maritima* (Fig. 17.3) [55]. This organism contains a standard Embden-Meyerhof glycolytic pathway that produces both NADH and reduced ferredoxin as electron carriers. The exergonic electron transfer from ferredoxin to the [FeFe]-hydrogenase active site is used to pull the endergonic transfer of electrons from NADH, ultimately producing H_2 from both reduced ferredoxin and NADH simultaneously. Interestingly, some of the Fe-S clusters that act as electron wires in the [FeFe]-hydrogenase are highly conserved in the present-day versions of Complex I, again emphasizing the evolutionary importance and the catalytic power of Fe-S clusters [52].

The current examples of bifurcation systems are highly evolved, indicating a long evolutionary history, although they are mostly found within strict anaerobic organisms. In methanogens, hydrogenase-heterodisulfide reductase (H_2 to heterodisulfide and ferredoxin) does not involve nicotinamide nucleotides, although the central methanogenic pathway uses the flavin-like cofactor F_{420}, supporting the notion that methanogens are present-day representatives of an ancient organism. Meanwhile, some butyrate-producing clostridial species use a bifurcating butyryl-CoA dehydrogenase (NADH to crotonyl-CoA and ferredoxin) that does not rely on Fe-S clusters (other than the ferredoxin) but rather contains only FAD as a cofactor [56]. Although an "all Fe-S" bifurcating system lacking flavin has yet to be identified, the ability of Fe-S clusters to carry out two-electron transfer reactions, e.g. $[4Fe\text{-}4S]^{1+,2+,3+}$, and to carry out proton-coupled (hydride) transfer reactions, e.g. in [FeFe]-hydrogenase, argues that

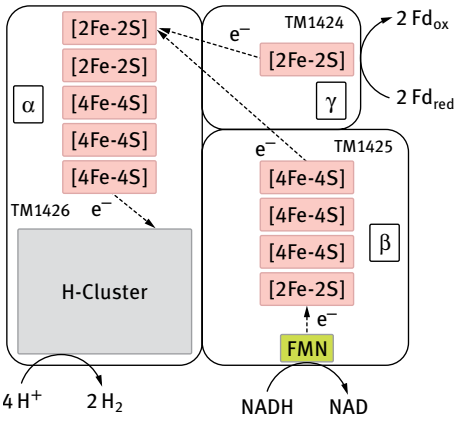

Fig. 17.3: The proposed cofactor content and pathway of electron flow in the bifurcating [FeFe]-hydrogenase of *T. maritima*. Reduced ferredoxin and NADH serve as electron sources, with the reducing equivalents shuttled among various Fe-S cluster centers until ultimately being delivered to the catalytic H-cluster site where H_2 is produced. The detailed structure of the H-cluster is shown in Fig. 17.1.

these moieties could have substituted for the role currently played by flavin in early bifurcating systems.

Electron bifurcation, together with substrate-level phosphorylation, and electron transport or chemiosmotic phosphorylation make up the three known mechanisms of biological energy conservation. Formally, substrate-level phosphorylation does not involve redox reactions *per se*, but the phosphorylating enzymes are typically part of oxidative pathways. In the case of the oxidation of glucose to acetate, the two oxidation steps [at the level of glyceraldehyde-3-phosphate (GAP) and pyruvate] were probably linked to ferredoxin reduction in the earliest forms of these pathways, such as those now present in several hyperthermophilic anaerobic microorganisms, which contain GAP and pyruvate oxidoreductases (GAPOR and POR). Note that GAPOR generates 3-phosphoglycerate, which cannot be used for substrate-level phosphorylation, rather than 1,3-bisphosphoglycerate, which can. Hence, energy is conserved in the GAPOR reaction in the form of a low-potential reductant (reduced ferredoxin), which uses the reducing equivalents to generate H_2 that is coupled to ion transport *via* the energy-conserving [NiFe]-MBH described in previous paragraphs. Most anaerobes have replaced GAPOR with GAP dehydrogenase (GAPDH) in which NAD is reduced (rather than ferredoxin) and energy is conserved in the form of 1,3-bisphosphoglycerate, which can be used for ATP synthesis. As discussed above, bifurcating [FeFe]-hydrogenase enables reductant from both reduced ferredoxin and NADH to be diposed of as H_2, as with the anaerobe *T. maritima*. Aerobes have similarly replaced POR with NAD-linked pyruvate dehydrogenase, but in this case, energy is conserved by aerobic respiration. In any event, electron transfer reactions involving Fe-S clusters dictate the mechanism in which energy can be conserved in pathways, for example, *via* GAPOR or GAPDH. Accordingly, a unifying theme among all three mechanisms of energy conservation in biological systems is oxidation-reduction chemistry mediated in part by Fe-S clusters that in many cases are ferredoxins.

A hallmark in much of this chemistry is the aforementioned pairing of Fe-S proteins and nucleotides, which reinforces the thought that the intimate relationship between Fe-S protein motifs and nucleotides as coenzymes and cofactors in metabolic pathways was forged very early. In the context of the origin of life, the Fe-S moieties in prebiotic energy-transducing reactions are attractive given their observed versatility in accessing a large range of oxidation-reduction potentials. This allows them to participate in a wide range of oxidation-reduction reactions, and as such, it is hard to imagine a nucleotide-based primordial energy metabolism that did not involve partnering with an Fe-S functionality. The aforementioned versatility of the simple Fe-S cluster cubanes in biology and their ubiquitous involvement in oxidative and reductive processes indeed place them at a seminal crossroads in the origin and evolution of early life on Earth.

17.5 Evolution of complex Fe-S cluster containing proteins

Our most recent work on Fe-S cluster biosynthesis has revealed that the parallels between the prebiotic Fe-S mineral reactivity and Fe-S enzymes go beyond common chemical reactivity. We have demonstrated that the stepwise modification of Fe-S clusters in biology occur by reactions of the type that can also be clearly rationalized in terms of the conditions on an early abiotic Earth [57]. These observations include radical-based reactions that transform Fe-S clusters by ligand modification and which tune their reactivity [13, 58–61]. Through the simple stepwise introduction of specific nonprotein ligands and other (non-iron) metals, simple Fe-S clusters are transformed into highly reactive metal sites that perform Hadean (representing the earliest eon in the Earth's history) chemistry. Such reactions are present today as the key fundamental biochemical transformations that support hydrogen, nitrogen, and carbon metabolism in microbial life. The results strongly suggest that the pathway from minerals to enzymes and the origin of simple metabolism is preserved in today's biochemistry.

Our work and the work of others suggest that there are two paradigms for generating the metal-containing enzyme active sites (Fig. 17.4) [57]. The first involves ancestral proteins with defined cavities serving as organic nests for the binding of reactive mineral clusters. In this model, these mineral clusters are refined stepwise through evolutionary time to improve reactivity through the synthesis of a well-defined cofactor with a combination of small molecule and chelating ligands. This paradigm appears to apply for nitrogenase and [FeFe]-hydrogenase. A second paradigm appears to exist for [NiFe]-hydrogenase and carbon monoxide dehydrogenase [62, 63]. These enzymes do not acquire an intact preformed metal cofactor, but rather each metal ion or a group of metal ions is modified on the pre-catalytic protein in a stepwise fashion. From our preliminary work, we have found that the apparently subtle differences in these paradigms have profound implications on the two types of biosynthetic pathways involved, the maturation proteins that these pathways contain, and consequently on how the two pathways involved in the synthesis of the

Fig. 17.4: (right) The path from mineral catalysis to biocatalysis represented to begin with Fe-S-based minerals (shown here as pyrite) and radiating out *via* hypothetical modified cluster intermediates to complex Fe-S enzymes. The top half depicts [FeFe]-hydrogenases (left) and [NiFe]-hydrogenases (right), which both catalyze reversible H_2 oxidation reactions. The bottom half shows nitrogenase catalyzing N_2 reduction (left) and carbon monoxide dehydrogenase catalyzing reversible CO oxidation (right). The representation is defined by the two evolutionary paradigms: paradigm 1, [FeFe]-hydrogenase and nitrogenase; paradigm 2: [NiFe]-hydrogenase and carbon monoxide dehydrogenase). Color scheme: red, iron; orange, sulfur; gray, carbon; cyan, molybdenum; green, nickel. (left) The maturation pathways of nitrogenase and [FeFe]-hydrogenase enzymes that represent paradigm 1. Importantly, the panel highlights the central role that radical SAM chemistry plays in the biosynthetic process. The term "sub" in the [FeFe]-hydrogenase pathway reflects synthesis of the [4Fe-4S] and 2Fe subclusters of the H-cluster, respectively.

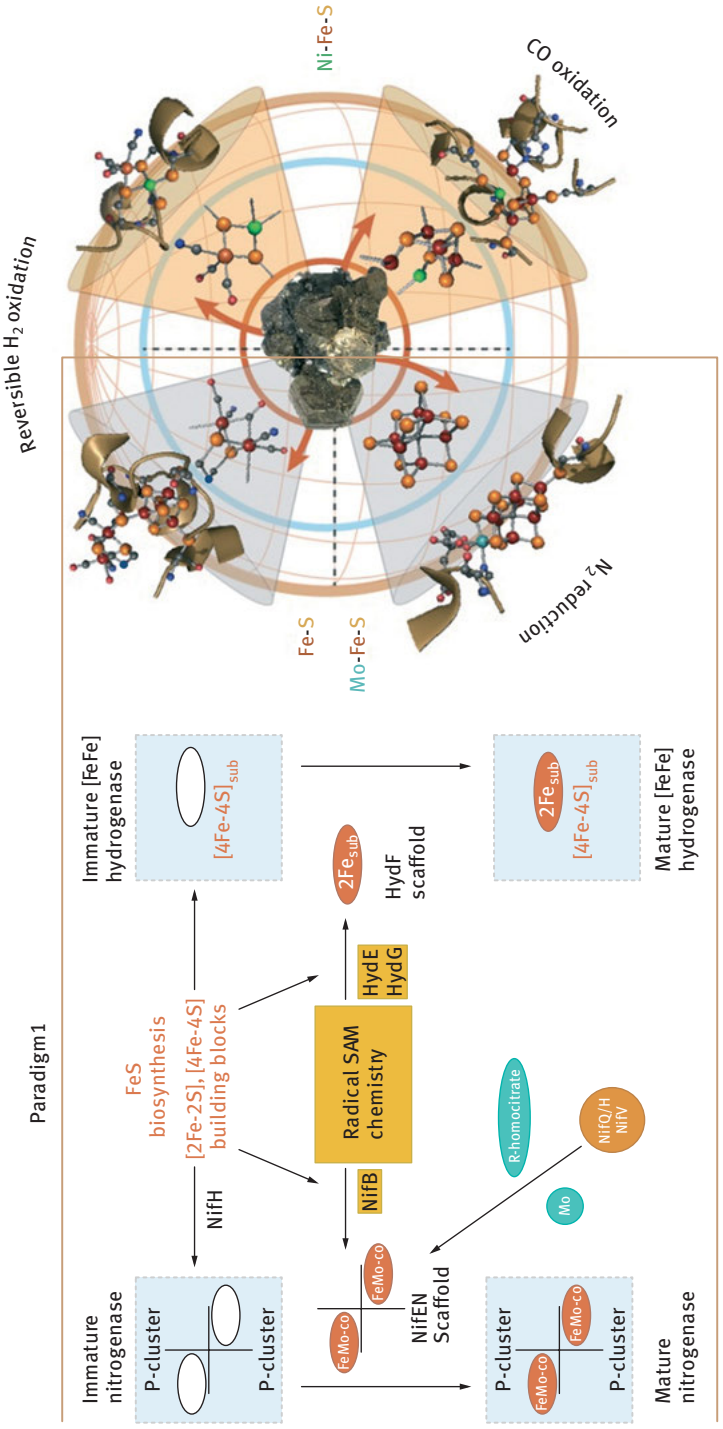

Fe-S-based catalytic sites likely evolved from abiotic mineral precursors. The fact that the biosynthesis of active site clusters in these two types of enzyme follow different paradigms is somewhat surprising especially for the [NiFe]- and [FeFe]-hydrogenases, which catalyze the same chemical reaction despite being evolutionarily unrelated (i.e. convergent evolution) [62]. Our studies suggest that the nitrogenase and [FeFe]-hydrogenase structural proteins observed in extant biology were later innovations in biological evolution, likely emerging to refine chemistry already catalyzed by unique radical-based enzymes [57, 64–66]. The radical enzymes involved in nitrogenase and [FeFe]-hydrogenase cofactor biosynthesis catalyze the key Fe-S modifications that are responsible for the specialized reactivity of these enzymes and are the key determinants of their ancestry [59]. Such radical-based enzymes are an interesting example of the marriage between elements of the Fe-S world and the RNA world where the nucleotide SAM promotes unique chemical reactivity that can be firmly placed as the type of reactivity that could have promoted mineral modifications in the prebiotic Earth to facilitate prebiotic chemistry [13, 40]. The radical SAM centric Fe-S cofactor reactivity underpins the first paradigm for cluster assembly. In contrast to the first paradigm, preliminary phylogenetic analysis of [NiFe]-hydrogenase, as an example of the second paradigm, appears to indicate that the structural proteins are more ancient than the biosynthetic components, and perhaps are primordial. In contrast to the synthesis and insertion of intact cofactors, the assembly of these proteins involves modification of metal ions that are already inserted into the protein and that will eventually become catalytic once those metal ions are suitably modified.

17.6 The path from minerals to Fe-S proteins and enzymes

Although the relationship between Fe-S minerals and protein-based Fe-S clusters is too strong to be coincidental, visualizing the series of steps that might link the two is not as clear-cut. We can perhaps envision a form of early life or protolife that might have lived vicariously off the capacity for oxidation-reduction reactions and the catalytic potential provided by a mineral surface. Life constrained to a mineral surface would be under constant selective pressure to generate mechanisms to effect a release from the dependency on the surface and as such expand its ecological distribution. From this perspective, initial levels of Fe homeostasis, cluster biosynthesis, and first generation functional metal clusters were likely satisfied simultaneously *via* the weathering of mineral surfaces and subsequent chelation of metals and clusters. Organic nesting of metal ions not only released reactive metal clusters from the surface but also concurrently brought about functional diversification. There likely would be ongoing selective pressure that would continue to drive the formation and refinement of such organically nested iron ions and the fact that many cofactors have a combination of protein and nonprotein organic ligand architectures may illustrate this sort of evolutionary progression.

References

[1] Wachtershauser G. Before enzymes and templates: theory of surface metabolism. Microbiol Rev 1988;52:452–84.
[2] Wachtershauser G. Groundworks for an evolutionary biochemistry: the iron-sulphur world. Prog Biophys Mol Biol 1992;58:85–201.
[3] Gilbert W. Origin of life: the RNA world. Nature 1986;319:618.
[4] Cech TR. The RNA worlds in context. Cold Spring Harbor Perspect Biol 2012;4:a006742.
[5] Wachtershauser G. Evolution of the first metabolic cycles. Proc Natl Acad Sci USA 1990;87:200–4.
[6] Russell MJ, Hall AJ. The emergence of life from iron monosulphide bubbles at a submarine hydrothermal redox and pH front. J Geol Soc 1997;154:377–402.
[7] Russell MJ, Daniel RM, Hall AJ, Sherringham JA. A hydrothermally precipitated catalytic iron sulphide membrane as a first step toward life. J Mol Evol 1994;39:231–43.
[8] Martin W, Russell MJ. On the origins of cells: a hypothesis for the evolutionary transitions from abiotic geochemistry to chemoautotrophic prokaryotes, and from prokaryotes to nucleated cells. Philos Trans R Soc London B Biol Sci 2003;358:59–83;discussion 83–55.
[9] Russell MJ, Martin W. The rocky roots of the acetyl-CoA pathway. Trends Biochem Sci 2004;29: 358–63.
[10] Nitschke W, McGlynn SE, Milner-White EJ, Russell MJ. On the antiquity of metalloenzymes and their substrates in bioenergetics. Biochim Biophys Acta 2013;1827:871–81.
[11] Hall DO, Cammack R, Rao KK. The iron-sulphur proteins: evolution of a ubiquitous protein from model systems to higher organisms. Orig Life 1974;5:363–86.
[12] Wachtershauser G. Origin of life in an iron-sulfur world. New York: Cambridge University Press; 1998.
[13] McGlynn SE, Mulder DM, Shepard EM, Broderick JB, Peters JW. Hydrogenase cluster biosynthesis: organometallic chemistry nature's way. Dalton Trans 2009:4274–85.
[14] Johnson MK, Smith AD. Iron-sulfur Proteins. In: King RB, ed. Encyclopedia of inorganic chemistry. 2nd ed. John Wiley & Sons; 2005;2589–619.
[15] Johnson DC, Dean DR, Smith AD, Johnson MK. Structure, function, and formation of biological iron-sulfur clusters. Annu Rev Biochem 2005;74:247–81.
[16] Drennan CL, Peters JW. Surprising cofactors in metalloenzymes. Curr Opin Struct Biol 2003;13:220–6.
[17] Bender G, Pierce E, Hill JA, Darty JE, Ragsdale SW. Metal centers in the anaerobic microbial metabolism of CO and CO_2. Metallomics 2011;3:797–815.
[18] Peters JW. Structure and mechanism of iron-only hydrogenases. Curr Opin Struct Biol 1999;9:670–6.
[19] Seefeldt LC, Hoffman BM, Dean DR. Electron transfer in nitrogenase catalysis. Curr Opin Chem Biol 2012;16:19–25.
[20] Igarashi RY, Seefeldt LC. Nitrogen fixation: the mechanism of the Mo-dependent nitrogenase. Crit Rev Biochem Mol Biol 2003;38:351–84.
[21] Russell MJ, Hall AJ, Cairns-Smith AG, Braterman PS. Submarine hot springs and the origin of life. Nature 1988;336:117.
[22] Wachtershauser G. Pyrite formation, the first energy source for life: a hypothesis. Microbiol Rev 1988;10:207–10.
[23] Daley CJ, Holm RH. Reactions of site-differentiated [Fe4S4]2+, 1+ clusters with sulfonium cations: reactivity analogues of biotin synthase and other members of the S-adenosyl-methionine enzyme family. J Inorg Biochem 2003;97:287–98.
[24] Daley CJ, Holm RH. Reactivity of [Fe4S4(SR)4]2-,3-clusters with sulfonium cations: analogue reaction systems for the initial step in biotin synthase catalysis. Inorg Chem 2001;40:2785–93.

[25] Hagen KS, Watson AD, Holm RH. Synthetic routes to Fe2S2, Fe3S4, Fe4S4, and Fe6S9 clusters from the common precursor [Fe(SC2H5)]4]2-: structures and properties. [Fe3S4(SR)4]3- and [Fe6S9(SC2H5)]2]4-, examples of the newest types of Fe-S-SR clusters. JACS 1983;105:3905–13.
[26] Shepard EM, Broderick JB. S-Adenosylmethionine and iron-sulfur clusters in biological radical reactions: the radical SAM superfamily. In: Comprehensive natural products chemistry. Elsevier; 2009.
[27] Horner DS, Heil B, Happe T, Embley TM. Iron hydrogenases – ancient enzymes in modern eukaryotes. Trends Biochem Sci 2002;27:148–53.
[28] Seefeldt LC, Yang ZY, Duval S, Dean DR. Nitrogenase reduction of carbon-containing compounds. Biochim Biophys Acta 2013;1827:1102–11.
[29] Doolittle WF, Brown JR. Tempo, mode, the progenote, and the universal root Proc Natl Acad Sci USA 1994;91:6721–8.
[30] Penny D, Poole A. The nature of the last universal common ancestor. Curr Opin Genet Dev 1999;9:672–7.
[31] Koonin EV. Comparative genomics, minimal gene-sets and the last universal common ancestor Nat Rev Microbiol 2003;1:127–36.
[32] Woese CR, Fox GE. Phylogenetic structure of the prokaryotic domain: the primary kingdoms. Proc Natl Acad Sci USA 1977;74:5088–90.
[33] Woese CR, Magrum LJ, Fox GE. Archaebacteria. J Mol Evol 1978;11:245–51.
[34] Fitch WM, Bruschi M. The evolution of prokaryotic ferredoxins – with a general method correcting for unobserved substitutions in less branched lineages. Mol Biol Evol 1987;4: 381–94.
[35] Meyer J. The evolution of ferredoxins. Trends Ecol Evol 1988;3:222–6.
[36] Sofia HJ, Chen G, Hetzler BG, Reyes-Spindola JF, Miller NE. Radical SAM, a novel protein superfamily linking unresolved steps in familiar biosynthetic pathways with radical mechanisms: functional characterization using new analysis and information visualization methods. Nucleic Acids Res 2001;29:1097–106.
[37] Frey PA, Hegeman AD, Ruzicka FJ. The radical SAM superfamily. Crit Rev Biochem Mol Biol 2008;43:63–88.
[38] Krebs C, Broderick WE, Henshaw TF, Broderick JB, Huynh BH. Coordination of adenosylmethionine to a unique iron site of the [4Fe-4S] of pyruvate formate-lyase activating enzyme: a Mossbauer spectroscopic study. J Am Chem Soc 2002;124:912–3.
[39] Vey JL, Drennan CL. Structural insights into radical generation by the radical SAM superfamily. Chem Rev 2011;111:2487–506.
[40] Stubbe J. Ribonucleotide reductases: the link between an RNA and a DNA world? Curr Opin Struct Biol 2000;10:731–6.
[41] Russell MJ. The alkaline solution to the emergence of life: energy, entropy and early evolution Acta Biotheor 2007;55:133–79.
[42] Drobner E, Huber H, Wachtershauser G, Rose D, Stetter KO. Pyrite formation linked with hydrogen evolution under anaerobic conditions. Nature 1990;346:742–4.
[43] Ayala-Castro C, Saini A, Outten FW. Fe-S cluster assembly pathways in bacteria. Microbiol Mol Biol Rev 2008;72:110–25.
[44] Bandyopadhyay S, Chandramouli K, Johnson MK. Iron-sulfur cluster biosynthesis. Biochem Soc Trans 2008;36:1112–9.
[45] Fontecave M, Ollagnier-de-Choudens S. Iron-sulfur cluster biosynthesis in bacteria: mechanisms of cluster assembly and transfer. Arch Biochem Biophys 2008;474:226–37.
[46] Zheng L, White RH, Cash VL, Jack RF, Dean DR. Cysteine desulfurase activity indicates a role for NIFS in metallocluster biosynthesis. Proc Natl Acad Sci USA 1993;90:2754–8.
[47] Yuvaniyama P, Agar JN, Cash VL, Johnson MK, Dean DR. NifS-directed assembly of a transient [2Fe-2S] cluster within the NifU protein. Proc Natl Acad Sci USA 2000;97:599–604.

[48] Liu Y, Sieprawska-Lupa M, Whitman WB, White RH. Cysteine is not the sulfur source for iron-sulfur cluster and methionine biosynthesis in the methanogenic archaeon Methanococcus maripaludis. J Biol Chem 2010;285:31923–9.
[49] David LA, Alm EJ. Rapid evolutionary innovation during an Archaean genetic expansion. Nature 2011;469:93–6.
[50] Anbar AD. Oceans. Elements and evolution. Science 2008;322:1481–3.
[51] Sapra R, Bagramyan K, Adams MW. A simple energy-conserving system: proton reduction coupled to proton translocation. Proc Natl Acad Sci USA 2003;100:7545–50.
[52] Schut GJ, Boyd ES, Peters JW, Adams MW. The modular respiratory complexes involved in hydrogen and sulfur metabolism by heterotrophic hyperthermophilic archaea and their evolutionary implications. FEMS Microbiol Rev 2013;37:182–203.
[53] Herrmann G, Jayamani E, Mai G, Buckel W. Energy conservation via electron-transferring flavoprotein in anaerobic bacteria. J Bacteriol 2008;190:784–91.
[54] Buckel W, Thauer RK. Energy conservation via electron bifurcating ferredoxin reduction and proton/Na(+) translocating ferredoxin oxidation. Biochim Biophys Acta 2013;1827:94–113.
[55] Schut GJ, Adams MW. The iron-hydrogenase of Thermotoga maritima utilizes ferredoxin and NADH synergistically: a new perspective on anaerobic hydrogen production. J Bacteriol 2009;191:4451–7.
[56] Li F, Hinderberger J, Seedorf H, Zhang J, Buckel W, Thauer RK. Coupled ferredoxin and crotonyl coenzyme A (CoA) reduction with NADH catalyzed by the butyryl-CoA dehydrogenase/Etf complex from Clostridium kluyveri. J Bacteriol 2008;190:843–50.
[57] Peters JW, Broderick JB. Emerging paradigms for complex iron-sulfur cofactor assembly and insertion. Annu Rev Biochem 2012;81:429–50.
[58] Driesener RC, Challand MR, McGlynn SE, Shepard EM, Boyd ES, Broderick JB, Peters JW, Roach PL. [FeFe]-hydrogenase cyanide ligands derived from S-adenosylmethionine-dependent cleavage of tyrosine. Angew Chemie 2010;49:1687–90.
[59] Shepard EM, Boyd ES, Broderick JB, Peters JW. Biosynthesis of complex iron-sulfur enzymes. Curr Opin Chem Biol 2011;15:319–27.
[60] Shepard EM, Duffus BR, George SJ, McGlynn SE, Challand MR, Swanson KD, Roach PL, Cramer SP, Peters JW, Broderick JB. [FeFe]-hydrogenase maturation: HydG-catalyzed synthesis of carbon monoxide. J Am Chem Soc 2010;132:9247–9.
[61] Wiig JA, Hu Y, Lee CC, Ribbe MW. Radical SAM-dependent carbon insertion into the nitrogenase M-cluster. Science 2012;337:1672–5.
[62] Swanson KD, Duffus BR, Beard TE, Peters JW, Broderick JB. Cyanide and Carbon monoxide ligand formation in hydrogenase biosynthesis. Eur J Inorg Chem 2011:935–47.
[63] Kung Y, Drennan CL. A role for nickel-iron cofactors in biological carbon monoxide and carbon dioxide utilization. Curr Opin Chem Biol 2011;15:276–83.
[64] Boyd ES, Anbar AD, Miller S, Hamilton TL, Lavin M, Peters JW. A late methanogen origin for molybdenum-dependent nitrogenase. Geobiology 2011;9:221–32.
[65] Boyd ES, Peters JW. New insights into the evolutionary history of biological nitrogen fixation. Front Microbiol 2013;4:201.
[66] Mulder DW, Boyd ES, Sarma R, et al. Stepwise [FeFe]-hydrogenase H-cluster assembly revealed in the structure of HydA(DeltaEFG). Nature 2010;465:248–51.

Index